CHE360: INORGANIC CHEMISTRY



LibreTexts™

CHE360: Inorganic Chemistry

This text is disseminated via the Open Education Resource (OER) LibreTexts Project (https://LibreTexts.org) and like the thousands of other texts available within this powerful platform, it is freely available for reading, printing, and "consuming."

The LibreTexts mission is to bring together students, faculty, and scholars in a collaborative effort to provide an accessible, and comprehensive platform that empowers our community to develop, curate, adapt, and adopt openly licensed resources and technologies; through these efforts we can reduce the financial burden born from traditional educational resource costs, ensuring education is more accessible for students and communities worldwide.

Most, but not all, pages in the library have licenses that may allow individuals to make changes, save, and print this book. Carefully consult the applicable license(s) before pursuing such effects. Instructors can adopt existing LibreTexts texts or Remix them to quickly build course-specific resources to meet the needs of their students. Unlike traditional textbooks, LibreTexts' web based origins allow powerful integration of advanced features and new technologies to support learning.



LibreTexts is the adaptable, user-friendly non-profit open education resource platform that educators trust for creating, customizing, and sharing accessible, interactive textbooks, adaptive homework, and ancillary materials. We collaborate with individuals and organizations to champion open education initiatives, support institutional publishing programs, drive curriculum development projects, and more.

The LibreTexts libraries are Powered by NICE CXone Expert and was supported by the Department of Education Open Textbook Pilot Project, the California Education Learning Lab, the UC Davis Office of the Provost, the UC Davis Library, the California State University Affordable Learning Solutions Program, and Merlot. This material is based upon work supported by the National Science Foundation under Grant No. 1246120, 1525057, and 1413739.

Any opinions, findings, and conclusions or recommendations expressed in this material are those of the author(s) and do not necessarily reflect the views of the National Science Foundation nor the US Department of Education.

Have questions or comments? For information about adoptions or adaptions contact info@LibreTexts.org or visit our main website at https://LibreTexts.org.

This text was compiled on 03/11/2026

TABLE OF CONTENTS

Licensing

1: Introduction to Inorganic Chemistry

- 1.1: What is Inorganic Chemistry?
- 1.2: History of Inorganic Chemistry

2: Atomic Structure

- 2.1: Historical Development of Atomic Theory
- 2.2: The Periodic Table
- 2.3: Discovery of Subatomic Particles and the Bohr Atom
- 2.4: The Schrödinger equation, particle in a box, and atomic wavefunctions
  - 2.4.1: Particle in a Box
- 2.5: Quantum Numbers and Atomic Wave Functions
- 2.6: Aufbau Principle
- 2.7: Shielding
- 2.8: Periodic Properties of Atoms
  - 2.8.1: Covalent and Ionic Radii
- 2.9: Ionization energy
- 2.10: Electron Affinity
- 2.11: Lanthanide Contraction

3: Simple Bonding Theory

- 3.1: Lewis Electron-Dot Diagrams
- 3.2: Resonance
- 3.3: Breaking the octet rule with higher electron counts (hypervalent atoms)
- 3.4: Formal Charge
- 3.5: Lewis Fails to Predict Unusual Cases - Boron and Beryllium
- 3.6: Valence Shell Electron-Pair Repulsion
- 3.7: Lone Pair Repulsion
- 3.8: Multiple Bonds
- 3.9: Electronegativity and Atomic Size Effects
- 3.10: Ligand Close Packing
- 3.11: Molecular Polarity
- 3.12: Hydrogen Bonding

4: Coordination Chemistry I- Structures and Isomers

- 4.1: Prelude to Coordination Chemistry I - Structure and Isomers
- 4.2: History
- 4.3: Nomenclature and Ligands
- 4.4: Isomerism
- 4.5: Coordination Numbers and Structures
- 4.6: Coordination Frameworks

5: Symmetry and Group Theory

- 5.1: Symmetry Elements and Operations
- 5.2: Point Groups
- 5.3: Groups of Low and High Symmetry
- 5.4: Other Groups
- 5.5: Properties and Representations of Groups
- 5.6: Matrices
- 5.7: Representations of Point Groups
- 5.8: Character Tables
- 5.9: Examples and Applications of Symmetry
- 5.10: Chirality
- 5.11: Molecular Vibrations

6: Molecular Orbitals

- 6.1: Formation of Molecular Orbitals from Atomic Orbitals
- 6.2: Molecular Orbitals from s Orbitals
- 6.3: Molecular Orbitals from p Orbitals
- 6.4: Molecular orbitals from d orbitals
- 6.5: Nonbonding Orbitals and Other Factors
- 6.6: Homonuclear Diatomic Molecules
- 6.7: Molecular Orbitals
- 6.8: Orbital Mixing
- 6.9: Diatomic Molecules of the First and Second Periods
- 6.10: Heteronuclear Diatomic Molecules
- 6.11: Orbital ionization energies
- 6.12: Polar bonds
- 6.13: Larger (Polyatomic) Molecules
- 6.14: Bifluoride anion
- 6.15: Carbon Dioxide
- 6.16: H_2O
- 6.17: NH_3
- 6.18: CO_2 (Revisted with Projection Operators)
- 6.19: BF_3
- 6.20: Ionic Compounds and Molecular Orbitals

7: Acid-Base and Donor-Acceptor Chemistry

- 7.1: Lewis Concept and Frontier Orbitals
- 7.2: The frontier orbital approach considers Lewis acid base reactions in terms of the donation of electrons from the base's highest occupied orbital into the acid's lowest unoccupied orbital.
- 7.3: All other things being equal electron withdrawing groups tend to make Lewis acids stronger and bases weaker while electron donating groups tend to make Lewis bases stronger and acids weaker
- 7.4: The electronic spectra of charge transfer complexes illustrate the impact of frontier orbital interactions on the electronic structure of Lewis-Acid base adducts
- 7.5: Hard and Soft Acids and Bases
- 7.6: Quantitative Measures of Hardness, Softness, and Acid-Base Interactions from a Hard Soft Acid-Base Principle perspective involve orbital energies and or apportioning acid-base bonding in terms of electrostatic and covalent factors
- 7.7: Hard-Hard and Soft-Soft preferences may be explained and quantified in terms of electrostatic and covalent and electronic stabilization on the stability of Lewis acid-base adducts

8: The Crystalline Solid State

- 8.1: Molecular Orbitals and Band Structure
- 8.2: Prelude to Electronic Properties of Materials - Superconductors and Semiconductors
- 8.3: Metal-Insulator Transitions
- 8.4: Periodic Trends- Metals, Semiconductors, and Insulators
- 8.5: Semiconductors- Band Gaps, Colors, Conductivity and Doping
- 8.6: Semiconductor p-n Junctions
- 8.7: Diodes, LEDs and Solar Cells
- 8.8: Lattice Structures in Crystalline Solids
- 8.9: Superconductors

9: Coordination Chemistry II- Bonding

- 9.1: Evidence for Electronic Structures
- 9.2: Thermodynamic Data
- 9.3: Magnetic Susceptibility
- 9.4: Crystal Field Theory
- 9.5: Ligand Field Theory
- 9.6: Ligand Field Theory - Molecular Orbitals for an Octahedral Complex
- 9.7: Orbital Splitting and Electron Spin
- 9.8: Ligand Field Stabilization Energy
- 9.9: Tetrahedral Complexes
- 9.10: Ligand Field Theory New Page
- 9.11: Angular Overlap
- 9.12: Sigma Bonding in the Angular Overlap Model
- 9.13: Pi Acceptors in the Angular Overlap Model
- 9.14: Pi Donors in the Angular Overlap Model
- 9.15: The Spectrochemical Series
- 9.16: The Magnitude of Parameters $e\sigma$, $e\pi$ and Δ
- 9.17: The Jahn-Teller Effect

Index

Glossary

Detailed Licensing

Licensing

*A detailed breakdown of this resource's licensing can be found in **Back Matter/Detailed Licensing**.*

CHAPTER OVERVIEW

1: Introduction to Inorganic Chemistry

1.1: What is Inorganic Chemistry?
1.2: History of Inorganic Chemistry

1: Introduction to Inorganic Chemistry is shared under a not declared license and was authored, remixed, and/or curated by LibreTexts.

1.1: What is Inorganic Chemistry?

Where did the name "Inorganic Chemistry" come from? Well, the term "Organic Chemistry" literally means the *chemistry of life*. Organic chemistry is the study of carbon-based molecules because the first molecules that were isolated from living organisms contained carbon. On the other hand, minerals and other non-living things seemed to be made of other elements. For some time in our history, scientists believed that the chemical difference between living and non-living things was carbon. So, if "organic" molecules are the molecules of life, then is "inorganic chemistry" the "chemistry of death"? Almost? "Inorganic" chemistry historically meant the chemistry of "non-living" things; and these were non-carbon based molecules and ions.

The names "organic" and "inorganic" come from science history, and still today a generally-accepted definition of *Inorganic Chemistry is the study of non-carbon molecules, or all the elements on the periodic table except carbon (*Figure **1.1.1**. But, this definition is not completely correct because the field of Inorganic Chemistry also includes organometallic compounds and the study of some carbon-based molecules that have properties that are familiar to metals (like conduction of electricity). This makes the field of inorganic chemistry very broad, and practically limitless. A great way to understand the breadth of the field is to take a look at the abstracts in the latest article of Inorganic Chemistry. Or, check out the 20 most-read articles from this past year using the links below.

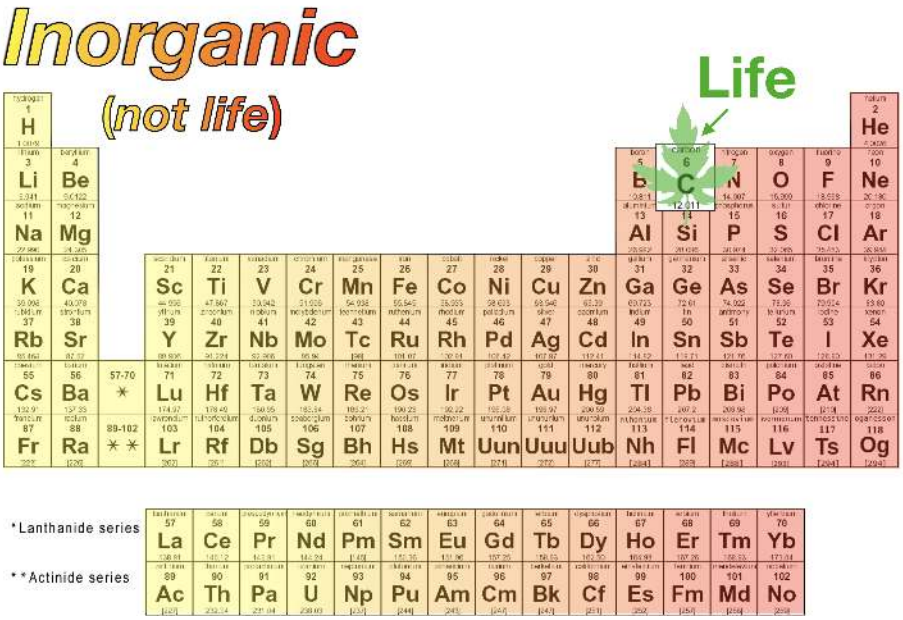


Figure **1.1.1**. An illustration of the historic meaning of "organic" and "inorganic". The modern understanding of organic and inorganic chemistry is not consistent with these historical meanings. (Kathryn Haas; CC-NC-BY-SA)

External links:

- The journal, Inorganic Chemistry: https://pubs.acs.org/journal/inocaj
- The latest issue of Inorganic chemistry: https://pubs.acs.org/toc/inocaj/current
- The most popular Inorganic Chemistry articles from the past month and the past year: https://pubs.acs.org/action/showMostReadArticles?journalCode=inocaj

Practice

? What are the Sub-Fields of Inorganic Chemistry?

To appreciate the breadth of Inorganic Chemistry, go to the most recent issue of Inorganic Chemistry and look at the titles and visual abstracts. Identify at least 4 sub-fields of Inorganic Chemistry.

Answer

> There are a lot of correct answers here! The point here is that you notice that Inorganic Chemistry is a very broad field. It has something for almost everyone because many other fields overlap with Inorganic Chemistry. You might notice that some of the sub-fields you identified are also interdisciplinary fields between inorganic chemistry and another discipline. For a list of some of the subfields of Inorganic Chemistry, check this Wikipedia article.

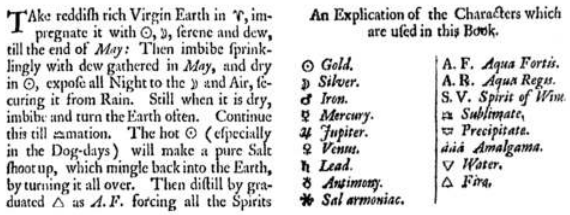
1.1: What is Inorganic Chemistry? is shared under a not declared license and was authored, remixed, and/or curated by LibreTexts.

- **1.1: What is Inorganic Chemistry?** by Kathryn Haas is licensed CC BY-NC-SA 4.0.

1.2: History of Inorganic Chemistry

Metals serve an essential role in many aspects of human civilization and have defined ages of human history. The period of time from about 3300 BC to 1200 BC is often referred to as the Bronze Age. During this period our ancestors first started using metal and learned to mix various elements with copper to make a strong alloy, called bronze. This age yielded significant advancement in the crafting of sharper knives and stronger weapons out of metal instead of rock, wood and bone. Around 1200 BC the human race found an even harder metal and discovered a much stronger alloy called steel. This period is known as the Iron Age. More recently, periods of time known as Gold Rushes have caused huge changes in population distributions and wealth in some countries. Metal has obvious importance in our modern way of life. Today, iron and steel are used for making buildings, machines, automobiles, jewelry, cooking pots, tools, weapons, vehicles, electronics, surgical instruments and symbolic structures like the Eiffel Tower and the Statue of Liberty. Gold, silver, and copper still serve as currency for trade and exchange of goods and services.

The existence of chemistry as a field of study owes much to the fact that gold was a valuable commodity throughout our history. In both the ancient Egyptian society and during the Roman Empire, gold mines were the property of the state, not an individual or group. So there were few ways for most people to legally get any gold for themselves. The Alchemists were a varied group of scholars and charlatans who aimed to solve this problem by creating the **Philosopher's Stone** (which caused the transmutation of lead into gold). Three major streams of alchemy are known: Chinese, Indian, and European, with all three streams having some factors in common. Techniques developed in the European stream ultimately influenced the development of the science of chemistry.


TAke reddiſh rich Virgin Earth in ♈, impregnate it with ☉, ☽, ſerene and dew, till the end of *May*: Then imbibe ſprinklingly with dew gathered in *May*, and dry in ☉, expoſe all Night to the ☽ and Air, ſecuring it from Rain. Still when it is dry, imbibe and turn the Earth often. Continue this till ♒mation. The hot ☉ (eſpecially in the Dog-days) will make a pure Salt ſhoot up, which mingle back into the Earth, by turning it all over. Then diſtill by graduated △ as *A. F.* forcing all the Spirits

An Explication of the Characters which are uſed in this Book.

☉ *Gold.*
☽ *Silver.*
♂ *Iron.*
☿ *Mercury.*
♃ *Jupiter.*
♀ *Venus.*
♄ *Lead.*
♁ *Antimony.*
❋ *Sal armoniac.*

A. F. *Aqua Fortis.*
A. R. *Aqua Regis.*
S. V. *Spirit of Wine.*
♒ *Sublimate.*
♈ *Precipitate.*
dia *Amalgama.*
▽ *Water.*
△ *Fire.*

Figure 1.2.1. Alchemist recipe. Many of the specific approaches that alchemists used when they tried changing lead into gold are vague and unclear. Each alchemist had his own code for recording his data. The processes were kept secret so others could not profit from them. Different scholars developed their own set of symbols as they recorded the information they came up with. Many alchemists were not very honest, taking money from a nobleman by claiming to be able to make gold from lead, then leaving town in the middle of the night. Sometimes the nobleman would detect the fraud and have the alchemist hung. By the 1300's, several European rules had declared alchemy to be illegal and set out strict punishments for those practicing the alchemical arts.

Although alchemists were never successful in changing lead into gold, they made several contributions to modern-day chemistry. Strong acids and bases were discovered, including nitric acid (*ce*$HNO3$), sulfuric acid (H_2SO_4), and hydrochloric acid (HCl), as well as sodium hydroxide ($NaOH$). Glassware for running chemical reactions was developed, as were methods for distillation, crystallization, and sublimation. Alchemy helped improve the study of metallurgy and the extraction of metals from ores. More systematic approaches to research were developed that allowed the discovery of atoms and laid the groundwork for development of the periodic table. For more about the History of Chemistry in general, try the LibreText page A Brief History of Chemistry.

Inorganic compounds have been known and used since antiquity; probably the oldest is the deep blue pigment called Prussian blue ($Fe_4[Fe(CN)_6]_3$). However, the chemical nature of these substances was unknown until the late nineteenth and early twentieth century when the modern field of coordination chemistry emerged. Much of what we know about inorganic chemistry is based largely on the work of and debates between Alfred Werner (1866–1919; Nobel Prize in Chemistry in 1913) and Sophus Mads Jørgensen (1837 –1914). After Werner succeeded in these debates, the field of inorganic chemistry declined in popularity until the mid-twentieth century, when the second world war stimulated renewed interest. During the post-war era, several important discoveries and theories were developed. For example, important theories of bonding in coordination compounds were developed.

Soon after World War II, Crystal Field Theory (CFT) and Ligand Field Theory (LFT) were developed. These are two critical and complimentary theories that provide explanations of spectroscopic, chemical, and structural properties of inorganic coordination compounds, CFT being more simple, and LFT more accurate. In the 1950's, organometallic catalysts were discovered that catalyzed important organic reactions and the Haber-Bosch Process was discovered. The Haber-Bosch Process is catalyzed by an inorganic oxide catalyst and is one of the world's most important industrial reactions. It provides for the synthesis of ammonia directly from elemental nitrogen, N_2, and hydrogen, H_2.

$$N_2(g) + 3H_2(g) \rightleftharpoons 2NH_3(g) \tag{1.2.1}$$

Since its development in the early twentieth century, it has led to the production of an enormous quantity of fertilizer, vastly increasing global food production. As a result, it is estimated that a significant fraction of the nitrogen content in the typical human body is ultimately derived from this process. Yet while the reaction must be run at high temperatures and pressures in the industrial setting, the nitrogenase enzyme in the roots of plants can carry out this reaction at the mild conditions within the soil. Intense investigations were then aimed at improving inorganic catalysts through understanding the metal cofactors in enzymes. The link between the Haber-Bosch industrial process and the nitrogenase enzyme was an early bridge between the fields of organometallic chemistry and biochemistry.

Contributions

Part of this page is adapted from K.Haas Ph.D. dissertation

Part of this page is adapted from the following LibreTexts pages

- Alchemy contributed by CK-12 Foundation by Sharon Bewick, Richard Parsons, Therese Forsythe, Shonna Robinson, and Jean Dupon.
- Werner's Theory of Coordination Compounds
- The Haber-Bosch Process Worksheet

1.2: History of Inorganic Chemistry is shared under a CC BY-NC-SA 4.0 license and was authored, remixed, and/or curated by LibreTexts.

- **1.3: History of Inorganic Chemistry** by Kathryn Haas is licensed CC BY-NC-SA 4.0.

CHAPTER OVERVIEW

2: Atomic Structure

2.1: Historical Development of Atomic Theory
2.2: The Periodic Table
2.3: Discovery of Subatomic Particles and the Bohr Atom
2.4: The Schrödinger equation, particle in a box, and atomic wavefunctions
2.4.1: Particle in a Box
2.5: Quantum Numbers and Atomic Wave Functions
2.6: Aufbau Principle
2.7: Shielding
2.8: Periodic Properties of Atoms
2.8.1: Covalent and Ionic Radii
2.9: Ionization energy
2.10: Electron Affinity
2.11: Lanthanide Contraction

2: Atomic Structure is shared under a not declared license and was authored, remixed, and/or curated by LibreTexts.

2.1: Historical Development of Atomic Theory

Notes about this page

The page below is a brief overview on the history of atomic theory. It contains lots of video media.

Alternatives pages on the history of atomic theory are:

- A more detailed overview that includes practice problems is here (click).
- Another brief overview is here (click).

Skills to Develop

By the end of this section, you will be able to:

- State the postulates of Dalton's atomic theory
- Use postulates of Dalton's atomic theory to explain the laws of definite and multiple proportions
- Outline milestones in the development of modern atomic theory
- Summarize and interpret the results of the experiments of Thomson, Millikan, and Rutherford

A Video Introduction to Atomic Theory through the Nineteenth Century From Crash Course Chemistry



***Video* 2.1.1*:* Lavoisier's discovery of The Law of Conservation of Matter led to the Laws of Definite and Multiple Proportions and eventually Dalton's Atomic Theory.**

Atomic Theory through the Nineteenth Century

The earliest recorded discussion of the basic structure of matter comes from ancient Greek philosophers, the scientists of their day. In the fifth century BC, Leucippus and Democritus argued that all matter was composed of small, finite particles that they called *atomos*, a term derived from the Greek word for "indivisible." They thought of atoms as moving particles that differed in shape and size, and which could join together. Later, Aristotle and others came to the conclusion that matter consisted of various combinations of the four "elements"—fire, earth, air, and water—and could be infinitely divided. Interestingly, these philosophers thought about atoms and "elements" as philosophical concepts, but apparently never considered performing experiments to test their ideas.

The Aristotelian view of the composition of matter held sway for over two thousand years, until English schoolteacher John Dalton helped to revolutionize chemistry with his hypothesis that the behavior of matter could be explained using an atomic theory. First published in 1807, many of Dalton's hypotheses about the microscopic features of matter are still valid in modern atomic theory. Here are the postulates of Dalton's atomic theory.

1. Matter is composed of exceedingly small particles called atoms. An atom is the smallest unit of an element that can participate in a chemical change.

2. An element consists of only one type of atom, which has a mass that is characteristic of the element and is the same for all atoms of that element (Figure **2.1.1**). A macroscopic sample of an element contains an incredibly large number of atoms, all of which have identical chemical properties.
3. Atoms of one element differ in properties from atoms of all other elements.
4. A compound consists of atoms of two or more elements combined in a small, whole-number ratio. In a given compound, the numbers of atoms of each of its elements are always present in the same ratio (Figure **2.1.2**).
5. Atoms are neither created nor destroyed during a chemical change, but are instead rearranged to yield substances that are different from those present before the change (Figure **2.1.3**).

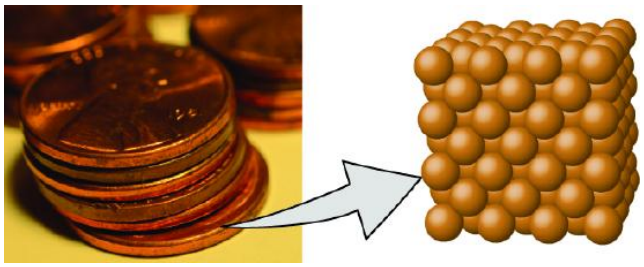


Figure* 2.1.1*: *A pre-1982 copper penny (left) contains approximately 3×10^{22} copper atoms (several dozen are represented as brown spheres at the right), each of which has the same chemical properties. (credit: modification of work by "slgckgc"/Flickr)*

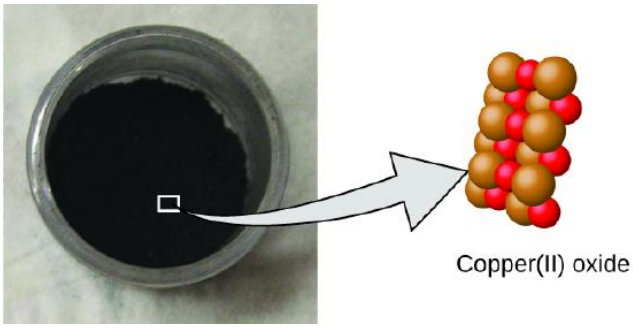


Figure* 2.1.2*: *Copper(II) oxide, a powdery, black compound, results from the combination of two types of atoms—copper (brown spheres) and oxygen (red spheres)—in a 1:1 ratio. (credit: modification of work by "Chemicalinterest"/Wikimedia Commons)*

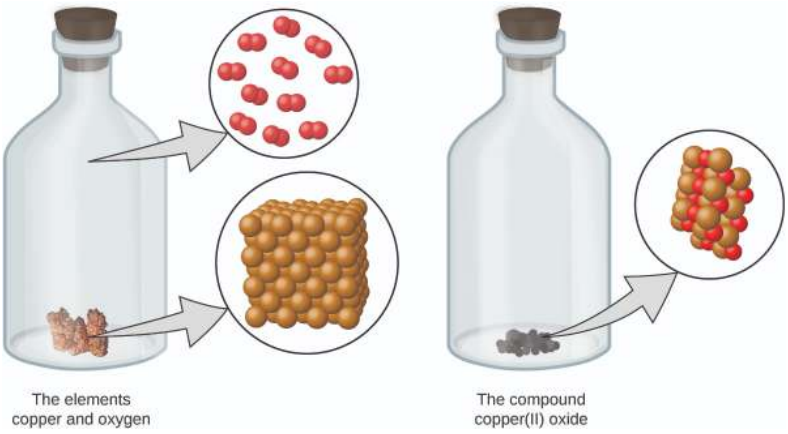


Figure* 2.1.3*: *When the elements copper (a shiny, red-brown solid, shown here as brown spheres) and oxygen (a clear and colorless gas, shown here as red spheres) react, their atoms rearrange to form a compound containing copper and oxygen (a powdery, black solid). (credit copper: modification of work by http://images-of-elements.com/copper.php).*

Dalton's atomic theory provides a microscopic explanation of the many macroscopic properties of matter that you've learned about. For example, if an element such as copper consists of only one kind of atom, then it cannot be broken down into simpler substances, that is, into substances composed of fewer types of atoms. And if atoms are neither created nor destroyed during a

chemical change, then the total mass of matter present when matter changes from one type to another will remain constant (the law of conservation of matter (or mass)).

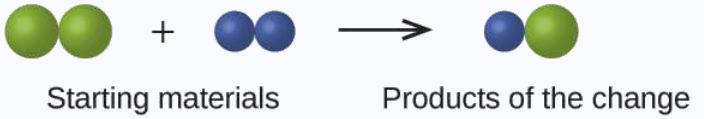
Want to learn more about the Law of Conservation of Mass?



Video 2.1.2: "We are made of star stuff" - Carl Sagan.

Example 2.1.1: Testing Dalton's Atomic Theory

In the following drawing, the green spheres represent atoms of a certain element. The purple spheres represent atoms of another element. If the spheres touch, they are part of a single unit of a compound. Does the following chemical change represented by these symbols violate any of the ideas of Dalton's atomic theory? If so, which one?



Solution

The starting materials consist of two green spheres and two purple spheres. The products consist of only one green sphere and one purple sphere. This violates Dalton's postulate that atoms are neither created nor destroyed during a chemical change, but are merely redistributed. (In this case, atoms appear to have been destroyed.)

Exercise 2.1.1

In the following drawing, the green spheres represent atoms of a certain element. The purple spheres represent atoms of another element. If the spheres touch, they are part of a single unit of a compound. Does the following chemical change represented by these symbols violate any of the ideas of Dalton's atomic theory? If so, which one



Answer

The starting materials consist of four green spheres and two purple spheres. The products consist of four green spheres and two purple spheres. This does not violate any of Dalton's postulates: Atoms are neither created nor destroyed, but are redistributed in small, whole-number ratios.

Dalton knew of the experiments of French chemist Joseph Proust, who demonstrated that *all samples of a pure compound contain the same elements in the same proportion by mass*. This statement is known as the law of definite proportions or the law of constant composition. The suggestion that the numbers of atoms of the elements in a given compound always exist in the same ratio is

consistent with these observations. For example, when different samples of isooctane (a component of gasoline and one of the standards used in the octane rating system) are analyzed, they are found to have a carbon-to-hydrogen mass ratio of 5.33:1, as shown in Table **2.1.1**.

***Table* 2.1.1**: *Constant Composition of Isooctane*

Sample	Carbon	Hydrogen	Mass Ratio
A	14.82 g	2.78 g	$\frac{14.82\text{ g carbon}}{2.78\text{ g hydrogen}} = \frac{5.33\text{ g carbon}}{1.00\text{ g hydrogen}}$
B	22.33 g	4.19 g	$\frac{22.33\text{ g carbon}}{4.19\text{ g hydrogen}} = \frac{5.33\text{ g carbon}}{1.00\text{ g hydrogen}}$
C	19.40 g	3.64 g	$\frac{19.40\text{ g carbon}}{3.63\text{ g hydrogen}} = \frac{5.33\text{ g carbon}}{1.00\text{ g hydrogen}}$

It is worth noting that although all samples of a particular compound have the same mass ratio, the converse is not true in general. That is, samples that have the same mass ratio are not necessarily the same substance. For example, there are many compounds other than isooctane that also have a carbon-to-hydrogen mass ratio of 5.33:1.00.

Dalton also used data from Proust, as well as results from his own experiments, to formulate another interesting law. The law of multiple proportions states that *when two elements react to form more than one compound, a fixed mass of one element will react with masses of the other element in a ratio of small, whole numbers*. For example, copper and chlorine can form a green, crystalline solid with a mass ratio of 0.558 g chlorine to 1 g copper, as well as a brown crystalline solid with a mass ratio of 1.116 g chlorine to 1 g copper. These ratios by themselves may not seem particularly interesting or informative; however, if we take a ratio of these ratios, we obtain a useful and possibly surprising result: a small, whole-number ratio.

$$\frac{\frac{1.116\text{ g Cl}}{1\text{ g Cu}}}{\frac{0.558\text{ g Cl}}{1\text{ g Cu}}} = \frac{2}{1} \tag{2.1.1}$$

This 2-to-1 ratio means that the brown compound has twice the amount of chlorine per amount of copper as the green compound.

This can be explained by atomic theory if the copper-to-chlorine ratio in the brown compound is 1 copper atom to 2 chlorine atoms, and the ratio in the green compound is 1 copper atom to 1 chlorine atom. The ratio of chlorine atoms (and thus the ratio of their masses) is therefore 2 to 1 (Figure **2.1.4**).

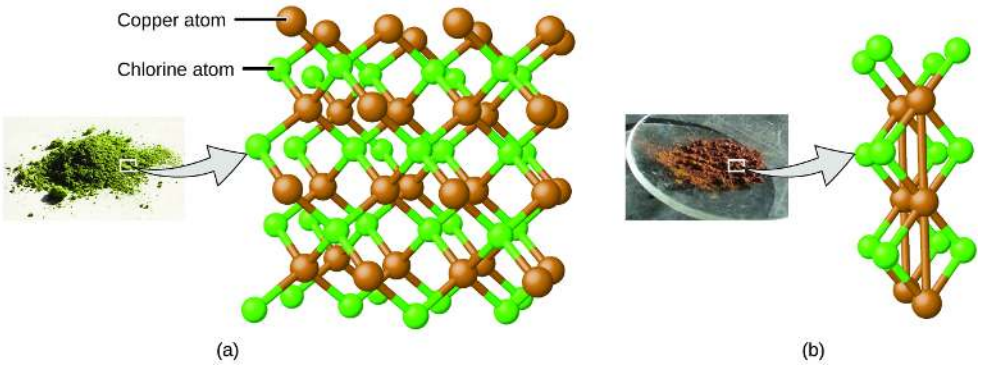


***Figure* 2.1.4**: *Compared to the copper chlorine compound in (a), where copper is represented by brown spheres and chlorine by green spheres, the copper chlorine compound in (b) has twice as many chlorine atoms per copper atom. (credit a: modification of work by "Benjah-bmm27"/Wikimedia Commons; credit b: modification of work by "Walkerma"/Wikimedia Commons)*

Example 2.1.2: Laws of Definite and Multiple Proportions

A sample of compound A (a clear, colorless gas) is analyzed and found to contain 4.27 g carbon and 5.69 g oxygen. A sample of compound B (also a clear, colorless gas) is analyzed and found to contain 5.19 g carbon and 13.84 g oxygen. Are these data an example of the law of definite proportions, the law of multiple proportions, or neither? What do these data tell you about substances A and B?

Solution

In compound A, the mass ratio of carbon to oxygen is:

$$\frac{1.33\text{ g O}}{1\text{ g C}}$$

In compound B, the mass ratio of carbon to oxygen is:

$$\frac{2.67\text{ g O}}{1\text{ g C}}$$

The ratio of these ratios is:

$$\frac{\frac{1.33\text{ g O}}{1\text{ g C}}}{\frac{2.67\text{ g O}}{1\text{ g C}}} = \frac{1}{2}$$

This supports the law of multiple proportions. This means that A and B are different compounds, with A having one-half as much carbon per amount of oxygen (or twice as much oxygen per amount of carbon) as B. A possible pair of compounds that would fit this relationship would be A = CO_2 and B = CO.

Exercise 2.1.2

A sample of compound X (a clear, colorless, combustible liquid with a noticeable odor) is analyzed and found to contain 14.13 g carbon and 2.96 g hydrogen. A sample of compound Y (a clear, colorless, combustible liquid with a noticeable odor that is slightly different from X's odor) is analyzed and found to contain 19.91 g carbon and 3.34 g hydrogen. Are these data an example of the law of definite proportions, the law of multiple proportions, or neither? What do these data tell you about substances X and Y?

Answer

In compound X, the mass ratio of carbon to hydrogen is $\frac{14.13\text{ g C}}{2.96\text{ g H}}$.

In compound Y, the mass ratio of carbon to oxygen is $\frac{19.91\text{ g C}}{3.34\text{ g H}}$.

The ratio of these ratios is

$$\frac{\frac{14.13\text{ g C}}{2.96\text{ g H}}}{\frac{19.91\text{ g C}}{3.34\text{ g H}}} = \frac{4.77\text{ g C/g H}}{5.96\text{ g C/g H}} = 0.800 = \frac{4}{5}.$$

This small, whole-number ratio supports the law of multiple proportions. This means that X and Y are different compounds.

In the two centuries since Dalton developed his ideas, scientists have made significant progress in furthering our understanding of atomic theory. Much of this came from the results of several seminal experiments that revealed the details of the internal structure of atoms. Here, we will discuss some of those key developments, with an emphasis on application of the scientific method, as well as understanding how the experimental evidence was analyzed. While the historical persons and dates behind these experiments can be quite interesting, it is most important to understand the concepts resulting from their work.

Atomic Theory after the Nineteenth Century

If matter were composed of atoms, what were atoms composed of? Were they the smallest particles, or was there something smaller? In the late 1800s, a number of scientists interested in questions like these investigated the electrical discharges that could be produced in low-pressure gases, with the most significant discovery made by English physicist J. J. Thomson using a cathode ray tube. This apparatus consisted of a sealed glass tube from which almost all the air had been removed; the tube contained two metal electrodes. When high voltage was applied across the electrodes, a visible beam called a cathode ray appeared between them.

This beam was deflected toward the positive charge and away from the negative charge, and was produced in the same way with identical properties when different metals were used for the electrodes. In similar experiments, the ray was simultaneously deflected by an applied magnetic field, and measurements of the extent of deflection and the magnetic field strength allowed Thomson to calculate the charge-to-mass ratio of the cathode ray particles. The results of these measurements indicated that these particles were much lighter than atoms (Figure **2.1.1**).

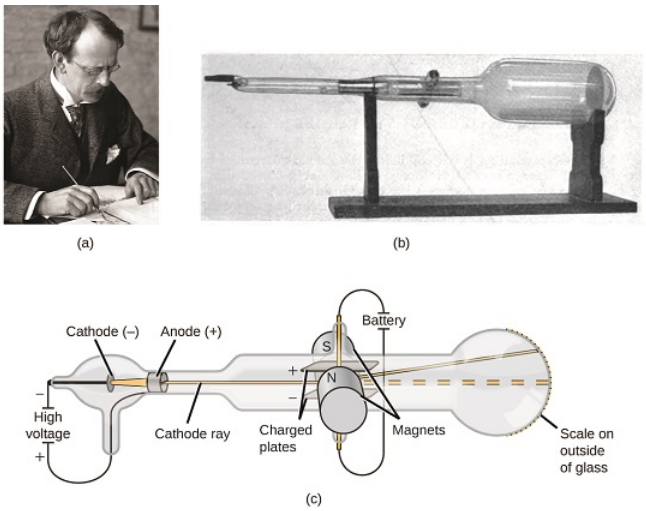
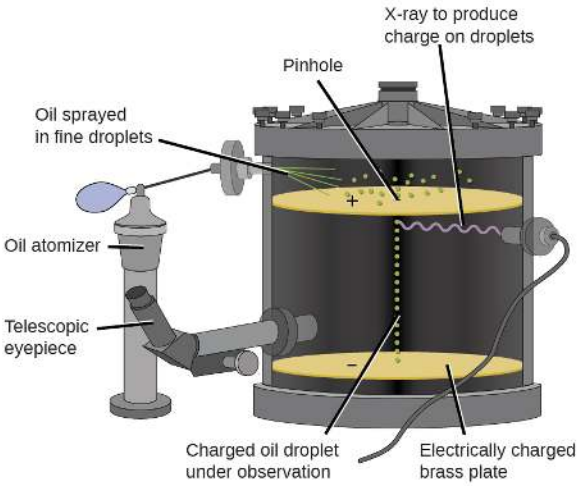


Figure* 2.1.5: (a) J. J. Thomson produced a visible beam in a cathode ray tube. (b) This is an early cathode ray tube, invented in 1897 by Ferdinand Braun. (c) In the cathode ray, the beam (shown in yellow) comes from the cathode and is accelerated past the anode toward a fluorescent scale at the end of the tube. Simultaneous deflections by applied electric and magnetic fields permitted Thomson to calculate the mass-to-charge ratio of the particles composing the cathode ray. (credit a: modification of work by Nobel Foundation; credit b: modification of work by Eugen Nesper; credit c: modification of work by "Kurzon"/Wikimedia Commons).*

Based on his observations, here is what Thomson proposed and why: The particles are attracted by positive (+) charges and repelled by negative (−) charges, so they must be negatively charged (like charges repel and unlike charges attract); they are less massive than atoms and indistinguishable, regardless of the source material, so they must be fundamental, subatomic constituents of all atoms. Although controversial at the time, Thomson's idea was gradually accepted, and his cathode ray particle is what we now call an electron, a negatively charged, subatomic particle with a mass more than one thousand-times less that of an atom. The term "electron" was coined in 1891 by Irish physicist George Stoney, from "*electr*ic i*on*."

In 1909, more information about the electron was uncovered by American physicist Robert A. Millikan via his "oil drop" experiments. Millikan created microscopic oil droplets, which could be electrically charged by friction as they formed or by using X-rays. These droplets initially fell due to gravity, but their downward progress could be slowed or even reversed by an electric field lower in the apparatus. By adjusting the electric field strength and making careful measurements and appropriate calculations, Millikan was able to determine the charge on individual drops (Figure **2.1.2**).



Oil drop	Charge in coulombs (C)
A	4.8×10^{-19} C
B	3.2×10^{-19} C
C	6.4×10^{-19} C
D	1.6×10^{-19} C
E	4.8×10^{-19} C

Figure 2.1.6: *Millikan's experiment measured the charge of individual oil drops. The tabulated data are examples of a few possible values.*

Looking at the charge data that Millikan gathered, you may have recognized that the charge of an oil droplet is always a multiple of a specific charge, 1.6×10^{-19} C. Millikan concluded that this value must therefore be a fundamental charge—the charge of a single electron—with his measured charges due to an excess of one electron (1 times 1.6×10^{-19} C), two electrons (2 times 1.6×10^{-19} C), three electrons (3 times 1.6×10^{-19} C), and so on, on a given oil droplet. Since the charge of an electron was now known due to Millikan's research, and the charge-to-mass ratio was already known due to Thomson's research (1.759×10^{11} C/kg), it only required a simple calculation to determine the mass of the electron as well.

$$\text{Mass of electron} = 1.602 \times 10^{-19} \cancel{\text{C}} \times \frac{1 \text{ kg}}{1.759 \times 10^{11} \cancel{\text{C}}} = 9.107 \times 10^{-31} \text{ kg} \tag{2.3.1}$$

Scientists had now established that the atom was not indivisible as Dalton had believed, and due to the work of Thomson, Millikan, and others, the charge and mass of the negative, subatomic particles—the electrons—were known. However, the positively charged part of an atom was not yet well understood. In 1904, Thomson proposed the "plum pudding" model of atoms, which described a positively charged mass with an equal amount of negative charge in the form of electrons embedded in it, since all atoms are electrically neutral. A competing model had been proposed in 1903 by Hantaro Nagaoka, who postulated a Saturn-like atom, consisting of a positively charged sphere surrounded by a halo of electrons (Figure 2.1.3).

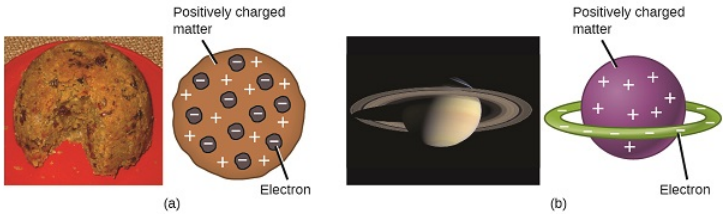


Figure 2.1.7*: (a) Thomson suggested that atoms resembled plum pudding, an English dessert consisting of moist cake with embedded raisins ("plums"). (b) Nagaoka proposed that atoms resembled the planet Saturn, with a ring of electrons surrounding a positive "planet." (credit a: modification of work by "Man vyi"/Wikimedia Commons; credit b: modification of work by "NASA"/Wikimedia Commons).*

The next major development in understanding the atom came from Ernest Rutherford, a physicist from New Zealand who largely spent his scientific career in Canada and England. He performed a series of experiments using a beam of high-speed, positively charged alpha particles (α particles) that were produced by the radioactive decay of radium; α particles consist of two protons and two neutrons (you will learn more about radioactive decay in the chapter on nuclear chemistry). Rutherford and his colleagues Hans Geiger (later famous for the Geiger counter) and Ernest Marsden aimed a beam of α particles, the source of which was

embedded in a lead block to absorb most of the radiation, at a very thin piece of gold foil and examined the resultant scattering of the α particles using a luminescent screen that glowed briefly where hit by an α particle.

What did they discover? Most particles passed right through the foil without being deflected at all. However, some were diverted slightly, and a very small number were deflected almost straight back toward the source (Figure **2.1.4**). Rutherford described finding these results: "It was quite the most incredible event that has ever happened to me in my life. It was almost as incredible as if you fired a 15-inch shell at a piece of tissue paper and it came back and hit you"[1] (p. 68).

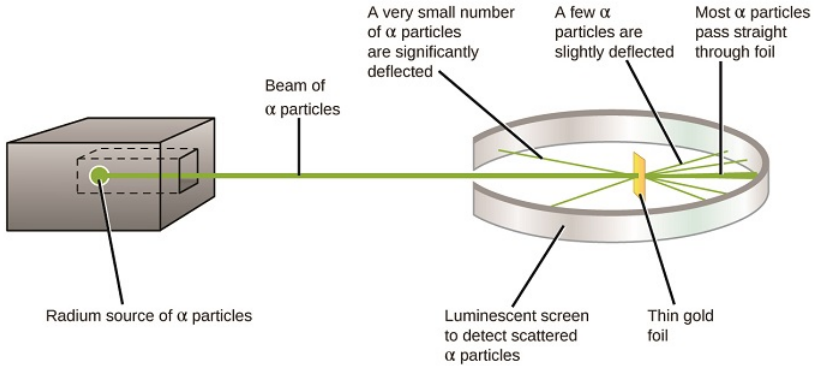


Figure* 2.1.8*: *Geiger and Rutherford fired α particles at a piece of gold foil and detected where those particles went, as shown in this schematic diagram of their experiment. Most of the particles passed straight through the foil, but a few were deflected slightly and a very small number were significantly deflected.*

Here is what Rutherford deduced: Because most of the fast-moving α particles passed through the gold atoms undeflected, they must have traveled through essentially empty space inside the atom. Alpha particles are positively charged, so deflections arose when they encountered another positive charge (like charges repel each other). Since like charges repel one another, the few positively charged α particles that changed paths abruptly must have hit, or closely approached, another body that also had a highly concentrated, positive charge. Since the deflections occurred a small fraction of the time, this charge only occupied a small amount of the space in the gold foil. Analyzing a series of such experiments in detail, Rutherford drew two conclusions:

1. The volume occupied by an atom must consist of a large amount of empty space.
2. A small, relatively heavy, positively charged body, the nucleus, must be at the center of each atom.

This analysis led Rutherford to propose a model in which an atom consists of a very small, positively charged nucleus, in which most of the mass of the atom is concentrated, surrounded by the negatively charged electrons, so that the atom is electrically neutral (Figure **2.1.5**).

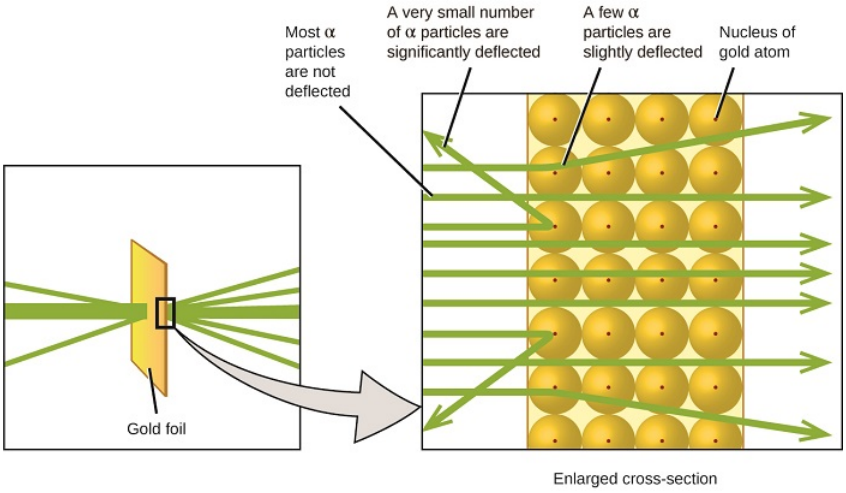
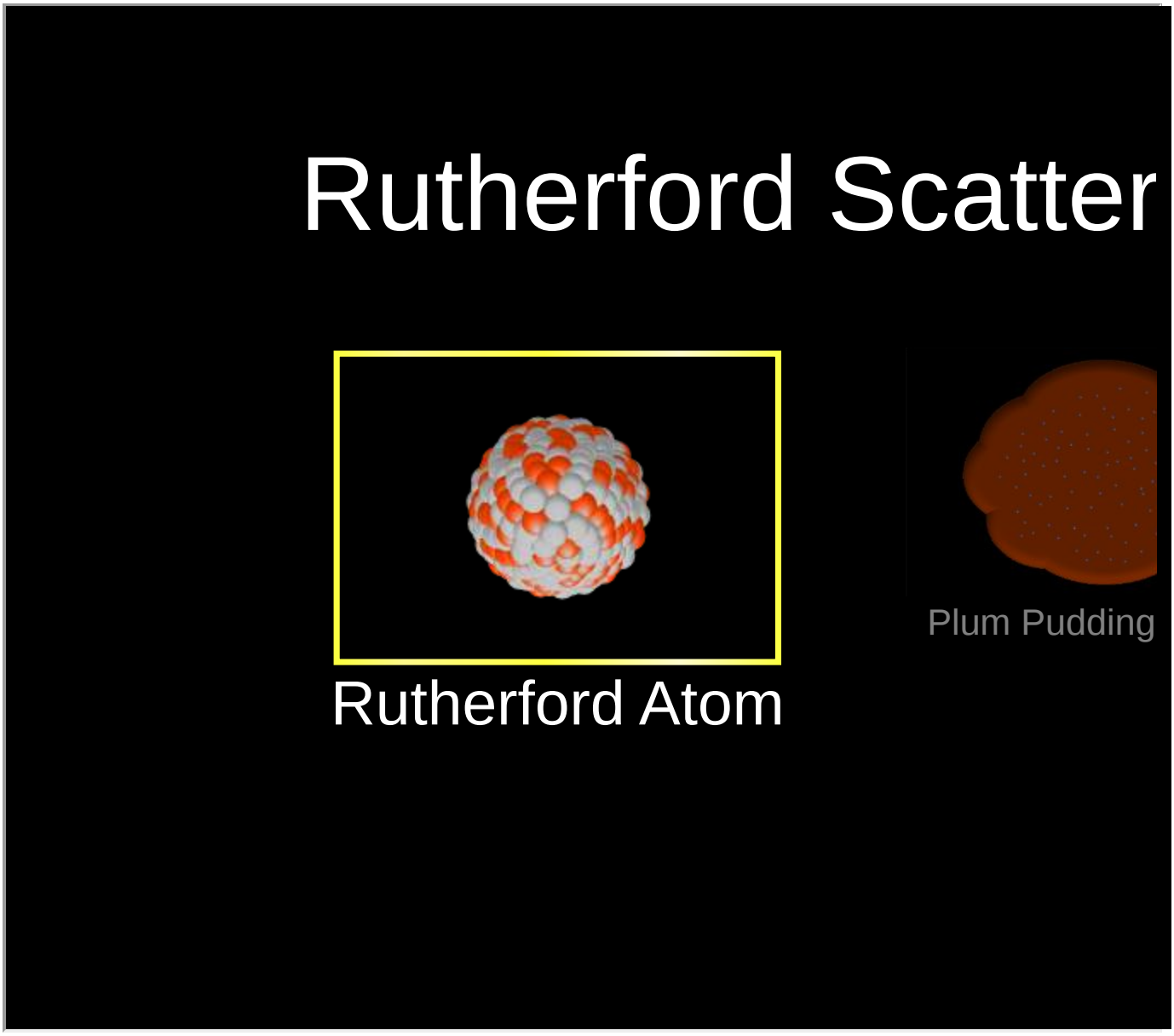


Figure* 2.1.9: The α particles are deflected only when they collide with or pass close to the much heavier, positively charged gold nucleus. Because the nucleus is very small compared to the size of an atom, very few α particles are deflected. Most pass through*

the relatively large region occupied by electrons, which are too light to deflect the rapidly moving particles.

After many more experiments, Rutherford also discovered that the nuclei of other elements contain the hydrogen nucleus as a "building block," and he named this more fundamental particle the proton, the positively charged, subatomic particle found in the nucleus. With one addition, which you will learn next, this nuclear model of the atom, proposed over a century ago, is still used today.



Another important finding was the discovery of isotopes. During the early 1900s, scientists identified several substances that appeared to be new elements, isolating them from radioactive ores. For example, a "new element" produced by the radioactive decay of thorium was initially given the name mesothorium. However, a more detailed analysis showed that mesothorium was chemically identical to radium (another decay product), despite having a different atomic mass. This result, along with similar findings for other elements, led the English chemist Frederick Soddy to realize that an element could have types of atoms with different masses that were chemically indistinguishable. These different types are called isotopes—atoms of the same element that differ in mass. Soddy was awarded the Nobel Prize in Chemistry in 1921 for this discovery.

One puzzle remained: The nucleus was known to contain almost all of the mass of an atom, with the number of protons only providing half, or less, of that mass. Different proposals were made to explain what constituted the remaining mass, including the

existence of neutral particles in the nucleus. As you might expect, detecting uncharged particles is very challenging, and it was not until 1932 that James Chadwick found evidence of neutrons, uncharged, subatomic particles with a mass approximately the same as that of protons. The existence of the neutron also explained isotopes: They differ in mass because they have different numbers of neutrons, but they are chemically identical because they have the same number of protons. This will be explained in more detail later in this unit.



Video* 2.1.2*: An Introduction to Subatomic Particles

Summary



***Video* 2.1.3*:** *A summary of discoveries in atomic theory.*



***Video* 2.1.4*:** *A different summary of discoveries in atomic theory.*

The ancient Greeks proposed that matter consists of extremely small particles called atoms. Dalton postulated that each element has a characteristic type of atom that differs in properties from atoms of all other elements, and that atoms of different elements can combine in fixed, small, whole-number ratios to form compounds. Samples of a particular compound all have the same elemental proportions by mass. When two elements form different compounds, a given mass of one element will combine with masses of the other element in a small, whole-number ratio. During any chemical change, atoms are neither created nor destroyed.

Although no one has actually seen the inside of an atom, experiments have demonstrated much about atomic structure. Thomson's cathode ray tube showed that atoms contain small, negatively charged particles called electrons. Millikan discovered that there is a fundamental electric charge—the charge of an electron. Rutherford's gold foil experiment showed that atoms have a small, dense, positively charged nucleus; the positively charged particles within the nucleus are called protons. Chadwick discovered that the nucleus also contains neutral particles called neutrons. Soddy demonstrated that atoms of the same element can differ in mass; these are called isotopes.

Footnotes

1. Ernest Rutherford, "The Development of the Theory of Atomic Structure," ed. J. A. Ratcliffe, in *Background to Modern Science*, eds. Joseph Needham and Walter Pagel, (Cambridge, UK: Cambridge University Press, 1938), 61–74. Accessed September 22, 2014, https://ia600508.us.archive.org/3/it...e032734mbp.pdf.

Glossary

Dalton's atomic theory
set of postulates that established the fundamental properties of atoms

law of constant composition
(also, law of definite proportions) all samples of a pure compound contain the same elements in the same proportions by mass

law of multiple proportions
when two elements react to form more than one compound, a fixed mass of one element will react with masses of the other element in a ratio of small whole numbers

law of definite proportions
(also, law of constant composition) all samples of a pure compound contain the same elements in the same proportions by mass

alpha particle (α particle)
positively charged particle consisting of two protons and two neutrons

electron
negatively charged, subatomic particle of relatively low mass located outside the nucleus

isotopes
atoms that contain the same number of protons but different numbers of neutrons

neutron
uncharged, subatomic particle located in the nucleus

proton
positively charged, subatomic particle located in the nucleus

nucleus
massive, positively charged center of an atom made up of protons and neutrons

Contributors

- Paul Flowers (University of North Carolina - Pembroke), Klaus Theopold (University of Delaware) and Richard Langley (Stephen F. Austin State University) with contributing authors. Textbook content produced by OpenStax College is licensed under a Creative Commons Attribution License 4.0 license. Download for free at http://cnx.org/contents/85abf193-2bd...a7ac8df6@9.110).
- Adelaide Clark, Oregon Institute of Technology
- Crash Course Chemistry: Crash Course is a division of Complexly and videos are free to stream for educational purposes.
- TED-Ed's commitment to creating lessons worth sharing is an extension of TED's mission of spreading great ideas. Within TED-Ed's growing library of TED-Ed animations, you will find carefully curated educational videos, many of which represent collaborations between talented educators and animators nominated through the TED-Ed website.

Feedback

Have feedback to give about this text? Click here.

Found a typo and want extra credit? Click here.

2.1: Historical Development of Atomic Theory is shared under a not declared license and was authored, remixed, and/or curated by LibreTexts.

- **2.1: Historical Development of Atomic Theory** is licensed CC BY-NC-SA 4.0.

2.2: The Periodic Table

Learning Objectives

- To become familiar with the history of the periodic table.

The modern periodic table has evolved through a long history of attempts by chemists to arrange the elements according to their reactivity and other properties as an aid in predicting chemical behavior. Now that we have arranged the table according to electronic structure, it makes sense to go back and look at earlier efforts in the light of what we know about electronic structure.

One of the first to suggest such an arrangement was the German chemist Johannes Dobereiner (1780–1849), who noticed that many of the known elements could be grouped in triads, sets of three elements that have similar properties—for example, chlorine, bromine, and iodine; or copper, silver, and gold. Dobereiner proposed that all elements could be grouped in such triads, but subsequent attempts to expand his concept were unsuccessful. We now know that portions of the periodic table—the *d* block in particular—contain triads of elements with substantial similarities. The middle three members of most of the other columns, such as sulfur, selenium, and tellurium in group 16 or aluminum, gallium, and indium in group 13, also have remarkably similar chemistry.

By the mid-19th century, the atomic masses of many of the elements had been determined. The English chemist John Newlands (1838–1898), hypothesizing that the chemistry of the elements might be related to their masses, arranged the known elements in order of increasing atomic mass and discovered that every seventh element had similar properties (Figure 3.4.1). Newlands therefore suggested that the elements could be classified into octaves: a group of seven elements (not counting the noble gases, which were unknown at the time) that correspond to the *horizontal* rows in the main group elements. Unfortunately, Newlands's "law of octaves" did not seem to work for elements heavier than calcium, and his idea was publicly ridiculed. At one scientific meeting, Newlands was asked why he didn't arrange the elements in alphabetical order instead of by atomic mass, since that would make just as much sense! Actually, Newlands was on the right track—with only a few exceptions, atomic mass does increase with atomic number, and similar properties occur every time a set of ns^2np^6 subshells is filled. Despite the fact that Newlands's table had no logical place for the *d*-block elements, he was honored for his idea by the Royal Society of London in 1887.

John Newlands (1838–1898)

Newlands noticed that elemental properties repeated every seventh (or multiple of seven) element, as musical notes repeat every eighth note.

No.	No.	No.	No.	No.	No.	No.	No.
H 1	F 8	Cl 15	Co & Ni 22	Br 29	Pd 36	I 42	Pt & Ir 50
Li 2	Na 9	K 16	Cu 23	Rb 30	Ag 37	Cs 44	Tl 51
G 3	Mg 10	Ca 17	Zn 25	Sr 31	Bd [sic-Cd] 38	Ba & V 45	Pb 54
Bo 4	Al 11	Cr 19	Y 24	Ce & La 33	U 40	Ta 46	Th 56
C 5	Si 12	Ti 18	In 26	Zr 32	Sn 39	W 47	Hg 52
N 6	**P 13**	Mn 20	**As 27**	Di & Mo 34	**Sb 41**	Nb 48	**Bi 55**
O 7	S 14	Fe 21	Se 28	Ro & Ru 35	Te 43	Au 49	Os 51

NOTE. Where two elements happen to have the same equivalent, both are designated by the same number.

Figure 3.4.1 The Arrangement of the Elements into Octaves as Proposed by **Newlands:** *The table shown here accompanied a letter from a 27-year-old Newlands to the editor of the journal Chemical News in which he wrote: "If the elements are arranged in the order of their equivalents, with a few slight transpositions, as in the accompanying table, it will be observed that elements belonging to the same group usually appear on the same horizontal line. It will also be seen that the numbers of analogous elements generally differ either by 7 or by some multiple of seven; in other words, members of the same group stand to each other in the same relation as the extremities of one or more octaves in music. Thus, in the nitrogen group, between nitrogen and phosphorus there are 7 elements; between phosphorus and arsenic, 14; between arsenic and antimony, 14; and lastly, between antimony and bismuth, 14 also. This peculiar relationship I propose to provisionally term the Law of Octaves. I am, &c. John A. R. Newlands, F.C.S. Laboratory, 19, Great St. Helen's, E.C., August 8, 1865."*

The periodic table achieved its modern form through the work of the German chemist Julius Lothar Meyer (1830–1895) and the Russian chemist Dimitri Mendeleev (1834–1907), both of whom focused on the relationships between atomic mass and various physical and chemical properties. In 1869, they independently proposed essentially identical arrangements of the elements. Meyer aligned the elements in his table according to periodic variations in simple atomic properties, such as "atomic volume" (Figure

3.4.2), which he obtained by dividing the atomic mass (molar mass) in grams per mole by the density of the element in grams per cubic centimeter. This property is equivalent to what is today defined as molar volume, the molar mass of an element divided by its density (measured in cubic centimeters per mole):

$$\frac{molar\ mass\ \left(g/mol\right)}{density\ \left(g/cm^3\right)} = molar\ volume\ \left(cm^3/mol\right)$$

As shown in Figure 3.4.2 , the alkali metals have the highest molar volumes of the solid elements. In Meyer's plot of atomic volume versus atomic mass, the nonmetals occur on the rising portion of the graph, and metals occur at the peaks, in the valleys, and on the down slopes.

Dimitri Mendeleev (1834–1907)

When his family's glass factory was destroyed by fire, Mendeleev moved to St. Petersburg, Russia, to study science. He became ill and was not expected to recover, but he finished his PhD with the help of his professors and fellow students. In addition to the periodic table, another of Mendeleev's contributions to science was an outstanding textbook, *The Principles of Chemistry*, which was used for many years.

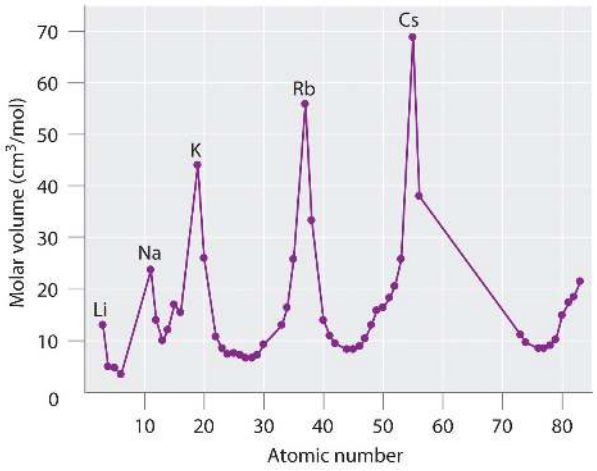


Figure 3.4.2 Variation of Atomic Volume with Atomic Number, Adapted from Meyer's Plot of **1870:** *Note the periodic increase and decrease in atomic volume. Because the noble gases had not yet been discovered at the time this graph was formulated, the peaks correspond to the alkali metals (group 1).*

Mendeleev's Periodic Table

Mendeleev, who first published his periodic table in 1869 (Figure 3.4.3), is usually credited with the origin of the modern periodic table. The key difference between his arrangement of the elements and that of Meyer and others is that Mendeleev did not assume that all the elements had been discovered (actually, only about two-thirds of the naturally occurring elements were known at the time). Instead, he deliberately left blanks in his table at atomic masses 44, 68, 72, and 100, in the expectation that elements with those atomic masses would be discovered. Those blanks correspond to the elements we now know as scandium, gallium, germanium, and technetium.

Reihen	Gruppe I. $\frac{}{R^2O}$	Gruppe II. $\frac{}{RO}$	Gruppe III. $\frac{}{R^2O^3}$	Gruppe IV. $\frac{RH^4}{RO^2}$	Gruppe V. $\frac{RH^3}{R^2O^5}$	Gruppe VI. $\frac{RH^2}{RO^3}$	Gruppe VII. $\frac{RH}{R^2O^7}$	Gruppe VIII. $\frac{}{RO^4}$
1	H=1							
2	Li=7	Be=9,4	B=11	C=12	N=14	O=16	F=19	
3	Na=23	Mg=24	Al=27,3	Si=28	P=31	S=32	Cl=35,5	
4	K=39	Ca=40	—=44	Ti=48	V=51	Cr=52	Mn=55	Fe=56, Co=59, Ni=59, Cu=63.
5	(Cu=63)	Zn=65	—=68	—=72	As=75	Se=78	Br=80	
6	Rb=85	Sr=87	?Yt=88	Zr=90	Nb=94	Mo=96	—=100	Ru=104, Rh=104, Pd=106, Ag=108.
7	(Ag=108)	Cd=112	In=113	Sn=118	Sb=122	Te=125	J=127	
8	Cs=133	Ba=137	?Di=138	?Ce=140	—	—	—	— — — —
9	(—)	—				—	—	
10	—	—	?Er=178	?La=180	Ta=182	W=184	—	Os=195, Ir=197, Pt=198, Au=199.
11	(Au=199)	Hg=200	Tl=204	Pb=207	Bi=208	—	—	
12	—	—	—	Th=231	—	U=240	—	— — — —

Figure 3.4.3 Mendeleev's Periodic Table, as Published in the German Journal *Annalen der Chemie und Pharmacie* in 1872: *The column headings "Reihen" and "Gruppe" are German for "row" and "group." Formulas indicate the type of compounds formed by each group, with "R" standing for "any element" and superscripts used where we now use subscripts. Atomic masses are shown after equal signs and increase across each row from left to right.*

The groups in Mendeleev's table are determined by how many oxygen or hydrogen atoms are needed to form compounds with each element. For example, in Group I, two atoms of hydrogen (H), lithium (Li), sodium (Na), and potassium (K) form compounds with one atom of oxygen. In Group VII, one atom of fluorine (F), chlorine (Cl), and bromine (Br), reacts with one atom of hydrogen. Notice how this approach has trouble with the transition metals. Until roughly 1960, a rectangular table developed from Mendeleev's table and based on reactivity was standard at the front of chemistry lecture halls.

The most convincing evidence in support of Mendeleev's arrangement of the elements was the discovery of two previously unknown elements whose properties closely corresponded with his predictions (Table 3.4.1). Two of the blanks Mendeleev had left in his original table were below aluminum and silicon, awaiting the discovery of two as-yet-unknown elements, *eka*-aluminum and *eka*-silicon (from the Sanskrit *eka*, meaning "one," as in "one beyond aluminum"). The observed properties of gallium and germanium matched those of *eka*-aluminum and *eka*-silicon so well that once they were discovered, Mendeleev's periodic table rapidly gained acceptance.



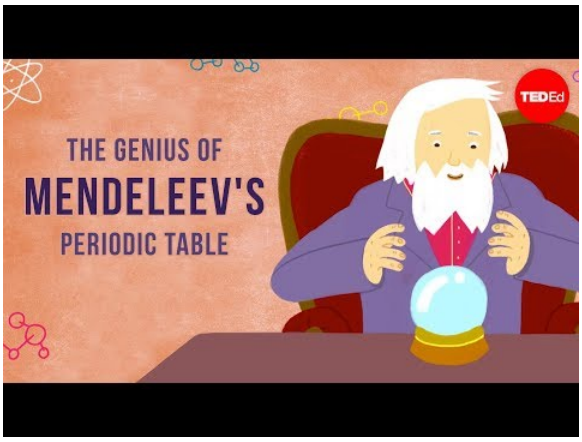


Table 3.4.1 Comparison of the Properties Predicted by Mendeleev in 1869 for *eka*-Aluminum and *eka*-Silicon with the Properties of Gallium (Discovered in 1875) and Germanium (Discovered in 1886)

Property	*eka*-Aluminum (predicted)	Gallium (observed)	*eka*-Silicon (predicted)	Germanium (observed)
atomic mass	68	69.723	72	72.64
element	metal	metal	dirty-gray metal	gray-white metal
	low mp*	mp = 29.8°C	high mp	mp = 938°C
	d = 5.9 g/cm^3	d = 5.91 g/cm^3	d = 5.5 g/cm^3	d = 5.323 g/cm^3
oxide	E_2O_3	Ga_2O_3	EO_2	GeO_2
	d = 5.5 g/cm^3	d = 6.0 g/cm^3	d = 4.7 g/cm^3	d = 4.25 g/cm^3
chloride	ECl_3	$GaCl_3$	ECl_4	$GeCl_4$
	volatile	mp = 78°C bp* = 201°C	bp < 100°C	bp = 87°C

*mp = melting point; bp = boiling point.

When the chemical properties of an element suggested that it might have been assigned the wrong place in earlier tables, Mendeleev carefully reexamined its atomic mass. He discovered, for example, that the atomic masses previously reported for beryllium, indium, and uranium were incorrect. The atomic mass of indium had originally been reported as 75.6, based on an assumed stoichiometry of InO for its oxide. If this atomic mass were correct, then indium would have to be placed in the middle of the nonmetals, between arsenic (atomic mass 75) and selenium (atomic mass 78). Because elemental indium is a silvery-white *metal*, however, Mendeleev postulated that the stoichiometry of its oxide was really In_2O_3 rather than InO. This would mean that indium's atomic mass was actually 113, placing the element between two other metals, cadmium and tin.

One group of elements absent from Mendeleev's table was the noble gases, all of which were discovered more than 20 years later, between 1894 and 1898, by Sir William Ramsay (1852–1916; Nobel Prize in Chemistry 1904). Initially, Ramsay did not know where to place these elements in the periodic table. Argon, the first to be discovered, had an atomic mass of 40. This was greater than chlorine's and comparable to that of potassium; so Ramsay, using the same kind of reasoning as Mendeleev, decided to place the noble gases between the halogens and the alkali metals.

The Role of the Atomic Number in the Periodic Table

Despite its usefulness, Mendeleev's periodic table was based entirely on empirical observation supported by very little understanding. It was not until 1913, when a young British physicist, H. G. J. Moseley (1887–1915), while analyzing the frequencies of x-rays emitted by the elements, discovered that the underlying foundation of the order of the elements was the

atomic number, not the atomic mass. Moseley hypothesized that the placement of each element in his series corresponded to its atomic number *Z*, which is the number of positive charges (protons) in its nucleus. Argon, for example, although having an atomic mass greater than that of potassium (39.9 amu versus 39.1 amu, respectively), was placed *before* potassium in the periodic table. While analyzing the frequencies of the emitted x-rays, Moseley noticed that the atomic number of argon is 18, whereas that of potassium is 19, which indicated that they were indeed placed correctly. Moseley also noticed three gaps in his table of x-ray frequencies, so he predicted the existence of three unknown elements: technetium (Z = 43), discovered in 1937; promethium (Z = 61), discovered in 1945; and rhenium (Z = 75), discovered in 1925.

H. G. J. Moseley (1887–1915)

Moseley left his research work at the University of Oxford to join the British army as a telecommunications officer during World War I. He was killed during the Battle of Gallipoli in Turkey.

Example 3.4.1

Before its discovery in 1999, some theoreticians believed that an element with a Z of 114 existed in nature. Use Mendeleev's reasoning to name element 114 as *eka*-_____; then identify the known element whose chemistry you predict would be most similar to that of element 114.

Given: atomic number

Asked for: name using prefix *eka*-

Strategy:

A Using the periodic table locate the n = 7 row. Identify the location of the unknown element with Z = 114; then identify the known element that is directly above this location.

B Name the unknown element by using the prefix *eka*- before the name of the known element.

Solution:

A The n = 7 row can be filled in by assuming the existence of elements with atomic numbers greater than 112, which is underneath mercury (Hg). Counting three boxes to the right gives element 114, which lies directly below lead (Pb). **B** If Mendeleev were alive today, he would call element 114 *eka*-lead.

Exercise

Use Mendeleev's reasoning to name element 112 as *eka*-_____; then identify the known element whose chemistry you predict would be most similar to that of element 112.

Answer: *eka*-mercury

Summary

The periodic table arranges the elements according to their electron configurations, such that elements in the same column have the same valence electron configurations. Periodic variations in size and chemical properties are important factors in dictating the types of chemical reactions the elements undergo and the kinds of chemical compounds they form. The modern periodic table was based on empirical correlations of properties such as atomic mass; early models using limited data noted the existence of **triads** and **octaves** of elements with similar properties. The periodic table achieved its current form through the work of Dimitri Mendeleev and Julius Lothar Meyer, who both focused on the relationship between atomic mass and chemical properties. Meyer arranged the elements by their atomic volume, which today is equivalent to the **molar volume**, defined as molar mass divided by molar density. The correlation with the electronic structure of atoms was made when H. G. J. Moseley showed that the periodic arrangement of the elements was determined by atomic number, not atomic mass.

Key Takeaways

- The elements in the periodic table are arranged according to their properties, and the periodic table serves as an aid in predicting chemical behavior.

Contributors and Attributions

- Anonymous

Modified by Joshua Halpern

Video from TED-Ed Lou Serocp

2.2: The Periodic Table is shared under a not declared license and was authored, remixed, and/or curated by LibreTexts.

- **2.1.1: The Periodic Table** is licensed CC BY-NC-SA 4.0.

2.3: Discovery of Subatomic Particles and the Bohr Atom

Hydrogen Absorption and Emission Spectra

When a high-voltage electrical discharge is passed through a sample of hydrogen gas (H_2) at low pressure, the result is individual isolated hydrogen atoms that emit a red light. Unlike blackbody radiation, the color of the light emitted by the hydrogen atoms does not depend greatly on the temperature of the gas in the tube. When the emitted light is passed through a prism, only a few narrow lines of particular wavelengths, called a line spectrum, are observed rather than a continuous range of wavelengths (Figure **2.3.1**). The light emitted by hydrogen atoms is red because, of its four characteristic lines, the most intense line in its spectrum is in the red portion of the visible spectrum, at 656 nm.

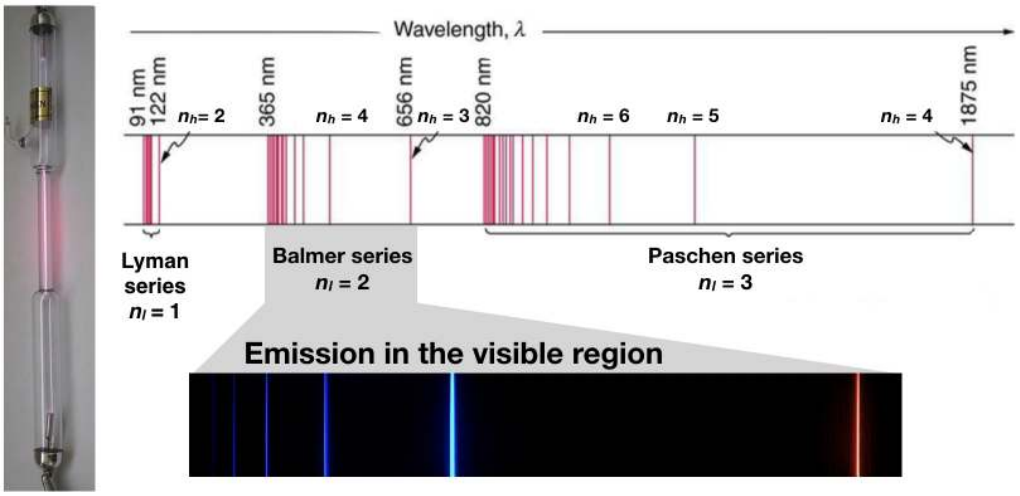


Figure **2.3.1**: The Emission of Light by Hydrogen Atoms. (left) A sample of excited hydrogen atoms emits a characteristic red light. (bottom) When the light emitted by a sample of excited hydrogen atoms is split into its component wavelengths by a prism, four characteristic violet, blue, green, and red emission lines can be observed, with the most intense at 656 nm. (top) A diagram showing extended regions of the electromagnetic spectrum and the hydrogen line spectra that are observed.

The Balmer Series

In 1885, a Swiss mathematics teacher, Johann Balmer (1825–1898), showed that the frequencies of the lines observed in the visible region of the hydrogen line spectrum fit a simple equation that can be expressed as follows:

$$u = constant\left(\frac{1}{2^2} - \frac{1}{n^2}\right) \tag{2.3.1}$$

where n = 3, 4, 5, 6. As a result, these lines are known as the *Balmer series*. The Swedish physicist Johannes Rydberg (1854–1919) subsequently restated and expanded Balmer's result in the *Rydberg equation*:

$$\frac{1}{\lambda} = R_H\left(\frac{1}{n_l^2} - \frac{1}{n_h^2}\right) \tag{2.3.2}$$

,

where n_l and n_h are positive integers, $n_h > n_l$, and R_H, the *Rydberg constant*, has a value of 1.09737 × 10^7 m^{-1}. Like Balmer's equation, Rydberg's simple equation described the wavelengths of the visible lines in the emission spectrum of hydrogen (with $n_l = 2, n_h = 3, 4, 5, ...$). More importantly, Rydberg's equation also predicted the wavelengths of other series of lines that would be observed in the emission spectrum of hydrogen: one in the ultraviolet ($n_l = 1, n_h = 2, 3, 4, ...$) and one in the infrared ($n_l = 3, n_h = 4, 5, 6$).

Other Series

The results given by Balmer and Rydberg for the spectrum in the visible region of the electromagnetic spectrum start with $n_h = 3$, and $n_l = 2$.

Is there a different series with the following formula (e.g., $n_l = 1$)?

$$\frac{1}{\lambda} = R_H \left(\frac{1}{1^2} - \frac{1}{n^2} \right) \tag{2.3.3}$$

The values for n_h and wavenumber u for this series would be:

Table **2.3.1**: The Lyman Series of Hydrogen Emission Lines ($n_l = 1$)

n_h	2	3	4	5
λ (nm)	121	102	97	94
$\tilde{u}$ (cm^{-1})	82,2291	97,530	102,864	105,332

Do you know what region of the electromagnetic radiation these lines are in? Of course, these lines are in the UV region, and they are not visible, but they are detected by instruments; these lines form a **Lyman series**. The existences of the Lyman series and Balmer's series suggest the existence of more series. For example, the series with $n_2^2 = 3$ and n_1^2 = 4, 5, 6, 7, ... is called the **Pashen series**.

Multiple series

The spectral lines are grouped into series according to n_1 values. Lines are named sequentially starting from the longest wavelength/lowest frequency of the series using Greek letters within each series. For example, the ($n_1 = 1/n_2 = 2$) line is called "Lyman-alpha" (Ly-α), while the ($n_1 = 3/n_2 = 7$) line is called "Paschen-delta" (Pa-δ). The first six series have specific names:

- Lyman series with $n_1 = 1$
- Balmer series with $n_1 = 2$
- Paschen series (or Bohr series) with $n_1 = 3$
- Brackett series with $n_1 = 4$
- Pfund series with $n_1 = 5$
- Humphreys series with $n_1 = 6$



The spectral series of hydrogen based on the Rydberg Equation (on a logarithmic scale).

Example 2.3.1: The Lyman Series

The so-called Lyman series of lines in the emission spectrum of hydrogen corresponds to transitions from various excited states to the *n* = 1 orbit. Calculate the wavelength of the lowest-energy line in the Lyman series to three significant figures. In what region of the electromagnetic spectrum does it occur?

Given: lowest-energy orbit in the Lyman series

Asked for: wavelength of the lowest-energy Lyman line and corresponding region of the spectrum

Strategy:

A. Substitute the appropriate values into Equation ***Ref*2.1.2.2** (the Rydberg equation) and solve for λ.
B. Locate the region of the electromagnetic spectrum corresponding to the calculated wavelength.

Solution:

We can use the Rydberg equation (Equation $Ref2.1.2.2$ to calculate the wavelength:

$$\frac{1}{\lambda} = R_H \left(\frac{1}{n_l^2} - \frac{1}{n_h^2} \right)$$

A For the Lyman series, $n_1 = 1$.

$$\begin{aligned} \frac{1}{\lambda} &= R_H \left(\frac{1}{n_l^2} - \frac{1}{n_h^2} \right) \\ &= 1.097 \times m^{-1} \left(\frac{1}{1} - \frac{1}{4} \right) \\ &= 8.228 \times 10^6 \; m^{-1} \end{aligned}$$

Spectroscopists often talk about energy and frequency as equivalent. The cm^{-1} unit (wavenumbers) is particularly convenient. We can convert the answer in part A to cm^{-1}.

$$\begin{aligned} \tilde{u} &= \frac{1}{\lambda} \\ &= 8.228 \times 10^6 \cancel{m^{-1}} \left(\frac{\cancel{m}}{100 \; cm} \right) \\ &= 82,280 \; cm^{-1} \end{aligned}$$

and

$$\lambda = 1.215 \times 10^{-7} \; m = 122 \; nm$$

This emission line is called Lyman alpha and is the strongest atomic emission line from the sun; it drives the chemistry of the upper atmosphere of all the planets producing ions by stripping electrons from atoms and molecules. It is completely absorbed by oxygen in the upper stratosphere, dissociating O_2 molecules to O atoms, which react with other O_2 molecules to form stratospheric ozone (O_3).

B This wavelength is in the ultraviolet region of the spectrum.

? Exercise 2.3.1: The Pfund Series

The Pfund series of lines in the emission spectrum of hydrogen corresponds to transitions from higher excited states to $n_1 = 5$. Calculate the wavelength of the *second* line in the Pfund series to three significant figures. In which region of the spectrum does it lie?

Answer

$4.65 \times 10^3 \; nm$; infrared

The above discussion presents only a phenomenological description of hydrogen emission lines. Balmer and Rydberg could predict where emission lines could occur, but they could not explain why lines followed this pattern using any useful theory. For an explanation of why atoms demonstrate discrete emission spectra, quantum theories were developed.

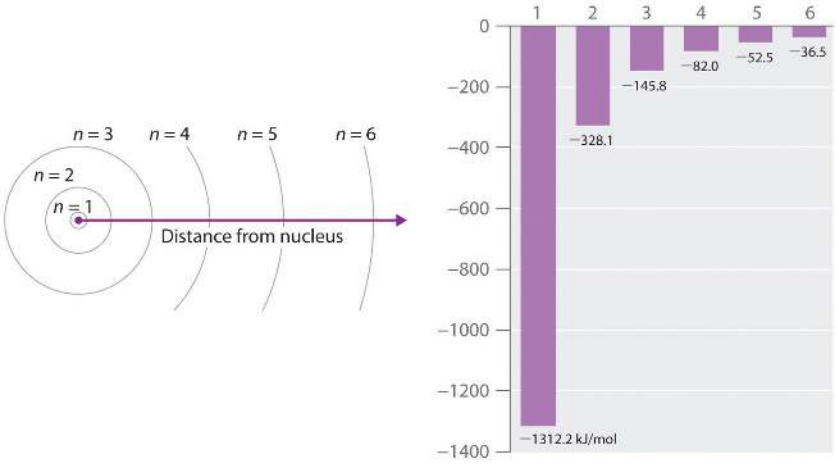
The Bohr Model

In 1913, a Danish physicist, Niels Bohr (1885–1962; Nobel Prize in Physics, 1922), proposed a theoretical model for the hydrogen atom that explained its emission spectrum. Bohr's model required only one assumption: *The electron moves around the nucleus in circular orbits that can have only certain allowed radii*. Rutherford's earlier model of the atom had also assumed that electrons moved in circular orbits around the nucleus and that the atom was held together by the electrostatic attraction between the positively charged nucleus and the negatively charged electron. Although we now know that the assumption of circular orbits was incorrect, Bohr's insight also posited that *the electron could occupy only certain regions of space*.

Using classical physics, Niels Bohr showed that the energy of an electron in a particular orbit is given by

$$E_n = \frac{-R_H hc}{n^2} \tag{2.3.4}$$

where R_H is the Rydberg constant, h is Planck's constant, c is the speed of light, and n is a positive integer corresponding to the number assigned to the orbit, with $n = 1$ corresponding to the orbit closest to the nucleus. In this model $n = \infty$ corresponds to the level where the energy holding the electron and the nucleus together is zero. In that level, the electron is unbound from the nucleus and the atom has been separated into a negatively charged (the electron) and a positively charged (the nucleus) ion. In this state the radius of the orbit is also infinite. The atom has been ionized.

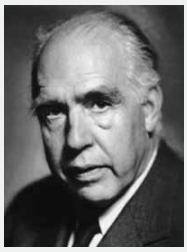


(a) Hydrogen orbits (Bohr model). Orbits are not drawn to scale. **(b) Hydrogen orbit energy (kJ/mol) vs. *n***

Figure **2.3.2**: *The Bohr Model of the Hydrogen Atom (a) The distance of the orbit from the nucleus increases with increasing n. (b) The energy of the orbit becomes increasingly less negative with increasing n.*

Niels Bohr (1885–1962)

During the Nazi occupation of Denmark in World War II, Bohr escaped to the United States, where he became associated with the Atomic Energy Project.



In his final years, he devoted himself to the peaceful application of atomic physics and to resolving political problems arising from the development of atomic weapons.

As n decreases, the energy holding the electron and the nucleus together becomes increasingly negative; the radius of the orbit shrinks and more energy is needed to ionize the atom. The orbit with n = 1 is the lowest lying and most tightly bound. The negative sign in Equation 2.3.4 indicates that the electron-nucleus pair is more tightly bound (i.e. at a lower potential energy) when they are near each other than when they are far apart. Because a hydrogen atom with its one electron in this orbit has the lowest possible energy, this is the **ground state** (the most stable arrangement of electrons for an element or a compound) for a hydrogen atom. As n increases, the radius of the orbit increases; the electron is farther from the proton, which results in a less stable arrangement with higher potential energy (Figure **2.3.2*a***). A hydrogen atom with an electron in an orbit with n > 1 is therefore in an **excited state**, defined as any arrangement of electrons that is higher in energy than the ground state. When an atom in an excited state undergoes a transition to the ground state in a process called decay, it loses energy by emitting a photon whose energy corresponds to the *difference* in energy between the two states (Figure **2.3.1**).

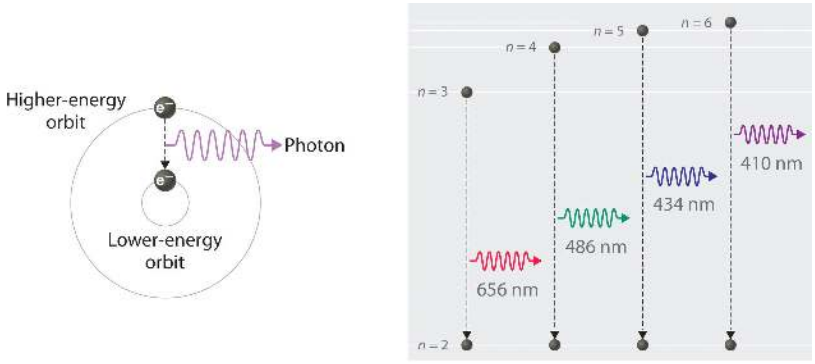


Figure **2.3.3**: *The Emission of Light by a Hydrogen Atom in an Excited State. (a) Light is emitted when the electron undergoes a transition from an orbit with a higher value of n (at a higher energy) to an orbit with a lower value of n (at lower energy). (b) The Balmer series of emission lines is due to transitions from orbits with n ≥ 3 to the orbit with n = 2. The differences in energy between these levels correspond to light in the visible portion of the electromagnetic spectrum.*

So the difference in energy (ΔE) between any two orbits or energy levels is given by $\Delta E = E_{n_l} - E_{n_h}$, where n_l is the final orbit and n_h the initial orbit. Substituting from Bohr's equation (Equation 2.1.2.4) for each energy value gives

$$\Delta E = E_{final} - E_{initial} = -\frac{R_H hc}{n_h^2} - \left(-\frac{R_H hc}{n_l^2}\right) = -R_H hc\left(\frac{1}{n_h^2} - \frac{1}{n_l^2}\right) \tag{2.3.5}$$

If $n_h > n_l$, the transition is from a higher energy state (larger-radius orbit) to a lower energy state (smaller-radius orbit), as shown by the dashed arrow in part (a) in Figure **2.3.3**. Substituting hc/λ for ΔE gives

$$\Delta E = \frac{hc}{\lambda} = -R_H hc\left(\frac{1}{n_h^2} - \frac{1}{n_l^2}\right) \tag{2.3.6}$$

Canceling *hc* on both sides gives

$$\frac{1}{\lambda} = -R_H\left(\frac{1}{n_h^2} - \frac{1}{n_l^2}\right) \tag{2.3.7}$$

Except for the negative sign, this is the same equation that Rydberg obtained experimentally. The negative sign in Equations 2.3.6 and 2.3.7 indicates that energy is released as the electron moves from orbit n_h to orbit n_l because orbit n_h is at a higher energy than orbit n_l. Bohr calculated the value of R_H from fundamental constants such as the charge and mass of the electron and Planck's constant and obtained a value of $1.0974 \times 10^7\ m^{-1}$, the same number Rydberg had obtained by analyzing the emission spectra.

We can now understand the physical basis for the Balmer series of lines in the emission spectrum of hydrogen (**2.3.3***b*); the lines in this series correspond to transitions from higher-energy orbits (n > 2) to the second orbit (n = 2). Thus, the hydrogen atoms in the sample have absorbed energy from the electrical discharge and decayed from a higher-energy excited state (n > 2) to a lower-energy state (n = 2) by emitting a photon of electromagnetic radiation whose energy corresponds exactly to the difference in energy between the two states (Figure **2.3.3***a*). The n = 3 to n = 2 transition gives rise to the line at 656 nm (red), the n = 4 to n = 2 transition to the line at 486 nm (green), the n = 5 to n = 2 transition to the line at 434 nm (blue), and the n = 6 to n = 2 transition to the line at 410 nm (violet). Because a sample of hydrogen contains a large number of atoms, the intensity of the various lines in a line spectrum depends on the number of atoms in each excited state. At the temperature in the gas discharge tube, more atoms are in the n = 3 than the n ≥ 4 levels. Consequently, the n = 3 to n = 2 transition is the most intense line, producing the characteristic red color of a hydrogen discharge (Figure **2.3.1***a*). Other families of lines are produced by transitions from excited states with n > 1 to the orbit with n = 1 or to orbits with n ≥ 3. These transitions are shown schematically in Figure **2.3.4** :

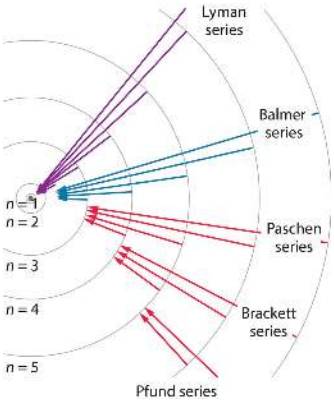


Figure 2.3.4: Electron Transitions Responsible for the Various Series of Lines Observed in the Emission Spectrum of Hydrogen. The Lyman series of lines is due to transitions from higher-energy orbits to the lowest-energy orbit (n = 1); these transitions release a great deal of energy, corresponding to radiation in the ultraviolet portion of the electromagnetic spectrum. The Paschen, Brackett, and Pfund series of lines are due to transitions from higher-energy orbits to orbits with n = 3, 4, and 5, respectively; these transitions release substantially less energy, corresponding to infrared radiation. (Orbits are not drawn to scale.)

Using Atoms to Time

In contemporary applications, electron transitions are used in timekeeping that needs to be exact. Telecommunications systems, such as cell phones, depend on timing signals that are accurate within a millionth of a second per day; the same goes for the devices that control the US power grid. Global positioning system (GPS) signals must be accurate within a billionth of a second per day, which is equivalent to gaining or losing no more than one second in 1,400,000 years. Quantifying time requires finding an event with an interval that repeats on a regular basis.

To achieve the accuracy required for modern purposes, physicists have turned to the atom. The current standard used to calibrate clocks is the cesium atom. Supercooled cesium atoms are placed in a vacuum chamber and bombarded with microwaves whose frequencies are carefully controlled. When the frequency is exactly right, the atoms absorb enough energy to undergo an electronic transition to a higher-energy state. Decay to a lower-energy state emits radiation. The microwave frequency is continually adjusted, serving as the clock's pendulum.

In 1967, the second was defined as the duration of 9,192,631,770 oscillations of the resonant frequency of a cesium atom, called the *cesium clock*. Research is currently under way to develop the next generation of atomic clocks that promise to be even more accurate. Such devices would allow scientists to monitor vanishingly faint electromagnetic signals produced by nerve pathways in the brain and allow geologists to measure variations in gravitational fields, which cause fluctuations in time, that would aid in the discovery of oil or minerals.

Example 2.3.1: The Lyman Series

The so-called Lyman series of lines in the emission spectrum of hydrogen corresponds to transitions from various excited states to the n = 1 orbit. Calculate the wavelength of the lowest-energy line in the Lyman series to three significant figures. In what region of the electromagnetic spectrum does it occur?

Given: lowest-energy orbit in the Lyman series

Asked for: wavelength of the lowest-energy Lyman line and corresponding region of the spectrum

Strategy:

A. Substitute the appropriate values into Equation 2.1.2.4 (the Rydberg equation) and solve for λ.
B. Use Figure 2.2.1 to locate the region of the electromagnetic spectrum corresponding to the calculated wavelength.

Solution:

We can use the Rydberg equation to calculate the wavelength:

$$\frac{1}{\lambda} = -R_H \left(\frac{1}{n_h^2} - \frac{1}{n_l^2} \right)$$

A For the Lyman series, /(n_l = 1\). The lowest-energy line is due to a transition from the n = 2 to n = 1 orbit because they are the closest in energy.

$$\frac{1}{\lambda} = -R_H \left(\frac{1}{n_h^2} - \frac{1}{n_l^2} \right) = 1.097 \times m^{-1} \left(\frac{1}{1} - \frac{1}{4} \right) = 8.228 \times 10^6 \; m^{-1}$$

It turns out that spectroscopists (the people who study spectroscopy) use cm^{-1} rather than m^{-1} as a common unit. Wavelength is inversely proportional to energy but frequency is directly proportional as shown by Planck's formula, E=hu.

Spectroscopists often talk about energy and frequency as equivalent. The cm^{-1} unit is particularly convenient. The infrared range is roughly 200 - 5,000 cm^{-1}, the visible from 11,000 to 25,000 cm^{-1} and the UV between 25,000 and 100,000 cm^{-1}. The units of cm^{-1} are called wavenumbers, although people often refer to the unit as inverse centimeters. We can convert the answer in part A to cm^{-1}.

$$\tilde{u} = \frac{1}{\lambda} = 8.228 \times 10^6 \; \cancel{m^{-1}} \left(\frac{\cancel{m}}{100 \; cm} \right) = 82,280 \; cm^{-1}$$

and

$$\lambda = 1.215 \times 10^{-7} \; m = 122 \; nm$$

This emission line is called Lyman alpha. As the strongest atomic emission line from the sun, it drives the chemistry of the upper atmosphere of all the planets, producing ions by stripping electrons from atoms and molecules. It is completely absorbed by oxygen in the upper stratosphere, dissociating O_2 molecules to O atoms which react with other O_2 molecules to form stratospheric ozone.

B This wavelength is in the ultraviolet region of the spectrum.

? Exercise 2.3.1: The Pfund Series

The Pfund series of lines in the emission spectrum of hydrogen corresponds to transitions from higher excited states to the n = 5 orbit. Calculate the wavelength of the *second* line in the Pfund series to three significant figures. In which region of the spectrum does it lie?

Answer

4.65 × 10^3 nm; infrared

Bohr's model of the hydrogen atom gave an exact explanation for its observed emission spectrum. The following are his key contributions to our understanding of atomic structure:

- Electrons can occupy only certain regions of space, called *orbits*.
- Orbits closer to the nucleus are lower in energy.
- Electrons can move from one orbit to another by absorbing or emitting energy, giving rise to characteristic spectra.

Unfortunately, Bohr could not explain *why* the electron should be restricted to particular orbits. Also, despite a great deal of conjecturing, such as assuming that orbits could be ellipses rather than circles, his model could not quantitatively explain the emission spectra of any element other than hydrogen (Figure **2.3.5**). In fact, Bohr's model worked only for species that contained just one electron: H, He^+, Li^{2+}, and so forth. Scientists needed a fundamental change in their way of thinking about the electronic structure of atoms to advance beyond the Bohr model.

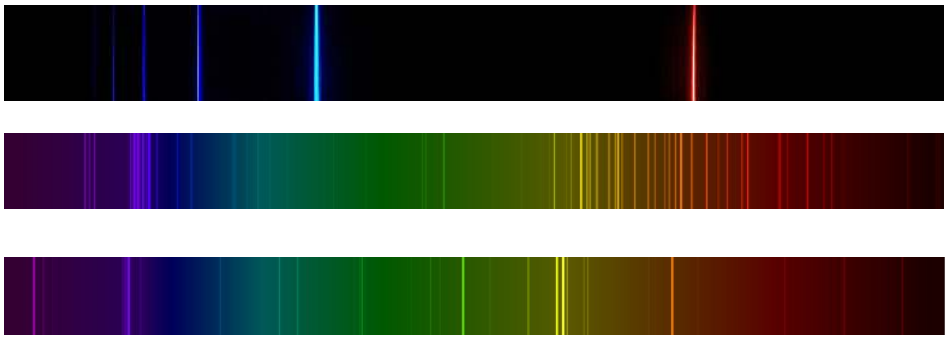


Figure 2.3.5: The Emission Spectra of Elements Compared to Hydrogen. **Top:** hydrogen gas (atomized to hydrogen atoms in the discharge tube). **Middle:** neon. **Bottom:** mercury. The strongest lines in the hydrogen spectrum are in the far UV Lyman series starting at 124 nm and below. The strongest lines in the mercury spectrum are at 181 and 254 nm, also in the UV. These are not shown. Attribution: Hydrogen (Jan Homann / CC BY-SA); Neon (Teravolt at en.Wikipedia / Public domain); Mercury (Teravolt at en.Wikipedia / Public domain)

The Energy States of the Hydrogen Atom

Thus far, we have explicitly considered only the emission of light by atoms in excited states, which produces an emission spectrum (a spectrum produced by the emission of light by atoms in excited states). The converse, absorption of light by ground-state atoms to produce an excited state, can also occur, producing an absorption spectrum (a spectrum produced by the absorption of light by ground-state atoms).

> When an atom emits light, it decays to a lower energy state; when an atom absorbs light, it is excited to a higher energy state.

If white light is passed through a sample of hydrogen, hydrogen atoms absorb energy as an electron is excited to higher energy levels (orbits with $n \geq 2$). If the light that emerges is passed through a prism, it forms a continuous spectrum with *black* lines (corresponding to no light passing through the sample) at 656, 468, 434, and 410 nm. These wavelengths correspond to the $n = 2$ to $n = 3$, $n = 2$ to $n = 4$, $n = 2$ to $n = 5$, and $n = 2$ to $n = 6$ transitions. Any given element therefore has both a characteristic emission spectrum and a characteristic absorption spectrum, which are essentially complementary images.

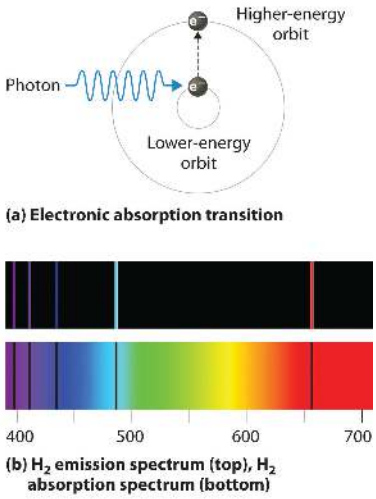


Figure 2.3.6: Absorption and Emission Spectra. Absorption of light by a hydrogen atom. (a) When a hydrogen atom absorbs a photon of light, an electron is excited to an orbit that has a higher energy and larger value of n. (b) Images of the emission and absorption spectra of hydrogen are shown here.

Emission and absorption spectra form the basis of *spectroscopy*, which uses spectra to provide information about the structure and the composition of a substance or an object. In particular, astronomers use emission and absorption spectra to determine the composition of stars and interstellar matter. As an example, consider the spectrum of sunlight shown in Figure 2.3.7. Since the sun is very hot, it emits light in the form of a continuous emission spectrum. Superimposed on the spectrum, however, is a series of

dark lines primarily resulting from the absorption of specific frequencies of light by cooler atoms in the outer atmosphere of the sun. By comparing these lines with the spectra of elements measured on Earth, we now know that the sun contains large amounts of hydrogen, iron, and carbon, along with smaller amounts of other elements. During the solar eclipse of 1868, the French astronomer Pierre Janssen (1824–1907) observed a set of lines that did not match those of any known element. He suggested that they were due to the presence of a new element, which he named *helium*, from the Greek *helios*, meaning "sun." Helium (He) was finally discovered in uranium ores on Earth in 1895. Alpha particles are helium nuclei. Alpha particles emitted by radioactive uranium nuclei pick up electrons from the rocks to form helium atoms.

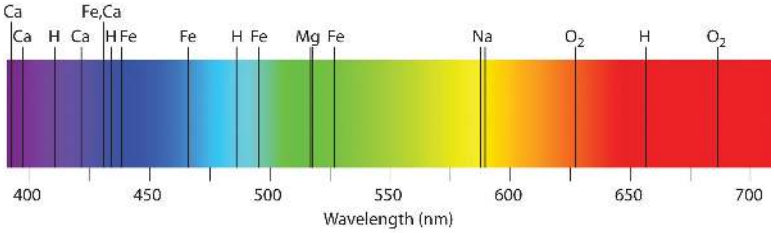


Figure **2.3.7**: *The Visible Spectrum of Sunlight. The characteristic dark lines are mostly due to the absorption of light by elements that are present in the cooler outer part of the sun's atmosphere; specific elements are indicated by the labels. The lines at 628 and 687 nm, however, are due to the absorption of light by oxygen molecules in Earth's atmosphere.*

The familiar red color of neon signs used in advertising is due to the emission spectrum of neon shown in part (b) in Figure **2.3.5**. Similarly, the blue and yellow colors of certain street lights are caused, respectively, by mercury and sodium discharges. In all these cases, an electrical discharge excites neutral atoms to a higher energy state, and light is emitted when the atoms decay to the ground state. In the case of mercury, most of the emission lines are below 450 nm, which produces a blue light (part (c) in Figure **2.3.5**). In the case of sodium, the most intense emission lines are at 589 nm, which produces an intense yellow light.

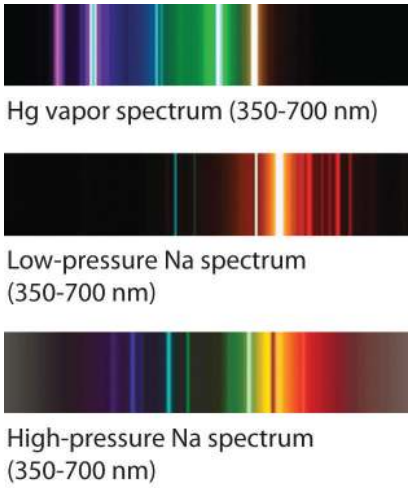


Figure **2.3.8**: *The emission spectra of sodium and mercury. Many street lights use bulbs that contain sodium or mercury vapor. Due to the very different emission spectra of these elements, they emit light of different colors. The lines in the sodium lamp are broadened by collisions. The dark line in the center of the high pressure sodium lamp where the low pressure lamp is strongest is caused by absorption of light in the cooler outer part of the lamp.*

Summary

There is an intimate connection between the atomic structure of an atom and its spectral characteristics. Atoms of individual elements emit light at only specific wavelengths, producing a **line spectrum** rather than the continuous spectrum of all wavelengths produced by a hot object. Niels Bohr explained the line spectrum of the hydrogen atom by assuming that the electron moved in circular orbits and that orbits with only certain radii were allowed. Lines in the spectrum were due to transitions in which an electron moved from a higher-energy orbit with a larger radius to a lower-energy orbit with smaller radius. The orbit closest to the nucleus represented the **ground state** of the atom and was most stable; orbits farther away were higher-energy **excited states**. Transitions from an excited state to a lower-energy state resulted in the emission of light with only a limited number of wavelengths. Atoms can also absorb light of certain energies, resulting in a transition from the ground state or a lower-energy

excited state to a higher-energy excited state. This produces an **absorption spectrum**, which has dark lines in the same position as the bright lines in the **emission spectrum** of an element. Bohr's model revolutionized the understanding of the atom but could not explain the spectra of atoms heavier than hydrogen.

Contributors and Attributions

- Modified by Joshua Halpern (Howard University)

This page titled 2.3: Discovery of Subatomic Particles and the Bohr Atom is shared under a CC BY-NC-SA 3.0 license and was authored, remixed, and/or curated by Anonymous.

- **2.1.2: Discovery of Subatomic Particles and the Bohr Atom** is licensed CC BY-NC-SA 3.0.

2.4: The Schrödinger equation, particle in a box, and atomic wavefunctions

Considering the failures of the Bohr model, Erwin Schrödinger and Werner Heisenberg proposed a major change in the paradigm regarding the electron. In several breakthrough papers (1925-1927) they attributed wave properties to electrons and they each received Nobel prizes for developing the theories of Wave Mechanics (or the "New Quantum Mechanics"). This approach treated electrons as having "dual" nature: possessing properties of *both* waves and particles.

Schrödinger's Equation describes the behavior of the electron (in a hydrogen atom) in three dimensions. It is a mathematical equation that defines the electron's position, mass, total energy, and potential energy. The simplest form of the Schrödinger Equation is as follows:

$$\hat{H}\psi = E\psi$$

where $\hat{H}$ is the **Hamiltonian operator**, E is the **energy of the electron**, and ψ is the **wavefunction**.

The Hamiltonian, $\hat{H}$

The Hamiltonian operator is like a set of instructions that tells us what to do with the function that follows it. A Hamiltonian operator is a function over three-dimensional space that corresponds to the sum of kinetic energies and potential energies of the particles in a system, one electron and its nucleus in this case. The Hamiltonian operator for a one-electron system is:

$$\hat{H} = \frac{-h^2}{8\pi^2 m_e}\left(\frac{\partial^2}{\partial x^2} + \frac{\partial^2}{\partial y^2} + \frac{\partial^2}{\partial z^2}\right) - \frac{Ze^2}{4\pi\epsilon_0 r},$$

where h is Planck's constant, m_e is the mass of the electron, e is the charge of the electron, r is the distance from the nucleus ($r = \sqrt{x^2+y^2+z^2}$), Z is the charge of the nucleus, and $4\pi\epsilon_0$ is the permittivity of a vacuum.

Kinetic Energy

The first part of the Hamiltonian written above, $\frac{-h^2}{8\pi^2 m_e}\left(\frac{\partial^2}{\partial x^2} + \frac{\partial^2}{\partial y^2} + \frac{\partial^2}{\partial z^2}\right)$ describes the kinetic energy of the electron. This is the energy due to motion of the electron.

Potential energy

The second part written above, $\frac{-Ze^2}{4\pi\epsilon_0 r}$, describes the potential energy of the electron, and is commonly written as $V(r)$ or $V(x,y,z)$.

$$V(x,y,x) = \frac{-Ze^2}{4\pi\epsilon_0 r} = \frac{-Ze^2}{4\pi\epsilon_0\sqrt{x^2+y^2+z^2}}$$

The potential energy depends on the attractive electrostatic force between the electron and the nucleus. You might notice that this attraction is essentially the same as the electrostatic force defined by Coulomb's law. And, just as in Coulomb's law, when two opposite charges are attracted to one another, the potential energy of the force is negative. Thus, when an electron is close to the nucleus, the potential energy is a large negative number corresponding to a strong attractive force. When an electron is farther from the nucleus, the potential energy is still negative but with a smaller magnitude, corresponding to a weaker attractive force. If the electron is very far from the nucleus ($r = \infty$) then the attractive force, and the potential energy, is zero.

The Wavefunction, ψ

In simple terms, the wavefunction (ψ) of an electron describes the electron's position in space, relative to the nucleus. The square of the ψ describes an atomic orbital. We can't define the position too exactly because we would violate the Heisenberg Uncertainty principle, but we can define its wave. A simple example of a ψ is described in the next section: Particle in a Box. Here, we will describe the ψ in general terms. Generally, in a one-electron atom, the electron ψ is defined by the wave's distance from the nucleus and its angle with respect to the x, y, and z axes of the atom's Cartesian coordinates (the nucleus is at the origin). The general form of the (ψ) for an electron in a hydrogen atom can be written as follows:

$$\psi_{n,l,m_l} = R_{n,l}(r) + Y_{l,m_l}(\theta,\phi)$$

Quantum Numbers define ψ

The (ψ) is defined by three of the quantum numbers: n, l, and m_l. These quantum numbers will be discussed more in a later section (2.2.2) The radial variation, R, depends on the electron's distance from the nucleus. The quantum numbers n (energy level) and l (orbital type) define R. Since n must be an integer, there are only certain allowed values for the solution to the wavefunction.

The angular variation, Y, depends on the angle with respect to the x, y, and z coordinates, and depends on the quantum numbers l (the orbital type) and m_l (the angular momentum, or the specific orbital). For example p_x lies along the x axis, while p_y points in a different direction in space.

For review, a list of the quantum numbers, their values, and meanings are in the table below.

SYMBOL	NAME	VALUES	MEANING
n	principal	$1, 2, 3...$(any integer)	energy level, shell
l	angular momentum	$0 \rightarrow n-1$	subshell, $0 = s, 1 = p, 2 = d, 3 = f...$ this is the angular dependence of the orbital, shape of the orbital *letters have historical meaning, sharp, principle, diffuse, fundamental
m_l	magnetic	$+l \rightarrow -l$	orientation of angular momentum in space, orbital
m_s	spin	$+\frac{1}{2}, -\frac{1}{2}$	the imaginary property we call "spin", up or down

Some important considerations and limitations

Although it might seem like there could be any value of x, y, and z for the Hamiltonian, these values are limited by the allowed positions of electrons according to ψ, which is limited by integer values of n. In other words the allowed solutions are *quantized*. However, there are an infinite number of values for n from $n = 1 \rightarrow \infty$, so there are also infinite solutions to the Schrödinger equation.

The ψ describes the wave properties of an electron. The probability of finding the electron somewhere in space is the square of the wavefunction (ψ^2 or $\psi\psi^*$). In other words, ψ^2 describes the shape and size of an electron's orbital (the shapes you already know).

There are some requirements for a physically realistic and meaningful solution for ψ, and thus ψ^2.

1. There is only one possible value for ψ for any set of the three quantum numbers n, l, m_l.
2. The ψ approaches zero as r approaches infinity, and so ψ^2 also approaches zero as $r \rightarrow \infty$.
3. The wavefunction must be normalized. In other words, the total probability of finding the electron in all of space must be 1.

$$\int_{\text{all space}} \psi_A \psi_A^* d\tau = 1$$

4. Any two orbitals must not occupy the same space. In other words, any two orbitals in an atom are orthogonal. If ψ_A and ψ_B are wavefunctions for different orbitals in the same atom,

$$\int_{\text{all space}} \psi_A \psi_B^* d\tau = 0$$

5. The probability of finding the electron anywhere in infinite space must be defined. This means that the wave functions and their first derivatives must be continuous (i.e. not change abruptly from one point to the next).

Awesome Sources for further reading

- +Plus: https://plus.maths.org/content/schrodinger-1

This page titled 2.4: The Schrödinger equation, particle in a box, and atomic wavefunctions is shared under a CC BY-NC-SA 4.0 license and was authored, remixed, and/or curated by Kathryn Haas.

- **2.2: The Schrödinger equation, particle in a box, and atomic wavefunctions** by Kathryn Haas is licensed CC BY-NC-SA 4.0.

2.4.1: Particle in a Box

The particle in the box is a model that can illustrate how a wave equation works. Although it does not represent a real situation, we can limit our model to just one dimension (the x-dimension, for instance) such that the Schrödinger equation becomes significantly simplified. Despite being unrealistic, this simplification is quite useful for gaining an understanding of the Schrödinger equation.

The model of a particle in a box

The particle in the box is a hypothetical situation with a particle trapped in a one-dimensional "box". Let's not get hung-up on the fact that the common object called a "box" is typically an object with three dimensions instead of just one dimension. And let's also not get hung up on the word "particle". This is a particle that has properties of a wave…so it is unlike the macroscopic particle that you're probably imagining. This "box" is more like a line, or an x-axis; it is just a one-dimensional space in which a particle-wave is trapped.

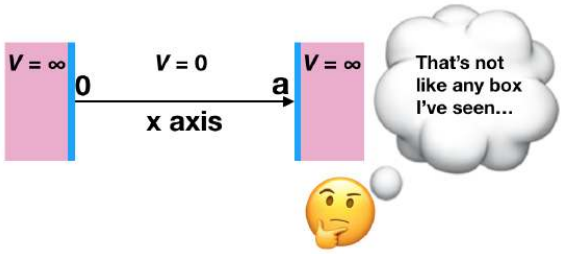


Figure 2.4.1.1. An illustration of the particle in the box model (particle not shown). The box is actually just a one-dimensional space, often assigned to the x-dimension (the x-axis). The particle has wave properties and is trapped in the box. Since no forces act on the particle inside the box, the particle's potential energy inside the box is zero ($V = 0$) and its potential energy outside the box is infinite ($V = \infty$). (CC-BY-NC-SA; Kathryn Haas)

The particle-wave can only exist inside the walls (where $0 < x < a$), along the x axis in the figure shown above. In terms of energy, the potential energy is zero ($V = 0$) because the particle is in an energetically-favorable position here. On the other hand, outside the box, the particle cannot exist and the potential energy is infinitely large ($V = \infty$) outside the walls (where $x < 0$ or $x > a$). This means that it is infinitely unfavorable for the particle-wave to exist outside the box, and so it never does. The particle-wave is trapped between the walls, along the 1-dimensional x axis, and there are no forces acting on the particle-wave inside this "box".

The Schrödinger wave equation for a particle in a box

The particle in a box model lets us consider a simple version of the Schrödinger equation. Before we simplify, let's take another look at the full Hamiltonian for a particle-wave in three dimensions (see equation 2.2.2) and the simplest form of the Schrödinger equation (see equation 2.2.1). Both of these equations are described in the previous section and are written below for convenience.

The Schrödinger Equation (from equation 2.2.1): $\hat{H}\psi = E\psi$

The Hamiltonian in three dimensions (from equation 2.2.2):

$$\hat{H} = \frac{-h^2}{8\pi^2 m_e}\left(\frac{\partial^2}{\partial x^2} + \frac{\partial^2}{\partial y^2} + \frac{\partial^2}{\partial z^2}\right) - \frac{Ze^2}{4\pi\epsilon_0 r}$$

In the particle in a box model, there is only one dimension, x. Because the y and z values are zero, we can drop y and z out of our Hamiltonian equation. And, since $V = 0$ inside the box, we can drop the whole part of the Hamiltonian equation that describes the potential energy ($\frac{-Ze^2}{4\pi\epsilon_0 r}$). This leaves us with a much simplified Hamiltonian operator, which we can then use to write the Schrödinger wave equation for a particle moving in one dimension. One last thing we'll do is use a more general value m for the mass of the particle, rather than m_e that specifically represents the mass of an electron. The Schrödinger equation for a particle-wave in a one-dimensional box is:

$$\frac{-h^2}{8\pi^2 m}\left(\frac{\partial^2\psi(x)}{\partial x^2}\right) = E\psi \qquad (2.4.1.1)$$

? Exercise 2.4.1.1

Follow the steps that were described in the last paragraph to find Equation 2.4.1.1 from equation 2.2.1 and 2.2.2. In other words, derive the Schrödinger Equation for the particle in a box given the three-dimensional Hamiltonian and Schrödinger Equations.

Answer

Here is the Hamitlonian Equation for in three dimensions.

$$\hat{H} = \frac{-h^2}{8\pi^2 m}\left(\frac{\partial^2}{\partial x^2} + \frac{\partial^2}{\partial y^2} + \frac{\partial^2}{\partial z^2}\right) - \frac{Ze^2}{4\pi\epsilon_0 r}$$

There are two parts to this equation: the kinetic energy contribution and the potential energy contribution. While the first part of this expression, $\frac{-h^2}{8\pi^2 m}\left(\frac{\partial^2}{\partial x^2} + \frac{\partial^2}{\partial y^2} + \frac{\partial^2}{\partial z^2}\right)$, is the **kinetic energy** contribution, the second part of the expression, $-\frac{Ze^2}{4\pi\epsilon_0 r}$, is the **potential energy (V)** contribution.

(1) Simplify the expression for kinetic energy

Your particle-wave is moving in only one dimension. We can arbitrarily choose the dimension x. This means that x is a variable and will have some value from 0 to a. On the other hand, the particle does not move in the other two dimensions, y and z. You can assign the position of the particle along x and y axes as zero or you can just understand that they do not exist in any significant capacity in our 1-D space. Either way, you can just drop them out of the kinetic energy part of the Hamiltonian, as so:

When $y = z = 0$ and the particle-wave only exists/moves in the x dimension, $\frac{-h^2}{8\pi^2 m}\left(\frac{\partial^2}{\partial x^2} + \frac{\partial^2}{\partial y^2} + \frac{\partial^2}{\partial z^2}\right) = \frac{-h^2}{8\pi^2 m}\left(\frac{\partial^2}{\partial x^2}\right)$

And the overall Hamiltonian is simplified:

$$\hat{H} = \frac{-h^2}{8\pi^2 m}\left(\frac{\partial^2}{\partial x^2}\right) - \frac{Ze^2}{4\pi\epsilon_0 r}$$

(2) Simplify the expression for potential energy (V).

The particle's potential energy inside the box is zero ($V = 0$). Therefore, $V = -\frac{Ze^2}{4\pi\epsilon_0 r} = 0$. We can simply drop the potential energy portion from the Hamiltonian because its value is zero.

The simplified Hamiltonian is now:

$$\hat{H} = \frac{-h^2}{8\pi^2 m}\left(\frac{\partial^2}{\partial x^2}\right)$$

(3) Substitute the simplified Hamiltonian into the Schrödinger Equation.

The Schrödinger is: $\hat{H}\psi = E\psi$

When the simplified Hamiltonian is substituted into this equation, the result is the 1-D Schrödinger Equation 2.4.1.1.

$$\left(\frac{-h^2}{8\pi^2 m}\left(\frac{\partial^2 \psi(x)}{\partial x^2}\right)\right) = E\psi$$

The wavefunction of a one-dimensional wave

Although we've simplified the Schrödinger Equation by considering the particle in the box, Equation 2.4.1.1 may still look mysterious to you. But it's simpler than you might realize. Let's unpack it! Here we'll go through the steps of deriving the 1-dimensional wavefunction for the particle in a box. We won't try to derive a three-dimensional wavefunction for a "real" electron, but when you understand how to find the 1-dimensional wavefunction, and what it tells us, then you can conceptually extend this to understand what the wavefunction tells us about electrons in three dimensions.

Let's dissect Equation 2.4.1.1. Here it is again for reference:

$$\frac{-h^2}{8\pi^2 m_e}\left(\frac{\partial^2\psi(x)}{\partial x^2}\right) = E\psi$$

The expression $\frac{-h^2}{8\pi^2 m_e}$ is just a negative constant. This negative constant is multiplied by the second derivative of the wavefunction in the expression above. And E is a constant multiplied by that same function. We can rearrange this equation as follows:

$$\frac{\partial^2\psi(x)}{\partial x^2} = \frac{-8\pi^2 m_e E}{h^2}\psi = -C\psi \tag{2.4.1.2}$$

where C is just the constant; $C = \frac{8\pi^2 m_e E}{h^2}$

To an expert in the mathematical field of Differential Equations, this expression 2.4.1.1 follows a familiar pattern that makes it easy to translate. If you're not an expert in differential equations, that is OK; you'll just have to bear with this while things get a little "hand-wavy" and try Exercise **2.4.1.2** to prove it to yourself that the following "hand waviness" is true. An expert in differential equations could tell you that when the second derivative of a function is equal to a negative constant times that same function, the function can be written in terms of ***sin*** and ***cos***, as shown in Equation 2.4.1.3 (that was the hand-wavy part...see, not so bad):

$$\psi = A\sin(rx) + B\cos(sx) \tag{2.4.1.3}$$

A, B, r, and s are constants in Equation 2.4.1.3. This expression is useful because it is in a form that we could plot with a graphing program (or calculator). However, to do so we must know the constants A, B, r, and s.

What are r and s?

If we substitute expression 2.4.1.3 into Equation 2.4.1.1 and solve for r and s, we find the expressions below.

$$r = s = \sqrt{2m_e E}\left(\frac{2\pi}{h}\right) \tag{2.4.1.4}$$

This shows us that r and s are equal and constant; we know the values for π, h, and m_e, and we can solve for the constant E.

? Exercise 2.4.1.2: Prove that Equation 2.4.1.3 is true

Show that Equation 2.4.1.3 is true in the case that Equation 2.4.1.2 ($\frac{\partial^2\psi(x)}{\partial x^2} = -C\psi$) is true. Also consider Equation 2.4.1.4 (r, s are constants and $r = s$) and explain why the constant r must equal s.

To do this problem, you'll also need to know the basic differentiation rules of **sin** and **cos** functions, given below for convenience.

Differentiation Rules for *sin* and *cos*:

$\frac{d}{dx}\left(\sin(rx)\right) = r\cos(rx)$, where r is a constant.

$\frac{d}{dx}\left(\cos(rx)\right) = -r\sin(rx)$, where r is a constant.

Answer

You can show that 2.4.1.3 is true by substituting 2.4.1.3 back into Equation 2.4.1.2; in other words take the second derivative of the function, $\psi = A\sin(rx) + B\cos(sx)$ to show that $\frac{\partial^2\psi(x)}{\partial x^2} = -C\psi$. C, r, and s are arbitrary constants, and $r = s$. The actual value of these constants is irrelevant for this problem. Here is one way to approach the problem:

(1) Substitute $\psi = A\sin(rx) + B\cos(sx)$ into $\frac{\partial^2\psi(x)}{\partial x^2} = -C\psi$.

$\frac{\partial^2}{\partial x^2}\left(A\sin(rx) + B\cos(sx)\right) = -C\psi$

(2) Take the first and second derivative of $A\sin(rx) + B\cos(sx)$.

The result of taking the first derivative...

$\frac{\partial}{\partial x}\left(rA\cos(rx) - sB\sin(sx)\right) = -C\psi$

...and the second derivative...

$-r^2 A\sin(rx) - s^2 B\cos(sx) = -C\psi$

This is where we see that the only way $\psi = A\sin(rx) + B\cos(sx)$ is if we can factor the values r^2 and s^2 out of the left side. We have a hint that $r = s$ from the discussion above and Equation 2.4.1.4. Now we see that this is a necessary condition for the expression $-r^2 A\sin(rx) - s^2 B\cos(sx) = -C\psi$ to be true.

(3) Simplify

If $r = s$, then $r^2 = s^2$ and we can replace s with r in the equation above, as so...

$$-r^2 A\sin(rx) - r^2 B\cos(sx) = -C\psi$$

Now, we can factor the constant, $-r^2$ out of the left side of this expression,

$$-r^2\left(A\sin(rx) + B\cos(sx)\right) = -C\psi$$

Now we see that $\psi = A\sin(rx) + B\cos(sx)$ when $-C = -r^2$. In other words, we have shown that $\psi = A\sin(rx) + B\cos(sx)$ is true.

Why is this a useful exercise?

Although it is difficult to explain the derivation of the expression $\psi = A\sin(rx) + B\cos(sx)$ without differential equations and only knowing that $\frac{\partial^2\psi(x)}{\partial x^2} = -C\psi$, to show this is true is as simple as solving this exercise. This exercise is here to help you review your calculus and to show you that the "hand waving" in the text above is not magic, but it is coming from math that you have seen in your calculus courses. Math is crucial for explaining the nature of the universe! Eat your vegetables and practice your math.

? Exercise 2.4.1.4

*Complete Exercise **2.4.1.2** before attempting this one.

Derive the expression for r below (from Equation 2.4.1.4) using the 1-D wavefunction (2.4.1.3: $\psi = A\sin(rx) + B\cos(sx)$) and the 1-D Schrödinger equation (2.4.1.1: $\left(\frac{-h^2}{8\pi^2 m_e}\left(\frac{\partial^2\psi(x)}{\partial x^2}\right) = E\psi\right)$).

$$r = \frac{2\pi}{h}\sqrt{2m_e E}$$

Answer

The steps below could be carried out in a different sequence:

(1) Rearrange

Let's move **all constants** to the right side of 2.4.1.1 so that we arrive at the expression that is shown in part of Equation 2.4.1.2 .

$$\frac{\partial^2\psi(x)}{\partial x^2} = \frac{-8\pi^2 m_e E}{h^2}\psi$$

(2) Take the second derivative of ψ, which we found in Exercise **2.4.1.2**.

$$\frac{\partial^2\psi(x)}{\partial x^2} = -r^2\left(A\sin(rx) + B\cos(sx)\right) = \frac{-8\pi^2 m_e E}{h^2}\psi$$

And since $\psi = A\sin(rx) + B\cos(sx)$, we can simplify this by dividing both sides by ψ (or by $A\sin(rx) + B\cos(sx)$).

**recall that $s = r$. So, you could have substituted r for s in the expression above, and you'd still be on the right track.*

$$-r^2 = \frac{-8\pi^2 m_e E}{h^2}$$

(3) Solve for r (*we already showed $r = s$ in the Exercise **2.4.1.2**).

$$r = \sqrt{\frac{8\pi^2 m_e E}{h^2}} = \frac{2\pi}{h}\sqrt{2m_e E}$$

What are A and B?

We can find the possible values of A and B by looking at the possible extremes for the value of x. In our model in Figure 2.4.1.1, we can see that x can have values from $0 \rightarrow a$. The two extremes, where $x = 0$ and $x = a$, lie at the walls of the box. The electron cannot exist beyond these values because it is trapped inside the walls, so its wavefunction must be zero at $x = 0$ and $x = a$.

The case where $x = 0$ can help us find the value of B. We just said that the wavefunction must be zero where $x = 0$. This means:

$$\psi_{x=0} = A\sin(rx) + B\cos(sx) = A\sin(0) + B\cos(0) = 0$$

Because $A\sin(0) = 0$, the expression can be simplified to:

$$\psi_{x=0} = B\cos(0) = B(1) = 0$$

Now we can see that there is only one possible value for the constant, B, that would allow this expression to be true, $B = 0$. And since B is constant then it will always be zero despite the value of x. This simplifies our 1-D wavefunction:

$$\psi = A\sin(rx) \tag{2.4.1.5}$$

The case where $x = a$ can help us find the value for A. Since the wavefunction must be zero where $x = a$:

$$\psi_{x=a} = A\sin(rx) = A\sin(ra) = 0$$

In this case, A cannot be zero because if both A and B are zero, the wavefunction is zero at all values of x, and so our wavefunction would not exist inside the box. So, let's assume A is not zero. Then, it must be the case that

$$\sin(ra) = 0$$

and then because of the way that $\sin$ functions work, the quantity ra must be an integer value of π if $\sin(ra) = 0$.

$$ra = \pm n\pi$$

where $n = 1, 2, 3...$ any non-zero integer. We can ignore negative values here since both positive and negative values of r will give the same value for $\sin(ra)$. We can then solve for r:

$$r = \frac{n\pi}{a} \tag{2.4.1.6}$$

and substitute the value $r = \frac{n\pi}{a}$ into Equation 2.4.1.5 to get:

$$\psi = A\sin\left(\frac{n\pi x}{a}\right) \tag{2.4.1.7}$$

Recall that the square of the wavefunction (ψ^2) gives the probability of finding the electron anywhere in space. In our model, the probability of finding the particle-wave inside the box is unity (it is 1). Mathematically, this is the normalizing requirement (expressed as $\int \psi_A \psi_A^* d\tau = 1$), which can be solved to find the value of A.

$$A = \sqrt{\frac{2}{a}}$$

Now, we can substitute the value of A into expression 2.4.1.7, and we have a wavefunction that can be visualized using any graphing program/calculator!

$$\psi = \sqrt{\frac{2}{a}}\left(\sin\left(\frac{n\pi x}{a}\right)\right) \tag{2.4.1.8}$$

What is the energy (E) of a particle in the box?

So, now you can see how a 1-D wavefunction can be solved. But how do we find the E of the electron from this? Well, in order to not distract you earlier, we skipped over a very simple way to do this. The E falls right out of the equations you just saw. We can set the two expressions we found above for the constant r, (equations 2.4.1.4 and 2.4.1.6) equal to one another and then solve for E:

$$r = \frac{n\pi}{a} = \sqrt{2mE}\left(\frac{2\pi}{h}\right)$$

$$E = \frac{n^2h^2}{8ma^2} \tag{2.4.1.9}$$

Expression 2.4.1.9 can be used to calculate the energy of a particle in a one-dimensional box of length a, given its integer energy level, n. Here we can see that the energy is quantized because n is an integer ($n = 1, 2, 3...$). In other words, n is a **quantum number**.

Making sense of the particle in a box: plotting the 1-D ψ and ψ^2.

No matter whether you're dealing with a 1-dimensional or 3-dimensional wave equation, the wavefunction itself (ψ) describes the particle's wave properties. This ψ doesn't have actual physical meaning, so it's hard to imagine what it "looks like" other than just plotting its function. However, the probability of finding the particle-wave at any specific position along the x-axis between $x = 0$ and $x = a$ is more physically meaningful. The probability of finding the particle is proportional to the square of the wave function, which is represented by either ψ^2 or, sometimes, $\psi\psi^*$. The plots of the functions for ψ and ψ^2 for the first three possible values of n are shown below in Figure 2.4.1.2. You could create plots similar to these simply by plotting the function shown in Equation 2.4.1.8. To plot, you just need to assign a value of n, and it is convenient to assign the length of the box as $a = 1$. The plot generated would have the general ratio of $\frac{x}{a}$ on the x axis, and thus would be relevant for any length box.

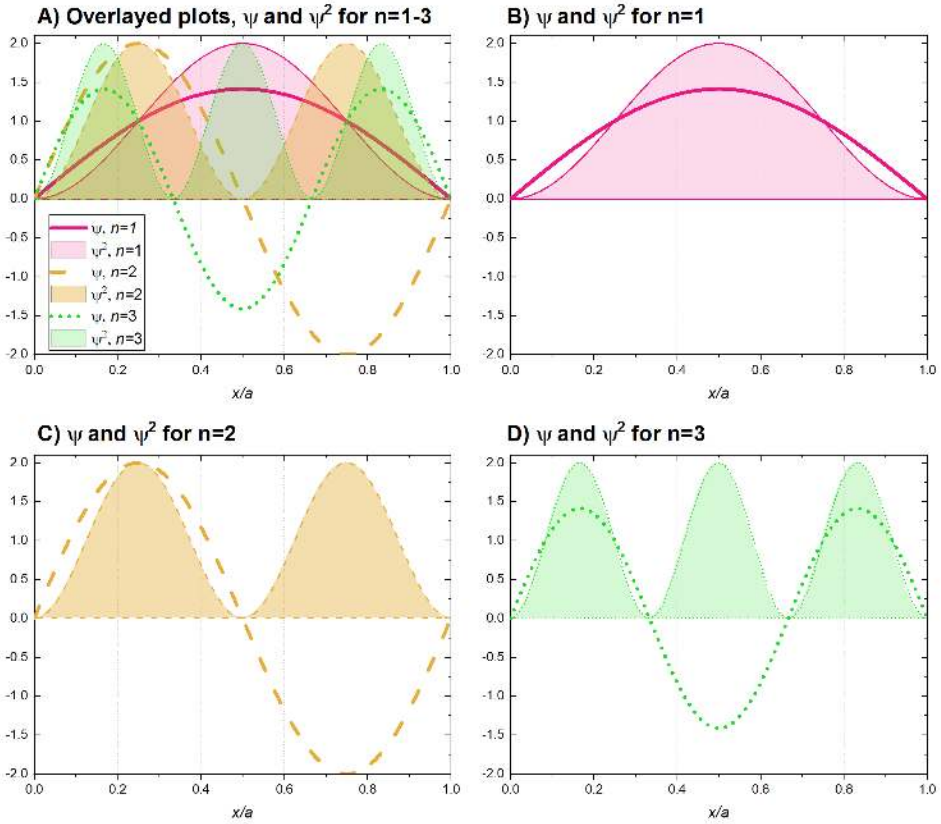


Figure 2.4.1.2. Plots of the 1-D ψ and ψ^2 for $n = 1$, $n = 2$, and $n = 3$ of a box of length a. The wavefunction (ψ) is plotted as a thick solid, dashed, or dotted line. The square of the wavefunction (ψ), which represents the probability of finding the particle at position x, is plotted as the thinner lines and is shaded. Solid lines represent $n = 1$, dashed lines represent $n = 2$, and dotted lines represent $n = 3$. (CC-BY-NC-SA; Kathryn Haas)

The graphs above represent "solutions" to the wave function. For example, the solution $n = 1$ gives the plot shown in Figure 2.4.1.2 B. The solution of $n = 2$ is plotted in Figure 2.4.1.2 C, and so on. These values for n are some of the possible solutions to the 1-dimensional ψ, and they yield descriptions of the wave behavior and probability of finding a particle in 1-dimensional space.

How does this apply to atoms?

The 1-dimensional particle in a box does not represent a real situation; but rather, it is a simple model that we can use to understand a more complex system, like a electron orbiting the nucleus in three dimensions. It's useful to recognize the analogies here that might represent something familiar in a real situation.

$x = 0$ is analogous to the nucleus in an atom. Here in the particle in a box model, $\psi = 0$ and there is zero probability of finding an electron. When this is extended to an atom, this position is analogous to the nucleus (at the origin of a coordinate system where $x = y = z = 0$. A 3-dimensional ψ is also zero at the nucleus and the electron cannot exist there; also, ψ approaches zero as it approaches this position in both the particle in a box model and in a more realistic case of an electron in an atom.

$x = a$ is analogous to a boundary surface far from the nucleus. In the particle in a box model, the 1-dimensional ψ is zero at $x = a$. This is analogous to an electron's ψ approaching zero as it gets further from the nucleus. There will be a more in depth description of boundary surface in the next section (2.2.2). You already know this as the outermost surface of an electron orbital. One minor but notable difference between the 1-dimensional particle in a box and the case of a real atom is that the ψ in three dimensions approaches but never quite reaches zero as distance from the nucleus increases, while $\psi = 0$ for $x = a$ in the more simple case of a 1-dimensional particle in a box.

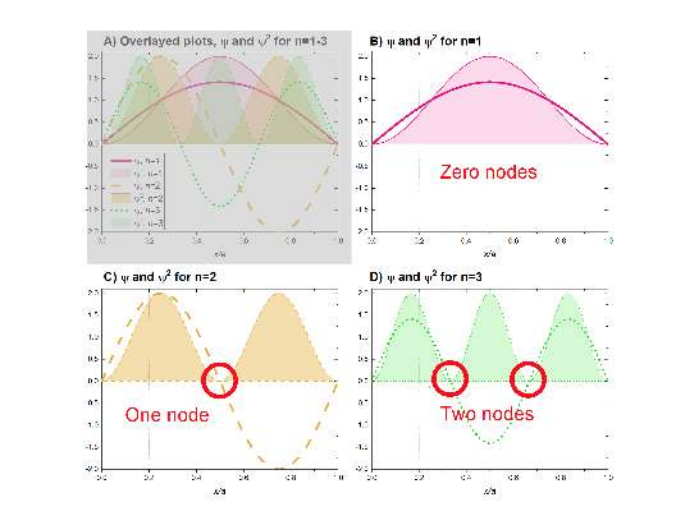
A change in sign of the ψ (and where both $psi = 0$ and $\psi^2 = 0$) is a node. In both the 1-dimensional particle in a box model and in the more realistic 3-dimensional case, a node is found where the ψ changes sign. At this point, $\psi = \psi^2 = 0$; in other words there is zero probability of finding the particle or electron at these points. It is easy to spot these points in the plots above because the wave function crosses the x-axis and the ψ^2 meets zero.

Exercise 2.4.1.4

Identify the points on plots B, C, and D in Figure **2.4.1.2** that are nodes. How many nodes are there for $n = 1, n = 2,$ and $n = 3$?

Answer

The nodes are annotated with red circles on the figure below. **Panel B** ($n = 1$) has zero nodes. There are two points where $\psi = 0$ in the case of $n = 1$, but these points are at the walls of the box and they are not nodes. The walls of the box are analogous to the nucleus and the boundary surface of an electron orbital. **Panel C** ($n = 2$) has one node where the ψ crosses zero. **Panel D** ($n = 3$) shows two nodes.



Exercise 2.4.1.5

Use a graphing program to plot the 1-dimensional ψ and ψ^2 for $n = 1, 2, 3, 4$. How many nodes are there for $n = 4$? Is this expected? Predict how many nodes we should expect for $n = 5$.

You can use any plotting program to do this, and if you aren't familiar with any, try this one: Desmos

Answer

You can use any plotting program to do this. This is the function you should plot (it is Equation 2.4.1.8):

$\psi = \sqrt{\frac{2}{a}}\left(\sin\left(\frac{n\pi x}{a}\right)\right)$

For n=1: Assign a value of $n = 1$, as stated in the problem. In the text above, it also states that it is convenient to assign a value of $a = 1$. Assigning these values results in the following function:

$\psi = \sqrt{\frac{2}{1}}\left(\sin\left(\frac{1\pi x}{1}\right)\right)$ and simplifying leads to $\psi = \sqrt{2}\left(\sin\left(\pi x\right)\right)$

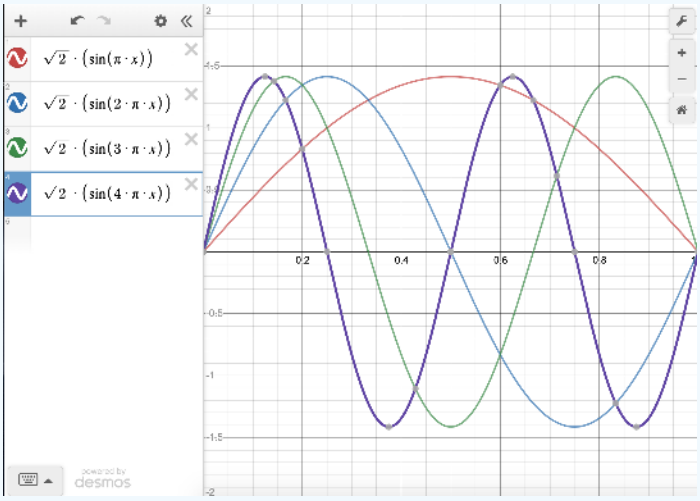
For n=2,3,4 you would repeat the process above. You will get the following functions:

For n=2: $\psi = \sqrt{2}\left(\sin\left(2\pi x\right)\right)$

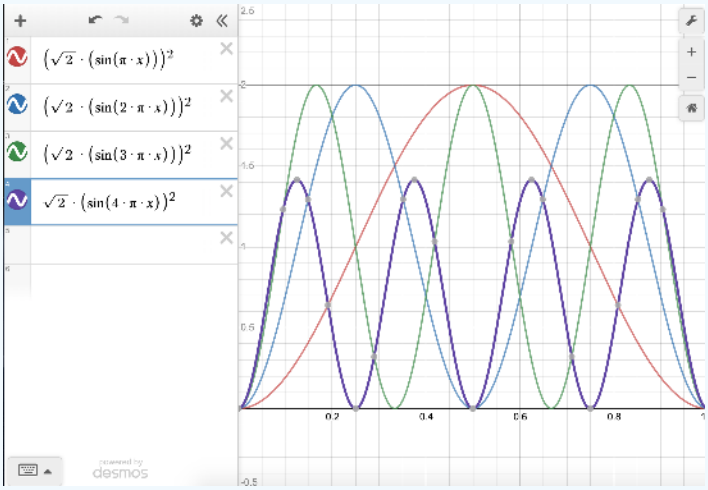
For n=3: $\psi = \sqrt{2}\left(\sin\left(3\pi x\right)\right)$

For n=4: $\psi = \sqrt{2}\left(\sin\left(4\pi x\right)\right)$

In a program like Desmos, you need to input the function correctly. It's useful to know the code for at least one graphing program. For Desmos, and most others, you can find help online. For example, the correct input for Desmos for the n=4 case is sqrt(2)*(sin(4*pi*x)). But, you have to type it in because copy/paste doesn't work. You'll also want to display your graph only from $x = 0$ to $x = 1$ by hitting the settings button (a little wrench in the upper right corner) and changing the x scale. Go ahead and change the y scale too, to $y = -2$ to $y = 2$. If you do this, you should get something that looks like this:



To graph the square of each wavefunction, you'd just square the functions that we just plotted:



> In both the case of ψ and ψ^2, the $n = 4$ function shows three nodes (see the bolded purple line, where nodes are tiny grey spots on the axis). This follows a pattern that you might have noticed with the cases of $n = 1, 2,$ and 3 where the number of nodes is $n - 1$ (nodes = $n - 1$). We should expect three nodes for $n = 4$ based on this pattern, and four nodes for $n = 5$.

In the next section, we will extend these ideas qualitatively to three dimensions. While there is only one quantum number in one dimension, there are three quantum numbers in three dimensions that (when combined) give discrete descriptions of an electron in three-dimensional space (plus a fourth quantum number that explains other properties of the electron).

This page titled 2.4.1: Particle in a Box is shared under a CC BY-NC-SA 4.0 license and was authored, remixed, and/or curated by Kathryn Haas.

- **2.2.1: Particle in a Box** by Kathryn Haas is licensed CC BY-NC-SA 4.0.

2.5: Quantum Numbers and Atomic Wave Functions

The one-dimensional particle in a box model from the previous section shows us how a wavefunction works in one dimension (the x-dimension). In one dimension, the wavefunction requires only one quantum number, n. A full explanation of the three-dimensional wavefunction for an electron is outside of the scope of this course. Instead, we will focus on gaining a conceptual understanding by extending knowledge of the one-dimensional wavefunction to a three-dimensional space.

Quantum numbers

Extending the wavefunction to three dimensions requires a total of three quantum numbers. In addition to n, which we saw in the one-dimensional case, we also need l and m_l to express the wavefunction in three dimensions. A complete solution to the Schrödinger equation, both the three-dimensional wavefunction and energy, includes a set of three quantum numbers (n, l, m_l). The wavefunction describes what we know as an atomic orbital; it defines the region in space where the electron is located. Additionally, there is a fourth quantum number, m_s. The m_s quantum number accounts for the observed interaction of electrons with an applied magnetic field; it is an additional postulate that is not part of the wavefunction. These four quantum numbers are described below.

The quantum number, n: This is the principle quantum number. This number represents the shell, including both the overall energy of the electron in that shell and the size of that shell. An allowed value for n is any non-zero, positive integer (1, 2, 3, 4, ... etc are allowed, but 4.1 is not allowed).

The quantum number, l: This is the angular momentum quantum number that corresponds to the subshell and its shape. It represents the angular dependence of the subshell, or the "shape" of the orbitals within a subshell. The allowed values of l depend on n. The allowed values of l for an electron in shell n are integer values between 0 to $n-1$, or $l = 0 \rightarrow n-1$. These values correspond to the orbital shape where $l = 0$ is an s-orbital, $l = 1$ is a p-orbital, $l = 2$ is a d-orbital, and $l = 3$ is an f-orbital.

The quantum number m_l: This is the magnetic quantum number. Its possible values give the number of orbitals within a subshell and its specific value gives the orbital's orientation in space. The allowed values of m_l depend on the value of l. The value of m_l is allowed to be any positive or negative integer between $+l$ and $-l$. In other terms, $m_l = +l \rightarrow -l$. For example, if the electron is in a 3-p-orbital, then $n = 3, l = 1$, and the possible values of m_l are $-1, 0,$ and $+1$. Since there are three possible values of m_l there are three orbitals in the p subshell. The specific m_l value defines in which of the three possible p-orbitals (p_x, p_y, or p_z) the electron exists. In the case of the s subshell, there is only one value, $m_l = 0$ because $l = 0$. The one value corresponds to the fact that there is only one s orbital in any shell.

The quantum number m_s: This quantum number accounts for the electron's "spin". In short, electrons interact with magnetic fields in a way that is similar to how a tiny bar magnet would interact with a magnetic field. The allowed values for m_s are $+\frac{1}{2}$ and $-\frac{1}{2}$.

Table 2.5.1. Quantum Numbers

SYMBOL	NAME	VALUES	MEANING
n	principal	$1, 2, 3...$(any integer)	energy level, shell
l	angular momentum	$0 \rightarrow n-1$	subshell, $0 = s, 1 = p, 2 = d, 3 = f...$ this is the angular dependence of the orbital, shape of the orbital *letters have historical meaning, sharp, principle, diffuse, fundamental
m_l	magnetic	$+l \rightarrow -l$	orientation of angular momentum in space, orbital
m_s	spin	$+\frac{1}{2}, -\frac{1}{2}$	the imaginary property we call "spin", up or down

1-Electron Wavefunctions (Atomic orbitals)

One simplified representation of the three-dimensional wavefunction is shown below. This representation breaks the wavefunction into two parts: the **radial contribution** ($R_{n,l}(r)$) and the **angular contribution** ($Y_{l,m_l}(\theta,\phi)$).

$$\psi_{(n,l,m_l)} = R_{n,l}(r) \times Y_{l,m_l}(\theta,\phi) \tag{2.5.1}$$

Allowed Energies

From the wavefunction, we can find the allowed energies of an electron in an atom. We have not given you the more complex form of the wavefunction where you'd need to derive 2.5.2 from 2.5.1 because it is outside the scope of this course. Instead, consider the process that we used to derive the energy of a particle in a one-dimensional box in the previous section. A similar process can be used to find the energy of an electron in three dimensions, shown in 2.5.2.

$$E_n = -\frac{hcRZ^2}{n^2} = -(13.607\,eV)\left(\frac{Z}{n}\right)^2 \tag{2.5.2}$$

,

where n is the principle quantum number, h is Planck's constant, c is the speed of light, R is the Rydberg constant, and Z is the charge of the nucleus. It is useful to know that the value of $hcR = 13.6eV$. This is also the value of the ionization energy of an electron in a hydrogen atom. This equation only works for **hydrogenic atoms** (atoms or ions that are "like" hydrogen in that they have only one electron).

? Exercise 2.5.1

The energy that it takes to eject a ground-state electron from a hydrogen atom (its ionization energy, IE) is measured to be approximately 13.6 eV, while the IE energy of a He^+ ion is four times greater at 54.4 eV. These values can be predicted using both Equation 2.5.2 and the Rydberg equation.

a. Using Equation 2.5.2 for allowed energies of electrons in a hydrogen atom, derive the energy of the ground state electron in H. Then repeat this process for a He^+ ion. What do the values indicate about the relative attraction between an electron and the nuclei of these two hydrogenic atoms?
b. Show that the IE of H's 1s electron can also be predicted by the Rydberg formula (equation 2.1.2.2).

Answer (a)

Use Equation 2.5.2 . For a hydrogen atom with one proton, $Z = 1$, and the ground state energy level is the lowest energy level, $n = 1$. Therefore, the energy of an electron in the ground state of a H atom is:

$E_n = -\frac{hcRZ^2}{n^2} = -13.607\ eV(\frac{1}{1})^2 = -13.607\ eV$, or *approximately* $-13.6\ eV$. Thus, the IE (energy necessary to remove that electron) is +13.6 eV.

We can use the same process to find the ground state energy of an electron in He^+. This time, $Z = 2$ because helium has two protons in its nucleus, and as before, the ground state is $n = 1$.

$E_n = -\frac{hcRZ^2}{n^2} = -13.607\,eV(\frac{2}{1})^2 = -54.428eV$, or *approximately* $-54.4\,eV$. Thus, the IE is +54.4 eV.

These ground-state energies are the same as the energy required to remove the ground state electron from H and He^+. In other words, these are the predicted ground state IE values for one electron in H and He^+. The *measured* IEs for these two species are in fact 13.6 eV and 54.4 eV, respectively.

The He^+ ion has a more negative value for its ground state energy with a magnitude four times greater than that of the ground state H electron. This means that the He^+ electron is more strongly attracted to the (+2) nucleus than the H electron is attracted to the (+1) nucleus, and more energy is required to eject the He^+ electron than the H electron. It takes more energy to remove the electron from He^+ than from H. This makes sense in light of Coulomb's law: The attractive force between the H nucleus (+1) and an electron (-1) would be weaker than that of a He nucleus (+2) and an electron (-1) because the positive charge of the He nucleus has a greater magnitude.

Answer (b)

The Rydberg equation is: $\frac{1}{\lambda} = E(cm^{-1}) = R_H \left(\frac{1}{n_l^2} - \frac{1}{n_h^2}\right)$ where n_l and n_h are positive integers, $n_h > n_l$, and the *Rydberg constant* (R_H), has a value of 1.09737 × $10^7 m^{-1}$. We should set $n_l = 1$ to represent the initial ground state, and $n_h = \infty$ to represent the removal of the electron from the atom.

Step 1.

Calculate Energy (in m^{-1}) using the Rydberg equation:

$$E = R_H \left(\frac{1}{n_l^2} - \frac{1}{n_h^2}\right) = 1.09737 \times 10^7 m^{-1} \left(\frac{1}{1^2} - \frac{1}{\infty^2}\right) = 1.09737 \times 10^7 m^{-1} (1 - 0) = 1.09737 \times 10^7 m^{-1}$$

Ultimately, we want a value of energy in units of eV so we can compare it to the answers in part (a), but our value here is in units of inverse meters (m^{-1}). A quick internet search can tell you the conversion between inverse centimeters (cm^{-1}) and eV is $1eV = 8065.6 cm^{-1}$.

Step 2.

Convert from m^{-1} to cm^{-1} to eV so that we can compare to the answer in part (a):

$1.09737 \times 10^7 \frac{1}{m} \times \frac{1m}{100cm} \times \frac{1eV}{8065.6 \frac{1}{cm}} = 13.6056eV$, or approximately 13.6 eV.

Exercise 2.5.2

Which of the following are hydrogenic atoms? H, H^+, H^-, He, He^{2+}, He^+, He^-, Li, Li^{3+}, Li^{2+}, Li^+, Li^- .

Answer

Hydrogenic atoms are atoms or ions that contain only one electron. H, He^+, and Li^{2+} are hydrogenic atoms/ions that contain only one electron.

Radial and Angular contributions to the wavefunction:

Radial contribution, $R_{n,l}(r)$

The radial part of the wavefunction, $R_{n,l}(r)$ gives the radial variation of ψ. In other words, $R_{n,l}(r)$ defines how the wavefunction depends on the distance of the electron from the nucleus (the radius). The $R_{n,l}(r)$ parts of the wavefunction for a hydrogenic atom are listed in Table **2.5.2**, and they are plotted in Figure **2.5.1**. Notice that the $R_{n,l}(r)$ of all s-orbitals (solid lines) reaches a maximum at $r = 0$. This is unique to the s-orbitals' $R_{n,l}(r)$. The $R_{n,l}(r)$ of p- and d-orbitals orbitals approaches zero as r approaches zero. This has important consequences for how closely an electron in these orbitals can approach the nucleus.

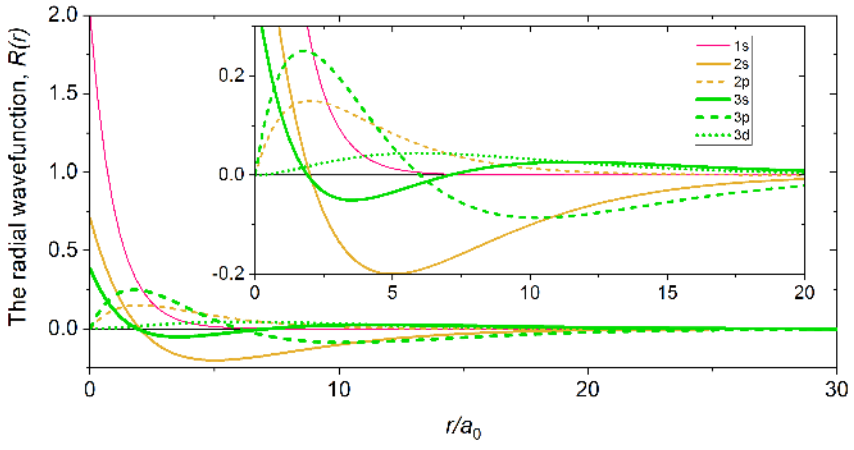


Figure **2.5.1**. Plots of the radial wavefunction, $R_{n,l}(r)$, for the first three shells. The wavefunctions are plotted relative to $\frac{r}{a_0}$, where $a_0 = 52.9pm = 0.529\text{Å}$ is the Bohr Radius (the radius of a hydrogen 1s orbital). The expressions for these radial wavefunctions ($R_{n,l}(r)$) are shown in Table **2.5.2**. (Kathryn Haas; CC-NC-BY-SA)

Table 2.5.2. Radial wavefunctions ($R(r)$) for the first three shells of a hydrogen atom. Z is the nuclear charge, and $a_0 = 52.9pm = 0.529\mathring{A}$ is the Bohr radius (the radius of a hydrogen 1s orbital). For the H atom, $Z = 1$ (the nuclear charge of hydrogen). Plotting of the functions can be simplified if we set $a_0 = 1$ and plot the functions with respect to r/a_0, which was done to find the plots shown in Figure 2.5.1.

Orbital	n	l	$R_{n,l}(r)$
1s	1	0	$2\left[\frac{Z}{a_0}\right]^{3/2} e^{-Zr/a_0}$
2s	2	0	$2\left[\frac{Z}{2a_0}\right]^{3/2}\left(2-\frac{Zr}{a_0}\right) e^{-Zr/2a_0}$
2p	2	1	$\frac{1}{\sqrt{3}}\left[\frac{Z}{3a_0}\right]^{3/2}\left(\frac{Zr}{a_0}\right) e^{-Zr/2a_0}$
3s	3	0	$\frac{2}{27}\left[\frac{Z}{3a_0}\right]^{3/2}\left(27-18\frac{Zr}{a_0}-2(\frac{Zr}{a_0})^2\right) e^{-Zr}$
3p	3	1	$\frac{1}{81\sqrt{3}}\left[\frac{2Z}{a_0}\right]^{3/2}\left(6-\frac{Zr}{a_0}\right)(\frac{Zr}{a_0})e^{-Zr/3a_0}$
3d	3	2	$\frac{1}{81\sqrt{15}}\left[\frac{2Z}{a_0}\right]^{3/2}\left(\frac{Zr}{a_0}\right)^2 e^{-Zr/3a_0}$

Radial probability function, $4\pi r^2(R_{n,l}(r))^2$

Just like in the particle-in-a-box model, the square of the wavefunction is proportional to the probability of finding a particle (electron) at some point in space. The square of the radial part of the wavefunction is called the radial distribution function $4\pi r^2(R_{n,l}(r))^2$, and it describes the probability of locating the electron at some distance r away from the nucleus. When we normalize the probability functions by dividing the function by its integral over all space, we get the plots shown in Figure 2.5.2. The normalized probability functions are compared to the original radial part of the wavefunctions in Figure 2.5.3. The most probable distance for finding an electron is shown by the maximum value of the function. For an electron in the 1s orbital of H, the most probable distance from the nucleus occurs at $r = 1a_0$. This is the Bohr Radius, and it has a value of $a_0 = 52.9pm = 0.529\mathring{A}$. It is convenient to plot the functions of the hydrogen atomic orbitals relative to the size of its smallest orbital, the 1s orbital; this is the reason we plot $R_{n,l}(r)$ and $4\pi r^2(R_{n,l}(r))^2$ relative to $\frac{r}{a_0}$.

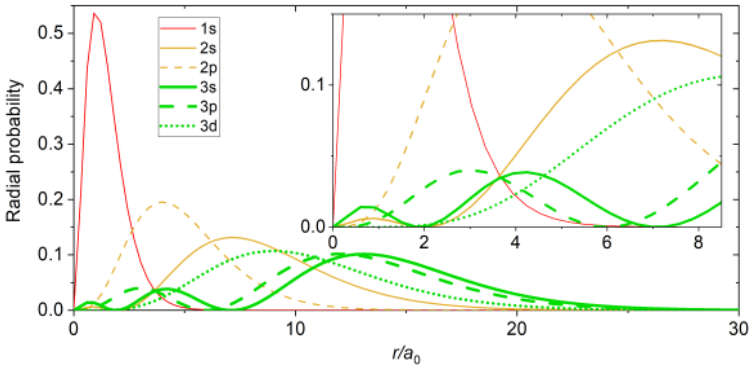


Figure 2.5.2: Plots of the normalized radial probability functions for the first three shells. The radial wavefunctions ($R_{n,l}(r)$) are shown in Table 2.5.2. (Kathryn Haas; CC-NC-BY-SA)

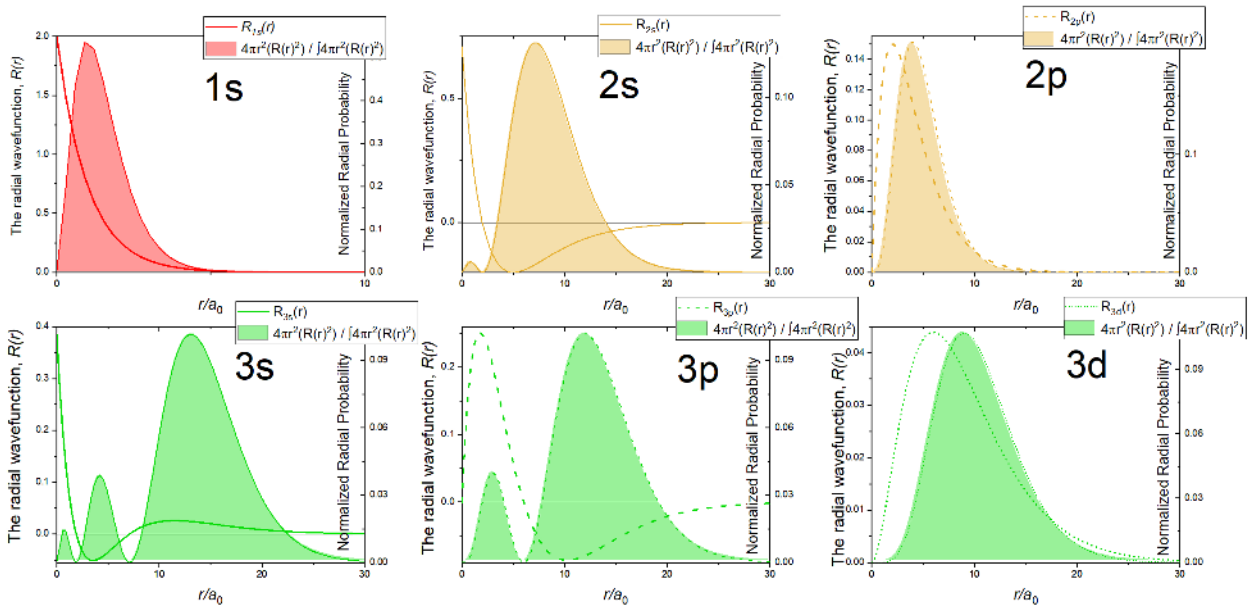


Figure **2.5.2**. Plots of the normalized radial probability function for each orbital in the first three shells (shaded curves). The radial wavefunctions are also shown (Table **2.5.2**). The y-axis on the left of each plot corresponds to the radial wavefunction (line); the y-axis on the right of each plot corresponds to the radial probability function (shaded). (Kathryn Haas; CC-NC-BY-SA)

Radial nodes

From the discussion of the 1-dimensional particle in a box, we learned that nodes exist where $\psi = 0$. In the case of the 3-dimensional wavefunction, there are two different types of nodes: radial nodes and angular nodes. **Radial nodes occur where the radial part of the wavefunction is zero ($R(x) = 0$)**. These are easy to find by plotting the radial part of the wavefunction and finding where the radial part of the wavefunction (and the radial probability function) is zero (where $R_{n,l}(r) = 0$) and where $4\pi r^2 (R_{n,l}(r))^2 = 0$. These nodes are spherical in shape and depend on the energy level and subshell (the values of n and l). **The number of radial nodes is $n - l - 1$**. An example of a radial node is the single node that occurs in the **2*s*** orbital ($2 - 0 - 1 = 1$ node). In contrast, the 1s orbital has zero radial nodes ($1 - 0 - 1 = 0$ nodes). Where there is a node, there is zero probability of finding an electron.

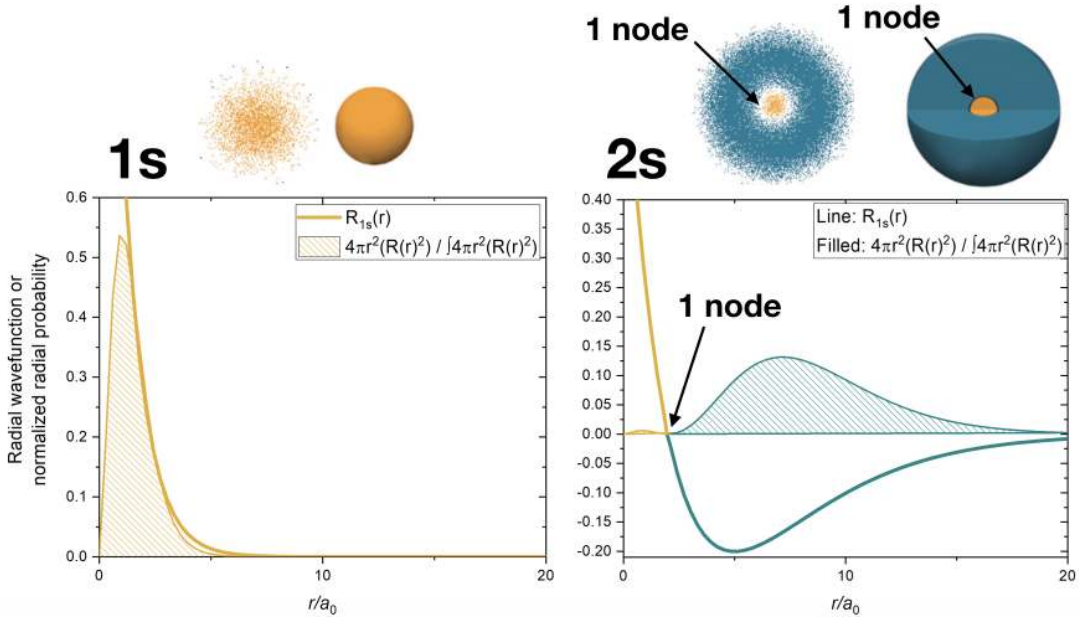


Figure **2.5.3**: Visualization of the 1s and 2s atomic orbitals. Each orbital is shown as both an electron probability density plot and a contour plot above its wavefunction and probability density function. The 1s orbital has zero radial nodes. The 2s orbital has one radial node where its wavefunction changes sign and its radial probability function is zero. (Kathryn Haas; CC-BY-SA)

Boundary surfaces

A true node occurs where the probability of finding an electron is zero. Nodes occur where $\psi = \psi^2 = 0$. Far from the nucleus, the probability of finding the electron rapidly approaches zero, but is never *exactly* zero. What this means is that it is rather improbable to find the electron at far distances from the nucleus, but it's not impossible. The rapid fall of probability creates a boundary surface rather than a node. The boundary surface represents the area around the nucleus where the electron exists most of the time.

? Exercise 2.5.1

How many radial nodes are in the s, p, d, and f orbitals in the first four shells? $n = 1, 2, 3, 4$?

Answer

You can approach this answer by using the mathematical relationship between the number of radial nodes and the values of n and l: **number of radial nodes is $n - 1 - l$**. You could also notice the pattern that the first orbital of any type (1s, 2p, 3d...) has zero radial nodes, the second orbital of a type (2s, 3p, 4d...) has one radial node, the third orbital of a type has two radial nodes (3s, 4p, 5d...)...etc.

A full list of all of the orbitals in the first four shells and their number of radial nodes is below. It's a good idea to prove to yourself that the numbers given below are consistent with the plots of the orbitals' wavefunctions for those orbitals in the first three shells:

s-orbitals:

1s: $n - 1 - l = 1 - 1 - 0 = 0$, zero radial nodes

2s: $n - 1 - l = 2 - 1 - 0 = 1$, one radial node

3s: $n - 1 - l = 3 - 1 - 0 = 2$, two radial nodes

4s: $n - 1 - l = 4 - 1 - 0 = 3$, three radial nodes

p-orbitals

2p: $n - 1 - l = 2 - 1 - 1 = 0$, zero radial nodes

3p: $n - 1 - l = 3 - 1 - 1 = 1$, one radial node

4p: $n - 1 - l = 4 - 1 - 1 = 2$, two radial nodes

d-orbitals

3d: $n-1-l=3-1-2=0$, zero radial nodes

4d: $n-1-l=4-1-2=1$, one radial nodes

f-orbital

4f: $n-1-l=4-1-3=0$, zero radial nodes

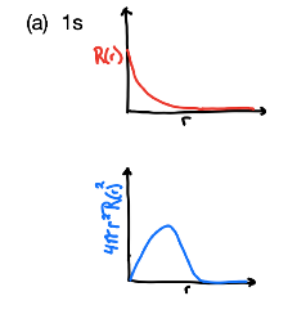
Exercise 2.5.1

Draw a rough plot of the following:

a. The radial wavefunction, $R_{n,l}(r)$ and the probability density function, $4\pi r^2(R_{n,l}(r))^2$, for the 1s orbital.
b. The radial wavefunction, $R_{n,l}(r)$ and the probability density function, $4\pi r^2(R_{n,l}(r))^2$, for the 4s orbital.

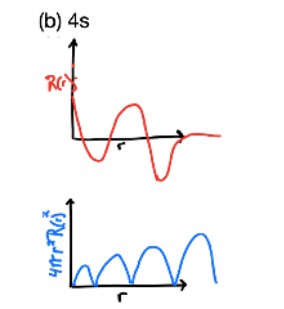
Answer, 1s

The 1s orbital's $R_{n,l}(r)$ reaches a maximum near the origin and approaches zero far from the nucleus. The $4\pi r^2(R_{n,l}(r))^2$ approaches zero at the origin, has a maximum intensity at the Bohr radius, and approaches zero far from the nucleus (its boundary surface).



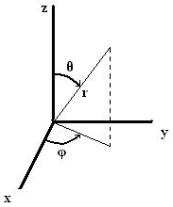
Answer, 4s

Like all s orbitals, the 4s orbital's $R_{n,l}(r)$ reaches a maximum near X=0, but it would be less intense than the function of the 1s, 2s, and 3s orbitals. It should have three radial nodes and so its wavefunction would change sign three times. This would give four regions of electron density in the probability function while the function would approach zero (boundary surface) far from the nucleus.



Angular contribution, $Y_{l,m_l}(\theta,\phi)$, and angular probability function, $(Y_{l,m_l}(\theta,\phi))^2$

The angular contribution to the wavefunction, $Y_{l,m_l}(\theta,\phi)$, describes the wavefunction's shape, or the angle with respect to a coordinate system. To describe the direction in space, we use spherical coordinates that tell us distance *and* orientation in 3-dimensional space. There are three spherical coordinates: r,ϕ, and θ. r is the radius, or the actual distance from the origin. ϕ and θ are angles. ϕ is measured from the positive x axis in the xy plane and may be between 0 and 2π. θ is measured from the positive z axis towards the xy plane and may be between 0 and π.

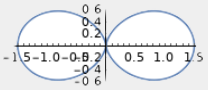
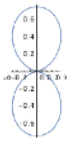
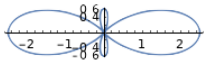
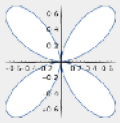
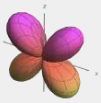
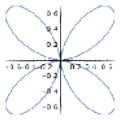
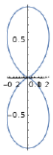
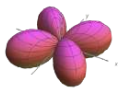


$$Y_{l,m_l}(\theta,\phi) = \left(\frac{1}{4\pi}\right)^{1/2} y(\theta,\phi)$$

$Y_{l,m_l}(\theta,\phi)$, is slightly more difficult to describe than the radial contribution was. This is partly because $Y_{l,m_l}(\theta,\phi)$ contains imaginary numbers, which have no real, physical meaning. However, the angular part of the wavefunction becomes more "real" when you square it to get angular probability density, a more tangible concept described as the **shapes of orbitals**.

The values of θ, ϕ, and $y(\theta,\phi)$ for orbitals in the hydrogen atom are listed in Table **2.5.3**. But $Y_{l,m_l}(\theta,\phi)$ is only a mathematical function and has no real physical meaning. The square of the radial wavefunction, $Y_{l,m_l}(\theta,\phi)^2$, gives the probability of finding the electron at a point in space on a ray described by (ϕ,θ). Thus $Y_{l,m_l}(\theta,\phi)^2$ describes the shape of the orbital.

Table **2.5.3**. Components of the angular wavefunction and the resulting orbital shapes. The plots in the two right hand columns were created using Desmos and Mathematica: specifically "Spherical Harmonics" from the Wolfram Demonstrations Project, http://demonstrations.wolfram.com/SphericalHarmonics/ and "Visualizing Atomic Orbitals" demonstrations.wolfram.com/Vi...tomicOrbitals/.

subshell	m_l (orbital)	θ	ϕ	Plots of θ^2	orbital shapes
$l = 0$, s	$m_l = 0$	$\frac{1}{\sqrt{2}}$	$\frac{1}{\sqrt{2\pi}}$		
$l = 1$, p	$m_l = 0$	$\frac{\sqrt{6}}{2}\cos\theta$	$\frac{1}{\sqrt{2\pi}}$		
$l = 1$, p	$m_l = +1$	$\frac{\sqrt{3}}{2}\sin\theta$	$\frac{1}{\sqrt{2\pi}}e^{i\phi}$		
$l = 1$, p	$m_l = -1$	$\frac{\sqrt{3}}{2}\sin\theta$	$\frac{1}{\sqrt{2\pi}}e^{-i\phi}$		
$l = 2$, d	0	$\frac{\sqrt{10}}{4}\left(3\cos^2\theta - 1\right)$	$\frac{1}{\sqrt{2\pi}}$		
$l = 2$, d	$m_l = +1$	$\frac{\sqrt{15}}{2}\sin\theta\cos\theta$	$\frac{1}{\sqrt{2\pi}}e^{i\phi}$		
$l = 2$, d	$m_l = -1$	$\frac{\sqrt{15}}{2}\sin\theta\cos\theta$	$\frac{1}{\sqrt{2\pi}}e^{-i\phi}$		
$l = 2$, d	$m_l = +2$	$\frac{\sqrt{15}}{4}\sin^2\theta$	$\frac{1}{\sqrt{2\pi}}e^{i2\phi}$		
$l = 2$, d	$m_l = -2$	$\frac{\sqrt{15}}{4}\sin^2\theta$	$\frac{1}{\sqrt{2\pi}}e^{-i2\phi}$		

Angular nodes

Angular nodes exist where $(Y_{l,m_l}(\theta,\phi))^2 = 0$. These nodes are planar in shape, and they depend on the value of l. The number of angular nodes in any orbital is equal to l. This means that s-orbitals ($l = 0$) have zero angular nodes, p-orbitals ($l = 1$) have one angular node, d-

orbitals ($l = 2$) have two angular nodes, and so on. Planar nodes can be flat planes (like the nodes in all p orbitals) or they can have a conical shape, like the two angular nodes in the d_{z^2} orbital. Angular nodes in some p and d orbitals are shown in Figure **2.5.4**.

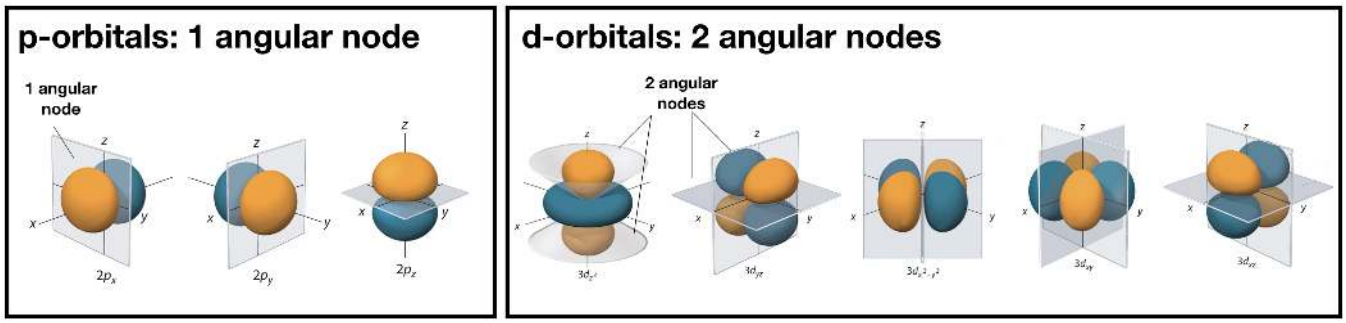
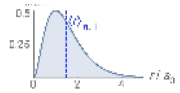
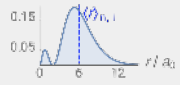
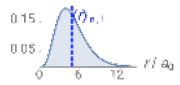
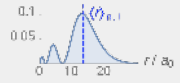
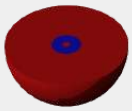
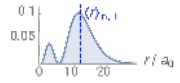
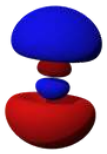
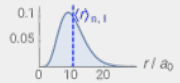
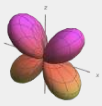


Figure **2.5.4**: The angular nodes in p-orbitals and d-orbitals are shown. Every p orbital has one angular node, and every d orbital has two angular nodes. The number of angular nodes in any orbital is equal to the value of the quantum number, l. (CC BY-NC-SA; anonymous by request)

Atomic Orbitals

Atomic orbitals result from a combination of both the radial and angular contributions of the wavefunction. Atomic orbitals can have both angular nodes and radial nodes, depending on the values of n and l.

The chart below compares the radial variation, angular variation, and their combinations (orbitals).

Orbital	Radial Probability	Radial Nodes	Angular Probability	Angular Nodes	Combination (Orbital)	Total Nodes
1s		0		0		0
2s		1		0		1
2p		0		1		1
3s		2		0		2
3p		1		1		2
3d		0		2		2

This page titled 2.5: Quantum Numbers and Atomic Wave Functions is shared under a CC BY-NC-SA 4.0 license and was authored, remixed, and/or curated by Kathryn Haas.

- **2.2.2: Quantum Numbers and Atomic Wave Functions** by Kathryn Haas is licensed CC BY-NC-SA 4.0.

2.6: Aufbau Principle

Introduction

The **Aufbau Principle** (also called the **building-up principle** or the **Aufbau rule**) states that, in the ground state of an atom or ion, electrons fill atomic orbitals of the lowest available energy level before occupying higher-energy levels. In general, an electron will occupy an atomic orbital with the lowest value of n, l, m_l, in that order of priority. The value of m_s for an unpaired electron is conventionally assigned a value of $+\frac{1}{2}$. Each electron in an atom/ion must have a unique set of values for all four quantum numbers.

The Ground State of Hydrogenic Atoms/Ions

In a hydrogenic atom/ion, there is only one electron. In this case, the *only factor determining energy is the value of* n. The ground state will always be the 1s orbital ($n = 1, l = 0, m_l = 0, m_s = +\frac{1}{2}$).

The Ground State of Multi-electron Atoms/Ions

In atoms/ions with two or more electrons, the ground state electron configuration (1) minimizes the total energy of the electrons, (2) obeys the Pauli exclusion principle, (3) obeys Hunds rule of maximum multiplicity, and (4) considers the exchange interaction. These "rules" are described below.

(1) Electrons will occupy the lowest energy orbitals in order to minimize the total energy. The two quantum numbers that are related to energy in multi-electron atoms are n, and l. Thus, orbitals with the lowest values of n and l will fill first.

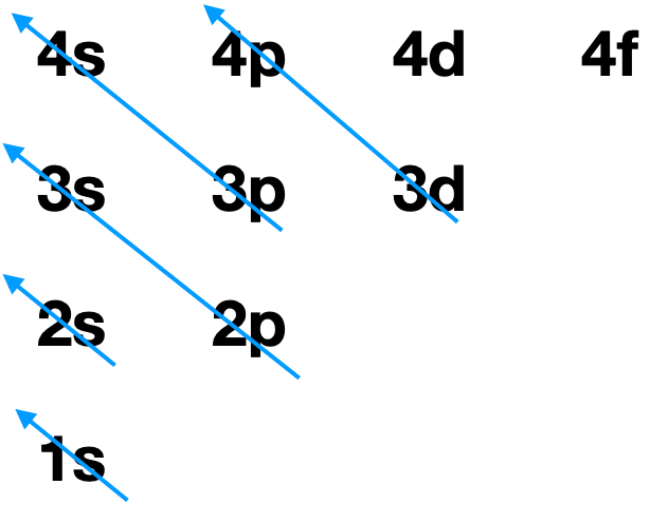


Figure **2.6.1**. The order of filling of ground state electron orbitals is 1s, 2s, 2p, 3s, 3p, 4s, 3d, 4p, etc... (CC-BY-NC-SA; Kathryn Haas)

(2) Hund's rule of maximum multiplicity states that for a given electron configuration, the lowest energy arrangement of electrons in degenerate orbitals is the one with the greatest "multiplicity," where multiplicity is the number of unpaired electrons (n) plus 1 (multiplicity = n + 1). This rule is used to predict the ground state of an atom or molecule with one or more open electronic shells.

Hund's rule is based on empirical observation of atomic spectra, and it is a consequence of the energy required to pair two electrons in the same orbital. This energy of repulsion between two electrons in the same orbitals is a Coulombic energy of repulsion, Π_c, caused by two electrons with like charge sharing the same area of space (an orbital). When more than one electron occupies a set of degenerate orbitals, the most favorable arrangement is one where the number of paired electrons is minimized.

A simplified definition of Hund's rule is that **the lowest energy arrangement is the one with the greatest number of unpaired electrons**. This implies that if two or more orbitals of equal energy are available, electrons will occupy them singly before filling them in pairs. Examples of ground

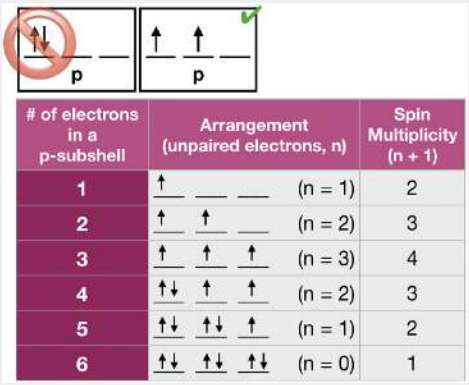


Figure 2.6.2. Hund's rule is that spin multiplicity must be maximized in the ground state.

(Kathryn Haas; CC-NC-BY-SA)

state arrangements of electrons in three degenerate p-orbitals is given in the figure shown here.

(3) The Pauli exclusion principle states that it is impossible for two electrons of a multi-electron atom to have the same set of values for all four quantum numbers. Two electrons in different orbitals will have a different set of n, l, and m_l values. When two electrons reside in the same orbital, they posses the same n, l, and m_l values, therefore their m_s must be different. Thus, two electrons in the same orbital must have opposite half-integer spin projections of $+\frac{1}{2}$ and $-\frac{1}{2}$.

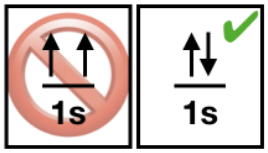


Figure 2.6.3. Pauli's principle tells us that paired electrons must have opposite spin. (Kathryn Haas; CC-NC-BY-SA)

(4) The exchange interaction is sometimes called the *exchange energy* or *exchange force*. However, it is not a true energy or force. Rather, it is a quantum mechanical effect that takes place between identical particles. The exchange interaction results in a ground state electron configuration with unpaired electrons all being of the same spin. Unpaired electrons are conventionally written in the "spin up" direction.

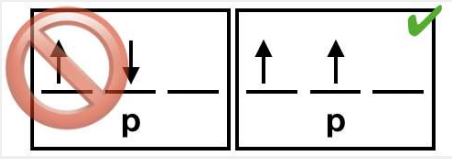


Figure 2.6.4. Unpaired electrons should have identical spins due to the exchange interaction. (Kathryn Haas; CC-NC-BY-SA)

Trends in Expected Electron Configuration

The four "rules" above can be used as guidelines to predict the ground state electron configuration of atoms, the filling of subshells, and the configuration of electrons in degenerate orbitals. However, the utility of these guidelines for predicting actual electron configurations requires more nuanced knowledge of the relative energy levels of orbitals.

Generally, orbital energy levels directly correspond to their shell number. Additionally, orbitals within a shell generally follow the energetic trend where s<p<d<f. Although these general trends for relative orbital energy levels hold true for most of the main block elements (the s - and p-blocks), there are important exceptions in the orbital energy levels of transition metal atoms and ions of the d- and f-blocks.

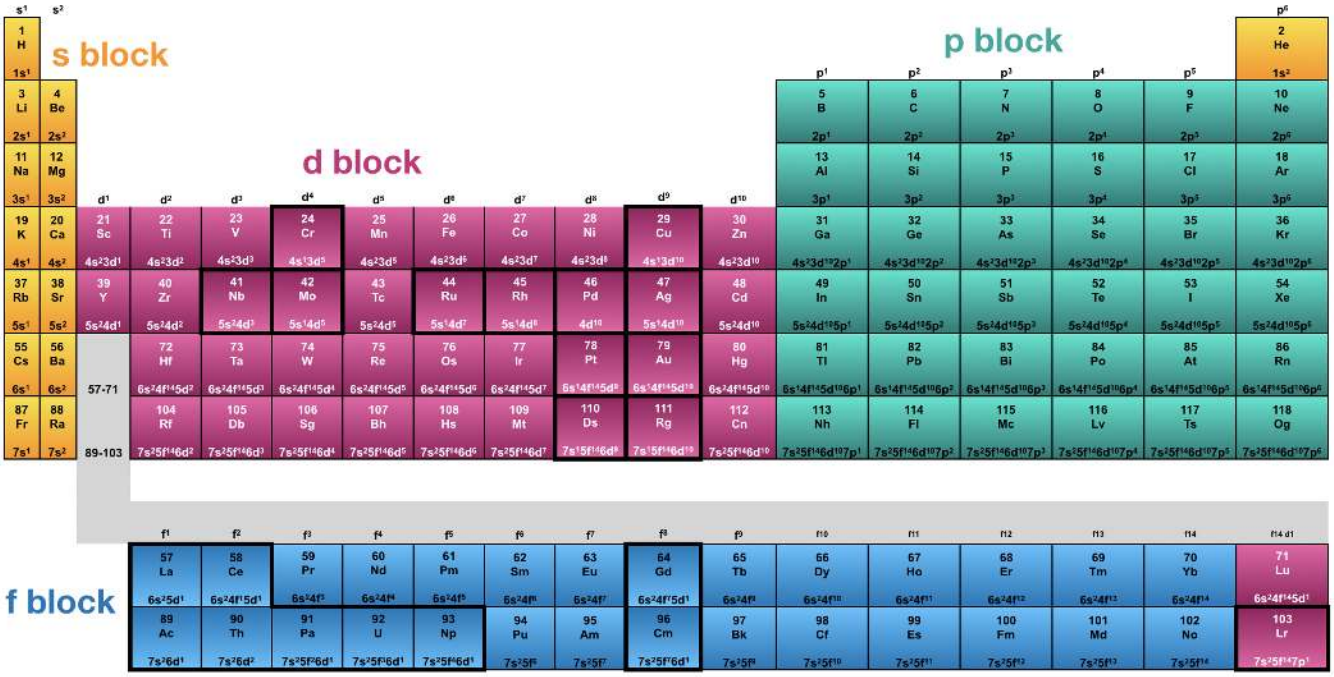


Figure **2.6.5**. This is a depiction of the periodic table that highlights the s-, p-, d-, and f- blocks in different colors. Violations of the expected trend in electron configurations are outlined in a heavy black line. Several elements of the d block and f block violate the general trends in electron configuration because their orbital energy levels do not follow *general* trends. (CC-BY-NC-SA; Kathryn Haas)

Elements that violate general trends in electron configuration are outlined with a dark line in Figure **2.6.5**. All of the exceptions are within the d- and f- blocks, and the violations are caused by an unexpected order of the orbital energy levels.

In the next section you will learn why the orbital energy levels correlate with shell number and why subshells within a shell usually follow the trend that s<p<d<f. You will also learn why there are occasional exceptions to this trend and how these exceptions influence elemental properties.

References

1. Miessler, Gary L., and Donald A. Tarr. *Inorganic Chemistry*. Upper Saddle River, NJ: Pearson Prentice Hall, 2010. Print.
2. Brown, Ian David. *The Chemical Bond in Inorganic Chemistry the Bond Valence Model*. Oxford: Oxford UP, 2006. Print.

This page titled 2.6: Aufbau Principle is shared under a CC BY-NC-SA 4.0 license and was authored, remixed, and/or curated by Kathryn Haas.

- **2.2.3: Aufbau Principle** by Kathryn Haas is licensed CC BY-NC-SA 4.0.

2.7: Shielding

Introduction

Coulomb's Law is from classical physics; it tells us that particles with opposite electrostatic charge are attracted to each other, and the larger the charge on either particle or the closer the distance between them, the stronger the attraction. Coulomb's law explains why atomic size decreases as the charge on the nucleus increases, but it can't explain the nuances and variations in size as we go across the periodic table. Coulomb's Law also explains why electrons in different shells (*n*), at different distances from the nucleus, have different energies. But on its own, Coulomb's law doesn't quite explain why electron subshells within a shell (like 2s vs. 2p) would have different energies. To explain these things, we need to consider how both electron **shielding** and **penetration** result in variations in effective nuclear charge (Z*) that depend on shell and subshell.

Effective Nuclear Charge (Z*)

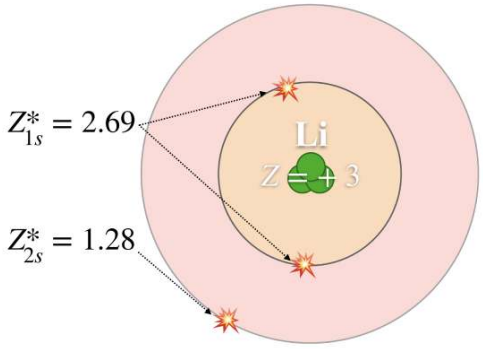


Figure 2.7.1. In a lithium atom, the nuclear charge (Z) is +3. 1s electrons experience an effective nuclear charge (Z*) of +2.69, and 2s electrons experience an Z* of +1.28. (CC-BY-NC-SA; Kathryn Haas)

Coulombs' law works well for predicting the energy of an electron in a hydrogen atom (because H has only one electron). It also works for hydrogen-like atoms: any nucleus with exactly one electron (a He^+ ion, for example, has one electron). However, Coulomb's law is insufficient for predicting the energies of electrons in multi-electron atoms and ions.

Electrons within a multi-electron atom interact with the nucleus and with all other electrons. Each electron in a multi-electron atom experiences both attraction to the nucleus and repulsion from interactions with other electrons. The presence of multiple electrons decreases the nuclear attraction to some extent. Each electron in a multi-electron atom experiences a different magnitude of (and attraction to) the nuclear charge depending on what specific shell and subshell the electron occupies. The amount of positive nuclear charge experienced by any individual electron is the **effective nuclear charge (Z*)**.

For example, in lithium (Li), none of the three electrons "feel" the full +3 charge from the nucleus (see Figure 2.7.1). Rather, each electron "feels" a Z* that is less than the actual Z and that depends on the electron's orbital. The actual nuclear charge in Li is $Z = +3$; the 1s electrons experience a $Z^* = +2.69$, and the 2s electron experiences a $Z^* = +1.28$. In general, core electrons (or the electrons closest to the nucleus), "feel" a Z* that is close to, but less than, Z. On the other hand, outer valence electrons experience a Z* that is much less than Z.

In summary:

- Core electrons: $Z^* \lessapprox Z$
- Valence electrons: $Z^* \ll Z$

Shielding:

Shielding is the reduction of true nuclear charge (Z) to the effective nuclear charge (Z*) by other electrons in a multi-electron atom or ion. Shielding occurs in all atoms and ions that have more than one electron. H is the only atom in which shielding does not occur.

Explanation of shielding: Electrons in a multi-electron atom interact with the nucleus and all other electrons in the atom. To describe shielding, we can use a simplified model of the atom: we will choose an electron-of-interest in a multi-electron atom and treat all the "other" electrons as a group of spherically-distributed negative charge. Classical electrostatics allows us to treat spherical distribution of charge as a point of charge at the center of the distribution. Thus, we consider all the "other" electrons in our atom as a point of negative charge in the center of the atom. While the positive charge of the nucleus provides an attractive force toward our electron, the negative charge distribution at the center of the atom would provide a repulsive force. The attractive and repulsive forces would partially cancel each other; but since there are less "other" electrons than there are protons in our atom, the nuclear charge is never completely canceled. The "other" electrons partially block, or shield, part of the nuclear charge so that our electron-of-interest experiences a partially-reduced nuclear charge, the Z*.

In reality, there is not a one-for-one "canceling" of the nuclear charge by each electron. Partly due to *penetration*, no single electron can completely shield a full unit of positive charge. Core electrons shield valence electrons, but valence electrons have little effect on the Z* of core electrons. The ability to shield, and be shielded by, other electrons strongly depends the electron orbital's average distance from the nucleus and its *penetration*; thus shielding depends on both shell (n) and subshell (l).

Shielding depends on electron penetration

Coulomb's law shows us that distance of an electron from its nucleus is important in determining the electron's energy (its attraction to the nucleus). The shell number (n) determines approximately how far an electron is from the nucleus *on average*. Thus, all orbitals in the same shell (s,p,d) have similar sizes and similar average distance of their electrons from the nucleus. But there is another distance-related factor that plays a critical role in determining orbital energy levels: *penetration*. **Penetration** describes the ability of an electron in a given subshell to penetrate into other shells and subshells to get close to the nucleus. Penetration is the **extent to which an electron can approach the nucleus**. Penetration depends on both the shell (n) and subshell (l).

The penetration of individual orbitals can be visualized using the radial probability functions. For example, Figure **2.7.2** below shows plots of the radial probability function of the 1s, 2s, and 2p orbitals. From these plots, we can see that the 1s orbital is able to approach the closest to the nucleus; thus it is the most penetrating. While the 2s and 2p have most of their probability at a farther distance from the nucleus (compared to 1s), the 2s orbital and the 2p orbital have different extents of penetration. Notice that the 2s orbital is able to penetrate the 1s orbital because of the central 2s lobe. The 2p orbital penetrates somewhat into the 1s, but it cannot approach the nucleus as closely as the 2s orbital can. While the 2s orbital penetrates more than 2p (the 2s orbital can approach closer to the nucleus), the 2p is slightly *closer on average* than 2s. The order of Z* in 2s and 2p subshells depends on which factor (average distance or penetration) is more important. In the first two rows of the periodic table, penetration is the dominant factor that results in 2s having a lower energy than 2p (see Figure **2.7.4** for values).

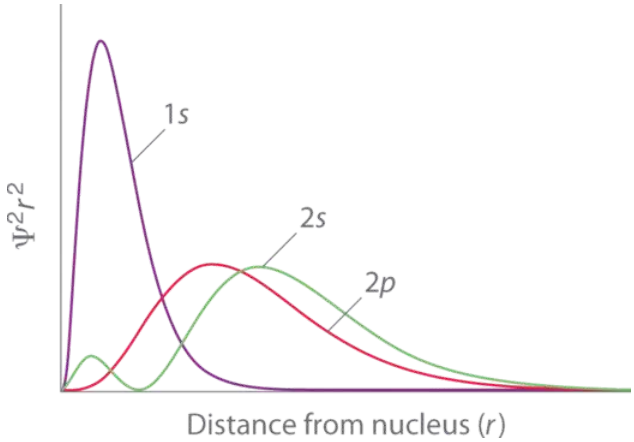


Figure **2.7.2**. Orbital Penetration. A comparison of the radial probability distribution of the 2s and 2p orbitals for various states of the hydrogen atom shows that the 2s orbital penetrates inside the 1s orbital more than the 2p orbital does. Consequently, when an electron is in the small inner lobe of the 2s orbital, it experiences a relatively large value of Z*, which causes the energy of the 2s orbital to be lower than the energy of the 2p orbital.

An electron orbital's penetration affects its ability to shield other electrons and affects the extent to which it is shielded by other electrons. In general, electron orbitals that have greater penetration experience stronger attraction to the nucleus and less shielding by other electrons; these electrons thus experience a larger Z*. Electrons in orbitals that have greater penetration also shield other electrons to a greater extent.

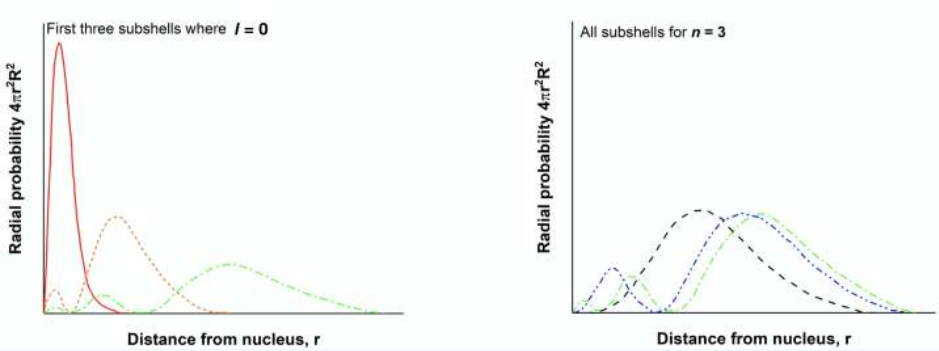
Within the same shell value (n), the penetrating power of an electron follows this trend in subshells (m_l):

s>p>d>f

Exercises

Exercises

1. Compare the 2s and 2p orbitals:
   (a) Which is closer to the nucleus on average?
   (b) Which is more penetrating?
   (c) Which orbital experiences a stronger Z* and is thus lower in energy (consider your experience, but also inspect Figures 1.1.2.3 and 1.1.2.4 from the previous page)? Please explain.
2. Peruse the Hyperphysics page (click) that shows radial probability functions of several orbitals (click around on various orbitals). Compare the 2p and 3s orbitals:
   (a) Which is farther from the nucleus on average?
   (b) Which is more penetrating?
   (c) Which orbital is lower in energy?
3. Which atom, Li, or N, has a stronger valence Z*? Explain why.
4. Explain why 2s and 2p subshells are completely degenerate in a hydrogen atom.
5. Which atom has a smaller radius: Be or F? Explain.
6. Which electrons shield others more effectively: 3p or 3d?
7. Use the clues given in the figures below to label the radial distribution functions shown.



8. Examine the plots on the right in the previous question, above. Note that this is a plot showing the probability density for the 3s, 3p, and 3d subshells.
(a) For which of these three functions is the highest probability density at the smallest r value (which is closest to the nucleus on average)? Is this the same subshell that penetrates most?
(b) Use this example to describe how penetration and shielding result in a splitting of subshell energy level in multi-electron atoms.

9. Explain why the ground state (most energetically favorable) electron configuration of Be is $1s^2 2s^2$ rather than alternative configurations like $1s^2 2s^1 2p^1$ or $1s^2 2p^2$.

Answer 1

(a) The 2s orbital is closer to the nucleus on average.

(b) The 2s orbital is more penetrating than 2p.

(c) You might "know" that the 2s orbital is lower in energy than 2p because 2s fills first. But a close inspection of Figures 1.1.2.3 and 1.1.2.4 from the previous page indicates that while the 2s and 2p elements are degenerate in Ne (element 10), for elements with atomic number 11 and greater 2p has a higher Z* than 2s! This example illustrates that both average distance and penetration are factors in determining Z*, and the factor that is more important may change as we increase in atomic number.

Answer 2

(a) The 3s orbital reaches farther away from the nucleus and is on average farther from the nucleus than 2p.

(b) The 3s orbital is more penetrating than 2p, even though 3s is farther on average!

(c) The 2p orbital is lower in energy than 3s; this is because 2p is still significantly closer to the nucleus on average and experiences a stronger Z*. (Penetration is not the only consideration!)

Answer 3

A nitrogen atom has a stronger effective nuclear charge (Z*) than lithium due to its greater number of protons; even though N also has more electrons that would shield the nuclear charge, each electron only partially shields each proton. This means that atoms with greater atomic number always have greater Z* for any given electron.

Answer 4

The hydrogen atom has only one electron; thus there is no shielding to consider. When there are not other electrons to shield the nucleus, penetration and shielding are irrelevant, and subshells within a shell are degenerate.

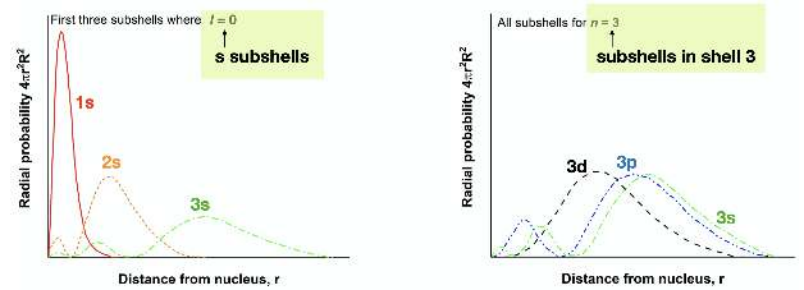
Answer 5

Fluorine has a smaller radius than beryllium because F has a greater valence Z* and therefore pulls the valence electrons closer to the nucleus and provides a smaller atomic radius.

Answer 6

3p shields better than 3d because p orbitals penetrate more than d orbitals within the same shell.

Answer 7



Answer 8

3d is closest on average, but 3s penetrates most. The three subshells of $n = 3$ differ in their average distance and in their ability to penetrate; these factors result in differences in the Z* experienced by electrons in each orbital. We would expect 3s to be lowest in energy followed by 3p and then 3d.

Answer 9

This question is asking why the 2s orbital fills in Be before 2p is occupied. This is a multi-electron atom, therefore core electrons shield the 2s and 2p orbitals to different extents. In Be we expect the 2s orbital to fill before 2p because 2s penetrates more and experiences a higher Z*.

Slater's rules for estimating Z*

The Z* can be estimated using a number of different methods; probably the best known and most commonly used method is known as **Slater's Rules**. Slater developed a set of rules to estimate Z* based on how many other electrons exist in the atom and on the

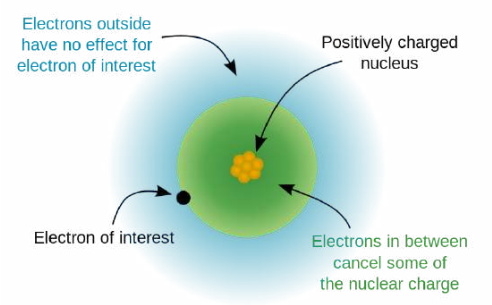


Figure **2.7.3**. Diagram illustrating effective nuclear charge according to Slater's rules.

orbital location of the electron-of-interest. These two factors are important determinants in shielding, and they are used to calculate a **shielding constant (S)** used in Slater's formula:

$$Z* = Z - S$$

where Z is the actual nuclear charge (the atomic number) and Z* is the effective nuclear charge.

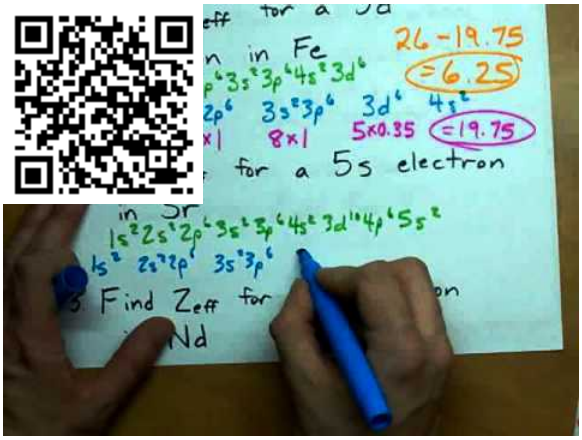
In the calculation of S, it is assumed that electrons closer to the nucleus than our electron-of-interest cancel some of the nuclear charge; those farther from the nucleus have no effect. To calculate S, all the relevant orbitals in an atom are written out in order of increasing energy, separating them into in "groups". Each change in shell number is a new group; s and p subshells are in the same group but d and f orbitals are their own group. You write out all the orbitals using parentheses until you get to the group of the electron-of-interest, like this:

(1s)(2s,2p)(3s,3p)(3d)(4s,4p)(4d)(4f)(5s,5p) etc.

**Critical: The orbitals must be written in order of increasing energy!

1. **Electrons in the same Group():** Each other electron (not counting the electron-of-interest) in the same group () as the chosen electron, contributes 0.35 to S.
   Conceptually, this means electrons in the same group shield each other 35%.
2. **Electrons in Groups() to the left:**
   - If the electron-of-interest is in a d or f subshell, every electron in groups () to the left contributes 1.00 to S.
     Conceptually, this means that d and f electrons are shielded 100% by all electrons in the same shell with a smaller value of l*, as well as all electrons in lower shells (*n*).*
   - If the electron-of-interest is in an s or p subshell, all electrons in the next lower shell (n - 1) contribute 0.85 to S. And all the electrons in even lower shells contribute 1.00 to S.
     Conceptually, this means that s and p electrons are shielded 85% by the electrons one shell lower, and 100% by all electrons in shells n - 2 or lower.
3. ***1s electrons:*** *S of a 1s electron is just S=0.3, no matter the element.*

A video explaining how to use Slater's Rules



Example 2.7.1: Fluorine, Neon, and Sodium

What is the Z* experienced by the valence electrons in the three isoelectronic species: fluorine anion (F^-), neutral neon atom (Ne), and sodium cation (Na^+)?

Solution

Each species has 10 electrons, and the number of core electrons is 2 (10 total electrons - 8 valence), but the effective nuclear charge varies because each has a different atomic number (Z). The approximate Z* can be found with Slater's Rules. For all of these species, we would calculate the same sigma value:

Calculating S: (1s)(2s,2p), $S = 2(0.85) + 7(0.35) = 1.7 + 2.45 = 4.15$

Fluorine anion: $Z* = 9 - S = 9 - 4.15 = 4.85$

Neon atom: $Z* = 10 - S = 10 - 4.15 = 5.85$

Sodium Cation: $Z* = 11 - S = 11 - 4.15 = 6.85$

So, the sodium cation has the greatest effective nuclear charge.

? Exercise 2.7.1

Calculate Z* for a 3d-electron in a zinc (Zn) atom.

Answer

Write out the relevant orbitals: (1s)(2s,2p)(3s,3p)(3d) ~~(4s)~~

Notice that although 4s is fully occupied, we don't include it because in Zn, 4s is higher in energy than 3d. Therefore, 4s is to the right of the d electrons we are considering. The electron-of-interest is in 3d, so the other nine electrons in 3d each contribute 0.35 to the value of S. The other 18 electrons each contribute 1 to the value of S.

$$S = 18(1) + 9(0.35) = 21.15$$

$$Z* = 30 - 21.15 = 8.85$$

So, although the nuclear charge of Zn is 30, the 3d electrons only experience a $Z* \approx 8.85$!

"Best" values for Z*

Slater's rules are a set of simple rules for predicting S and Z* based on empirical evidence from quantum mechanical calculations. In other words, the Z* calculated from Slater's rules are approximate values. The values considered to be the most accurate are derived from quantum mechanical calculations directly. You can find these values in a nice chart on the Wikipedia article of Effective Nuclear Charge. The chart is recreated here in Figure 2.7.3 for convenience:

Z or Z_{eff}	H																	He
Z	1.00																	2.00
1s	1.00																	1.69
	Li	Be											B	C	N	O	F	Ne
Z	3.00	4.00											5.00	6.00	7.00	8.00	9.00	10.00
1s	2.69	3.69											4.68	5.67	6.67	7.66	8.65	9.64
2s	1.28	1.91											2.58	3.22	3.85	4.49	5.13	5.76
2p													2.42	3.14	3.83	4.45	5.10	5.76
	Na	Mg											Al	Si	P	S	Cl	Ar
Z	11.00	12.00											13.00	14.00	15.00	16.00	17.00	18.00
1s	10.63	11.61											12.59	13.58	14.56	15.54	16.52	17.51
2s	6.57	7.39											8.21	9.02	9.83	10.63	11.43	12.23
2p	6.80	7.83											8.96	9.95	10.96	11.98	12.99	14.01
3s	2.51	3.31											4.12	4.90	5.64	6.37	7.07	7.76
3p													4.07	4.29	4.89	5.48	6.12	6.76
	K	Ca	Sc	Ti	V	Cr	Mn	Fe	Co	Ni	Cu	Zn	Ga	Ge	As	Se	Br	Kr
Z	19.00	20.00	21.00	22.00	23.00	24.00	25.00	26.00	27.00	28.00	29.00	30.00	31.00	32.00	33.00	34.00	35.00	36.00
1s	18.49	19.47	20.46	21.44	22.43	23.41	24.40	25.38	26.37	27.35	28.34	29.33	30.31	31.29	32.28	33.26	34.25	35.23
2s	13.01	13.78	14.57	15.38	16.18	16.98	17.79	18.60	19.41	20.21	21.02	21.83	22.60	23.37	24.13	24.89	25.64	26.40
2p	15.03	16.04	17.06	18.07	19.07	20.08	21.08	22.09	23.09	24.10	25.10	26.10	27.09	28.08	29.07	30.07	31.06	32.05
3s	8.68	9.60	10.34	11.03	11.71	12.37	13.02	13.68	14.32	14.96	15.59	16.22	17.00	17.79	18.60	19.40	20.22	21.03
3p	7.73	8.66	9.41	10.10	10.79	11.47	12.11	12.78	13.44	14.09	14.73	15.37	16.20	17.01	17.85	18.71	19.57	20.43
4s	3.50	4.40	4.63	4.82	4.98	5.13	5.28	5.43	5.58	5.71	5.84	5.97	7.07	8.04	8.94	9.76	10.55	11.32
3d			7.12	8.14	8.98	9.76	10.53	11.18	11.86	12.53	13.20	13.88	15.09	16.25	17.38	18.48	19.56	20.63
4p													6.22	6.78	7.45	8.29	9.03	9.34
	Rb	Sr	Y	Zr	Nb	Mo	Tc	Ru	Rh	Pd	Ag	Cd	In	Sn	Sb	Te	I	Xe
Z	37.00	38.00	39.00	40.00	41.00	42.00	43.00	44.00	45.00	46.00	47.00	48.00	49.00	50.00	51.00	52.00	53.00	54.00
1s	36.21	37.19	38.18	39.16	40.14	41.13	42.11	43.09	44.08	45.06	46.04	47.03	48.01	48.99	49.97	50.96	51.94	52.92
2s	27.16	27.90	28.62	29.37	30.13	30.88	31.63	32.38	33.16	33.88	34.63	35.39	36.12	36.86	37.60	38.33	39.07	39.80
2p	33.04	34.03	35.00	35.99	36.98	37.97	38.94	39.95	40.94	41.93	42.92	43.91	44.90	45.89	46.87	47.86	48.85	49.84
3s	21.84	22.66	23.55	24.36	25.17	25.98	26.79	27.60	28.44	29.22	30.03	30.84	31.63	32.42	33.21	34.00	34.79	35.58
3p	21.30	22.17	23.09	23.85	24.62	25.47	26.38	27.22	28.15	29.02	29.81	30.69	31.52	32.35	33.18	34.01	34.84	35.67
4s	12.39	13.44	14.26	14.90	15.28	16.10	17.20	17.66	18.58	18.99	19.87	20.87	21.76	22.66	23.54	24.41	25.30	26.17
3d	21.68	22.73	25.40	25.57	26.25	27.23	28.35	29.36	30.41	31.45	32.54	33.61	34.68	35.74	36.80	37.84	38.90	39.95
4p	10.88	11.93	12.75	13.46	14.08	14.98	15.81	16.44	17.14	17.72	18.56	19.41	20.37	21.27	22.18	23.12	24.03	24.96
5s	4.99	6.07	6.26	6.45	5.92	6.11	7.23	6.49	6.64	(empty)	6.76	8.19	9.51	10.63	11.62	12.54	13.40	14.22
4d			15.96	13.07	11.24	11.39	12.88	12.81	13.44	13.62	14.76	15.88	16.94	17.97	18.97	19.96	20.93	21.89
5p													8.47	9.10	10.00	10.81	11.61	12.43

Figure 2.7.4. This chart shows Z* values calculated by Clementi et al. in 1963 and 1967 that are consistent with SCF Calculations. This chart was created using data from the Wikipedia article on Effective Nuclear Charge. (Kathryn Haas; CC-NC-BY-SA)

Z* modulates attraction

When valence electrons experience less nuclear charge than core electrons, different electrons experience different magnitudes of attraction to the nucleus. A modified form of Coulomb's Law is written below, where e is the charge of an electron, Z* is the effective nuclear charge experienced by that electron, and r is the radius (distance of the electron from the nucleus).

$$F_{eff} = k\frac{Z* e^2}{r^2}$$

This formula suggests that if we can estimate Z*, then we can predict the attractive force experienced by, and the energy of, an electron in a multi-electron atom (ex. Li).

The attraction of the nucleus to valence electrons determines the atomic or ionic size, ionization energy, electron affinity, and electronegativity. The stronger the attraction, and the stronger Z*, the closer the electrons are pulled toward the nucleus. This in turn results in a smaller size, higher ionization energy, higher electron affinity, and stronger electronegativity.

General Periodic Trends in Z*

Close inspection of Figure **2.7.3** and analysis of Slater's rules indicate that there are some predictable trends in Z*. The data from Figure **2.7.3** is plotted below in Figure **2.7.4** to provide a visual aid to the discussion below.

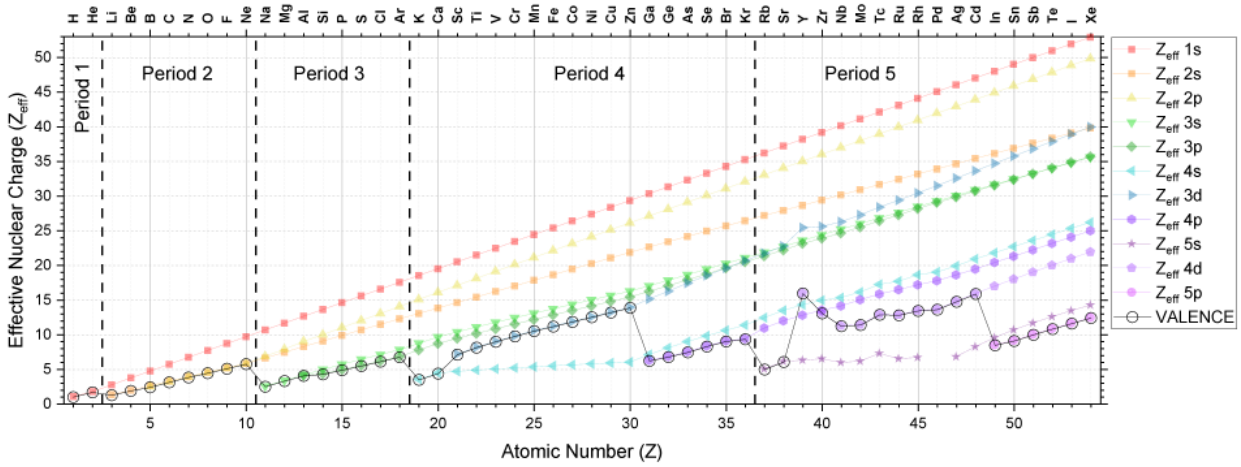


Figure **2.7.5**: The Z* values for electrons in each subshell of the first 54 elements (H to Xe). Each subshell is plotted as a different series (see legend) and the valence shell is highlighted by a solid black line with open circles. (Kathryn Haas; CC-NC-BY-SA)

Trends in Z* for electrons in a specific shell and subshell

The Z* for electrons in a given shell and subshell generally increases as atomic number increases; this trend holds true going across the periodic table and down the periodic table. Convince yourself that this is true for any subshell by examining Figure **2.7.4**. (CC-BY-NC-SA; Kathryn Haas)

Do you notice any exceptions to this general trend?

Inspection of Figure **2.7.4** should confirm for you that the Z* increases as Z increases for electrons in any subshell (like the 1s subshell for example, which is plotted above as a red line with square points). You can see this trend as the positive slope in each series. There is one obvious exception in Period 5 in elements 39 (Y) to 41 (Nb; the Z* of 4s actually decreases across these three elements as atomic number increases. There is also an exception between Y and Zr in the 3d subshell, and between Tc and Ru in the 5s subshell.

For valence electrons:

It is useful to understand trends in valence Z* because the valence Z* determines atomic/ionic properties and chemical reactivity. The trends in the valence Z* are not simple because as atomic number increases, the valence shell and/or subshell also changes. The valence Z* is indicated in Figure **2.7.4** as a black line with open circles.

Down the table: As we go down a column of the periodic table, the valence Z* increases. This is a simple trend because type of subshell is consistent and there is an increase only in shell and in atomic number, Z. This trend is best illustrated by inspection of Figure **2.7.3**.

Across the table: the trend depends on shell and subshell, but generally Z* increases across a period.

Periods 1-3 (s and p only): As we go across the table in periods 1-3, the shell stays constant as Z increases and the subshell changes from s to p. In these periods, there is a gradual increase in valence Z* as we move across any of the

first three periods.

Periods 4 and 5 (s, p, and d): Now we have some more complex trends because valence subshell and shell are changing as we increase in atomic number. Notice that the valence Z* generally increases going across a period as long as the subshell isn't changing; the exception is within the 4d subshell (elements 39-44 or Y-Ru). In general, going from an $(n)s$ subshell to an $(n-1)d$ subshell, there a relatively large increase in valence Z*. And in going from an $(n-1$d\) subshell to an $(n)p$ subshell, there is a relatively large decrease in Z*.

From one period to another: From Figure **2.7.4**, we can see that as we increase Z by one proton, going from one period to the next, there is a relatively large decrease in Z* (from Ne to Na, for example). This is because as Z increases by a small interval, the shell number increases, and so the electrons in the valence shell are much farther from the nucleus and are more shielded by all the electrons in the lower shell numbers.

Exercises

? Exercise 2.7.2

1. Compare trends in Z* and atomic size. Explain how and why atomic size depends on Z*.
2. Compare trends in Z* and ionization energy. Explain how and why ionization energy depends on Z*.

Answer

1. On the periodic table, atomic radius generally decreases across the periods (left to right) and increases down the groups. As atomic number increases across the periodic table, nuclear charge (Z) increases and Z* increases. In turn, the atomic radius decreases because the higher nuclear charge (and thus higher Z*) pulls electrons closer to the nucleus. Atomic radius increases down the periodic table because the shell number increases. Despite an increase in Z* going down the periodic table, larger atomic radii result from electrons occupying higher shells.

2. Ionization energies (IE) are inversely related to atomic radius; IE increases across the periods and decreases down the groups. Since the nucleus holds valence electrons more strongly (due to higher Z*) across the periods, IE increases because valence electrons are harder to remove. Down the periodic table, larger atomic radii cause electrons in valence orbitals to be shielded by core electrons. Recall that shielding reduces the nuclear charge available to electrons in higher orbital levels, resulting in a lower Z*. With more shielding and lower Z*, the valence electrons are held less tightly by the nucleus such that ionization energy decreases (i.e., valence electrons are easier to remove).

References

1. Petrucci, Ralph H., William S. Harwood, F. Geoffrey Herring, and Jeffry D. Madura. General Chemistry: Principles and Modern Applications, Ninth Edition. Pearson Education Inc. Upper Saddle River, New Jersey: 2007.
2. Raymond Chang. Physical Chemistry for Biological Sciences. Sausalito, California: University Science Books, 2005
3. R. S. Mulliken, Electronic Structures of Molecules and Valence. II General Considerations, Physical Review, vol. 41, pp. 49-71 (1932)
4. Anastopoulos, Charis (2008). *Particle Or Wave: The Evolution of the Concept of Matter in Modern Physics*. Princeton University Press. pp. 236–237. ISBN 0691135126. http://books.google.com/?id=rDEvQZhpltEC&pg=PA236.

Contributors and Attributions

- Sidra Ayub (UCD), Alan Chu (UCD)
- Emily V Eames (City College of San Francisco)
- Curated or created by Kathryn Haas

2.7: Shielding is shared under a CC BY-NC-SA 4.0 license and was authored, remixed, and/or curated by LibreTexts.

- **2.2.4: Shielding** by Kathryn Haas is licensed CC BY-NC-SA 4.0.

SECTION OVERVIEW

2.8: Periodic Properties of Atoms

General periodic trends are specific patterns that are present within the periodic table; these are patterns in properties like electronegativity, ionization energy, electron affinity, atomic radius, melting point, and metallic character. General periodic trends provide chemists with an invaluable tool to quickly predict an element's properties. These trends exist because of the similar atomic structure of the elements within their respective group families or periods, and because of the periodic nature of the elements. Some of the general periodic trends are described in this section.

2.8.1: Covalent and Ionic Radii

References

1. Russo, Steve, and Mike Silver. Introductory Chemistry. San Francisco: Pearson, 2007.
2. Petrucci, Ralph H, et al. General Chemistry: Principles and Modern Applications. 9th Ed. New Jersey: Pearson, 2007.
3. Atkins, Peter et. al, *Physical Chemistry*, 7th Edition, 2002, W.H Freeman and Company, New York, pg. 390.
4. Alberty, Robert A. et. al, *Physical Chemistry*, 3rd Edition, 2001, John Wiley & Sons, Inc, pg. 380.
5. Kots, John C. et. al, *Chemistry & Chemical Reactivity*, 5th Edition, 2003, Thomson Learning Inc, pg. 305-309.

2.8: Periodic Properties of Atoms is shared under a not declared license and was authored, remixed, and/or curated by LibreTexts.

2.8.1: Covalent and Ionic Radii

Measurement of Radius

There are several methods that can be used to determine radii of atoms and ions:

- **Nonpolar atomic radii:** The radius of an atom is derived from the bond lengths within nonpolar molecules; one-half the distance between the nuclei of two atoms within a covalent bond.
- **van der Waals radius:** The radius of an atom is determined by collision with other atoms.
- **Crystal radii**: The atomic or ionic radius is determined using electron density maps from X-ray data.

The measurement of atomic or ionic size will depend on a number of factors, including the covalent character of bonding in any particular molecule, coordination number, physical state (liquid, solid, gas), the identity of nearby atoms/ions, variation in crystal structure, and distortions within regular crystal structures. You should keep in mind that the size of an atom or ion is a "fuzzy" measure, and the radius under a different set of conditions will probably change slightly.

Regardless, measured atomic and ionic radii reveal obvious trends across the periodic table and between atoms and ions. The relative atomic sizes shown in Figure **2.8.1.1** were derived from crystallographic data.[1]

Trends in Atomic Radius

Atomic size generally decreases gradually from left to right across a period of elements. As nuclear charge (Z) increases, we expect the effective nuclear charge (Z*) of the valence electrons to also increase. Increasing Z pulls electrons closer to the nucleus. However, with each additional unit of Z, there is also an additional electron. The change in size is a balance of a compression caused by increasing Z and an expansion in the number of electrons. As a result, the atomic radius decreases *gradually* across a period.

Atomic size generally increases going down a group. As valence electrons occupy higher level shells due to the increasing quantum number (n), size increases despite the fact that Z and Z* are increasing going down the group.

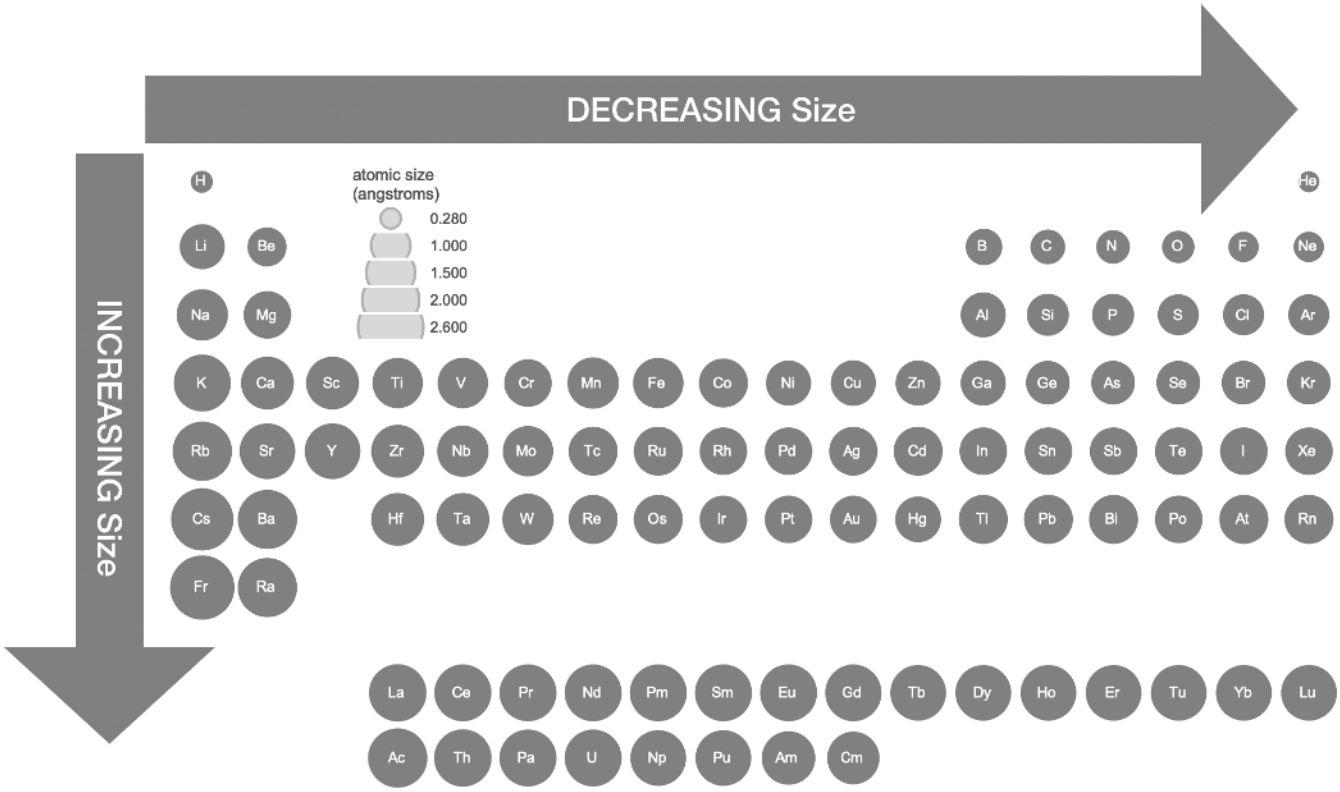


Figure **2.8.1.1**. *Atomic Radii Calculated from Crystalographic Data. Data from Cordero, Beatriz, Veronica Gomez, Ana E. Platero-Prats, Marc Reves, Jorge Echeverria, Eduard Cremades, Flavia Barragan, and Santiago Alvarez. "Covalent Radii Revisited." Dalton Transactions, no. 21 (2008): 2832–38. doi:10.1039/b801115j.* (Kathryn Haas; CC-NC-BY-SA)

Trends in Ionic Radius

Trends in ionic radius follow general trends in atomic radius for ions of the same charge. Ionic radius varies with the charge of the ion (and number of electrons) and the electron configuration (e.g. high spin or low spin).

Cations

Compared to their atoms, cations have the same Z but fewer electrons. Removal of electrons from an atom to form a cation results in a significant increase in effective nuclear charge, resulting in all other electrons being more strongly attracted to the nucleus, and having a lower energy level. The result is a contraction in size from the atom to cation. Figure **2.8.1.2** visually illustrates the relative size of atoms and some cations of the first four periods; the data is available in tabular format in Figure **2.8.1.3**.

Anions

Compared to their atoms, anions have the same Z but more electrons. Addition of electrons to an atom to form an anion results in a decrease in effective nuclear charge, which corresponds to a decrease in attractive force between the nucleus and electrons. Lower attractive force leads to expansion, where the size of the atom becomes larger in the formation of an anion. Figure **2.8.1.2** visually illustrates the relative size of atoms and some anions of the first four periods, while the data is available in tabular format in Figure **2.8.1.3**.

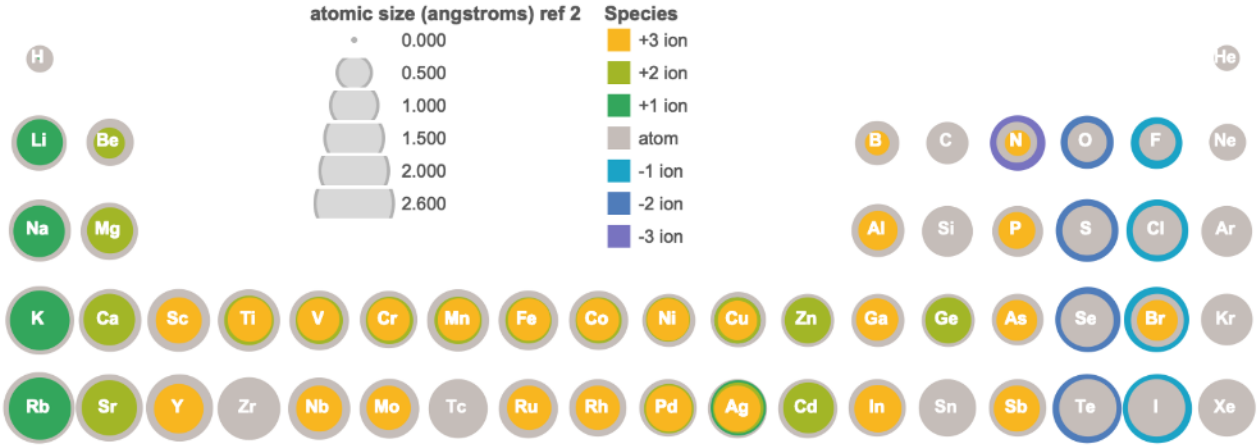


Figure **2.8.1.2**. This figure illustrates relative size of atoms and ions of the first four periods of the periodic table. Atomic radius is indicated by grey circles. Radius of cations is shown in green (+1), lime (+2), and yellow (+3) circles. Radius of anions are shown as aqua (-1), blue (-2), and purple (-3) circles. Data from sources 1-3. (Kathryn Haas; CC-NC-BY-SA)

H																	He
0.31 (atom) 0 (+1)																	0.28 (atom)
Li	Be											B	C	N	O	F	Ne
1.28 (atom) 0.9 (+1) -	0.96 (atom) 0.41 (+2) -											0.84 (atom) 0.25 (+1)	0.76 (atom) 0.29 (+4)	1.32 (-3) 0.71 (atom) 0.3 (+3) 0.27 (+5)	1.21 (-2) 0.66 (atom)	1.145 (-1) 0.57 (atom)	0.58 (atom)
Na	Mg											Al	Si	P	S	Cl	Ar
1.66 (atom) 1.16 (+1)	1.41 (atom) 0.86 (+2)											1.21 (atom) 0.675 (+3)	1.11 (atom) 0.4 (+4)	1.07 (atom) 0.58 (+3) 0.31 (+5)	1.7 (-2) 1.05 (atom) 0.51 (+4) 0.26 (+6)	1.67 (-1) 1.02 (atom)	1.06 (atom)
K	Ca	Sc	Ti	V	Cr	Mn	Fe	Co	Ni	Cu	Zn	Ga	Ge	As	Se	Br	Kr
2.03 (atom) 1.52 (+1)	1.76 (atom) 1.14 (+2)	1.7 (atom) 0.885 (+3)	1.6 (atom) 1 (+2) 0.81 (+3) 0.745 (+4)	1.53 (atom) 0.93 (+2) 0.78 (+3) 0.72 (+4)	1.39 (atom) 0.94 (+2 hs) 0.87 (+2 ls) 0.7555 (+3) 0.69 (+4) 0.63 (+5) 0.58 (+6)	1.61 (atom) 0.97 (+2 hs) 0.81 (+2 ls) 0.785 (+3 hs) 0.72 (+3 ls) 0.67 (+4) 0.47 (+5) 0.395 (+6) 0.39 (+7)	1.52 (atom) 0.92 (+2 hs) 0.765 (+3 hs) 0.75 (+2 ls) 0.725 (+4) 0.69 (+3 ls) 0.39 (+6)	1.5 (atom) 0.885 (+2 hs) 0.79 (+2 ls) 0.75 (+3 hs) 0.685 (+3 ls) 0.67 (+4 hs)	1.24 (atom) 0.83 (+2) 0.74 (+3 hs) 0.7 (+3 ls) 0.62 (+4)	1.32 (atom) 0.91 (+1, cn6) 0.87 (+2, cn6) 0.68 (+3, cn6)	1.22 (atom) 0.88 (+2)	1.22 (atom) 0.76 (+3)	1.2 (atom) 0.87 (+2) 0.67 (+4)	1.19 (atom) 0.72 (+3) 0.6 (+5)	1.84 (-2) 1.2 (atom) 0.64 (+4) 0.56 (+6)	1.82 (-1) 1.2 (atom) 0.73 (+3) 0.53 (+7) 0.45 (+5)	1.16 (atom)
Rb	Sr	Y	Zr	Nb	Mo	Tc	Ru	Rh	Pd	Ag	Cd	In	Sn	Sb	Te	I	Xe
2.2 (atom) 1.66 (+1)	1.95 (atom) 1.32 (+2)	1.9 (atom) 1.04 (+3)	1.75 (atom) 0.86 (+4)	1.64 (atom) 0.86 (+3) 0.82 (+4) 0.78 (+5)	1.54 (atom) 0.83 (+3) 0.79 (+4) 0.75 (+5) 0.73 (+6)	1.47 (atom) 0.785 (+4) 0.74 (+5) 0.7 (+7)	1.46 (atom) 0.82 (+3) 0.76 (+4) 0.705 (+5) 0.52 (+7) 0.5 (+8)	1.42 (atom) 0.805 (+3) 0.74 (+4) 0.69 (+5)	1.39 (atom) 0.73 (+1) 1 (+2) 0.9 (+3) 0.755 (+4)	1.45 (atom) 1.29 (+1) 1.08 (+2) 0.89 (+3)	1.44 (atom) 1.09 (+2)	1.42 (atom) 0.94 (+3)	1.39 (atom) 0.83 (+4)	1.39 (atom) 0.9 (+3) 0.74 (+5)	2.07 (-2) 1.38 (atom) 1.1 (+4) 0.7 (+6)	2.06 (-1) 1.39 (atom) 1.09 (+5) 0.67 (+7)	1.4 (atom) 0.62 (+8)

Figure 2.8.1.3.

This figure shows radii (in Angstroms) of atoms and ions of the first four periods of the periodic table. Radii from each element are listed from largest to smallest, ionic charge indicated in parentheses (); hs = high spin, ls = low spin, cn6 = coordination number is 6. Data from sources 1-3. (Kathryn Haas; CC-NC-BY-SA)

References

1. Cordero, Beatriz, Veronica Gomez, Ana E. Platero-Prats, Marc Reves, Jorge Echeverria, Eduard Cremades, Flavia Barragan, and Santiago Alvarez. *"Covalent Radii Revisited." Dalton Transactions, no. 21 (2008): 2832–38. doi:10.1039/b801115j.*
2. R. D. Shannon (1976). "Revised effective ionic radii and systematic studies of interatomic distances in halides and chalcogenides". *Acta Crystallogr A.* **32** (5): 751–767. Bibcode:1976AcCrA..32..751S. doi:10.1107/S0567739476001551.
3. Wikipedia articles on Atomic Radius and Ionic Radius.

2.8.1: Covalent and Ionic Radii is shared under a CC BY-NC 4.0 license and was authored, remixed, and/or curated by Kathryn Haas, Swetha Ramireddy, Bingyao Zheng, Emily Nguyen, & Emily Nguyen.

- **2.3.3: Covalent and Ionic Radii** by Bingyao Zheng, Emily Nguyen, Kathryn Haas, Swetha Ramireddy is licensed CC BY-NC-SA 4.0.

2.9: Ionization energy

Ionization energy (IE) is the energy required to **remove an electron from a neutral atom or cation in its gaseous phase**. IE is also known as *ionization potential*.

$$A^{n+}_{(g)} \longrightarrow A^{(n+1)+}_{(g)} + e^- \qquad IE = \Delta U$$

Conceptually, ionization energy is the affinity of an element for its outermost electron (an electron it already has in its valence shell).

1st, 2nd, and 3rd Ionization Energies

The symbol I_1 stands for the ***first ionization energy*** (energy required to take away an electron from a neutral atom, where $n = 0$). The symbol I_2 stands for the ***second ionization energy*** (energy required to take away an electron from an atom with a +1 charge, $n = 2$.)

- **First Ionization Energy,** I_1 (general element, A):

$$A_{(g)} \rightarrow A^{1+}_{(g)} + e^-$$

- **Second Ionization Energy,** I_2 (general element, A):

$$A^{1+}_{(g)} \rightarrow A^{2+}_{(g)} + e^-$$

- **Third Ionization Energy,** I_3 (general element, A):

$$A^{2+}_{(g)} \rightarrow A^{3+}_{(g)} + e^-$$

Each succeeding ionization energy is larger than the preceding energy. This means that $I_1 < I_2 < I_3 < ... < I_n$ will always be true. For example, ionization energy increases as succeeding electrons are taken away from **Mg**.

$$Mg_{\,(g)} \rightarrow Mg^{+}{}_{(g)} + e^- \quad I_1 = 738\,kJ/mol$$

$$Mg^{+}{}_{(g)} \rightarrow Mg^{2+}{}_{(g)} + e^- \quad I_2 = 1451\,kJ/mol$$

Ionization energy is correlated with the strength of attraction between the positively-charged nucleus and the negatively-charged valence electrons. The higher the ionization energy, the stronger the attractive force between nucleus and valence electrons, and the more energy is required to remove a valence electron. The lower the ionization energy, the weaker the attractive force between nucleus and valence electrons, and the less energy required to remove a valence electron.

General periodic trends in electron affinity

In general, ionization energies increase from left to right and decrease down a group; however, there are variations in these trends that would be expected from the effects of penetration and shielding. The trends in **first ionization energy** are shown in Figure 2.9.1 and are summarized below.

- **Across a period:** As Z* increases across a period, the ionization energy of the elements generally increases from left to right. However there are breaks or variation in the trends in the following cases:
  - IE is especially low when removal of an electron creates a newly empty p subshell (examples include I_1 of B, Al, Sc)
  - IE energy is especially low where removal of an electron results in a half-filled p or d subshell (examples include I_1 of O, S)
  - IE increases more gradually across the d- and f-subshells compared to s- and p- subshells. This is because d- and f- electrons are weakly penetrating and experience especially low Z*.
- **From one period to the next:** There is an especially large decrease in IE with the start of every new period (from He to Li or from Ne to Na for example). This is consistent with the idea that IE is especially low when removal of an electron creates a newly empty s-subshell.
- **Noble gases:** The noble gases posses very high ionization energies. Note that helium has the highest ionization energy of all the elements.

- **Down a group:** Although Z* increases going down a group, there is no reliable trend in IE going down any group; in some cases IE increases going down a group, while in other cases IE decreases going down a group.

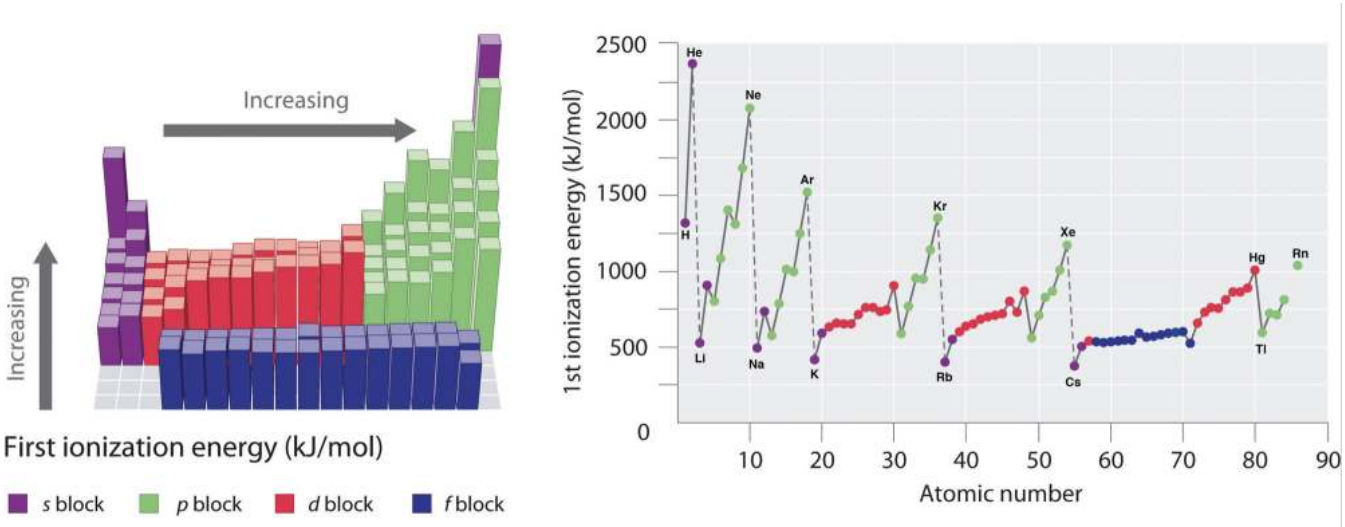


Figure 2.9.1: Graph showing the First Ionization Energy of the Elements. Left: ionization energies are mapped onto the periodic table, where the magnitude of ionization energy is depicted as a bar graph. Right: the first ionization energy is plotted against atomic number. In both panels the elements of the s-block are shown in purple, p-block are shown in green, d-block are shown in red, and f-block are shown in blue. (CC BY-NC-SA 3.0; anonymous)

Plots of the I_1, I_2, and I_3 of elements from hydrogen to krypton (first four periods) are shown in Figure 2.9.2. Notice that $I_3 > I_2 > I_1$. Also notice that trends mentioned above for I_1 hold true for subsequent ionizations when electron configurations are considered!

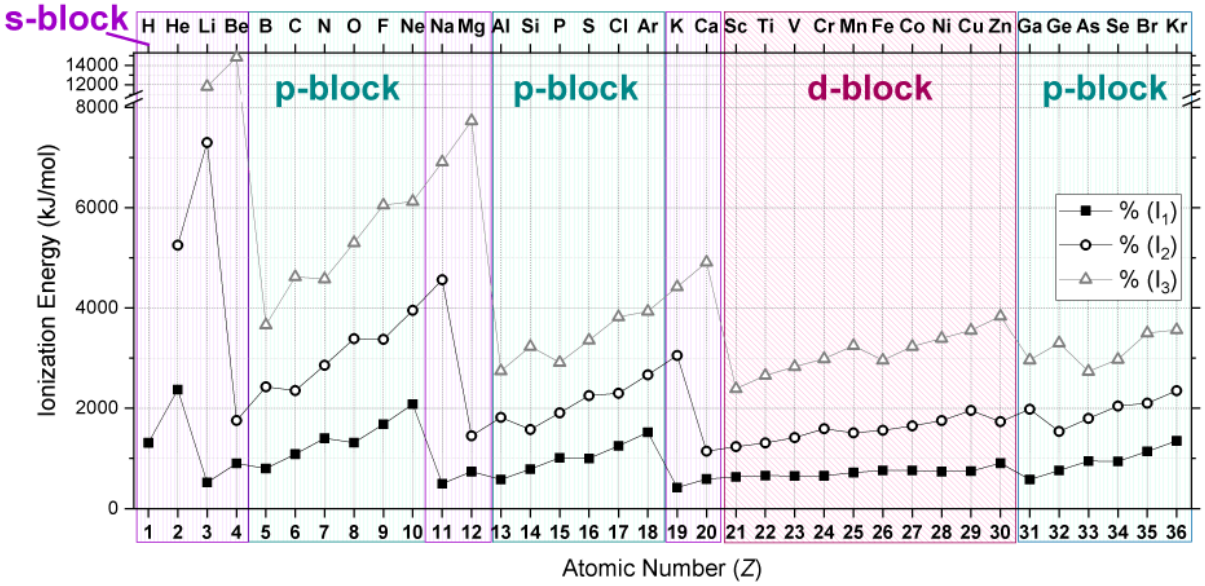


Figure 2.9.2. The first (I_1), second (I_2), and third (I_3) ionization energies plotted for elements with Z = 1 to 36 (H to Kr). The position of each element in its atomic form is indicated as s- p- or d-block. (CC-BY-NC-SA; Kathryn Haas)

2.9: Ionization energy is shared under a not declared license and was authored, remixed, and/or curated by LibreTexts.

- **2.3.1: Ionization energy** by Bingyao Zheng, Emily Nguyen, Kathryn Haas, Swetha Ramireddy is licensed CC BY-NC-SA 3.0.

2.10: Electron Affinity

Definitions of Electron Affinity

According to IUPAC, there are two different, but equivalent, definitions of **electron affinity (EA)**.[1]

Definition: Electron Affinity defined as removal of an electron

Electron affinity can be defined as the energy *required* when an electron is removed from a gaseous anion. The reaction as shown in equation 2.10.1 is *endothermic* (positive ΔU) for elements except noble gases and alkaline earth metals. Under this definition, the more positive the EA value, the higher an atom's affinity for electrons.

$$A^-_{(g)} \longrightarrow A_{(g)} + e^- \qquad EA = \Delta U \tag{2.10.1}$$

The reaction shown in Equation 2.10.1 is similar those that define ionization energy. For this reason, the EA is also described as the *zeroth ionization energy*.

Definition: Electron Affinity defined as addition of an electron

An alternate and more common definition is the microscopic reverse of Equation 2.10.1. This more common definition states that electron affinity is the energy *released* when an electron is added to a gaseous atom, as shown in Equation 2.10.2. The reaction as shown in equation 2.10.2 is *exothermic* (negative ΔU) for elements except noble gases and alkaline earth metals. The more negative this EA value, the higher an atom's affinity for electrons.

$$A_{(g)} + e^- \longrightarrow A^-_{(g)} \qquad EA = \Delta U \tag{2.10.2}$$

Conceptually, this second definition is quite similar to the concept of electronegativity; but unlike electronegativity, EA is a well-defined quantitative measurement.

Trends in Electron Affinity

For this discussion, we will use the definition of EA that is consistent with it being a *zeroth ionization energy:* a more positive (larger) value means that the EA is higher (meaning stronger affinity toward an electron).

- **Across a period**: Similar to ionization energy, EA generally increases across a row of the periodic table; this observation is consistent with the increase in effective nuclear charge (Z*) from left to right across a period. However, there are variations across a period that are similar to variations in ionization energy and that can be explained by shielding, penetration, and electron configuration.
- **Down a group**: Like the case of ionization energy trends, EA does not consistently decrease going down a column of the periodic table despite the fact that Z^* increases down a group.

The trend in EA follows a zig-zag pattern similar to the one seen with ionization energies, except that it is displaced by one unit from the trend in I_1, two units from I_2, and so on. For example, EA peaks at F, while I_1 peaks at Ne, I_2 peaks at Na, and I_3 peaks at Mg. A plot of EA for the first 13 elements is shown overlaid on plots of I_1, I_2 and I_3 in Figure 2.10.1., where the shifts in the peaks and valleys within each zig-zag trend are indicated.

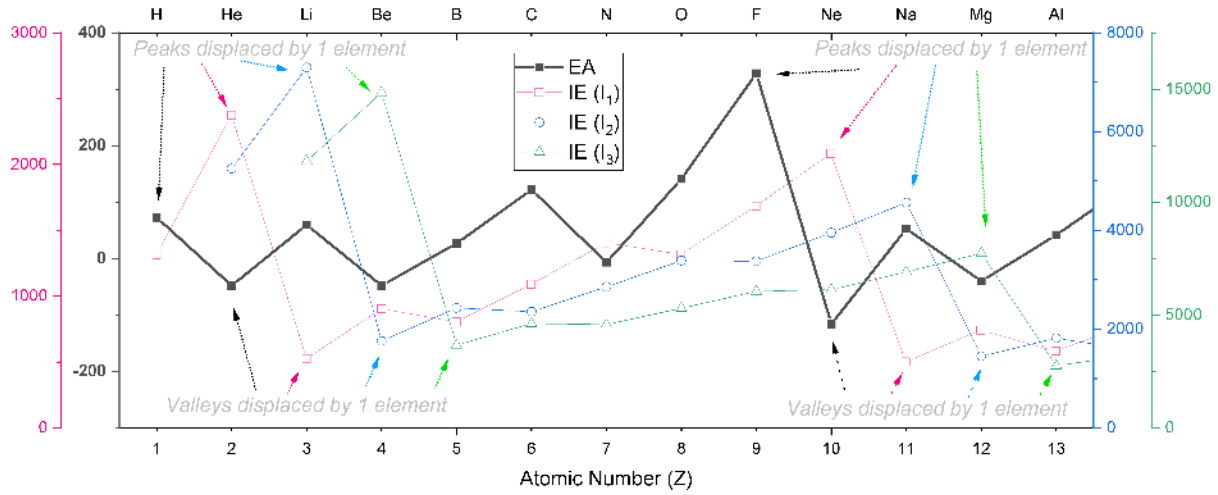


Figure **2.10.1**. A plot of electron affinity (the zeroth ionization energy) is overlaid on plots of the first (I_1), second (I_2), and third (I_3) ionization energies. Each plot is shown using separate y-axes. Trends in EA are similar to those in ionization energies, except that the peaks and valleys of the trends are shifted by one unit, as indicated. These plots are shown in units of kJ/mole. (CC-BY-NC-SA; Kathryn Haas)

Sources

1. IUPAC. Compendium of Chemical Terminology, 2nd ed. (the "Gold Book"). Compiled by A. D. McNaught and A. Wilkinson. Blackwell Scientific Publications, Oxford (1997). Online version (2019-) created by S. J. Chalk. ISBN 0-9678550-9-8. doi.org/10.1351/goldbook.
2. Electron Affinity (data page), Wikipedia. en.Wikipedia.org/wiki/Electron_affinity_(data_page) Accessed 12/3/19.

2.10: Electron Affinity is shared under a CC BY-NC 4.0 license and was authored, remixed, and/or curated by Kathryn Haas.

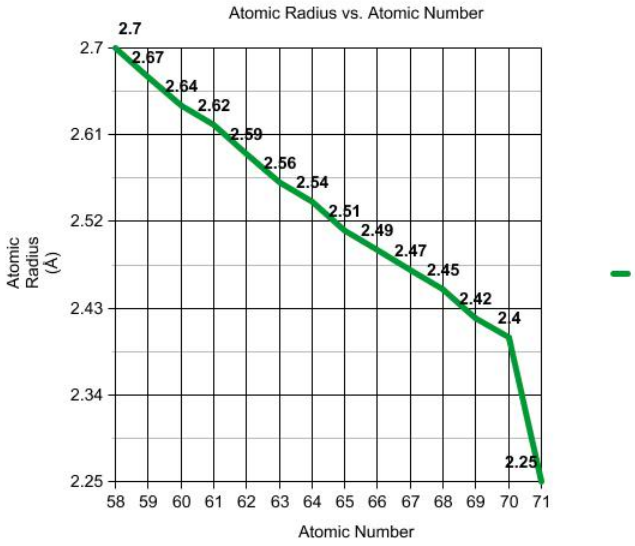
- **2.3.2: Electron Affinity** by Kathryn Haas is licensed CC BY-NC-SA 4.0.

2.11: Lanthanide Contraction

The Lanthanide Contraction describes the atomic radius trend that the Lanthanide series exhibit. Another important feature of the The Lanthanide Contraction refers to the fact that the 5s and 5p orbitals penetrate the 4f sub-shell so the 4f orbital is not shielded from the increasing nuclear change, which causes the atomic radius of the atom to decrease. This decrease in size continues throughout the series.

Introduction

The Lanthanide Contraction applies to all 14 elements included in the Lanthanide series. This series includes Cerium(Ce), Praseodymium(Pr), Neodymium(Nd), Promethium(Pm), Samarium(Sm), Europium(Eu), Gadolinium(Gd), Terbium(Tb), Dysprosium(Dy), Holmium(Ho), Erbium(Er), Thulium(Tm), Ytterbium(Yb), and Lutetium(Lu). The atomic radius, as according to the Lanthanide Contraction, of these elements decreases as the atomic number increases. We can compare the elements Ce and Nd by looking at a periodic table. Ce has an atomic number of 58 and Nd has an atomic number of 60. Which one will have a smaller atomic radius? Nd will because of its larger atomic number.

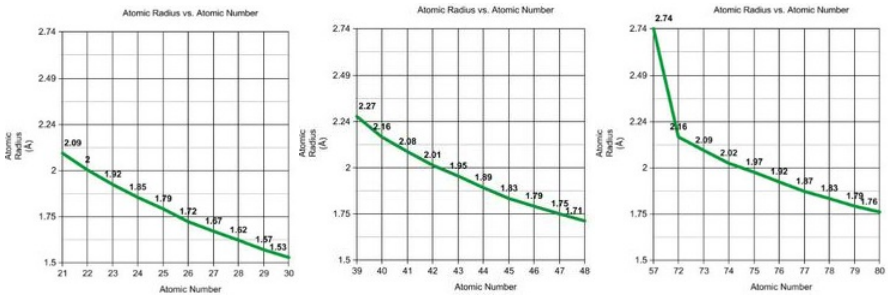


The graph shows the atomic radius decreasing as the atomic number is increasing, Lanthanide Contraction.

Shielding and its Effects on Atomic Radius

The Lanthanide Contraction is the result of a poor shielding effect of the 4f electrons. The shielding effect is described as the phenomenon by which the inner-shell electrons shield the outer-shell electrons so they are not effected by nuclear charge. So when the shielding is not as good, this would mean that the positively charged nucleus has a greater attraction to the electrons, thus decreasing the atomic radius as the atomic number increases. The s orbital has the greatest shielding while f has the least and p and d in between the two with p being greater than d.

The Lanthanide Contraction can be seen by comparing the elements with f electrons and those without f electrons in the d block orbital. Pd and Pt are such elements. Pd has 4d electrons while Pt has 5d and 4f electrons. These 2 elements have roughly the same atomic radius. This is due to Lanthanide Contraction and shielding. While we would expect Pt to have a significantly larger radius because more electrons and protons are added, it does not because the 4f electrons are poor at shielding. When the shielding is not good there will be a greater nuclear charge, thus pulling the electrons in closer, resulting in a smaller than expected radius.



Row 1 of Periodic Table D block Row 2 Row 3

The graphs depict the atomic radii of the first three rows of transition metals. We can apply the same principle as applied with the elements Pd and Pt to whole rows and columns. As we can see by comparing Row 1 with Row 2, the atomic radii differ greatly between the elements, but if we compare Row 2 with Row 3, the atomic radii do not have much difference. Elements with atomic number 23 and 41 lie in the same column of the periodic table and have a significantly large difference in atomic radii (atomic radii increases from Row 1 to Row 2), but elements 41 and 73, also in the same column, only differ slightly. This is the cause of introducing 4f electrons in Row 3. In Row 3, we would expect the elements to carry on the same trend as was witnessed between Rows 1 and 2 (large increase in atomic radii) but we do not. This is because the 4f orbitals are not doing a great job of shielding.

D Block Contraction (Scandide Contraction)

The d block contraction, also known as the Scandide Contraction, describes the atomic radius trend that the d block elements (Transition metals) experience. Normally the trend for atomic radius, moving across the periodic table is that the atomic radius decreases significantly. In the transition metals with D electrons as we move from left to right across the periodic table, the element's atomic radius only decreases slightly. This is because they have the same amount of s electrons, but are only differing in d electrons. These d electrons are in an inner shell (penultimate shell) and electrons are getting added to this shell, another shell is not created. The d electrons are not good at shielding the nuclear charge, so the atomic radius does not change much as electrons are added. Almost like disregarding the D electrons being added.

Effects on Ionization Energy and Properties

As the proton number increases and the atomic radius decreases, the ionization energy increases. This is due to a more positively charged nucleus and a greater pull on the electrons by the nucleus. A greater pull is the result of an increased effective nuclear charge. Effective nuclear charge is caused by the nucleus having a more positive charge than the negative charge on the electron (net positive charge). The density, melting point, and hardness increase from left to right throughout the Lanthanide Series. The Lanthanide Contraction makes chemical separation of the Lanthanides easier. The Lanthanide Contraction, while making the chemical separation of Lanthanides easier, it makes the separation of elements following the series a bit more difficult.

References

1. Petrucci, Harwood, Herring, and Madura. *General Chemistry Principles & Modern Applications*. 9th ed. Prentice Hall. Print.
2. Cotton, Simon. *Lanthanide and Actinide Chemistry*. Wiley. Print.

Problems

1. What is the cause of Lanthanide Contraction?
2. Which element has a greater atomic radius Gd or Tb and why?
3. Which element has a smaller atomic radius Dy or Yb and why?
4. Why do elements in Rows 2 and 3 that are in the same column have similar atomic radii?
5. Place the following elements in order of increasing atomic radius: Eu, Ce, Pr, Ho.
6. Which one of the following has the lowest density: Tb, Pm, Er, Tm, Ce

Answers:

1. The Lanthanide Contraction is caused by a poor shielding effect of the 4f electrons.
2. Gd because as atomic number increases, the atomic radius decreases.

3. Yb because it has a larger atomic number.
4. Because the elements in Row 3 have 4f electrons. These electrons are do not shield good, causing a greater nuclear charge. This greater nuclear charge has a greater pull on the electrons.
5. Ho, Eu, Pr, Ce
6. Ce

Contributors and Attributions

- Amrit Paul Bains (UCD)

2.11: Lanthanide Contraction is shared under a not declared license and was authored, remixed, and/or curated by LibreTexts.

- **Lanthanide Contraction** is licensed CC BY-NC-SA 4.0.

CHAPTER OVERVIEW

3: Simple Bonding Theory

3.1: Lewis Electron-Dot Diagrams
3.2: Resonance
3.3: Breaking the octet rule with higher electron counts (hypervalent atoms)
3.4: Formal Charge
3.5: Lewis Fails to Predict Unusual Cases - Boron and Beryllium
3.6: Valence Shell Electron-Pair Repulsion
3.7: Lone Pair Repulsion
3.8: Multiple Bonds
3.9: Electronegativity and Atomic Size Effects
3.10: Ligand Close Packing
3.11: Molecular Polarity
3.12: Hydrogen Bonding

3: Simple Bonding Theory is shared under a not declared license and was authored, remixed, and/or curated by LibreTexts.

3.1: Lewis Electron-Dot Diagrams

In 1916, Gilbert Lewis Newton introduced a simple way to show the bonding between atoms in a molecule though Lewis electron dot diagrams. Creating Lewis diagrams is rather simple and requires only a few steps and some accounting of the valence electrons on each atom. Valence electrons are represented as dots. When two electrons are paired (lone pairs), they are represented by two adjacent dots located on an atom, and when two paired electrons are shared between atoms (bonds), they are shown as lines. For example, below are the electron dot structures of atoms and the Lewis electron dot structures of the molecules.

These diagrams are helpful because they allow us to show how atoms are connected, and when coupled with Valence Shell Electron Repulsion Theory (VSEPR), we can use Lewis structures to predict the shape of the molecule.

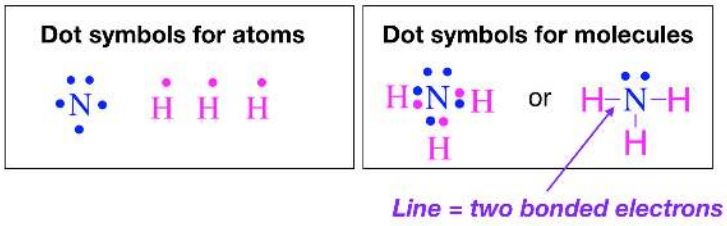


Figure 3.1.1: Lewis dot structure of atoms comprising ammonia and the dot structure of the molecule. (Kathryn Haas; CC-NC-BY-SA)

The drawing of Lewis electron-dot structures is guided largely by the **octet rule**: that atoms form bonds to achieve eight electrons in their valence shell. For many elements, a full valence shell has an electron configuration of s^2p^6, or eight electrons. A common exception to this rule is the first row elements, H and He. These two elements have $n = 1$ as their valence shell, and so they have only two electrons in a full valence shell ($1s^2$ electron configuration). Although H and He are exceptions to the "octet rule", they still form bonds to achieve a full valence shell. It may be better to think of this as the "full valence" rule of bonding. We will see many more violations to the "octet" rule as we progress through this course. In the case of metals and metalloids, breaking of the rules is particularly common. (CC-BY-NC-SA; Kathryn Haas)

Common violations of the octet rule

- **Less than eight electrons (hypovalency)**: H and He are examples of elements that cannot have more than two electrons in their full valence shell. Additionally, there are cases where a valid Lewis structure contains atoms with ***hypovalency:*** *partially-filled valence shells*. An example of this is a *carbocation, a positively charged carbon with only six electrons in its valence shell.* Carbocations are important intermediates in organic chemistry, and they are highly reactive (unstable) Lewis acids (electrophiles). Another example of hypovalency is the Lewis structure for BH_3, which shows boron with three bonds, and only six electrons in its valence shell. Boron hydride is a strong Lewis Acid. (Side note: the actual chemical form of BH_3 is not well-predicted by the Lewis structure and we'll see more about this in Section 3.1.4.)
- **More than eight electrons (hypervalency)**: This is a case where an element has more than eight electrons in its valence shell. It is common for larger atoms ($n \geq 3$), and it is discussed further in Section 3.1.2.

Pitfall alert! There are different rules for counting electrons depending on the purpose of the counting. These are the rules for counting for "octets". The rules for counting for calculation of an atom's formal charge are !!different!! and are described in Section 3.1.1. When an atom is part of a molecule, all electrons that are associated with the atom are counted as contributing to the atom's valence. This includes electrons that are lone pairs on the atoms, and *all* electrons that are shared in bonds. If four electrons are shared between two atoms, it is a double bond. If six electrons are shared between atoms, it is a triple bond.

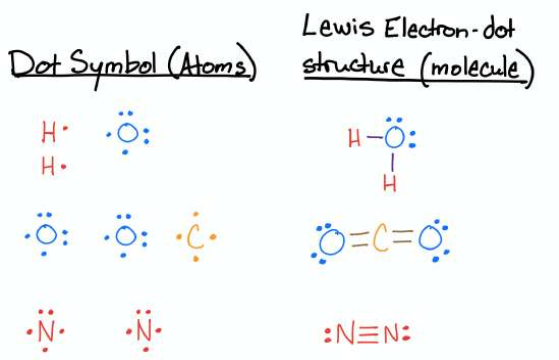
Electrons in valence (octet) = total unbonded electrons on the atom + total bonded electrons (2 electrons per bond)

Even if you're an old pro at drawing Lewis structures, it's a good idea to polish up. Please complete the practice exercises below. You should get out an actual piece of paper (I know...just do it. It's good for you.) and a writing tool and try to complete each problem before checking the answer.

Exercise 3.1.1

Draw the Lewis structures for H_2O, CO_2, and N_2.

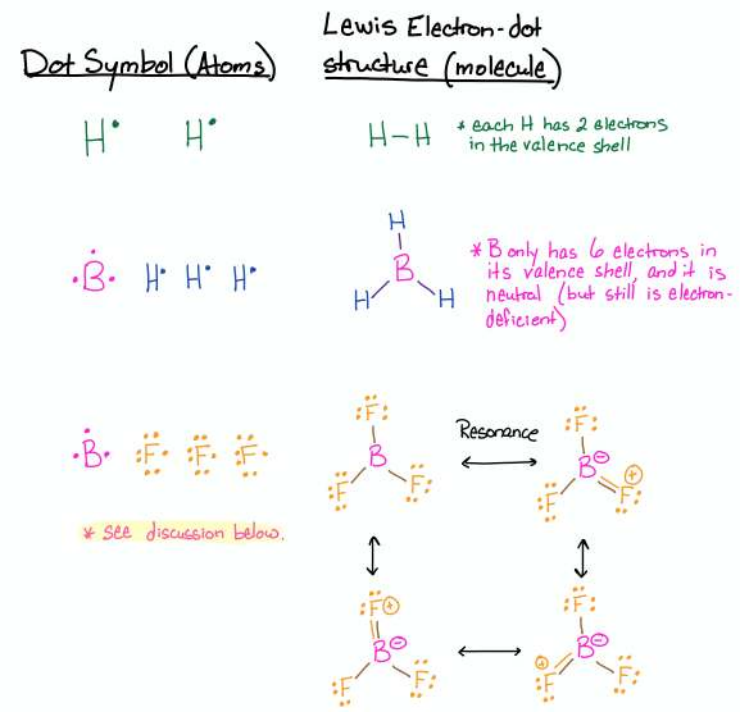
Answer



Exercise 3.1.2

Draw the Lewis structures for H_2, BH_3 and BF_3.

Answer



These three examples include atoms that have less than eight electrons in their valence shell. In the case of H, it is satisfied with only two electrons in its valence, as was discussed earlier in this section. The case of BH_3 was also discussed above. In the Lewis structure of BH_3, the boron can only have six electrons in its octet and it is neutral in charge. The boron is electron deficient even though it has neutral charge.

The case of BF_3 deserves a discussion: If you are unfamiliar with resonance and formal charge, see Sections 3.1.1 (Resonance) and 3.1.3 (Formal Charge) first and come back to this afterward. You might have drawn the BF_3 structure similar to the one that is drawn for BH_3, where boron has three bonds and only six electrons in its valence shell. If you did that, then you are correct; but if you only gave this structure, then your answer is not complete. There are three other correct

ways to draw the structure. Since F has lone pairs of electrons, other valid Lewis structures would each have a double bond to one of the fluorines (three total). All of these structures are called resonance structures, and based on the four of them, we could predict that BF_3 would have B-F bonds that have some double-bond character. If fact, this is the case for BF_3; it has bond lengths that are shorter than single bonds, but longer than double bonds. Read more about it on its Wikipedia page here (click).

Outside Links

- en.Wikipedia.org/wiki/Lewis_structures
- http://www.ausetute.com.au/lewisstr.html
- cost.georgiasouthern.edu/chem...cule/lewis.htm

This page titled 3.1: Lewis Electron-Dot Diagrams is shared under a CC BY-NC 4.0 license and was authored, remixed, and/or curated by Kathryn Haas.

- **3.1: Lewis Electron-Dot Diagrams** by Kathryn Haas is licensed CC BY-NC-SA 4.0.
- **2.1B: Lewis Structures** by Andrew Iskandar is licensed CC BY 4.0.

3.2: Resonance

Learning Objectives

- To understand the concept of resonance.

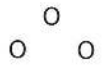
Resonance structures are a set of two or more Lewis Structures that collectively describe the electronic bonding of a single polyatomic species including fractional bonds and fractional charges. Resonance structures are capable of describing delocalized electrons that cannot be expressed by a single Lewis formula with an integral number of covalent bonds.

Sometimes one Lewis Structure is not Enough

Sometimes, even when formal charges are considered, the bonding in some molecules or ions cannot be described by a single Lewis structure. Resonance is a way of describing delocalized electrons within certain molecules or polyatomic ions where the bonding cannot be expressed by a single Lewis formula. A molecule or ion with such delocalized electrons is represented by several contributing structures (also called resonance structures or canonical forms). Such is the case for ozone ($\mathbf{O_3}$), an allotrope of oxygen with a V-shaped structure and an O–O–O angle of 117.5°.

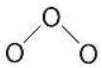
Ozone (O_3)

1. We know that ozone has a V-shaped structure, so one O atom is central:



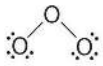
2. Each O atom has 6 valence electrons, for a total of 18 valence electrons.

3. Assigning one bonding pair of electrons to each oxygen–oxygen bond gives



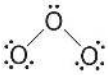
with 14 electrons left over.

4. If we place three lone pairs of electrons on each terminal oxygen, we obtain

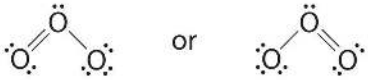


and have 2 electrons left over.

5. At this point, both terminal oxygen atoms have octets of electrons. We therefore place the last 2 electrons on the central atom:

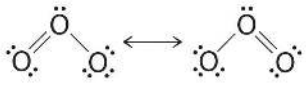


6. The central oxygen has only 6 electrons. We must convert one lone pair on a terminal oxygen atom to a bonding pair of electrons —but which one? Depending on which one we choose, we obtain either



Which is correct? In fact, neither is correct. Both predict one O–O single bond and one O=O double bond. As you will learn, if the bonds were of different types (one single and one double, for example), they would have different lengths. It turns out, however, that both O–O bond distances are identical, 127.2 pm, which is shorter than a typical O–O single bond (148 pm) and longer than the O=O double bond in O_2 (120.7 pm).

Equivalent Lewis dot structures, such as those of ozone, are called **resonance structures**. The position of the *atoms* is the same in the various resonance structures of a compound, but the position of the *electrons* is different. Double-headed arrows link the different resonance structures of a compound:



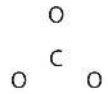
The double-headed arrow indicates that the actual electronic structure is an *average* of those shown, not that the molecule oscillates between the two structures.

> *When it is possible to write more than one equivalent resonance structure for a molecule or ion, the actual structure is the average of the resonance structures.*

The Carbonate (CO_3^{2-}) Ion

Like ozone, the electronic structure of the carbonate ion cannot be described by a single Lewis electron structure. Unlike O_3, though, the actual structure of CO_3^{2-} is an average of *three* resonance structures.

1. Because carbon is the least electronegative element, we place it in the central position:



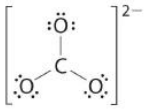
The three oxygens are drawn in the shape of a triangle with the carbon at the center of the triangle.

2. Carbon has 4 valence electrons, each oxygen has 6 valence electrons, and there are 2 more for the −2 charge. This gives 4 + (3 × 6) + 2 = 24 valence electrons.

3. Six electrons are used to form three bonding pairs between the oxygen atoms and the carbon:



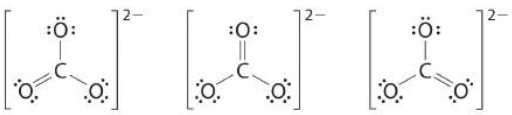
4. We divide the remaining 18 electrons equally among the three oxygen atoms by placing three lone pairs on each and indicating the −2 charge:



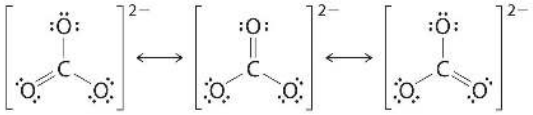
The Lewis dot structure has a central carbon that is bonded to 3 oxygens. Each oxygen has 3 lone pairs. The molecule is inside square brackets and has a charge of minus 2.

5. No electrons are left for the central atom.

6. At this point, the carbon atom has only 6 valence electrons, so we must take one lone pair from an oxygen and use it to form a carbon–oxygen double bond. In this case, however, there are *three* possible choices:



As with ozone, none of these structures describes the bonding exactly. Each predicts one carbon–oxygen double bond and two carbon–oxygen single bonds, but experimentally all C–O bond lengths are identical. We can write resonance structures (in this case, three of them) for the carbonate ion:



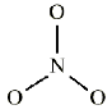
The resonance structure includes all three Lewis dot structures with double headed arrows between them.

The actual structure is an average of these three resonance structures.

The Nitrate (NO_3^-) ion

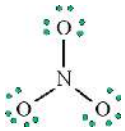
1. Count up the valence electrons: (1*5) + (3*6) + 1(ion) = **24** electrons

2. Draw the bond connectivities:

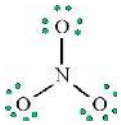


The three oxygens are drawn in the shape of a triangle with the nitrogen at the center of the triangle.

3. Add octet electrons to the atoms bonded to the center atom:

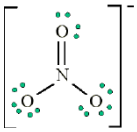


4. Place any leftover electrons (24-24 = **0**) on the center atom:



5. Does the central atom have an octet?

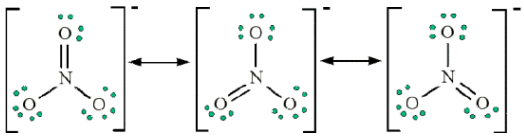
- **NO**, it has 6 electrons
- Add a multiple bond (first try a double bond) to see if the central atom can achieve an octet:



A double bond is added between one oxygen and the central nitrogen. The molecule has a negative charge.

6. Does the central atom have an octet?

- YES
- Are there possible resonance structures? YES



Note: We would expect that the bond lengths in the $\mathbf{NO_3^-}$ ion to be somewhat shorter than a single bond.



Example 3.2.1: Benzene

Benzene is a common organic solvent that was previously used in gasoline; it is no longer used for this purpose, however, because it is now known to be a carcinogen. The benzene molecule (C_6H_6) consists of a regular hexagon of carbon atoms, each of which is also bonded to a hydrogen atom. Use resonance structures to describe the bonding in benzene.

Given: molecular formula and molecular geometry

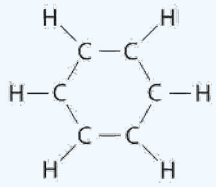
Asked for: resonance structures

Strategy:

A. Draw a structure for benzene illustrating the bonded atoms. Then calculate the number of valence electrons used in this drawing.
B. Subtract this number from the total number of valence electrons in benzene and then locate the remaining electrons such that each atom in the structure reaches an octet.
C. Draw the resonance structures for benzene.

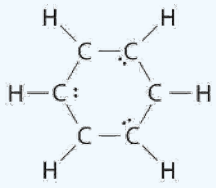
Solution:

A Each hydrogen atom contributes 1 valence electron, and each carbon atom contributes 4 valence electrons, for a total of (6 × 1) + (6 × 4) = 30 valence electrons. If we place a single bonding electron pair between each pair of carbon atoms and between each carbon and a hydrogen atom, we obtain the following:



Each carbon atom in this structure has only 6 electrons and has a formal charge of +1, but we have used only 24 of the 30 valence electrons.

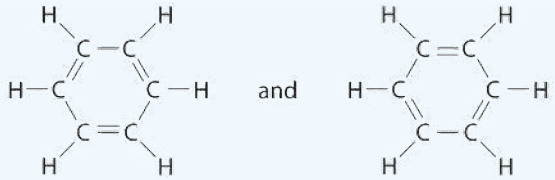
B If the 6 remaining electrons are uniformly distributed pairwise on alternate carbon atoms, we obtain the following:



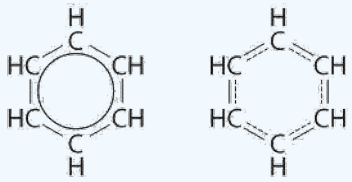
Three carbon atoms now have an octet configuration and a formal charge of −1, while three carbon atoms have only 6 electrons and a formal charge of +1. We can convert each lone pair to a bonding electron pair, which gives each atom an octet of

electrons and a formal charge of 0, by making three C=C double bonds.

C There are, however, two ways to do this:



Each structure has alternating double and single bonds, but experimentation shows that each carbon–carbon bond in benzene is identical, with bond lengths (139.9 pm) intermediate between those typically found for a C–C single bond (154 pm) and a C=C double bond (134 pm). We can describe the bonding in benzene using the two resonance structures, but the actual electronic structure is an average of the two. The existence of multiple resonance structures for aromatic hydrocarbons like benzene is often indicated by drawing either a circle or dashed lines inside the hexagon:

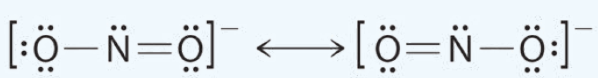


Benzene

? Exercise 3.2.1: Nitrite Ion

The sodium salt of nitrite is used to relieve muscle spasms. Draw two resonance structures for the nitrite ion (NO_2^-).

Answer



There is a double bond between one oxygen and the nitrogen, It can be found on the left oxygen or the right oxygen.

Resonance structures are particularly common in oxoanions of the *p*-block elements, such as sulfate and phosphate, and in aromatic hydrocarbons, such as benzene and naphthalene.

Warning

If several reasonable resonance forms for a molecule exists, the "actual electronic structure" of the molecule will probably be intermediate between all the forms that you can draw. The classic example is benzene in Example **3.2.1**. One would expect the double bonds to be shorter than the single bonds, but if one overlays the two structures, you see that one structure has a single bond where the other structure has a double bond. The best measurements that we can make of benzene do not show two bond lengths - instead, they show that the bond length is intermediate between the two resonance structures.

Resonance structures is a mechanism that allows us to use all of the possible resonance structures to try to predict what the actual form of the molecule would be. Single bonds, double bonds, triple bonds, +1 charges, -1 charges, these are our limitations in explaining the structures, and the true forms can be in between - a carbon-carbon bond could be mostly single bond with a little bit of double bond character and a partial negative charge, for example.

Summary

Some molecules have two or more chemically equivalent Lewis electron structures, called resonance structures. Resonance is a mental exercise and method within the Valence Bond Theory of bonding that describes the delocalization of electrons within molecules. These structures are written with a **double-headed arrow** between them, indicating that none of the Lewis structures accurately describes the bonding but that the actual structure is an average of the individual resonance structures. Resonance

structures are used when one Lewis structure for a single molecule cannot fully describe the bonding that takes place between neighboring atoms relative to the empirical data for the actual bond lengths between those atoms. The net sum of valid resonance structures is defined as a resonance hybrid, which represents the overall delocalization of electrons within the molecule. A molecule that has several resonance structures is more stable than one with fewer. Some resonance structures are more favorable than others.

3.2: Resonance is shared under a CC BY-NC 3.0 license and was authored, remixed, and/or curated by LibreTexts.

- **8.6: Resonance Structures** is licensed CC BY-NC-SA 3.0.

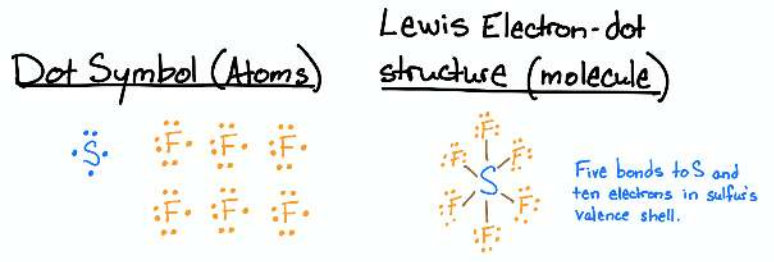
3.3: Breaking the octet rule with higher electron counts (hypervalent atoms)

The octet rule applies well to atoms in the second row of the periodic table, where a full valence shell includes eight electrons with an electron configuration of s^2p^6. Even elements in the third and fourth row are known to follow this rule *sometimes*, but not always. In larger atoms, where $n \geq 3$ the valence shell contains additional subshells: the $d, f, g...$ subshells. Therefore, atoms with $n \geq 3$ can have higher valence shell counts by "expanding" into these additional subshells. When atoms contain more than eight electrons in their valence shell, they are said to be **hypervalent**. Hypervalency allows atoms with $n \geq 3$ to break the octet rule by having more than eight electrons. This also means they can have five or more bonds; something that is nearly unheard of for atoms with $n \leq 2$. Complete the exercises below to see examples of molecules containing hypervalent atoms.

? Exercise 3.3.1

Draw the Lewis structures for SF_6.

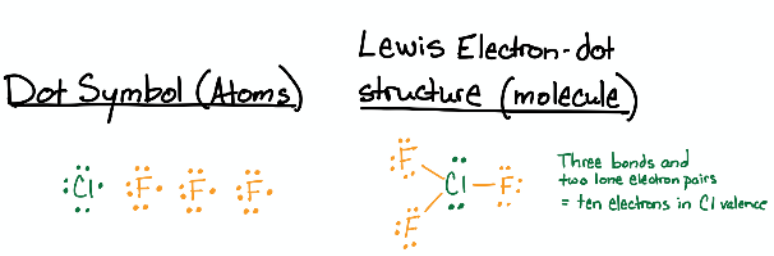
Answer



? Exercise 3.3.1

Draw the Lewis structure for ClF_3.

Answer



Is hypervalency real? Not exactly. Hypervalency is a concept associated with hybrid orbital theory and Lewis theory. It's useful for some simple things, like predicting how atoms are connected and predicting molecular shape. But the idea that the d-orbitals are involved in bonding isn't accurate according to wave mechanics.

For main group molecules, chemists (like Pauling) thought a long time ago that hypervalence is due to expanded s^2p^6 octets. The consensus is now clear that d orbitals are NOT involved in bonding in molecules like SF_6 any more than they are in SF_4 and SF_2. In all three cases, there is a small and roughly identical participation of d-orbitals in the wavefunctions. This has been established in both MO and VB theory. However using Hybrid orbitals with d-orbital contributions equips us with a language which can pragmatically describe the geometries of highly coordinated substances.

Hybrid orbitals are a powerful tool to describe the geometries and shape of molecules and metal complexes. However, in "real" molecules, their significance may be debated. Often a more realistically (and more complicated) molecular orbitals approach is needed. However, from an epistemologically simple point of view, bonding theories can only be judged by their predictions. To the extent that hybridization can explain the shapes of PF_5 and SF_6, valence bond theory is a perfectly good theory. To the extent that if

you write out the valence bond wavefunction using hybridized orbitals and calculate energies and other properties à la Pauling (i.e., ionization energy and electron affinities) and find them to be off from experimental results (by tens of kcals/mol), then valence bond theory is not accurate.

> *Bonding theories can only be judged by their predictions.*

A simple explanation that can be given is that molecular wavefunctions constructed out of hybridized atomic orbitals is accurate enough to predict some things, but not others. Predictions of any theory must be compared with empirical evidence to assess when they work and when they fail. When a theory gives the wrong answer, at least one assumption must not hold. In this case, the valence bond wavefunction is not accurate enough to capture some important features of a system's electronic structure. It may not be the most intellectually satisfying answer, but to say more would result in a much more complicated answer and certainly far beyond the level reasonably expected from general chemistry discussions.

This page titled 3.3: Breaking the octet rule with higher electron counts (hypervalent atoms) is shared under a CC BY-NC 4.0 license and was authored, remixed, and/or curated by Kathryn Haas.

- **3.1.2: Breaking the octet rule with higher electron counts (hypervalent atoms)** by Kathryn Haas is licensed CC BY-NC-SA 4.0.

3.4: Formal Charge

The formal charge of an atom in a molecule is the *hypothetical* charge the atom would have if we could redistribute the electrons in the bonds evenly between the atoms. Another way of saying this is that formal charge results when we take the number of valence electrons of a neutral atom, subtract the nonbonding electrons, and then subtract the number of bonds connected to that atom in the Lewis structure.

Calculating Formal Charges

We calculate the formal charge of an atom in a molecule or polyatomic ions as follows:

$$\text{Formal Charge} = (\text{valence electrons of the "free" element}) - (\text{unshared electrons}) - (\text{bonds}).$$

We can double-check formal charge calculations by determining the sum of the formal charges for the whole structure. The sum of the formal charges of all atoms in a molecule must be zero; the sum of the formal charges in an ion should equal the charge of the ion.

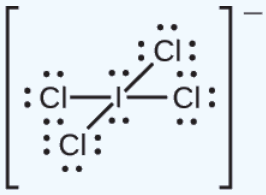
We must remember that the formal charge calculated for an atom is not the *actual* charge of the atom in the molecule. Formal charge is only a useful bookkeeping procedure; it does not indicate the presence of actual charges.

Calculating Formal Charge from Lewis Structures

Assign formal charges to each atom in the interhalogen ion $\mathrm{ICl_4^-}$.

Solution

We divide the bonding electron pairs equally for all I–Cl bonds:



We assign lone pairs of electrons to their atoms. Each Cl atom now has seven electrons assigned to it, and the I atom has eight.

Subtract this number from the number of valence electrons for the neutral atom:

- I: 7 – 8 = –1
- Cl: 7 – 7 = 0

The sum of the formal charges of all the atoms equals –1, which is identical to the charge of the ion (–1).

Exercise 3.4.1

Calculate the formal charge for each atom in the carbon monoxide molecule:



Answer

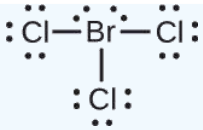
C −1, O +1

Example: Calculating Formal Charge from Lewis Structures

Assign formal charges to each atom in the interhalogen molecule $\mathrm{BrCl_3}$.

Solution

Assign one of the electrons in each Br–Cl bond to the Br atom and one to the Cl atom in that bond:



Assign the lone pairs to their atom. Now each Cl atom has seven electrons and the Br atom has seven electrons.

Subtract this number from the number of valence electrons for the neutral atom. This gives the formal charge:

- Br: 7 – 7 = 0
- Cl: 7 – 7 = 0

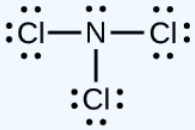
All atoms in $\mathbf{BrCl_3}$ have a formal charge of zero, and the sum of the formal charges totals zero, as it must in a neutral molecule.

? Exercise 3.4.2

Determine the formal charge for each atom in $\mathbf{NCl_3}$.

Answer

N: 0; all three Cl atoms: 0



This page titled 3.4: Formal Charge is shared under a CC BY-NC 4.0 license and was authored, remixed, and/or curated by OpenStax.

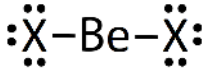
- **7.5: Formal Charges and Resonance** by OpenStax is licensed CC BY 4.0. Original source: https://openstax.org/details/books/chemistry-2e.

3.5: Lewis Fails to Predict Unusual Cases - Boron and Beryllium

Two notable cases where Lewis theory fails to predict structure are the cases of beryllium (**Be**) and boron (**B**). These two atoms are in period 2 ($n = 2$) of the periodic table and their atoms have the valence electron configurations of $2s^2$ and $2s^2 2p^1$, respectively.

Beryllium

The Lewis electron dot structures are shown below for BeX_2, where **X** is one of the halogens, **F** or **Cl**.



Each of the structures above would predict a linear geometry for the BeX_2 molecule. Together the three resonance structures suggest partial double-bond character in the Be-X bond, which results in an intermediate bond length between a single and double bond.

There are issues with each of these resonance structures. The structure on the left would predict only four electrons around **Be**; thus, the atom does not fulfill the octet rule. The structure on the left suggests multiple bonds for the halogen (**X**) and high separation of charge with formal charge on each atom. The structure in the middle is a mix of these problems. None of these situations is ideal according to Lewis theory. Further, experimental data is not consistent with any of these structures or their resonance hybrid (except in the case of $BeCl_2$ at very high temperatures).

It turns out that the monomer of BeX_2 does exist, but only at very high temperatures and low pressures. Even under extreme conditions, the monomer is not particularly stable due to the electron deficiency around **Be**.

BeF_2

At ambient temperature and pressure, BeF_2 is a solid that looks similar to quartz (Figure **3.5.1**) The Be is four-coordinate with tetrahedral geometry; each F is two-coordinate and the Be-F bond length is 1.54 Å. This structure is possible due to an extended 3-dimensional network in the solid where adjacent BeF_2 units are bonded to one another, as shown in Figure **3.5.1**.

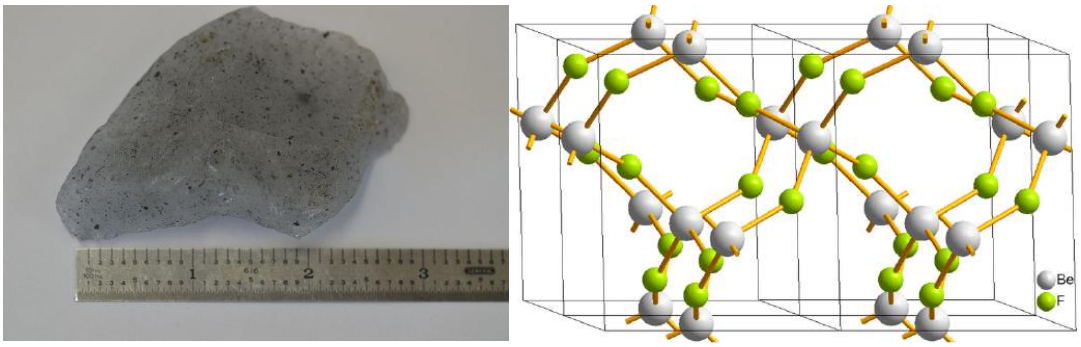


Figure **3.5.1**: (left) A nugget of beryllium fluoride obtained from Materion. Black spots are carbon (CC BY-SA 3.0; Bckelleher via Wikipedia). (right) BeF2 structure (CC BY-SA 3.0 Unported; Materialscientist via Wikipedia)

In the liquid phase, BeF_2 has a fluctuating tetrahedral structure where Be and F ions exchange. The vapor phase is reached at temperatures higher than 1000 °C (at ~ 1 atm). In the vapor phase, BeF_2 exists as a monomer with linear geometry and a bond length of 1.43 Å, consistent with a double bond between **Be** and **F**.

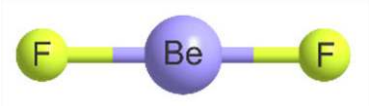


Figure **3.5.2**: Geometries of BeF_2. (CC BY; Ibon Alkorta and Anthony C. Legoe via Inorganics)

$BeCl_2$

At ambient temperature and pressure, $BeCl_2$ is a solid. As in BeF_2 described above, $BeCl_2$ has four-coordinate, tetrahedral Be and two-coordinate Cl. In contrast to BeF_2, solid $BeCl_2$ is a 1-dimensional polymer consisting of edge-shared tetrahedral.

In the gas phase, $BeCl_2$ exists as a dimer with two chlorine atoms bridging two Be atoms. In the dimer, the Be atoms are 3-coordinate. Bridging Cl atoms are two-coordinate, while terminal Cl atoms are one-coordinate. At higher temperatures in the vapor phase, the linear monomer also exists.

Boron ($2s^2 2p^1$)

Prediction based on Lewis structures:

Lewis structures of $\mathbf{BH_3}$ and $\mathbf{BF_3}$ were described in Exercise 3.1.2, and are drawn again below for convenience.

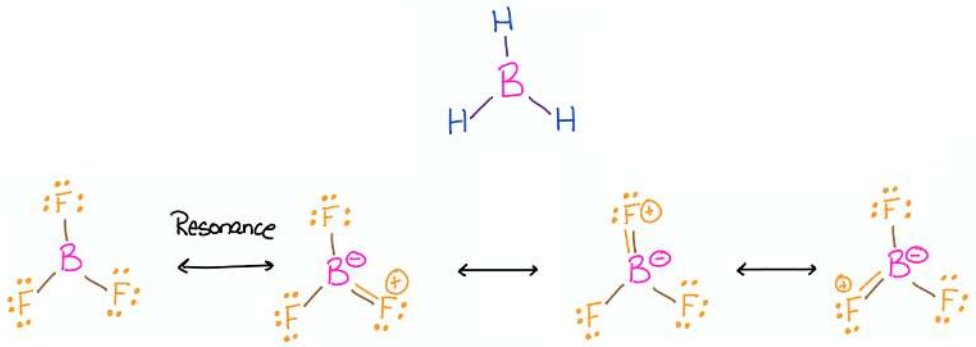


Figure 3.5.2: Lewis structures of $\mathbf{BH_3}$ and $\mathbf{BF_3}$. (Kathryn Haas; CC-NC-BY-SA)

Boron trihalides

Boron trihalides, like $\mathbf{BF_3}$, have properties that are largely predicted by Lewis structures and VSEPR theory. The Lewis structure for $\mathbf{BF_3}$ includes several resonance structures. The structure with only single bonds is the most common representation for this molecule because the charge separation shown in the other structures is considered to be unfavorable. The highly polarized B-F bond has a dipole moment that lies opposite to the indicated formal charges shown in the resonance structures with double bonds between boron and fluorine.

The resonance hybrid of $\mathbf{BF_3}$ predicts partial double bond character between boron and fluorine, thus a bond length shorter than a single bond. Using the Lewis structures and VSEPR theory, we would predict a trigonal planar geometry around boron. In fact, the actual structure of $\mathbf{BF_3}$ is a monomer with trigonal planar geometry and with bond length that is shorter than a single bond. The case is similar to structures of other boron trihalides as well.

Boron trihalides are electron deficient at the boron center and react readily with Lewis bases. In other words they are strong Lewis acids (electrophiles).

Boron trihydride (BH_3 is really B_2H_6)

The properties of boron trihydride ($\mathbf{BH_3}$) are not predicted by the simple predictions made through Lewis structures and VSEPR. The monomer, BH_3, is not stable, but when dissolved in the presence of a Lewis base, BH_3 can form a stable acid-base adduct. In its pure form, the compound actually exists as a dimeric gas with a molecular unit of B_2H_6 (try drawing a valid Lewis structure for that!). Its unexpected structure includes two H's that bridge the two boron atoms in 3-center-2-electron bonds. You can read more about B_2H_6 on the Wikipedia page for Diborane(6). The unique bonding observed for boron is described more in Chapter 8 and Chapter 15.

This page titled 3.5: Lewis Fails to Predict Unusual Cases - Boron and Beryllium is shared under a CC BY-NC 4.0 license and was authored, remixed, and/or curated by Kathryn Haas.

- **3.1.4: Lewis Fails to Predict Unusual Cases - Boron and Beryllium** by Kathryn Haas is licensed CC BY-NC-SA 4.0.

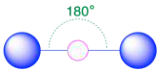
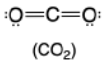
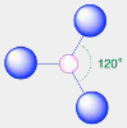
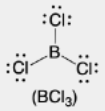
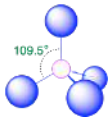
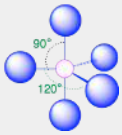
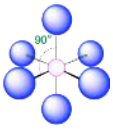
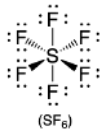
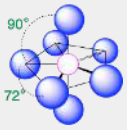
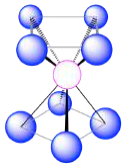
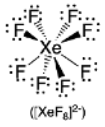
3.6: Valence Shell Electron-Pair Repulsion

Introduction to VSEPR

The **Valence Shell Electron Repulsion (VSEPR)** model can predict the structure of most molecules and polyatomic ions in which the central atom is a nonmetal; it also works for some structures in which the central atom is a metal. VSEPR builds on Lewis electron dot structures (discussed in Section 3.1); Lewis structures alone predict only connectivity while the Lewis structure and VSEPR together can predict the geometry of each atom in a molecule. The main idea of VSEPR theory is that pairs of electrons (in bonds and in lone pairs) repel each other. The pairs of electrons (in bonds and in lone pairs) are called "groups". Because electrons repel each other electrostatically, the most stable arrangement of electron groups (i.e., the one with the lowest energy) is the one that minimizes repulsion. Groups are positioned around the central atom in a way that produces the molecular structure with the lowest energy. In other words, the repulsion between groups around an atom favors a geometry in which the groups are as far apart from each other as possible. Although VSEPR is simplistic because it does not account for the subtleties of orbital interactions that influence molecular shapes, it accurately predicts the three-dimensional structures of a large number of compounds.

We can use the VSEPR model to predict the geometry around the atoms in a polyatomic molecule or ion by focusing on the number of electron pairs (groups) around a *central atom* of interest. Groups include bonded and unbonded electrons; a single bond, a double bond, a triple bond, a lone pair of electrons, or even a single unpaired electron each count as one group. The molecule or polyatomic ion is given an AX_mE_n designation, where **A is the central atom**, **X is a bonded atom**, **E is a nonbonding** valence electron group (usually a lone pair of electrons), and m and n are integers. The number of groups is equal to the sum of m and n. Using this information, we can describe the molecular geometry around a central atom, that is, the arrangement of the *bonded atoms* in a molecule or polyatomic ion. The geometries that are predicted from VSEPR when a central atom has only bonded groups ($n = 0$) are listed below in Table **3.6.1**. The cases where lone pairs contribute to the total groups ($n \geq 1$) are discussed in the next section about lone pair repulsion.

Table **3.6.1**. Geometries predicted using VSEPR theory (bonded groups only).

Groups around central atom (m + n)	Geometry Name	Geometry Sketch	Predicted bond Angle	Example
2	linear		180°	 (CO_2)
3	trigonal plane		120°	 (BCl_3)
4	tetrahedron		109.5°	 (CH_4)
5	trigonal bipyramid		90° and 120°	 (PF_5)
6	octahedron		90°	 (SF_6)
7	pentagonal bipyramid		90° and 72°	 ($[ZrF_7]^{3-}$)
8	square antiprism		70.5°, 99.6° and 109.5°	 ($[XeF_8]^{2-}$)

Practice

VSEPR to predict Molecular Geometry

You can follow these four steps to predict the geometry around an atom using VSEPR:

1. Draw the Lewis electron structure of the molecule or polyatomic ion.
2. For the central atom of interest, assign the AX_mE_n designation and the total number of groups (m+n).
3. Determine the electron group arrangement around the central atom that minimizes repulsions.
4. Describe the molecular geometry.

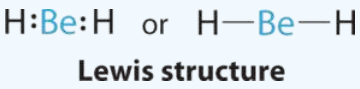
Use the procedure above to complete the exercises below

Exercise 3.6.1

Predict the geometry around the central atom in BeH_2 and CO_2.

Answer BeH_2

1. The central atom, beryllium, contributes two valence electrons, and each hydrogen atom contributes one. The Lewis electron structure is



Lewis structure

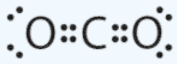
2. There are two groups around the central atom, and both groups are single bonds. Thus BeH_2 is designated as AX_2.

3. We see from Table **3.6.1** that the arrangement that minimizes repulsions places the groups 180° apart.

4. From Table **3.6.1** we see that with two bonding pairs, the molecular geometry that minimizes repulsions in BeH_2 is *linear.*

Answer CO_2

1. The central atom, carbon, contributes four valence electrons, and each oxygen atom contributes six. The Lewis electron structure is



2. The carbon atom forms two double bonds. Each double bond is counted as one group, so there are two groups around the central atom. Once again, both groups around the central atom are bonds, so CO_2 is designated as AX_2.

3. Like BeH_2, the arrangement that minimizes repulsions places the groups 180° apart.

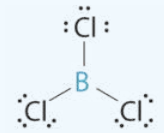
4. VSEPR only recognizes groups around the *central* atom (the carbon). Thus the lone pairs on the oxygen atoms do not influence the molecular geometry. With two bonded groups on the central atom and no lone pairs, the molecular geometry of CO_2 is linear (Table **3.6.1**). The structure of CO_2 is shown in Table **3.6.1**.

? Exercise 3.6.2

Predict the geometry around the central atom in BCl_3 and CO_3^{2-}.

Answer BCl_3

1. The central atom, boron, contributes three valence electrons, and each chlorine atom contributes seven valence electrons. The Lewis electron structure is



Lewis structure

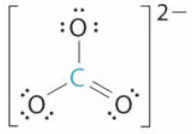
2. There are three groups around the central atom and all are single bonds. The structure is designated as AX_3.

3. To minimize repulsions, the groups are placed 120° apart (Table **3.6.1**).

4. From Table **3.6.1** we see that with three bonding pairs around the central atom, the molecular geometry of BCl_3 is *trigonal planar*.

Answer CO_3^{2-}

1. The central atom, carbon, has four valence electrons, and each oxygen atom has six valence electrons. The Lewis electron structure of one of three resonance forms is represented as

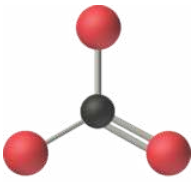


Lewis structure

2. The structure of CO_3^{2-} is a resonance hybrid. It has three identical bonds, each with a bond order of $1\frac{1}{3}$. All electron groups are bonds. With three bonding groups around the central atom, the structure is designated as AX_3.

3. We minimize repulsions by placing the three groups 120° apart (Table **3.6.1**).

4. We see from Table **3.6.1** that the molecular geometry of CO_3^{2-} is trigonal planar with bond angles of 120°.



Molecular geometry
(trigonal planar)

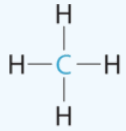
In our next example we encounter the effects of lone pairs and multiple bonds on molecular geometry for the first time.

? Exercise 3.6.3

Predict the geometry around the central atom in CH_4, PCl_5 and SF_6.

Answer CH_4

1. The central atom, carbon, contributes four valence electrons, and each hydrogen atom has one valence electron, so the full Lewis electron structure is

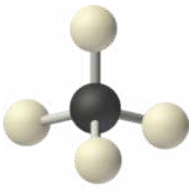


Lewis structure

2. There are four electron groups around the central atom. All electron groups are bonding pairs, so the structure is designated as AX_4.

3. As shown in Table **3.6.1**, repulsions are minimized by placing the groups in the corners of a tetrahedron with bond angles of 109.5°.

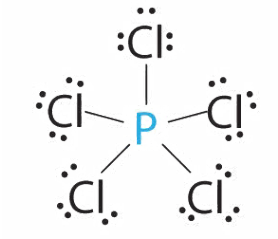
4. With four bonding pairs, the molecular geometry of methane is *tetrahedral* (Table **3.6.1**).



Molecular geometry
(tetrahedral)

Answer PCl_5

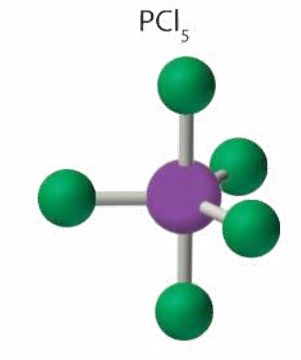
1. Phosphorus has five valence electrons and each chlorine has seven valence electrons, so the Lewis electron structure of PCl_5 is



2. There are five bonding groups around phosphorus, the central atom. All electron groups are bonds, so the structure is designated as AX_5.

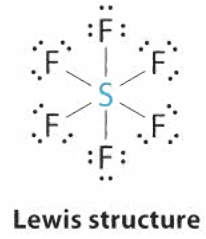
3. The structure that minimizes repulsions is a *trigonal bipyramid*, which consists of two trigonal pyramids that share a base (Table **3.6.1**).

4. The molecular geometry of PCl_5 is *trigonal bipyramidal*, as shown below. The molecule has three atoms in a plane in *equatorial* positions and two atoms above and below the plane in *axial* positions. The three equatorial positions are separated by 120° from one another, and the two axial positions are at 90° to the equatorial plane. The axial and equatorial positions are not chemically equivalent.



Answer SF_6

1. The central atom, sulfur, contributes six valence electrons, and each fluorine atom has seven valence electrons, so the Lewis electron structure is

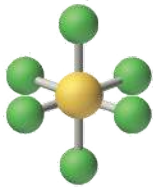


With an expanded valence, this species is an exception to the octet rule.

2. There are six electron groups around the central atom, each a bonding pair. We see from Figure **3.6.2** that the geometry that minimizes repulsions is *octahedral*.

3. With only bonding pairs, SF_6 is designated as AX_6. All positions are chemically equivalent, so all electronic interactions are equivalent.

4. There are six nuclei, so the molecular geometry of SF_6 is octahedral.



Molecular geometry
(octahedral)

This page titled 3.6: Valence Shell Electron-Pair Repulsion is shared under a CC BY-NC-SA 4.0 license and was authored, remixed, and/or curated by Kathryn Haas.

- **3.2: Valence Shell Electron-Pair Repulsion** by Kathryn Haas is licensed CC BY-NC-SA 4.0.

3.7: Lone Pair Repulsion

In the previous section, we saw how to use VSEPR to predict the geometry around a central atom based on the number of groups attached to a central atom. However, our previous discussion was limited to the simple cases where all of the groups were bonded groups (i.e., in the designation AX_mE_n , n=0). When all of the groups are bonds, the geometries can be predicted using information in Table 3.2.1 in the previous section. Now we will consider cases where one or more of these groups are lone pairs.

Lone pairs have stronger repulsive forces than bonded groups.

When one or more of the groups is a lone pair of electrons (non-bonded electrons), the experimentally-observed geometry around an atom is slightly different than in the case where all groups are bonds. The actual bond angles are similar, but not exactly the same, as those predicted based on the *total number of groups* (the "parent" geometry). When there is a mixture of group types (**lone pairs (E)** ***and*** **bonded groups (X)**) there are three different types of angles to consider: bond angles between two bonded atoms (**X-X** angles), angles between a bonded atom and a lone pair (**X-E** angles), and angles between two lone pairs (**E-E** angles). Empirical evidence shows the following trend in the degree of bond angles around atoms with a mixture of group types:

Trend in bond angles:

E-E >**X-E** >**X-X**

Using empirical evidence as a guide, we can predict that lone pairs repel other electron groups more strongly than bonded pairs. The molecular geometry of molecules with lone pairs of electrons is better predicted when we consider that electronic repulsion created by lone pairs is stronger than the repulsion from bonded groups. It is difficult to predict the exact bond angle based on this principle, but we can predict approximate angles, as described and summarized below in Table **3.7.1**.

Table **3.7.1**: Predictions of molecular geometry and bond angles around atoms with a mixture of bonded (X) and unbonded (E) electron groups.

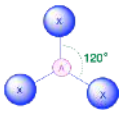
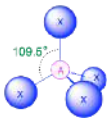
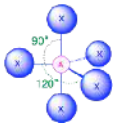
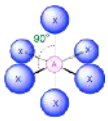
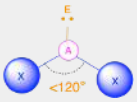
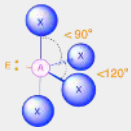
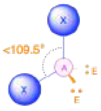
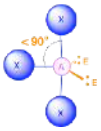
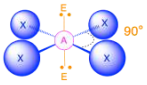
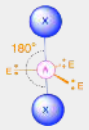
Electron Groups (m + n)					
	2 (steric number = 2)	**3** (steric number = 3)	**4** (steric number = 4)	**5** (steric number = 5)	**6** (steric number = 6)
Parent Geometry (0 lone pairs) AX_m	 AX_2, linear 180°	 AX_3, trig. plane 120°	 $AX4$, tetrahedron 109.5°	 AX_5, trig. bipyramid 90°, 120°	 AX_6, octahedron 90°
1 lone pair AX_mE_1		 $AX2E_1$, bent <120°	 AX_3E_1, trig. pyramid <109.5°	 AX_4E_1, see-saw <90°, <120°	 AX_5E_1, square pyramid 90°, <90°
2 lone pairs AX_mE_2			 AX_2E_2, bent <109.5°	 AX_3E_2, T-shape <90°	 AX_4E_2, square plane 90°
3 lone pairs AX_mE_3				 AX_2E_3, linear 180°	

Table **3.7.1** summarizes the geometries and bond angles predicted for nearest-neighbor bonded groups on central atoms with a mixture of lone pairs and bonded groups. The table does not cover all possible situations; it only includes cases where there are two bonded groups in which an X-X angle is measurable between nearest-neighbors. A more detailed description of some selected cases is given below.

Two Electron Groups (m + n = 2)

(Steric number = 2) In the case that there are only two electron groups around a central atom, those groups will lie 180° from one another. This results in a linear molecular geometry with 180° bond angles.

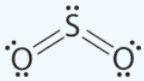
Three Electron Groups (m + n = 3)

(Steric number = 3) In the case that there are three electron groups around a central atom, those groups will lie approximately 120° from one another in space. This results in an electronic geometry that is approximately **trigonal planar**. There are two different molecular geometries that are possible in this category:

- When all of the electron groups are bonds (m = 3 or AX_3), the molecular geometry is a ***trigonal plane*** with **120°** bond angles.
- When there is one lone pair (m=2, n=1 or AX_2E_1), the molecular geometry is ***bent*** with a bond angle that is slightly **less than 120°**.

✔ AX_2E Molecules: Example SO_2

1. The central atom, sulfur, has 6 valence electrons, as does each oxygen atom. With 18 valence electrons, the Lewis electron structure is shown below.



2. There are three electron groups around the central atom: two double bonds and one lone pair. We initially place the groups in a trigonal planar arrangement to minimize repulsions (Table **3.7.1**).

3. With two bonding pairs and one lone pair, the structure is designated as AX_2E. This designation has a total of three electron pairs, two X and one E. The lone pair occupies more space around the central atom than a bonding pair (even double bonds!). Bonding pairs and lone pairs repel each other electrostatically in the order BP–BP < LP–BP < LP–LP. In SO_2, we have one BP–BP interaction and two LP–BP interactions.

4. The molecular geometry is described only by the positions of the nuclei, *not* by the positions of the lone pairs. Thus, with two nuclei and one lone pair the shape is *bent*, or *V shaped*, which can be viewed as a trigonal planar arrangement with a missing vertex. The O-S-O bond angle is expected to be *less than* 120° because of the extra space taken up by the lone pair.

Four Electron Groups (m + n = 4)

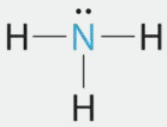
(Steric number = 4) In the case that there are four electron groups around a central atom, those groups will lie approximately 109.5° from one another in space. This results in an electronic geometry that is approximately **tetrahedral**. There are three different molecular geometries that are possible in this category:

- When all electron groups are bonds (m=4 or AX_4), the molecular geometry is a ***tetrahedron*** with bond angles of **109.5°**.
- When there is one lone pair (m=3, n=1 or AX_3E_1), the molecular geometry is a ***trigonal pyramid*** with bond angles of **slightly less than 109.5°**.
- When there are two lone pairs (m=2, n=2 or AX_2E_2), the molecular geometry is ***bent*** with bond angles of **slightly less than 109.5°**.

📌 AX_3E Molecules: Example NH_3

One of the limitations of Lewis structures is that they depict molecules and ions in only two dimensions. With four electron groups, we must learn to show molecules and ions in three dimensions.

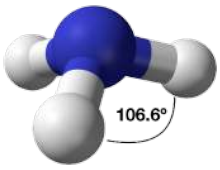
1. In ammonia, the central atom, nitrogen, has five valence electrons and each hydrogen donates one valence electron, producing the Lewis electron structure



Lewis structure

2. There are four electron groups around nitrogen, three bonding pairs and one lone pair. Repulsions are minimized by directing each hydrogen atom and the lone pair to the corners of a tetrahedron.

3. With three bonding pairs and one lone pair, the structure is designated as AX_3E. This designation has a total of four electron pairs, three X and one E. We expect the LP–BP interactions to cause the bonding pair angles to deviate significantly from the angles of a perfect tetrahedron.



The Difference in the Space Occupied by a Lone Pair of Electrons and by a Bonding Pair

As with SO_2, this composite model of electron distribution and negative electrostatic potential in ammonia shows that a lone pair of electrons occupies a larger region of space around the nitrogen atom than does a bonding pair of electrons that is shared with a hydrogen atom.

4. There are three nuclei and one lone pair, so the molecular geometry is *trigonal pyramidal*. In essence, this is a tetrahedron with a vertex missing. However, the H–N–H bond angles are less than the ideal angle of 109.5° because of LP–BP repulsion. The bond angles in ammonia are 106.6°.

AX_2E_2 Molecules: Example H_2O

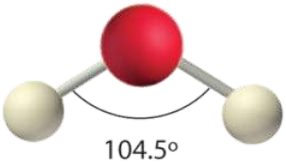
1. Oxygen has six valence electrons and each hydrogen has one valence electron, producing the Lewis electron structure



2. There are four groups around the central oxygen atom, two bonding pairs and two lone pairs. Repulsions are minimized by directing the bonding pairs and the lone pairs to the corners of a tetrahedron.

3. With two bonding pairs and two lone pairs, the structure is designated as AX_2E_2 with a total of four electron pairs. Due to LP–LP, LP–BP, and BP–BP interactions, we expect a significant deviation from idealized tetrahedral angles.

4. With two hydrogen atoms and two lone pairs of electrons, the structure has significant lone pair interactions. There are two nuclei about the central atom, so the molecular shape is *bent*, or *V shaped*, with an H–O–H angle that is even less than the H–N–H angles in NH_3, as we would expect because of the presence of two lone pairs of electrons on the central atom rather than one. This molecular shape is essentially a tetrahedron with two missing vertices.



Five Electron Groups (m + n = 5)

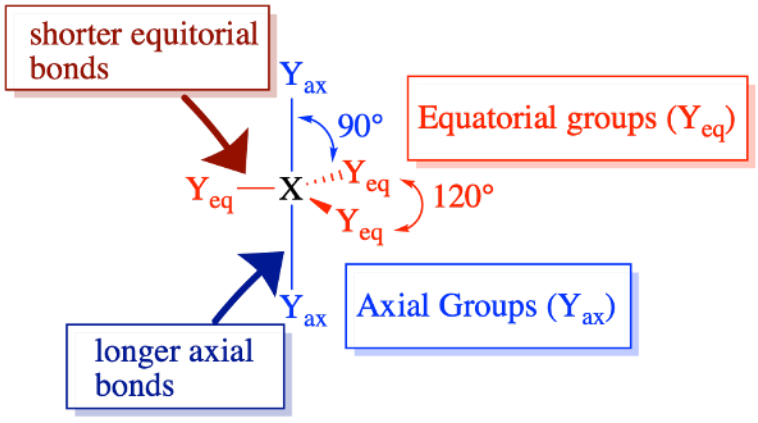


Figure: Trigonal pyramidal molecules (steric number 5) possess different bond angles and lengths for axial (ax) and equatorial (eq) pendant atoms. (CC-BY-NC-SA; Kathryn Haas).

(Steric number = 5) In the case that there are five electron groups around a central atom, there are two different types of positions around the central atom: equatorial positions and axial positions. The three equatorial ligands are 120° from one another and are 90° from each of the two axial ligands. The axial positions have three adjacent groups oriented 90° away in space. Axial groups are thus more crowded than the equatorial positions with only two adjacent groups at 90°. The crowding of axial positions results in slight differences in bond distances; crowded axial groups have longer bonds than the less crowded equatorial groups. Lone pairs of electrons generally prefer to occupy equatorial positions rather than axial positions. The justification for this preference, according to VSEPR theory, is that the lone electron pairs are more repulsive than bonding electron pairs, and thus the lone pairs prefer the less crowded equatorial positions.

The arrangement of five groups around a central atom results in a **trigonal bipyramidal** electronic geometry. There are four different molecular geometries that are possible in this category, depending upon the number of bonded groups and lone pairs of electrons:

- When all electron groups are bonds (m=5 or AX_5), the molecular geometry is a ***trigonal bipyramid*** with bond angles of **120°** and **90°** between adjacent ligands.
- When there is one lone pair (m=4, n=1 or AX_4E_1), the lone pair occupies one of the equatorial positions. The molecular geometry is called a ***see saw*** with bond angles of **slightly less than 120°** and **slightly less than 90°**.
- When there are two lone pairs (m=3, n=2 or AX_3E_2), each lone pair occupies one of the three equatorial positions. The molecular geometry is ***T-shaped*** with bond angles of **slightly less than 120°** and **slightly less than 90°**.
- When there are three lone pairs (m=1, n=3 or AX_3E_2), the lone pairs occupy the three equatorial positions. The molecular geometry is ***linear*** with bond angles of **180°**.

AX_4E Molecules: SF_4

1. The sulfur atom has six valence electrons and each fluorine has seven valence electrons, so the Lewis electron structure is



Lewis structure

With an expanded valence, this species is an exception to the octet rule.

2. There are five groups around sulfur, four bonding pairs and one lone pair. With five electron groups, the lowest energy arrangement is a trigonal bipyramid.

3. We designate SF_4 as AX_4E; it has a total of five electron pairs. However, because the axial and equatorial positions are not chemically equivalent, where do we place the lone pair? If we place the lone pair in the axial position, we have three LP–BP repulsions at 90°. If we place it in the equatorial position, we have two 90° LP–BP repulsions at 90°. With fewer 90° LP–BP repulsions, we can predict that the structure with the lone pair of electrons in the *equatorial position is more stable than the one with the lone pair in the axial position*. We also expect a deviation from ideal geometry because a lone pair of electrons occupies more space than a bonding pair.

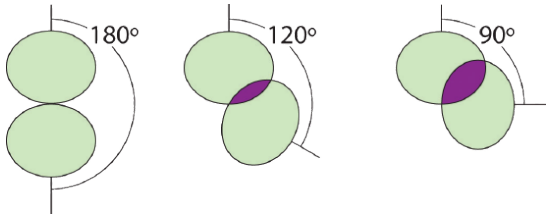
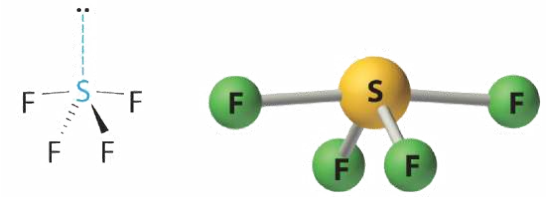


Illustration of the Area Shared by Two Electron Pairs versus the Angle between Them

At 90°, the two electron pairs share a relatively large region of space, which leads to strong repulsive electron–electron interactions.

4. With four nuclei and one lone pair of electrons, the molecular structure is based on a trigonal bipyramid with a missing equatorial vertex; it is described as a *seesaw*. The F_{axial}–S–F_{axial} angle is 173° rather than 180° because of the lone pair of electrons

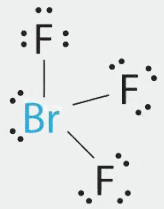
in the equatorial plane.



Molecular geometry (seesaw)

AX_3E_2 Molecules: BrF_3

1. The bromine atom has seven valence electrons, and each fluorine has seven valence electrons, so the Lewis electron structure is



Lewis structure

Once again, we have a compound that is an exception to the octet rule.

2. There are five groups around the central atom, three bonding pairs and two lone pairs. We again direct the groups toward the vertices of a trigonal bipyramid.

3. With three bonding pairs and two lone pairs, the structural designation is AX_3E_2 with a total of five electron pairs. Because the axial and equatorial positions are not equivalent, we must decide how to arrange the groups to minimize repulsions. If we place both lone pairs in the axial positions, we have six LP–BP repulsions at 90°. If both are in the equatorial positions, we have four LP–BP repulsions at 90°. If one lone pair is axial and the other equatorial, we have one LP–LP repulsion at 90° and three LP–BP repulsions at 90°:



Lone pairs axial (a) | Lone pairs equatorial (b) | Lone pairs axial and equatorial (c)

Interactions			
90° LP–LP	0	0	1
90° LP–BP	6	4	3

Structure (c) can be eliminated because it has a LP–LP interaction at 90°. Structure (b), with fewer LP–BP repulsions at 90° than (a), is lower in energy. However, we predict a deviation in bond angles because of the presence of the two lone pairs of electrons.

4. The three nuclei in BrF_3 determine its molecular structure, which is described as *T shaped*. This is essentially a trigonal bipyramid that is missing two equatorial vertices. The F_{axial}–Br–F_{axial} angle is 172°, less than 180° because of LP–BP repulsions.

Because lone pairs occupy more space around the central atom than bonding pairs, electrostatic repulsions are more important for lone pairs than for bonding pairs.

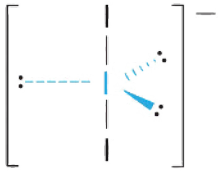
AX_2E_3 Molecules: I_3^-

1. Each iodine atom contributes seven electrons and the negative charge one, so the Lewis electron structure is



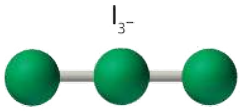
2. There are five electron groups about the central atom in I_3^-, two bonding pairs and three lone pairs. To minimize repulsions, the groups are directed to the corners of a trigonal bipyramid.

3. With two bonding pairs and three lone pairs, I_3^- has a total of five electron pairs and is designated as AX_2E_3. We must now decide how to arrange the lone pairs of electrons in a trigonal bipyramid in a way that minimizes repulsions. Placing them in the equatorial positions eliminates 90° LP–LP repulsions and minimizes the number of 90° LP–BP repulsions.



The three lone pairs of electrons have equivalent interactions with the three iodine atoms, so we do not expect any deviations in bonding angles.

4. With three nuclei and three lone pairs of electrons, the molecular geometry of I_3^- is linear. This can be described as a trigonal bipyramid with three equatorial vertices missing. The ion has an I–I–I angle of 180°, as expected.



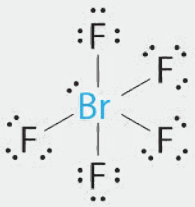
Six Electron Groups (m + n = 6)

(Steric number = 6) In the case that there are six electron groups around a central atom, the nearest groups will lie approximately 90° from one another in space. This results in an electronic geometry that is approximately **octahedral**. There are three relevant molecular geometries in this category:

- When all electron groups are bonds (m=6 or AX_6), the molecular geometry is an ***octahedron*** with bond angles of **90°** between adjacent bonds.
- When there is one lone pair (m=5, n=1 or AX_5E_1) we now distinguish between the axial and equitorial positions; the lone pair is considered to be in one of the axial positions, while the bond directly opposite of the lone pair is the axial bond. The molecular geometry is a ***square pyramid*** with bond angles of **90°** between adjacent equatorial bonds and **slightly less than 90°** between the axial bond and equatorial groups.
- When there are two lone pairs (m=4, n=2 or AX_4E_2), the lone pairs are opposite of one another and each occupy an axial position. The molecular geometry is ***square planar*** with bond angles of **90°**.

AX_5E Molecules: BrF_5

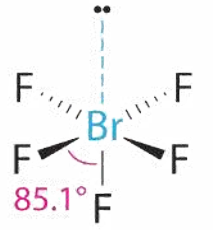
1. The central atom, bromine, has seven valence electrons, as does each fluorine, so the Lewis electron structure is



Lewis structure

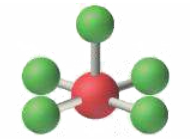
With its expanded valence, this species is an exception to the octet rule.

2. There are six electron groups around the Br, five bonding pairs and one lone pair. Placing five F atoms around Br while minimizing BP–BP and LP–BP repulsions gives the following structure:



3. With five bonding pairs and one lone pair, BrF_5 is designated as AX_5E; it has a total of six electron pairs. The BrF_5 structure has four fluorine atoms in a plane in an equatorial position and one fluorine atom and the lone pair of electrons in the axial positions. We expect all F_{axial}–Br–$F_{equatorial}$ angles to be less than 90° because of the lone pair of electrons, which occupies more space than the bonding electron pairs.

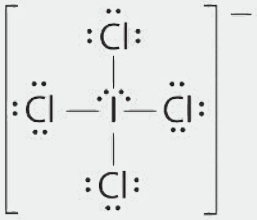
4. With five nuclei surrounding the central atom, the molecular structure is based on an octahedron with a vertex missing. This molecular structure is *square pyramidal*. The F_{axial}–B–$F_{equatorial}$ angles are 85.1°, less than 90° because of LP–BP repulsions.



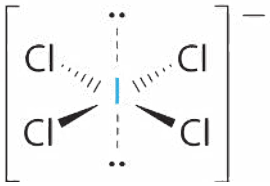
Molecular geometry
(square pyramidal)

AX_4E_2 Molecules: ICl_4^-

1. The central atom, iodine, contributes seven electrons. Each chlorine contributes seven, and there is a single negative charge. The Lewis electron structure is

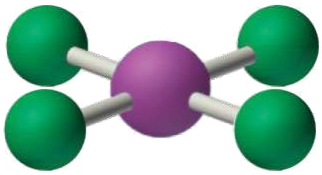


2. There are six electron groups around the central atom, four bonding pairs and two lone pairs. The structure that minimizes LP–LP, LP–BP, and BP–BP repulsions is



3. ICl_4^- is designated as AX_4E_2 and has a total of six electron pairs. Although there are lone pairs of electrons, with four bonding electron pairs in the equatorial plane and the lone pairs of electrons in the axial positions, all LP–BP repulsions are the same. Therefore, we do not expect any deviation in the Cl–I–Cl bond angles.

4. With five nuclei, the ICl4− ion forms a molecular structure that is *square planar*, an octahedron with two opposite vertices missing.



Summary

The arrangement of bonded atoms in a molecule or polyatomic ion is crucial to understanding the chemistry of a molecule, but Lewis electron structures give no information about **molecular geometry**. The **valence-shell electron-pair repulsion (VSEPR) model** allows us to predict which of the possible structures is actually observed in most cases. VSEPR is based on the assumption that pairs of electrons occupy space, and the lowest-energy structure is the one that minimizes repulsions between electron pairs. In the VSEPR model, the molecule or polyatomic ion is given an AX_mE_n designation, where A is the central atom, X is a bonded atom, E is a nonbonding valence electron group (usually a lone pair of electrons), and *m* and *n* are integers. Each group around the central atom is designated as a bonding pair (BP) or lone (nonbonding) pair (LP). From the BP and LP interactions we can predict both the relative positions of the atoms and the angles between the bonds, called the **bond angles**. From this we can describe the **molecular geometry**. The VSEPR model can be used to predict the shapes of many molecules and polyatomic ions, but it gives no information about bond lengths and the presence of multiple bonds. A combination of VSEPR and a bonding model, such as Lewis electron structures, is necessary to understand the presence of multiple bonds.

The relationship between the number of electron groups around a central atom, the number of lone pairs of electrons, and the molecular geometry is summarized in Table **3.7.1**.

Example Excercises

✔ Example 3.7.1

Using the VSEPR model, predict the molecular geometry of each molecule or ion.

1. PF_5 (phosphorus pentafluoride, a catalyst used in certain organic reactions)
2. H_3O^+ (hydronium ion)

Given: two chemical species

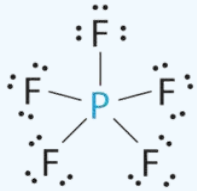
Asked for: molecular geometry

Strategy:

A. Draw the Lewis electron structure of the molecule or polyatomic ion.
B. Determine the electron group arrangement around the central atom that minimizes repulsions.
C. Assign an AX_mE_n designation; then identify the LP–LP, LP–BP, or BP–BP interactions and predict deviations in bond angles.
D. Describe the molecular geometry.

Solution:

1. **A** The central atom, P, has five valence electrons and each fluorine has seven valence electrons, so the Lewis structure of PF_5 is



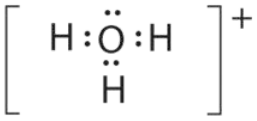
B There are five bonding groups about phosphorus. The structure that minimizes repulsions is a trigonal bipyramid.

C All electron groups are bonding pairs, so PF_5 is designated as AX_5. Notice that this gives a total of five electron pairs. With no lone pair repulsions, we do not expect any bond angles to deviate from the ideal.

D The PF_5 molecule has five nuclei and no lone pairs of electrons, so its molecular geometry is trigonal bipyramidal.



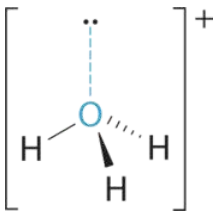
- **A** The central atom, O, has six valence electrons, and each H atom contributes one valence electron. Subtracting one electron for the positive charge gives a total of eight valence electrons, so the Lewis electron structure is



B There are four electron groups around oxygen, three bonding pairs and one lone pair. Like NH_3, repulsions are minimized by directing each hydrogen atom and the lone pair to the corners of a tetrahedron.

C With three bonding pairs and one lone pair, the structure is designated as AX_3E and has a total of four electron pairs (three X and one E). We expect the LP–BP interactions to cause the bonding pair angles to deviate significantly from the angles of a perfect tetrahedron.

D There are three nuclei and one lone pair, so the molecular geometry is *trigonal pyramidal*, in essence a tetrahedron missing a vertex. However, the H–O–H bond angles are less than the ideal angle of 109.5° because of LP–BP repulsions:



? Exercise 3.7.1

Using the VSEPR model, predict the molecular geometry of each molecule or ion.

a. XeO_3
b. PF_6^-
c. NO_2^+

Answer a

trigonal pyramidal

Answer b

octahedral

Answer c

linear

Example 3.7.2

Predict the molecular geometry of each molecule.

1. XeF_2
2. $SnCl_2$

Given: two chemical compounds

Asked for: molecular geometry

Strategy:

Use the strategy given in Example **3.7.1**.

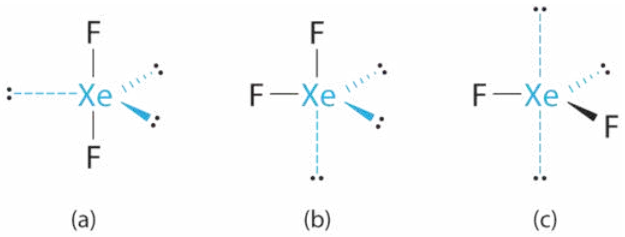
Solution:

1. **A** Xenon contributes eight electrons and each fluorine seven valence electrons, so the Lewis electron structure is



B There are five electron groups around the central atom, two bonding pairs and three lone pairs. Repulsions are minimized by placing the groups in the corners of a trigonal bipyramid.

C From B, XeF_2 is designated as AX_2E_3 and has a total of five electron pairs (two X and three E). With three lone pairs about the central atom, we can arrange the two F atoms in three possible ways: both F atoms can be axial, one can be axial and one equatorial, or both can be equatorial:

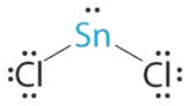


Interactions			
90 LP–LP	0	2	2

The structure with the lowest energy is the one that minimizes LP–LP repulsions. Both (b) and (c) have two 90° LP–LP interactions, whereas structure (a) has none. Thus both F atoms are in the axial positions, like the two iodine atoms around the central iodine in I_3^-. All LP–BP interactions are equivalent, so we do not expect a deviation from an ideal 180° in the F–Xe–F bond angle.

D With two nuclei about the central atom, the molecular geometry of XeF_2 is linear. It is a trigonal bipyramid with three missing equatorial vertices.

- **A** The tin atom donates 4 valence electrons and each chlorine atom donates 7 valence electrons. With 18 valence electrons, the Lewis electron structure is



B There are three electron groups around the central atom, two bonding groups and one lone pair of electrons. To minimize repulsions the three groups are initially placed at 120° angles from each other.

C From B we designate $SnCl_2$ as AX_2E. It has a total of three electron pairs, two X and one E. Because the lone pair of electrons occupies more space than the bonding pairs, we expect a decrease in the Cl–Sn–Cl bond angle due to increased LP–BP repulsions.

D With two nuclei around the central atom and one lone pair of electrons, the molecular geometry of $SnCl_2$ is bent, like SO_2, but with a Cl–Sn–Cl bond angle of 95°. The molecular geometry can be described as a trigonal planar arrangement with one vertex missing.

? Exercise 3.7.2

Predict the molecular geometry of each molecule.

a. SO_3
b. XeF_4

Answer a

trigonal planar

Answer b

square planar

This page titled 3.7: Lone Pair Repulsion is shared under a not declared license and was authored, remixed, and/or curated by Kathryn Haas.

- **3.2.1: Lone Pair Repulsion** by Kathryn Haas is licensed CC BY-NC-SA 4.0.
- **3.2.2: Multiple Bonds** by Kathryn Haas is licensed CC BY-NC-SA 4.0.

3.8: Multiple Bonds

In the previous sections, we saw how to predict the approximate geometry around an atom using VSEPR theory, and we learned that lone pairs of electrons slightly distort bond angles from the "parent" geometry. This page discusses the effect of multiple (double and triple) bonds between bonded atoms.

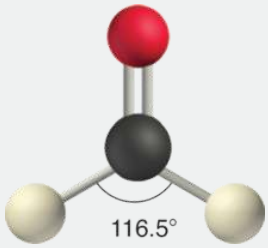
Double and triple bonds are more repulsive than single bonds

VSEPR theory predicts that double and triple bonds have stronger repulsive forces than single bonds. Like lone pairs of electrons, multiple bonds occupy more space around the central atom than a single bond. The result is that bond angles are slightly distorted compared to the parent geometry. Since a multiple bond has a higher electron density than a single bond, its electrons occupy more space than those of a single bond. Double and triple bonds distort bond angles in a way similar to what lone pairs do. Due to the stronger repulsion, double and triple bonds occupy positions similar to those of lone pairs in groups with 5 and 6 electron groups.

Examples 3.8.1

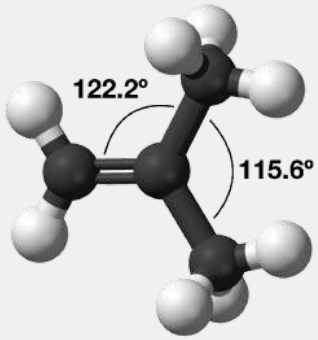
CH_2O

In a molecule such as CH_2O (AX_3), whose structure is shown below, the double bond repels the single bonds more strongly than the single bonds repel each other. This causes a deviation from ideal geometry (an H–C–H bond angle of 116.5° rather than 120°).



2-methybutene

In the molecule, $CH_2C(CH_3)_2$, the methyl—C—methyl bond angle is 115.6°, which is less than the 120° bond angle that would be expected of the parent geometry. On the other hand, the acetyl—C—methyl bond angle is greater than 120°, with an actual bond angle of 122.2°.



Atoms with both lone pairs and multiple bonds

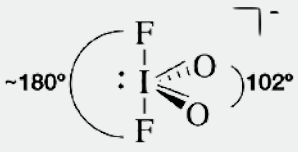
In general, we expect that a lone pair has slightly greater repulsive force than a multiple bond, and that a multiple bond has slightly greater repulsive force than a single bond. The **order of expected repulsive force** is:

$$\text{lone pair} > \text{double or triple bond} > \text{single bond}$$

Examples3.8.1

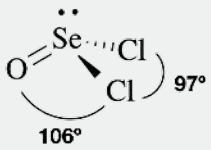
$IO_2F_2^-$

With five electron groups, the IO_2F_2 molecule has an approximately trigonal bipyramidal electronic (parent) geometry. The central iodine atom has a single bond to each of the fluorine atoms, a double bond to each oxygen, and a lone pair. The lone pair and the double bonds will occupy more space around iodine than each of the single bonds. Thus, we expect the lone pair and double bonds to occupy equatorial positions around the central iodine. The O=I=O bond angle is 102° (*much* smaller than the 120° angle expected from the parent geometry). This dramatically smaller angle is a result of the increased repulsion between the lone pair and the double bond.



$SeOCl_2$

With four electron groups, the $SeOCl_2$ molecule has four electron groups and approximately tetrahedral electronic (parent) geometry. It has both a lone pair and a double bond on the central selenium atom. The two chlorine atoms are singly bonded to selenium, while the oxygen is double bonded. The lone pair is most repulsive, followed by the double bonded oxygen, and then the chlorine bonds. This gives a Cl—Se—Cl bond angle of 97° and a Cl—Se—O bond angle of 106°; both angles are less than the 109.5° angles expected for the ideal tetrahedral geometry.



Practice

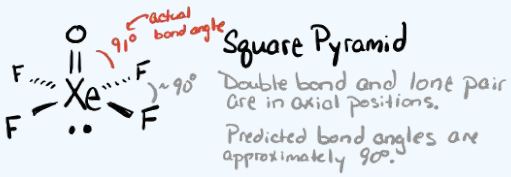
Exercise 3.8.1

Use VSEPR theory to predict the geometries and draw the structures of the following.

a. $XeOF_4$
b. NO_2^-
c. $SOCl_2$
d. IOF_3^-

Answer a

This molecule has six electron groups around the central Xe atom (steric number 6), and thus has an approximately octahdral electronic (parent) geometry. There is a double bond to O and a lone pair, both of which are more strongly repulsive than the single bonds to F. The double bond and lone pair will be directly opposite to each other, designated as axial positions. The result is a square pyramidal molecular geometry. VSEPR theory predicts F—Xe—F bond angles of 90°. As a general rule, lone pairs are slightly more repulsive than multiple bonds, and so we might expect the O—Xe—F bond angles to be <90°; *however in this case the actual O—Xe—F bond angle is observed to be 91°* (you could not have predicted the latter).



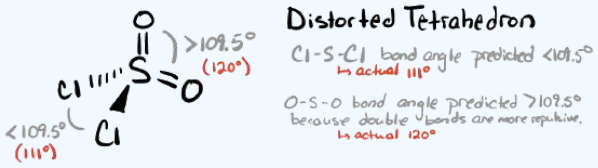
Answer b

This molecule has three electron groups around the central atom: one lone pair and two double bonds to oxygen atoms. This results in an approximately trigonal planar electronic (parent geometry). We expect the lone pair to be slightly more repulsive than double bonds, and so we expect the O—N—O bond angle to be slightly less than 120°. *The actual O—N—O angle is 115°.*



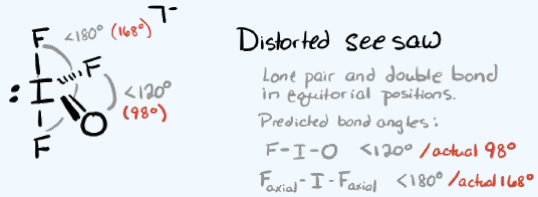
Answer c

This molecule has four electron groups (steric number 4) with an approximately tetrahedral electronic (parent) geometry. Each double bonded oxygen will take up more space around the central S than the single bonded Cl atoms. We should expect the double bonds to repel each other more strongly than they repel each single bond, with the least repulsive interaction being between the two single bonds. The bond angle for Cl—S—Cl is expected to be <109.5° according to VSEPR theory (however, it is actually 111°). We would expect the bond angle for O—S—O to be larger than the angle for Cl—S—Cl and for Cl—S—O. The O—S—O bond angle is predicted to be >109.5° (and the actual bond angle is 120°). The molecular geometry is a distorted tetrahedron.



Answer d

This molecule has five electron groups (steric number 5) with an approximately trigonal bipyramidal electronic (parent) geometry. There is one lone pair, a double bond to O, and three single bonds to F atoms around the central I atom. The lone pair and double bond are most repulsive, and should occupy the less crowded equatorial positions rather than the more crowded axial positions. This results in a seesaw molecular geometry. With the more repulsive lone pair and the strongest equatorial repulsive force being between the double bond and lone pair, we should expect the $F_{equatorial}$—I—O bond angle to be less than the 120° angle expected for the parent geometry (*it is actually much less, at 98°*). Due to repulsion between the axial F atoms and both the lone pair and double bond, we should expect the F—S—F bond angles to be compressed. The F_{axial}—I—F_{axial} is actually 168°.



References

- Miessler, G.; Fischer, P.J.; Tarr, D. (2014). Inorganic Chemistry. New Jersey: Prentice-Hall. pp. 55

This page titled 3.8: Multiple Bonds is shared under a not declared license and was authored, remixed, and/or curated by Kathryn Haas.

- **3.2.2: Multiple Bonds** by Kathryn Haas is licensed CC BY-NC-SA 4.0.

3.9: Electronegativity and Atomic Size Effects

Introduction

We saw in previous sections how lone pairs of electrons and multiple bonds distort bond angles between non-central atoms (ligands) around a central atom. This section describes how ligand **electronegativity and size also influence bond angles and molecular geometry**. Electronegativity is generally correlated with atomic size going down any group of the periodic table. There are some cases where bond angles can be predicted by these correlations. However, size and electronegativity can also work as competing factors in determining bond angles.

Definitions of Electronegativity

Linus Pauling introduced the first electronegativity scale in 1932 in order to explain the extra stability of molecules with polar bonds.[1] The electronegativity of an atom, represented by the Greek letter χ (chi), can be defined as the tendency of an atom to draw electrons to itself in a chemical bond. On the Pauling scale, the electronegativity difference between two atoms A and B was defined in terms of the dissociation energies E_d of the A-A, B-B, and A-B bonds:

$$\chi_A - \chi_B = \sqrt{E_d(AB) - [E_d(AA) + E_d(BB)]/2}$$

where the energies are expressed in electron volts. Pauling's scale of electronegativity ranges from Fluorine (most electronegative = 4.0) to Francium (least electronegative = 0.7). [2,3] The polarity of bonds and assignment of formal charges is predicted by electronegativity differences.

Periodic table of electronegativity using the Pauling scale

→ Atomic radius decreases → Ionization energy increases → Electronegativity increases →

Group →	1	2	3	4	5	6	7	8	9	10	11	12	13	14	15	16	17	18
↓ Period																		
1	H 2.20																	He
2	Li 0.98	Be 1.57											B 2.04	C 2.55	N 3.04	O 3.44	F 3.98	Ne
3	Na 0.93	Mg 1.31											Al 1.61	Si 1.90	P 2.19	S 2.58	Cl 3.16	Ar
4	K 0.82	Ca 1.00	Sc 1.36	Ti 1.54	V 1.63	Cr 1.66	Mn 1.55	Fe 1.83	Co 1.88	Ni 1.91	Cu 1.90	Zn 1.65	Ga 1.81	Ge 2.01	As 2.18	Se 2.55	Br 2.96	Kr 3.00
5	Rb 0.82	Sr 0.95	Y 1.22	Zr 1.33	Nb 1.6	Mo 2.16	Tc 1.9	Ru 2.2	Rh 2.28	Pd 2.20	Ag 1.93	Cd 1.69	In 1.78	Sn 1.96	Sb 2.05	Te 2.1	I 2.66	Xe 2.60
6	Cs 0.79	Ba 0.89	*	Hf 1.3	Ta 1.5	W 2.36	Re 1.9	Os 2.2	Ir 2.20	Pt 2.28	Au 2.54	Hg 2.00	Tl 1.62	Pb 1.87	Bi 2.02	Po 2.0	At 2.2	Rn 2.2
7	Fr 0.7	Ra 0.9	**	Rf	Db	Sg	Bh	Hs	Mt	Ds	Rg	Cn	Uut	Fl	Uup	Lv	Uus	Uuo
* Lanthanoids			La 1.1	Ce 1.12	Pr 1.13	Nd 1.14	Pm 1.13	Sm 1.17	Eu 1.2	Gd 1.2	Tb 1.1	Dy 1.22	Ho 1.23	Er 1.24	Tm 1.25	Yb 1.1	Lu 1.27	
** Actinoids			Ac 1.1	Th 1.3	Pa 1.5	U 1.38	Np 1.36	Pu 1.28	Am 1.13	Cm 1.28	Bk 1.3	Cf 1.3	Es 1.3	Fm 1.3	Md 1.3	No 1.3	Lr 1.3	

Figure 3.9.1: Table of Pauling electronegativities from Wikipedia's Electronegativity page (click).

While directly relevant to the strength of chemical bonds, the Pauling definition of electronegativity has a significant limitation: calculating each value requires data from several compounds in which specific atoms are bonded. This means that the scale cannot be successfully applied to all situations. To overcome this limitation, alternative electronegativity scales were developed based on different thermochemical measurements or calculations. These other scales are listed in the table below. More thorough descriptions of how values in each scale are calculated are described on Wikipedia's Electronegativity page (click) and a concise history of electronegativity scales is summarized in ref 4.

Scale Developer	Year first described	Characteristics
Linus Pauling[1]	1932	Based on bond energies
Robert S. Mulliken[5,6]	1934	Based on valence electron properties of atoms (electron affinity and ionization energy)
Louis Allred & Eugene G. Rochow[7]	1958	Based on electrostatic force (effective nuclear charge)
Robert T. Sanderson[8]	1983	Based on atomic electron density
Ralph G. Pearson[9]	1985	Related to Hard-Soft Acid-Based theory
Leland C. Allen, Joseph Mann, Terry L. Meek[10,11,12]	1989, 2000	Average ionization energies of valence shell electrons, configuration energies (CE) $$\mathrm{CE} = \frac{n\varepsilon_s + m\varepsilon_p}{n+m}$$ n = number of s electrons m = number of p electrons $\varepsilon_s, \varepsilon_p$ = experimental 1-electron s and p energies

The primary advantage to this scale developed by Mann, Meek, and Allen[12] is that it is based on configuration energy (CE), the average ionization energies of valence electrons in ground state free atoms. A scale based on ionization energies can be calculated more directly for any element. However, a critique of all electronegativity scales, including this one, is that they are all based on assumptions that fail in some cases.

There is a relationship between electronegativity and atomic size because both are related to ionization energy. Like ionization energy, there is a general trend across the periodic table for both electronegativity and atomic size; in general, smaller atoms toward the top right-hand side of the periodic table have greater electronegativity values and smaller atomic size. We will see below that both electronegativity and atomic size influence bond angles and absolute molecular geometry around a central atom. In some cases, the size and electronegativity affects are aligned; in some cases these effects compete.

Electronegativity and Size Influence Bond Angles

Let's begin by examining the bond angles of several trigonal pyramidal molecules. The molecules shown in Figure **3.9.2** each have three identical "pendant groups" on the central atom (Figure **3.9.2**). *Pendant atoms* or *pendant groups* are the atoms, or groups of atoms, that are bonded directly to the central atom. The molecules shown here are arranged according to the size of the central and pendant atoms. Central atoms increase in size going down this figure, and pendant atoms increase in size going across from left to right. The bond angles and bond lengths are labeled in each case.

What trends can you identify?

Trends in Size

First, let's examine how the size of the central and pendant groups might influence bond angle. In VSEPR theory, **the size of atoms (or groups of atoms) will affect bond angles due to changes in steric interactions between pendant groups.**

Size of the central atom

Examine the relationship between the size of the central atom and the bond angles in Figure **3.9.2** (go down any column in the figure). For example, compare NH_3, PH_3, AsH_3, and SbH_3, with bond angles 106.6°, 93.2°, 92.1°, and 91.6°, respectively. In this series, the size of the central atom increases from N to Sb while the size of the pendant atom (hydrogen) remains constant. *As the size of the central atom increases, the bond angles decrease; thus, we observe a negative relationship between size of the central atom and the bond angle in these molecules*. This relationship is explained by sterics. As the central atom increases in size, the

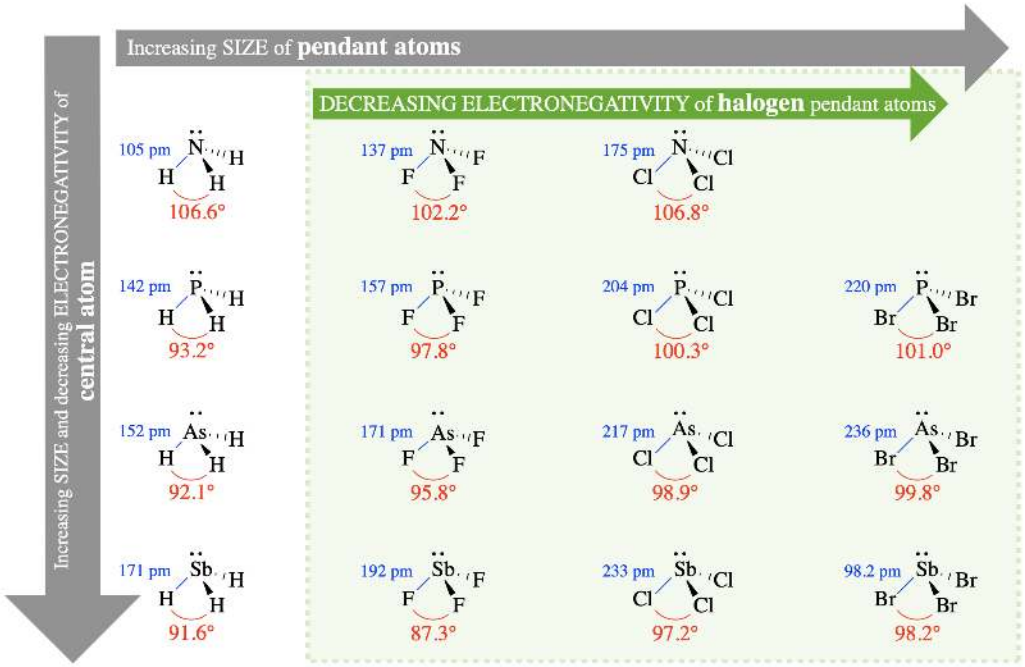


Figure **3.9.2**: Several molecules with trigonal pyramidal electronic geometry are shown arranged according to size of the central atom (increasing size of central atom from top to bottom) and pendant atom (increasing size of pendant atoms from left to right). Bond angles and bond lengths are indicated. (Kathryn Haas; CC-NC-BY-SA)

bond lengths also increase and the pendant atoms are farther from each other in space. In VSEPR theory, this will reduce steric interactions between the pendant groups. Since the lone pair on these molecules is more repulsive than bonded groups, the decrease in steric interactions between bonded groups results in a decrease in bond angles.

Size of the pendant atoms (or groups)

Examine the relationships between size of the halogen pendant atoms and bond angle in Figure **3.9.2** (go across any row within the shaded region). For example, compare PF_3, PCl_3, and PBr_3, with bond angles 97.8°, 100.3°, and 101.0°, respectively. In this series, the size of the pendant atom increases from F to Br while the central atom remains constant (phosphorous). *As the size of pendant atoms increases, the bond angle increases; thus, we observe a direct relationship between size of the pendant group and the bond angle in these molecules*. Again, we can explain this using sterics. As the size of the pendant atoms increases, sterics between the pendant groups will increase (despite small changes in bond length). Increased steric interactions between pendant groups will prefer larger bond angles between the groups.

This trend fails, however, if we consider the molecules with hydrogen as the pendant atoms. Notice, for example, that H is the smallest pendant atom. If we consider the trend described above, we should assume that XH_3 (where X is a variable atom) would have the smallest bond angle in the series of XH_3, XF_3, XCl_3, and XBr_3. However this is not the case of NH_3, NF_3, and NCl_3, with bond angles 106.6°, 102.2°, and 106.8°, respectively. To explain the variation in these bond angles, we need to consider electronegativity.

Trends in Electronegativity

Now let's examine how electronegativity influences bond angles around a central atom. In VSEPR theory, **electronegativity of atoms/groups will affect bond angles due to changes in the distribution of electron pairs around the central atom (and thus changes in the severity of electron pair repulsion).** This really comes down to bond polarity caused by the difference in electronegativity between the central atom and pendant groups (bond polarity in the context of valence bond theory). In a polar bond, the more electronegative atom will pull electron density towards itself. When a pendant atom is more electronegative, it will pull the bonded electron pair towards itself and away from the central atom; this will reduce the electron pair repulsion between bonded electron pairs on the central atom. A decrease in electron pair repulsion on the central atom should decrease bond angles between the groups (Figure **3.9.3**).

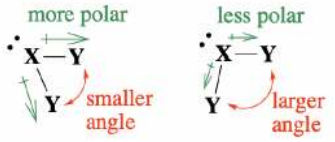


Figure **3.9.3**. When electron pairs are distributed away from the central atom, repulsions are decreased, allowing smaller bond angles. (Kathryn Haas; CC-NC-BY-SA)

Electronegativity is an alternative explanation to the trends we already examined above in Figure **3.9.2** . For example, when we compare the halogen pendant atoms (shaded region in Figure **3.9.2**) , the electronegativity of pendant groups decreases, bond polarity of the bonds decreases, and bond angles increase going from left to right and from F to Br. As more electron density remains on the central atom, electron repulsion between the bonded pairs increases and bond angles increase.

The electronegativity argument can also be used to explain the fact that NH_3 (106.6°) has a larger bond angle than NF_3 (102.2°). This particular case illustrates how electronegativity and size can be competing factors. While electronegativity differences seem to dominate in the case of NH_3 (106.6°) compared to NF_3 (102.2°), size differences still dominate in the cases of other XH_3 and XF_3 examples in Figure **3.9.2**).

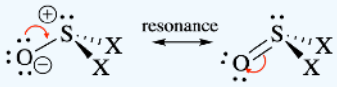
? Exercise 3.9.1

Predict the geometry and approximate bond angles. Then put the molecules in each series in order of smallest to largest bond angle. Defend your answer.

a. The X-S-X bond angle in OSF_2, $OSCl_2$, $OSBr_2$
b. H_2O, H_2S, H_2Se, H_2Te
c. H_2O, OF_2, OCl_2

Answer (a)

Geometry and predicted bond angles: These are molecules with steric number 4. They can be written as two different resonance structures, and the resonance hybrid would have double bond character between S and O.



We would expect a trigonal pyramidal geometry with all bond angles <109.5° because the lone pair is more repulsive than bonds. Because the double bond is more repulsive than single bonds, we should also expect the O-S-X bond angles to be greater than the X-S-X bond angles.

Trend: This is a series of molecules that varies in the identity of the pendant atoms; the variation is within the halogens. The size of the halogens increases, and the electronegativity decreases in the order F, Cl, Br. Both size and electronegativity would lead us to conclude that the X-S-X bond angles would increase in the order $OSF_2 < OSCl_2 < OSBr_2$

Explanation: (1) Increasing electonegativity of the pendant atom (F > Cl > Br) increases the polarity of the bond and reduces the electron density of the bonded pair on the central atom. This reduces the e-e repulsions of adjacent bonded electron pairs on S, allowing the halogens to become closer. The more electronegative pendant atoms can have smaller bond angles. (2) Increasing size of pendant atoms (F < Cl < Br) increases steric repulsions and increases bond angle. Both explanations lead to the same predicted trend.

The actual measured X-S-X bond angles are OSF_2 (92.3°) / $OSCl_2$ (96.2°) / $OSBr_2$ (98.2°). The trend in these bond angles is consistent with the prediction.

Answer (b)

Geometry and predicted bond angles: These are molecules with steric number 4, bent molecular geometry, with predicted bond angles <109.5° because the two lone pairs are each more repulsive than the bonds. There are two lone pairs and two single bonds to H around each central atom.

Trend: This is a series of molecules that varies in the identity of the central atom. The central atom increases in the order O < S < Se < Te, where Te is the largest element and O is the smallest. Arguments based on size would lead us to predict that the pendant groups of H_2Te would be less sterically crowded and thus have a smaller bond angle than the pendant groups of H_2O. The electronegativity decreases in the order O > S > Se > Te, where O is the most electronegative element and Te is the least. Thus, we expect the bonding electro pairs to be closer to the central atom on O than they would be on Te; we should expect H_2Te to have the least electron pair repulsions and thus smallest bond angle in this series, while H_2O would have the strongest electron pair repulsions and largest bond angles.

Both arguments lead to the same conclusion, that the order of increasing bond angle is $H_2Te < H_2Se < H_2S < H_2O$.

The actual measured bond angles are H_2Te (90.2°) / H_2Se (90.6°) / H_2S (92.1°) / H_2O (104.5). The trend in these bond angles is consistent with prediction.

Answer (c)

Geometry and predicted bond angles: These are molecules with steric number 4, bent molecular geometry, with predicted bond angles <109.5° because the two lone pairs are each more repulsive than the bonds. There are two lone pairs and two single bonds to H around each central atom. (This is similar to the case in (b)).

Trend: This is a series of molecules that varies in the identity of the pendant atoms; two of the molecules have halogens, and the other has hydrogen pendant atoms. This is a case where size and electronegativity will be conflicting factors because trends in electronegativity do not mirror the trend in size.

- *Size:* The size of pendant atoms increases in the order H < F < Cl where H is smallest and Cl is largest. Prediction of bond angles based on size alone would lead to the predicted order of increasing bond angle $H_2O < OF_2 < OCl_2$.
- *Electronegativity*: The electronegativity decreases in the order F > Cl > H where F has the greatest electronegativity and H has the least. Since we expect the most electronegative pendant atoms to have the smallest bond angles, prediction based on electronegativity alone would lead to the predicted order of increasing bond angle $OF_2 < OCl_2 < H_2O$.

The points above illustrate how the two different arguments would lead to different predictions about the trend in bond angle. This makes it difficult to predict the actual order of increasing bond angle. However, we saw above in the example of NH_3 vs NF_3 that electronegativity is more important than size; yet in the case of NH_3 vs NCl_3, the much larger size of the pendant atom is more important. If we apply this lesson to the current problem, we might predict the order $OF_2 < H_2O < OCl_2$, and in fact this more nuanced prediction, based on a similar case, matches the actual order for measured bond angles: OF_2 (103.3°) < H_2O (104.5°) < OCl_2 (110.9°).

Group Electronegativities

You probably heard the terms "electron donating group" and "electron withdrawing group" from your coursework in Organic Chemistry. For example, the acid trifluoroacetic acid (TFA) is more acidic than acetic acid due to the electron withdrawing effects of the CF_3 group compared to CH_3. CF_3 is an electron withdrawing group, while CH_3 is an electron donating group. In other words, CF_3 is more electronegative than CH_3.

The electron withdrawing ability (electronegativity) of groups can be estimated and compared, just as they are with atoms. Although there is no one scale that is used for group electronegativities, and published values even for the same groups vary widely, there are reliable trends within similar groups. The same size and electronegativity factors discussed above that affect bond angles for *pendant atoms*, also can be used to rationalize distorted bond angles for *pendant groups* around a central atom.

? Exercise 3.9.2

Consider the relative electronegativities and sizes of the pendant atoms/groups in the following examples. Is the trend in bond angles what you would expect from the relative group electronegativities and relative sizes? What, if any, is the more dominant factor in determining the trend?

a. $N(CH_3)_3$ has an C-N-C bond angle of 110.9°, while $N(CF_3)_3$ has a bond angle of 117.9°.
b. The X-S-X bond angles in molecules of the form $SO_2(X)_2$ are: $SO_2(OH)_2$ 101.3°; $SO_2(CF_3)_2$ 102.0°; $SO_2(CH_3)_2$ 102.6°.

Answer (a)

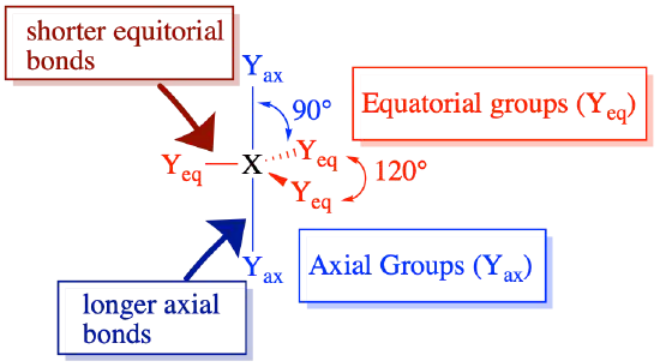
Add texts here. Do not delete this text first.

Answer (b)

Add texts here. Do not delete this text first.

Special case of electronegativity and size in steric number 5 (trigonal bypyramid)

Molecules with steric number 5 are interesting because they posses two different types of positions (equatorial and axial). These positions have unique bond angles and bond lengths. Pendant atoms/groups have different preferences for the axial and equatorial positions that depend somewhat on their electronegativity.



Molecules with steric number 5 possess different bond angles and lengths for axial (ax) and equatorial (eq) pendant atoms. (CC-BY-NC-SA; Kathryn Haas)

In a previous section, we discussed the preference of lone pairs and multiple bonds for the equatorial positions in trigonal bipyramidal molecules. VSEPR theory rationalizes this by assuming that lone pairs and multiple bonds are more repulsive than the electron pairs in single bonds. Equatorial positions are less crowded (with only two closest neighbors at 90°, and two farther neighbors at 120°) compared to axial positions (with three closest neighbors at 90°), thus the more repulsive groups prefer the less crowded equatorial positions.

Pendant groups that are more electronegative result in weaker electron pair repulsion around the central atom, while groups that are less electronegative result in stronger electron-pair repulsion around the central atom (as described above). The result for steric number 5: **bonding pairs to *less electronegative elements* are *more repulsive,* and *generally prefer equatorial* positions.** Still, lone pairs and multiple bonds are more repulsive than single bonds and would show a stronger preference for equatorial positions.

Examples and Nuances

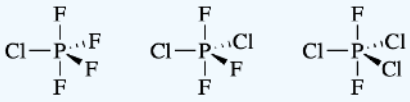
? Exercise 3.9.3

Some examples of molecule that demonstrate the equatorial preference of less electronegative groups are below. Predict (draw) their structures.

a. PF_4Cl, PF_3Cl_2, and PF_2Cl_3
b. $PF_4(CH_3)$ $PF_3(CH_3)_2$, and $PF_2(CH_3)_3$

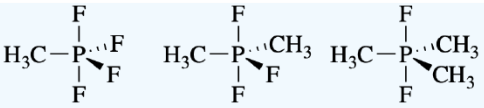
Answer (a)

Cl is less electronegative than F; thus we expect Cl to have stronger preference for the equatorial positions.

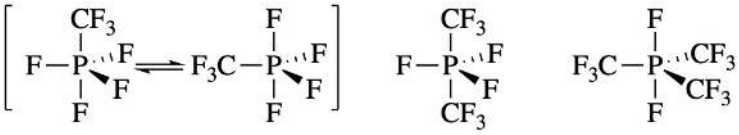


Answer (b)

CH_3, an electron donating group, is less electronegative than F. We expect CH_3 to have a stronger preference for the equatorial positions.



In the exercise above, the structures can be explained by the electronegativity of the pendant groups; less electronegative groups prefer the equatorial positions. There are other similar molecules for which explanations (or predictions) are difficult. For example, the series of molecules below seems to have completely random placement of F and CF_3 groups. **These structures could not be predicted based on VSEPR theory.** It seems that in this case, the more symmetrical arrangements of pendant groups is preferred.



References and resources

1. Pauling, L. (1932). "The Nature of the Chemical Bond. IV. The Energy of Single Bonds and the Relative Electronegativity of Atoms". *J. Am. Chem. Soc.* **54**(9): 3570–3582. doi:10.1021/ja01348a011.
2. Housecroft, Catherine E. et. al. "Inorganic Chemistry" 3rd Edition. Pearson Education Limited 2008. Chapter 2.5 "Electronegativity Values" pgs. 42-44
3. International Union of Pure and Applied Chemistry. "Electronegativity". goldbook.iupac.org/E01990.html.
4. Pearson, R.G. *Acc. Chem. Res.* 1990, 23, 1, 1–2. https://doi.org/10.1021/ar00169a001
5. Mulliken, R. S. (1934). "A New Electroaffinity Scale; Together with Data on Valence States and on Valence Ionization Potentials and Electron Affinities". *J. Chem. Phys.***2** (11): 782–793. doi:10.1063/1.1749394.
6. Mulliken, R. S. (1935). "Electronic Structures of Molecules XI. Electroaffinity, Molecular Orbitals and Dipole Moments". J. Chem. Phys. **3** (9): 573–585. doi:10.1063/1.1749731.
7. Allred, A. L.; Rochow, E. G. (1958). "A scale of electronegativity based on electrostatic force". *Journal of Inorganic and Nuclear Chemistry*. **5** (4): 264–268. doi:10.1016/0022-1902(58)80003-2
8. Sanderson, R. T. (1983). "Electronegativity and bond energy". *Journal of the American Chemical Society*. **105** (8): 2259–2261. doi:10.1021/ja00346a026
9. Pearson, R. G. (1985). "Absolute electronegativity and absolute hardness of Lewis acids and bases". J. Am. Chem. Soc. 107 (24): 6801. doi:10.1021/ja00310a009.
10. Allen, Leland C. (1989). "Electronegativity is the average one-electron energy of the valence-shell electrons in ground-state free atoms". Journal of the American Chemical Society. 111 (25): 9003–9014. doi:10.1021/ja00207a003.
11. Mann, Joseph B.; Meek, Terry L.; Allen, Leland C. (2000). "Configuration Energies of the Main Group Elements". Journal of the American Chemical Society. 122 (12): 2780–2783. doi:10.1021/ja992866e.
12. Mann, Joseph B.; Meek, Terry L.; Knight, Eugene T.; Capitani, Joseph F.; Allen, Leland C. (2000). "Configuration energies of the d-block elements". Journal of the American Chemical Society. 122 (21): 5132–5137. doi:10.1021/ja9928677

Acknowledgment

- Matthew Salem (UC Davis) (Pauling Electronegativity)
- Introduction to Inorganic Chemistry Wikibook (https://chem.libretexts.org/Bookshel..._Bond_Strength)
- Curated or created by Kathryn Haas

This page titled 3.9: Electronegativity and Atomic Size Effects is shared under a not declared license and was authored, remixed, and/or curated by Kathryn Haas.

- **3.2.3: Electronegativity and Atomic Size Effects** by Kathryn Haas is licensed CC BY-NC-SA 4.0.

3.10: Ligand Close Packing

Introduction

Ligand Close Packing (LCP) theory is complimentary to VSEPR, except that LCP focuses on repulsions between pendant *atoms* ("outer" atoms that are not directly bonded to one another), rather than focusing on the chemical environment around the central atom in a molecule. Both LCP and the VSEPR models were developed by Robert Gillespie.

The LCP model assumes that ligands (or pendant atoms) "pack" as closely as possible around a central atom. A given ligand will have a specific atomic radius when bound to a central atom. The distance between two ligands around the same central atom is simply the sum of the atomic radii of the pendant atoms. Therefore for a specific set of ligands around a specific central atom, the ligand-ligand distances are constant despite the coordination number or bond angles. In other words, for a series of similar molecules with the same central atom, while bond angles and bond distances of pendant atoms may change, the distances between two pendant atoms remain the same.

Ligand Close Packing Theory

According to LCP, distances between two pendant atoms are similar...

- even when steric number changes
- even when bond angles change
- Reason: pendant atoms "pack" around the central atom.

Ligand Close Packing and Bond Distances

If the distance between non-bonded atoms remains constant even while bond angles change, then the bond length between the pendant and central atom must change to accommodate. For example, $\mathbf{PF_4^+}$ and $\mathbf{PF_3O}$ have almost identical $\mathbf{F-F}$ distances of 238 and 237 pm, respectively. As expected from VSEPR, the $\mathbf{F-P-F}$ bond angle in $\mathbf{PF_4^+}$ is 109.5°. The $\mathbf{F-P-F}$ bond angle in $\mathbf{PF_3O}$ (101.1°) is smaller due to the increased repulsion of the oxygen double bond. Therefore the P-F bond lengths must be different. In fact, the P-F bond distances are 145.7 pm in $\mathbf{PF_4^+}$ and 154 pm in $\mathbf{PF_3O}$.

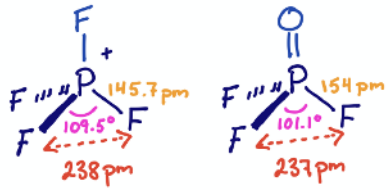


Figure **3.10.1**: The molecular structures of $\mathbf{PF_4^+}$ and $\mathbf{PF_3O}$. The distances between neighboring F atoms are similar in the two molecules, while bond lengths and angles differ. The $\mathbf{PF_4^+}$ ion has a $\mathbf{P-F}$ bond length of 145.7 pm, an $\mathbf{F-P-F}$ bond angle of 109.5°, and a distance of 238 pm between neighboring F atoms. The $\mathbf{PF_3O}$ molecule has a $\mathbf{P-F}$ bond length of 154 pm, an $\mathbf{F-P-F}$ bond angle of 101.1°, and a distance of 237 pm between neighboring F atoms. (CC-BY-NC-SA; Kathryn Haas)

The relationship between bond angles, bond lengths, and close-packing distance is described by right angle trigonometry (recall SOA-CAH-TOA). In a right triangle, the hypotenuse is the longest side, opposite to the right angle. For either of the other two angles in the triangle, the angle (θ) and lengths of the sides (*opposite* and *adjacent* to θ) are related by the trigometric functions shown in Figure **3.10.2** .



Figure **3.10.2**: Visual depiction of SOA-CAH-TOA. (CC-BY-NC-SA; Kathryn Haas)

In the case of a molecule, we can apply right angle trigonometry by imagining that the bond angle is divided into two right angles, as illustrated in Figure **3.10.2**. The hypotenuse of the triangles is the bond length, the opposite side is one half of the close-packing

distance, and θ is one half the bond angle.

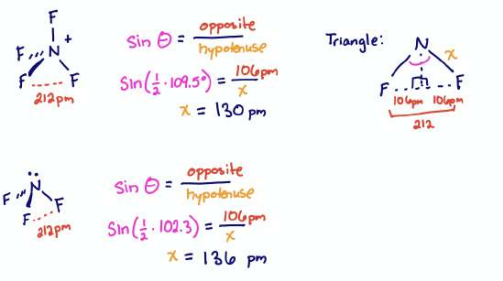


Figure 3.10.1: Illustration of how right angle trigonometry can be applied to determine bond angle, bond length, or distance between neighboring atoms: any bond angle can be divided into two right angles where the bond length is the hypotenuse, the distance between neighbors is twice the opposite side, and the bond angle is twice θ. (CC-BY-NC-SA; Kathryn Haas)

Exercise 3.10.1

The distance between F atoms is 212 pm in both NF_4^+ and NF_3. The bond angles are 109.5° and 102.3°, respectively. What are the expected $N-F$ bond lengths?

Answer



The actual measured bond lengths are 130 pm for NF_4^+ and 136.5 pm for NF_3.

Sources and Resources

- https://en.Wikipedia.org/wiki/LCP_th...ieNyholm1957-3

This page titled 3.10: Ligand Close Packing is shared under a not declared license and was authored, remixed, and/or curated by Kathryn Haas.

- **3.2.4: Ligand Close Packing** by Kathryn Haas is licensed CC BY-NC-SA 4.0.

3.11: Molecular Polarity

Dipole moments occur when there is a separation of charge. They can occur between two ions in an ionic bond or between atoms in a covalent bond; dipole moments arise from differences in electronegativity. The larger the difference in electronegativity, the larger the dipole moment. The distance between the charge separation is also a deciding factor in the size of the dipole moment. The dipole moment is a measure of the polarity of the molecule.

Introduction

When atoms in a molecule share electrons unequally, they create what is called a dipole moment. This occurs when one atom is more electronegative than another, resulting in that atom pulling more tightly on the shared pair of electrons, or when one atom has a lone pair of electrons and the difference of electronegativity vector points in the same way. One of the most common examples is the water molecule, made up of one oxygen atom and two hydrogen atoms. The differences in electronegativity and lone electrons give oxygen a partial negative charge and each hydrogen a partial positive charge.

Dipole Moment

When two electrical charges, of opposite sign and equal magnitude, are separated by a distance, an electric dipole is established. The size of a dipole is measured by its dipole moment (μ). Dipole moment is measured in Debye units, which is equal to the distance between the charges multiplied by the charge (1 Debye equals $3.34 \times 10^{-30}\ C\,m$). The dipole moment of a molecule can be calculated by Equation 3.11.1:

$$\vec{\mu} = \sum_i q_i \vec{r}_i \tag{3.11.1}$$

where

- $\vec{\mu}$ is the dipole moment vector
- q_i is the magnitude of the i^{th} charge, and
- $\vec{r}_i$ is the vector representing the position of i^{th} charge.

The dipole moment acts in the direction of the vector quantity. An example of a polar molecule is H_2O. Because of the lone pair on oxygen, the structure of H_2O is bent (via VSEPR theory), which means that the vectors representing the dipole moment of each bond do not cancel each other out. Hence, water is polar.

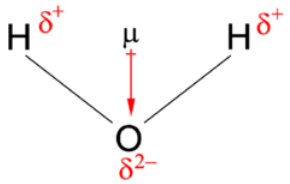


Figure 3.11.1: Dipole moment of water. The convention in chemistry is that the arrow representing the dipole moment goes from positive to negative. Physicist tend to use the opposite orientation.

The vector points from positive to negative, on both the molecular (net) dipole moment and the individual bond dipoles. Table A2 shows the electronegativity of some of the common elements. The larger the difference in electronegativity between the two atoms, the more electronegative that bond is. To be considered a polar bond, the difference in electronegativity must be large. The dipole moment points in the direction of the vector quantity of each of the bond electronegativities added together.

It is relatively easy to measure dipole moments: just place a substance between charged plates (Figure 3.11.2); polar molecules increase the charge stored on the plates, and the dipole moment can be obtained (i.e., via the capacitance of the system). Nonpolar CCl_4 is not deflected; moderately polar acetone deflects slightly; highly polar water deflects strongly. In general, polar molecules will align themselves: (1) in an electric field, (2) with respect to one another, or (3) with respect to ions (Figure 3.11.2).

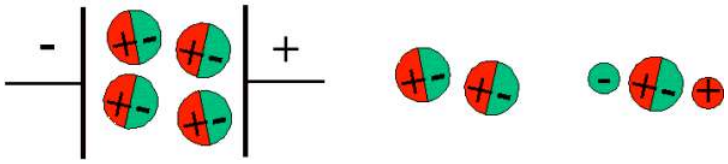


Figure **3.11.2**: Polar molecules align themselves in an electric field (left), with respect to one another (middle), and with respect to ions (right)

Equation 3.11.1 can be simplified for a simple separated two-charge system like diatomic molecules or when considering a bond dipole within a molecule

$$\mu_{diatomic} = Q \times r \tag{3.11.2}$$

This bond dipole is interpreted as the dipole from a charge separation over a distance r between the partial charges Q^+ and Q^- (or the more commonly used terms δ^+ - δ^-); the orientation of the dipole is along the axis of the bond. Consider a simple system of a single electron and proton separated by a fixed distance. When the proton and electron are close together, the dipole moment (degree of polarity) decreases. However, as the proton and electron get farther apart, the dipole moment increases. In this case, the dipole moment is calculated as (via Equation 3.11.2):

$$\begin{aligned} \mu &= Qr \\ &= (1.60 \times 10^{-19}\, C)(1.00 \times 10^{-10}\, m) \\ &= 1.60 \times 10^{-29}\, C \cdot m \end{aligned}$$

The Debye characterizes the size of the dipole moment. When a proton and electron are 100 pm apart, the dipole moment is $4.80\ D$:

$$\begin{aligned} \mu &= (1.60 \times 10^{-29}\, C \cdot m)\left(\frac{1\ D}{3.336 \times 10^{-30}\, C \cdot m}\right) \\ &= 4.80\ D \end{aligned}$$

$4.80\ D$ is a key reference value and represents a pure charge of +1 and -1 separated by 100 pm. If the charge separation is increased then the dipole moment increases (linearly):

- If the proton and electron are separated by 120 pm:

$$\mu = \frac{120}{100}(4.80\ D) = 5.76\ D \tag{3.11.3}$$

- If the proton and electron are separated by 150 pm:

$$\mu = \frac{150}{100}(4.80\ D) = 7.20\ D \tag{3.11.4}$$

- If the proton and electron are separated by 200 pm:

$$\mu = \frac{200}{100}(4.80\ D) = 9.60\ D \tag{3.11.5}$$

Example 3.11.1: Water

The water molecule in Figure **3.11.1** can be used to determine the direction and magnitude of the dipole moment. From the electronegativities of oxygen and hydrogen, the difference in electronegativity is 1.2e for each of the hydrogen-oxygen bonds. Next, because the oxygen is the more electronegative atom, it exerts a greater pull on the shared electrons; it also has two lone pairs of electrons. From this, it can be concluded that the dipole moment points from between the two hydrogen atoms toward the oxygen atom. Using the equation above, the dipole moment is calculated to be 1.85 D by multiplying the distance between the oxygen and hydrogen atoms by the charge difference between them and then finding the components of each that point in the direction of the net dipole moment (the angle of the molecule is 104.5˚).

The bond moment of the O-H bond =1.5 D, so the net dipole moment is

$$\mu = 2(1.5)\cos\left(\frac{104.5^\circ}{2}\right) = 1.84\ D$$

Polarity and Structure of Molecules

The shape of a molecule and the polarity of its bonds determine the OVERALL POLARITY of that molecule. A molecule that contains polar bonds might not have any overall polarity, depending upon its shape. The simple definition of whether a complex molecule is polar or not depends upon whether its overall centers of positive and negative charges overlap. If these centers lie at the same point in space, then the molecule has no overall polarity (and is non polar). If a molecule is completely symmetric, then the dipole moment vectors on each molecule will cancel each other out, making the molecule nonpolar. A molecule can only be polar if the structure of that molecule is not symmetric.

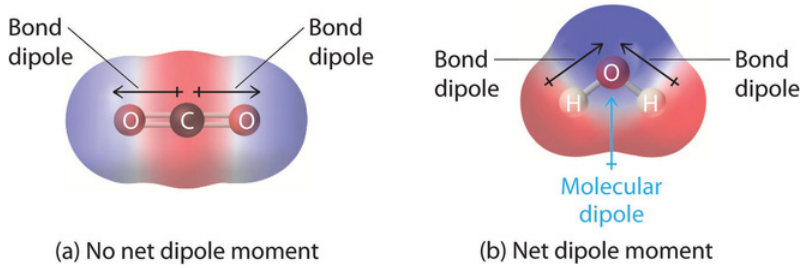


Figure 3.11.3: Charge distributions of CO_2 and H_2O\). Blue and red colored regions are negatively and positively signed regions, respectively. (CC BY-SA-NC 3.0; anonymous)

A good example of a nonpolar molecule that contains polar bonds is carbon dioxide (Figure 3.11.3*a*). This is a linear molecule and each C=O bond is, in fact, polar. The central carbon will have a net positive charge, and the two outer oxygen atoms a net negative charge. However, since the molecule is linear, these two bond dipoles cancel each other out (i.e. the vector addition of the dipoles equals zero) and the overall molecule has a zero dipole moment ($\mu = 0$).

> *Although a polar bond is a prerequisite for a molecule to have a dipole, not all molecules with polar bonds exhibit dipoles*

For AB_n molecules, where A is the central atom and B are all the same types of atoms, there are certain molecular geometries which are symmetric. Therefore, they will have no dipole even if the bonds are polar. These geometries include linear, trigonal planar, tetrahedral, octahedral and trigonal bipyramid.

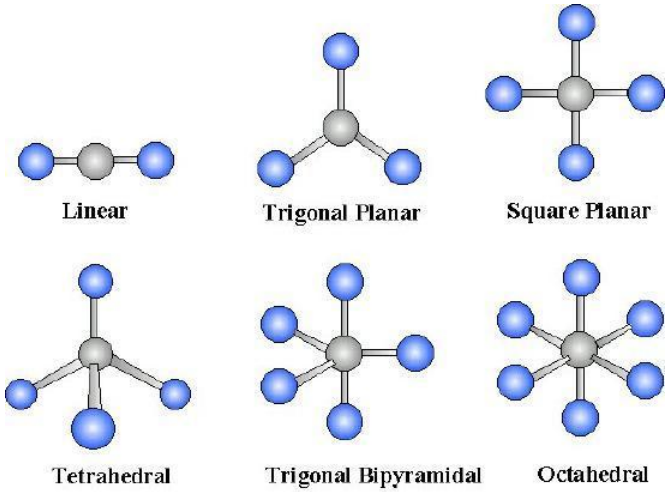
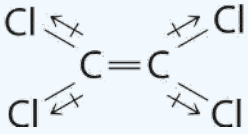


Figure 3.11.4: Molecular geometries with exact cancellation of polar bonding to generate a non-polar molecule ($\mu = 0$)

Example 3.11.3: C_2Cl_4

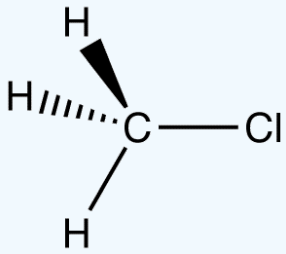
Although the C–Cl bonds are rather polar, the individual bond dipoles cancel one another in this symmetrical structure, and $Cl_2C{=}CCl_2$ does not have a net dipole moment.



Example 3.11.3: CH_3Cl

C-Cl, the key polar bond, is 178 pm. Measurement reveals 1.87 D. From this data, % ionic character can be computed. If this bond were 100% ionic (based on proton & electron),

$$\mu = \frac{178}{100}(4.80\ D)$$
$$= 8.54\ D$$



Although the bond length is ***increasing***, the dipole is ***decreasing*** as you move down the halogen group. The electronegativity decreases as we move down the group. Thus, the greater influence is the electronegativity of the two atoms (which influences the ***charge*** at the ends of the dipole).

Table **3.11.1**: Relationship between Bond length, Electronegativity and Dipole moments in simple Diatomics

Compound	Bond Length (Å)	Electronegativity Difference	Dipole Moment (D)
HF	0.92	1.9	1.82
HCl	1.27	0.9	1.08
HBr	1.41	0.7	0.82
HI	1.61	0.4	0.44

References

1. *Housecroft, Catherine E. and Alan G. Sharpe. Inorganic Chemistry. 3rd ed. Harlow: Pearson Education, 2008. Print. (Pages 44-46)*
2. *Tro, Nivaldo J. Chemistry: A Molecular Approach. Upper Saddle River: Pearson Education, 2008. Print. (Pages 379-386)*

This page titled 3.11: Molecular Polarity is shared under a not declared license and was authored, remixed, and/or curated by Kathryn Haas.

- **Dipole Moments** by Delmar Larsen, Mike Blaber is licensed CC BY 4.0.

3.12: Hydrogen Bonding

A hydrogen bond is an intermolecular force (IMF) that forms a special type of dipole-dipole attraction when a hydrogen atom bonded to a strongly electronegative atom exists in the vicinity of another electronegative atom with a lone pair of electrons. Intermolecular forces (IMFs) occur between molecules. Other examples include ordinary dipole-dipole interactions and dispersion forces. Hydrogen bonds are are generally stronger than ordinary dipole-dipole and dispersion forces, but weaker than true covalent and ionic bonds.

The evidence for hydrogen bonding

Many elements form compounds with hydrogen. If you plot the boiling points of the compounds of the group 14 elements with hydrogen, you find that the boiling points increase as you go down the group.

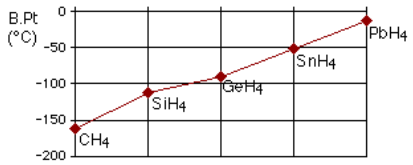


Figure 1: Boiling points of group 14 elemental halides.

The increase in boiling point happens because the molecules are getting larger with more electrons, and so van der Waals dispersion forces become greater. If you repeat this exercise with the compounds of the elements in groups 15, 16, and 17 with hydrogen, something odd happens.

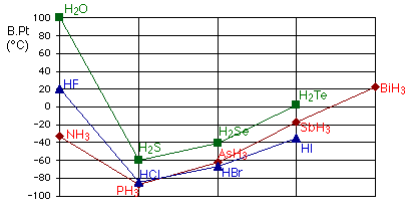


Figure 2: Boiling points of group 15-17 elemental halides.

Although the same reasoning applies for group 4 of the periodic table, the boiling point of the compound of hydrogen with the first element in each group is abnormally high. In the cases of NH_3, H_2O and HF there must be some additional intermolecular forces of attraction, requiring significantly more heat energy to break the IMFs. These relatively powerful intermolecular forces are described as hydrogen bonds.

Origin of Hydrogen Bonding

The molecules capable of hydrogen bonding include the following:

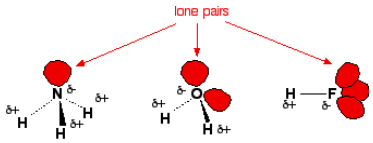


Figure 3: The lone pairs responsible for hydrogen bonding in NH_3, H_2O, and HF. The solid line represents a bond in the plane of the screen or paper. Dotted bonds are going back into the screen or paper away from you, and wedge-shaped ones are coming out towards you.

Notice that in each of these molecules:

- The hydrogen is attached directly to a highly electronegative atoms, causing the hydrogen to acquire a highly positive charge.
- Each of the highly electronegative atoms attains a high negative charge and has at least one "active" lone pair. Lone pairs at the 2-level have electrons contained in a relatively small volume of space, resulting in a high negative charge density. Lone pairs at higher levels are more diffuse and, resulting in a lower charge density and lower affinity for positive charge.

> *If you are not familiar with electronegativity, you should follow this link before you go on.*

Consider two water molecules coming close together.

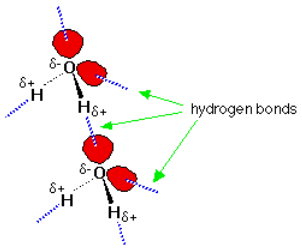


Figure 4: Hydrogen bonding in water

The δ^+ hydrogen is so strongly attracted to the lone pair that it is almost as if you were beginning to form a co-ordinate (dative covalent) bond. It doesn't go that far, but the attraction is significantly stronger than an ordinary dipole-dipole interaction. Hydrogen bonds have about a tenth of the strength of an average covalent bond, and are constantly broken and reformed in liquid water. If you liken the covalent bond between the oxygen and hydrogen to a stable marriage, the hydrogen bond has "just good friends" status.

Water is an ideal example of hydrogen bonding. Notice that each water molecule can potentially form four hydrogen bonds with surrounding water molecules: two with the hydrogen atoms and two with the with the oxygen atoms. There are exactly the right numbers of δ^+ hydrogens and lone pairs for every one of them to be involved in hydrogen bonding.

This is why the boiling point of water is higher than that of ammonia or hydrogen fluoride. In the case of ammonia, the amount of hydrogen bonding is limited by the fact that each nitrogen only has one lone pair. In a group of ammonia molecules, there are not enough lone pairs to go around to satisfy all the hydrogens. In hydrogen fluoride, the problem is a shortage of hydrogens. In water, two hydrogen bonds and two lone pairs allow formation of hydrogen bond interactions in a lattice of water molecules. Water is thus considered an ideal hydrogen bonded system.

More complex examples of hydrogen bonding

The hydration of negative ions

When an ionic substance dissolves in water, water molecules cluster around the separated ions. This process is called hydration. Water frequently attaches to positive ions by co-ordinate (dative covalent) bonds. It bonds to negative ions using hydrogen bonds.

> *If you are interested in the bonding in hydrated positive ions, you could follow this link to co-ordinate (dative covalent) bonding.*

The diagram shows the potential hydrogen bonds formed with a chloride ion, Cl-. Although the lone pairs in the chloride ion are at the 3-level and would not normally be active enough to form hydrogen bonds, they are made more attractive by the full negative charge on the chlorine in this case.

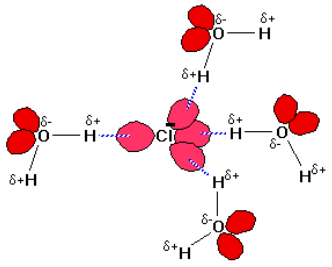


Figure 5: Hydrogen bonding between chloride ions and water.

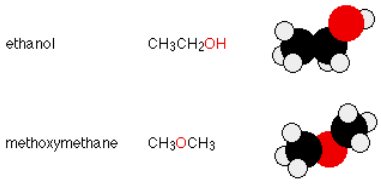
However complicated the negative ion, there will always be lone pairs that the hydrogen atoms from the water molecules can hydrogen bond to.

Hydrogen bonding in alcohols

An alcohol is an organic molecule containing an -OH group. Any molecule which has a hydrogen atom attached directly to an oxygen or a nitrogen is capable of hydrogen bonding. Hydrogen bonds also occur when hydrogen is bonded to fluorine, but the HF

group does not appear in other molecules. Molecules with hydrogen bonds will always have higher boiling points than similarly sized molecules which don't have an -O-H or an -N-H group. The hydrogen bonding makes the molecules "stickier," such that more heat (energy) is required to separate them. This phenomenon can be used to analyze boiling point of different molecules, defined as the temperature at which a phase change from liquid to gas occurs.

Ethanol, $\mathbf{CH_3CH_2{-}O{-}H}$, and methoxymethane, $\mathbf{CH_3{-}O{-}CH_3}$, both have the same molecular formula, $\mathbf{C_2H_6O}$.

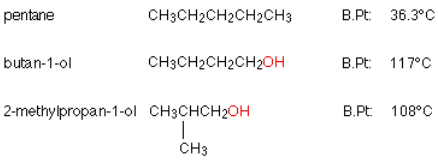


They have the same number of electrons, and a similar length. The van der Waals attractions (both dispersion forces and dipole-dipole attractions) in each will be similar. However, ethanol has a hydrogen atom attached directly to an oxygen; here the oxygen still has two lone pairs like a water molecule. Hydrogen bonding can occur between ethanol molecules, although not as effectively as in water. The hydrogen bonding is limited by the fact that there is only one hydrogen in each ethanol molecule with sufficient $\delta+$ charge.

In methoxymethane, the lone pairs on the oxygen are still there, but the hydrogens are not sufficiently $\delta+$ for hydrogen bonds to form. Except in some rather unusual cases, the hydrogen atom has to be attached directly to the very electronegative element for hydrogen bonding to occur. The boiling points of ethanol and methoxymethane show the dramatic effect that the hydrogen bonding has on the stickiness of the ethanol molecules:

ethanol (with hydrogen bonding)	78.5°C
methoxymethane (without hydrogen bonding)	-24.8°C

The hydrogen bonding in the ethanol has lifted its boiling point about 100°C. It is important to realize that hydrogen bonding exists in addition to van der Waals attractions. For example, all the following molecules contain the same number of electrons, and the first two have similar chain lengths. The higher boiling point of the butan-1-ol is due to the additional hydrogen bonding.



Comparing the two alcohols (containing -OH groups), both boiling points are high because of the additional hydrogen bonding; however, the values are not the same. The boiling point of the 2-methylpropan-1-ol isn't as high as the butan-1-ol because the branching in the molecule makes the van der Waals attractions less effective than in the longer butan-1-ol.

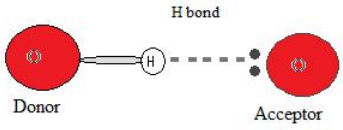
Hydrogen bonding in organic molecules containing nitrogen

Hydrogen bonding also occurs in organic molecules containing N-H groups; recall the hydrogen bonds that occur with ammonia. Examples range from simple molecules like CH_3NH_2 (methylamine) to large molecules like proteins and DNA. The two strands of the famous double helix in DNA are held together by hydrogen bonds between hydrogen atoms attached to nitrogen on one strand, and lone pairs on another nitrogen or an oxygen on the other one.

Donors and Acceptors

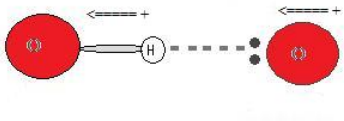
In order for a hydrogen bond to occur there must be both a hydrogen donor and an acceptor present. The donor in a hydrogen bond is usually a strongly electronegative atom such as N, O, or F that is covalently bonded to a hydrogen bond.

The hydrogen acceptor is an electronegative atom of a neighboring molecule or ion that contains a lone pair that participates in the hydrogen bond.



Why does a hydrogen bond occur?

Since the hydrogen donor (N, O, or F) is strongly electronegative, it pulls the covalently bonded electron pair closer to its nucleus, and away from the hydrogen atom. The hydrogen atom is then left with a partial positive charge, creating a dipole-dipole attraction between the hydrogen atom bonded to the donor and the lone electron pair of the acceptor. This results in a hydrogen bond.(see Interactions Between Molecules With Permanent Dipoles)

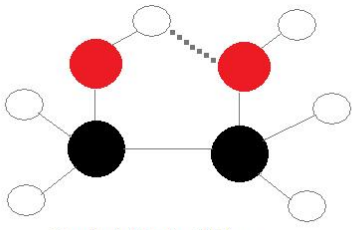


Types of hydrogen bonds

Although hydrogen bonds are well-known as a type of IMF, these bonds can also occur within a single molecule, between two identical molecules, or between two dissimilar molecules.

Intramolecular hydrogen bonds

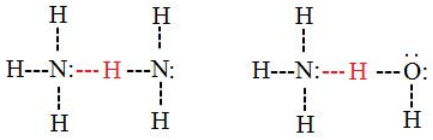
Intramolecular hydrogen bonds are those which occur *within* one single molecule. This occurs when two functional groups of a molecule can form hydrogen bonds with each other. In order for this to happen, both a hydrogen donor a hydrogen acceptor must be present within one molecule, and they must be within close proximity of each other in the molecule. For example, intramolecular hydrogen bonding occurs in ethylene glycol ($C_2H_4(OH)_2$) between its two hydroxyl groups due to the molecular geometry.



Intramolecular h-bonding in Ethylene Glycol molecule

Intermolecular hydrogen bonds

Intermolecular hydrogen bonds occur *between* separate molecules in a substance. They can occur between any number of like or unlike molecules as long as hydrogen donors and acceptors are present in positions where they can interact with one another. For example, intermolecular hydrogen bonds can occur between NH_3 molecules alone, between H_2O molecules alone, or between NH_3 and H_2O molecules.



Properties and effects of hydrogen bonds

On Boiling Point

When we consider the boiling points of molecules, we usually expect molecules with larger molar masses to have higher normal boiling points than molecules with smaller molar masses. This, without taking hydrogen bonds into account, is due to greater dispersion forces (see Interactions Between Nonpolar Molecules). Larger molecules have more space for electron distribution and thus more possibilities for an instantaneous dipole moment. However, when we consider the table below, we see that this is not always the case.

Compound	Molar Mass	Normal Boiling Point
H_2O	18 g/mol	373 K
HF	20 g/mol	292.5 K
NH_3	17 g/mol	239.8 K
H_2S	34 g/mol	212.9 K
HCl	36.4 g/mol	197.9 K
PH_3	34 g/mol	185.2 K

We see that H_2O, HF, and NH_3 each have higher boiling points than the same compound formed between hydrogen and the next element moving down its respective group, indicating that the former have greater intermolecular forces. This is because H_2O, HF, and NH_3 all exhibit hydrogen bonding, whereas the others do not. Furthermore, H_2O has a smaller molar mass than HF but partakes in more hydrogen bonds per molecule, so its boiling point is higher.

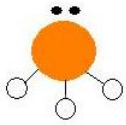
On Viscosity

The same effect that is seen on boiling point as a result of hydrogen bonding can also be observed in the viscosity of certain substances. Substances capable of forming hydrogen bonds tend to have a higher viscosity than those that do not form hydrogen bonds. Generally, substances that have the possibility for multiple hydrogen bonds exhibit even higher viscosities.

Factors preventing Hydrogen bonding

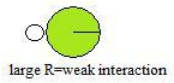
Electronegativity

Hydrogen bonding cannot occur without significant electronegativity differences between hydrogen and the atom it is bonded to. Thus, we see molecules such as PH_3, which do not participate in hydrogen bonding. PH_3 exhibits a trigonal pyramidal molecular geometry like that of ammonia, but unlike NH_3 it cannot hydrogen bond. This is due to the similarity in the electronegativities of phosphorous and hydrogen. Both atoms have an electronegativity of 2.1, and thus, there is no dipole moment. This prevents the hydrogen atom from acquiring the partial positive charge needed to hydrogen bond with the lone electron pair in another molecule. (see Polarizability)



Atom Size

The size of donors and acceptors can also affect the ability to hydrogen bond. This can account for the relatively low ability of Cl to form hydrogen bonds. When the radii of two atoms differ greatly or are large, their nuclei cannot achieve close proximity when they interact, resulting in a weak interaction.

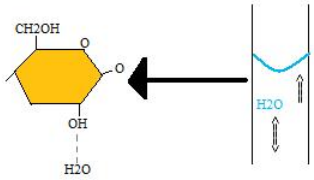


Hydrogen Bonding in Nature

Hydrogen bonding plays a crucial role in many biological processes and can account for many natural phenomena such as the Unusual properties of Water. In addition to being present in water, hydrogen bonding is also important in the water transport system of plants, secondary and tertiary protein structure, and DNA base pairing.

Plants

The cohesion-adhesion theory of transport in vascular plants uses hydrogen bonding to explain many key components of water movement through the plant's xylem and other vessels. Within a vessel, water molecules hydrogen bond not only to each other, but also to the cellulose chain that comprises the wall of plant cells. Since the vessel is relatively small, the attraction of the water to the cellulose wall creates a sort of capillary tube that allows for capillary action. This mechanism allows plants to pull water up into their roots. Furthermore, hydrogen bonding can create a long chain of water molecules, which can overcome the force of gravity and travel up to the high altitudes of leaves.



Proteins

Hydrogen bonding is present abundantly in the secondary structure of proteins, and also sparingly in tertiary conformation. The secondary structure of a protein involves interactions (mainly hydrogen bonds) between neighboring polypeptide backbones which contain nitrogen-hydrogen bonded pairs and oxygen atoms. Since both N and O are strongly electronegative, the hydrogen atoms bonded to nitrogen in one polypeptide backbone can hydrogen bond to the oxygen atoms in another chain and vice-versa. Though they are relatively weak, these bonds offer substantial stability to secondary protein structure because they repeat many times and work collectively.

In tertiary protein structure, interactions are primarily between functional R groups of a polypeptide chain; one such interaction is called a hydrophobic interaction. These interactions occur because of hydrogen bonding between water molecules around the hydrophobe that further reinforces protein conformation.

References

1. Brown, et al. Chemistry:The Central Science. 11th ed. Upper Saddle River, New Jersey: Pearson/Prentice Hall, 2008.
2. Chang, Raymond. General Chemistry:The Essential Concepts. 3rd ed. New York: Mcgraw Hill, 2003
3. Petrucci, et al. General Chemistry: Principles & Modern Applications. 9th ed. Upper Saddle River, New Jersey: Pearson/Prentice Hall, 2007.

3.12: Hydrogen Bonding is shared under a not declared license and was authored, remixed, and/or curated by LibreTexts.

- **Hydrogen Bonding** by Jim Clark, Jose Pietri is licensed CC BY-NC-SA 4.0.

CHAPTER OVERVIEW

4: Coordination Chemistry I- Structures and Isomers

4.1: Prelude to Coordination Chemistry I - Structure and Isomers

4.2: History

4.3: Nomenclature and Ligands

4.4: Isomerism

4.5: Coordination Numbers and Structures

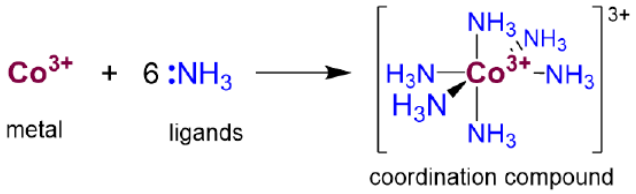
4.6: Coordination Frameworks

4: Coordination Chemistry I- Structures and Isomers is shared under a not declared license and was authored, remixed, and/or curated by LibreTexts.

4.1: Prelude to Coordination Chemistry I - Structure and Isomers

What is a coordination compound?

Coordination compounds consist of one or more **metals** bound to one or more Lewis base **ligands**. For example, hexammineruthenium (3+) ion is a coordination complex in which six ammonia ligands coordinate a Co^{3+} ion, as shown in Scheme **4.1.1**.



Scheme **4.1.1**: Formation of hexammineruthenium(3+) ion from Co^{3+} and NH_3. (CC BY 4.0; Stephen Contakes)

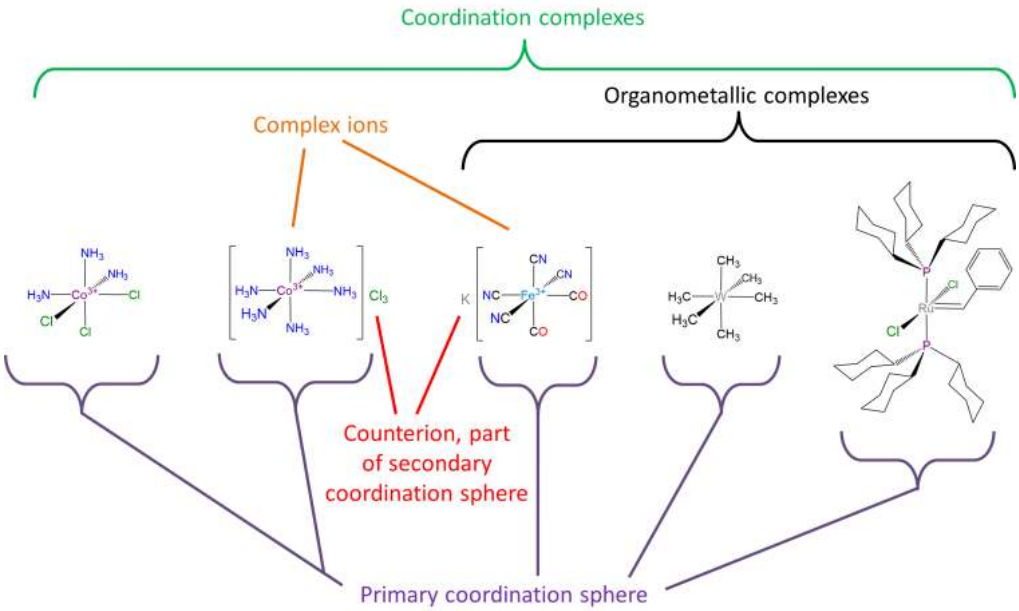
Such complexes are called coordination complexes because the ligand-metal bond may be thought of as a **coordinate covalent bond** in which both of the bonding electrons come from the ligand, which is then said to **coordinate** the metal. This coordinate covalent model is a very useful formalism for understanding the basic features of coordination chemistry, although it does not always accurately reflect the actual details of the bonding in every coordination complex. Nevertheless, even in those cases where the simple coordinate covalent bond model breaks down, the coordinate covalent bond concept supplies the language sophisticated models employ to describe the more complex bonding involved.

Additional important terms

Some of the common widely used terms that follow from the coordinate covalent model of bonding in coordination complexes include:

- Coordination compounds are also called **coordination complexes**, **metal complexes**, or just **complexes**. The term **complex** refers to coordination compounds' composite nature, in that they may be thought of as comprising multiple ligand and metal ion parts that can be restored by breaking the coordinate covalent bonds holding the complex together. This is in contrast to inorganic or organic molecules which are more commonly thought about as whole molecules held together by the sharing of electrons contributed by all the atoms.
- Coordination complexes that are ions are called **complex ions.**
- Ligands bound to the coordination complex are said to reside in the **primary** or **inner coordination sphere**. These bound ligands are not readily exchangeable, in contrast to nearby counterions and solvent molecules, which are said to reside in the **secondary** or **outer coordination sphere**.
- The portion of the complex contributing the electron pairs is said to be the **donor** and the portion which receives them the **acceptor**. In conventional coordination compounds the ligand is the donor and the metal the acceptor. In these cases it would be equally convenient to refer to the ligand donor as the Lewis base and the metal acceptor as the Lewis acid. However, in more complex bonding scenarios there may be multiple electron pair donation and acceptance interactions taking place between each pair of atoms and donor-acceptor language will be more convenient.
- The number of ligand sites donating lone pairs to the central atom is referred to as the **coordination number**. For most complexes this will just be equal to the number of ligand atoms bound to the metal. In simple complexes it is just equal to the number of ligands. For instance, the cobalt in Scheme **4.1.1** has a coordination number of six.
- Although technically compounds with metal-carbon bonds are coordination complexes, the term coordination complex is sometimes used to refer to complexes which do not possess metal-carbon bonds in their primary coordination sphere. Complexes which possess metal-carbon bonds are called **organometallic compounds** instead. The use of the terms organometallic and coordination to distinguish organometallic compounds from other types of coordination compounds is often convenient since many organometallic ligands engage in more than simple σ donor-acceptor coordinate covalent bond formation with the metal center. However, this is true of some wholly inorganic ligands too, so it should always be kept in mind that organometallic compounds are just a type of coordination compound and that inorganic ligands can in principle be tuned to interact with a metal center in much the same way an organic ligand does.

A summary of some of the concepts and terms used to describe coordination compounds is given in Scheme **4.1.2**.



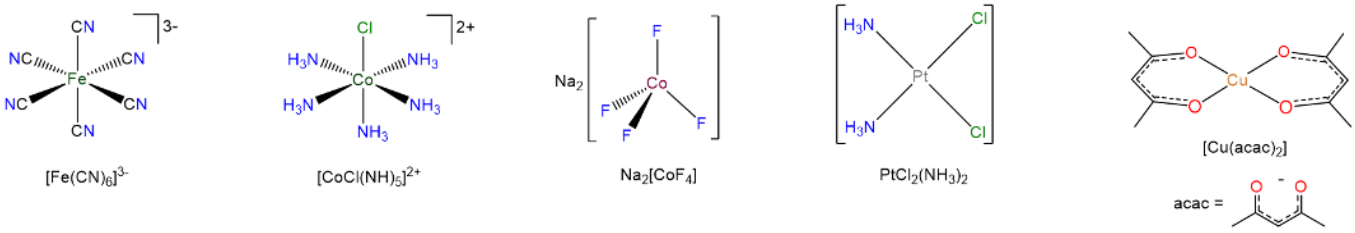
Scheme **4.1.2**: Some terms used to describe coordination compounds. (CC BY 4.0; Stephen Contakes)

The formulae of coordination complexes

The way the formulae of coordination complexes are written reflects the fact that it is often convenient to think of coordination compounds as a composite of metals and ligands. When writing the formula of a complex

- the atoms of a ligand are not added to those of the rest of the compound. Instead, the ligand atoms are kept together, if necessary by enclosing the ligand formula in parentheses or giving an abbreviation for the ligand.
- For complex ions the metal and ligands are enclosed in square brackets. Sometimes this is also done for neutral coordination compounds as well. In either case the brackets enclose those parts of the compound which comprise the primary coordination sphere; anything else is in the secondary coordination sphere outside.

A careful perusal of the examples in Scheme **4.1.3** should make the important features of this system clear.



Scheme **4.1.3**: Formulae of coordination compounds and complex ions. (CC BY 4.0; Stephen Contakes)

4.1: Prelude to Coordination Chemistry I - Structure and Isomers is shared under a CC BY 4.0 license and was authored, remixed, and/or curated by Stephen M. Contakes.

- **9.1: Prelude to Coordination Chemistry I - Structure and Isomers** by Stephen M. Contakes is licensed CC BY 4.0.

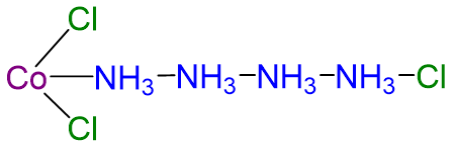
4.2: History

History of the Coordination Compounds

Coordination compounds have been known and used since antiquity; one of the oldest synthetic pigments is the blue pigment Egyptian blue, a copper complex of formula $CaCuSi_4O_{10}$ used by the Egyptians since the third Millenium B.C. (in ancient China the Ba analogue, Han blue, was discovered independently). The blue color of Egyptian blue is due to interlocked $Cu(Si_2O_7)_4$ units in which each copper is coordinated by four O atoms in a square planar arrangement. Later, in 1706, the Berlin painter Diesbach would discover another deep blue pigment, Prussian blue: $KFe_2(CN)_6$.

Despite their long use, the chemical nature of coordination compounds was unclear for a number of reasons. For example, many compounds called "double salts" were known, such as $AlF_3 \cdot 3\,KF$, $Fe(CN)_2 \cdot 4\,KCN$, and $ZnCl_2 \cdot 2\,CsCl$, which were combinations of simple salts in fixed and apparently arbitrary ratios. Why should $AlF_3 \cdot 3\,KF$ exist but not $AlF_3 \cdot 4\,KF$ or $AlF_3 \cdot 2\,KF$? And why should a 3:1 KF:AlF_3 mixture have different chemical and physical properties than either of its components? Similarly, adducts of metal salts with neutral molecules such as ammonia were also known—for example, $CoCl_3 \cdot 6\,NH_3$, which was first prepared sometime before 1798. Like the double salts, the compositions of these adducts exhibited fixed and apparently arbitrary ratios of the components. For example, $CoCl_3 \cdot 6\,NH_3$, $CoCl_3 \cdot 5\,NH_3$, $CoCl_3 \cdot 4\,NH_3$, and $CoCl_3 \cdot 3\,NH_3$ were all known and had very different properties, but despite all attempts, chemists could not prepare $CoCl_3 \cdot 2\,NH_3$ or $CoCl_3 \cdot NH_3$.

Although the chemical composition of such compounds was readily established by existing analytical methods, their chemical nature was puzzling and highly controversial. The major problem was that what we now call valence (i.e., the oxidation state) and coordination number were thought to be identical. As a result, highly implausible (to modern eyes at least) structures were proposed for such compounds. Of these the most influential was the Blomstrand-Jørgensen chain theory of bonding in coordination compounds, which predicted the "Chattanooga choo-choo" model for $CoCl_3{\cdot}4NH_3$ shown in Scheme **4.2.I**.



Scheme **4.2.I**. Blomstrand-Jørgensen chain theory model of bonding in $CoCl_3{\cdot}4NH_3$.

Nevertheless, this theory was not wholly illogical and, in fact, explained much of the analytical data on coordination compounds available to chemists of the time. This data included the electrical conductivity of aqueous solutions of these compounds, which was roughly proportional to the number of ions formed per mole, and the number of free chloride ions present, which could be determined by precipitating them gravimetrically as AgCl. In the case of $CoCl_3{\cdot}4NH_3$, two ions and one chloride were produced when the compound was dissolved in water, which Jørgensen was able to explain using the chain structure shown above by postulating that chlorides attached to NH_3 could dissociate while those attached to Co could not. The modern theory of coordination chemistry, which overthrew the chain theory, is based largely on the work of Alfred Werner (1866–1919; Nobel Prize in Chemistry in 1913). In a series of careful experiments carried out in the late 1880s and early 1890s, he examined the properties of several series of metal halide complexes with ammonia. For example, five different "adducts" of ammonia with $PtCl_4$ were known at the time: $PtCl_4{\cdot}nNH_3$ (n = 2–6). Some of Werner's original data on these compounds are shown in Table **4.2.1**. Werner's data on $PtCl_4{\cdot}6NH_3$ in Table **4.2.1** showed that all the chloride ions were present as free chloride. In contrast, $PtCl_4{\cdot}2NH_3$, was a neutral molecule that did not give free chloride ions when dissolved in water.

Alfred Werner (1866–1919)

Werner, the son of a factory worker, was born in Alsace. He developed an interest in chemistry at an early age, and he did his first independent research experiments at age 18. While doing his military service in southern Germany, he attended a series of chemistry lectures, and he subsequently received his PhD at the University of Zurich in Switzerland, where he was appointed professor of chemistry at age 29. He won the Nobel Prize in Chemistry in 1913 for his work on coordination compounds, which he performed as a graduate student and first presented at age 26. Apparently, Werner was so obsessed with solving the riddle of the structure of coordination compounds that his brain continued to work on the problem even while he was asleep. In

1891, when he was only 25, he woke up in the middle of the night and, in only a few hours, had laid the foundation for modern coordination chemistry.

Table **4.2.1**: Werner's Data on Complexes of Ammonia with $PtCl_4$

Complex	Conductivity (ohm^{-1})	Number of Ions per Formula Unit	Number of Cl^- Ions Precipitated by Ag^+
$PtCl_4 \cdot 6NH_3$	523	5	4
$PtCl_4 \cdot 5NH_3$	404	4	3
$PtCl_4 \cdot 4NH_3$	299	3	2
$PtCl_4 \cdot 3NH_3$	97	2	1
$PtCl_4 \cdot 2NH_3$	0	0	0

These data led Werner to postulate that metal ions have two different kinds of valence: (1) a primary valence (oxidation state) that corresponds to the positive charge on the metal ion and (2) a secondary valence (coordination number) that is the total number of ligands bound to the metal ion. If Pt had a primary valence of 4 and a secondary valence of 6, Werner could explain the properties of the $PtCl_4 \cdot NH_3$ adducts by the following reactions, where the metal complex is enclosed in square brackets:

$$[Pt(NH_3)_6]Cl_4 \rightarrow [Pt(NH_3)_6]^{4+}(aq) + 4Cl^-(aq) \quad (4.2.1)$$

$$[Pt(NH_3)_5Cl]Cl_3 \rightarrow [Pt(NH_3)_5Cl]^{3+}(aq) + 3Cl^-(aq) \quad (4.2.2)$$

$$[Pt(NH_3)_4Cl_2]Cl_2 \rightarrow [Pt(NH_3)_4Cl_2]^{2+}(aq) + 2Cl^-(aq) \quad (4.2.3)$$

$$[Pt(NH_3)_3Cl_3]Cl \rightarrow [Pt(NH_3)_3Cl_3]^{+}(aq) + Cl^-(aq) \quad (4.2.4)$$

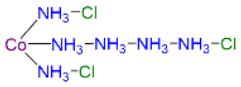
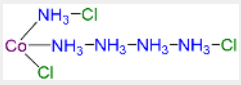
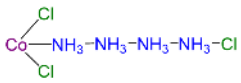
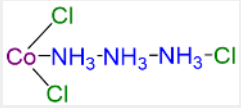
$$[Pt(NH_3)_2Cl_4] \rightarrow [Pt(NH_3)_2Cl_4]^{0}(aq) \quad (4.2.5)$$

Further work showed that the two missing members of the series—$[Pt(NH_3)Cl_5]^-$ and $[PtCl_6]^{2-}$—could be prepared as their mono- and dipotassium salts, respectively. Similar studies established coordination numbers of 6 for Co^{3+} and Cr^{3+} and 4 for Pt^{2+} and Pd^{2+}.

? Exercise 4.2.1. The $CoCl_3 x NH_3$ series.

The series $CoCl_3 \cdot xNH_3$ was particularly important in establishing the correctness of Werner's coordination theory over the rival chain theory. By ~1900 conductivity measurements suggested that the members of the series gave the number of ions shown in Table **4.2.1**.

Table **4.2.1**. The CoCl3·xNH3 series according to coordination theory, chain theory, and experiment.

Compound	Color	Werner formulation	Blomstrand-Jørgensen chain theory formulation	Number of ions in solution
$CoCl_3 \cdot 6NH_3$	yellow	$[Co(NH_3)_6]Cl_3$		4
$CoCl_3 \cdot 5NH_3$	violet	$[Co(NH_3)_5Cl]Cl_2$		3
$CoCl_3 \cdot 4NH_3$	green	$[Co(NH_3)_4Cl_2]Cl$		2
$CoCl_3 \cdot 3NH_3$	orange	$[Co(NH_3)_4Cl_3]$		0

What does this data suggest about the relative explanatory power of Werner's coordination theory and chain theory? Explain.

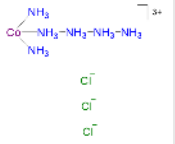
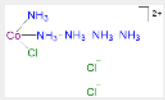
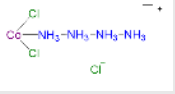
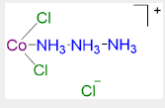
Answer

Remember that

- chain theory predicts that the number of ions is the number formed when the Cl atoms bound in a chain with NH_3 dissociate.
- coordination theory predicts the number of ions based on the number of complex ions and their counterions.

Based on this the predictions of coordination theory and chain theory can be compared with the experimental data, as is done in Table **4.2.2**.

Table **4.2.2**: Comparison of ions predicted for the $CoCl_3 \cdot xNH_3$ series by coordination theory and chain theory with the number observed experimentally.

Compound	Color	Ions predicted by Werner's coordination theory	Number of ions predicted by coordination theory	Ions predicted by Blomstrand-Jørgensen chain theory	Number of ions predicted by chain theory	Observed Number of ions in solution
$CoCl_3 \cdot 6NH_3$	yellow	$[Co(NH_3)_6]^{3+}$ Cl^- Cl^- Cl^-	4		4	4
$CoCl_3 \cdot 5NH_3$	violet	$[Co(NH_3)_5Cl]^{2+}$ Cl^- Cl^-	3		3	3
$CoCl_3 \cdot 4NH_3$	green	$[Co(NH_3)_4Cl_2]^+$ Cl^-	2		2	2
$CoCl_3 \cdot 3NH_3$	orange	None	0		2	0

As can be seen by comparing the number of ions predicted by coordination and chain theory in Table **4.2.2**, coordination theory successfully explains all the observed ion counts, while chain theory fails to explain the lack of ions observed for $CoCl_3 \cdot 3NH_3$.

Nevertheless, as is often the case when developing theoretical models using data from real experimental investigations, these observations did not convince Jørgensen, who could point to the experimental difficulty of determining the number of ions present from solution conductivity data.

What ultimately convinced Jørgensen of the correctness of Werner's coordination model over his own chain theory was how Werner's explanation of the structure of cobalt coordination complexes using an octahedral coordination geometry explained the existence of isomers in Co complexes containing Cl and NH_3 ligands. In the case of $[Co(NH_3)_4Cl_2]Cl$ two isomers were known: one red and the other green. Because both compounds had the same chemical composition and the same number of groups of the same kind attached to the same metal, there had to be something different about the arrangement of the ligands around the metal ion. Werner's key insight was that the six ligands in $[Co(NH_3)_4Cl_2]Cl$ had to be arranged at the vertices of an octahedron because that was the only structure consistent with the existence of two, and only two, stereoisomers (Figure **4.2.1**). His conclusion was also corroborated by the existence of two and only two stereoisomers of the next compound in the series: $Co(NH_3)_3Cl_3$.

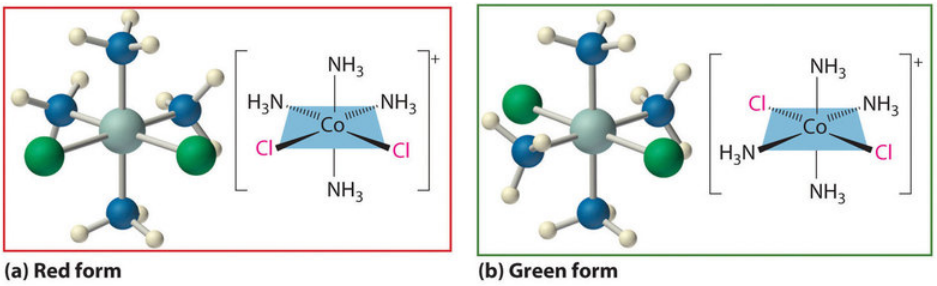


Figure **4.2.1**. The $[Co(NH_3)_4Cl_2]^+$ ion can have two different arrangements of the ligands, which results in different colors: if the two Cl^- ligands are next to each other (*cis*), the complex is red (a), but if they are opposite each other (*trans*), the complex is green (b).

Example 4.2.1: Why did Werner propose an octahedral geometry for 6-coordinate complexes?

In Werner's time, many complexes of the general formula MA_4B_2 were known, but no more than two different compounds with the same composition had been prepared for any metal. To confirm Werner's reasoning that this suggests these complexes possess an octahedral geometry, calculate the maximum number of different structures possible for six-coordinate MA_4B_2 complexes with each of the three most symmetrical possible structures the ligands will form about the central metal - a hexagon, a trigonal prism, and an octahedron.

Assuming that the absence of evidence for additional compounds in this case serves as reasonable circumstantial evidence for their absence, what does the fact that no more than two forms of any MA_4B_2 complex were known suggest about the three-dimensional structures of these complexes?

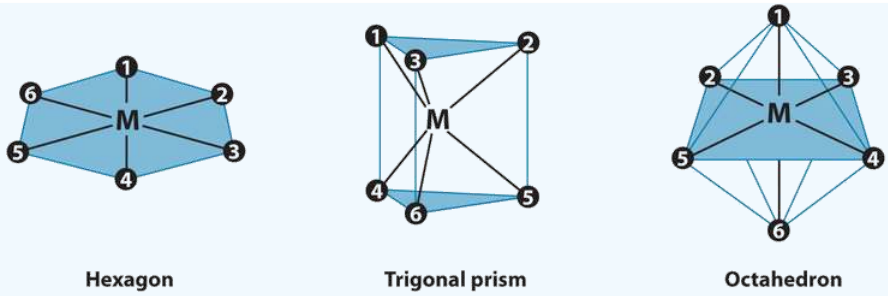
Solution

In this problem you are given

- the stochiometry of the complexes, MA_4B_2
- three possible coordination geometries - hexagonal, trigonal prismatic, and octahedral.

In order to calculate the number of isomers that could be present for each geometry it is best to follow a systematic approach. Since there are fewer B type ligands than A type ligands, the easiest way to do this for each geometry is to start by placing a B ligand at one vertex and then to determine how many different positions are available for the second B ligand.

The three regular six-coordinate structures are shown here, with each coordination position numbered so that we can keep track of the different arrangements of ligands. For each structure, all vertices are equivalent. We begin with a symmetrical MA_6 complex and simply replace two of the A ligands in each structure to give an MA_4B_2 complex:



For the hexagon, we place the first B ligand at position 1. There are now **three** possible places for the second B ligand:

- position 2 (or 6)
- position 3 (or 5)
- position 4

The (1, 2) and (1, 6) arrangements are chemically identical because the two B ligands are adjacent to each other. The (1, 3) and (1, 5) arrangements are also identical because in both cases the two B ligands are separated by an A ligand. Those of you who remember your ogranic chemistry might recognize that this situation is formally analogous to the *ortho-*, *meta-*, and *para-* isomerism in disubstituted benzenes.

Turning to the trigonal prism, we place the first B ligand at position 1. Again, there are three possible choices for the second B ligand:

- at position 2 or 3 on the same triangular face
- position 4 (on the other triangular face but adjacent to 1)
- position 5 or 6 (on the other triangular face but not adjacent to 1).

The (1, 2) and (1, 3) arrangements are chemically identical, as are the (1, 5) and (1, 6) arrangements.

In the octahedron, however, if we place the first B ligand at position 1, then we have only two choices for the second B ligand:

- position 2 (or 3 or 4 or 5)
- position 6.

In the latter, the two B ligands are at opposite vertices of the octahedron, with the metal lying directly between them. Although there are four possible arrangements for the former, they are chemically identical because in all cases the two B ligands are adjacent to each other.

The number of possible MA_4B_2 arrangements for the three geometries is thus: hexagon, 3; trigonal prism, 3; and octahedron, 2. The fact that only two different forms were known for all MA_4B_2 complexes that had been prepared suggested that the correct structure was the octahedron but did not prove it. For some reason one of the three arrangements possible for the other two structures could have been less stable or harder to prepare and had simply not yet been synthesized. When combined with analogous results for other types of complexes (e.g., MA_3B_3), however, the data were best explained by an octahedral structure for six-coordinate metal complexes.

? Exercise 4.2.1

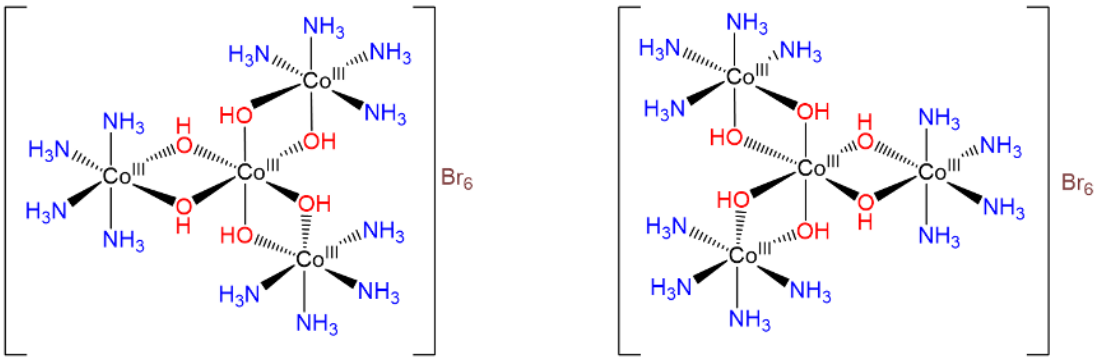
Determine the maximum number of structures that are possible for a four-coordinate MA_2B_2 complex with either a square planar or a tetrahedral symmetrical structure.

Answer

square planar, 2; tetrahedral, 1

Even Werner's explanation of isomerism in coordination complexes in terms of octahedral and other recognized coordination geometries did not convince all chemists until he was able to resolve a racemic mixture of *d*- and *l*-$[Co\{Co(NH3)_4(OH)_2\}_3]$ into its

enantiomers, which are shown in Scheme **4.2.II**. By doing so Werner demonstrated to chemists of his time (virtually none of whom knew group theory) that tetrahedral carbon atoms were not required for chirality; D_3 octahedral complexes were also chiral.



Scheme **4.2.II**: d- and l-enantiomers of [Co{Co(NH3)$_4$(OH)$_2$}$_3$], colloquially referred to as hexol. This work by Stephen Contakes is licensed under a Creative Commons Attribution 4.0 International License.

4.2: History is shared under a CC BY-NC-SA 4.0 license and was authored, remixed, and/or curated by Stephen M. Contakes.

- **24.1: Werner's Theory of Coordination Compounds** by Anonymous is licensed CC BY-NC-SA 4.0.

4.3: Nomenclature and Ligands

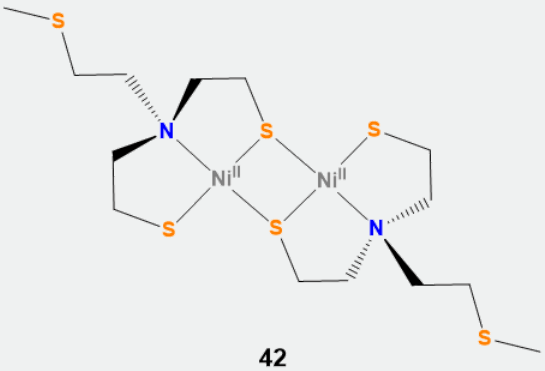
Systems of nomenclature and formulae are intended as tools, to be employed insofar as they are useful

There are well-established rules for both naming and writing the formulae of coordination compounds. The purpose of these rules is to facilitate clear and precise communication among chemists. As with all such rules, some are more burdensome than others to employ, and some serve more crucial roles in the communication process while others are more peripheral - and all are poorly used in the service of pedantic tyranny, especially when used against those who are otherwise doing good work. For this reason, you are urged to approach the rules in a spirit of generosity towards others in

- naming and writing formulas as reasonably accurately as you can so that ligands and metals are where readers expect them and thus can understand what you mean more easily.
- being gracious towards the many professional inorganic chemists who adhere loosely to some of the rules you are about to learn.
- recognizing that in cases when a structure is particularly complex and a picture may make be particularly useful, you should supply one (See the note below).

Note 4.3.1: Sometimes the most helpful name to give a compound is 42.

Even though the IUPAC nomenclature rules permit specification of even the most complex structures, it is often much easier and more effective to supply a numbered structure that can be referred to instead of the IUPAC name. Consider bis{[(μ-2-mercaptoethyl)(2-mercaptoethyl)-methylthioethylaminato (2-)]Nickel(II)}. Which is easier, to expect readers and hearers to work out the structure from that name or to just refer them to compound **42** in Scheme **4.3.I**?



42

Scheme **4.3.I**. Structure of bis{[(μ-2-mercaptoethyl)(2-mercaptoethyl)-methylthioethylaminato (2-)]Nickel(II)}. The authors of the synthesis of this compound in Inorganic syntheses1 may have had to figure out an IUPAC name for this compound but if you have this scheme in your paper and your instructor is OK with it you can just call it **42**

Coordination Complexes are named as the ligand derivatives of a metal

A variety of systems have been used for naming coordination compounds since the development of the discipline in the time of Alfred Werner. In this section the most common approaches as they are currently used by practicing chemists will be described. Those who need a more thorough and accurate acquaintance with the full IUPAC nomenclature rules are encouraged to consult the IUPAC brief guide to inorganic nomenclature followed by complete guidelines, commonly known as the IUPAC red book. If those are still not enough a careful read of note **4.3.1** is suggested.

The systems for naming coordination compounds used at present are additive, meaning that they consider coordination compounds as comprising a central metal to which are added ligands. To specify the structure and bonding in this metal-ligand complex then involves:

1. when there are several different ways of attaching the metal and ligands, specifying the structural or stereoisomer
2. systematically listing the ligands in a way that, as necessary, conveys information about how they are linked to the metal and their stereochemistry

3. providing the identity of the metal and its oxidation state, or if the oxidation state is unclear, at least the overall charge on the complex
4. specifying any counterions present

Since the stereochemistry of coordination compounds forms the subject of the next section, in this section it will be addressed by simply giving the prefixes that designate stereochemistry as if they were self-evident. Do not worry about these for now. They will make sense after you have learned more about stereochemistry in the next section. At that time, you can go back over the examples in that section to solidify your understanding of how to name coordination compounds.

However, in order to name coordination compounds accurately you will need to learn how to think about and name ligands first.

Ligands

Ligands are classified based on whether they bind to the metal center through a single site on the ligand or whether they bind at multiple sites. Ligands that bind through only a single site are called **monodentate** from the Latin word for tooth; in contrast, those which bind through multiple sites are called **chelating** after the Greek $\chi\alpha\lambda\epsilon$ for "claw". These relationships are summarized in Figure **4.3.1**.

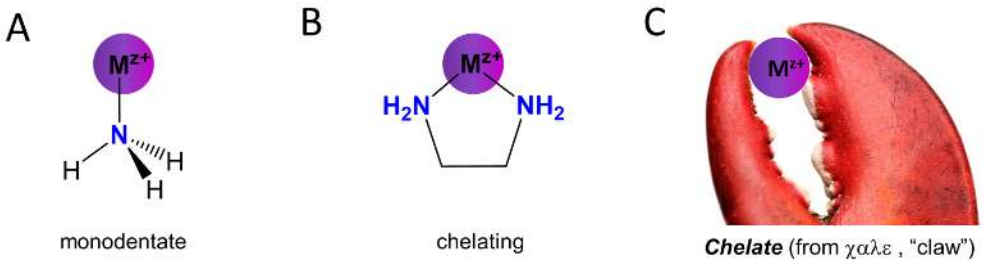
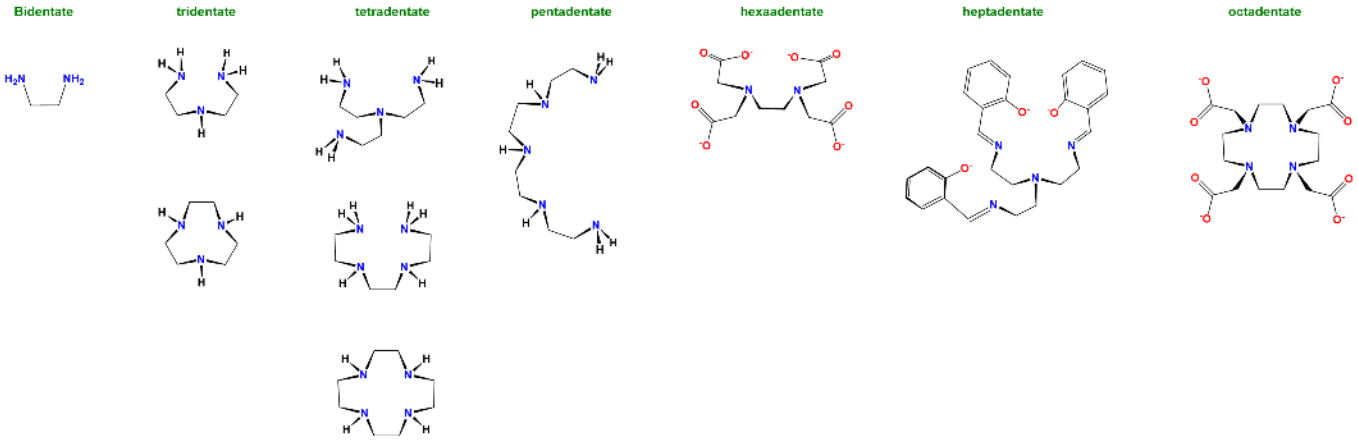


Figure **4.3.1**. (A) Ammonia is a monodentate ligand while (B) ethylene diamine is a chelating ligand owing to its capacity to bind metals via its two amine functional groups. (C) Chelating ligands act like a lobster claw in attaching to the metal via multiple sites. The lobster claw image is adapted from https://www.clipart.email/download/1127636.html. Otherwise this work by Stephen Contakes is licensed under a Creative Commons Attribution 4.0 International License.

Following naturally from the classification of non-chelating ligands as monodentate, chelating ligands are further classified according to the number of sites which they can use to bind a metal center. This number of binding sites is called the denticity and ligands are referred to as monodentate (non- chelating), bidentate, tridentate, etc., based on the number of sites available. Ligands with two binding sites have a denticity of two and are said to be bidentate; those with three are tridentate, four tetradentate, and so on. To illustrate this classification system examples of chelating ligands classified according to denticity are given in Scheme **4.3.I**.

Scheme 4.3.I. A selection of chelating ligands classified according to denticity.

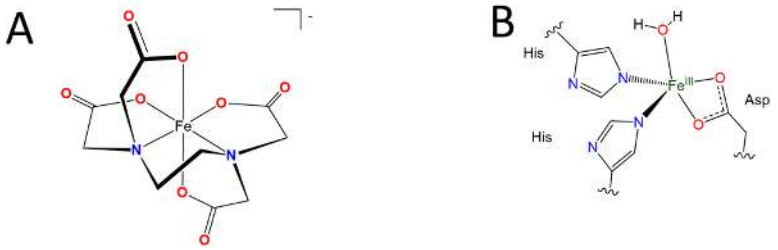


Scheme **4.3.IIA**. Because only one oxygen per carboxylate *typically* binds, only one is counted when assigning a ligand's denticity. This work by Stephen Contakes is licensed under a Creative Commons Attribution 4.0 International License.

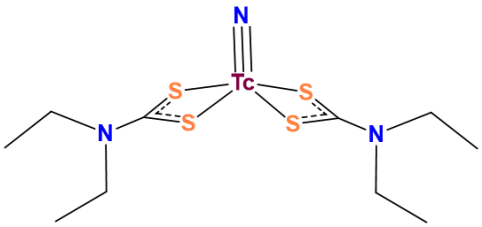
Although only one carboxylate oxygen *usually* binds to a metal, it is still possible to bind for both oxygens to bind to a single metal. As shown in Scheme **4.3.IIB**, complexes in which both carboxylates bind to a metal are known, and in fact are common in the

active sites of some enzymes. It is just that the binding of both oxygens gives a strained four-membered ring that is usually unstable.

Scheme 4.3.II. (A) Only one oxygen per carboxylate counts towards the denticity of EDTA since on binding the other oxygen generally points away from the metal center, as in the structure of $Fe(EDTA)^-$. (B) In some enzyme active sites both oxygens of a carboxylic acid (aspartate or Asp in this example) bind to a metal. The aspartate carboxylic acid group is bidentate while the EDTA carboxlic acid groups in A are monodentate. This work by Stephen Contakes is licensed under a Creative Commons Attribution 4.0 International License.



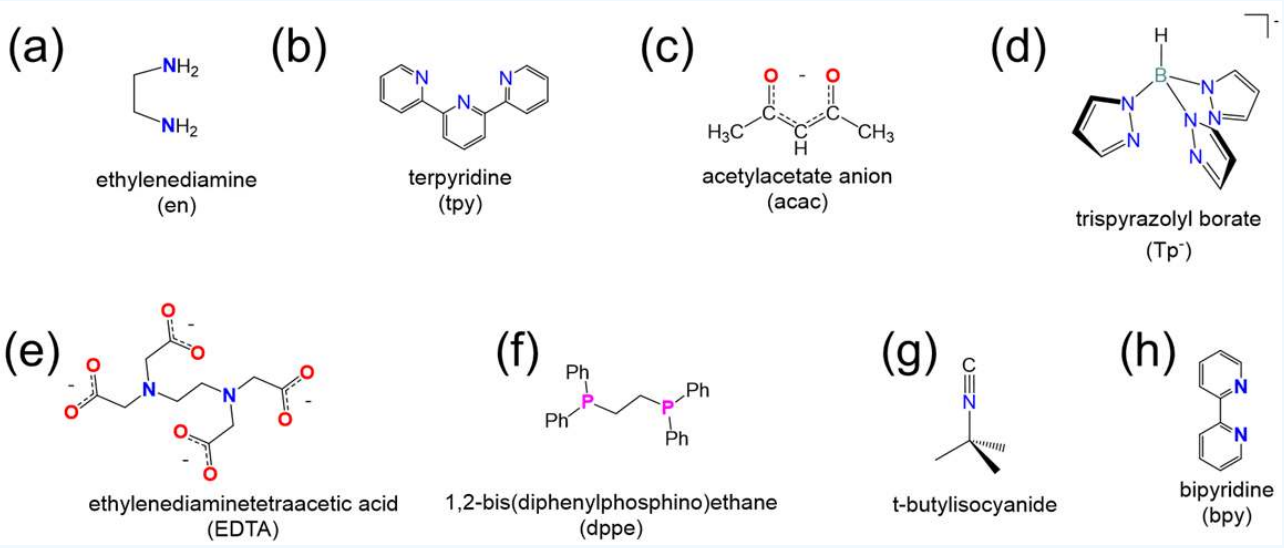
Scheme 4.3.III. As in this complex, dithiocarbamates commonly bind metals through both sulfur atoms. Consequently, dithiocarbamates are classified as bidentate. This work by Stephen Contakes is licensed under a Creative Commons Attribution 4.0 International License.



Because of these factors it is technically more correct to say that carboxylates *usually act as* monodentate ligands and dithiocarbamates bidentate ones than it is to say that carboxylates *are* monodentate ligands and dithiocarbamates bidentate ones. So in other words the ligand classifications presented here just represent common binding modes.

? Exercise 4.3.1

Determine the denticity of each ligand in the list below and classify them as monodentate, tridentate, etc.



Answer

(a) bidentate

(b) tridentate

(c) bidentate

(d) tridentate (only the lower N on each ring has a lone pair that can be used to bind the metal)

(e) hexadentate (remember that each carboxylate only counts as one point of attachment)

(f) bidentate

(g) monodentate (through the lone pair on the isocyanide C)

(h) bidentate

This experimentally-based classification of dithiocarbamates as bidentate and carboxylates as monodentate can be confusing to a beginner. Fortunately, such experimentally based classifications are embedded in the lists of common monodentate ligands as given in Table **4.3.1** and common chelating ligands in Table **4.3.2**.

A perusal of the ligands in Table **4.3.1** reveals that several can bind to a metal in multiple ways. For example, thiocyanate, SCN^- can bind metals through its S or N atoms. Such ligands are called **ambidentate ligands**. In naming an ambidentate ligand, the atom through which it attaches to the metal is commonly specified after the ligand name using the italicized element symbol or, more formally, a κ followed by the italicized element symbol. An example is given in Scheme **4.3.I**.[2]

Scheme 4.3.I. Two possible binding modes of nitrite acting as a ligand.[3]

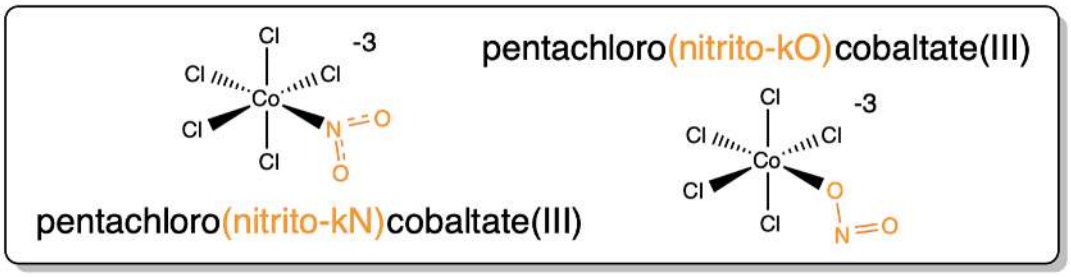
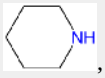
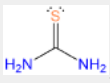
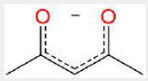
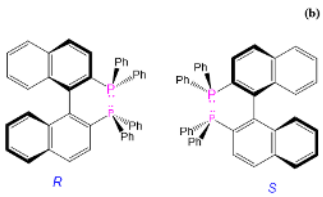
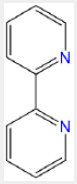
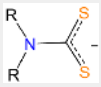
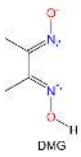
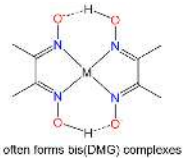
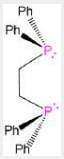
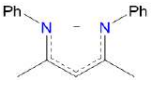


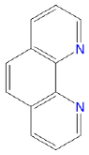
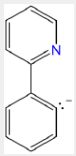
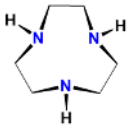
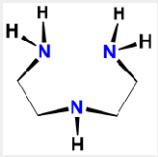
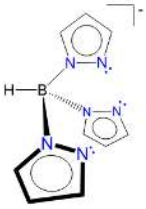
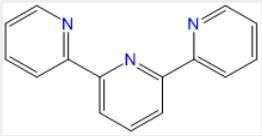
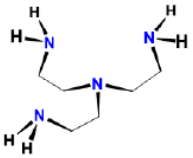
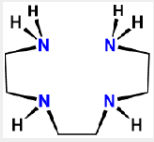
Table **4.3.1**. Common monodentate ligands. Most chemists still prefer common names over the IUPAC ones.

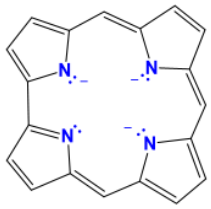
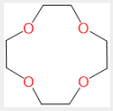
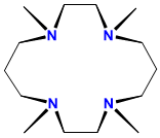
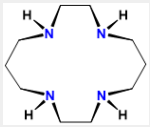
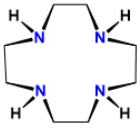
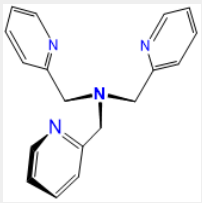
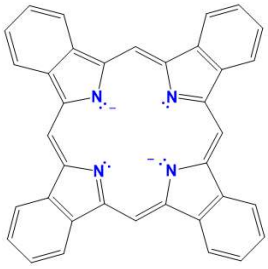
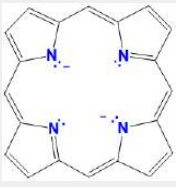
Ligand	Common name	IUPAC name
H^- (H ligands are always considered anions for naming purposes)	hydrido	hydrido
F^-	fluoro	fluorido
Cl^-	chloro	chlorido
Br^-	bromo	bromido
I^-	iodo	iodido
CN^-, as M-CN	cyano	cyanido or cyanido-κC or cyanido-*C*
CN^-, as M-NC	isocyano	isocyanido or cyanido-κN or cyanido-*N*
CH_3NC	methylisocyanide	methylisocyanide
N_3^-	azido	azido
SCN^-, *e.g.* thiocyanate as M-SCN	thiocyanato	thiocyanato-κS or thiocyanato-*S*
NCS^-, *e.g.* thiocyanate as M-NCS	isothiocyanato	thiocyanato-κN or thiocyanato-*N*
$CH_3CO_2^-$	acetato	ethanoato
N^{3-}	nitrido	nitrido
NH^{2-}	imido	azanediido
NH_2^-	amido	azanido
NH_3	ammine	ammine
RNH_2, R_2NH, R_3N	alkylamine, dialkylamine, trialkalyamine (*e.g.* methylamine for CH_3NH_2)	alkylamine, dialkylamine, trialkalyamine (*e.g.* methylamine for CH_3NH_2)
 , piperidine, abbreviated pip	piperidine	piperidine
 , pyridine, abbreviated py	pyridine	pyridine
CH_3CN, acetonitrile, abbreviated MeCN	acetonitrile	acetonitrile
P^{3-}	phosphido	phosphido
PH_3	phosphine	phosphane
PR_3	trialkylphosphine (*e.g.* trimethylphosphine for Me_3P)	trialkylphosphane (*e.g.* trimethylphosphane for Me_3P)
PAr_3	triarylphosphine (*e.g.* triphenylphosphine for Ph_3P)	triarylphosphine (*e.g.* triphenylphosphane for Ph_3P)
 , dimethylsulfoxide or DMSO or dmso	dimethylsulfoxide (sometimes called dimethylsulfoxo but this usage is rare and violates the nomenclature rules for neutral ligands)	(methanesulfinyl)methane or dimethyl(oxido)sulfur
 , thiourea or tu	thiourea	thiourea

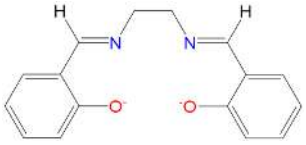
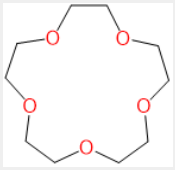
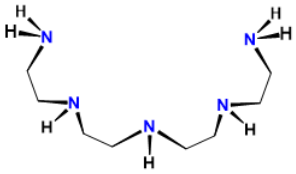
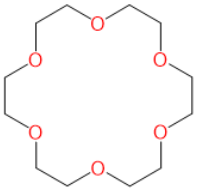
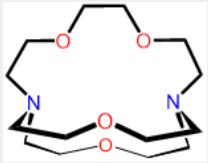
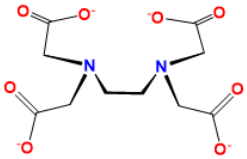
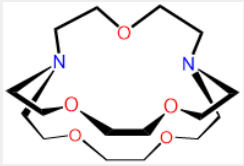
Ligand	Common name	IUPAC name
O^{2-}	oxo	oxido
OH^-	hydroxo	hydroxido
H_2O	aqua	aqua
S^{2-}	sulfo	sulfo
HS^-	hydrosulfido	hydrosulfido
RS^-	alkanethiolate (*e.g.* ethanthiolate for EtS^-)	thioalkanoate
H_2S	hydrogen sulfide	hydrogen sulfide
R_2S	alkylsulfanylalkane (*e.g.* ethylsulfanylethane for Et_2S)	dialkyl sulfide
O_2	dioxygen	dioxygen
O_2^-, superoxide	superoxido	dioxido(1-) or superoxido
O_2^{2-}, peroxide	peroxido	dioxido(2-) or peroxido
N_2	dinitrogen	dinitrogen
NO (are always considered neutral for naming purposes)	nitrosyl	nitrosyl
CO	carbonyl	carbonyl
CS	thiocarbonyl	thiocarbonyl
SO, as M-SO	sulfino	sulfur monoxide-κS or sulfur monoxide-*S*
NO_2, as M-NO_2	nitryl	nitrogen dioxide-κN or nitrogen dioxide-*N*
CO_3^{2-}	carbonato	carbonato
NO_2^-, as M-NO_2	nitro or nitrito-*N*	nitrito-κN or nitrito-*N*
NO_2^-, as M-ONO	nitrito or nitrito-*O*	nitrito-κO or nitrito-*O*
NO_3^-	nitrato	nitrato
SO_3^{2-}	sulfito	sulfito
SO_4^{2-}	sulfato	sulfato
$S_2O_3^{2-}$, as M-S-SO_2-O^-	thiosulfato-*S*	thiosulfato-κS or thiosulfato-*S*
$S_2O_3^{2-}$, as M-O-SO_2-S^-	thiosulfato-*O*	thiosulfato-κO or thiosulfato-*O*

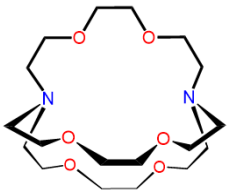
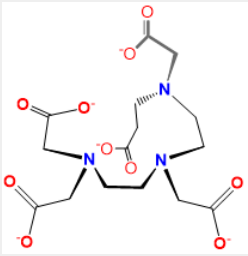
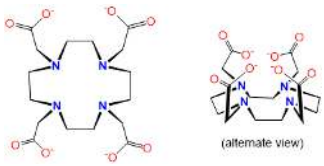
Table **4.3.2**. Common chelating ligands organized by denticity. Most chemists use the common names and abbreviations to describe these ligands.

Common Ligand name	IUPAC ligand name	abbreviation (if applicable)	structure or representative/parent structure (shown in the ionization state in which they bind to a metal)
bidentate ligands			
acetylacetonato	2,4-pentanediono	acac	
R-BINAP and *S*-BINAP	*R*- or *S*-2,2'-bis(diphenylphosphino)-1,1'-binapthyl	BINAP	
2,2'-bipyridine	2,2'-bipyridine	bpy or bipy	
cyclooctadiene	1,5-cyclooctadiene	COD	 (binding to the metal occurs through the alkene π cloud)
dialkyldithiocarbamato	dialkylcarbamodithiolato	$R_2NCS_2^-$ or dtc	
dimethylgloximato	butanedienedioxime	Hdmg or DMG	 
diphenylphosphinoethane or 1,2-(diphenylphosphino)ethane	Ethane-1,2-diylbis(diphenylphosphane)	dppe	
ethylenediamine	Ethane-1,2-diamine	en	
ethylenedithiolato	Ethane-1,2-dithiolato	$C_2H_2S_2^{2-}$	
nacnac	*N*,*N*'-diphenyl-2,4-pentanediiminato	nacnac	
oxalato	oxalato	ox	

Common Ligand name	IUPAC ligand name	abbreviation (if applicable)	structure or representative/parent structure (shown in the ionization state in which they bind to a metal)
1,10-phenanthroline or *o*-phenanthroline	1,10-phenanthroline	phen or *o*-phen	
phenylpyridinato	2-phenylpyridinato-C^2,*N* or 2-phenylpyridinato-κC^2,*N*	ppy	
tridentate ligands			
triazacyclononane	1,4,7-triazacyclononane	tacn	
diethylenetriamine	1,4,7-triazaheptane	dien	
pyrazoylborato (scorpionate)	hydrotris(pyrazo-1-yl)borato	Tp	
terpyridine or 2,2';6',2"-terpyridine	1^2,2^2:2^6,3^2-terpyridine or 2,6-bis(2-pyridyl)pyridine, tripyridyl, 2,2′:6′,2″-terpyridine	tpy or terpy	
tetradentate ligands			
β, *β*', *β*"-triaminotriethylamine	*β*, *β*', *β*"-tris(2-aminoethyl)amine	tren	
triethylenetetramine	1,4,7,10-tetraazadecane	trien	

Common Ligand name	IUPAC ligand name	abbreviation (if applicable)	structure or representative/parent structure (shown in the ionization state in which they bind to a metal)
corroles	variable and generally not used	cor or Cor	
12-crown-4	1,4,7,10-tetraoxacyclododecane	12-crown-4	
tetramethylcyclam	1,4,8,11-tetramethyl-1,4,8,11-tetraazacyclotetradecane	TMC or cyclam	
cyclam	1,4,8,11-tetraazacyclotetradecane	cyclam	
cyclen	1,4,7,10-tetraazacyclododecane	cyclen	
tris(2-pyridylmethyl)amine	1-pyridin-2-yl-*N*,*N*-bis(pyridin-2-ylmethyl)methanamine	tpa or TPA	
phthalocyanines	variable and generally not used	variable, usually a modified Pc	
porphyrins	variable and generally not used	variable, usually a modified por, Por, or P (e.g. TPP = tetraphenylporphyrin)	

Common Ligand name	IUPAC ligand name	abbreviation (if applicable)	structure or representative/parent structure (shown in the ionization state in which they bind to a metal)
salen	2,2'-ethylenebis(nitrilomethylidene) diphenoxido	salen	
pentadentate ligands			
15-crown-5	1,4,7,10,13-Pentaoxacyclopentadecane	15-crown-5	
tetraethylenepentamine	1,4,7,10,13-pentaazatridecane	tepa or TEPA	
hexadentate ligands			
18-crown-6	1,4,7,10,13,16-hexaoxacyclooctadecane	18-crown-6	
2,1,1-cryptand	4,7,13,18-Tetraoxa-1,10-diazabicyclo[8.5.5]icosane	2,1,1-crypt or [2.1.1]-cryptand kryptofix 211 and variations thereof	
ethylenediaminetetraaceto	2,2′,2″,2‴-(Ethane-1,2-diyldinitrilo)tetraaceto	EDTA, edta, Y^{4-}	
heptadentate ligands			
2,2,1-cryptand	4,7,13,16,21-pentaoxa-1,10-diazabicyclo[8.8.5]icosane	2,2,1-crypt or [2.2.1]-cryptand kryptofix 221 and variations thereof	

Common Ligand name	IUPAC ligand name	abbreviation (if applicable)	structure or representative/parent structure (shown in the ionization state in which they bind to a metal)
octadentate ligands			
2,2,2-cryptand	4,7,13,16,21,24-Hexaoxa-1,10-diazabicyclo[8.8.8]hexacosan	2,2,2-crypt or [2.2.2]-cryptand kryptofix 222 and variations thereof	
pentetato acid or diethylenetriaminepentaacetato or DTPA	2-[bis[2-[bis(carboxylatomethyl)amino]ethyl]amino]acetato	DTPA	
DOTA or tetraxetan	1,4,7,10-Tetraazacyclododecane-1,4,7,10-tetraacetic acid	Dota, DOTA	

Rules for Naming Coordination Compounds

As explained above, the name of a coordination compound communicates

- as appropriate, information about isomerism
- systematically listing the ligands in a way that as necessary conveys information about their oxidation state and how they are linked to the metal
- the identity of the metal and its oxidation state
- any counterions present

Before going into these rules it is worth pointing out a few things.

1. It is easiest to learn these rules by starting with one or two of the rules, learning how to apply them, and then adding additional rules one at a time. To that end, instructors who wish to use a more programmed approach may find it convenient to first direct their students to this page which focuses on getting the names of the ligands and metal right, without worrying about isomerism or stereochemistry.

2. The rules also assume some familiarity with common coordination geometries and patterns of isomerism in metal complexes. Thus it might be easiest to learn about common coordination geometries first, followed by common patterns of isomerism in metal complexes before beginning this section. If you decide to dive right in to this section you might find it helpful to know that when applying nomenclature and formula rules most textbooks *assume*

- complexes in which the metal has a coordination number of six are octahedral
- complexes in which the metal has a coordination number of five are trigonal bipyramidal
- complexes in which Pt^{II} , Pd^{II} , or Rh^{I}, or Ir^{I} have a coordination number of four are square planar
- other complexes in which the metal has a coordination number of four are tetrahedral

Like all assumptions these don't always work in real life but they should be good enough to get you through your first inorganic chemistry course.

For the pedants among you, note that the complexes given as examples and in exercises on this page have been selected for pedagogical utility. Although many are well-known compounds, others are hypothetical.

Now on to the rules.

Rule 1: If ions are present, name the cation first, followed by the anion.

Examples:

$K_2[Pt^{II}Cl_4]$ potassium tetrachloroplatinate(2-)

$[Co^{III}(NH_3)_6](NO_3)_3$ hexaamminecobalt(3+) nitrate

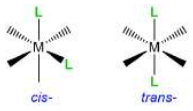
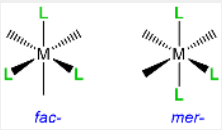
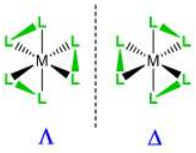
$[Co^{III}(NH_3)_6][Cr^{III}(C_2O_4)_3]$ hexaamminecobalt(3+) tris(oxalato)chromium(3-)

Rule 2: When multiple isomers are possible, designate the particular isomer in italics at the front of the name of each complex

If you have not yet learned about isomerism in coordination compounds skip this rule for now and return to it after you have.

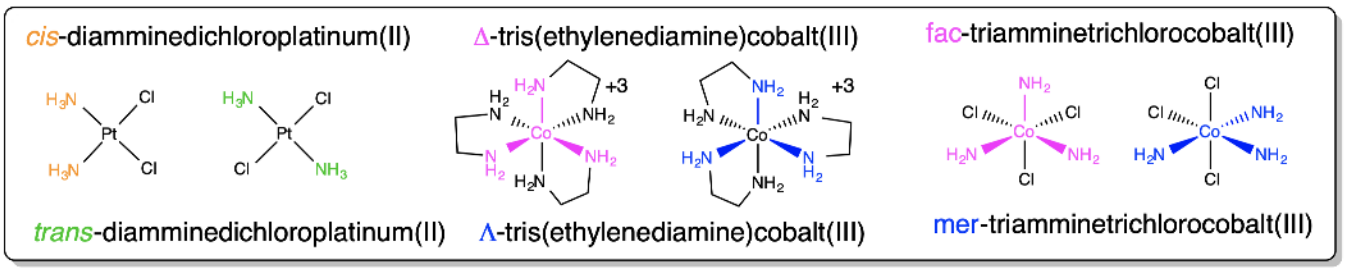
When a complex might exist as one of two stereoisomers, prefixes are commonly used to designate which isomer is present. The most common cases are listed in Table **4.3.3**.

Table **4.3.3**. Prefixes used to specify isomerism about a metal center when naming and writing coordination compounds' formulae.

Type of isomerism	Graphical reminder	Prefixes
Geometric, *cis-* , *trans-*		*cis-* or *trans-*
Geometric, *fac- /mer-*		*fac-* or *mer-*
Enantiomers, **Λ-**, **Δ-**		**Λ-** or **Δ-**

Examples of how isomerism about a metal center is designated are given in Scheme **4.3.II**.

Scheme 4.3.II. Application of nomenclature rules for stereosimerism about a metal.[3]



There are a number of other cases where it might be advisable to specify the stereochemistry of a complex. These cases involve specifying

- the coordination geometry about a metal center (octahedral, trigonal prismatic, tetrahedral, square planar, etc.)

- the geometry cannot be unambigouously described by a single *cis/trans* or *fac/mer* relaionship of ligands

These cases may also be handled by using a designator to specify the coordination geometry and, as necessary, giving the position of ligated atoms in terms of designated numbered positions for that geometry. See the IUPAC red book for details as such cases fall outside the scope of what is normally advisable for an undergraduate course.

Rule 3: Specify the identity, number, and as appropriate, isomerism of the ligands present in alphabetical order by ligand name.

Before specifying the metal, the ligands are written as prefixes of the metal.

In specifying the ligands several rules are followed.

1. The ligands are written in alphabetical order by the ligand name only; symbols are not considered and prefixes do not count in determining alphabetical order.

   Example: In the name of the complex ion $[Co(NH_3)_5Cl]^{2+}$, pentamminechlorocobalt(II), the ammine ligand is named before the chloro ligand because the order is alphabetical by the ligand name by virtue of which ammine comes before chloro.

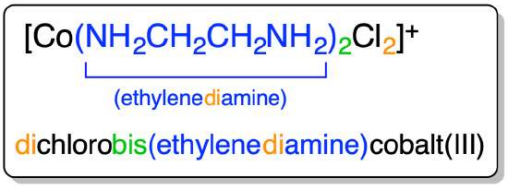
2. Prefixes are used to indicate the number of each ligand present. Specifically, *di-*, *tri-*, *tetra-* , *penta-*, *hexa-*, *etc.* prefixes are used to indicate multiple ligands of the same type EXCEPT when the ligand is polydentate or its name already has a *di-*, *tri-*, *tetra-* etc. In that case *bis-*,*tris-*, *tetrakis-*, etc. are used instead. These prefix rules are summarized in Table **4.3.3**.

Table **4.3.3**. Prefixes used to specify the number of a given ligand present.

Number of identical ligands	prefix used when the ligand name is simple	prefix used when the ligand is polydentate or its name already has a *di-*, *tri-*, *tetra-* etc.
2	di-	bis-
3	tri-	tris-
4	tetra-	tetrakis-
5	penta-	pentakis-
6	hexa-	hexakis-
7	hepta-	heptakis-
8	octa-	octakis-
9	nona-	nonakis-
10	deca-	decakis-

An example of the application of the prefix rule is given in Scheme **4.3.III**.

Scheme 4.3.III. Example of the use of prefixes to specify the number of ligands of each type in a complex.[3]



3. Ligand names are based on their charge.

   - Neutral and cationic ligand names are the same as the names of their neutral compounds with two caveats:

     i. names that involve spaces should either be put in parentheses or the spaces should be eliminated (preferred)

     Example: cis-dichlorobis(**dimethyl sulfoxide**)platinum(II) or *cis*-dichlorobis(**dimethylsulfoxide**)platinum(II)

ii. A few ligands are given common names.

- H_2O = aqua
- NH_3 = ammine (notice that there are two n's)
- CO = carbonyl
- CS = thiocarbonyl
- NO = nitrosyl

- For anionic ligands, the vowel at the end of their anion names is changed to an -"o"

  Examples: Cl^- = chloro, NH_2^- = amido, N_3^- = azido

  Caveat: some anionic ligands have common names that may also be used

  Examples:

  I^- = iodo or iodino

  CN^- = cyano or cyanido

  O^{2-} = oxo or oxido

The IUPAC and common names of many ligands are given in Tables **4.3.1**. and **4.3.2**.

4. When an ambidentate ligand is present, the atom through which it is bound to the metal is indicated by giving either its element symbol or a κ and its element symbol in italics after the ligand name.

   Example:

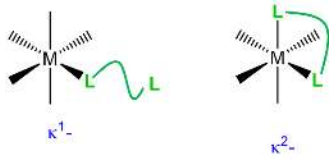
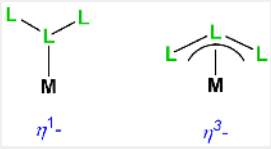
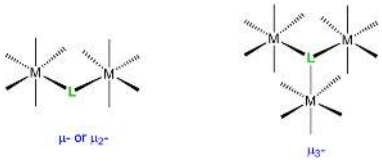
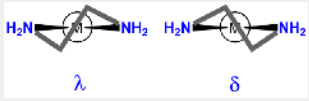
   M-SCN is thiocyanato-*S* or thiocyanato-κ*S*

   M-NCS = thiocyanato-*N or* thiocyanato-κ*N*

   The use of κ and an element symbol to indicate how a ligand and metal are linked is called a **k-term**. More complex k-terms might also involve specifying the atoms by number, though their use is outside the scope of this text.

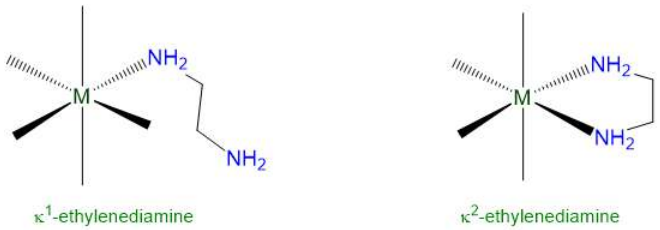
5. As appropriate, additional information about the way a ligand is bound to the metal center and/or its stereochemistry is specified using a prefix. The prefixes to provide linkage and stereochemistry for ligands are given in Table **4.3.4**.

Table **4.3.4**. Prefixes used to specify ligands' isomerism when naming and writing coordination compounds' formulae. Some of these types of isomerism will be discussed in later pages.

Type of isomerism	Graphical reminder	Prefixes
when a multidentate ligand binds through less than the full number of atoms		κ^n where n is the number of attached atoms; used when the attached atoms are not directly connected by a chemical bond. The metal-ligand bonding usually involves σ-type coordination.
hapticity		η^n where n is the number of attached atoms; used when the coordinated atoms are all connected by bonds. Usually the metal-ligand bonding involves π-type coordination. In speech, η^1=monohapto; η^2=dihapto; η^3=trihapto, etc.
bridging ligands		μ_n where n is the number of atoms bridged. The number n is usually omitted when n =2.
chelating ligand ring twist		λ- or δ-

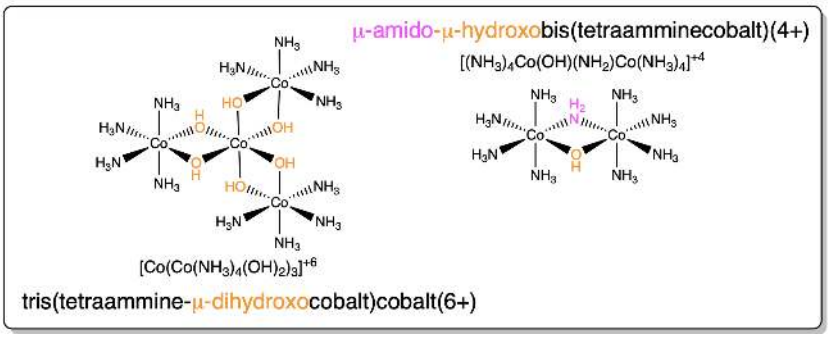
A example showing how the nomenclature rule is applied to a ligand that can have two coordination modes is given in Scheme **4.3.IV**.

Scheme 4.3.IV. Use of the κ notation to specify the number of attached groups in a multidentate ligand.



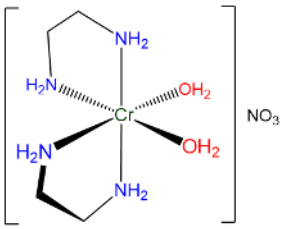
Scheme **4.3.V**. The names of the complexes follow the rules described in 9.2.6: multinuclear coordination complexes.

Scheme 4.3.V. Use of the μ notation to specify bridging ligands in metal complexes.[3]



6. If desired, parentheses *may* be used to delineate a ligand name to make it easier to identify in the name of the complex. This can be particularly helpful when the entire name contains a lot of information to keep track of. An example is given in Scheme **4.3.VI**.

Scheme 4.3.VI. When naming the complex shown, *cis*-diaquabis(ethylenediamine)chromium(III) nitrate is easier to read than *cis*-diaquabisethylenediaminechromium(III) nitrate.



Rule 4: Specify the identity of the metal

- In neutral and cationic complexes the metal's name is used directly

  - *e.g.* as in hexammineruthenium(III) for $[Ru(NH_3)_6]^{3+}$

- In anionic complexes, *-ate* replaces *-ium*, *-en*, or *–ese* or adds to the metal name,

  e.g., as in hexachloromanganate(IV) for $MnCl_6^{2-}$

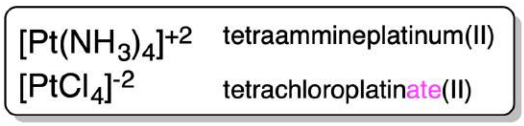
- In anionic complexes of some metals a Latin-derived name is used instead of the element's English name. These names are given in Table **4.3.5**.

Table **4.3.5**. Latin terms for select metal Ions. Redrawn from this page describing the nomenclature of coordination complexes.

Transition Metal	Latin
Copper	Cuprate
Gold	Aurate
Iron	Ferrate
Lead	Plumbate
Silver	Argentate
Tin	Stannate

An example of the application of the metal naming rules is given in Scheme \sf{\PageIndex{VII}}\).

Scheme 4.3.VII. Example of the application of the metal specification rules to a cationic and an anionic platinum complex.[3]



Rule 5: Specify the oxidation state of the metal.

Two different systems are used to specify the oxidation state of the metal.

1. In the **Stock system** the metal's oxidation state is indicated in Roman numerals after the metal name.

   Examples:

   $[CoCl(NH_3)_5]Cl_2$ = pentamminechlorocobalt(III) chloride

   $[PtBr_2(bpy)]$ = dibromobipyridineplatinium(II)

   $K[Ag(SCN)_2]$ = potassium di-*S*-thiocyanatoargentate(I)

2. In the **Ewing-Bassett system** the charge on the complex is specified in Arabic numerals after the complex name. This provides a way of specifying a complex even when the oxidation state of the metal isn't known and, in cases where it is known, the value

of the metal's oxidation state may be inferred from the complex ion's charge.

$[CoCl(NH_3)_5]Cl_2$ = pentamminechlorocobalt(2+) chloride

$[PtBr_2(bpy)]$ = dibromobipyridineplatinium(0)

$K[Ag(SCN)_2]$ = potassium di-*S*-thiocyanatoargentate(1-)

Summary of rules for naming coordination complexes.

A graphical summary of the **rules for naming complexes** along with a few examples that you can use to review the nomenclature rules is given in Figure **4.3.1**. This work by Stephen Contakes is licensed under a Creative Commons Attribution 4.0 International License.

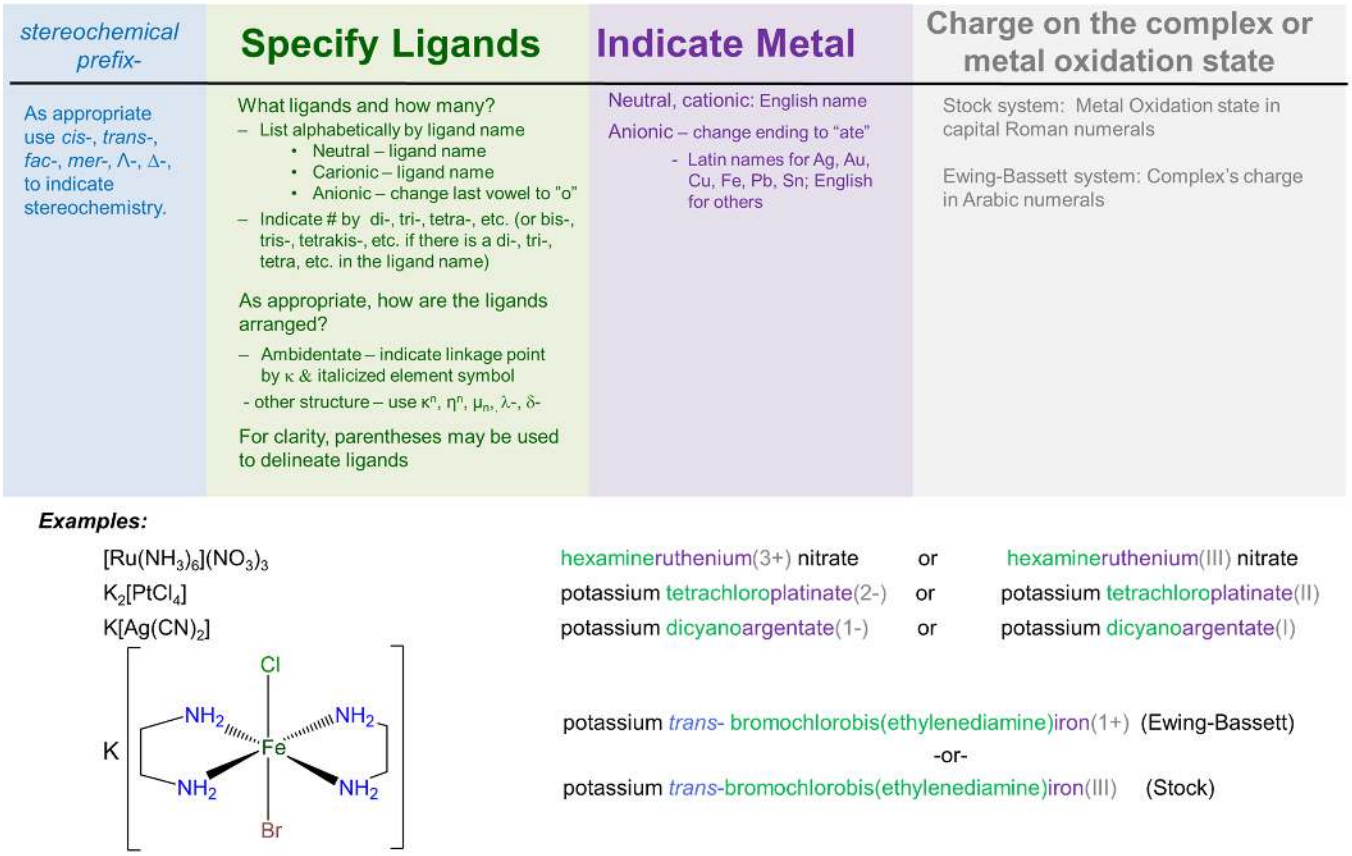


Figure **4.3.1**. Summary of nomenclature rules for coordination complexes along with a few examples of their application.

When learning chemical nomenclature, practice makes perfect. The following examples and exercises are provided to give you this practice. Additional examples and exercises on the https://chem.libretexts.org/ site include a set of simple examples with explained solutions, a set of simple exercises with solutions, and a set of more challenging exercises without solutions.

? Exercise **4.3.2**. Assigning metal oxidation states in a complex

In order to name a complex in the Stock system it is necessary to assign a formal oxidation state to the metal. For this reason it is important to be able to assign the oxidation state of a metal in a complex. Fortunately, this is easy to do if you remember

1. The sum of all atoms' oxidation states will equal the overall charge on the complex
2. When determining the metal's oxidation state the ligands can be treated as having an oxidation state equal to their charge - *i.e.*, the charge they possess in the form in which they coordinate the metal, so if they need to lose a proton to bind, don't forget to account for that.

Given the above, assign the oxidation state of the metal in the following real and hypothetical complexes.

a. $K_3[Fe(CN)_6]$

b. $[CoCl(NH_3)_5](NO_3)_2$
c. $K_2[PtCl_4]$
d. [MnCl(por)]
e. $[Ru(bpy)_3]Cl_2$
f. $[PdCl_2(dppe)]$
g. $[Mn(en)_2(SCN)_2]$

Answer for $K_3[Fe(CN)_6]^{3-}$.

This contains $[Fe(CN)_6]^{3-}$; so O.S.$_{Fe}$ + 6 x (-1) (for CN^-) = -3 (the complex's charge) so O.S.$_{Fe}$ = +3 or Fe^{3+}.

Answer for $[CoCl(NH_3)_5](NO_3)_2$.

This contains $[CoCl(NH_3)_5]^{2+}$; so O.S.$_{Co}$ + 1 x (-1) (for Cl^-) + 0 x 5 (for NH_3) = +2 (the complex's charge) so O.S.$_{Co}$ = +3 or Co^{3+}.

Answer for $K_2[PtCl_4]$.

This contains $2K^+$ and $[PtCl_4]^{2-}$; so O.S.$_{Pt}$ + 4 x (-1) (for Cl^-) = -2 (the complex's charge) so O.S.$_{Pt}$ = +2 or Pt^{2+}.

Answer for [MnCl(por)].

O.S.$_{Pt}$ + 1 x (-2) (for por; see table 9.2.2) + 1 x (-1) (for Cl^-) = +0 (the complex's charge) so O.S.$_{Mn}$ = +3 or Mn^{3+}.

Answer $[Ru(bpy)_3]Cl_2$.

The complex is $[Ru(bpy)3]^{2+}$ so O.S.$_{Ru}$ + 0 x 3 (for bpy) = +2 (the complex's charge) so O.S.$_{Ru}$ = +2 or Ru^{2+}.

Answer $[PdCl_2(dppe)]$.

O.S.$_{Pd}$ + 2 x (-1) (for Cl^-) + 0 x 3 (for dppe) = +0 (the complex's charge) so O.S.$_{Pd}$ = +2 or Pd^{2+}.

Answer $[Mn(en)_2(SCN)_2]$.

O.S.$_{Mn}$ + (2 x 0) (for en) + 2 x (-1) (for SCN^-) = +0 (the complex's charge) so O.S.$_{Mn}$ = +2 or Mn^{2+}.

? Exercise 4.3.3: Simple Nomenclature Problems.

Name the following compounds in both the Stock and Ewing-Bassett systems:

a. $[Ru(NH_3)_6](NO_3)_3$
b. $K_2[PtCl_4]$
c. $K[Ag(CN)_2]$
d. $Cs[CuBrCl_2F]$
e. $[Cu(acac)_2]$

Answer

	Complex	Stock system name	Ewing-Bassett System name
a	$[Ru(NH_3)_6](NO_3)_3$	hexammineruthenium(III) nitrate	hexammineruthenium(3+) nitrate
b	$K_2[PtCl_4]$	potassium tetrachloroplatinate(II)	potassium tetrachloroplatinate(2-)
c	$K[Ag(CN)_2]$	potassium dicyanoargentate(I)	potassium dicyanoargentate(1-)
d	$Cs_2[CuBrCl_2F]$	cesium bromodichlorofluorocuprate(II)	cesium bromodichlorofluorocuprate(2-)
e	$[Cu(acac)_2]$	bis(acetylacetonato)copper(II)	bis(acetylacetonato)copper(0)

? Exercise 4.3.4: More simple nomenclature problems.

Name the following compounds and ions in both the Stock and Ewing-Bassett systems.

a. $Cu(OH)_4^-$
b. $[AuXe_4]^{2+}$
c. $AuCl_4^-$
d. $Fe(CN)_6^{3-}$
e. $K_4[Fe(CN)_6]$
f. *trans*-$[Cu(en)_2(NO_2)_2]$ (the N is bound to Cu)
g. cis-$IrCl_2(CO)(PPh_3)$ (ignore stereochemistry)
h. $IrCl(PPh_3)_3$

Answer

	Compound	Stock System Name	Ewing-Bassett System Name
a	$Cu(OH)_4^-$	tetrahydroxidocuprate(III) or tetrahydroxidocuprate(III)	tetrahydroxidocuprate(1-) or tetrahydroxidocuprate(1-)
b	$[AuXe_4]^{2+}$	tetraxenongold(II)	tetraxenongold(2+)
c	$AuCl_4^-$	tetrachloroaurate(III)	tetrachloroaurate(1-)
d	$Fe(CN)_6^{3-}$	hexacyanoferrate(III) or hexacyanidoferrrate(III)	hexacyanoferrate(3-) or hexacyanidoferrate(3-)
e	$K_4[Fe(CN)_6]$	potassium hexacyanoferrate(II) or potassium hexacyanidoferrrate(II)	potassium hexacyanoferrate(4-) or potassium hexacyanidoferrrate(4-)
f	*trans*-$[Cu(en)_2(NO_2)_2]$ (the N is bound to Cu)	bis(ethylenediamine)bisnitrocopper(II) or bis(ethylenediamine)bis(nitrito-*κN*)copper(II)	bis(ethylenediamine)bisnitrocopper(0) or bis(ethylenediamine)bis(nitrito-*κN*)copper(0)
g	*cis*-$IrCl_2(CO)(PPh_3)$	*cis*-dichlorocarbonyltriphenylphosphineiridium(I) or *cis*-dichloro(carbonyl)(triphenylphosphine)iridium(I)	*cis*-dichlorocarbonyltriphenylphosphineiridium(0) or *cis*-dichloro(carbonyl)(triphenylphosphine)iridium(0)
h	$IrCl(PPh_3)_3$	chlorotris(triphenylphosphine)iridium(I)	chlorotris(triphenylphosphine)iridium(0)

? Exercise 4.3.5: Even more simple nomenclature problems.

Name the following compounds and ions in both the Stock and Ewing-Bassett systems. Ignore prefixes for designating isomers if you haven't learned about those.

a. $Fe(acac)_3$
b. $K_2[CuBr_4]$
c. ReH_9
d. $[Ag(NH_3)_2]BF_4$
e. $[Ag(NH_3)_2][Ag(CN)_2]$
f. $[Ni(CN)_4]^{2-}$
g. $[Co(N_3)(NH_3)_5]SO_4$
h. $[CoBrCl(H_2O)(NH_3)]I$ (ignore stereochemistry)

Sample Answers

	Complex	Stock system name	Ewing-Bassett System name
a	$Fe(acac)_3$	tris(acetoacetato)iron(III)	tris(acetoacetato)iron(0)
b	$Na_2[CuBr_4]$	sodium tetrabromocuprate(II)	sodium tetrabromocuprate(2-)
c	$[Co(NH_3)_6][Co(ox)_3]$	hexamminecobalt(III) tris(oxalato)cobalt(III)	hexamminecobalt(3+) tris(oxalato)cobalt(3-)
d	$[Ag(NH_3)_2]BF_4$	diamminesilver(I) tetrafluoroborate	diamminesilver(1+) tetrafluoroborate
e	$[Ag(NH_3)_2][Ag(CN)_2]$	diamminesilver(I) dicyanoargentate(I) or diamminesilver(I) dicyanidoargentate(I)	diamminesilver(1+) dicyanoargentate(1-) or diamminesilver(1+) dicyanidoargentate(1-)
f	$[Ni(CN)_4]^{2-}$	tetracyanonickelate(II) or tetracyanonickelate(II) ion	tetracyanonickelate(2-) or tetracyanonickelate(2-) ion
g	$[Co(N_3)(NH_3)_5]SO_4$	pentammineazidocobalt(III) sulfate	pentammineazidocobalt(2+) sulfate
h	$[CoBrCl(H_2O)(NH_3)]I$ (ignore stereochemistry)	ammineaquabromochlorocobalt(III) iodide	ammineaquabromochlorocobalt(1+) iodide

? Exercise 4.3.6: Nomenclature problems, some of which involve consideration of isomerism.

Name the following compounds and ions in both the Stock and Ewing-Bassett systems. Ignore prefixes for designating isomers if you haven't learned about those.

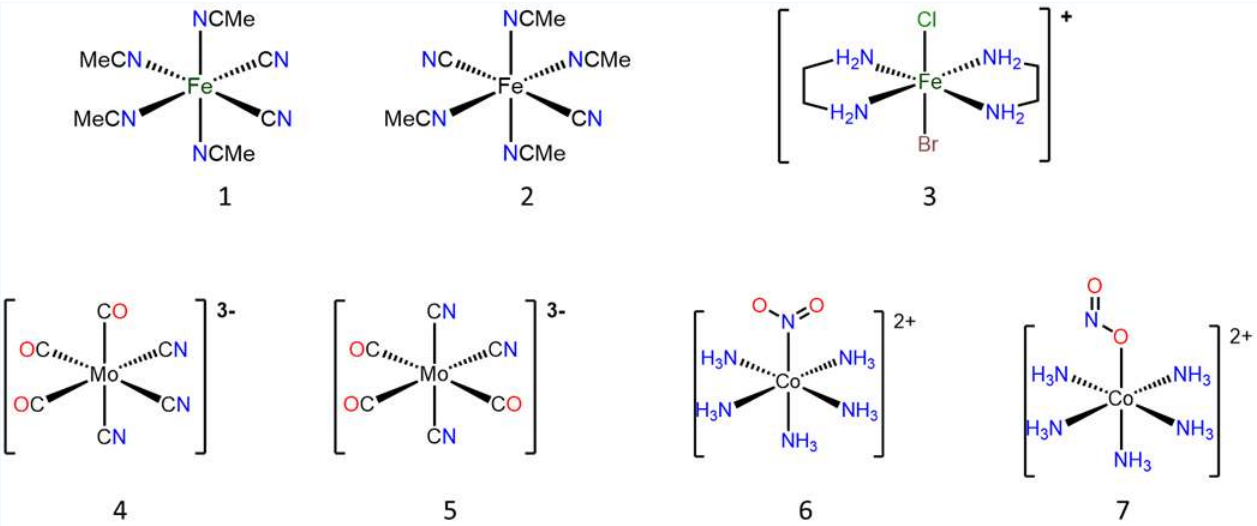
a. *trans*-$[Cu(dppe)_2(NO_2)_2]$ (the N is bound to Cu)
b. $[Pd(en)_2(SCN)_2]$, with the thiocyanates bound Pd-SCN
c. $[Mn(CO)_6]BPh_4$ (BPh_4 = tetraphenylborate)
d. $Rb[AgF_4]$
e. K_2ReH_9
f. K_3CrCl_6
g. $[Ru(H_2O)_6]Cl_2$
h. [*cis*-$Fe(CO)_4I_2$]
i. K_2[*trans*-$Fe(CN)_4(CO)_2$]
j. [*cis*-$MnCl(H_2O)_4(NH_3)](NO_3)$
k. K_3[*fac*-$RuCl_3(PMe_3)_3$]

Answer

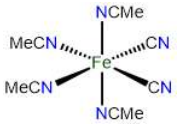
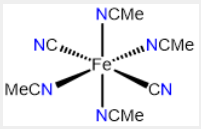
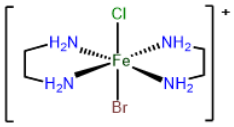
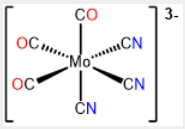
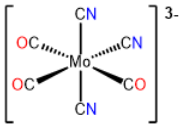
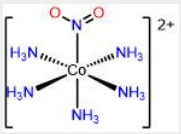
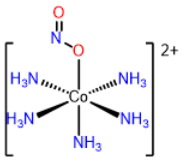
	Complex	Stock system name	Ewing-Bassett System name
a	*trans*-$[Cu(dppe)_2(NO_2)_2]$	*trans*-bis(diphenylphosphinoethane)bisnitrocopper(II) or *trans*-bis(diphenylphosphinoethane)bis(nitrito-κN)copper(II)	*trans*-bis(diphenylphosphinoethane)bisnitrocopper(0) or *trans*-bis(diphenylphosphino)ethane bis(nitrito-κN)copper(0)
b	$[Pd(en)_2(SCN)_2]$, with the thiocyanates bound Pd-SCN	bis(ethylenediamine)bisthiocyanatopalladium(II) or bis(ethylenediamine)bis(thiocyanato-*S*)palladium(II) or bis(ethylenediamine)bis(thiocyanato-κS)palladium(II)	bis(ethylenediamine)bisthiocyanatopalladium(0) or bis(ethylenediamine)bis(thiocyanato-*S*)palladium(0) or bis(ethylenediamine)bis(thiocyanato-κS)palladium(0)
c	$[Mn(CO)_6]BPh_4$	hexacarbonylmanganese(I) tetraphenylborate	hexacarbonylmanganese(1+) tetraphenylborate
d	$Rb[AgF_4]$	rubidium tetrafluoroargentate(III)	rubidium tetrafluoroargentate(1-)
e	K_2ReH_9	potassium nonahydridorhenium(VII)	potassium nonahydridorhenium(2-)
f	K_3CrCl_6 or $K_3[CrCl_6]$	potassium hexachlorochromium(III) or potassium hexachloridochromium(III)	potassium hexachlorochromium(3-) or potassium hexachloridochromium(3-)
g	$[Ru(H_2O)_6]Cl_2$	hexaaquaruthenium(II) chloride	hexaaquaruthenium(2+) chloride
h	[*cis*-$Fe(CO)_4I_2$]	*cis*-tetracarbonyldiiodoiron(II)	*cis*-tetracarbonyldiiodoiron(0)
i	K_2[*trans*-$Fe(CN)_4(CO)_2$]	potassium *trans*-dicarbonyltetracyanoferrate(II)	potassium *trans*-dicarbonyltetracyanoferrate(2-)
j	[*cis*-$MnCl(H_2O)_4(NH_3)$] (NO_3)	*cis*-amminetetraaquachloromanganese(0) nitrate	*cis*-amminetetraaquachloromanganese(1+) nitrate
k	K[*fac*-$RuCl_3(PMe_3)_3$]	potassium *fac*-trichlorotris(triphenylphosphine)ruthenium(II)	potassium *fac*-trichlorotris(triphenylphosphine)ruthenium(1-)

? Exercise 4.3.7

Name the compounds and ions below using both the Stock and Ewing-Bassett systems. Ignore prefixes for designating isomers if you haven't learned about those.


NCMe
MeCN
CN
Fe
MeCN
CN
NCMe
1
NCMe
NC
NCMe
Fe
MeCN
CN
NCMe
2
Cl
+
H2N
NH2
Fe
H2N
NH2
Br
3
CO
OC
CN
3-
Mo
OC
CN
CN
4
CN
OC
CN
3-
Mo
OC
CO
CN
5
O
N
O
2+
H3N
NH3
Co
H3N
NH3
NH3
6
O
N
O
2+
H3N
NH3
Co
H3N
NH3
NH3
7

Answer

#	Structure	Stock system name	Ewing-Bassett system name
1		*cis*-tetraacetonitriledicyanoiron(II) or *cis*-tetraacetonitriledicyanidoiron(II)	*cis*-tetraacetonitriledicyanoiron(0) or *cis*-tetraacetonitriledicyanidoiron(0)
2		*trans*-tetraacetonitriledicyanoiron(II) or *trans*-tetraacetonitriledicyanidoiron(II)	*trans*-tetraacetonitriledicyanoiron(0) or *trans*-tetraacetonitriledicyanidoiron(0)
3		*trans*-bromochlorobis(ethylenediamine)iron(III) or *trans*-bromidochloridobis(ethylenediamine)iron(III)	*trans*-bromochlorobis(ethylenediamine)iron(1+) or *trans*-bromidochloridobis(ethylenediamine)iron(1+)
4		*fac*-tricarbonyltricyanomolybdate(0) or *fac*-tricarbonyltricyanidomolybdate(0)	*fac*-tricarbonyltricyanomolybdate(3-) or *fac*-tricarbonyltricyanidomolybdate(3-)
5		*mer*-tricarbonyltricyanomolybdate(0) or *mer*-tricarbonyltricyanidomolybdate(0)	*mer*-tricarbonyltricyanomolybdate(3-) or *mer*-tricarbonyltricyanidomolybdate(3-)
6		pentamminenitrito-*N*-cobalt(III), pentamminenitrito-**κ***N*-cobalt(III), or pentamminenitrocobalt(III)	pentamminenitrito-*N*-cobalt(2+), pentamminenitrito-**κ***N*-cobalt(2+), or pentamminenitrocobalt(2+)
7		pentamminenitrito-*O*-cobalt(2+), pentamminenitrito-**κ***O*-cobalt(2+), or pentamminenitritocobalt(2+)	pentamminenitrito-*O*-cobalt(2+), pentamminenitrito-**κ***O*-cobalt(2+), or pentamminenitritocobalt(2+)

? Exercise 4.3.8

Draw structural formulae for the following compounds and ions. You may assume that

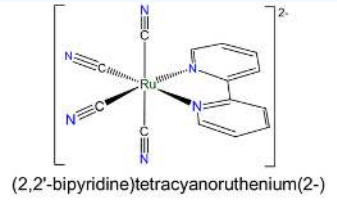
- complexes in which the metal has a coordination number of six are octahedral
- complexes in which the metal has a coordination number of five are trigonal bipyramidal

- complexes in which Pt^{II} , Pd^{II} , or Rh^{I}, or Ir^{I} have a coordination number of four are square planar
- other complexes in which the metal has a coordination number of four will be tetrahedral

a. (2,2'-bipyridine)tetracyanoruthenium(2-)
b. sodium tetrachloroaluminate (note that since Al is a main group metal with a generally fixed oxidation state no oxidation state is given)
c. pentaamminechlorocobalt(2+) sulfate
d. carbonylhydridotris(triphenylphosphine)rhodium(I) (the ligands in this complex occupy sterically preferred positions)
e. bromotrichlorocobaltate(III)
f. hexaaquacopper(2+) sulfate
g. sodium tris(oxalato)cobalt(III)
h. *fac*-(1,10-phenanthroline)tricarbonylchlororhenium(I)
i. *mer*-triaquatrichlorochromium(III)
j. *trans*-dichlorobis(ethylenediamine)platinum(IV)

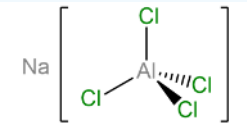
Answers

a



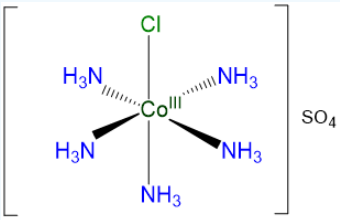
(2,2'-bipyridine)tetracyanoruthenium(2-)

b



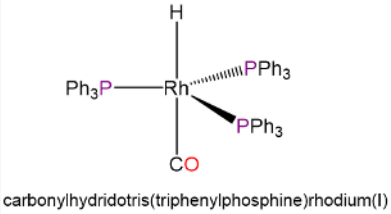
Sodium tetrachloroalumnate

c



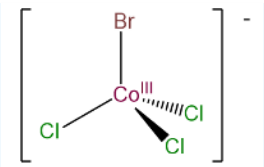
pentaamminechlorocobalt(2+) sulfate

d



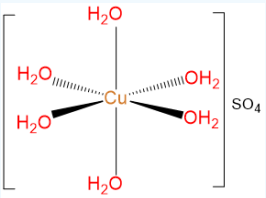
carbonylhydridotris(triphenylphosphine)rhodium(I)

e



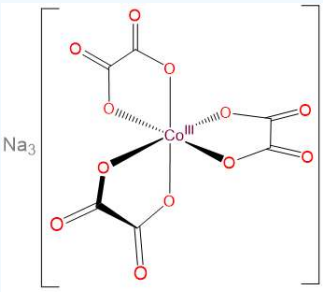
bromotrichlorocobaltate(III)

f



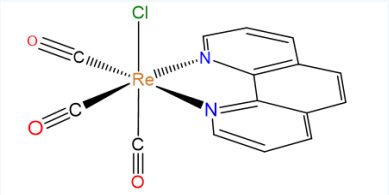
hexaaquacopper(2+) sulfate

g



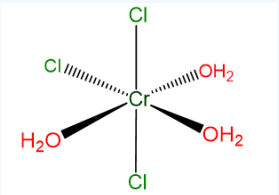
sodium tris(oxalato)cobalt(III)
Λ-enantiomer shown

h



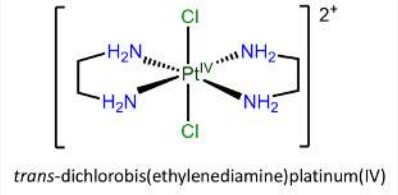
fac-(1,10-phenanthroline)tricarbonylchlororhenium(I)

i



mer-triaquatrichlorochromium(III)

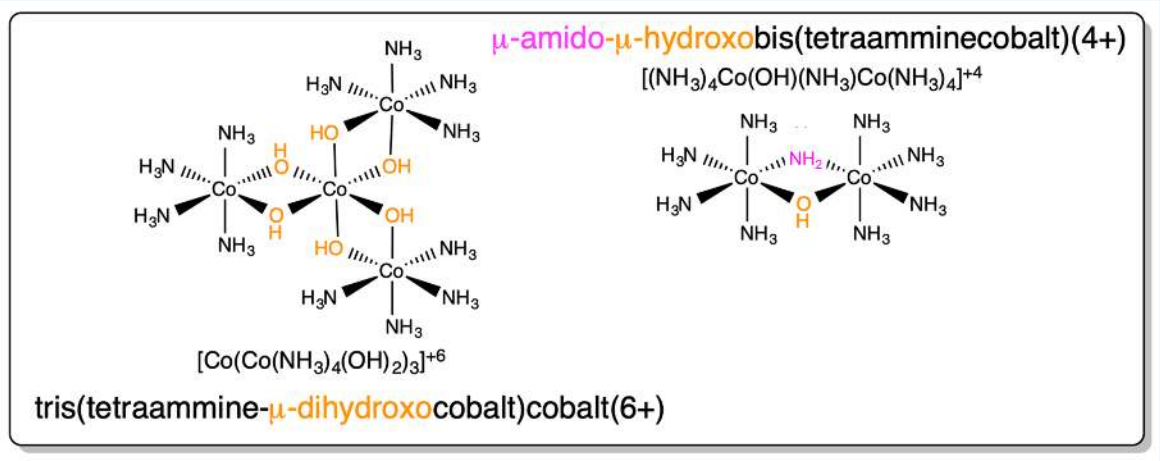
j



trans-dichlorobis(ethylenediamine)platinum(IV)

Exercise 4.3.9.

The name of the structure named tris(tetraammine-μ-dihydroxocobalt)cobalt(6+) in Scheme **4.3.III** (reproduced below) is incomplete. Give the complete name of the structure in both the Stock and Ewing-Basset systems.



Answer

Δ-tris(tetraammine-μ-dihydroxocobalt)cobalt(6+) or **Δ**-tris(tetraammine-μ-dihydroxocobalt(III)cobalt(III)

Note: Rules for Writing the Formulae of Coordination Copounds

Rules for writing the formulae of coordination compounds

As organized predictable formulae can be easier to read and understand than haphazardly written ones, the rules for writing the formulae of coordination compounds have value. To support those who wish to employ them they are given in this section. The rules as given here are adapted from a summary by Robert Lancashire.

The rules for writing the formulae of coordination compounds follow the same convention used to specify their names.

1. If there are multiple ions present list the cations before anions.
2. Enclose all the constituents of each complex ion in square brackets.
3. For each complex ion,
   - Give the **central metal** atom first.
   - Then **ligands** next, listed in alphabetical order, ignoring prefixes according to the first letters in the ligand's symbol as written. This is true regardless of whether the symbol is an element symbol (like C, N, O, etc.) or a symbol for the ligand name (bpy, en, MeCN, etc.). Contrary to widely-circulated myths, the ligand's charge does not matter.[4]
   - The formulae or abbreviations (*e.g.* en) for all polyatomic ligands should be enclosed in ordinary parentheses.
   - As appropriate, use italicized atom symbols to indicate linkage isomerism and prefixes such as *cis*-, *trans*-, *fac*-, *mer*-, **Λ**-, **Δ**-, κ^n, η^n , μ_n, **λ**-, or **δ**- to indicate stereochemistry.
   - When a ligand is bound to a metal through a particular atom, preferably place that atom closest to the metal - *e.g.*, $[Fe(CN)_6]^{3-}$ not $[Fe(NC)_6]^{3-}$ (Note: this rule is used primarily for ambidentate ligands; although IUPAC recommends that aqua ligands be written as OH_2 when the O would be closest to its coordinated metal, they are still usually written as H_2O).

These rules are graphically summarized in Figure **4.3.2**.

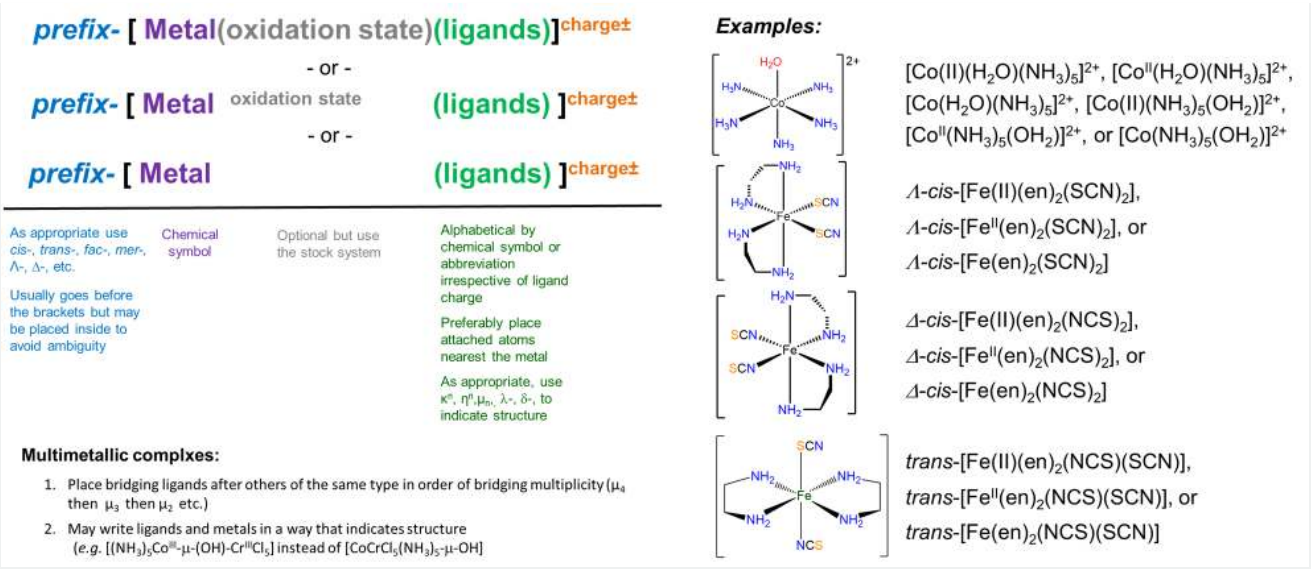
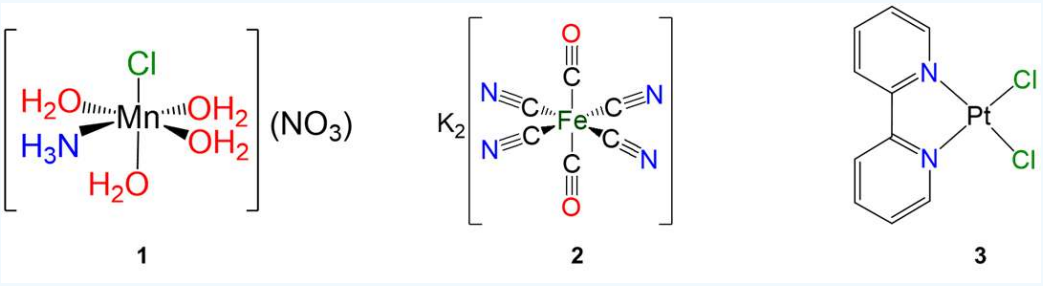


Figure **4.3.2**. Summary of the rules for writing the formula of a coordination complexes along with a few examples of their application. This work by Stephen Contakes is licensed under a Creative Commons Attribution 4.0 International License.

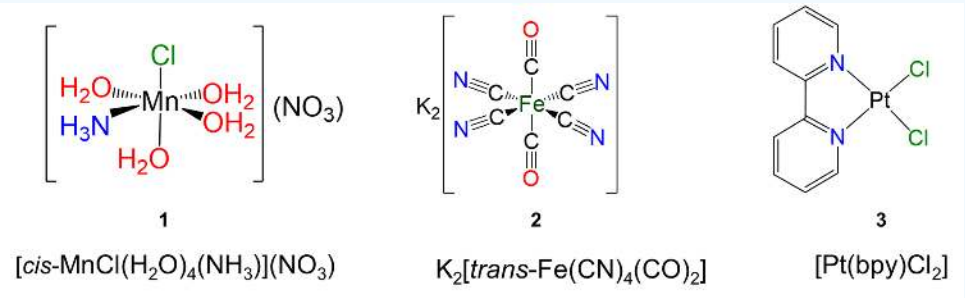
? Exercise 4.3.10

Give the formulae of the following complexes.



.

Answer

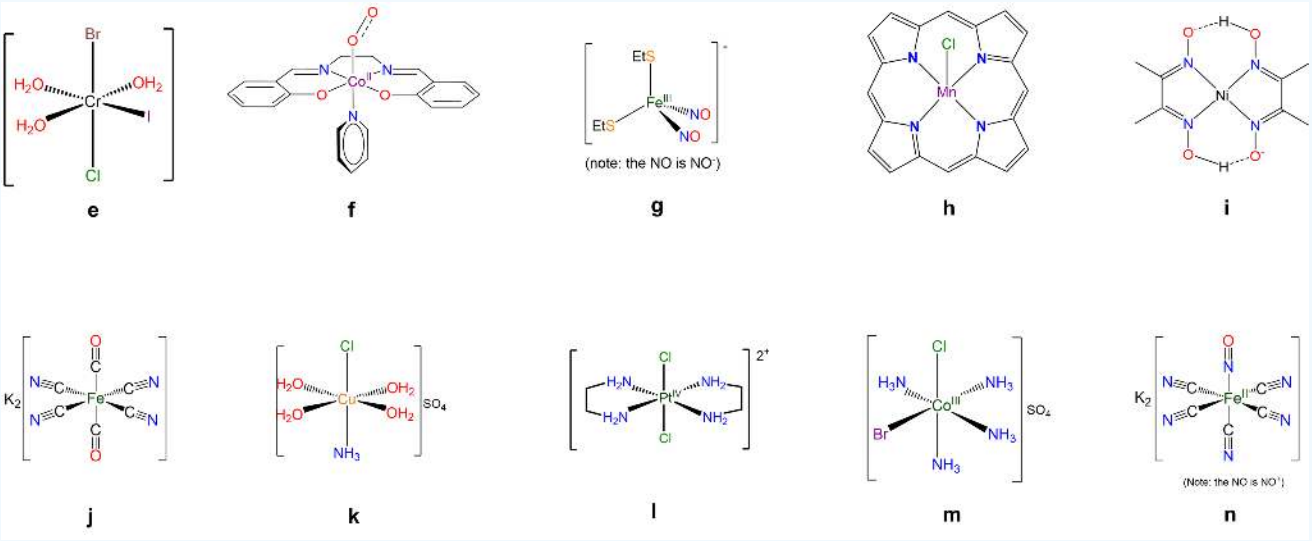


? Exercise 4.3.11

Write formulae for each of the following compounds and ions. When multidentate ligands are present use suitable abbreviations.

a. pentaamminechlorocobalt(2+) sulfate
b. **Δ**-diamminebis(oxalato)manganate(III)
c. *trans*-tetraacetonitriledicyanoiron(II)

d. tricarbonyldichlorobis(triphenylphosphine)molybdenum



Answers

a.

$[CoCl(NH_3)_5](SO_4)$

b.

Δ-$[Mn(NH_3)_2(ox)_2]^-$

c.

trans-$[Fe(CN)_2(NCMe)_4]$

d.

$[MoCl_2(CO)_3(PPh_3)]$ or $MoCl_2(CO)_3(PPh_3)$

e.

mer-$[CrBrCl(H_2O)_3I]$

f.

$[Co(O_2)py(salen)]$

g.

$[Fe(NO)_2(SEt)_2]^-$

h.

$[MnCl(por)]^-$ or $[MnCl(porphyrin)]^-$

i.

$[Ni(DMG)_2]$ or $[Ni(Hdmg)_2]$

j.

potassium *trans*-$[Fe(CN)_2(CO)_4]$

k.

trans-$[CuCl(H_2O)_4(NH_3)]SO_4$

l.

trans-$[PtCl_2(en)_2]^{2+}$

m.

cis-$[CoBrCl(NH_3)_4]SO_4$

n.

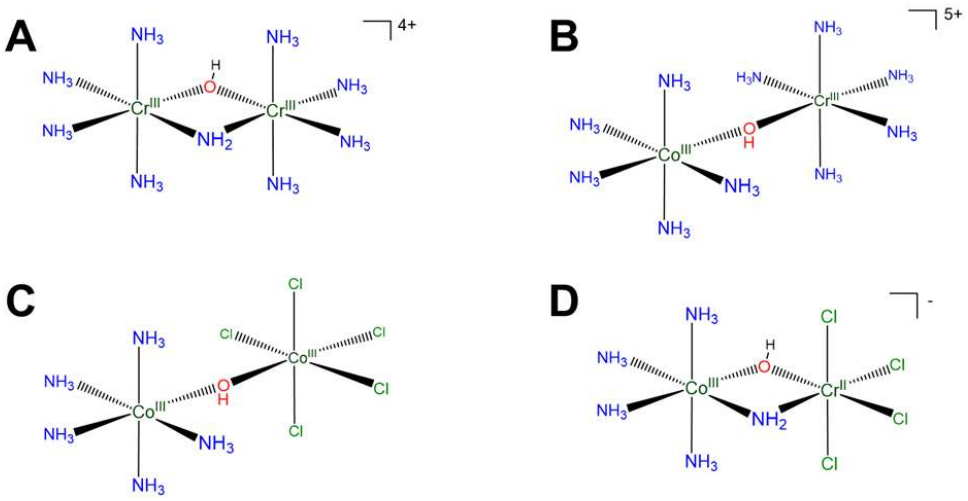
$K_2[Fe(CN)_5NO]$

Multinuclear coordination complexes

Multinuclear coordination complexes contain multiple metals connected by one or more bridging ligands. The structures of bridging complexes can usually be inferred from their μ-tagged ligands in their names and formulae. For the benefit of instructors who wish to have their students name multinuclear complexes, the rules are presented below.

Multinuclear complexes are named differently depending on whether the groups on either side of the bridging ligands are identical or different, as shown in Scheme **4.3.VIII**.

Scheme 4.3.VIII. Multinuclear coordination complexes may be named differently depending on whether the groups on either side of the bridging ligands are the same or different. The groups are the same if the metal, ligands, and ligand arrangement are identical. This is true in A but in B the metals differ, in C the ligands differ, and in D both the metal and ligands differ.



Naming multinuclear complexes

Let's look at the rules for naming symmetric and asymmetric multinuclear complexes.

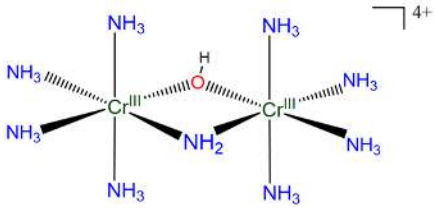
Application of the IUPAC system and variants thereof to symmetric complexes

The IUPAC naming system helpfully avoids the sort of ambiguities and *ad hoc* choices involved in most textbook-level nomenclature systems for multimetallic complexes. Unfortunately, it is correspondingly difficult for beginners to employ. Thus it will only be applied in depth to the case of symmetric complexes. Symmetric complexes are particularly easy to name in the IUPAC system and several of its variants that find common use. In these

1. The ligands are given in alphabetical order. When there are bridging and non-bridging ligands of the same type the bridging ligands are given first. When there are multiple bridging ligands of the same type but which use different bridging modes (*e.g.*, μ_4-, μ_3-, μ_2-), the bridging ligands are specified in decreasing order of bridging multiplicity, *e.g.*, μ_3 -sulfido-di-μ-sulfido.
2. The groups bridged are given afterwards using names that follow the ordinary rules. Generally this involves either
   a. naming all the ligands followed by all the metals, in both cases using prefixes to indicate the number of each, or
   b. naming each group of atoms individually as in the less formal naming system, using prefixes to indicate the number of ligands (this is an unofficial variant of the IUPAC system that some textbook authors seem to prefer).

These two rules are sufficient to describe simple symmetric bridging complexes.

Example: The compound in Scheme **4.3.VIIIA**



may be named

[μ-amido-μ-hydroxo-octaamminedichromium(4+)] ion

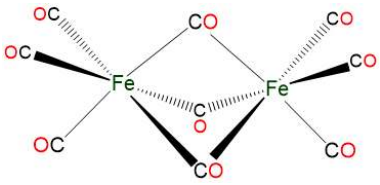
or

[μ-amido-μ-hydroxo-bis(tetraamminechromium(III))] ion

or

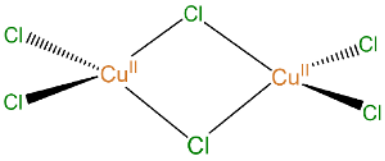
[μ-amido-μ-hydroxo-bis(tetraamminechromium)(4+)] ion

Example: The complex[5]



may be named [tri-μ-carbonyl-bis(tricarbonyliron)(0)], [tri-μ-carbonyl-bis(tricarbonyliron(0))], or [tri-μ-carbonyl-hexacarbonyldiiron)(0)]

Example: The complex



may be named di-μ-chlorido-tetrachloridodicopper(II), di-μ-chlorido-bis(dichlorocopper(II)), or di-μ-chlorido-bis(dichlorocopper)(0)

A note on the application of the IUPAC system and variants thereof to asymmetric complexes

For a symmetrical complex like the $[Cu_2Cl_4(\mu\text{-}Cl)_2]$ considered above it is enough to specify the existence of the two bridging and four terminal chloro ligands; there is no need to number the chloro ligands or to specify exactly which ones are involved in bridging or to clarify that the bridging involves κ^2 coordination of the chloro ligands. In cases where the two metal centers or the chloro ligands differ it is necessary to specify the exact ligands and metals involved and how they are connected.

For example, a more extensive IUPAC name for $[Cu_2Cl_4(\mu\text{-}Cl)_2]$ in which the chloro ligands are individually and more completely specified would read di-μ_2-chlorido-tetrachlorido-1κ^2Cl,2κ^2Cl-dicopper(II).

Even more extensive systems would involve numbering the metals and specifying how they are connected together too. The details of how this is done are typically beyond the level of most undergraduate and graduate courses in inorganic chemistry. Those who want to know the details should consult the red book. In many cases it is sufficient to reserve the use of formal IUPAC names for use in publications and to employ a convenient shorthand naming system for everyday use. An example of one type of system that is sometimes employed is given next.

Unofficial but commonly used methods applicable to complexes in which the groups bridged are identical or different.

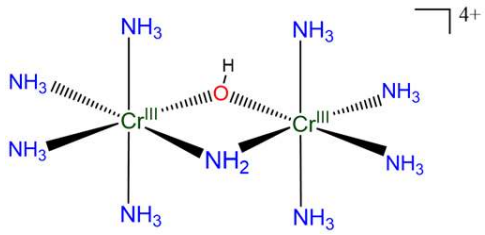
It can be quite complicated to use the IUPAC system to name asymmetric multinuclear coordination complexes. Fortunately it is rarely necessary and there are a variety of simpler somewhat *ad hoc* methods that work well for such cases. Since these methods

are commonly used by textbooks and inorganic instructors it is likely worth your while to learn about their general features. In these methods

1. A multinuclear complex is named as a derivative of one of the metal centers and the other metal centers and their ligands are treated as ligands to the prioritized metal center.
2. Unfortunately, most of the time the choice of which metals are part of the ligands and which one is central is made haphazardly. In other words, there is no agreed upon system for assigning which metal center is the central metal and which should be regarded as part of the ligands around it. One way to be more systematic about the selection of the central and ligand-embedded metals is to assign the central metal as the metal of highest priority in the IUPAC priority rules. In the IUPAC priority rules, the central metal is the highest priority metal alphabetically by name; then if there is a tie the ligands on each tied metal center are ranked alphabetically and the tied metal center with the highest priority (or most highest priority) ligands wins.
3. The metal centers not chosen as the primary metal center and all ligands around them, including those bridging to the winning metal center, are then treated as a single ligand that coordinates the winning metal center.
4. When naming the ligands and the overall complex, again there is much that is haphazard. However, in the best systems each coordination sphere is named using the same rules as for mononuclear complexes - *i.e.*, the ligands are given in alphabetical order, etc.
    - This is true of any metal center-containing ligands.
    - When there is a bridging and non-bridging ligand of the same type, the bridging ligands are given first. When there are multiple bridging ligands of the same type but which use different bridging modes (*e.g.* μ_4-, μ_3-, μ_2-), the ligands are specified in decreasing order of bridging multiplicity, *e.g.* μ_3 -sulfido-di-μ-sulfido.

Let's apply these rules to the examples in Scheme **4.3.VIII**.

Compound A:



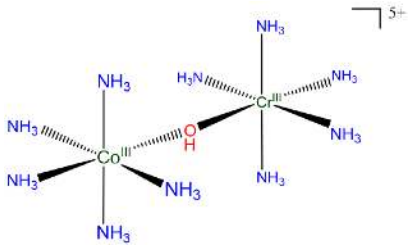
Using hydroxo for the OH^-, it may be named

[(μ-amido-tetraammine-μ-hydroxochromium(III))tetraamminechromium(III)] ion

or

[(μ-amido-tetraammine-μ-hydroxochromium)chromium(4+)] ion

Compound B:



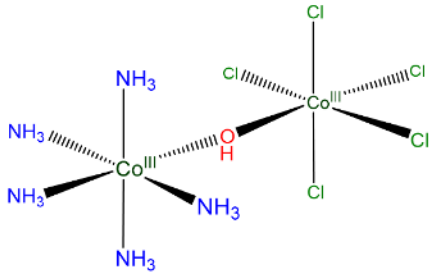
Using hydroxo for the OH^-, it may be named

[(pentaammine-μ-hydroxocobalt(III))tetraamminechromium(III)] ion

or

[(pentaammine-μ-hydroxocobalt)tetraamminechromium(5+)] ion

Compound C:



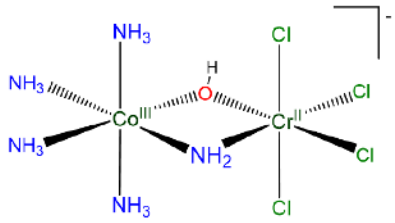
Using hydroxo for OH^-, it may be named

[pentaammine(pentachloro-μ-hydroxocobalt(III))cobalt(III)]

or

[pentaammine(pentachloro-μ-hydroxocobalt)cobalt](0)]

Compound D:



Using hydroxo for OH^- and chloro for Cl^-, it may be named

[pentaammine(pentachloro-μ-hydroxocobalt(III))chromate(III)] ion

or

[(tetrammine-μ-ammine-μ-hydroxocobalt)tetrachlorochromate](1-)] ion

As can be seen from the examples above this system gives serviceable names for multimetallic complexes but those names are not the IUPAC names and so should not be used to describe complexes outside of pedagogical and informal settings.

Writing and interpreting formulae for multinuclear complexes

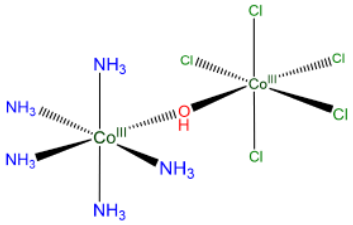
The rules for writing formulae for multinuclear complexes are the same as for mononuclear ones with two added details:

1. Write bridging ligands after nonbridging ligands of the same type. For example, Cu_2Cl_6 should be written as $[Cu_2Cl_4\text{-}(\mu\text{-}Cl)_2]$
2. However, you may ignore that and other rules if you find it helpful to keep groups of metals and ligands together in a way that better conveys how the atoms are connected. Just as the structure of ethane may be more clearly conveyed as H_3CCH_3 instead of CH_3CH_3, the complex $[Cu_2Cl_4(\mu\text{-}Cl)_2]$ may be written as $[(Cl_2Cu)(\mu\text{-}Cl)_2(CuCl_2)]$.

Other Examples:

For dichromate write, $[Cr_2O_6(\mu\text{-}O)]^{2-}$ or $[O_5Cr\text{-}\mu\text{-}O\text{-}CrO_5]^{2-}$

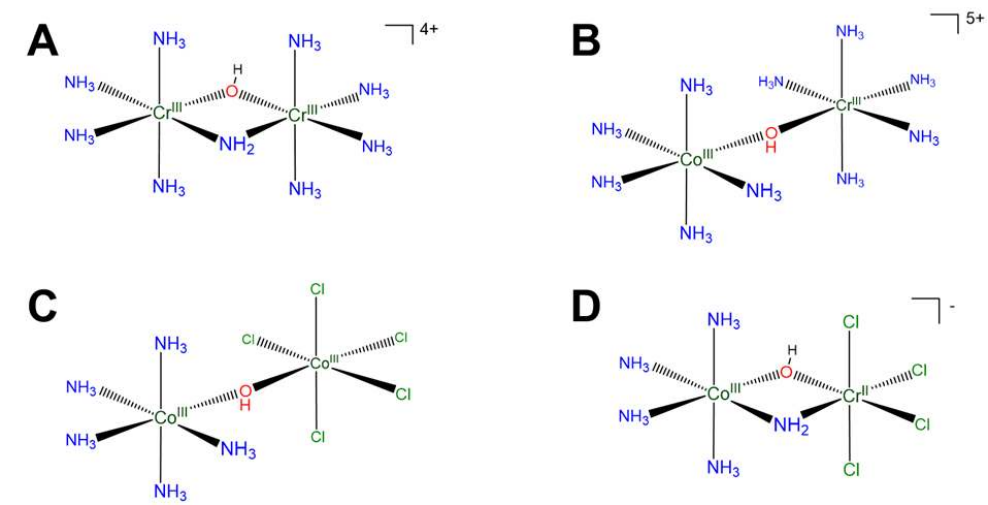
For compound C of Scheme **4.3.VIII**.



write $[Co_2Cl_5(NH_3)_5(\mu\text{-}OH)]$ or, even better, $[(H_3N)_5Co(\mu\text{-}OH)CoCl_5]$.

Exercise 4.3.10

Write reasonable formulae for complexes A, B, and D in Scheme **4.3.VIII**, which for convenience is reproduced below.



Sample answers for A

$[Cr_2(NH_3)_8\text{-}\mu(NH_2)\text{-}\mu(OH)]^{4+}$ or $[(H_3N)_4Cr^{III}\text{-}\mu(NH_2)\text{-}\mu(OH)\text{-}Cr^{II}(NH_3)_4]$ and variants thereof involving writing the H_3N as NH_3, μ as μ_2, etc.

Sample answers for B

$[CoCr(NH_3)_{10}\text{-}\mu(OH)]^{5+}$ or, better, $[(H_3N)_5Co^{III}\text{-}\mu(OH)\text{-}Cr^{III}(NH_3)_5]^{5+}$

Sample answers for C

This was already done as an example above, $[Co_2Cl_5(NH_3)_5\text{-}\mu(OH)]$ or, better, $[(NH_3)_5Co^{III}\text{-}\mu(OH)\text{-}Co^{III}Cl_5]$ and variants thereof

Sample answers for D

$[CoCrCl_4(NH_3)_4\text{-}\mu(NH_2)\text{-}\mu(OH)]$ or, better, $[(H_3N)_4Co^{III}\text{-}\mu(NH_2)\text{-}\mu(OH)\text{-}Cr^{II}Cl_4]$

References

1. International Union of Pure and Applied Chemistry *Nomenclature of Inorganic Chemistry* Cambridge, UK, 2005.

2. The structure and name is taken from Choudhury, S. B.; Allan, C. B.; Maroney, M.; Wodward, A. D.; Lucas, C. R. *Inorg. Synth.* **1998**, *32*, 98-107.

3. Haas, K. Naming Transition Metal Complexes. https://chem.libretexts.org/Courses/Saint_Mary's_College%2C_Notre_Dame%2C_IN/CHEM_342%3A_Bio-inorganic_Chemistry/Readings/Week_2%3A_Introduction_to_Metal-Ligand_Interactions_and_Biomolecules/2.1_Transition_metal_complexes/2.1.6%3A_Naming_Transition_Metal_Complexes

4. There is a widely-circulated myth that anionic ligands should be named before neutral ones. This myth is false. According to the IUPAC red book (bolding mine):

> IR-2.15.3.4: Ordering ligands in formulae and names in formulae of coordination compounds,
>
> The formulae or abbreviations representing the ligands **are cited in alphabetical order as the general rule**. Bridging ligands are cited immediately after terminal ligands of the same kind, if any, and in increasing order of bridging multiplicity. (See also Sections IR-9.2.3 and IR-9.2.5.)
>
> IR-9.2.3.1 Sequence of symbols within the coordination formula

(i) The central atom symbol(s) is (are) listed first.

(ii) The **ligand symbols (line formulae, abbreviations or acronyms) are then listed in alphabetical order** (see Section IR-4.4.2.2).5 Thus, CH_3CN, MeCN and NCMe would be ordered under C, M and N respectively, and CO precedes Cl because single letter symbols precede two letter symbols. **The placement of the ligand in the list does not depend on the charge of the ligand.**

(iii) More information is conveyed by formulae that show ligands with the donor atom nearest the central atom; this procedure is recommended wherever possible, even for coordinated water.

5. Technically organometallic complexes are named according to slightly different rules but the coordination compound naming system works here. Note that this complex was once thought to possess an Fe-Fe bond, in accordance with the predictions of the 18-electron rule. Consequently, older sources often give an [*Fe-Fe*] after the name to reflect the presence of that bond. However, as the complex is no longer thought to possess an Fe-Fe bond it is omitted here.

Contributors and Attributions

Stephen Contakes, Westmont College, to whom comments, corrections, and criticisms should be addressed.

with some examples taken from Naming Transition Metal Complexes by Kathryn Haas.

Consistent with the policy for original artwork made as part of this project, all unlabeled drawings of chemical structures are by Stephen Contakes and licensed under a Creative Commons Attribution 4.0 International License.

4.3: Nomenclature and Ligands is shared under a not declared license and was authored, remixed, and/or curated by Stephen M. Contakes.

- **9.3: Nomenclature and Ligands** by Stephen M. Contakes has no license indicated.

4.4: Isomerism

Metal complexes present a rich, interesting, and diverse structural chemistry. Major points of variation in the structural chemistry of metal complexes include

1. **coordination number** and **coordination geometry**, which involve differences in how many ligands surround a central metal and their overall geometric arrangement. Examples of the latter include the tetrahedral and square planar geometries commonly observed for four-coordinate metal centers. Tetrahedral, square planar, and octahedral coordination serve as a backdrop to the discussion of isomerism on this page. Readers who are unfamiliar with these structures might consider reading the section on coordination geometries before this one.
2. **structural iosmerism** involves differences in how potential ligand atoms are bound to metals in a complex. Possibilities for structural isomerism include
   - linkage or ambidentate isomerism
   - hydrate/solvate isomerism
   - ionization isomerism
   - coordination isomerism.

   Of these, linkage isomerism should always be considered when working with ambidentate ligands. As classifications, the last three forms of structural isomerism are mainly of academic interest since they represent permutations of ordinary structure patterns for solvates, salts, and coordination complexes, respectively.
3. **stereochemistry**, which includes
   - which coordination geometry is adopted for a metal with a given set of ligands in a particular oxidation state. For instance, $[Ni^{II}Cl_4]^{2-}$ is tetrahedral while $[Pt^{II}Cl_4]^{2-}$ is square planar. Since this geometry is usually fixed by the metal and ligands it is typically not a source of stereoisomeric varierty.
   - metal-centric stereoisomerism involving possible variations in where ligands are located relative to one another around the metal. The possibilities depend on the coordination number, geometry, and number of different types of ligands. For instance, square planar complexes can exhibit *cis-/trans-* isomerism while tetrahedral ones cannot. Tetrahedral complexes with four different ligands exhibit *R* and *S* chirality but complexes of that type are relatively rare. The more common cases include *cis* and *trans* isomerism in square planar complexes and *cis* & *trans-*, *mer* & *fac-*, and Λ & Δ isomerism in octahedral ones, although some multidentate ligands present additional possibilities for stereochemical variation
   - Stereoisomerism centered on the ligands bound to a metal center. Possibilities include
     - stereoisomerism inherent to a ligand. This would include cases where the ligand itself is chiral or, as in the case of amines, exists as a rapidly interconverting mixture of isomers. Thus this sort of stereoisomerism is an extension of the isomerism encountered in ordinary organic and other main group compounds. The main new issues introduced by binding of such ligands to a metal center involve the creation of new possibilities for diastereoisomerism based on the stereochemistry of the metal center and the freezing out of stereocenter inversion on binding to a metal. The latter is particularly important for amines, which as free amines racemize rapidly by nitrogen inversion.
     - or conformational isomerism involving five-membered **chelate rings** created when a multidentate ligand binds to a metal. This isomerism is often called chelate ring twist since individual rings can exhibit one of two conformations depending on how they twist on binding.

A summary of these forms of isomerism is given in Figure **4.4.1**.

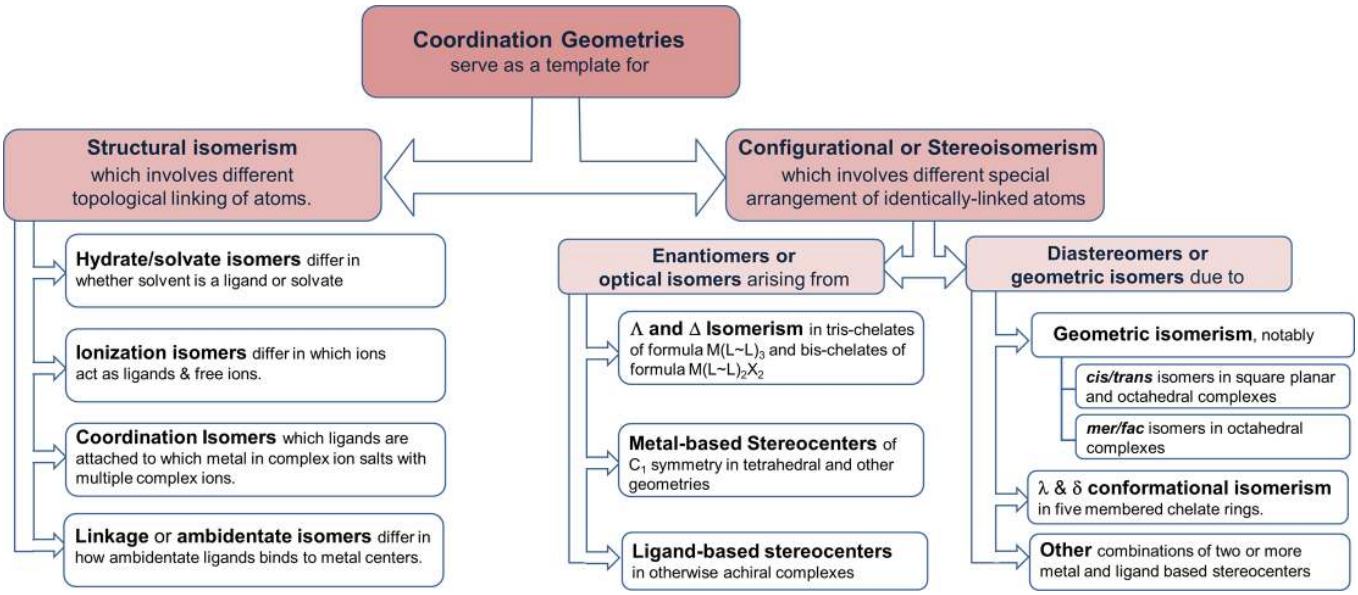


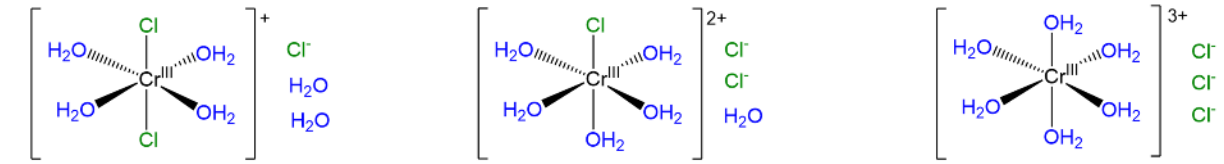
Figure **4.4.1**. Relationship among the common types of isomerism in metal complexes. This work by Stephen Contakes is licensed under a Creative Commons Attribution 4.0 International License.

Structural isomers

Structural isomerism involves different topological linkages of atoms. Differences in atomic linkages distinctive to coordination chemistry involve the linkages between metals and ligands. The main variations are:

1. Hydrate/solvate isomerism

Solvate isomers differ in terms of whether a molecule acts as a ligand or whether it acts as a solvate by occupying a lattice site in the crystal. Among solvate isomers, the case in which water is the ligand or solvate is the best known. The resulting isomers are called **hydrate isomers** after the term for water acting as a solvate, hydrate. A well-known example that illustrates how solvate isomerism works is the series $[CrCl_x(H_2O)_{6-x}]Cl_{3-x}{\cdot}xH_2O$, for which x = 0-2. The structures of the complex ions involved in this series are shown in Figure **4.4.2**.[1]



***trans*- $[CrCl_2(H_2O)_4]Cl{\cdot}2H_2O$**
bright-green
"tetraaqua-dihydrate"

$[CrCl(H_2O)_5]Cl_2{\cdot}H_2O$
grey-green
"pentaaqua-monohydrate"

$[Cr(H_2O)_6]Cl_3$
violet
"hexaaqua-"

Figure **4.4.2**. Complexes of the hydrate isomer series $[CrCl_x(H_2O)_{6-x}]Cl_{3-x}{\cdot}xH_2O$ (x = 0-2). This work by Stephen Contakes is licensed under a Creative Commons Attribution 4.0 International License.

As can be seen from the compounds in Figure **4.4.2**, hydrate isomers differ both in terms of whether water acts as a ligand or hydrate *and* in terms of whether a potential counterion acts as a counterion or ligand. Thus, in *trans*-$[CrCl_2(H_2O)_4]Cl{\cdot}2H_2O$ two chlorides act as chloro ligands and four waters as aqua ligands while in $[CrCl(H_2O)_5]Cl_2{\cdot}H_2O$ five water molecules act as aqua ligands while only one chloride acts as a chloro ligand. In this way, solvate isomers simply represent cases in which two or more of the possible permutations for metal ligand binding among a set of solvent and counterion molecules are stable.

2. Ionization isomerism

In **ionization isomerism** there are two or more potential ions that can act as ligands. The ionization isomers differ in terms of which of these ions act as counterions and which act as ligands. Consider, for instance, the complexes shown in Figure **4.4.3**. These complexes differ in terms of whether the chloride or sulfate acts as a ligand, with the other acting as a counterion.

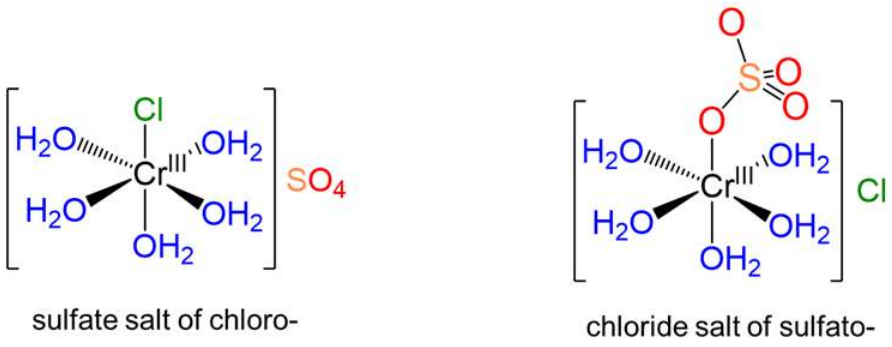


Figure **4.4.3**. Ionization isomers comprising a pentaaquachromium(III) fragment and the anions chloride and sulfate. As with all ionization isomers, the isomers differ in terms of which anion acts as a ligand and which a counterion. This work by Stephen Contakes is licensed under a Creative Commons Attribution 4.0 International License.

3. Coordination isomerism

Coordination isomers exist in compounds containing two or more complexes, each of which possesses a different set of ligands that can in principle be swapped with a ligand of the other complex. An example involves $[Co^{III}(NH_3)_6][Cr^{III}(ox)_3]$, depicted in Figure **4.4.4A**.[1] Coordination isomers of this complex involve swapping the ammine ligands around the Co^{3+} center for oxalato ligands surrounding the Cr^{3+} center. For instance, swapping all the ammine and oxalato ligands between the metal centers gives the coordination isomer $[Cr^{III}(NH_3)_6][Co^{III}(ox)_3]$ shown in Figure **4.4.4B**.

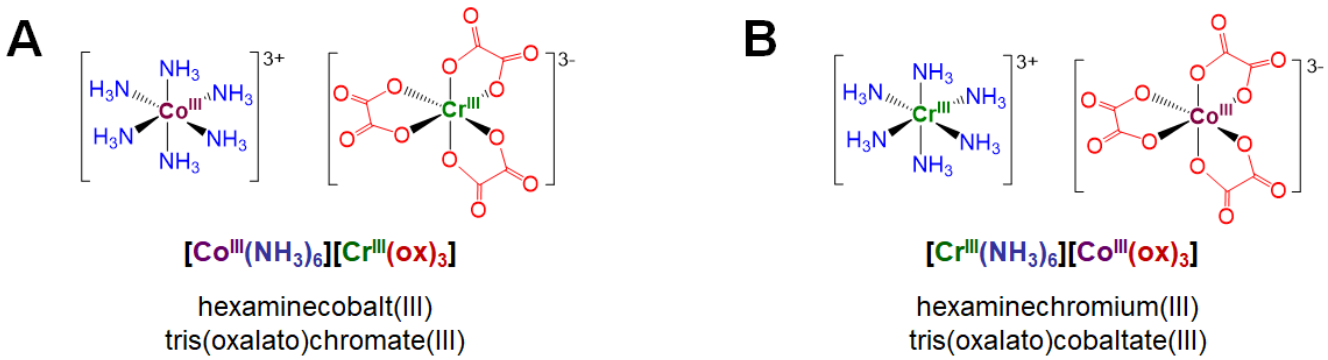
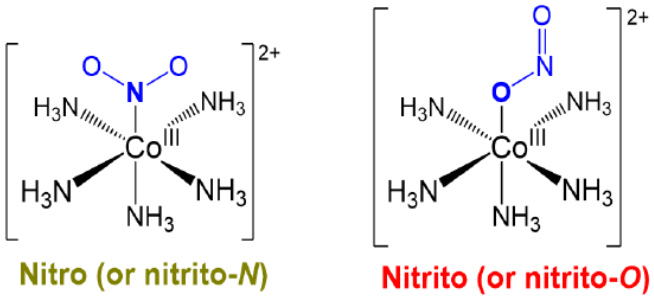


Figure **4.4.4**. Two coordination isomers comprising a Co^{3+} ,Cr^{3+}, six NH_3. and three oxalato ligands. The isomers differ in terms of which ligand type is bound to which metal. This work by Stephen Contakes is licensed under a Creative Commons Attribution 4.0 International License.

As classifications, hydrate/solvate, ionization, and coordination isomerism represent permutations of ordinary structure patterns for solvates, salts, and coordination complexes, respectively. As a result these forms of isomerism are rarely used as independent conceptual frameworks when thinking and talking about the structure of coordination compounds. Not so the final type of structural isomerism, linkage isomerism. That is because linkage isomerism has to do with the special *capacity* of ambidentate ligands to bind metals in multiple ways.

4. Linkage or ambidentate isomerism

Linkage or ambidentate isomers differ in how one or more ambidentate ligands bind to metal centers in a complex. The classic example dating from the work of Jørgensen and Werner is given in Scheme **4.4.I**.



Scheme **4.4.I**. Linkage isomers of penaamminenitritocobalt(III) ion. This work by Stephen Contakes is licensed under a Creative Commons Attribution 4.0 International License.

Just as alkenes exist as *E* and *Z* isomers, compounds possessing ambidentate ligands exist as one among the possible linkage isomers. As such, when working with ambidentate ligands the particular linkage isomer formed should be determined experimentally and considered when interpreting the complex's chemical and physical behavior.

The main ambidentate ligands which give rise to linkage isomerism are

- cyanide, CN^-
- thiocyanate, SCN^-, and the O and Se analogues, OCN^- and $SeCN^-$
- nitrite, NO_2^-
- sulfite, SO_3^-
- nitrosyl, NO

Although ambidentate ligands can bind metals in multiple ways, most exhibit a preferred binding mode (*i.e.*, prefer to bind metal centers in one of the possible ways). For instance, cyanide almost always binds through its carbon atom and thiocyanate almost always binds through its nitrogen (*μ-N*). However, the other binding mode can sometimes be formed kinetically or by using conditions that particularly favor its formation. Thus thiocyanate forms M-SCN^- linkages in the presence of exceptionally soft metal centers or in hard polar solvents (in which Lewis acid groups can stablize the terminal nitrogen of a bound thiocyanate ligand).

Ambidentate ligands are of significant research interest because many don't just bind to metal centers in two ways; the linkage isomers sometimes have significantly different physical properties. In addition, the possibility of two binding modes introduces the possibility of exploiting linkage isomerism to take advantage of some of these ligands:

a. different structural chemistry in different coordination modes. In mononuclear complexes the coordination mode influences which side of the ligand faces away from the complex and might be susceptible to stabilization by interaction with solvent. Additionally, the orientation of the ligand relative to the metal center might differ between one coordination mode and another. For instance, as predicted from the minor contributor to its resonance structure, thiocyanate binds nonlinearly via its S atom and linearly via its N (Figure **4.4.5**). Because of this the apparent steric bulk of the ligand around the metal center might differ between forms.

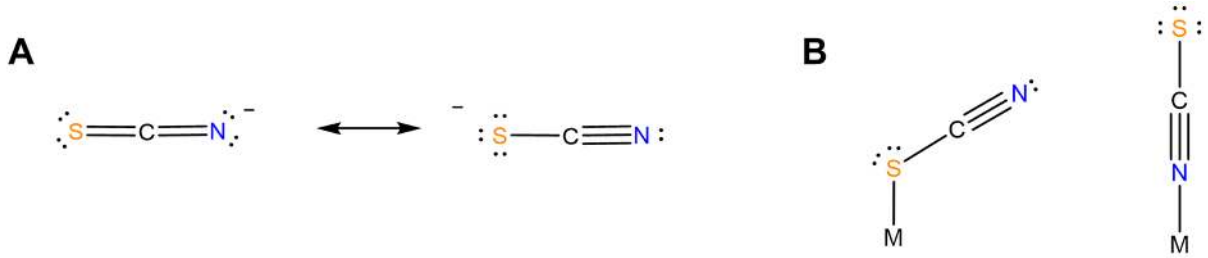


Figure **4.4.5**. Thiocyanate generally prefers to bind metals nonlinearly but in some cases forms linear M-SCN bonds. This work by Stephen Contakes is licensed under a Creative Commons Attribution 4.0 International License.

b. bind two different metal centers at the same time, linking them together. Perhaps the best-known examples involve thiocyanate and cyanide. The latter forms linkages of the type M-C≡N-M'. In the dye Prussian blue these take the form Fe^{II}-C≡N-Fe^{III}. An example from the author's graduate research involved tetrahedral clusters containing four metal atoms linked by six cyano ligands, as shown in Figure **4.4.6**.

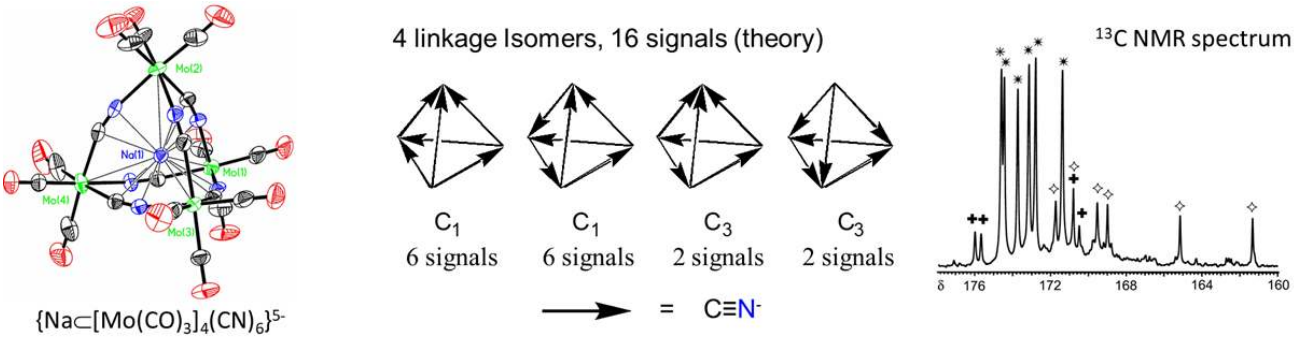


Figure **4.4.6**. (A) Structure of $\{Na@[Mo(CO)_3]_4(CN)_6\}$ showing the linking of four Mo centers by six CN ligands. Thermal ellipsoids for the C atoms are shown in black; those of the N atoms in blue. (B) The complex exists as a mixture of four linkage isomers in which the bridging CN^- ligands are oriented in different ways, as may be seen from the presence of the expected sixteen signals in its ^{13}C NMR spectrum. Based on work reported in reference 2.

c. can be induced to change from one binding mode to another in response to a stimulus. The classic example involves the light-driven transformation of the thermodynamically more stable yellow nitro complex of pentamminecobalt(III), $[Co(NH_3)_5NO_2]^{2+}$ to the less stable red *O*-nitrito complex, $[Co(NH_3)_5ONO]^{2+}$. Less stable cyanometallate coordination networks like those in the red $K\{Fe^{II}[Cr^{III}(CN)_6]\}$ transform into the more stable green $K\{Fe^{II}[Cr^{III}(NC)_6]\}$ form on heating, as shown in Figure **4.4.7**.[3]

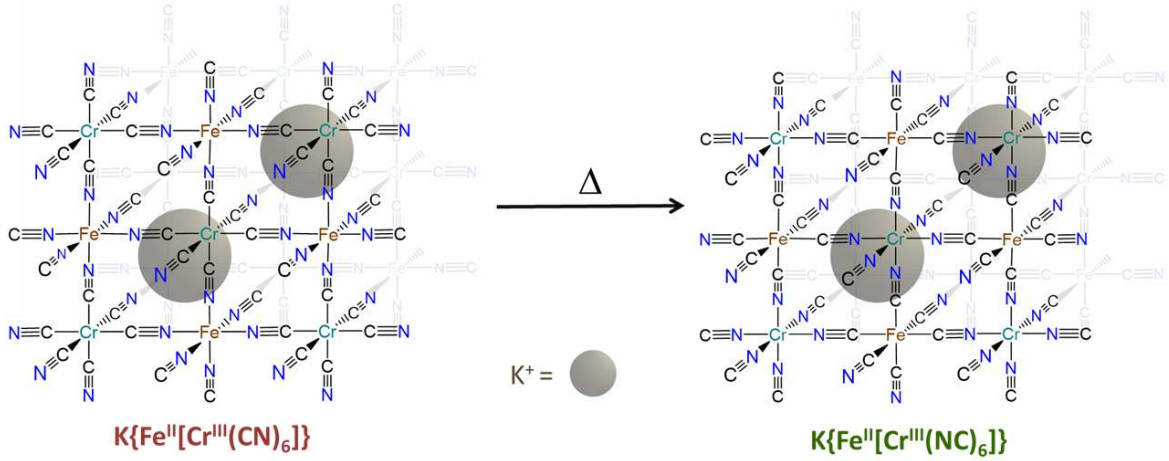


Figure **4.4.7**. Thermally-induced transformation of one $K\{Fe^{II}[Cr^{III}(CN)_6]\}$ into its more stable green linkage isomer $K\{Fe^{II}[Cr^{III}(NC)_6]\}$ involves "flipping" the cyano ligands. This work by Stephen Contakes is licensed under a Creative Commons Attribution 4.0 International License.

? Exercise 4.4.1: Bridging ambidentate ligands and the Hard-Soft Acid- Base Principle.

The hard-soft acid-base principle helps explain the preference of bridging ambidentate ligands for particular binding modes. How might the greater stability of the green $K\{Fe^{II}[Cr^{III}(NC)_6]\}$ over red $K\{Fe^{II}[Cr^{III}(CN)_6]\}$ be explained in terms of the hard and soft acid-base concept?

Answer

The greater stability of $K\{Fe^{II}[Cr^{III}(NC)_6]\}$ over $K\{Fe^{II}[Cr^{III}(CN)_6]\}$ reflects the greater stability of the Fe^{II}-CN-Cr^{III} linkages in the former over the Fe^{II}-NC-Cr^{III} linkages in the latter. This is consistent with the preference for hard-hard and soft-soft Lewis acid-base interactions of the Hard-Soft Acid-Base Principle.

The Fe^{II}-CN-Cr^{III} linkages are more stable because they possess bonds between

- the softer Lewis acid (Fe^{II}) and Lewis base (the C end of CN^-)
- the harder Lewis acid (Cr^{III}) and Lewis base (the N end of CN^-)

In contrast, the Fe^{II}-NC-Cr^{III} linkages in the less stable linkage isomer involve bonds between

- the softer base (the C end of CN^-) and harder acid (Cr^{III})
- the harder base (the N end of CN^-) and softer acid (Fe^{II})

Stereoisomerism

Optical Isomerism/Chirality

Molecules of D_n, C_n, or C_1 symmetry with only proper rotation axes (including $E = C_1$) are chiral and exhibit optical isomerism. As described in Figure **4.4.1**, the main sources of such optical isomerism in coordination chemistry are:

1. Chirality inherent to an organic or main group ligand.

   This type of isomerism is just an extension of the sort described in undergraduate organic texts and consequently does not merit separate discussion here, other than to note that some forms of optical isomerism which are of little importance in organic chemistry lead to optical activity in coordination compounds. In particular, the nitrogen inversion process which serves to rapidly racemize chiral amines is frozen out on formation of a metal-ligand bond. Because of this chiral amine, ligands bound to a metal form non-interconvertible *R* and *S* enantiomers, as shown in Figure **4.4.8**.

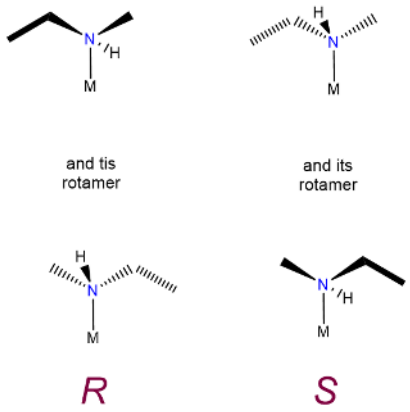


Figure **4.4.8**. Two views of *R* and *S* enantiomers formed when the chiral amine ethylmethylamine binds a metal that are commonly used to represent chiral amines in complexes. This work by Stephen Contakes is licensed under a Creative Commons Attribution 4.0 International License.

2. Chirality arising from the symmetry of ligands about a metal center.

   The two common situations through which such chirality arises involve:

   i. Chirality at a tetrahedral metal center surrounded by four different ligand attachment points.

   Such cases are often referred to as MABCD or Mabcd where M stands for the metal and a, b, c, and d the four different ligand attachment points. An example of such a complex is given in Figure **4.4.9A**. The chirality of such complexes is analogous to the chirality arising from a tetrahedral carbon stereocenter. There are two caveats, though. First, it is not enough to have a four-coordinate complex; the metal must possess tetrahedral symmetry since, as shown in Figure **4.4.9B**, square planar M complexes with four different ligands are identical to their mirror images. Second, such chirality is most easily realized using macrocyclic ligands like proteins. Metal ligand bonds involving sterically unhindered monodentate complexes like that in the example of Figure **4.4.9A** are in general weaker and more flexible than analogous carbon-carbon bonds. Consequently, in such cases it is likely that the enantiomers would interconvert through a fluxional process, making their resolution difficult if not impossible.

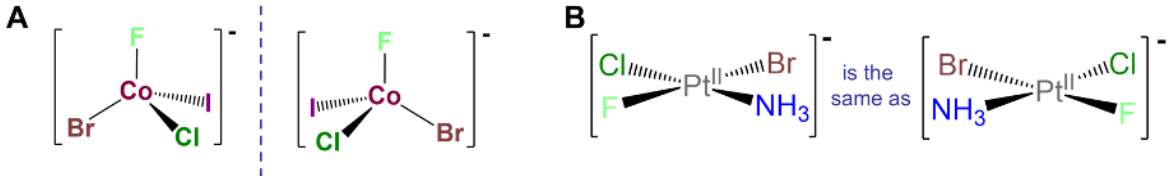


Figure **4.4.9**. (A) In principle tetrahedral metal centers surrounded by four different ligands (Mabcd) exhibit chirality analogous to the chirality of tetrahedral carbon stereocenters; (B) in contrast, square planar Macbd complexes like $[PtBrClF(NH_3)]^-$ are not chiral since they are the same as their mirror images. (It is easiest to see this by either working out its point group (C_s) or by rotating the left $[PtBrClF(NH_3)]^-$ structure clockwise 180 degrees to give its mirror image. This work by Stephen Contakes is licensed under a Creative Commons Attribution 4.0 International License.

ii. **Λ** and **Δ** isomerism at octahedral metal centers surrounded by two or three chelating ligands.

Specifically,

a. Octahedral tris-chelates of formula $M(L\sim L)_3$ exhibit D_3 symmetry.
b. cis-octahedral bis-chelates of formula $M(L\sim L)_2XY$ exhibit C_2 or C_1 symmetry: C_2 if X = Y and C_1 if $X \neq Y$.

As shown in Figure **4.4.10A**, octahedral tris-chelates like $[V(ox)_3]^{3-}$ are chiral and can exist as nonsuperimposable **Λ** and **Δ** enantiomers. The chirality of these tris-chelates is analogous to that of pinwheels. As shown in Figure **4.4.10B**, when looking directly at the head of any individual pinwheel from above, the blades will be angled from back to front going around the pinwheel in either the clockwise or counterclockwise direction. As shown in Figure **4.4.10C**, the case for which the blades are angled in the clockwise direction is analogous to the **Λ** enantiomer and the case when they are angled in the counterclockwise direction the **Δ**.

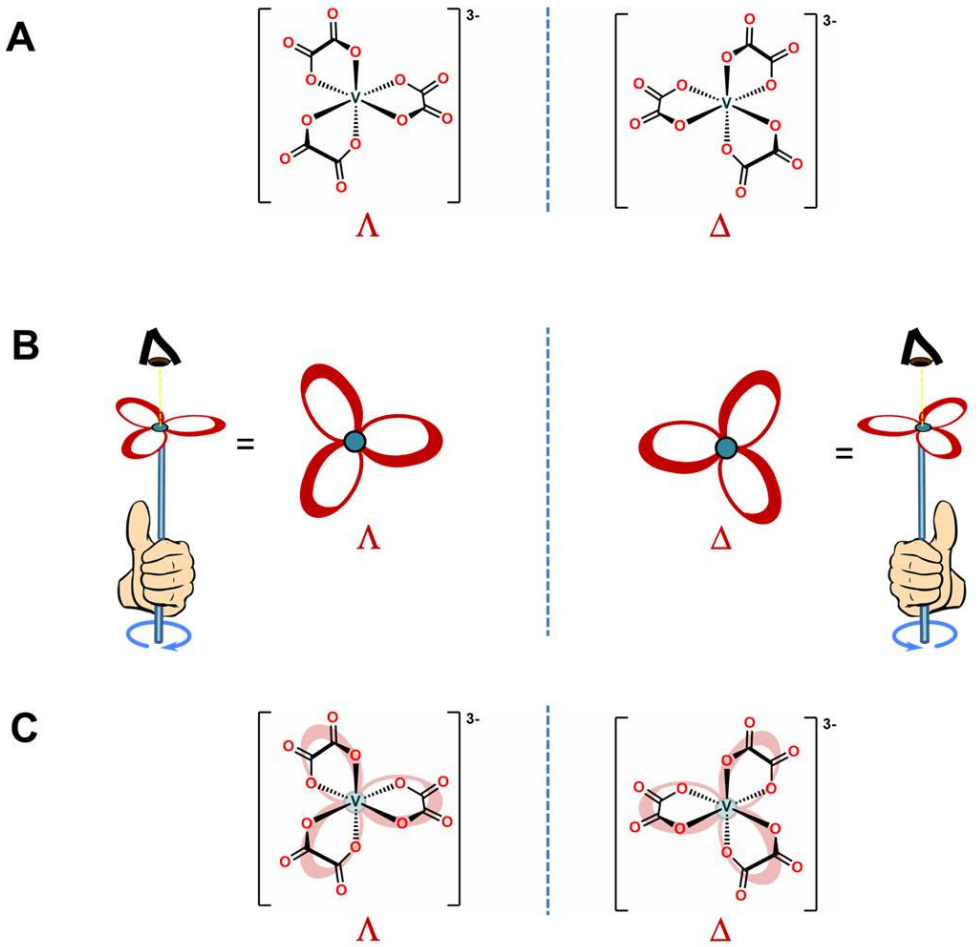


Figure **4.4.10**. (A) Octahedral tris-chelates like $[V(ox)_3]^{3-}$ are chiral and can exist as **Λ** and **Δ** enantiomers. (B) The chirality in these systems is analogous to that of a pinwheel, with the **Λ** enantiomer exhibiting the symmetry of a left-handed pinwheel and the **Δ** enantiomer that of a right handed one. (C) The pinwheel-like nature of **Λ** and **Δ** enantiomers is easiest to see by overlaying the structures of $[V(ox)_3]^{3-}$ from A with the pinwheel structures of B. One way to recognize **Λ** and **Δ** enantiomers is to draw them in these projections. If a left hand is curled around the **Λ** enantiomer with the thumb facing up the curl of the fingers will flow from the back of each ligand towards the front. The same will be true if the right hand is curled around the **Δ** enantiomer. Credits: Although the image is largely an original drawing, the hand images used in part B are adapted from an image by SVGguru / CC BY-SA (https://creativecommons.org/licenses/by-sa/4.0). Otherwise this work by Stephen Contakes is licensed under a Creative Commons Attribution 4.0 International License.

The **Λ** and **Δ** chirality in octahedral bis-chelates is analogous to that in the tris-chelates except this time the third chelating ligand is replaced by an arbitrary pair of ligands. This lowers the symmetry of the complex to either C_2 or C_1, as shown for the C_2 complex $[CoCl_2(en)_2]^+$ in Figure **4.4.11A**. In either case the result is that such complexes exist as **Λ** and **Δ** enantiomers analogous to those in the metal tris-chelates, as shown in Figure **4.4.11B**.

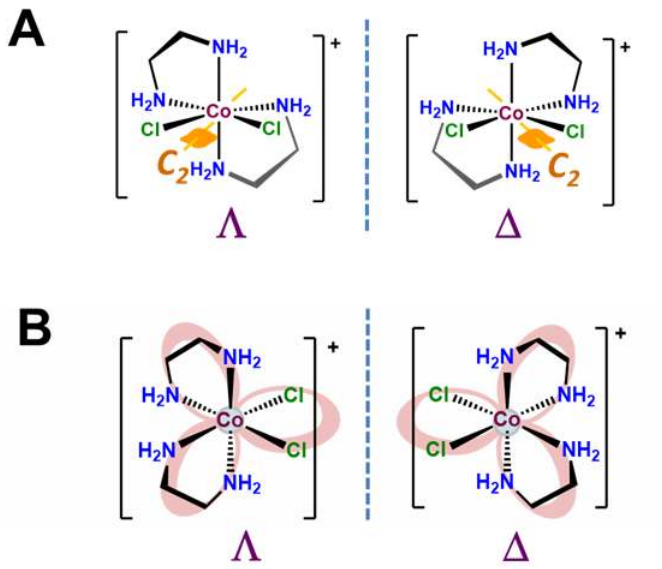


Figure **4.4.9C**. This work by Stephen Contakes is licensed under a Creative Commons Attribution 4.0 International License.

Octahedral complexes containing ligands with denticities of four or more also exhibit **Λ** and **Δ** chirality; it is just that in such cases the bound ligand defines multiple rings within the complex that can be defined as existing in either **Λ** or **Δ** orientations relative to each other. The procedure for making these assignments is beyond the scope of most introductory inorganic courses but the result is that such complexes are designated as **ΛΛ**, **ΔΔ**, **ΔΛ**, **ΔΔΔ**, etc., depending on the number of relationships involving the rings defined by the bound ligand. Interested readers should consult reference 4 for more details.

Circular dichroism may be used to characterize optically active metal complexes.

At the present the most definitive way to determine the absolute configuration of an optically active coordination compound is to determine its 3D molecular structure using single crystal X-ray crystallography.[5] However, as that is not always possible or convenient, the optical activity of coordination complexes is also commonly studied using circular dichroism (CD) spectroscopy. CD spectroscopy is used because, unlike most chiral organics, optically active coordination complexes possess low-energy electronic transitions that occur in the far UV and visible range. This means that it is often convenient to use the ability of a complex to refract and absorb different circular polarizations of light to derive information about both the configuration of an optically active complex and its electronic structure. The focus of this section will be to explain how the determination of absolute configuration by circular dichroism and optical rotatory dispersion work, as well as the relationship of these techniques to the more ordinary sort of polarimetry used to measure optical rotation in organic systems. Only brief notes will be made about the instrumental and electronic structure applications of these techniques since the electronic spectra of metal complexes will be discussed in Chapter 11: Coordination Chemistry III - Electronic Spectra and the instrumental aspects of CD are well-treated elsewhere.

Both polarimetry and circular dichroism spectroscopy are grounded in the recognition that plane polarized light is equivalent to a superposition of left and right circularly polarized light, as shown in Figure **4.4.12**.

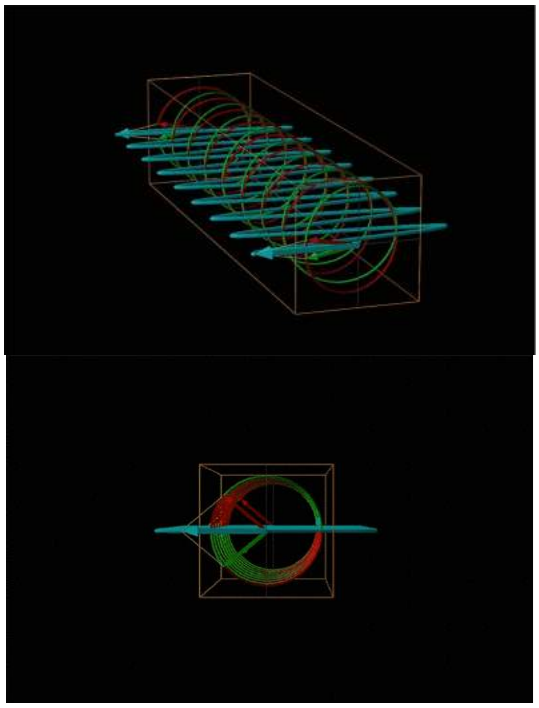


Figure **4.4.12**. Angled and front view of plane polarized light (light blue) as the vector sum of left circularly polarized light (red) and right circularly polarized light (green). Created using EMANIM Version 1.2 (2011 July) by Andras Szilagyi (www.enzim.hu/~szia/emanim). This work by Stephen Contakes is licensed under a Creative Commons Attribution 4.0 International License.

When plane polarized light passes through a chiral medium, its left and right circularly polarized components move at different rates (*i.e.*, have different indices of refraction). This causes the plane of polarization to rotate in the direction of the faster component according to the relationship

$$\alpha = \frac{n_l - n_r}{\lambda}$$

where α is the angle of rotation, λ the light's wavelength, and n_l and n_r the refractive indices experienced by left and right circularly polarized light.

An example of such a rotation is shown in Figure **4.4.13**.

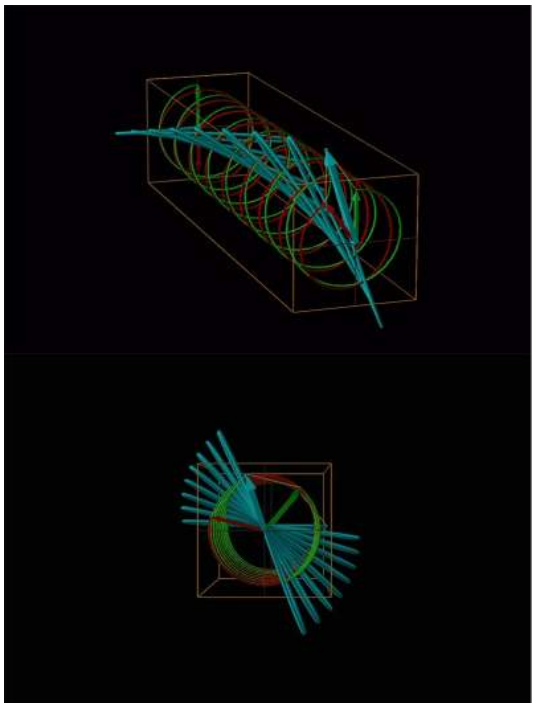


Figure **4.4.13**. Angled and front view of plane polarized light (light blue) as it passes through a medium (represented by the orange box) in which left circularly polarized light (red) experiences a higher refractive index (and so moves slower) than right circularly polarized light (green). Created using EMANIM Version 1.2 (2011 July) by Andras Szilagyi (www.enzim.hu/~szia/emanim) with a refractive index of 1.05 for left circularly polarized light and 1.00 for right circularly polarized light. This work by Stephen Contakes is licensed under a Creative Commons Attribution 4.0 International License.

Chemists typically call this rotation of light by a chiral medium optical rotation. In organic chemistry it is common to measure the optical rotation at the sodium D wavelength of 589.29 nm, a much longer wavelength than most organics are able to absorb. Because of this the optical rotations commonly measured by organic chemists are largely independent of absorption and mainly serve as a characteristic physical property similar to melting points or are used to establish the purity of a mixture of enantiomers. The sort of spectroscopic data used to characterize chiral coordination compounds more commonly makes use of the relationship between absorption and optical rotation.

In coordination chemistry the wavelength-dependence of optical rotation is used to discern information about compounds' electronic spectra. This measurement of the wavelength dependence of optical rotation is called **optical rotatory dispersion (ORD)** and the resulting plots are called optical rotatory dispersion or ORD spectra or curves. Such ORD curves are useful for characterizing the chiral environment in a coordination complex because the ORD curves exhibit a characteristic shape. This characteristic shape is because according to the **Cotton Effect,** the optical rotation changes sign at the absorption maximum of a chromophore in the compound. For one configuration the rotation will go from negative to positive with increasing wavelength and is called a **positive cotton effect**; for the other configuration the rotation will go from positive to negative or exhibit a **negative cotton effect**. This behavior is summarized in the top two curves of Figure **4.4.14**.

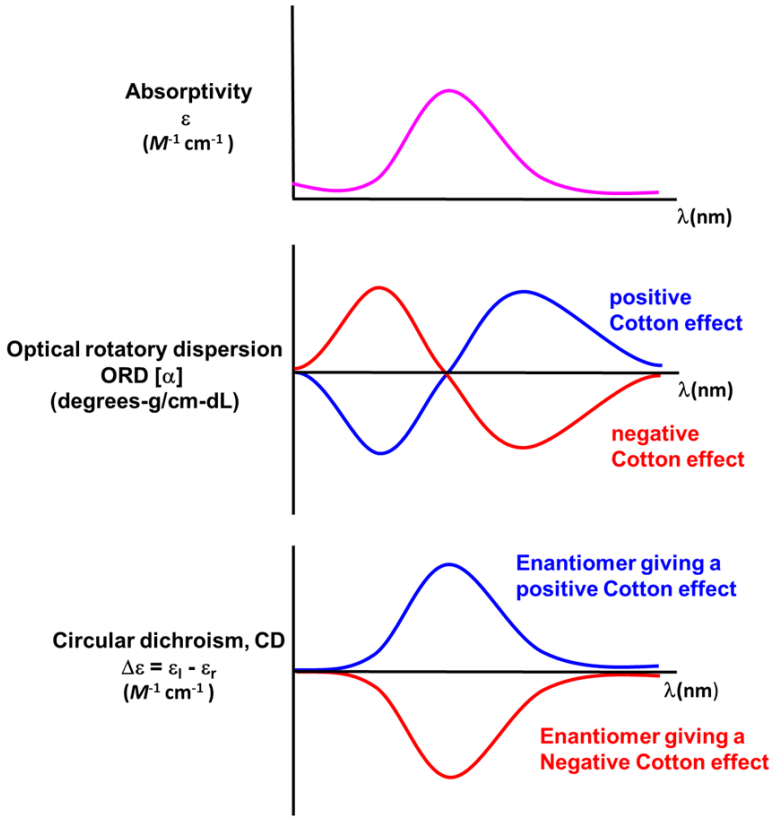


Figure **4.4.14**. Idealized relationship between absorbance, ORD, and CD spectra for enantiomers exhibiting a positive and negative Cotton effect. This work by Stephen Contakes is licensed under a Creative Commons Attribution 4.0 International License.

A technique used even more often than ORD is **circular dichroism (CD)**, represented by the lowest spectrum in Figure **4.4.14**. Circular dichroism arises from the differential absorption of left and right circularly polarized light by a chiral compound. This gives elliptically polarized light as shown in Figure **4.4.15**.

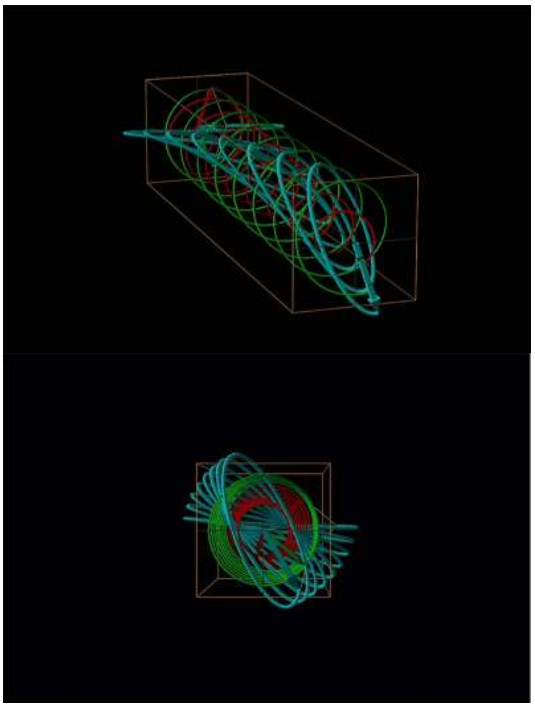


Figure **4.4.15**. Angled and front view of plane polarized light (light blue) as it passes through a medium (represented by the orange box) in which left circularly polarized light (red) both experiences a higher refractive index and greater absorption than right circularly polarized light (green). Created using EMANIM Version 1.2 (2011 July) by Andras Szilagyi (www.enzim.hu/~szia/emanim) with a refractive index of 1.05 and an extinction coefficient of 0.05 for left circularly polarized light and a refractive index of 1.00 and extinction coefficient of 0 for right circularly polarized light. This work by Stephen Contakes is licensed under a Creative Commons Attribution 4.0 International License.

In circular dichroism (CD) spectroscopy a sample is irradiated with polarized light resulting in the transmission of elliptically polarized light due to differential refraction and absorption of the polarized light's left and right circularly polarized components. For achiral molecules the handedness doesn't affect absorbance, but for chiral molecules, which chiral ground and excited states the handedness of an EM wave affects can determine how readily that wave can distort the chiral ground state into the chiral excited one. For this reason chiral molecules absorb left and right circularly polarized light differently.

In CD spectroscopy the magnitudes of the left and right circularly polarized components of light that is transmitted by the sample are measured and used to determine how much light of each was absorbed (just as in regular absorbance spectroscopy). The difference in absorption between left and right circularly polarized light constitutes the primary signal in CD spectroscopy. More specifically, circular dichroism spectra (CD spectra) show the difference in extinction coefficients for left and right circularly polarized light, $\Delta\epsilon$, as a function of wavelength, where

$$\Delta\epsilon = \epsilon_l - \epsilon_r$$

where Missing open brace for subscript and Missing open brace for subscript are the extinction coefficients observed with left and right circularly polarized light, respectively.

As with ORD spectra, the signs of the features in CD spectra like that of Δ–$[Co(en)_3]Cl_3$ given in Figure **4.4.16** are enantiomer-dependent. As illustrated in the lower spectrum in Figure **4.4.14** , the CD spectra of enantiomers mirror one another. Because of this difference in behavior it is possible in principle to determine the absolute configuration of a complex from its CD spectrum.

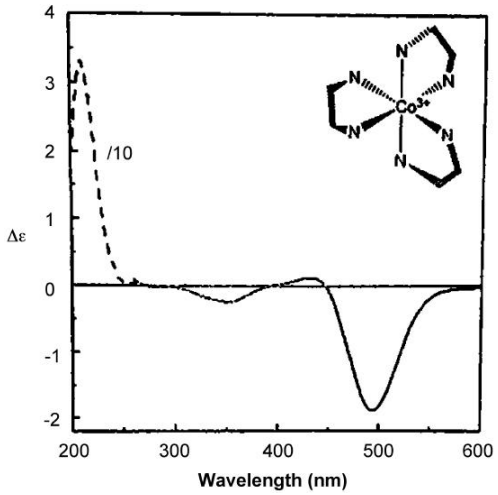


Figure **4.4.16**. CD spectrum of Δ–$[Co(en)_3]Cl_3$. Taken from reference 6.

There are several ways that ORD and CD spectra can be useful for determining the absolute configuration of a chiral complex.

1. First, the sign of the Cotton effect and peaks in CD spectra exhibited by a given absolute configuration is often consistent across a series of compounds. Thus if a new member of the series is isolated, its configuration can be determined based on which enantiomer has the same Cotton effect. For instance, if both the **Λ** isomer of a metal diimine complex like $[Ru(bpy)_3]^{2+}$ exhibit a positive Cotton effect and a newly resolved metal diimine exhibits a negative Cotton effect it might reasonably be inferred that the newly-resolved complex is in the opposite or **Δ** configuration.
2. Second, for some systems the expected sign of the Cotton effect and CD peaks for each enantiomer may be predicted semi-empirically based on the spatial locations of substituents relative to the chromophore (the part of the molecule that changes electronic structure during the transition), although the details are beyond the scope of the present discussion.
3. Consideration of interactions between multiple chromophores in a compound can be used to infer absolute configuration. Again, the details are beyond the scope of the present discussion. Interested readers are referred to reference 7 for details.

Common patterns of Diastereomerism

Geometric isomerism

Geometric isomerism involves differences in the geometric placement of atoms in a compound. In coordination chemistry, geometric isomerism involves differences in the relative placement of a set of ligands about a metal center. There are two main types:

cis and *trans* isomerism

This type of isomerism has to do with how two ligands are oriented relative to one another in a square planar or octahedral complex. As shown in Figure **4.4.17**, ligands that are next to one another with a L-M-L bond angle of 90° are said to be *cis*; those on opposite sides of the metal with a L-M-L bond angle of 180° are in the *trans* arrangement.



Figure **4.4.17**. *cis* and *trans* arrangement of ligands around (A) square planar and (B) octahedral metal centers. Since both types of complexes feature 90° L-M-L bond angles, the arrangements are fundamentally the same in both cases. This work by Stephen Contakes is licensed under a Creative Commons Attribution 4.0 International License.

Simple *cis* and *trans* geometric isomers can be identified when there are two identical ligands (A) or chelating ligands with distinguishable attachment points (A~B) oriented about either a square planar or octahedral center. Examples are given in Figure

4.4.18. Notice from the example given in Figure 4.4.18C that multidentate ligands have the potential to constrain complexes to adopt a particular geometry.

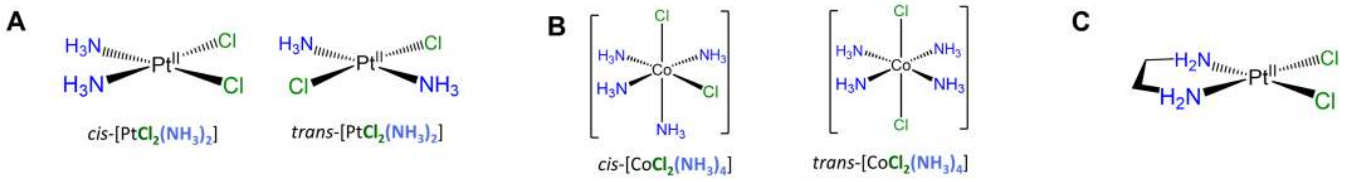


Figure 4.4.18. Examples of square planar and octahedral *cis* and *trans* isomers. (A) *cis* and *trans* isomers of $[PtCl_2(NH_3)_2]$; the former is medicinally important. Sold under the name cisplatin, the *cis* isomer is used as a chemotheraphy against various forms of cancer. (B) *cis* and *trans* isomers of $[CoCl_2(NH_3)_4]$, a compound of more academic interest. (C) $PtCl_2$(en) only exists as the *cis* isomer because the chelating en ligand can only bind in a *cis* arrangement. This work by Stephen Contakes is licensed under a Creative Commons Attribution 4.0 International License.

Slightly more involved examples involve perturbations of the simple cases above in which there are multiple distinguishable *cis* and/or *trans* relationships. Two square planar examples are given in Figure 4.4.19.

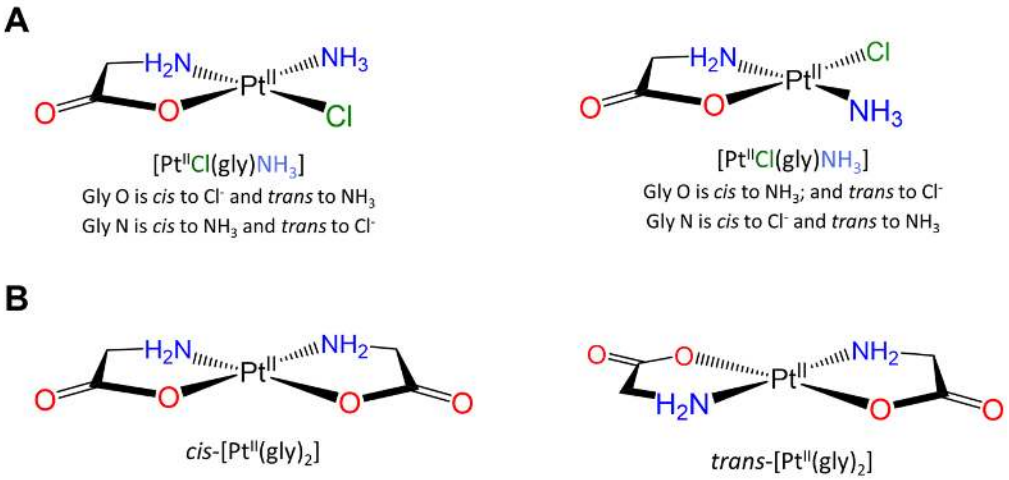


Figure 4.4.19. Examples of more complex square planar systems. (A) Geometric isomers of $[PtCl(gly)NH_3]$, a MA_2BC system for which A = gly^-, B = Cl^-, and C = NH_3. Swapping of the ammine and chloro ligands changes both the *cis* and *trans* relationships involving the Gly ligand. (B) Geometric isomers of $[Pt(gly)_2]$, an $M(A\sim B)_2$ system for which A = the *κO* glycine carboxy group and B its *κN* amine. The only possible geometric isomerism involves swapping the orientation of one glycine relative to the other. For this reason the two complexes shown can be designated as *cis* and *trans* isomers based on whether the *κO* and *κ*N ends of the glycine are *cis* or *trans* to one another. This work by Stephen Contakes is licensed under a Creative Commons Attribution 4.0 International License.

More complex examples of *cis* and *trans* relationships between ligands in octahedral complexes are given in the exercises that conclude this page, which also demonstrates how a systematic approach may be used to identify isomers.

mer and *fac* isomerism

This type of isomerism has to do with how three ligands are oriented relative to one another in an octahedral complex. The arrangements are represented in Figure 4.4.20.

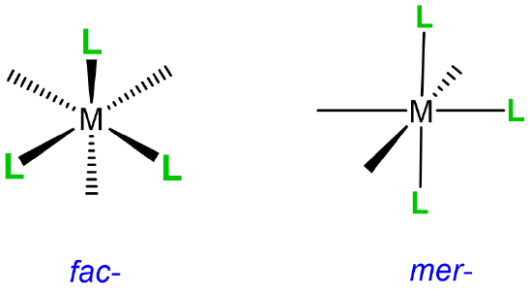


Figure 4.4.20. Simple representation of the *fac* and *mer* arrangements of ligands around an octahedral metal center. This work by Stephen Contakes is licensed under a Creative Commons Attribution 4.0 International License.

Since it can help to visualize the *mer* and *fac* geometry from multiple points of view, several representations are given in Figure 4.4.21. As shown in Figure 4.4.21, in ***fac*** or **facial arrangements**, the ligands occupy the same "face" of the octahedral coordination sphere, while in the ***mer*** or **meridional geometry** the ligands form a T shape in the same plane or its "meridian."[8]

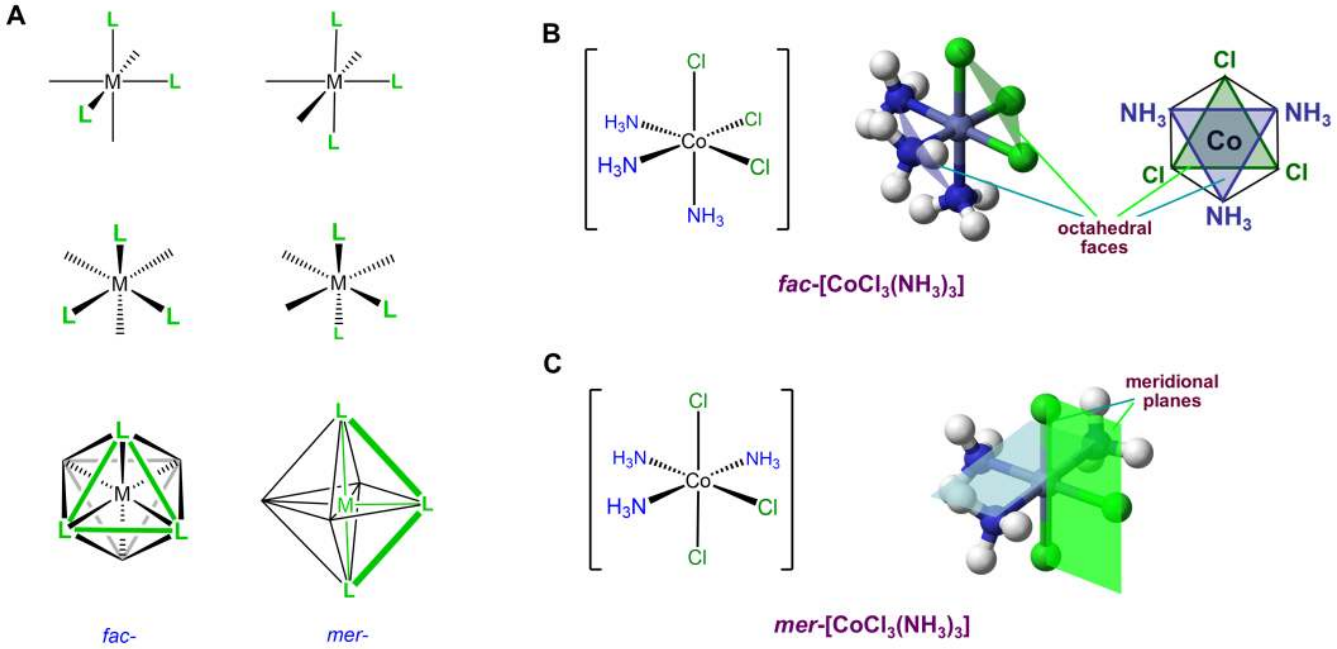
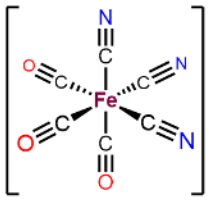
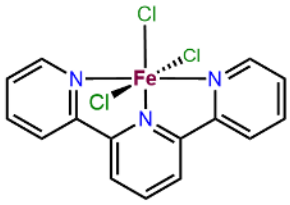
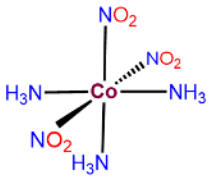


Figure 4.4.21. (A) Three projections of *fac* and *mer* arrangements of ligands around an octahedral metal center emphasizing that in the *fac* arrangement the ligands are oriented along a face of the octahedron while in the *mer* arrangement they are oriented in a plane. (B) Structure of *fac*-$[CoCl_3(NH_3)_3]$ showing the octahedral faces occupied by the chloro and amine ligands. (C) Structure of *mer*-$[CoCl_3(NH_3)_3]$ showing the planar arrangement of the chloro and ammine ligands. The ball and stick models are modified from images by Benjah-bmm27 - Own work, Public Domain, https://commons.wikimedia.org/w/inde...?curid=1874872 and curid=1874873. Otherwise this work by Stephen Contakes is licensed under a Creative Commons Attribution 4.0 International License.

Octahedral complexes with three identical ligands oriented about an octahedral center can only exist in *mer* and *fac* arrangements. Consequently, such complexes can be designated as *mer* and *fac* isomers. Examples are given in Figure 4.4.22.







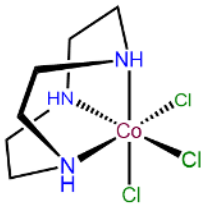


Figure **4.4.22**. Examples of *fac* and *mer* octahedral complexes. Note how some chelating ligands preferentially bind to the metal in a *fac* or *mer* arrangement and, in so doing, force the other ligands to also form a *mer* or *fac* arrangement. This work by Stephen Contakes is licensed under a Creative Commons Attribution 4.0 International License.

Diastereomerism arising from multiple ligand-associated chiral centers

Diastereomerism can also arise when two or more chiral ligands bind to a metal center. Such cases typically give rise to a complex mixture of isomers, as shown by the example in Figure **4.4.23**. As may be seen from Figure **4.4.23**, the differences between these isomers can arise from both changes in the stereochemical configuration of the ligand and the relationship of particular ligand centers relative to one another. For instance, the leftmost two structures in Figure **4.4.23** possess one *R* and *S* nitrogen center each but differ in whether the centers are oriented so that the *R* and *S* centers on the two ligands are *trans* or *cis* to one another.

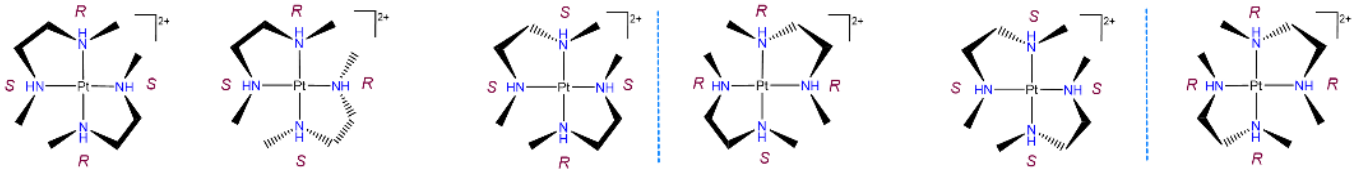


Figure **4.4.23**. Diastereomers that can in principle be formed when two *N*,*N*′-dimethylethylenediamine ligands coordinate a Pt^{2+} center. This work by Stephen Contakes is licensed under a Creative Commons Attribution 4.0 International License.

Diastereomerism arising from λ and δ ring conformation isomerism.

Chelate rings are formed when a chelating ligand binds a metal

As may also be seen from the structures in Figure **4.4.23**, when a multidentate ligand coordinates a metal, the ligand and metal center comprise one or more **chelate rings**. Examples of such chelate rings are shown in Figure **4.4.24**.

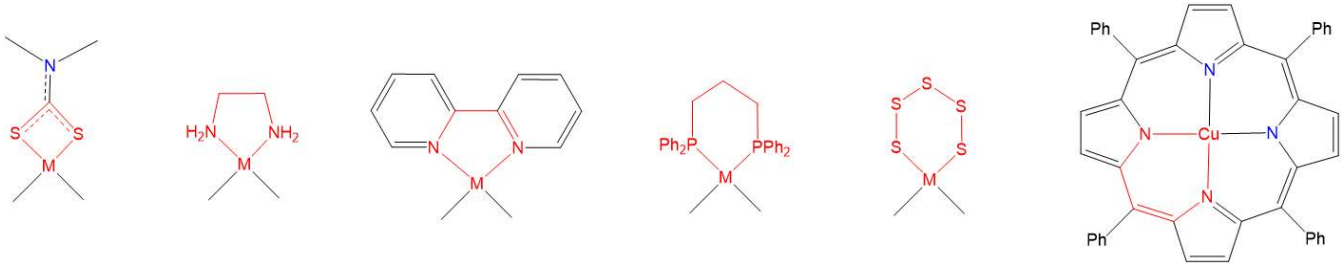


Figure **4.4.24**. Four, five, and six-membered chelate rings (shown in red) formed by coordination of selected bidentate ligands to a metal center. This work by Stephen Contakes is licensed under a Creative Commons Attribution 4.0 International License.

As may be inferred from the examples in Figure **4.4.24**, chelate rings may be of different sizes, although four, six, and especially five-membered rings are particularly common. Exactly which ring sizes will be more stable for a given system depends on the

coordination geometry and, due to differences in M-L bond lengths, to a lesser degree on the metal. As a result, for octahedral and square planar complexes with 90° L-M-L bond angles between *cis* ligands, *five-membered rings tend to be especially stable* (Figure **4.4.25**).

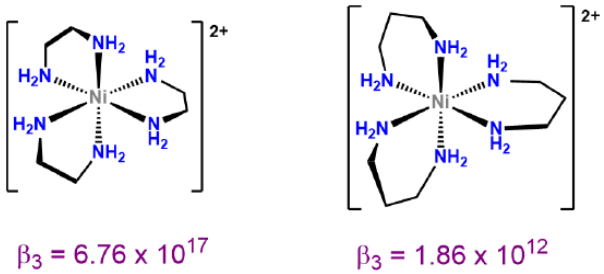


Figure **4.4.25**. The greater stability of five-membered chelate rings involving Ni^{2+} and organic ligands is reflected in the higher overall formation constant (β_3) for the five-membered chelate rings contained in $[Ni(en)_3]^{2+}$ compared to that of $[Ni(et)_3]^{2+}$, which has six-membered rings. The data in this figure is taken from Stability of Metal Complexes and Chelation by Robert Lancashire. This work by Stephen Contakes is licensed under a Creative Commons Attribution 4.0 International License.

Not all metal chelates prefer to form five-membered rings. The steric requirements of chelate rings depend on both the preferred coordination geometry of the metal center and the stereochemistry of the ligand. Both of these effects are typically considered in terms of preferred L-M-L bond angles. From the perspective of the metal center, the preferred bond angle is determined by the coordination geometry. Octahedral and square planar metals prefer 90° L-M-L bond amgles, trigonal bipyramidal systems 90 and 120° L-M-L bond angles, and tetrahedral complexes 109.5° L-M-L angles. The larger preferred bond angles in tetrahedral and trigonal bipyramidal systems often require the formation of larger six or seven-membered chelate rings for maximum stability. The size of the chelate ring actually formed between a metal and ligand is determined by the ligand's structure. As the contributor of all the atoms in the chelate ring but one, the ligand directly determines the chelate ring size. More subtly, ligands naturally prefer to coordinate metals at a particular L-M-L angle, called the **bite angle**, as shown in Figure **4.4.26A**. Ligands with bite angles corresponding to the ideal L-M-L angle for a metal's preferred geometry tend to form more stable complexes, although in turn ligand bite angles can cause metals with a weak coordination geometry preference to adopt the ligand's preferred geometry instead.[10] As may be seen from the values in Figure **4.4.26B**, bite angles roughly increase with the size of the chelate ring formed but are also influenced by the types of structures used to connect the ligand's Lewis base sites. This facilitates the use of diphosphine ligands to tailor the structure and reactivity of phosphine-containing organometallic catalysts.



Figure **4.4.26**. (A) Definition of the bite angle as the angle at which the ligand's preferred L-M-L angle when coordinating a metal center. (B) Bite angles of selected diphosphines.[9] The bite angles of many such diphosphines have been determined to facilitate the design of phosphine-containing organometallic catalysts. This work by Stephen Contakes is licensed under a Creative Commons Attribution 4.0 International License.

λ and δ isomerism involves differences in the conformation of nonplanar five-membered chelate rings

As shown in Figure **4.4.27**, some chelate ring systems are planar while others are not.

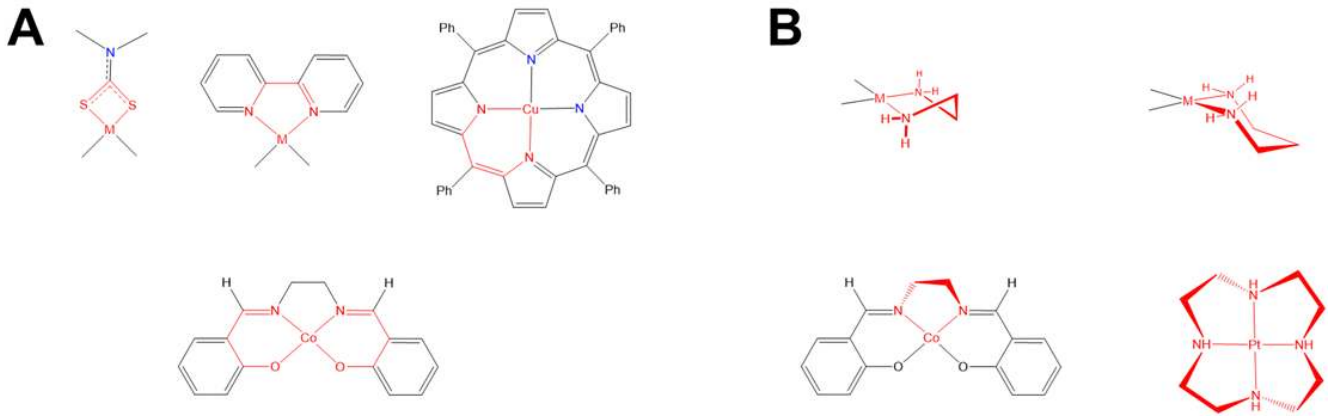


Figure 4.4.27. (A) Planar and (B) Nonplanar chelate rings shown highlighted in red. Notice how [Co(salen)] possesses a nonplanar chelate ring and two planar ones. This work by Stephen Contakes is licensed under a Creative Commons Attribution 4.0 International License.

Among the nonplanar chelate ring systems are ligands like en and dppe, which contain tetrahedral C, N, O, P, and S atoms. Because these atoms create kinks in the chelate ring they introduce additional opportunities for diastereomerism due to differences in the chelate ring conformation, called **ring twist**. Ring twist in nonplanar systems has been most extensively explored for five-membered chelates like those formed by dppe and by en and other chelating amines. Unlike the more rigid four-membered chelate rings, five-membered chelates tend to be conformationally flexible, but not so conformationally flexible that their conformers are rapidly interconverting at room temperature (at least not when the rings are substituted to introduce additional steric strain). This balance between flexibility and rigidity enables some five-membered chelate rings to exist as mixtures of distinguishable conformational isomers at room temperature.

To understand the two most stable conformers that five-membered chelates rings tend to form, it is helpful to think of five-membered chelate rings as involving two components (Figure 4.4.28):

- a planar L-M-L group, where L are the atoms directly attached to the metal, M, and
- the remaining two ring atoms, E, which form a rigid E-E bar across the back of the chelate ring.

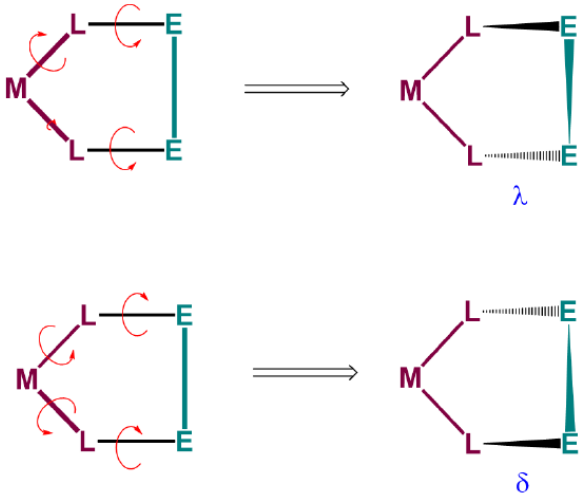


Figure 4.4.28. Five-membered chelate rings consist of a planar L-M-L group connected to a rigid E-E bar. Conformers arise as rotation about the M-L and L-E bonds causes twisting of the E-E bar relative to the L-M-L plane. This work by Stephen Contakes is licensed under a Creative Commons Attribution 4.0 International License.

As can be seen from Figure 4.4.28 , rotation about the M-L and L-E bonds causes twisting of the E-E bar relative to the L-M-L plane. The two most stable conformers produced by these motions are the λ or δ conformations as shown in Figures 4.4.29 and 4.4.29.

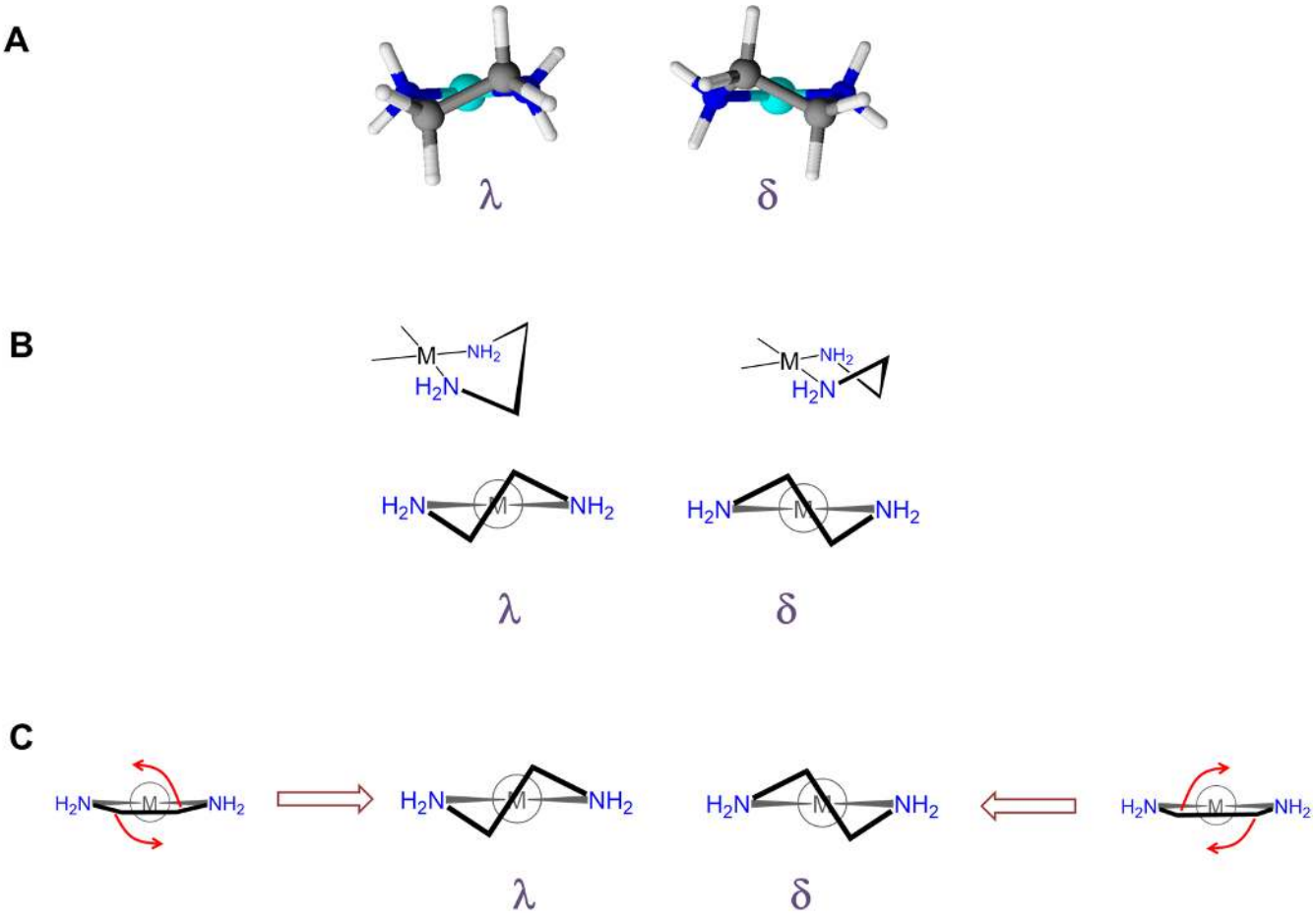


Figure **4.4.29**. (A) **λ** and **δ** ring twist in a square planar metal ethylenediamine complex (B) along with several ways to represent it in line drawing form. (C) Of these, the projection looking down an axis bisecting the chelate ring makes it easiest to see that, starting with a planar chelate ring the **λ** conformer corresponds to a counterclockwise twist of the CH_2CH_2 bond relative to the N-M-N plane and the **δ** conformer a clockwise twist relative to the N-M-N plane. This work by Stephen Contakes is licensed under a Creative Commons Attribution 4.0 International License.

The relative stability of the **λ** and **δ** conformers will depend on the configuration of any stereocenters present and steric factors. As with organic ring systems, steric effects tend to favor conformers in which bulky groups are placed in the less sterically strained equatorial positions while the configuration of the stereocenters present can serve to restrict the allowable ring twist conformations, as illustrated in Figure **4.4.30**. A detailed treatment of such systems is beyond the scope of this page. Interested readers are referred to reference 12 for more details.

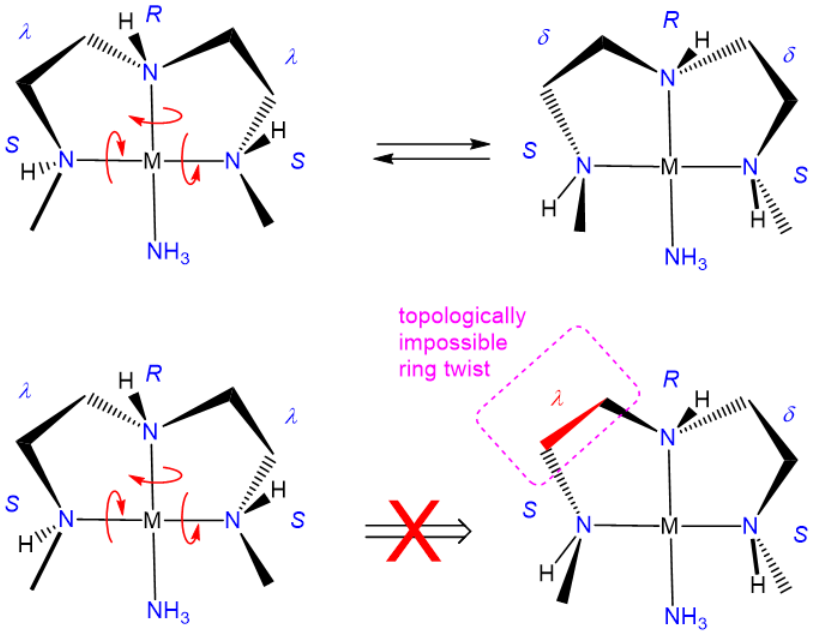


Figure 4.4.30. The configurations at nitrogen in the complex shown restrict the chelate ring conformations to either a λλ or δδ conformation because the rotations needed to enable a λδ configuration are topologically impossible. This work by Stephen Contakes is licensed under a Creative Commons Attribution 4.0 International License.

In closing, it should be noted that it might seem to be making much of small effects in pointing out that one source of diastereomerism in metal complexes involves the freezing out of chelate ring conformations. However, that would be to mistake the impacts that ring conformations can have on the steric accessibility of a coordination site and shaping the course of processes that might occur there. As illustrated in Figure 4.4.31, a simple shift in the conformation of one ring in a square planar, pyramidal, or octahedral complex containing coplanar ethylene diamine ligands can exert a significant effect on the steric profile of the complex perpendicular to the MN_4 square plane. Because of effects like these, ring conformation isomerism plays a role in the design of stereoselective transition metal catalysts.

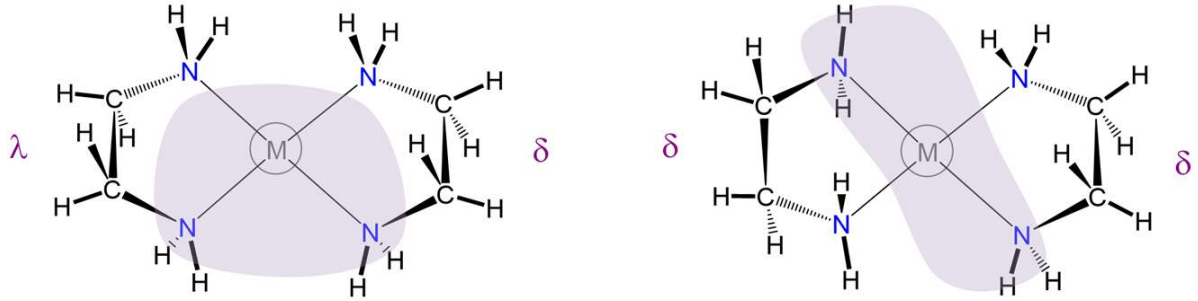


Figure 4.4.31. Schematic illustrating how the conformation of ethlyenediamine ligands bound to a metal center affects the steric accessibility of the metal (shown shaded in violet) to potential ligands attempting to bind from above the MN_4 plane. This work by Stephen Contakes is licensed under a Creative Commons Attribution 4.0 International License.

Exercises

? Exercise 4.4.1. Identify the type of isomerism

What type of isomers are

a. $[CoCl(NH_3)_5](NO_3)$ and $[Co(NH_3)_5(N\text{-}NO_2)]Cl$?
b. $[Co(NH_3)_5\text{-}CN\text{-}Ru(NH_3)_5]^{4+}$ and $[Co(NH_3)_5\text{-}NC\text{-}Ru(NH_3)_5]^{4+}$
c. $[Cr(CN)_5\text{-}CN\text{-}Co(NH_3)_5]$ and $[Co(CN)_5\text{-}CN\text{-}Cr(NH_3)_5]$
d. *cis*-$[Mn(en)_2(CN)_2]$ and *trans*-$[Mn(en)_2(CN)_2]$

Answer a.

Ionization isomers.

Answer b.

Linkage isomers.

Answer c.

Coordination isomers.

Answer d.

Geometric isomers, specifically *cis*/*trans* isomers.

? Exercise 4.4.2. Assigning metal oxidation states in a complex

Many properties of transition metal complexes depend on the metal's oxidation state. For instance,

- octahedral complexes of Co^{II} lose and gain ligands rapidly
- octahedral complexes of Co^{III} lose and gain ligands very slowly
- four-coordinate complexes are generally tetrahedral
- EXCEPT four-coordinate complexes of metals like Pt^{II} , Pd^{II} , Rh^{I}, and Ir^{I}, among others, are square planar

For this reason it is important to be able to estimate the formal oxidation state of a metal in a complex. Fortunately, this is easy to do if you remember

1. The sum of all atoms' oxidation states will equal the overall charge on the complex
2. When determining the metal's oxidation state, the ligands can be treated as having an oxidation state equal to their charge - *i.e.*, the charge they possess in the form in which they coordinate the metal - so if they need to lose a proton to bind, don't forget to account for that.

Given the above, estimate the oxidation state of the metal in the following real and hypothetical complexes.

a. $Na_4[Fe(CN)_6]$
b. $[Cu(phen)_2]BF_4$
c. $[PtF_4(NH_3)_2]$
d. $[Ni(en)_2]SO_4$
e. $Co(acac)_3$
f. [MnCl(O)(salen)]

Answer for $Na_4[Fe(CN)_6]$.

This contains $[Fe(CN)_6]^{4-}$; so $O.S._{Fe}$ + 6 x (-1) (for CN^-) = -4 (the complex's charge) so $O.S._{Fe}$ = +2 or Fe^{2+}.

Answer for $[Cu(phen)_2]BF_4$.

Since tetrafluoroborate is a monoanion, the complex is $[Cu(phen)_2]^+$ so $O.S._{Cu}$ + 0 x 2 (for phen) = +1 (the complex's charge) so $O.S._{Cu}$ = +1 or Cu^+.

Answer for $[PtF_4(NH_3)_2]$.

$O.S._{Pt}$ + 4 x (-1) (for F^-) + 0 x 2 (for NH_3) = +0 (the complex's charge) so $O.S._{Pt}$ = +4 or Pt^{4+}.

Answer $[Ni(en)_2]SO_4$.

The complex is $[Ni(en)_2]^+$ so $O.S._{Ni}$ + 0 x 2 (for en) = +2 (the complex's charge) so $O.S._{Ni}$ = +2 or Ni^{2+}.

Answer $Co(acac)_3$.

$O.S._{Co}$ + 3 x (-1) (for acac; see table 9.2.2) = +0 (the complex's charge) so $O.S._{Co}$ = +3 or Co^{3+}.

Answer [MnCl(O)(salen)].

$O.S._{Mn}$ + 1 x (-1) (for Cl^-) + 1 x (-2)(for oxo) + 1 x (-2) (for salen; see table 9.2.2) = +0 (the complex's charge) so $O.S._{Mn}$ = +5 or Mn^{5+}.

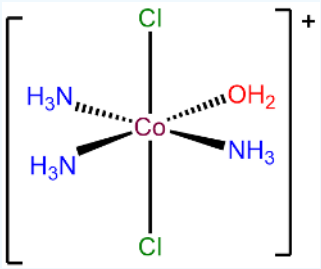
? Exercise 4.4.3. Drawing isomers from descriptions

Draw structures that match the descriptions given, assuming that

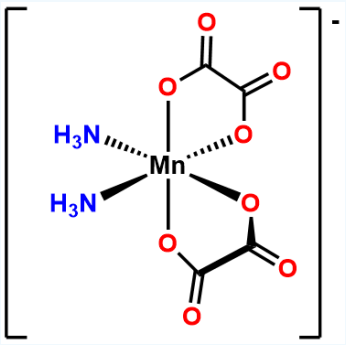
- complexes in which the metal has a coordination number of six are octahedral
- complexes in which the metal has a coordination number of five are trigonal bipyramidal
- complexes in which Pt^{II} , Pd^{II} , or Rh^{I}, or Ir^{I} have a coordination number of four are square planar
- other complexes in which the metal has a coordination number of four will be tetrahedral

a. *mer*-triammineaqua-*trans*-dichlorocobalt(III) ion
b. **Δ**-diaminebis(oxalato)manganate(III)
c. $[CoCl_4]^{2-}$
d. *trans*-diamminebis(ethylenediamine)Nickel(2+) tetracyanopalladate(2-)
e. **Λ**-bis(ethylenediamine)cobalt(III)- μ-amido μ-hydroxo-**Δ**-bis(ethylenediamine)cobalt(III)

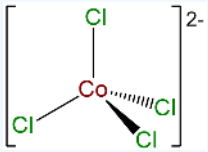
Answer a. *mer*-triammineaqua-*trans*-dichlorocobalt(III) ion.



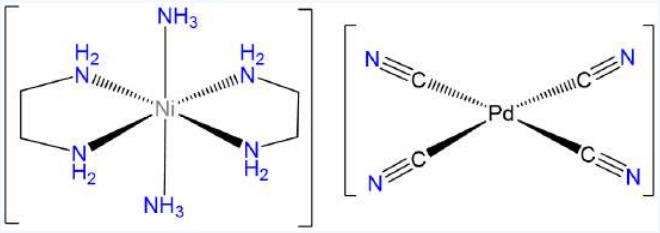
Answer b. Δ-diaminebis(oxalato)manganate(III).



Answer c. $[CoCl_4]^{2-}$.



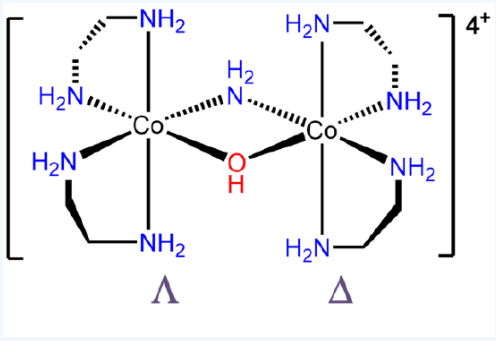
Answer d. *trans*-diamminebis(ethylenediamine)Nickel(2+) tetracyanopalladate(2-).



Note that since the Pd in $[Pd(CN)_4]^{2-}$ is Pd^{2+} it will be square planar.

https://chem.libretexts.org/@go/page/403023

Answer e. Λ-bis(ethylenediamine)cobalt(III)- μ-amido μ-hydroxo-Δ-bis(ethylenediamine)cobalt(III).



? Exercise 4.4.4. Stereoisomers of complexes containing only monodentate ligands.

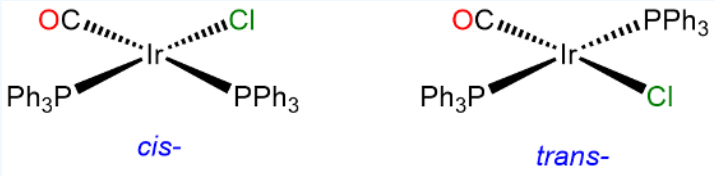
Draw all the stereoisomers of the following real and hypothetical complexes. You may assume that

- complexes in which the metal has a coordination number of six are octahedral
- complexes in which the metal has a coordination number of five are trigonal bipyramidal
- complexes in which Pt^{II} , Pd^{II} , or Rh^{I}, or Ir^{I} have a coordination number of four are square planar
- other complexes in which the metal has a coordination number of four will be tetrahedral

a. $[IrCl(CO)(PPh_3)_2]$
b. $[CoCl_3(NH_3)_3]$
c. $[CoCl_2(H_2O)_2(NH_3)_2]^+$
d. $[CoBrCl(H_2O)_2(NH_3)_2]^+$
e. $[CoBrClI(NH_3)_3]$

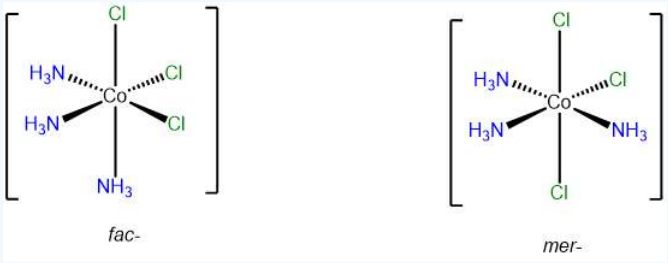
Answer a. $[IrCl(CO)(PPh_3)_2]$

This is a 4-coordinate Ir^{I} complex and, as such will be square planar. Since two of the ligands are identical, it will have *cis* and *trans* isomers. The *trans* isomer is famous for its ability to form adducts and is called Vaska's complex.



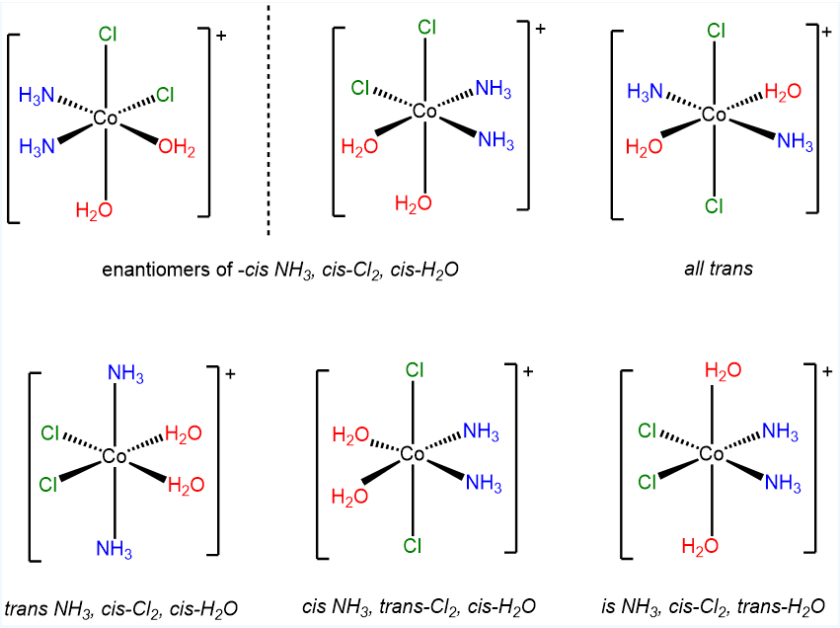
Answer b. $[CoCl_3(NH_3)_3]$

This complex contains three ammine and three chloro ligands and so will have *fac* and *mer* isomers.



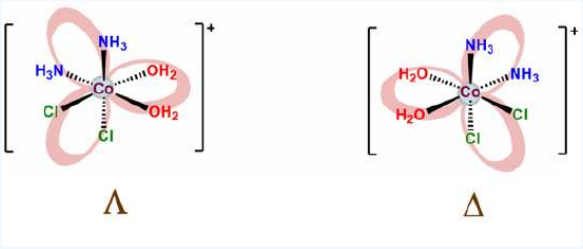
Answer c. $[CoCl_2(H_2O)_2(NH_3)_2]^+$

This is a case of an $MA_2B_2C_2$ system (A = Cl^-, B = H_2O, C = NH_3) involving multiple *cis* and *trans* relationships. The six stereoisomers are shown below.



Since it may not be obvious how to arrive at a set of isomers like the ones above, it is worth considering how one might work through the possibilities for a system of ligands like this one. Several systems may be used to systematically identify isomers. Once approach is the Macbdef system described in Note **4.4.1** at the end of these exercises. The solutions presented here and in subsequent problems employ a variant of that approach.

- Start by fixing one set of ligands. In this case the chloro ligands were first fixed as *cis* to one another. Then the remaining ligands might be *cis* or *trans* to one another, although since the *chloro* ligands are already *cis*, the ammine and aqua ligands cannot both be *trans* at the same time. Thus for *cis* chloro ligands the possibilities for the others are:
  - *cis*-H_2O ,*cis*-NH_3,
  - *cis*--H_2O, *trans*-NH_3
  - *trans*-H_2O, *cis*-NH_3
- Swap the configuration of the ligand set you started with. In this case it means placing the chloro ligands *trans* to one another. From that configuration, the possibilities for the ammine and aqua ligands are
  - *cis*-H_2O ,*cis*-NH_3,
  - *trans*-H_2O, *trans*-NH_3
- Check for enantiomers and create mirror images of any chiral complexes you drew. The easiest way to do this is to assign point groups. However, it turns out that the octahedral all-*cis* case is D_3 and formally equivalent to the symmetry of a tris chelate, as shown below.

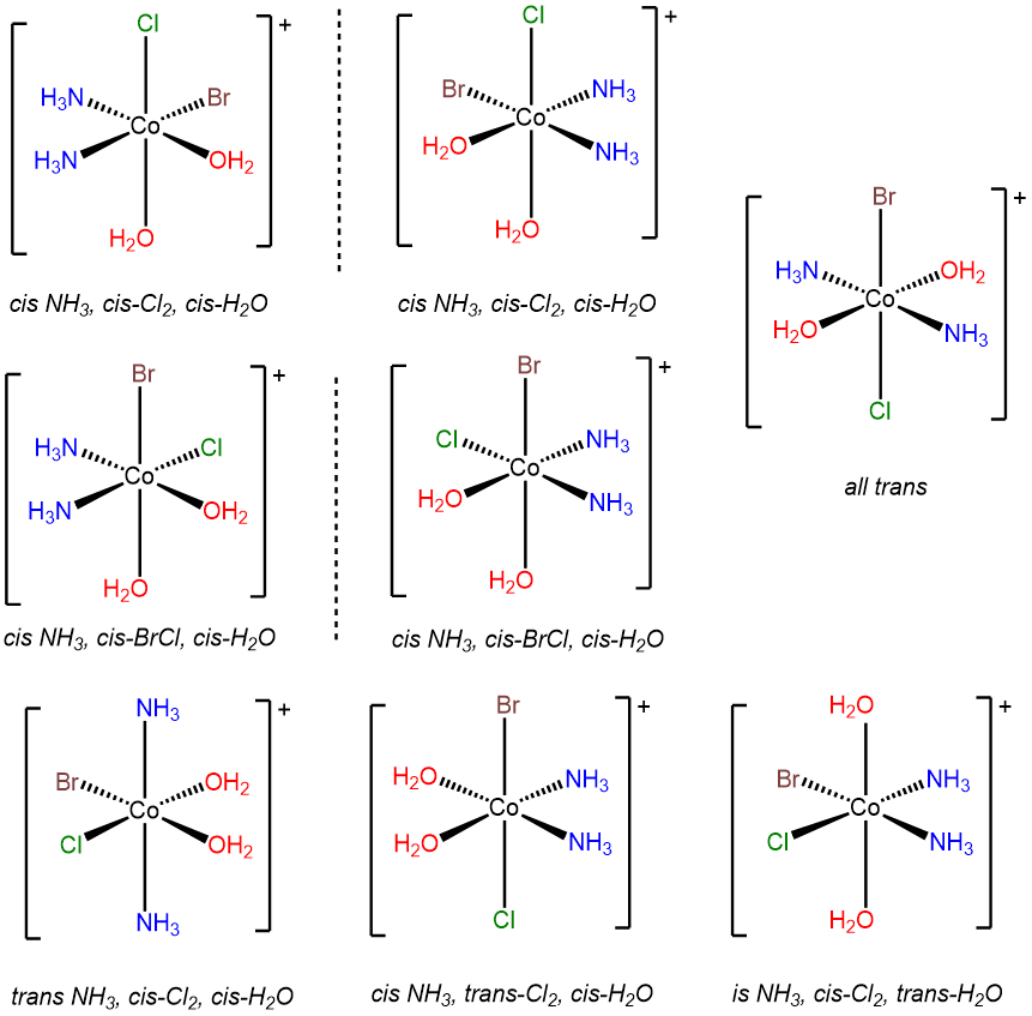


- finally, check to make sure you didn't include the same complex twice. Humans do make mistakes after all.

Answer d. $[CoBrCl(H_2O)_2(NH_3)_2]^+$

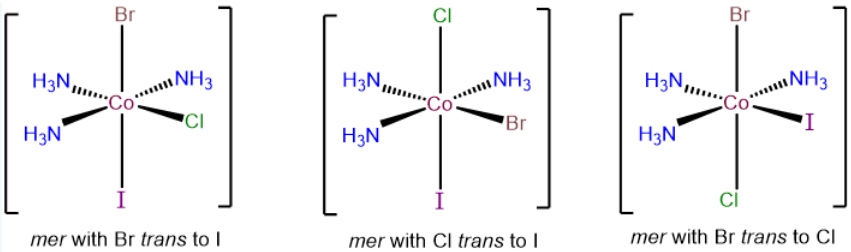
This problem is analogous to the one above except that this complex contains a bromo and chloro ligand in place of the two chloro ligands in $[CoCl_2(H_2O)_2(NH_3)_2]^+$. Consequently, when the bromo and chloro ligands are *cis* to one

another, additional possibilities for isomers arise based on whether ammine or aqua ligands are *trans* to the chloro and bromo. The result is eight isomers.

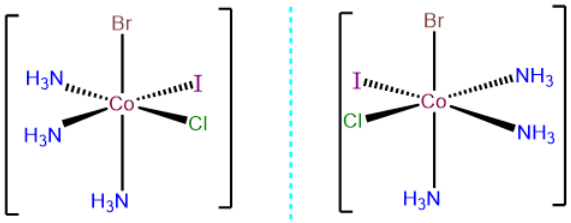


Answer e. [CoBrClI(NH_3)$_3$]

There are two possibilities for this complex - a *fac*-(NH_3)$_3$ and a *mer*-(NH_3)$_3$ arrangement. These may be taken as starting points for examining the possible permutations for the Cl^-, Br^-, and I^- ligands. The top row presents the three possibilities within the *mer*-(NH_3)$_3$ arrangement; each corresponds to a different ligand *trans* to an ammine ligand. The bottom row presents the two possible isomers with a *fac*-(NH_3)$_3$ arrangement. In each, the Cl^-, Br^-, and I^- ligands are *trans* to ammine ligands. However, the complexes possess C_1 symmetry and so are chiral and exist as enantiomers.

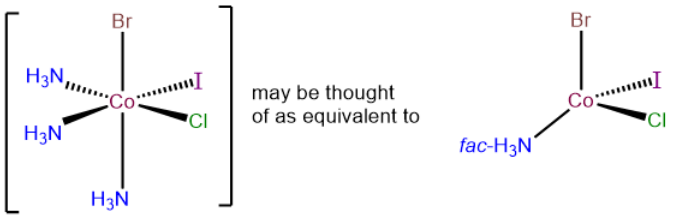


mer with Br *trans* to I | *mer* with Cl *trans* to I | *mer* with Br *trans* to Cl



fac enantiomers

(C_1 symmetry or it you think of the *fac*-$(H_3N)_3$ as being "one uniform group" then the symmetry is equivalent to that of a chiral carbon)



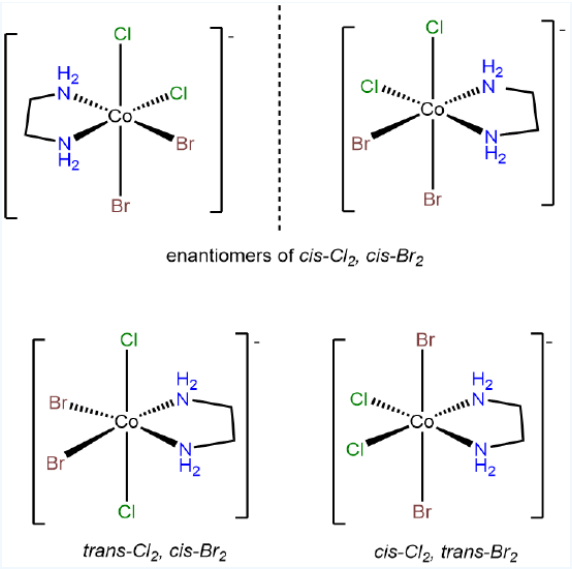
? Exercise 4.4.5. Stereoisomers of complexes with bidentate ligands (ignoring ring twist).

Ignoring ring twist, draw all the stereoisomers of the following real and hypothetical octahedral complexes.

a. $[CoBr_2Cl_2(en)]^-$
b. $[CoBrCl(en)_2]^+$
c. $[CoBrCl(gly)_2]^-$
d. $[Co(en)_3]^{3+}$
e. $[Co(gly)_3]$

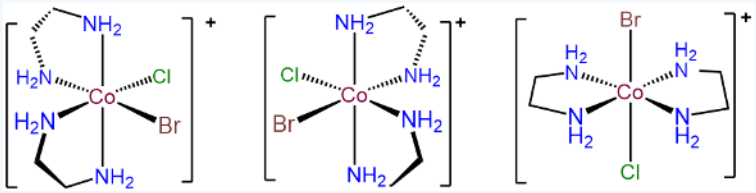
Answer a. $[CoBr_2Cl_2(en)]^-$

This complex is analogous to $[CoCl_2(H_2O)_2(NH_3)_2]^+$ in possessing pairs of identical ligating groups. The main difference is that in $[CoBr_2Cl_2(en)]^-$ the two amine ligating group of the en ligand are restricted to a *cis* arrangement. Under the MABCDEF system explained in Note **4.4.1**, $[CoCl_2(H_2O)_2(NH_3)_2]^+$ may be $MA_2B_2C_2$, but this complex, $[CoBr_2Cl_2(en)]^-$, is $M(AA)B_2C_2$. The isomers are:



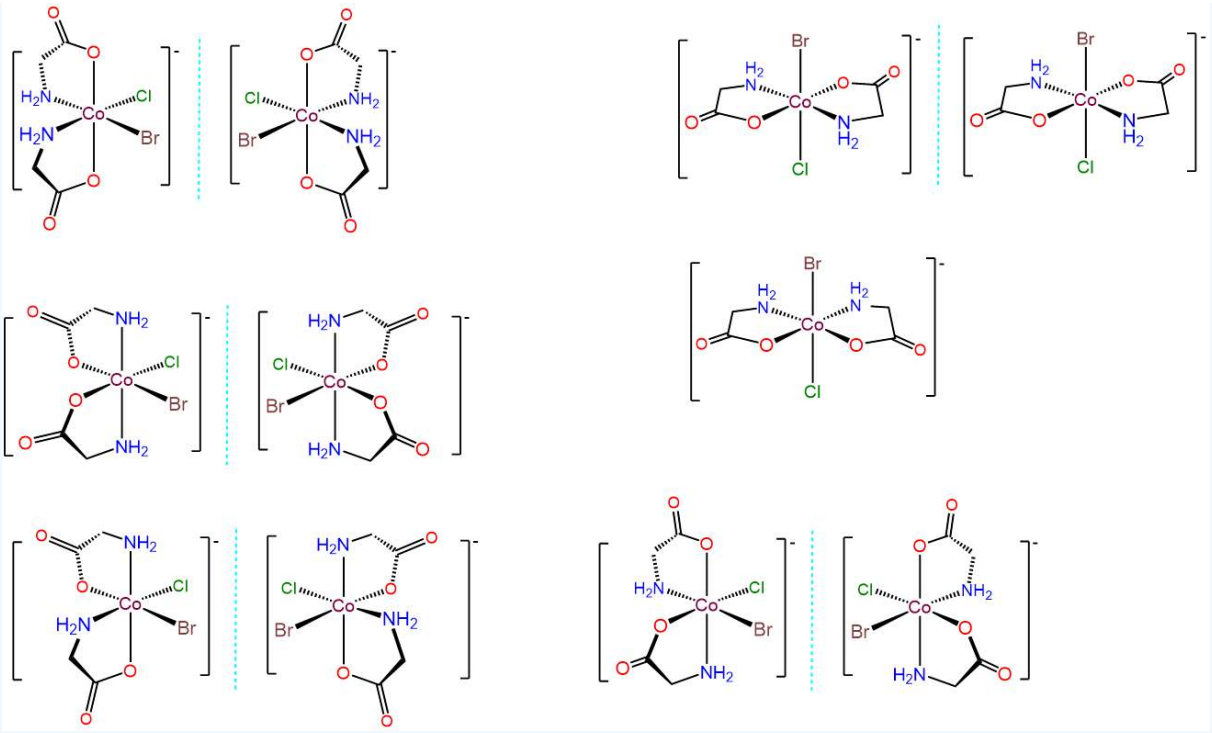
Answer b. $[CoBrCl(en)_2]^+$

The key to problems like this is to focus on the unique ligands, in this case Br^- and Cl^-. These can exist in either a *cis* or *trans* arrangement. The *trans* form is achiral, but in the case where Br^- and Cl^- are *cis*, **Λ** and **Δ** enantiomers are possible. The result is three isomers.



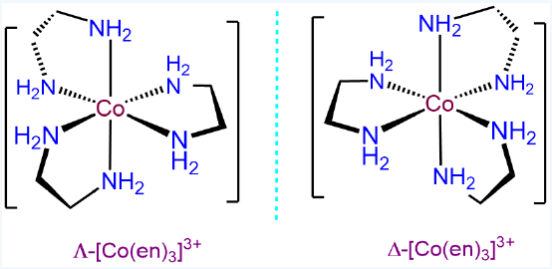
Answer c. $[CoBrCl(gly)_2]^-$

This case is analogous to the one above, but this time the bidentate ligand, gly, possesses distinguishable binding sites. Thus there are additional permutations involving how the gly ligands are bound relative to one another and/or whether the O or N end of the gly is bound *trans* to Br or Cl. The result is 11 different isomers, which are given below.



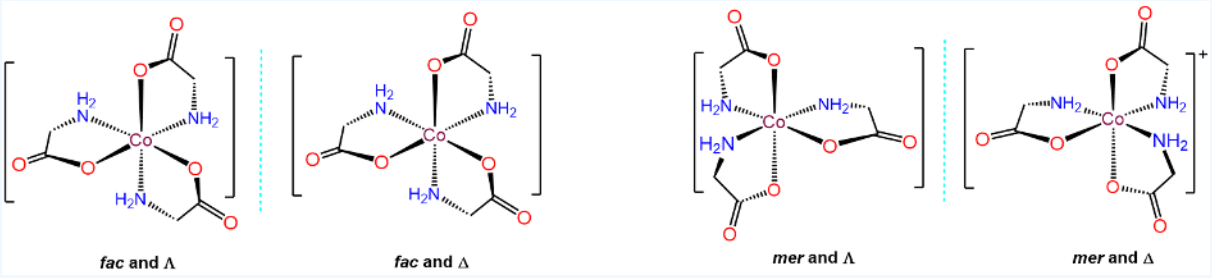
Answer d. $[Co(en)_3]^{3+}$

As a tris-chelate of symmetric bidentate ligands, ignoring ring twist, $[Co(en)_3]^{3+}$ will only exhibit **Λ** and **Δ** isomerism.



Answer e. $[Co(gly)_3]$

Since there are three gly ligands, each of which have carboxy and amine ends, the allowable arrangements involve whether the resulting three carboxy and three amine ends are oriented in a *mer* or *fac* arrangement. This gives two possibilities, each of which can exist as either the **Λ** or **Δ** enantiomer, for a total of four isomers, which are given below.



Exercise 4.4.6. More stereoisomers: Now featuring linkage isomerism

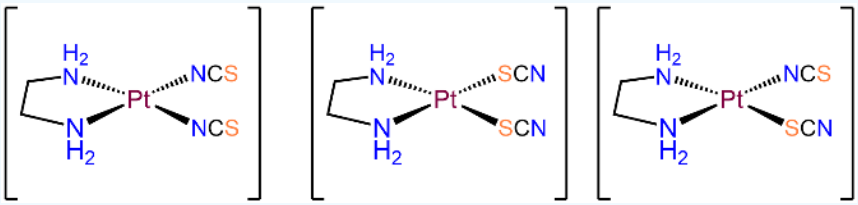
Ignoring ring twist, draw all chemically reasonable stereoisomers for the following real and hypothetical complexes. You may assume that

- complexes in which the metal has a coordination number of six are octahedral
- complexes in which the metal has a coordination number of five are trigonal bipyramidal
- complexes in which Pt^{II} , Pd^{II} , or Rh^{I}, or Ir^{I} have a coordination number of four are square planar
- other complexes in which the metal has a coordination number of four will be tetrahedral

a. $[Pt(en)(SCN)_2]$
b. $[Pt(NH_3)_2(SCN)_2]$
c. $[Co(en)_2(SCN)_2]^+$

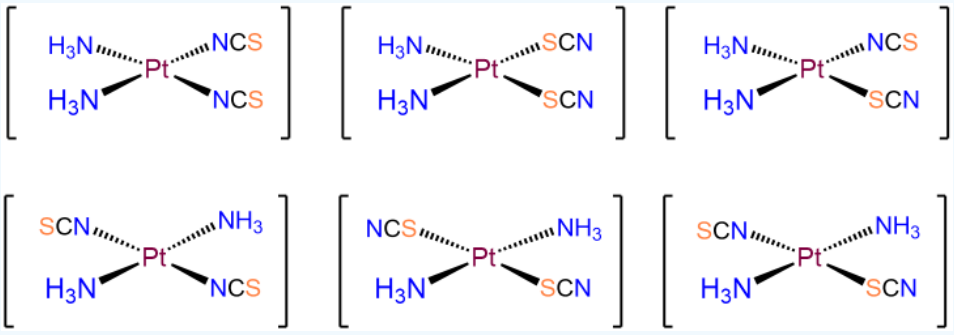
Answer a. $[Pt(en)(SCN)_2]$

The Pt in this neutral complex must be Pt^{2+} to balance the negative charges of the two SCN^- ligands. Complexes of Pt^{2+} are square planar and four coordinate, consistent with the bidentate en and two thiocyanato ligands. Of the ligands, the en ligand must bind in a *cis* arrangement. Consequently, the two SCN^- ligands will be in a *cis* arrangement as well. The isomers will therefore only differ in whether the two SCN^- bind κN or κS. The possibilities are:



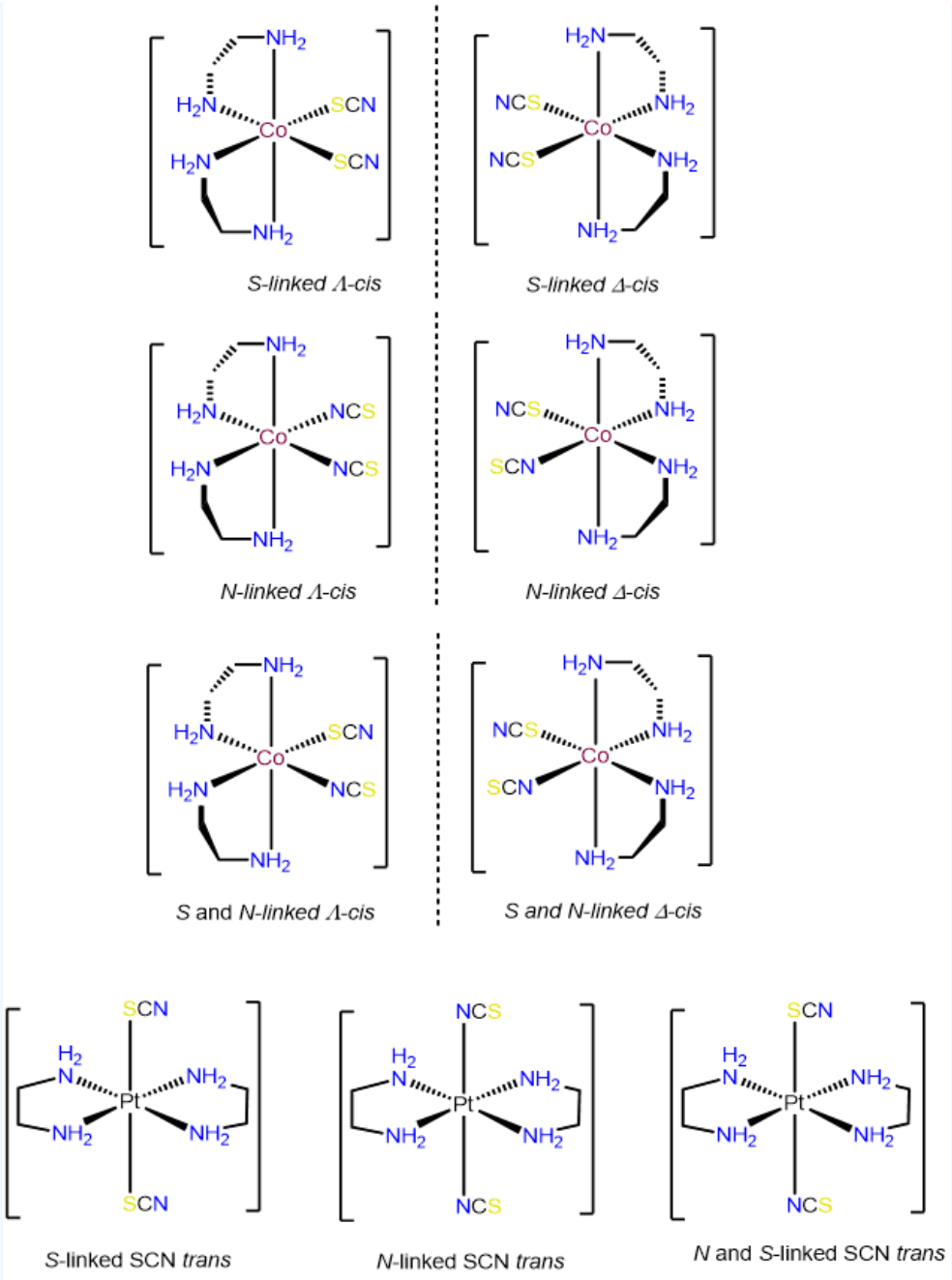
Answer b. $[Pt(NH_3)_2(SCN)_2]$

As with the preceding example, this will be a square planar Pt^{2+} complex. The main difference is that this time the coordinated nitrogens are not constrained to adopt a *cis* arrangement so there will be both *cis* and *trans* isomers.



Answer c. $[Co(en)_2(SCN)_2]^+$

https://chem.libretexts.org/@go/page/403023



? Exercise 4.4.7. Stereoisomer free for all.

Ignoring ring twist, draw all chemically reasonable stereoisomers for the following real and hypothetical complexes. You may assume that

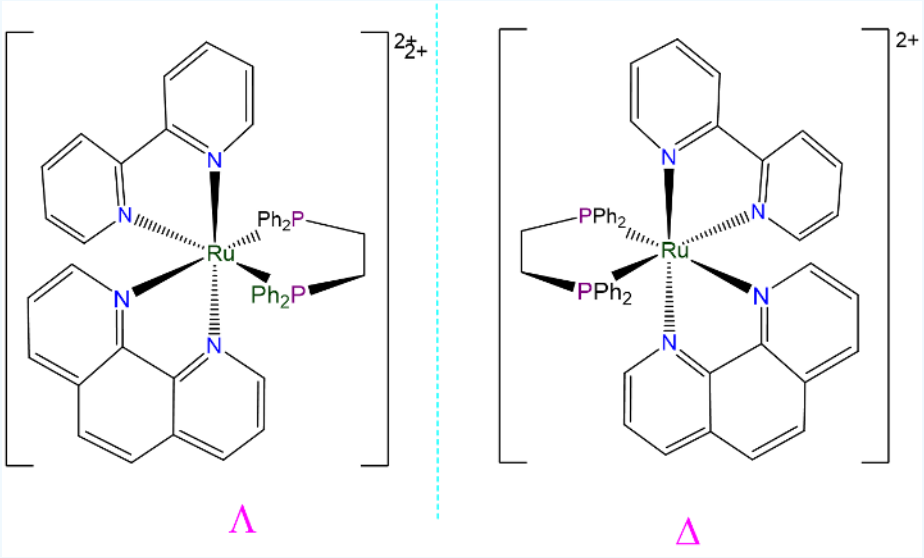
- complexes in which the metal has a coordination number of six are octahedral
- complexes in which the metal has a coordination number of five are trigonal bipyramidal
- complexes in which Pt^{II} , Pd^{II} , or Rh^{I}, or Ir^{I} have a coordination number of four are square planar
- other complexes in which the metal has a coordination number of four will be tetrahedral

a. $[Ru(bpy)(phen)(dppe)]^{2+}$
b. $[CoClF(PPh_3)(py)]^{-}$
c. $[Ni(en)_2(NO_2)_2]$

d. $[Fe(H_2O)_3(SCN)_3]$
e. $[PtClF(PPh_3)(py)]$
f. $[CoBr_2Cl(NH_3)_3]$

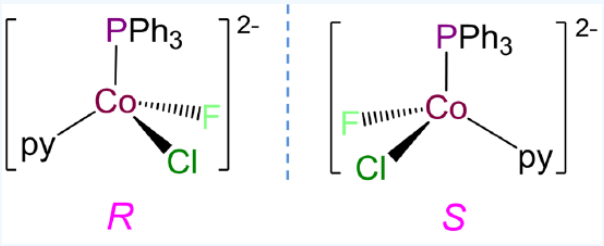
Answer a. $[Ru(bpy)(phen)(dppe)]^{2+}$

This complex is an octahedral tris-chelate containing symmetric ligands. As such it will exhibit **Λ** and **Δ** isomers:



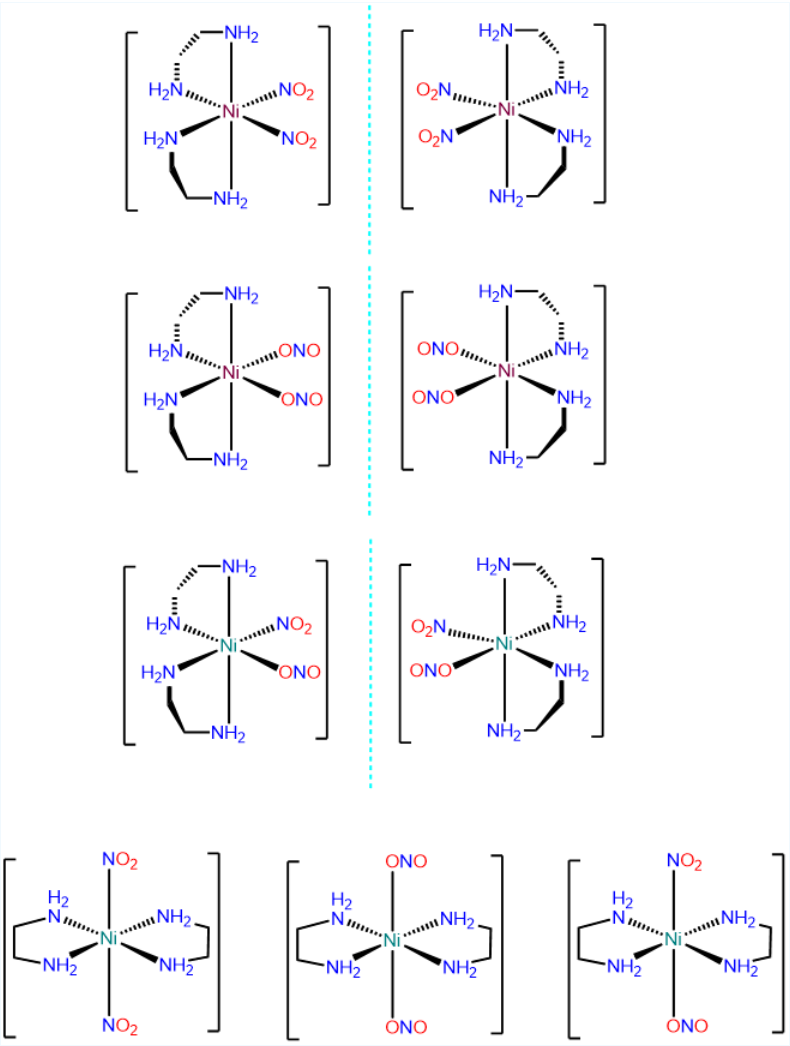
Answer b. $[CoClF(PPh_3)(py)]^-$

This complex has a coordination number of 4 and contains a Co^{2+} ion with a d^7 electron configuration, so a tetrahedral geometry is expected. Tetrahedral complexes like this one with four different ligands are chiral and can form *R* and *S* enantiomers.



Answer c. $[Ni(en)_2(NO_2)_2]$

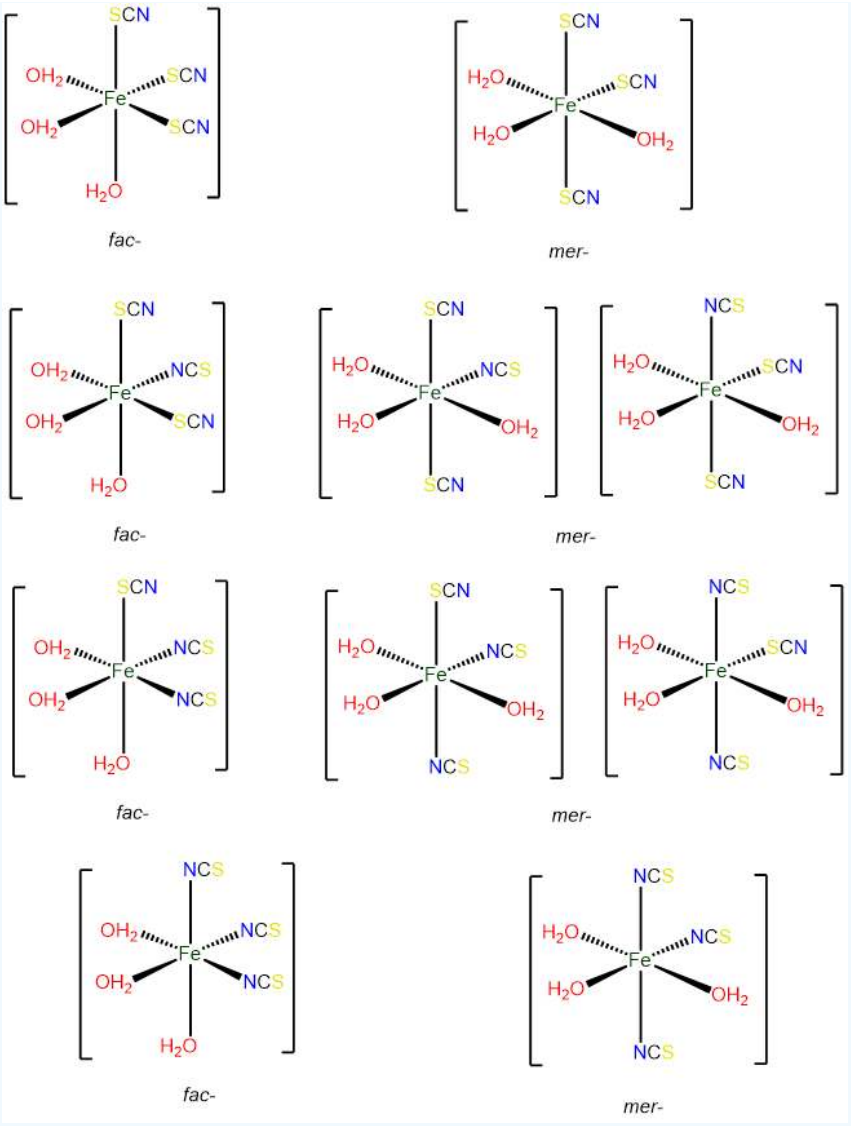
This is an octahedral bis-chelate and will exist in **Λ** and **Δ** configurations. Within each configuration the NO_2^- ligands can exist as *κN* and *κO*, leading to the following possibilities:



Answer d. $[Fe(H_2O)_3(SCN)_3]$

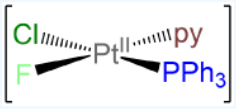
As an octahedral complex with three identical ligands it can exist in *mer* and *fac* configurations, with the ambidentate SCN ligand providing additional possibilities for isomerism.

https://chem.libretexts.org/@go/page/403023



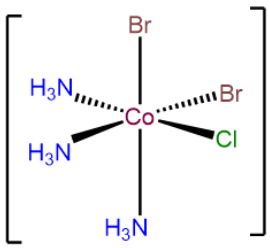
Answer e. [PtClF(PPh$_3$)(py)]

As a square planar complex with four nonidentical ligands, this complex exists as a single isomer.

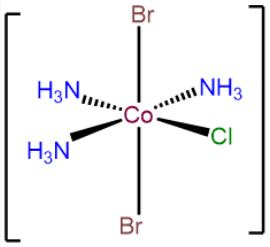


Answer f. [CoBr$_2$Cl(NH$_3$)$_3$]

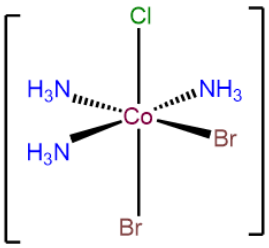
As an octahedral complex with three identical ligands it will exhibit *mer* and *fac* isomerism. In addition, it will have two *mer* configurations that differ in terms of the cis and trans relationships between the bromo and chloro ligands.



fac



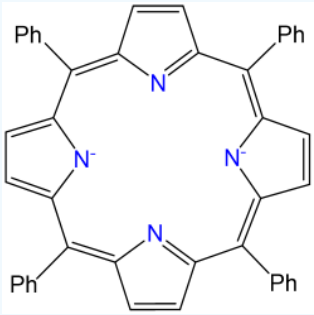
mer with Br *trans* to Br



mer with Cl *trans* to Br

Exercise 4.4.8

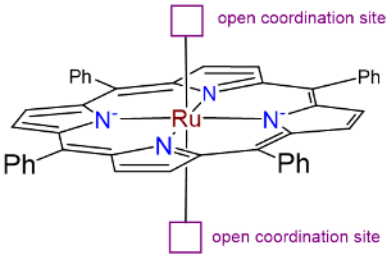
Complexes of formula Ru(TPP)py_2 have been prepared, in which TPP is tetraphenylporphyrin, which binds metals in the form given below. Draw all isomers of Ru(TPP)py_2.

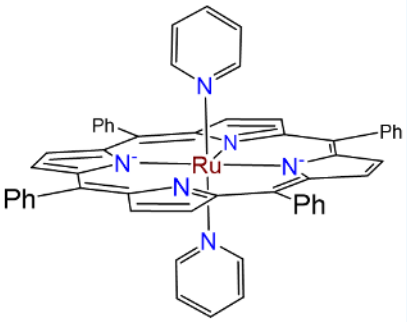


Answer

There is only one isomer. While normally complexes containing two identical ligands (in this case py) can exhibit *cis* and *trans* isomerism, in this case the planar tetraphenylporphyrin ring ligates the Ru^{2+} ion in a square planar arrangement, as shown at left in the image below. This leaves only a pair of *trans* coordination sites for the chloro ligands to occupy, giving the isomer shown at right below.

When TPP ligates Ru^{2+} it leaves only *trans* open coordination sites so only the *trans* isomer can form.

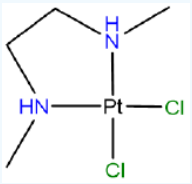




trans-[Ru(py)$_2$(TPP)]

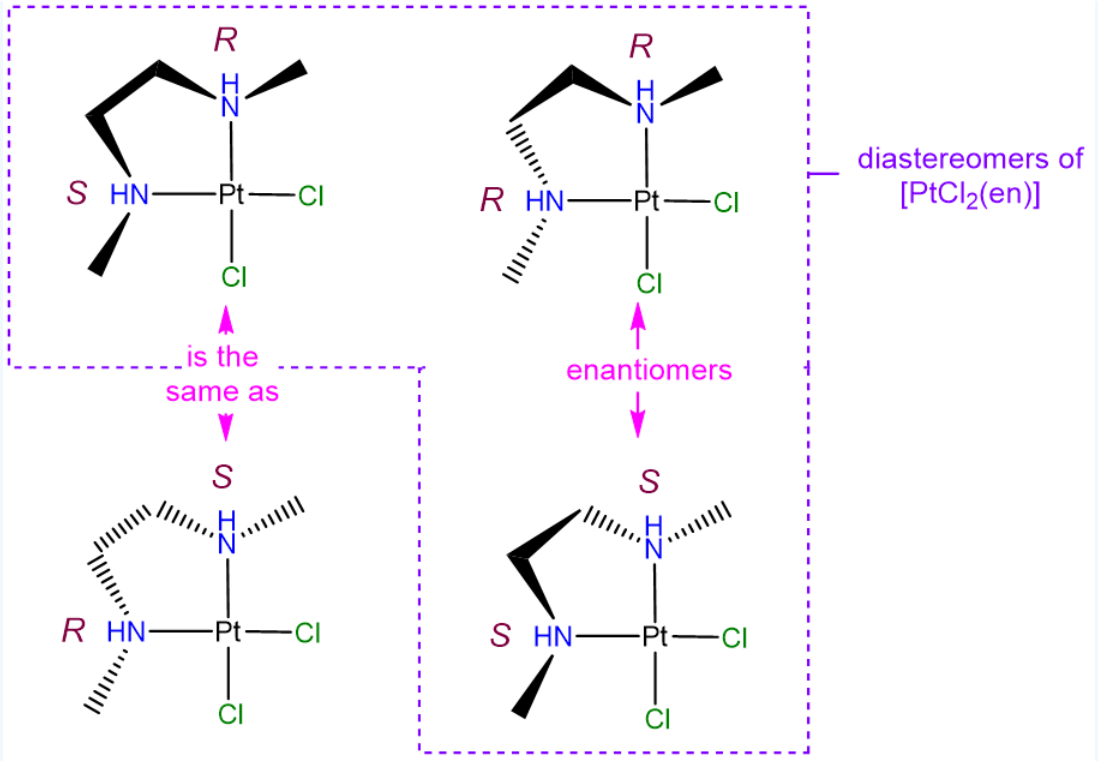
Exercise 4.4.9

Draw the diastereomers formed due to the chirality of the amine nitrogen atoms in [$PtCl_2$(*N*,*N*'-dimethylethane-1,2-diamine)] which has the atomic connectivity represented below



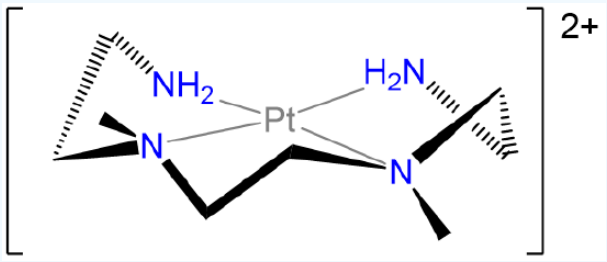
Answer

The diastereomers will differ in whether the N atoms adopt an *R* or *S* configuration at the nitrogen atoms. The possible permutations are (*R*,*R*), (S,*S*), (*R*,*S*), and (S,*R*). However, as may be seen from the image below, the (*R*,*S*) and (S,*R*) configurations are identical (the two projections shown can be interconverted through a C_2 rotation along an axis bisecting the Cl-Pt-Cl unit). As a result there are only three unique isomers. Of these, the (*R*,*R*) and (S,*S*) configurations are enantiomers (they are mirror images by reflection in the $PtCl_2N_2$ plane). Note that in solving problems like this one it can be helpful to keep track of possible isomers by assigning the stereochemistry at each chiral center as *R* or *S* using the Cahn-Ingold-Prelog-convention, though it is not strictly necessary to do so.

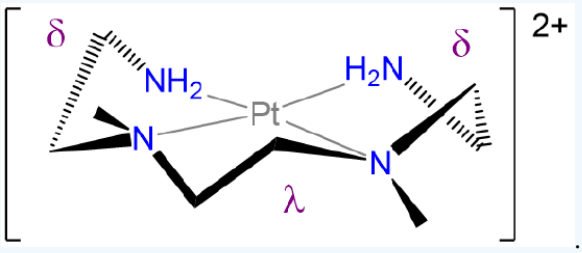


? Exercise 4.4.10

Label the conformations of all chelate rings in the structure below.



Answer



Appendix: The MABCDEF bookkeeping system for identifying isomers

The Mabcdef or MABCDEF system is one method for identifying the number of isomers in an octahedral complex, although since it is really just a bookkeeping and organizational system it can easily be extended to other geometries as well. The M in Mabcdef stands for metal and the other letters are used to stand in for ligands. The basic approach involves

- classifying the ligands as A, B, C, D, E, or F in order of multiplicity. Thus for

$[Cr(NH_3)_6]^{3+}$ A = NH_3; there are no B, C, D,E, or F ligands; and the complex is classified as MA_6

$[CoCl(NH_3)_5]^{2+}$ A = NH_3, B = Cl^-, and the complex is MA_5B

$[CrCl_2(H_2O)_2(NH_3)_2]^+$ A = Cl^-, B = H_2O, C = NH_3, and the complex is $MA_2B_2C_2$

- in the classification above, multidentate ligands are typically classified before monodentate ones and are designated AA, AB, ABC, ABA, etc. based on the symmetry of the attachment points. Thus

  en has identical attachment amine points and is AA

  gly has a carboxy and amine attachment points and is AB

  trien is ABA

  $CoCl_2(en)_2^+$ is $M(AA)_2B_2$

  $CoCl_2(gly)_2^-$ is $M(AB)_2C_2$

  $CoCl_2(en)(gly)$ is $M(AA)(AB)C_2$

- Systematically list out the possible *trans* arrangements of ligands by
  1. assigning one pair of ligands to be *trans* to one another.
  2. Then systematically list out the other possible *trans* pairs by permuting the remaining trans arrangements. It can help to organize the permutations in a table, such as that shown below for an MABCDEF complex where A and B are assigned *trans*. In looking at the table notice how the second set of trans permutations is systematically varied. This helps ensure that no possibility is skipped.
  3. Go through the list of isomers and remove any duplicates you generated so far. For instance, notice in the table below that the last three stereoisomers are identical with the first three (*e.g.*, stereoisomer 4 is identical to stereoisomer 3, 5 with 2, and 6 with 1).

Stereoisomer 1	Stereoisomer 2	Stereoisomer 3	Stereoisomer 4 (same as isomer 3)	Stereoisomer 5 (same as isomer 2)	Stereoisomer 6 (same as isomer 1)
trans AB (fixed)	*trans* AB (fixed)	*trans* AB (fixed)	*trans* AB (fixed)	*trans* AB (fixed)	*trans* AB (fixed)
trans CD	*trans* CE	*trans* CF	*trans* DE	*trans* DF	*trans* EF
trans EF	*trans* DF	*trans* DE	*trans* CF	*trans* CE	*trans* CD

  4. If the complex possesses multidentate ligands that demand that certain groups exist and *cis* pairs, then also remove any configurations which do not agree with the known binding capability of the ligand (*e.g.*, the two amine groups of ethylenediamine cannot be *trans* to one another, so if you have an en ligand, remove configurations like that from the list).

5. Next, swap or permute the original *trans* pair and repeat the process you just followed. In the case of Mabcdef this gives the following results:

Isomer	"fixed" trans pair	Additional trans pairs	
1	AB	CD	EF
2	AB	CE	DF
3	AB	CF	DE
4	AC	BD	EF
5	AC	BE	BF
6	AC	BF	DE
7	AD	BC	EF
8	AD	BE	CF
9	AD	BF	CE
10	AE	BC	DF
11	AE	BD	CF
12	AE	BF	CD
13	AF	BC	DE
14	AF	BD	CE
15	AF	BE	CD

- Since the procedure explained above only identifies isomers based on unique *trans* pairings, **it does not identify when a configuration is chiral and corresponds to a pair of enantiomers.** Any enantiomers can be identified by drawing out the complexes and either classifying their point groups or by drawing their mirror images and checking if they are superimposable. In the MABCDEF case - *i.e.*, where all the ligands are different - all of the isomers identified have C_1 symmetry so are chiral. This means there will be a pair of enantiomers for each, giving 15 x 2 = 30 different stereoisomers.

References

1. These examples are taken from http://wwwchem.uwimona.edu.jm/courses/inorgnom.html

2. Contakes S. M.; Rauchfuss, T.B. *Chem. Commun.* 2001, 553-554.

3. Shriver, D. F.; Shriver, S. A.; Anderson, S. E., *Inorg. Chem.* 1965, *4(5)*, 725-730.

4. Zelewsky, A. v., *Stereochemistry of Coordination Compounds* Wiley, 1996.

5. In the past it was difficult to determine absolute configurations from X-ray data alone, but recent advances have made it easier to do so.

6. Pavan M. V. Raja & Andrew R. Barron "Circular Dichroism Spectroscopy and its Application for Determination of Secondary Structure of Optically Active Species" in *Physical Methods in Chemistry and Nano Science* https://chem.libretexts.org/Bookshelves/Analytical_Chemistry/Book%3A_Physical_Methods_in_Chemistry_and_Nano_Science_(Barron)/07%3A_Molecular_and_Solid_State_Structure/7.07%3A_Circular_Dichroism_Spectroscopy_and_its_Application_for_Determination_of_Secondary_Structure_of_Optically_Active_Species

7. Berova, N.; Bari, L. D.; Pescitelli, G., *Chemical Society Reviews* 2007, 36 (6), 914-931.

8. Of course, if one set of ligands occupies a meridional plane, then the other three ligands will be oriented in an equatorial one. The reason they may both be considered meridional is because if the complex were rotated, the equatorial plane would be meridional and vice versa. From that point of view both might be considered meridional planes - albeit not at the same time.

9. Bite angles are taken from Mansell, S. M., Catalytic applications of small bite-angle diphosphorus ligands with single-atom linkers. Dalton Transactions 2017, 46 (44), 15157-15174.

10. Hancock, R. D., The pyridyl group in ligand design for selective metal ion complexation and sensing. Chemical Society Reviews 2013, 42 (4), 1500-1524.

11. Sasi, D.; Ramkumar, V.; Murthy, N. N., Bite-Angle-Regulated Coordination Geometries: Tetrahedral and Trigonal Bipyramidal in Ni(II) with Biphenyl-Appended (2-Pyridyl)alkylamine N,N'-Bidentate Ligands. ACS Omega 2017, 2 (6), 2474-2481.

12. Ehnbom, A.; Ghosh, S. K.; Lewis, K. G.; Gladysz, J. A., Octahedral Werner complexes with substituted ethylenediamine ligands: a stereochemical primer for a historic series of compounds now emerging as a modern family of catalysts. Chemical Society Reviews 2016, 45 (24), 6799-6811.

4.4: Isomerism is shared under a CC BY 4.0 license and was authored, remixed, and/or curated by Stephen M. Contakes.

- **9.4: Isomerism** by Stephen M. Contakes is licensed CC BY 4.0.

4.5: Coordination Numbers and Structures

4.5.1 Why do coordination complexes form the structures they do?

As with all chemical structure, coordination complexes form the structures they do so as to best stabilize the metal center and ligands through the formation of metal-ligand bonds while avoiding destabilizing interactions like steric repulsions. The issue then is how many metal-ligand bonds should be formed and how those bonds should be arranged spatially to give the largest net stabilization possible. This question will eventually be considered in detail in connection with the nature of bonding in coordination compounds. For now, it will be helpful to think about it in terms of seven factors:

4.5.1.1 The stabilizing effect of metal-ligand bond formation.

The driving force for complex formation is the stabilization of electrons in covalent chemical bonds. In the vast majority of cases, this largely involves stabilization of the ligand lone pair as it experiences the effective nuclear charge of the metal, although a few instances involve stabilization of metal electrons by ligand nuclei (inverse ligand fields). Regardless, metal-ligand bond formation is stabilizing and classified by the way it preferences the addition of ligands to the complex.

4.5.1.2 Steric effects, specifically steric repulsions between ligands.

One reason coordination numbers do not increase indefinitely is that only so many ligands can fit around a metal. Exactly how many depends on

- *the size of the metal center.* This is one of the more important factors. Many metals tend to exhibit preferred coordination numbers, which depend on their oxidation state and size as shown in Figure **4.5.1**. Larger inner transition metals like the Lanthanides and Actinides can accommodate 9-12 sterically undemanding ligands, while the smaller transition metals tend to accommodate up to six, although larger coordination numbers are more common for low valent metals and as size increases on moving from right to left across the transition metal block of the periodic table. Thus, the early transition metal molybdenum forms seven- and eight-coordinate $[Mo^{III}(CN)_7]^{4-}$ and $[Mo^{IV}(CN)_8]^{4-}$ with the sterically undemanding cyano ligand.
- *the size of the ligands.* As long as ligands are not excessively rigid and bulky, their size is less important than the size of the metal in determining the number of ligands that coordinate. Ligands' ability to donate electrons to the metal center also tends to influence coordination number more than ligand size. However, all other things being equal for a given metal and ligand donor ability, small ligands allow higher coordination numbers while fewer bulky ligands will fit around the metal center.
- *how the ligand bonds to the metal.* Again, all other things being equal, ligands that are more sterically demanding in the vicinity of the metal center tend to limit the ability of other ligands to bind more than those which bind through a small extended group. For example, a bulky isocyanide like t-BuCN will sterically crowd the metal less than a bulky phosphine like t-BuH_2P would. For this reason the effective size of a ligand is sometimes rated in terms of either a cone angle of space they are estimated to occupy around the metal (called the Tolman cone angle, it is commonly used to evaluate phosphines' steric bulk) or in terms of the percentage of the metal's coordination sphere the ligand occupies (called the percent buried volume, it is used to estimate the steric impact of *N*-heterocyclic carbenes).

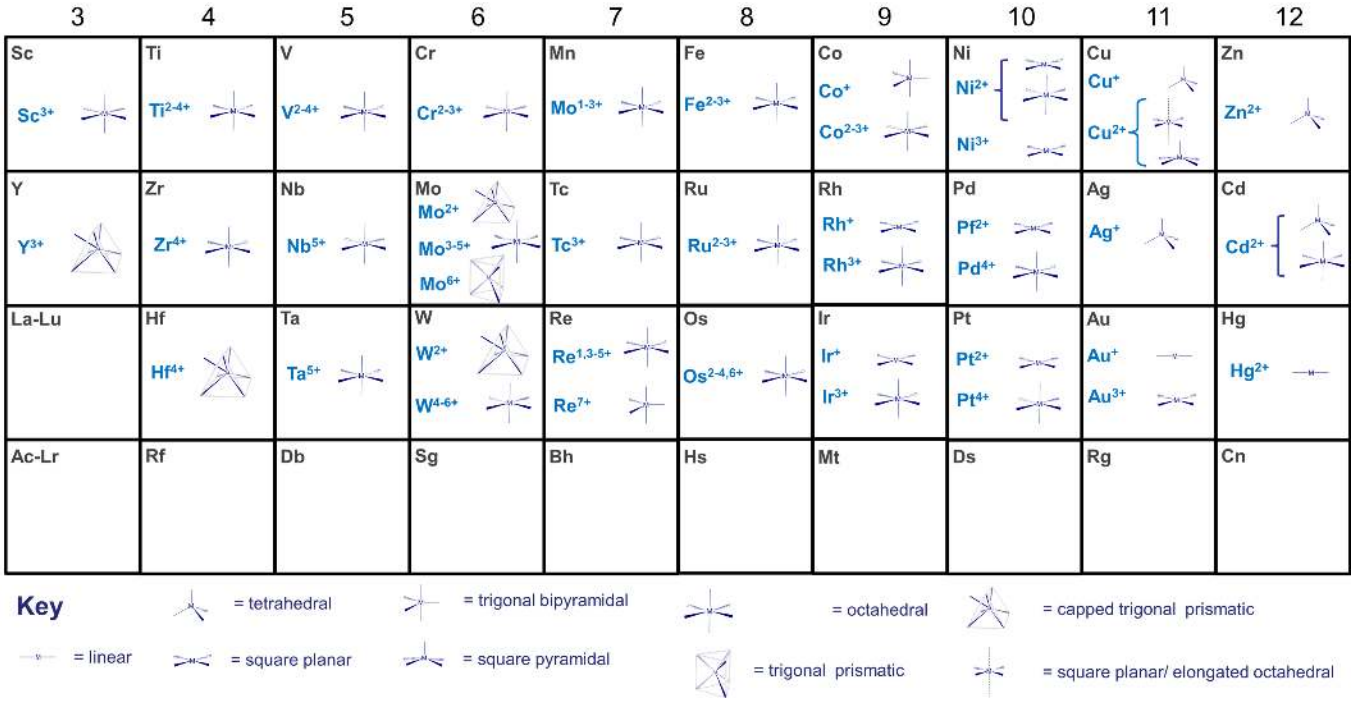


Figure **4.5.1**. Preferred coordination geometries of the transition elements. Assignments are as reported in reference 1 except for Cu^{2+}, which is assigned above as square planar/elongated octahedral instead of the square planar assignment given in that work. This work by Stephen Contakes is licensed under a Creative Commons Attribution 4.0 International License.

4.5.1.3 Repulsion between M-L bonding electrons on different ligands.

For many complexes, steric effects are neither the only effects nor the most important. Among the additional factors that should be considered are the repulsions that occur between the electrons that different ligands donate to the metal-ligand bonding. These electron-electron repulsions affect the

a. **Coordination number.** When a ligand donates its electrons to a metal center to form a new metal-ligand bond, the electron density around the metal increases, raising the overall energy of the other M-L bonding electrons. This increased repulsion often limits the number of coordinated ligands. As more ligands are added, the electron-electron repulsions keep increasing until the lowering of energy of the ligand electrons in the new bond is insufficient to compensate for the raising of energy of the existing M-L bonding electrons. Based on this effect alone,
   - larger metals tend to achieve higher coordination numbers than smaller ones because the electron-electron repulsions are spread across a larger coordination sphere.
   - With a given metal, ligands that are more electron donating have a greater tendency to form complexes with lower coordination numbers with a given metal than similar neutral ones do. This is why anionic ligands (which tend to be better electron donors) tend to give lower coordination numbers than comparable neutral ligands (which tend to be weaker donors). Thus Co^{2+} forms $CoCl_4^{2-}$ with chloro ligands but $[Co(H_2O)_6]^{2+}$ with aqua ligands.

b. **Coordination geometry.** In the **Kepert model** for the shapes of coordination complexes, this intraligand repulsion determines the most stable coordination geometry by causing the ligands to move as far apart from one another on the metal's coordination sphere as possible.

Formally, according to the **Kepert model**

- any of the metal's valence electrons not involved in metal-ligand bonds occupy (n-1)*d* orbitals and function as core electrons. As core electrons they do not influence the molecular shape.
- electrons involved in bonding to a given ligand constitute an electron group that repels all other electron groups around the metal.
- all other things being equal, the complex will form the geometry that maximizes the intra-electron group repulsions.

Notice the similarities of these postulates to those of VSEPR theory. In predicting coordination geometries in terms of electron-electron repulsions, the Kepert model is just an extension of VSEPR theory to coordination compounds. The difference between VSEPR theory and the Kepert model is that in the Kepert model, only electrons involved in metal-ligand bonds count.

Coordination geometries predicted by the Kepert model for coordination numbers two through nine are given in Figure **4.5.2**. As may be seen from the geometries listed in Figure **4.5.2**, these are just equivalent to VSEPR geometries for cases in which the number of electron groups is equal to the coordination number.

The difference between optimal and suboptimal coordination geometries is greater with few ligands, and becomes smaller as ligands become increasingly dispersed across the metal's coordination sphere. In complexes containing five, seven, eight, or higher coordinate metals, there are a number of geometries that are similar in energy to the preferred geometry. These geometries, which should be regarded as accessible, are also listed in Figure **4.5.2**.

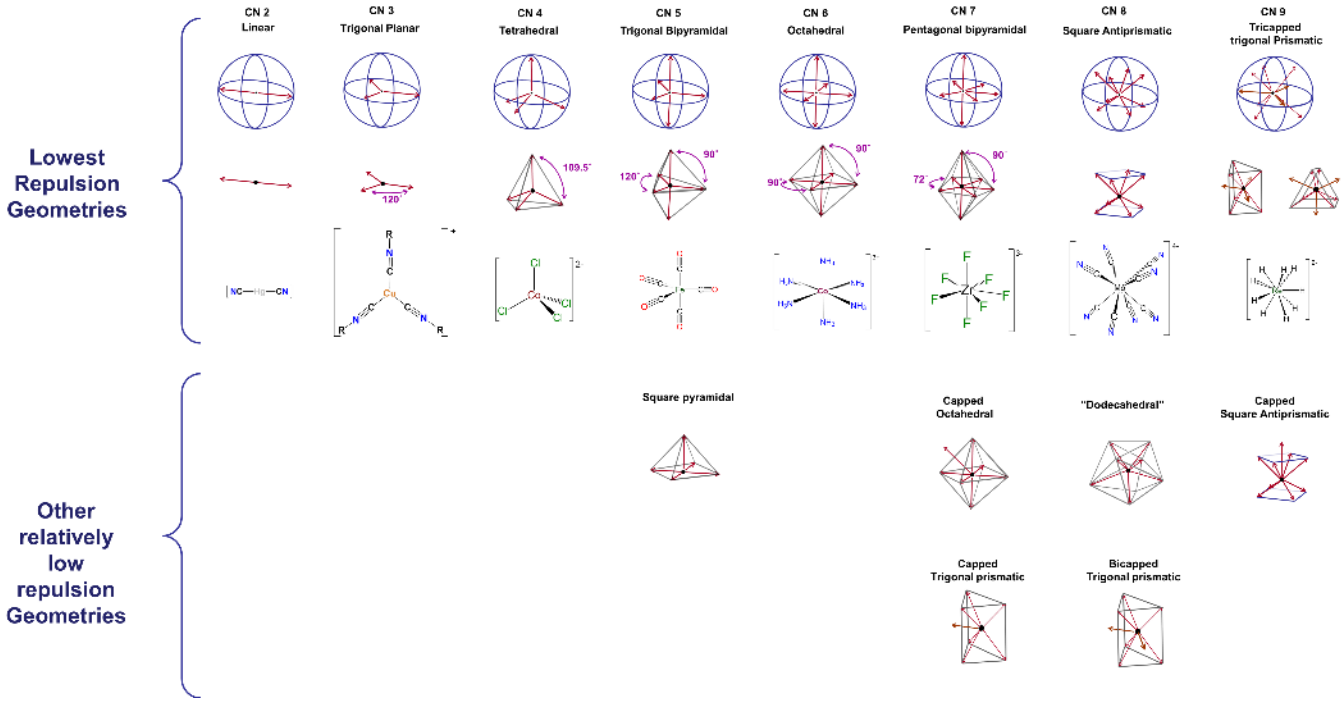


Figure **4.5.2**. Coordination geometries predicted by the Kepert model for coordination numbers two through nine along with other coordination geometries similar in energy to the lowest repulsion geometry. This work by Stephen Contakes is licensed under a Creative Commons Attribution 4.0 International License.

4.5.1.4 d-electron effects

A few coordination geometries are noticeably absent from the Kepert-preferred and Kepert-accessible geometries in Figure **4.5.1**. These include the trigonal prismatic geometries formed by compounds like $W(CH_3)_6$ and the very common square planar geometry illustrated by complexes like $[PtCl_4]^{2-}$ and $[IrClH(PPh_3)_2]$. One of the reasons the Kepert model fails to predict the existence of such structures is its neglect of directional interactions involving *d* electrons on the metal center. Metal *d* electrons exert a profound influence on almost all properties of transition metal complexes, including their structures. The way in which this occurs will be explored at length in the next chapter. For now, it is enough to note that both the ligand-donated electrons surrounding a metal center and the electrons occupying particular *d* orbitals on that metal are oriented in specific directions relative to one another. Because of this, the strength of the interactions between the ligand and metal *d* electrons depends on the number of *d* electrons present, how strongly metal-ligand binding affects their energy, and how the ligands are arranged about the metal center. The impact of these effects, here termed ligand field effects, differs from case to case and can include

- distortions of the complex's geometry. For instance, an ideal octahedral coordination geoemtry might be tetragonally distorted by flattening or elongating it.
- imparting a strong preference for non-Kepert coordination geometries. This is why, for example, 2nd and 3rd row complexes in which the metal has a d^8 electron configuration are almost always square planar.

- stabilizing non-Kepert geometries enough to permit complexes to adopt them in the presence of a rigid or semirigid ligand that prefers to coordinate the metal in that geometry.[3]

Because of these effects, square planar and trigonal prismatic geometries are also observed, and the list of coordination geometries given in Figure **4.5.2** may be extended to that shown in Figure **4.5.3**.

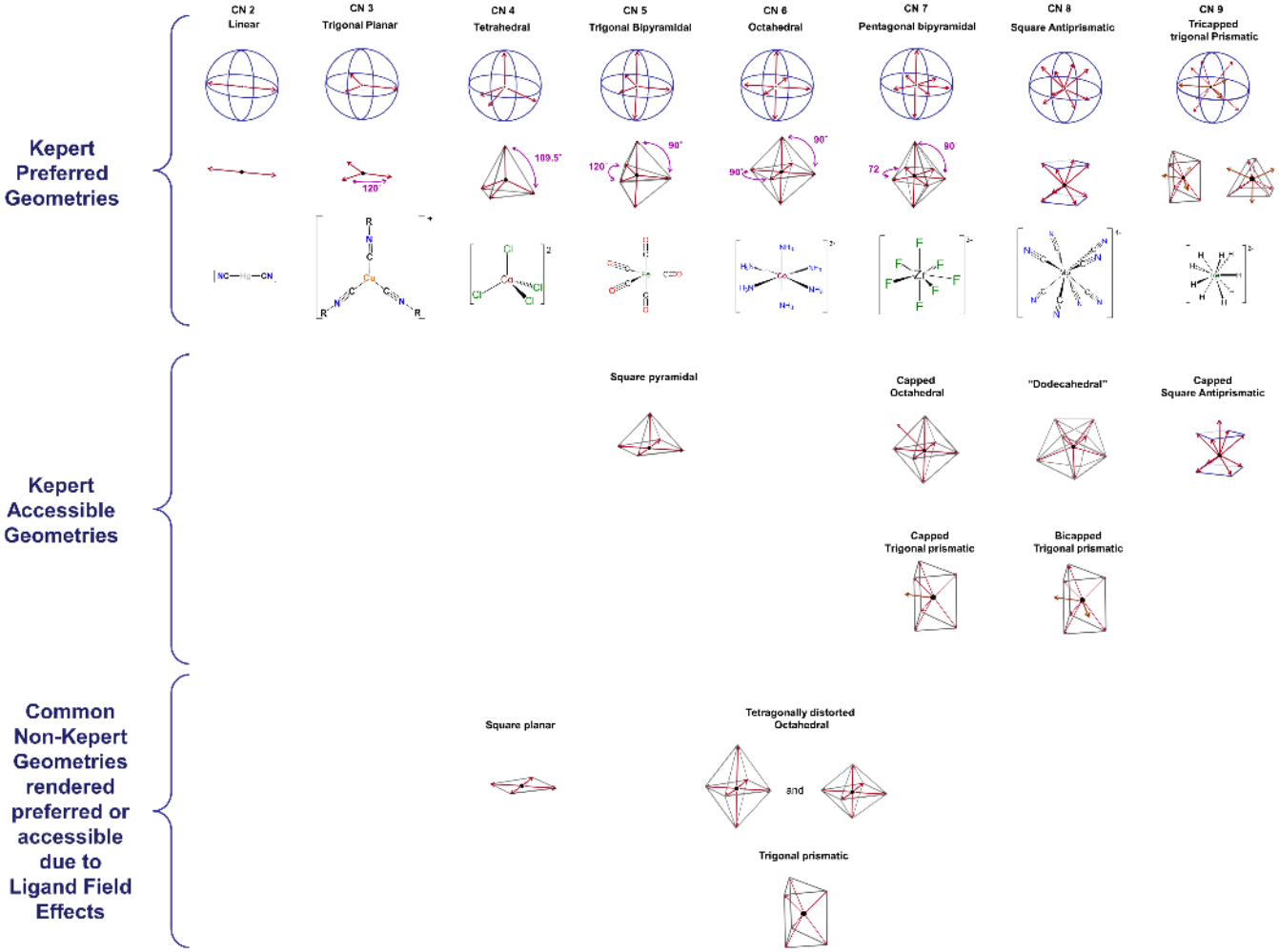


Figure **4.5.3**. Coordination geometries accessible for 2-9 coordinate complexes even without constraint by rigid or semirigid ligands. This work by Stephen Contakes is licensed under a Creative Commons Attribution 4.0 International License.

4.5.1.5 Ligand constraints imposed by rigid or semirigid ligands

Rigid or semirigid ligands influence the coordination geometry of metal complexes in two main ways:

a. Bulky rigid ligands that crowd the metal center prevent other ligands from binding. Thus such ligands are useful for preparing low-coordinate complexes.
b. Rigid and semirigid ligands can impose their preferred coordination geometry on a metal center. This is because these ligands energetically prefer to adopt a particular conformation when they bind a metal center. In doing so they shift the coordination geometry energy landscape toward that preferred geometry. If the shift is large enough relative to the native preference due to ligand repulsion and ligand field effects, the complex will either adopt the ligand-preferred geometry or be distorted in the direction of the ligand-preferred geometry. Examples are given in Figure **4.5.4**.

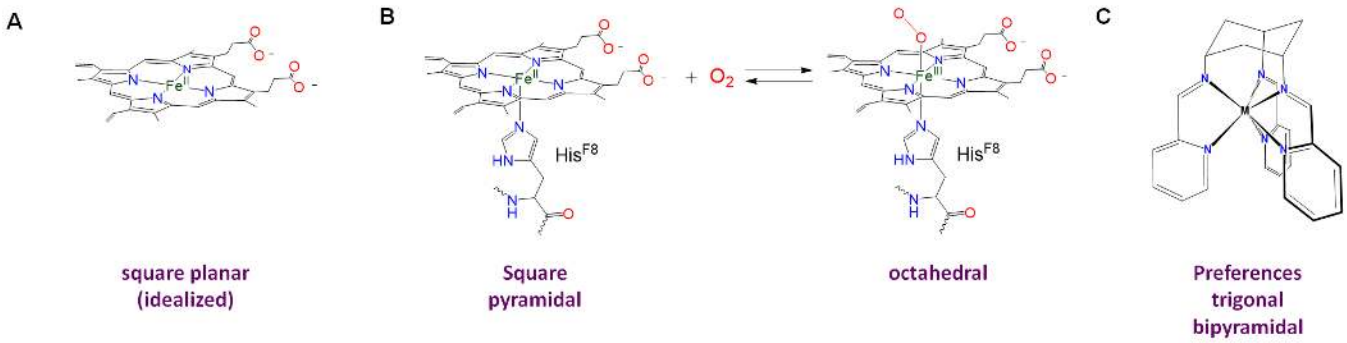


Figure **4.5.4**. Examples of rigid/semirigid ligands that can impose their preferred coordination geometry on a metal center. Porphyrins, phyhalocyanines and related macrocycles tend to impose a slightly bent square planar coordination geometry, although (B) many such complexes, including the iron of myoglobin's heme cofactor, coordinate additional ligands to give square planar or octahedral complexes. (C) Synthetic multidentate ligands have been developed to preference trigonal prismatic coordination geometries, including the one shown here. It forms roughly trigonal prismatic complexes with Co^{II} and $Zn^{II,}$ albeit imperfect ones.[3]
This work by Stephen Contakes is licensed under a Creative Commons Attribution 4.0 International License.

The influence of ligands on coordination geometry is important in living systems, in which proteins and nucleic acids can act as rigid or semirigid ligands. The ability of these ligands to distort the coordination geometries of metal atoms in ways that enable them to perform specific functions is so common that the resulting distorted geometries are termed entactic states. A particularly spectacular case of an entactic state involves the blue copper proteins azurin and plastocyanin, the structure of which is given in Figure **4.5.5**.

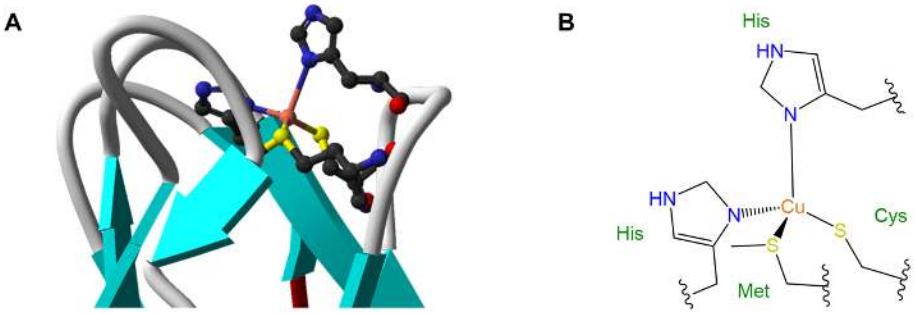


Figure **4.5.5**. (A) Structure and (B) schematic of the plastocyanin active site showing the distorted tetrahedral coordination environment that the protein imposes on the copper center (tan), which is most evident from the long vertically oriented Cu-Histidine bond. The image in part A is cropped from an original image by Ben Mills - Own work, Public Domain, https://commons.wikimedia.org/w/inde...?curid=6202620. The image in part B is by Stephen Contakes and licensed under a Creative Commons Attribution 4.0 International License.

As may be seen from the structure in Figure **4.5.5**, the copper in plastocyanin exibits a distorted tetrahedral coordination geometry. The protein is said to act like a medieval torture device called a rack in stretching the metal into its distorted geometry. This distortion makes it easier for the copper center to undergo facile redox reactions, enabling it to better function as an electron carrier.

4.5.1.6 Crystal packing effects, in which the energy-lowering packing of molecules and ions in a crystal drives the distortion of a complex's structure away from what it would adopt in the gas phase or solution

This effect is similar to that of ligand constraints except that in this case it arises not from the structure internal to a ligand but out of the forces involves in maximizing the stabilization energy of a crystal. With lower coordination number complexes, packing effects can shift the conformations of flexible ligands but only give rise to very small distortions of the overall coordination geometry. Packing effects can drive a shift in the overall coordination geometry of higher coordination number complexes, for which packing effects are significant relative to the small difference in energy between geometries. Thus while $[Mo(CN)_8]^{4-}$ has a square antiprismatic coordination geometry, in solution it exhibits a dodecahedral coordination geometry in the crystals of many of its salts.

4.5.1.7 Relativistic effects on orbital energies

The proximity of fast moving electrons to massive nuclei in the heavier transition elements results in relativistic expansion and contraction of orbitals. The net results are that

- heavier elements tend to be smaller than expected. This effect preferences lower coordination numbers.
- the relative energies of orbitals shift. Orbitals which become contracted are lowered in energy while those which are expanded increase in energy, as shown for the case of gold in Figure **4.5.6A**.

The combination of smaller sizes and altered orbital energies affects coordination preferences. Relativistic effects contribute to the greater tendency of Au^{I} relative to other group 11 metals to form linear two-coordinate complexes. As shown in Figure **4.5.6B**, the relative closeness in energy of the 6*s* and 5*d* orbitals of gold makes mixing of these orbitals more favorable, facilitating the ability of gold to form two-coordinate complexes with strong sigma bonds oriented 180/(^{\circ}\) from one another.

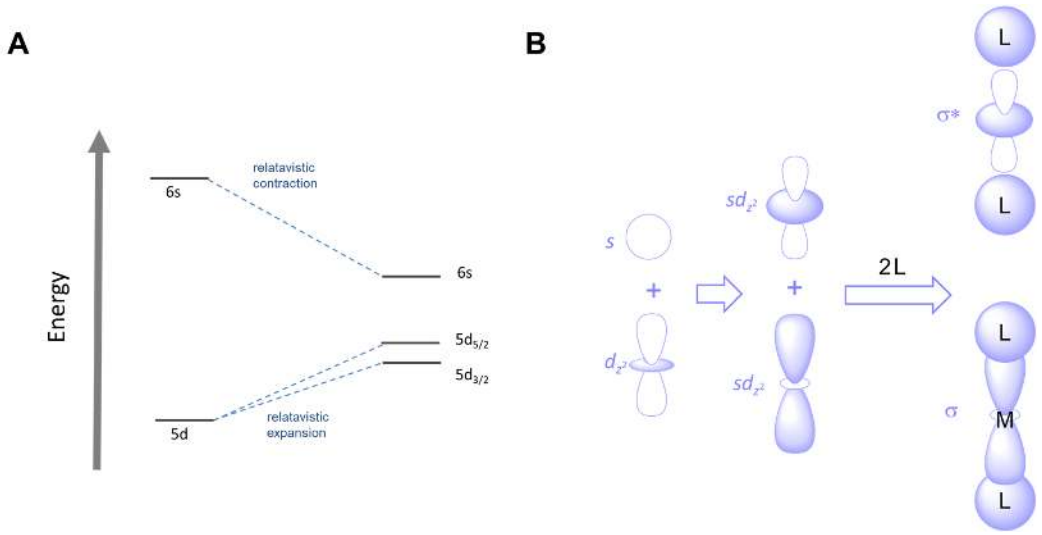


Figure **4.5.6**. (A) Gold experiences relativistic expansion and contraction of its 5*d* and 6*s* orbitals, resulting in shifts to their relative energies. (B) This makes mixing of these orbitals more favorable, facilitating the ability of gold to form two-coordinate complexes with strong sigma bonds that involve considerable sd_{z^2} character. This work by Stephen Contakes is licensed under a Creative Commons Attribution 4.0 International License.

4.5.2 What structures do coordination complexes form?

Metal complexes with coordination numbers ranging from one to 16 are known, although values greater than seven are rare for the transition metals. In this section, examples of common coordination geometries will be presented in order of coordination number.

4.5.2.1 Coordination Number 1.

Condensed phase monocoordinate complexes are unknown for the transition metals, although the post-transition metals Tl and In form monocoordinate complexes with the bulky ligands triazapentadienyl and 2,6-tris(2,4,6-triisopropylphenyl)benzene as shown in Figure **4.5.7**.

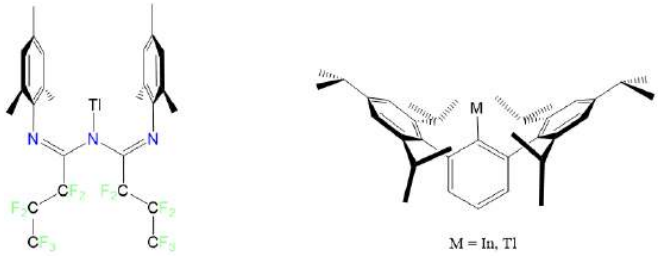
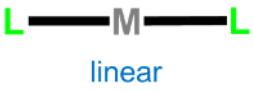


Figure **4.5.7**. No monocoordinate transition metal complexes are known, but Tl^{+} and In^{+} form monocoordinate complexes with extremely bulky ligands. This work by Stephen Contakes is licensed under a Creative Commons Attribution 4.0 International License.

4.5.2.2 Coordination Number 2.

A coordination number of 2 is rare outside of ***d*^{10} complexes of the group 11 metals and mercury**, specifically, Cu^+, Ag^+, Au^+, and Hg^{2+}. In accordance with the predictions of the Kepert model these give **linear complexes.**



Among these,

- Cu^+ more commonly gives tetrahedral complexes but can be coaxed to give linear ones. The most prominent example is $[CuCl_2]^-$, which forms when CuCl is treated with concentrated HCl under anerobic conditions.
- Ag^+ also commonly forms tetrahedral or trigonal planar complexes but can give linear ones. The most prominent example is $[Ag(NH_3)_2]^+$, which can be formed by treating silver slats with concentrated aqueous or liquid ammonia.
- Au^+ almost always forms linear complexes, but many of these formally two-coordinate complexes associate as depicted in Figure **4.5.8**. The ability of Au^+ to form linear complexes with cyanide is even used to selectively extract metallic gold from low grade ores. The stability of $[Au(CN)_2]^-$ means that the dissolution of metallic gold in aqueous cyanide is thermodynamically favorable under aerobic conditions.

$$4\ Au + 8\ CN^- + O_2 + 2\ H_2O \longrightarrow 4\ [Au(CN)_2]^- + 4\ OH^-$$

- Hg^{2+}, like Au^+, benefits from relativistic effects and more commonly forms two-coordinate complexes with a linear geometry. Among these is $[Hg(CN)_2]$. However, its preference for linearity is not as rigid as for Au^+, and so complexes with a variety of coordination geometries are known.

And by means of honorary mention, the mercury(I) ion, Hg_2^{2+}, forms linear complexes of the type L-Hg-Hg-L, although since Hg_2^{2+} is often considered as a single unit, these aren't always considered to be two-coordinate complexes.

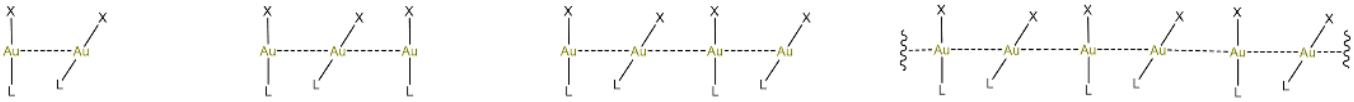
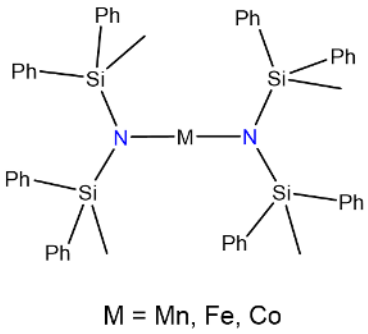


Figure **4.5.8**. Many "linear" gold complexes associate side-on to form dimers, trimers, tetramers, and chains. Although in this chapter L is usually taken to represent a generic ligand, in this scheme L represents a neutral ligand that donates two electrons to the metal (py, PR_3, CO, etc.) and X an anionic one (*e.g.*, Cl^-, CN^-, etc.). Exactly which structure forms depends on the identity of L and X. Redrawn from reference 5. This work by Stephen Contakes is licensed under a Creative Commons Attribution 4.0 International License.

Two-coordinate complexes may also be formed through the use of bulky ligands that only allow for the binding of two to the metal center. The classic examples are given in Figure **4.5.9**.

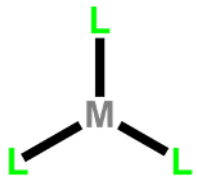


M = Mn, Fe, Co

Figure **4.5.9**. Two-coordinate complexes form between Mn^{2+}, Fe^{2+}, and Co^{2+} with $N(SiMePh_2)_2$.[6] This work by Stephen Contakes is licensed under a Creative Commons Attribution 4.0 International License.

4.5.2.3 Coordination Number 3

Three-coordinate complexes are similar to two-coordinate ones in that they are rare and, aside from the constraining influence of ligands, usually limited to d^{10} metal ions such as Cu^+ , Ag^+, Au^+, Hg^{2+}, and Pt(0). As expected from the Kepert model, in the absence of constraining ligands, three-coordinate complexes are trigonal planar.



Trigonal planar

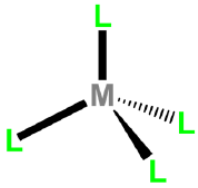
Figure **4.5.10**.



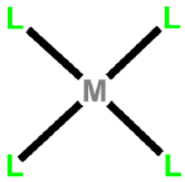
Figure **4.5.10**. Three-coordinate complexes prepared using bulky and semirigid ligands. This work by Stephen Contakes is licensed under a Creative Commons Attribution 4.0 International License.

4.5.2.4 Coordination Number 4

The two common four-coordinate geometries are tetrahedral and square planar.



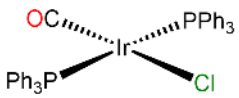
tetrahedral



Square planar

Tetrahedral complexes are commonly formed by metals possessing either a d^0 or d^{10} electron configuration. Monometallic examples of d^0 configurations include $TiCl_4$, VO_4^{3-}, WS_4^{2-}, MnO_4^-, CrO_4^{2-}, and OsO_4, while d^{10} examples are $[Ni(CO)_4]$, $[HgBr_4]^{2-}$, $[ZnCl_4]^{2-}$, and $[CdI_4]^{2-}$. For other electron configurations, tetrahedral complexes are known but much less common. Examples usually involve good donor ligands and include $[FeCl_4]^-$ (d^5), $[CoCl_4^{2-}]$ (d^6), and $[NiCl_4]^{2-}$ (d^7).

Second and third row transition metal centers with d^8 electron configurations like Rh^+, Ir^+, Pd^{2+}, Pt^{2+}, and Au^{3+} almost exclusively exhibit **square planar geometries**. Beyond this, square planar geometries are often formed by Ni^{2+} (d^8), Ni^{3+} (d^7), and Cu^{2+} (d^9). Examples of square planar complexes include $[Cu(acac)_2]$; $[PtCl_4]^{2-}$;Wilkinson's catalyst, $[RhCl(PPh_3)_3]$; and Vaska's complex, *trans*-$[Ir(CO)Cl(PPh_3)_2]$.



Vaska's Complex

4.5.2.5 Coordination Number 5

The two common coordination geometries for five-coordinate complexes are trigonal bipyramidal and square pyramidal.



Figure **4.5.11**.

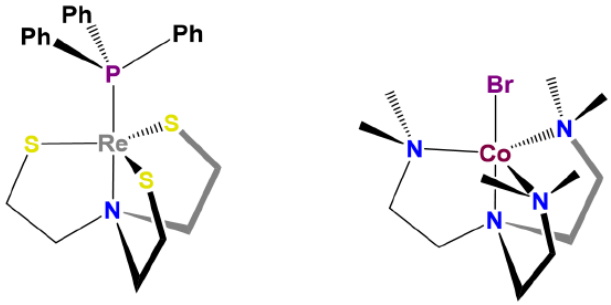


Figure **4.5.11**. Some tripodal ligands preference the formation of trigonal bipyramidal complexes. This work by Stephen Contakes is licensed under a Creative Commons Attribution 4.0 International License.

Homoleptic $[Ni(CN)_5]^{3-}$ possesses a square pyramidal structure, although the geometry is more common for macrocyclic complexes like the iron protoporphyrin of deoxymyoglobin shown in figure **4.5.4** and for complexes containing oxo and nitrido ligands, examples of which are shown in Figure **4.5.12**.

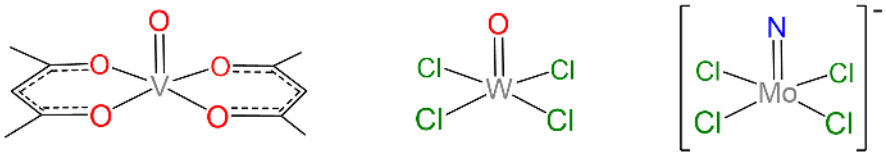


Figure **4.5.12**. Some square pyramidal oxo and nitrido complexes. This work by Stephen Contakes is licensed under a Creative Commons Attribution 4.0 International License.

In the absence of rigid constraining ligands, the relatively low energy difference between the trigonal bipyramidal and square pyramidal coordination geometries provides a mechanism for interconversion of the axial and equatorial ligands in a trigonal planar complex. For example, pentacarbonyliron(0) exhibits fluxionality involving a square pyramidal intermediate via a Berry pseudorotation mechanism, as shown in Figure **4.5.13**.

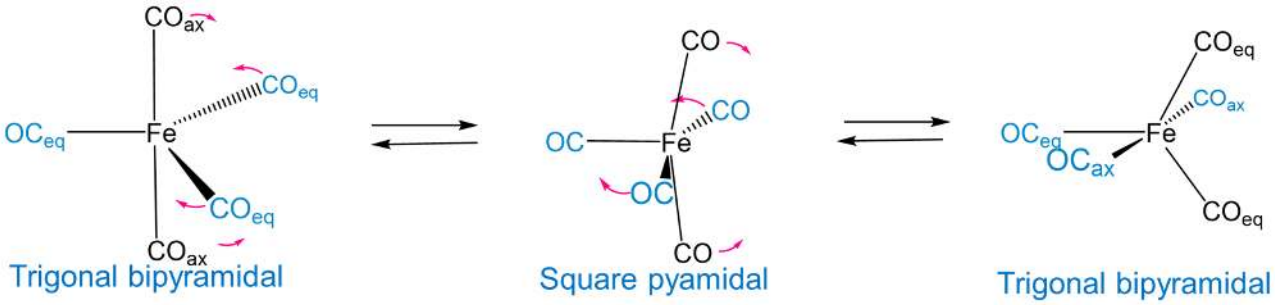


Figure **4.5.13**. Fluxionality in pentacarbonyliron(0) involves exchange of axial and equatorial carbonyl ligands via Berry pseudorotation. Interconversion of the axial and equatorial carbonyl groups occurs faster than the NMR timescale at room temperature. As a result the ^{13}C NMR spectrum of $Fe(CO)_5$ exhibits a single signal rather than two separate signals for the axial and equatorial carbonyl carbons. This work by Stephen Contakes is licensed under a Creative Commons Attribution 4.0 International License.

4.5.2.6 Coordination Number 6

The two common coordination geometries for coordination number 8 are octahedral and trigonal prismatic.

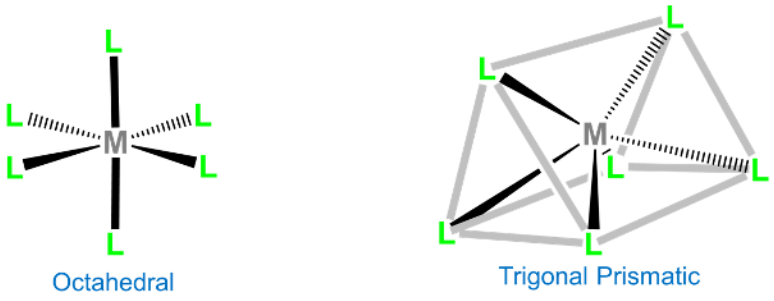


Figure **4.5.14**.

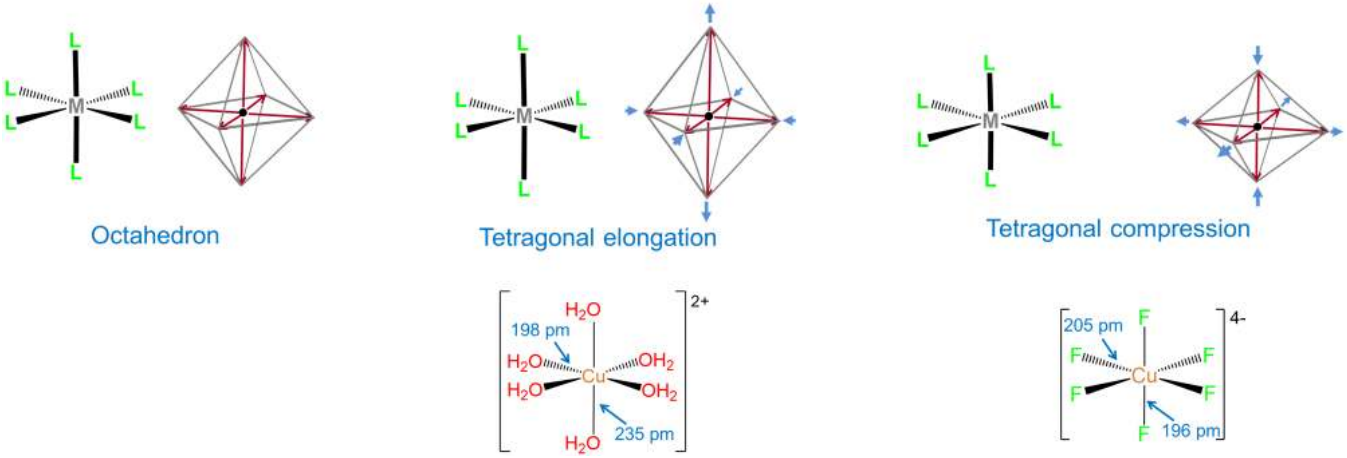


Figure **4.5.14**. Tetragonal distortions commonly occur for d^4, d^7 , and d^9 octahedral complexes. The most common type involves axial elongation in which the octahedron is stretched along a single *trans*-L-M-L axis, but axial compressions in which the octahedron is compressed along such an axis instead are sometimes observed. An example of an axial elongated complex is $[Cu(H_2O)_6]^{2+}$ in solution, while $[CuF_6]^{4-}$ is axially compressed when doped into a Ba_2ZrF_6 lattice (it is elongated when doped into a -----. Bond distances are taken from references 7 and 8. This work by Stephen Contakes is licensed under a Creative Commons Attribution 4.0 International License.

Trigonal prismatic coordination is related to octahedral coordination as shown in Figure **4.5.15**. As may be seen in Figure **4.5.15**, an octahedral coordination sphere is just a trigonal antiprism in which all edge lengths are identical. Rotation of one triangular face relative to its opposite until the two are eclipsed gives a trigonal prismatic geometry. In fact, since continuation of this rotation gives another octahedral complex, the trigonal prismatic geometry is an intermediate in isomerization reactions involving octahedral complexes.

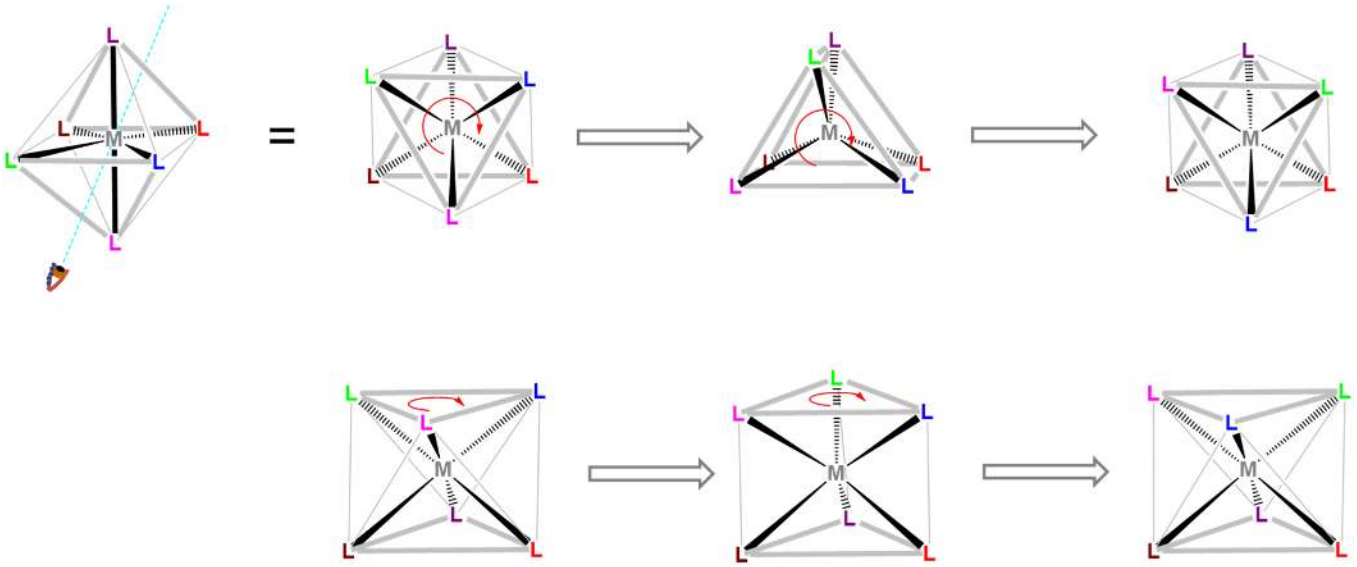


Figure 4.5.15. Since an octahedron is a trigonal antiprism, a trigonal prism may be produced by rotating or "twisting" one face of the octahedron relative to its opposite. Since continuation of the rotation gives an isomer of the original octahedron, when the energy landscape for twists like these is thermally or photochemically accessible, such twists provide one pathway for isomerization reactions involving octahedral complexes. In tris- and bis-chelates, such isomerizations are said to occur by Bailar and Ray-Dutt twists, which differ only in the relationship between the chelate rings and the faces twisted. Top: View looking down an axis bisecting a pair of opposing faces. Bottom: View perpendicular to that shown at top. This work by Stephen Contakes is licensed under a Creative Commons Attribution 4.0 International License.

In contrast to octahedral coordination geometries, trigonal prismatic coordination (and distorted versions thereof) are rare and occur mostly for d^0, d^1, and d^2 configurations. Examples of trigonal prismatic metal centers include the d^2 Mo^{4+} centers in MoS_2, d^1 $[Re(S_2C_2Ph_2)_3]^-$, and d^0 $[Ta(CH_3)_6]^-$, of which the latter two structures are given in Figure 4.5.16. Semirigid ligands like that shown in Figure 4.5.4C may be used to encourage the adoption of a trigonal prismatic geometry, although once the number of *d* electrons present exceeds two, the preference for octahedral coordination is too great for a trigonal prismatic geometry to occur.

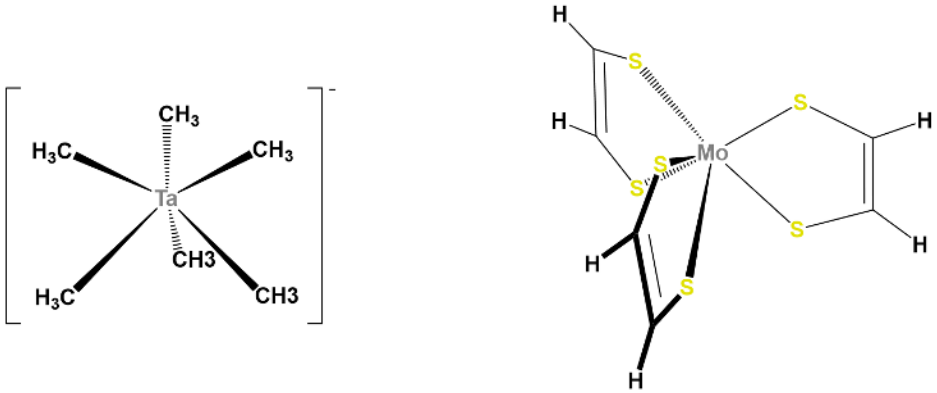
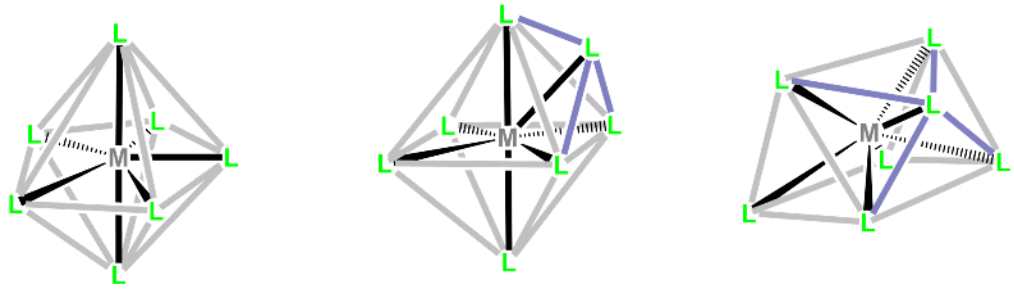


Figure 4.5.16. The complexes $[Ta(CH_3)_6]^-$ and $[Mo(S_2C_2H_2)_3]$ adopt a trigonal prismatic geometry. Trigonal prismatic coordination is common for d^0 and d^1 complexes with alkyl and dithiolene ligands. It is also typical for the dithiolene ligands to coordinate along the rectangular edges of the trigonal prism instead of the triangular ones. This work by Stephen Contakes is licensed under a Creative Commons Attribution 4.0 International License.

4.5.2.7 Coordination Number 7

Seven-coordinate complexes are rare outside of the relatively large early transition metals, lanthanides, and actinides. The three common seven-coordinate geometries are pentagonal bipyramidal, monocapped octahedral, and monocapped trigonal prismatic. The latter two are often called capped octahedral and capped trigonal prismatic, with the mono- prefix being understood.



Although intraligand repulsions are smaller in the pentagonal bipyramidal coordination geometry than the capped octahedral and capped trigonal prismatic geometries, the difference is small, and the three structures are often close in energy. As a result the structure observed is often dependent on ligand-based constraints, crystal packing, and solvent effects that preference one geometry over the others.

Heptacyano complexes are often pentagonal bipyramidal. Examples include $[Mo(CN)_7]^{3-}$, $[W(CN)_7]^{3-}$, and $[Os(CN)_7]^{3-}$. Seven-coordinate complexes containing oxo ligands commonly are pentagonal bipyramidal with the oxo ligand(s) in the less sterically hindered axial position. Examples include $[NbOF_6]^{3-}$ and, for the inner transition metals, $[UO_2F_5]^{3-}$. Ligands that have been used to promote formation of seven-coordinate species include 15-crown-5 and 2,2':6',2":6",2"'-quaterpyridine. Representative complexes are given in Figure **4.5.17**.

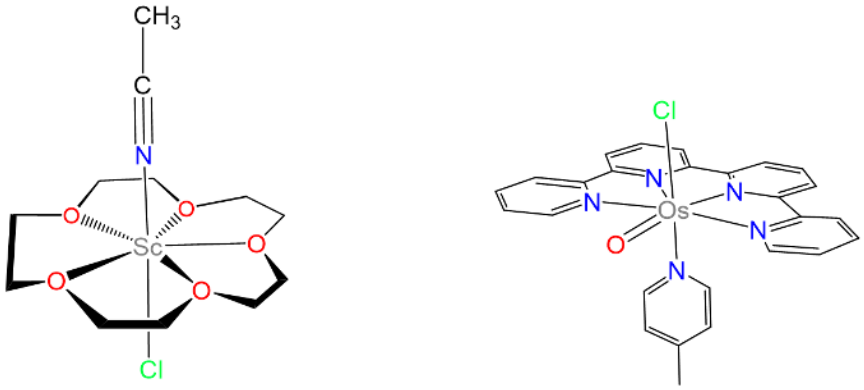


Figure **4.5.17**. Seven-coordinate complexes containing ligands that encourage the formation of seven-coordinate geometries. Note that while in $[NbOF_6]^{3-}$ and $[UO_2F_5]^{3-}$ the oxo ligands occupy axial positions, the Osmium complex shown possesses an oxo ligand in an equatorial position. This is likely because the parent octahedral complex, in which the oxo ligand is not present, possesses an expanded outer N-Os-N angle of 121.655° that opens to 154.161° to accommodate the oxo group. Drawn based on the structures reported in references 9 and 10. This work by Stephen Contakes is licensed under a Creative Commons Attribution 4.0 International License.

Capped trigonal prismatic geometries are common for complexes of the early transition metals. Examples include $[NbF_7]^{2-}$, $[TaF_7]^{2-}$, and $[ZrF_7]^{3-}$ in $(NH_4)_3[ZrF_7]$.

Capped octahedral geometries are found in $[MoMe_7]^-$, $[WMe_7]^-$, and $[WBr_3(CO)_4]$, which contains three pairs of *trans*-Br and CO with the final CO capping the octahedron's $(CO)_3$ face, as shown in Figure **4.5.18**.

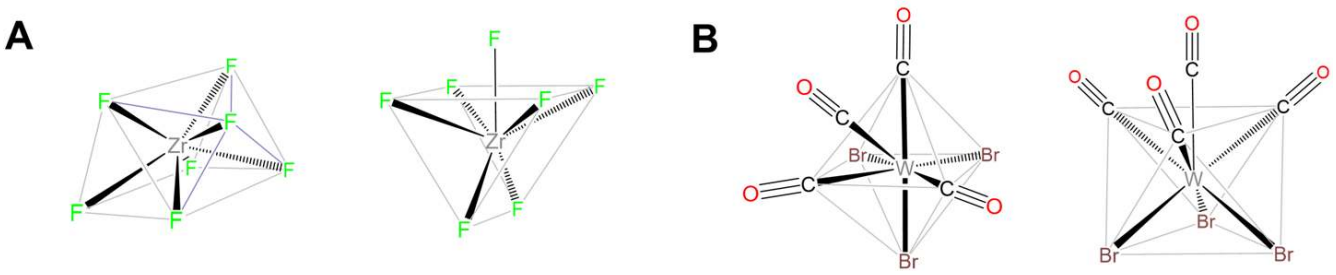


Figure **4.5.18**. Examples of complexes that adopt monocapped triconal prismatic and monocapped octahedral geometries.(A) Two views of the structure of (A) capped trigonalprismatic $[ZrF_7]^{3-}$ and (B) capped octahedral $[WBr_3(CO)_4]$. This work by Stephen Contakes is licensed under a Creative Commons Attribution 4.0 International License.

In seven- and higher-coordinate complexes, ligand and crystal packing effects frequently give distorted coordination geometries. These geometries are intermediate between two or more of the idealized seven coordinate geometries, making it difficult to tell exactly which structure they are a distortion of (Figure **4.5.19**).

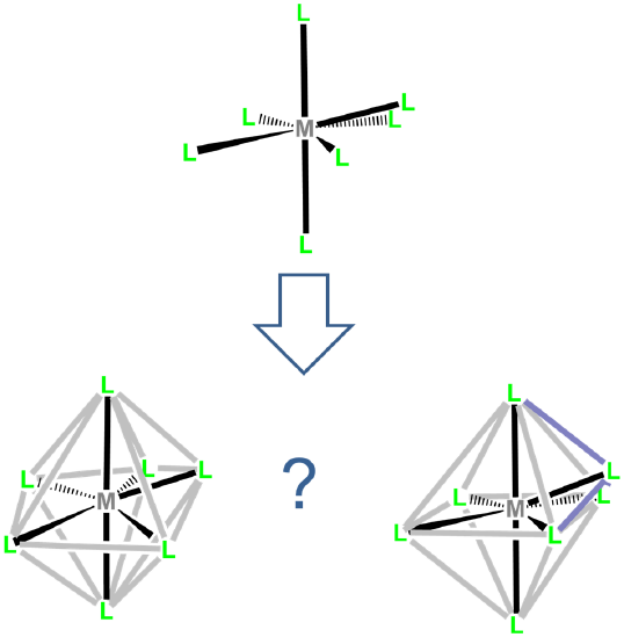


Figure **4.5.19**. Many seven-coordinate structures are distorted and can be difficult to classify. For example, how should the geometry of this complex be described - as distorted trigonal bipyramidal or distorted monocapped octahedral? This work by Stephen Contakes is licensed under a Creative Commons Attribution 4.0 International License.

4.5.2.8 Coordination Number 8

Eight-coordinate complexes are rare and occurs in discrete molecules and ions only for the relatively large early transition metals, lanthanides, and actinides. The three common eight-coordinate geometries are square antiprismatic, dodecahedral, and bicapped trigonal prismatic. In contrast, the cubic coordination geometry is only found in ionic lattices like that of CsCl and in complexes of the inner transition metals such as $Na_3[UF_8]$.

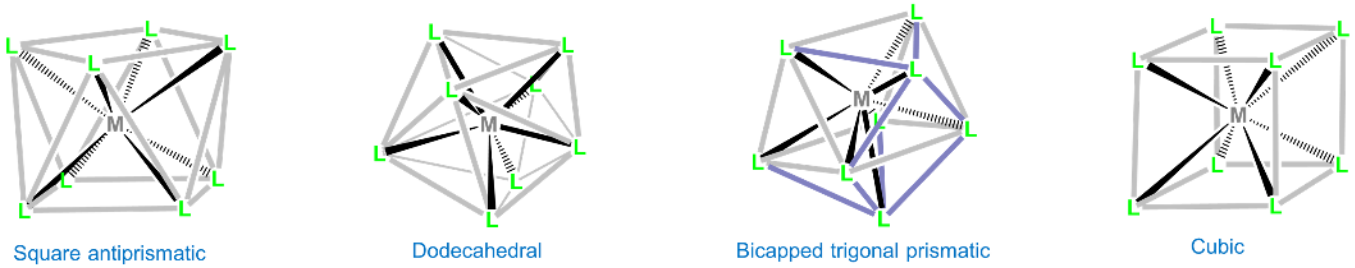


Figure **4.5.20**. The square antiprism may be made by twisting one face of a cube relative to another, and the dodecahedron by folding opposing faces towards one another.

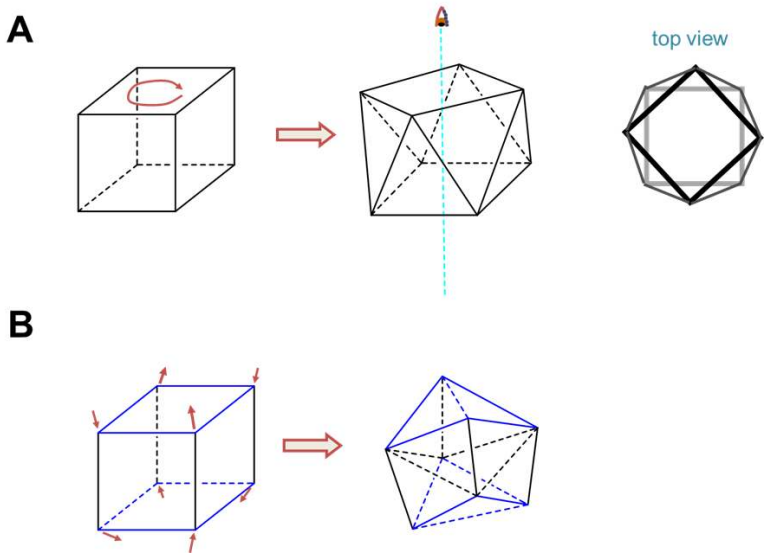


Figure **4.5.20**. The (A) square antiprismatic and (B) dodecahedral coordination geometries are distorted cubic geometries. (A) The square antiprismatic coordination geometry is just a cubic coordination geometry in which one face has been rotated 45° relative to its opposite (and for which the distance between those faces need not be equal to the distance between adjacent atoms within a face) (B) The dodecahedral geometry may be thought of as a cube in which opposing faces are folded up and down relative to one another as shown. This work by Stephen Contakes is licensed under a Creative Commons Attribution 4.0 International License.

As with other high-coordinate structures, the energy difference between these eightfold coordination geometries is small enough that packing effects can significantly influence the observed structure. For example, octacyanomolybdates commonly adopt a square antiprismatic coordination geometry but depending on the counterions present can give dodecahedral or bicapped trigonal prismatic complexes. Examples are given in Figure **4.5.21**.

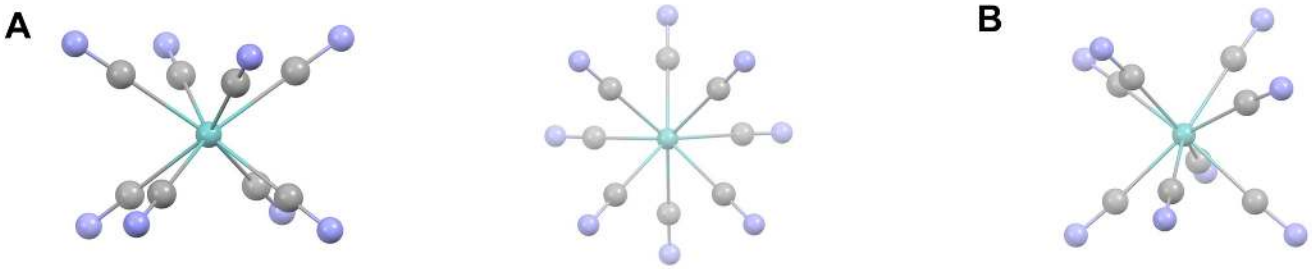


Figure **4.5.21**: Structures reported for (A) square antiprismatic $[Mo(CN)_8]^{3-}$ as a solid 4,4'-Diazenediyldipyridinium salt and (B) dodecahedral $[Mo(CN)_8]^{4-}$ as a solid tetra-n-butylammonium salt.

4.5.2.9 Coordination Number 9

Again, nine-coordinate complexes typically require larger transition metals, lanthanides, and actinides. Coordination geometries are typically either tricapped trigonal prismatic or idiosyncratically determined by the ligands. Simple examples include the aqua complexes $[Sc(H_2O)_9]^{3+}$, $[Y(H_2O)_9]^{3+}$, and $[La(H_2O)_9]^{3+}$, as well as $[TcH_9]^{2-}$ and $[ReH_9]^{2-}$.

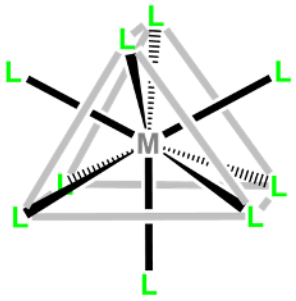


Figure **4.5.22**.

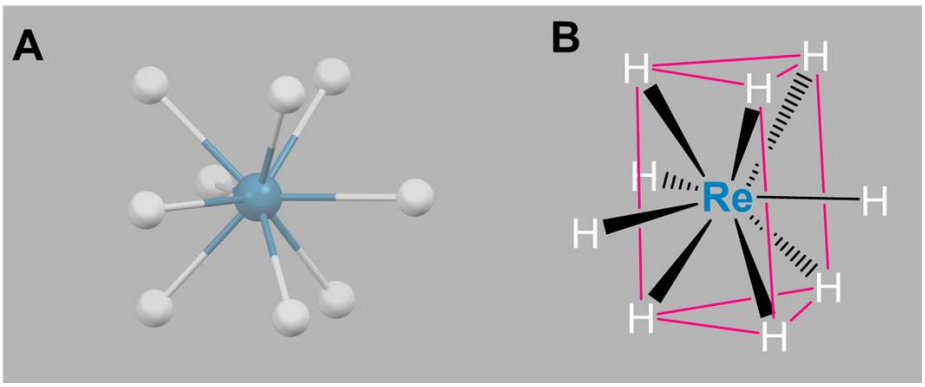


Figure **4.5.22**. (A) Structure of $[ReH_9]^{2-}$ in $K_2[ReH_9]$ and (B) schematic showing how the structure maps onto a tricapped trigonal pyramidal coordination geometry. This work by Stephen Contakes is licensed under a Creative Commons Attribution 4.0 International License.

4.5.2.10 Coordination Numbers 10-16

Coordination numbers higher than nine are extremely rare for compounds that bind in κ fashion (form conventional metal-ligand bonds)[14] and usually involve some combination of large metals, sterically undemanding ligands, and special ligand structures that promote higher coordination. Noteworthy examples include

1. Twelve-coordinate $[Hf(BH_4)_4]$, which illustrates how small multidentate ligands promote higher coordination numbers. As shown in Figure **4.5.23**, $[Hf(BH_4)_4]$ has a cubooctahedral structure in which BH_4^- acts as a tridentate ligand, with BH_3 units occupying triangular faces of the cubooctahedron to give a tetrahedron of BH_4^- ligands around the Hf.

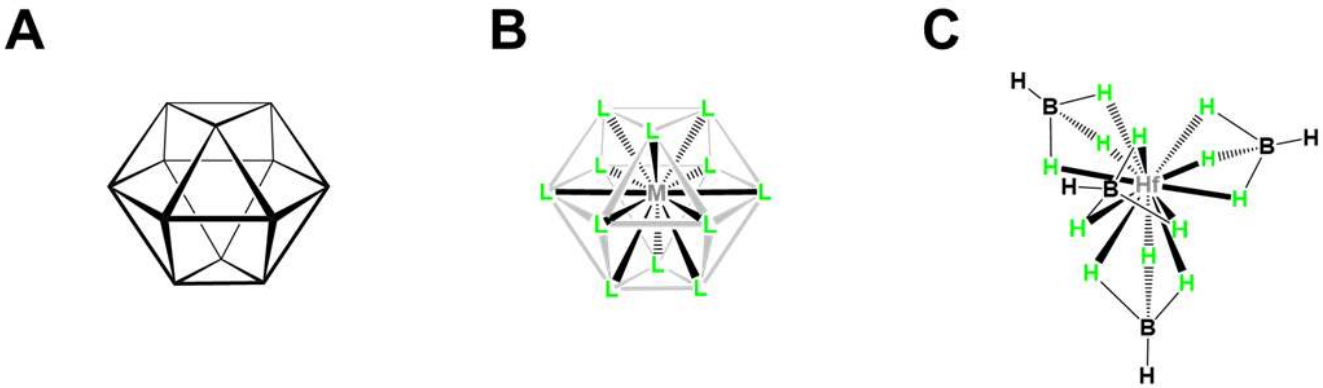


Figure **4.5.23**. The anticubooctahedral coordination geometry is observed for $[Hf(BH_4)_4]$. (A) An anticubooctahedron consists of a hexagonal ring capped with antiparallel triangles above and below the ring. (B) Idealized anticubooctahedral complex. (C) Structure of $[Hf(BH_4)_4]$. This work by Stephen Contakes is licensed under a Creative Commons Attribution 4.0 International License.

2. Twelve-coordinate $[Ce(NO_3)_6]^{2-}$, in which the nitrate oxygens define an icosahedral coordination geometry as shown in Figure **4.5.24**. The nitrates in the structure bind the Ce center in bidentate fashion in an octahedral array.

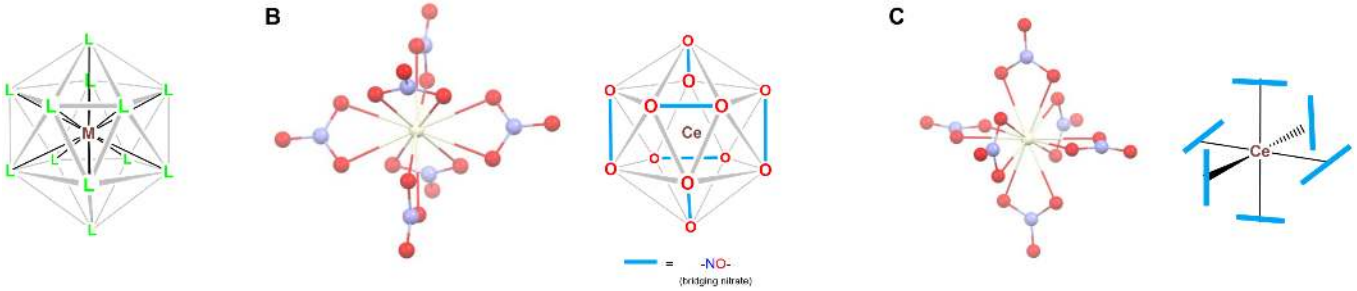


Figure **4.5.24**. Coordination geometry of $[Ce(NO_3)_6]^{2-}$ in $[Mg(H_2O)_6][Ce(NO_3)_6]\cdot H_2O$. (A) Idealized icosahedral coordination. (B) View of the structure of $[Ce(NO_3)_6]^{2-}$ showing how it maps onto the icosahedral coordination geometry. (C) The structure may also be thought of as comprising an octahedral geometry in which each vertex of the octahedron is occupied by a κ^2-NO_3^-. The structure of $[Ce(NO_3)_6]^{2-}$ is rendered in Mercury from the cif data in reference 15. This work by Stephen Contakes is licensed under a Creative Commons Attribution 4.0 International License.

3. Fifteen-coordinate $[Th(H_3BNMe_2BH_3)_4]$, which also uses bridging H-B-H units that occupy little of the coordination sphere. In $[Th(H_3BNMe_2BH_3)_4]$, three of the four $H_3BNMe_2BH_3$ ligands bind in κ^4 fashion and one binds κ^3, giving the fifteen fold coordination.[16]

4. Sixteen-coordinate $[CoB_{16}]^-$, which possesses the highest coordination number yet observed. Its structure is given in Figure **4.5.25**. The coordination geometry is an octahedral antiprism, and the complex should be considered to involve a Co center in the midst of a B_{16}^- "molecular drum" held together by cluster bonds.

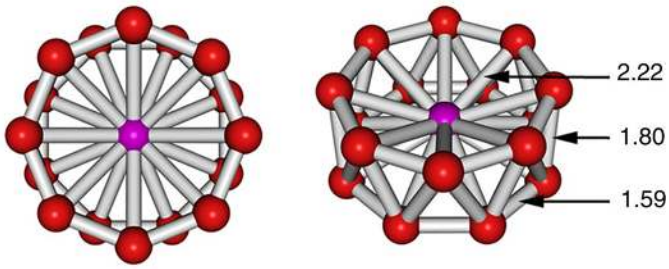


Figure 2A from Popov, I., Jian, T., Lopez, G. *et al.* Cobalt-centered boron molecular drums with the highest coordination number in the CoB_{16}^- cluster. *Nat Commun* **6,** 8654 (2015). https://doi.org/10.1038/ncomms9654, which is is licensed in that publication under a Creative Commons Attribution 4.0 International License.

4.5.3 References

1. Dudev, M.; Wang, J.; Dudev, T.; Lim, C., Factors Governing the Metal Coordination Number in Metal Complexes from Cambridge Structural Database Analyses. *The Journal of Physical Chemistry B* **2006**, *110(4)*, 1889-1895.
2. Kuppuraj, G.; Dudev, M.; Lim, C., Factors Governing Metal−Ligand Distances and Coordination Geometries of Metal Complexes. *The Journal of Physical Chemistry B* 2009, 113 (9), 2952-2960.
3. Cremades, E.; Echeverría, J.; Alvarez, S., The Trigonal Prism in Coordination Chemistry. *Chemistry – A European Journal* 2010, 16 (34), 10380-10396.
4. Xiong, X.-G.; Wang, Y.-L.; Xu, C.-Q.; Qiu, Y.-H.; Wang, L.-S.; Li, J., On the gold–ligand covalency in linear $[AuX_2]^-$ complexes. *Dalton Transactions* 2015, 44 (12), 5535-5546.
5. Concepción Gimeno, M. The Chemistry of Gold in Laguna, Antonio (ed.) *Modern Supramolecular Gold Chemistry: Gold-Metal Interactions and Applications*. Wiley, 2008.
6. Andersen, R. A.; Faegri, K.; Green, J. C.; Haaland, A.; Lappert, M. F.; Leung, W. P.; Rypdal, K., Synthesis of bis[bis(trimethylsilyl)amido]iron(II). Structure and bonding in M[N(SiMe3)2]2 (M = manganese, iron, cobalt): two-coordinate transition-metal amides. *Inorganic Chemistry* 1988, 27 (10), 1782-1786.
7. Persson, I., Hydrated metal ions in aqueous solution: How regular are their structures? Pure and Applied Chemistry 2010, 82*(10)*, 1901.

8. Aramburu, J. A.; García-Fernández, P.; García-Lastra, J. M.; Moreno, M., Jahn–Teller and Non-Jahn–Teller Systems Involving CuF_6^{4-} Units: Role of the Internal Electric Field in Ba2ZnF6:Cu2+ and Other Insulating Systems. *The Journal of Physical Chemistry C* 2017, *121(9)*, 5215-5224.
9. Brown, M. D.; Levason, W.; Murray, D. C.; Popham, M. C.; Reid, G.; Webster, M., Primary and secondary coordination of crown ethers to scandium(iii). Synthesis, properties and structures of the reaction products of ScCl3(thf)3, ScCl3·6H2O and Sc(NO3)3·5H2O with crown ethers. Dalton Transactions 2003, (5), 857-865.
10. Liu, Y.; Ng, S.-M.; Lam, W. W. Y.; Yiu, S.-M.; Lau, T.-C., A Highly Reactive Seven-Coordinate Osmium(V) Oxo Complex: [OsV(O)(qpy)(pic)Cl]2+. Angewandte Chemie International Edition 2016, 55 (1), 288-291.
11. Popov, I., Jian, T., Lopez, G. *et al.* Cobalt-centred boron molecular drums with the highest coordination number in the CoB_{16}^- cluster. *Nat Commun* **6,** 8654 (2015). https://doi.org/10.1038/ncomms9654
12. The structures are rendered from cif data reported in the following publications: (A) square antiprismatic $[Mo(CN)_8]^{3-}$: Wen-Yan Liu, Hu Zhou, Ai-Hua Yuan, *Acta Crystallographica Section E: Structure Reports Online*, 2008, 64, m1151, (B) dodecahedral $[Mo(CN)_8]^{4-}$: B.J.Corden, J.A.Cunningham, R.Eisenberg, *Inorganic Chemistry*, 1970, 9, 356.
13. The structure of ReH_9^{2-} is rendered from the structure reported in Abrahams, S.C.; Ginsberg, A.P.; Knox, K. Transition metal-hydrogen compounds. II. The crystal and molecular structure of potassium rhenium hydride, K_2ReH_9 *Inorganic Chemistry*, **1964**, *3*, 558-567.
14. There are other complexes in which a metal may be said to interact with more than sixteen "ligand atoms", but these are not usually considered to possess a higher coordination number. For example, in some π complexes like η^5-Cp_4U, technically there are 20 C atoms fastened to the U, but these complexes are better considered as 12-coordinate than twenty (since each cyclopentadienyl ring is isolobal with a *fac*-coordinated set of 3 L ligands), while the metal centers in endohedral fullerene species like $La@C_{60}$ do not interact with all sixty carbon atoms at once, and so are better thought of as a metal trapped in a spacious sixty-carbon cage.
15. Zalkin, A.; Forrester, J.D.; Templeton, D.H. Crystal structure of cerium magnesium nitrate hydrate *Journal of Chemical Physics*, **1963**, *39*, 2881-2891.
16. Daly, S. R.; Piccoli, P. M. B.; Schultz, A. J.; Todorova, T. K.; Gagliardi, L.; Girolami, G. S., Synthesis and Properties of a Fifteen-Coordinate Complex: The Thorium Aminodiboranate [Th(H3BNMe2BH3)4]. Angewandte Chemie International Edition 2010, 49 (19), 3379-3381.
17. Popov, I., Jian, T., Lopez, G., Boldyrev, A. I.; Wang, L-S. Cobalt-centred boron molecular drums with the highest coordination number in the CoB_{16}^- cluster. *Nat Commun* **6,** 8654 (2015).

4.5: Coordination Numbers and Structures is shared under a CC BY 4.0 license and was authored, remixed, and/or curated by Stephen M. Contakes.

- **9.5: Coordination Numbers and Structures** by Stephen M. Contakes is licensed CC BY 4.0.

4.6: Coordination Frameworks

Bridging ligands link metals in multicenter coordination complexes

Some ambidentate and multidentate ligands have the capacity to bridge two metal centers. For instance, the cyano ligands can bridge two metal centers by forming linear links of the type

$$M{-}CN{-}M'$$

Linkages like these can be used to bridge multiple metal centers in a cluster or network solid, the latter of which is sometimes called a coordination framework. When the cyano ligand is combined with octahedral metal centers possessing 90° L-M-L bond angles, a cubic coordination network results. An example is the Prussian Blue coordination framework, which possesses the unit cell depicted in Figure **4.6.1A**.

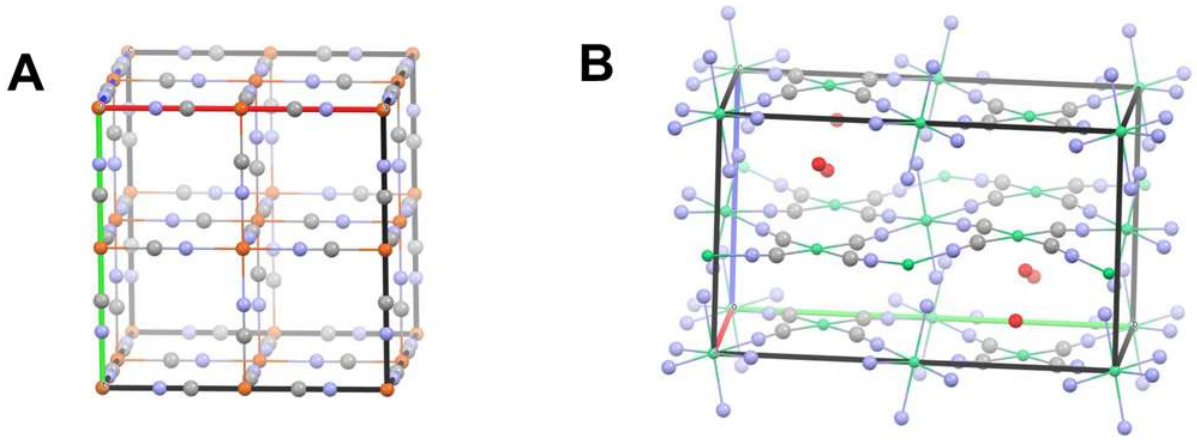


Figure **4.6.1**. (A) Idealized unit cell of Prussian Blue showing the cubic coordination framework of interconnected $[Fe^{II}(CN)_6]^{4-}$ and Fe^{3+} units. Because the ratio of Fe^{3+} to $[Fe^{II}(CN)_6]^{4-}$ is 4:3, some of the $[Fe^{II}(CN)_6]^{4-}$ sites are occupied by aqua ligands. (B) Structure of a Hofmann-type clathrate consisting of layers of square planar $[Ni(CN)_4]^{2-}$ units linked by $Ni(NH_3)_2^{2+}$ units. In this structure water occupies the sites between the layers, but structures like these can adjust to accommodate a variety of organic molecules. Hydrogen atoms are omitted for clarity. Rendered from the structures reported in references 1. This work by Stephen Contakes is licensed under a Creative Commons Attribution 4.0 International License.

The cubic network shown in Figure **4.6.1A** reflects the 3D structure of the octahedron, in which the M-L bonds point along the x, y, and z axes. If a square planar metal center is used, a 2D coordination network comprising interlinked squares is produced instead. An example is the Hofmann clathrate shown in Figure **4.6.1B**, which depicts a Hofmann clathrate in which square planar $[Ni(CN)_4]^{2-}$ units are linked by *trans*-$Ni(NH_3)_2^{2+}$ units (which are octahedral but have a square plane of open coordination sites perpendicular to the NH_3-Ni-NH_3 axis).

The structures of coordination polyhedra and frameworks reflect ligand and metal coordination geometries

As illustrated by the Prussian Blue and Hofmann clathrate coordination networks shown in Figure **4.6.1**, the structures formed when a bridging ligand links multiple metal centers depends on the geometry of the centers, the ligand, and the metal-ligand bonds formed. Because the directionality of metal-ligand bonding in many types of complexes is well-characterized and predictable, it is possible to design metal complexes and linkers that can serve as building blocks for clusters and networks. In particular

- metal complexes with combinations of labile (substitutable) ligands in particular topologies. These insure that the linking ligand will be arranged around the metal center in those defined directions.
- Ligands that possess binding sites oriented in defined directions so that they link the metal centers together in particular topologies.

Examples of the sort of metal centers that can be used and examples of linking ligands are given in Figure **4.6.2**.

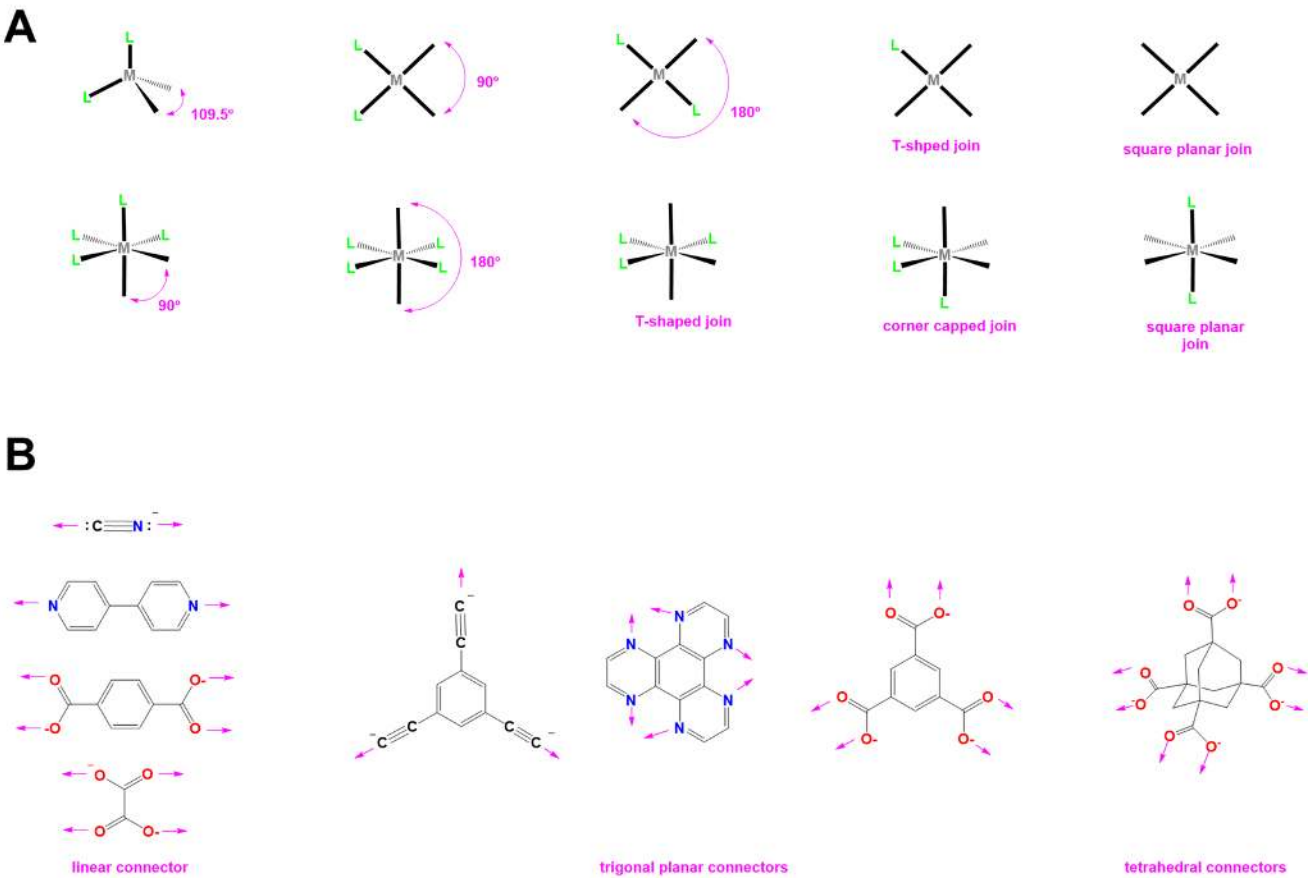


Figure **4.6.2**. The directionality of M-L bonding permits the rational construction of structures using metal and ligand "building blocks". For example, (A) Tetrahedral, octahedral, and square planar metal centers alone can be used to connect sets of ligands at 90°, 109.5°, and 180° bond angles in a variety of arrangements while (B) the selection of organic linkers shown can be used as linear, trigonal planar, and tetrahedral linkers.

Examples of how the building blocks shown in Figure **4.6.2** might be used to prepare molecular polyhedra and coordination networks are depicted schematically as shown in Figure **4.6.3**. Among the examples shown in Figure **4.6.3**, those depicted on the right schematize the Hofmann clathrate (top) and Prussian Blue (bottom) coordination networks of Figure **4.6.1**.

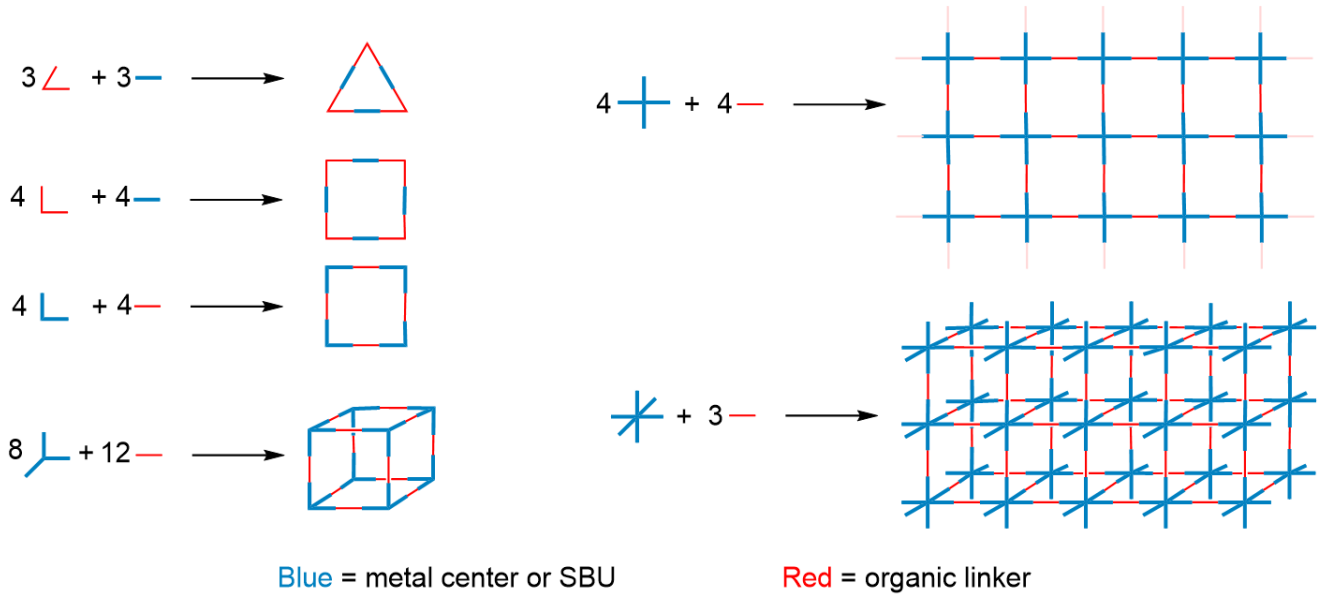


Figure **4.6.3**. Examples illustrating how the combination of metal and organic linker units gives rise to polyhedral and network structures that reflect the geometry of the building blocks used.

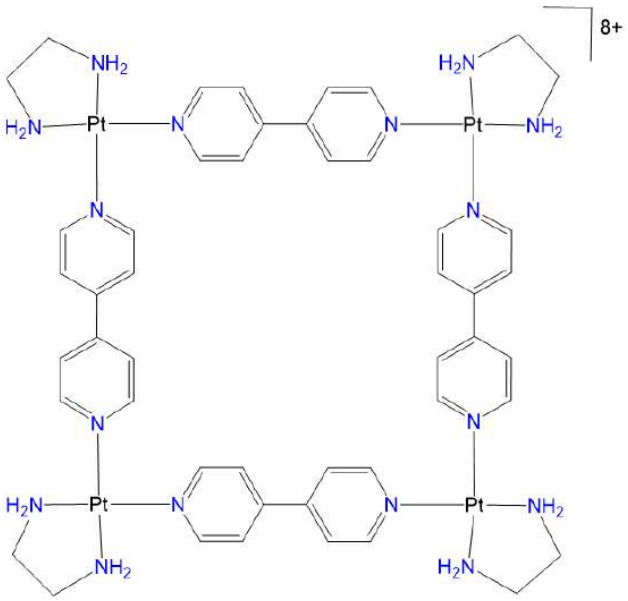


Figure **4.6.4**. In its structure, the $Pt(en)^{2+}$ centers possess *cis*-90° coordination sites linked by the linear linker 4,4'-bipyridine.

A wider variety of structures are possible than those hinted at by the building blocks and structures shown in Figures **4.6.2** and **4.6.3**. More may be obtained using the principles of molecular structure outlined in the sections on coordination geometry, ligands, and isomerism. In fact, one of the first coordination polyhedra prepared involved Jean-Marie Lehn's recognition that planar bidentate ligands in a tetrahedral bis-chelate are oriented perpendicular to one another, as shown in Figures **4.6.5A**. This enabled him to prepare a molecular trigonal prism by combining a source of Cu^{2+} with the trigonal planar and linear-capable organic linkers that bind the Cu^{2+} in bidentate fashion, as shown in Figure **4.6.5B**.

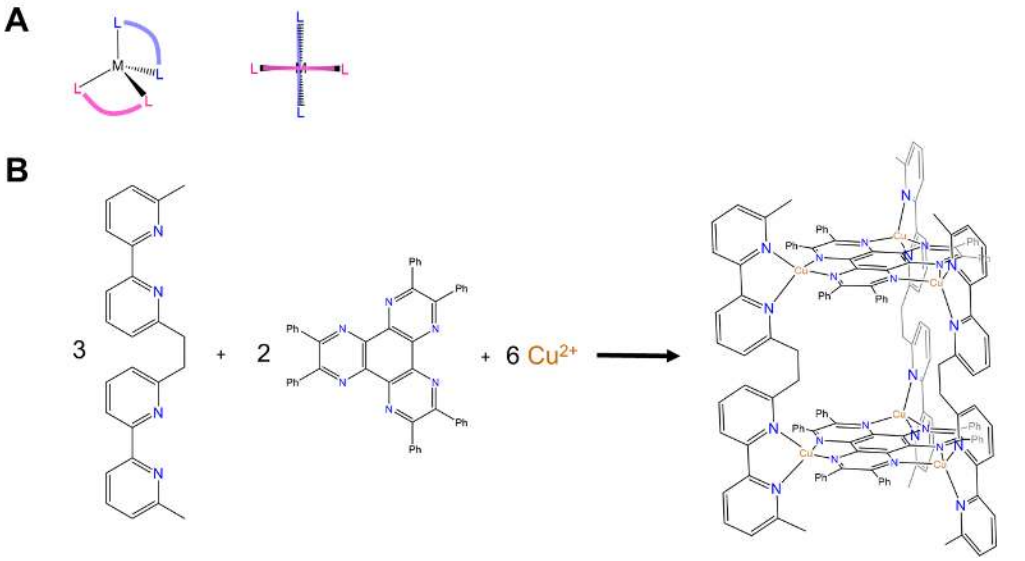


Figure **4.6.5**. (A) When a tetrahedral metal center is coordinated by two planar bidentate ligands, the ligands are oriented at 90° to one another. (B) This permitted Jean Marie-Lehn and his cowokers to prepare a molecular trigonal prism consisting of six Cu^{2+} ions linked by the rigid and semirigid nitrogen-containing ligands on the prism's trigonal faces and rectangular edges as shown. Redrawn from structures given in reference 3.

Metal Organic Frameworks (MOFs) are porous coordination polymers in which metal "building units" are connected by rigid organic ligand "struts"

One class of coordination frameworks that has received much attention over the past 25 years is the metal organic frameworks (MOFs). These consist of metal centers linked by rigid organic ligands to give a porous structure similar to those of the aluminosilicate-based zeolites. The structure of one MOF, called MIL-53, is given in Figure **4.6.6A**.

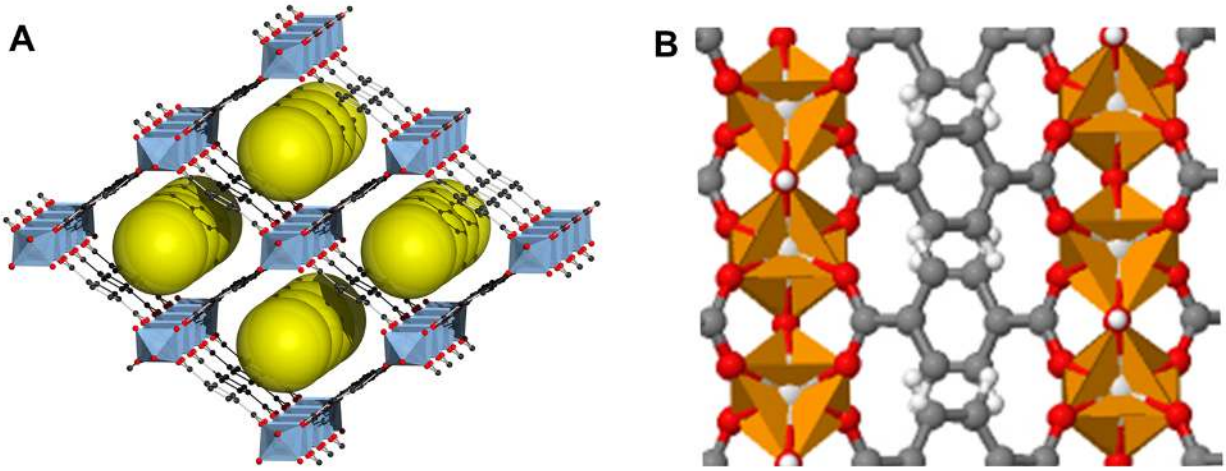


Figure **4.6.6**. In metal organic frameworks containing carboxylate ligands, the two oxygens in each carboxylate usually bind to different metal centers. A simple example involves the structure of MIL-53, in which linear *p*-terephthalato (1,4'-benzenedicarboxylato or BDC) ligands bridge chains of linked MO_6 octahedra. (A) Structure of MIL-53 showing the open structure of the MOF, indicated by the yellow spheres. (B) Top-down image of an MIL-53 structure showing how the carboxylic acid oxygens in the BDC ligands coordinate two different metals. The image in part A is by Tony Boehle - Tony Boehle, Public Domain, https://commons.wikimedia.org/w/inde...curid=10328580 The image in part B is rendered from the jmol structure of MIL-53(Sc) at https://www.chemtube3d.com/mof-mil53sc-2/

As can be seen from the overall structure of MIL-53 depicted in Figure **4.6.6A**, the structure possesses large rhombic prismatic voids, represented by the yellow spheres. These voids can in principle be occupied by small molecule substrates. Because of MOF's potential to bind and store substrates, there is considerable interest in developing MOFs that are useful for storing and separating particular gases.

A closer look at the structure of MIL-53 reveals that the carboxylate oxygens in the benzenedicarboxylato (BDU) linkers span two different metal centers rather than binding to only one. As explained in Figure **4.6.7**, this binding mode enables the formation of rigid stable networks, although it requires the use of metal building blocks in which two or more metal centers are held in close proximity.

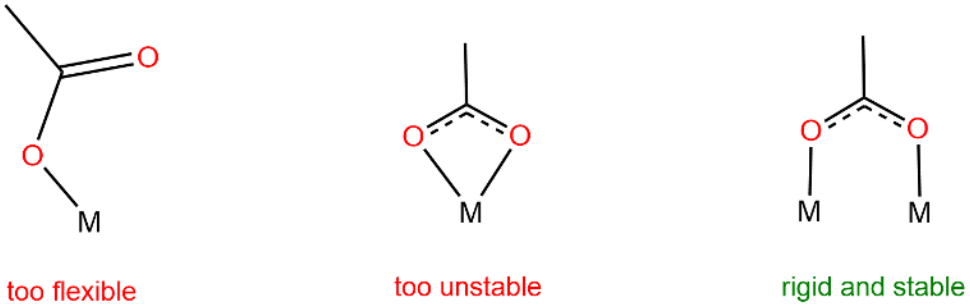


Figure **4.6.7**. The carboxylate groups in the ligands of metal organic frameworks commonly bind κ^1 to two different metal centers rather than κ^1 or κ^2 to a single center because the single metal κ^1 binding mode is too flexible to give rigid networks while the small chelate rings and narrow bite angles of the κ^2 chelate rings make them less stable.

In MIL-53, the metal centers that the DBU ligands coordinate are chains of octahedral metal centers bridged by μ_2 hydroxo ligands. These chains form spontaneously as the network forms under the high temperature conditions of its synthesis. In other cases, metal secondary building units (SBUs) containing the necessary bridging dicarboxylate ligands are used. One common class of metal SBUs used is the paddlewheel carboxylates shown in Figure **4.6.8A**. These consist of two metals spanned by a square plane of four carboxylates in a paddlewheel arrangment.

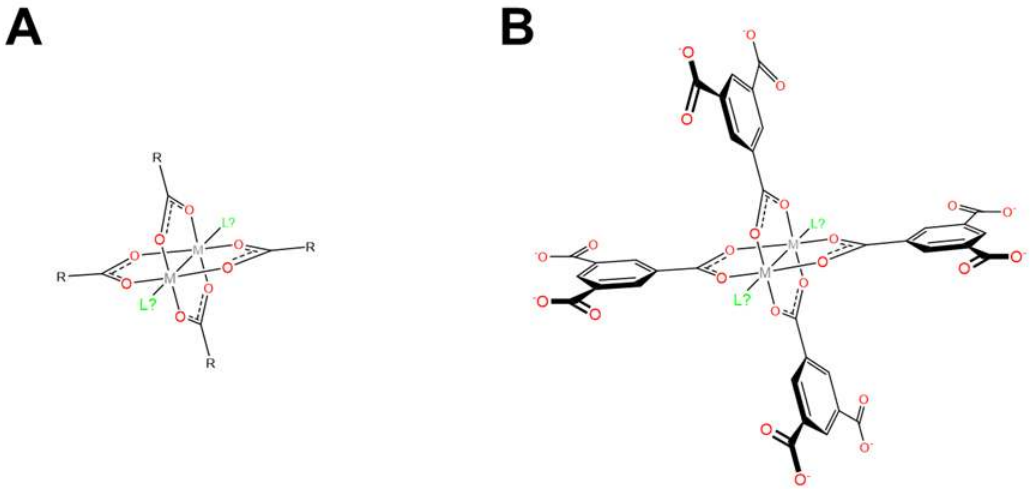


Figure **4.6.8**. Metal organic frameworks do not use a metal center directly but instead employ a metal cluster as a secondary building unit (SBU). (A) Paddlewheel carboxylates are a common SBU. They consist of two metals surrounded by four carboxylato ligands in a square planar "paddlewheel" arrangement. (B) In complexes where the ligands contain additional carboxylates, they function as a planar center in a MOF. An example is the paddlewheel carboxylate present in the HKUST class of MOFs, in which each carboxylato ligand is capable of bridging to three dimetal units. Note that in the structures shown, the axial ligands shown in green may be present or absent depending on the specific metal carboxylate used and/or whether the ligand was removed during processing of the MOF.

The use of paddlewheel carboxylate metal SBUs and bridging organic carboxylate ligands enables the construction of coordination frameworks like that of HKUST-1 shown in Figure **4.6.9**. The structure of these networks depends on the geometry of the linking ligand. For instance, in HKUST-1 the 1,3,5-benzenetricarboxylato bridging ligands each link three paddlewheel SBUs to give the cubic network shown in Figure **4.6.9**. Other organic carboxylate ligands give different network topologies. In addition, the ability of some paddlewheel carboxylates to coordinate ligands perpendicular to the carboxylates, represented by the ligands marked L? in Figure **4.6.8**, affords additional opportunities to use these networks to bind substrates that can coordinate those sites.

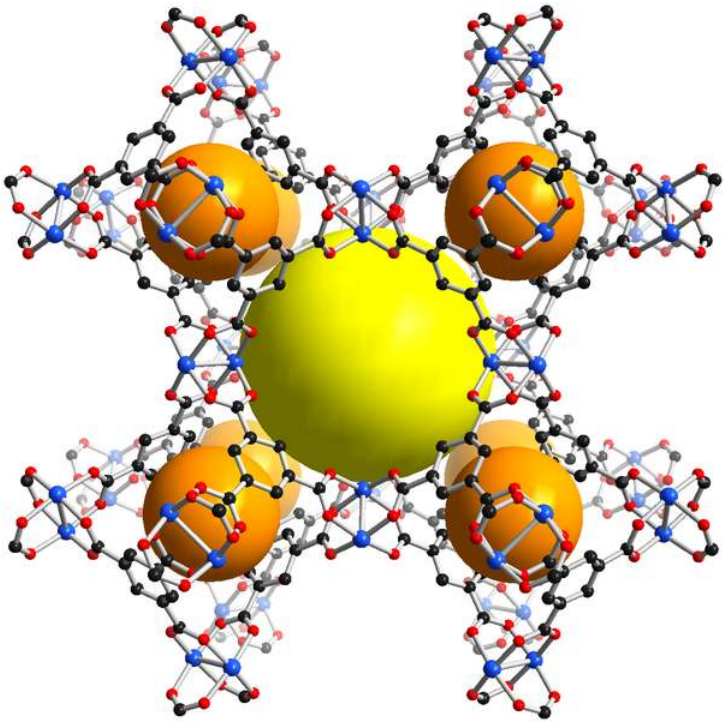


Figure 4.6.9. Desolvated HKUST-1 member of the HKUST class of MOFs showing open regions in the structure. The structure consists of paddlewheel carboxylates linked by trigonal planar tricarboxylate organic SBUs. The image is by Tony Boehle - Own work, CC BY-SA 3.0, https://commons.wikimedia.org/w/inde...curid=27424501

Another common metal SBU is the basic zinc acetate structure shown in Figure 4.6.10. As shown in Figure 4.6.10A, the structure is analogous to those of the basic beryllium acetates and involves an OZn_4 tetrahedron in which the tetrahedrally arranged Zn^{2+} are connected by carboxylate ligands spanning the tetrahedron's six edges. When these carboxylate ligands are replaced by rigid dicarboxylates (Figure 4.6.10B), the result is that the Zn_4O core is surrounded by an octahedral coordination sphere of carboxylate ligands (Figure 4.6.10C).

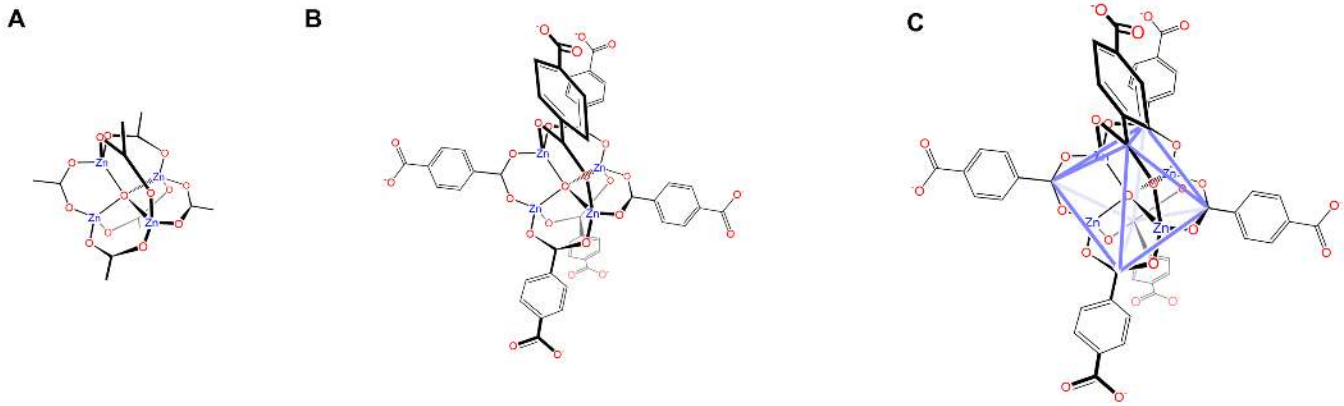


Figure 4.6.10. (A) Basic zinc acetate is a common SBU used as a pseudooctahedral center in MOFs. (B) Exchange of its acetate ligands with *p*-terephthalate (1,4-benzenedicarboxylate) linkers gives a complex in which the free dicarboxylates are oriented towards the vertices of an octahedron (C).

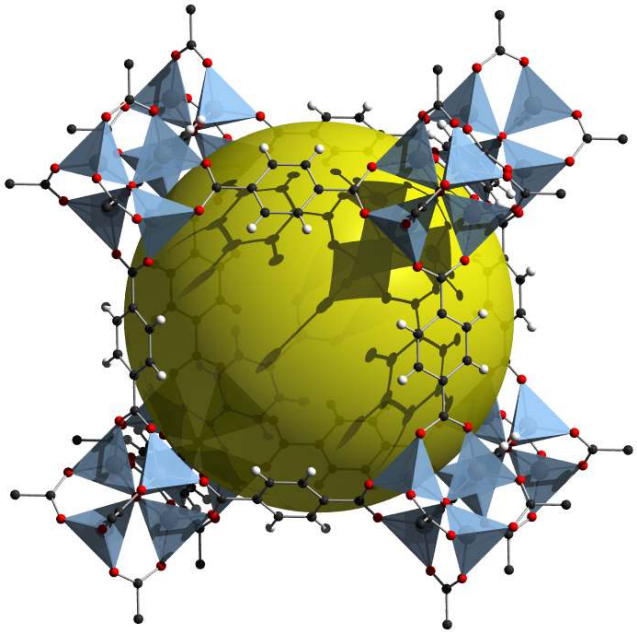


Figure **4.6.11**. A cubic metal organic framework derived from the basic zinc acetate SBU. The structure is called MOF-5 and consists of Zn_4O^{6+} pseudooctahedra linked by linear *p*-terephthalate (1,4-benzenedicarboxylate) ligands. The large golden sphere inside the unit cell has a radius of 12 Angstroms (defined with the aromatic rings oriented as shown) and represents the space available for the framework to accommodate guest molecules. By Tony Boehle - Own work, Public Domain, https://commons.wikimedia.org/w/inde...curid=10319204.

The structure of MOF-5 also illustrates how the size of the pores in an MOF structure may be tailored by lengthening or shortening the organic linker. In particular, from Figure **4.6.11** it can be seen that the size of the MOF-5's cubic unit cell depends on the length of the organic portion of the carboxylate linker. In MOF-5 this linker consists of a single benzene unit and gives 9-Angstrom pores, while the use of two and three benzene rings increases the pore size to 13 and 16 Angstroms, respectively, as shown in **4.6.12**.

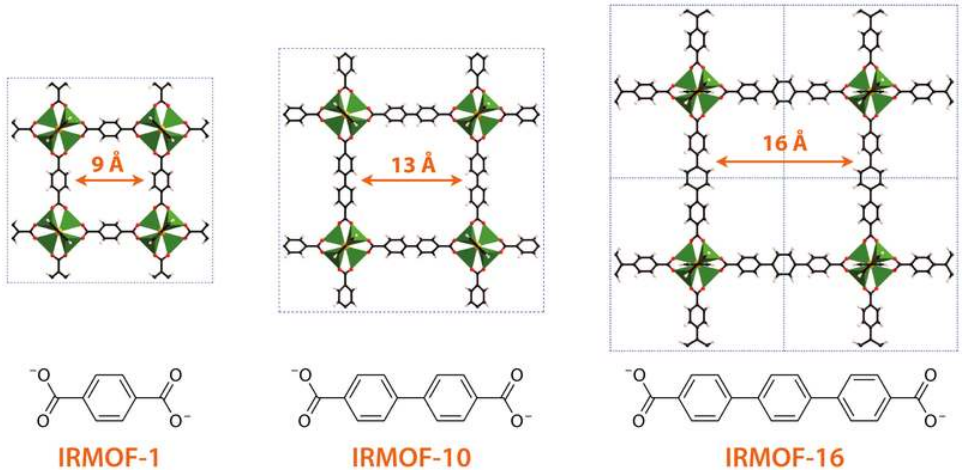


Figure **4.6.12**. The spacing between metal centers in a coordination network may be tailored by the use of organic linkers of differing lengths. By François-Xavier Coudert - Own work, CC BY 4.0, https://commons.wikimedia.org/w/inde...curid=89656071

References

1. The structure of Prussian blue is rendered from that reported in Buser, H. J.; Schwarzenbach, D.; Petter, W.; Ludi, A., The crystal structure of Prussian Blue: $Fe_4[Fe(CN)_6]_3.xH_2O$. *Inorganic Chemistry* 1977, *16(11)*, 2704-2710; to simplify depiction of the coordination framework, water molecules were removed. The structure of the Hofmann-type clathrate is rendered from that reported in Rayner, J. H.; Powell, H. M., 688. Crystal structure of a hydrated nickel cyanide ammoniate. *Journal of the Chemical Society (Resumed)* 1958, 3412-3418.

2. (a) Fujita, M.; Ogura, K., Transition-metal-directed assembly of well-defined organic architectures possessing large voids: From macrocycles to [2] catenanes. *Coordination Chemistry Reviews* 1996, *148*, 249-264. (b) Leininger, S.; Olenyuk, B.; Stang, P. J., Self-Assembly of Discrete Cyclic Nanostructures Mediated by Transition Metals. *Chemical Reviews* 2000, *100(3)*, 853-908.

3. Machado, V. G.; Baxter, P. N. W.; Lehn, J.-M., Self-assembly in self-organized inorganic systems: a view of programmed metallosupramolecular architectures. Journal of the Brazilian Chemical Society 2001, 12, 431-462.

4. Yaghi, O. M.; O'Keeffe, M.; Ockwig, N. W.; Chae, H. K.; Eddaoudi, M.; Kim, J., Reticular synthesis and the design of new materials. Nature 2003, 423 (6941), 705-714.

4.6: Coordination Frameworks is shared under a CC BY 4.0 license and was authored, remixed, and/or curated by Stephen M. Contakes.

- **9.6: Coordination Frameworks** by Stephen M. Contakes is licensed CC BY 4.0.

CHAPTER OVERVIEW

5: Symmetry and Group Theory

5.1: Symmetry Elements and Operations
5.2: Point Groups
5.3: Groups of Low and High Symmetry
5.4: Other Groups
5.5: Properties and Representations of Groups
5.6: Matrices
5.7: Representations of Point Groups
5.8: Character Tables
5.9: Examples and Applications of Symmetry
5.10: Chirality
5.11: Molecular Vibrations

5: Symmetry and Group Theory is shared under a not declared license and was authored, remixed, and/or curated by LibreTexts.

5.1: Symmetry Elements and Operations

Click here to see a lecture on this topic.

Introduction

The symmetry of a molecule consists of **symmetry operations** and **symmetry elements**. A symmetry operation is an operation that is performed to a molecule which leaves it indistinguishable and superimposable on the original position. Symmetry operations are performed with respect to symmetry elements (points, lines, or planes).

An example of a symmetry operation is a 180° rotation of a water molecule in which the resulting position of the molecule is indistinguishable from the original position (see Figure **5.1.1**). In this example, the symmetry operation is the rotation and the symmetry element is the axis of rotation.

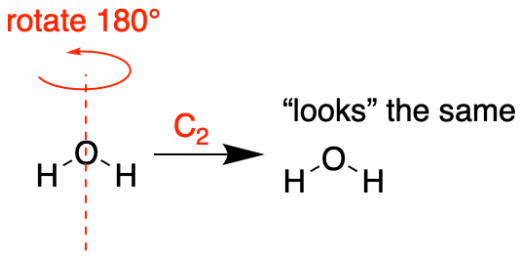


Figure **5.1.1**: An example of a symmetry operation is a 180° rotation where the resulting position is indistinguishable from the original. A 180° rotation is called a C_2 operation; the axis of rotation is the symmetry element. (Kathryn Haas; CC-NC-BY-SA)

There are five types of symmetry operations including **identity**, **reflection**, **inversion**, **proper rotation**, and **improper rotation**. The improper rotation is the sum of a rotation followed by a reflection. The symmetry elements that correspond to the five types of symmetry operations are listed in Table **5.1.1**.

Table **5.1.1**: Table of elements and operations

Element	Operation	Symbol
Identity	identity	E
Proper axis	rotation by (360/n)°	C_n
Symmetry plane	reflection in the plane	σ
Inversion center	inversion of a point at (x,y,z) to (-x,-y,-z)	*i*
Improper axis	rotation by (360/n)°, followed by reflection in the plane perpendicular to the rotation axis	S_n

Symmetry Operations and Elements

Identity (E)

All molecules have the identity element. The identity operation is doing nothing to the molecule (it doesn't rotate, reflect, or invert...it just is).

Proper Rotation and Proper Axis (C_n)

A "proper" rotation is just a simple rotation operation about an axis. The symbol for any proper rotation or proper axis is $C_{(360/n)}$, where n is the degree of rotation. Thus, a 180° rotation is a C_2 rotation around a C_2 axis, and a 120° rotation is a C_3 rotation about a C_3 axis.

PRINCIPAL AXIS: The principal axis of a molecule is the highest order proper rotation axis. For example, if a molecule had C_2 and C_4 axes, the C_4 is the principal axis.

Reflection and Symmetry Planes (σ)

Symmetry planes are mirror planes within the molecule. A reflection operation occurs with respect to a plane of symmetry. There are three classes of symmetry elements:

1. σ_h (horizontal): horizontal planes are perpendicular to principal axis
2. σ_v (vertical): vertical planes are parallel to the principal axis
3. σ_d (dihedral): dihedral planes are parallel to the principal axis and bisecting two C_2' axes

Inversion and Inversion Center (i)

The inversion operation requires a point of symmetry (a center of symmetry within a molecule). In other words, a point at the center of the molecule that can transform (x,y,z) into (-x,-y,-z) coordinate. Structures of tetrahedrons, triangles, and pentagons lack an inversion center.

Improper rotation (S_n)

Improper rotation is a combination of a rotation with respect to an axis of rotation (C_n), followed by a reflection through a plane perpendicular to that C_n axis. In short, an S_n operation is equivalent to C_n followed by σ_h.

References

1. Introduction to Molecular Symmetry by J. S Ogden
2. Inorganic Chemistry by Catherine Housecroft And Alan G. Sharpe.

5.1: Symmetry Elements and Operations is shared under a not declared license and was authored, remixed, and/or curated by LibreTexts.

- **4.1: Symmetry Elements and Operations** by Kathryn Haas has no license indicated.

5.2: Point Groups

Click here to see a lecture on this topic.

Introduction

A **Point Group** describes all the symmetry operations that can be performed on a molecule that result in a conformation indistinguishable from the original. Point groups are used in Group Theory, the mathematical analysis of groups, to determine properties such as a molecule's molecular orbitals.

Assigning Point Groups

While a point group contains all of the symmetry operations that can be performed on a given molecule, it is not necessary to identify all of these operations to determine the molecule's overall point group. Instead, a molecule's point group can be determined by following a set of steps which analyze the presence (or absence) of particular symmetry elements.

Steps for assigning a molecule's point group:

1. Determine if the molecule is of high or low symmetry.
2. If not, find the highest order rotation axis, C_n.
3. Determine whether the molecule has any C_2 axes perpendicular to the principal C_n axis. If so, then there are n such C_2 axes, and the molecule is in the D set of point groups. If not, it is in either the C or S set of point groups.
4. Determine whether the molecule has a horizontal mirror plane (σ_h) perpendicular to the principal C_n axis. If so, the molecule is either in the C_{nh} or D_{nh} set of point groups.
5. Determine whether the molecule has a vertical mirror plane (σ_v) containing the principal C_n axis. If so, the molecule is either in the C_{nv} or D_{nd} set of point groups. If not, and if the molecule has n perpendicular C_2 axes, then it is part of the D_n set of point groups.
6. Determine whether there is an improper rotation axis, S_{2n}, collinear with the principal C_n axis. If so, the molecule is in the S_{2n} point group. If not, the molecule is in the C_n point group.

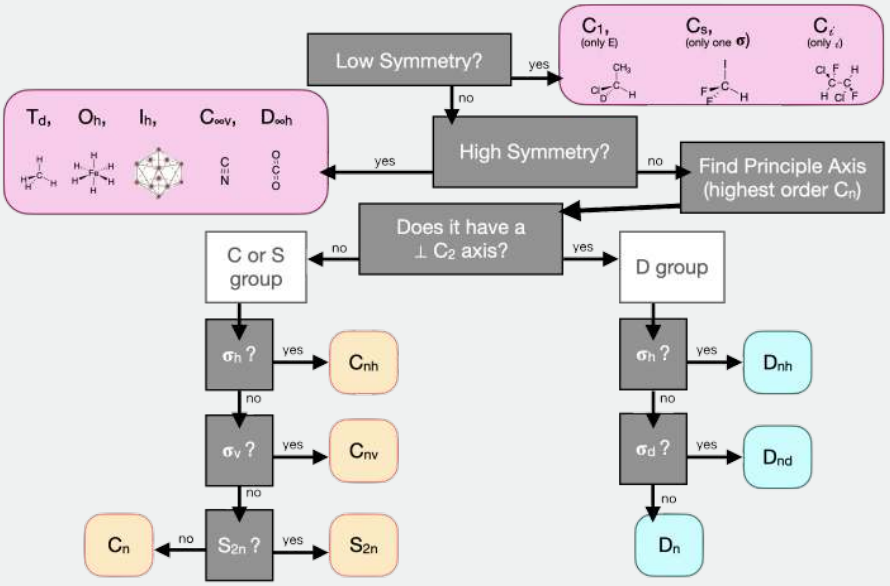


Figure **5.2.1**: Decision tree for determining a molecule's point group (CC-BY-NC-SA; Kathryn Haas)

Example 5.2.1

Find the point group of benzene (C_6H_6).

Answer

Solution

1. Benzene is neither high nor low symmetry
2. Highest order rotation axis: C_6
3. There are 6 C_2 axes perpendicular to the principal axis
4. There is a horizontal mirror plane (σ_h)

Benzene is in the D_{6h} point group.

See Also

Symmetry Gallery

5.2: Point Groups is shared under a not declared license and was authored, remixed, and/or curated by LibreTexts.

- **4.2: Point Groups** by Kathryn Haas has no license indicated.

5.3: Groups of Low and High Symmetry

Click here to see a lecture on this topic.

Low Symmetry Point Groups

Low symmetry point groups include the C_1, C_s, and C_i groups

Group	Description	Example
C_1	only the identity operation (E)	CHFClBr
C_s	only the identity operation (E) and one mirror plane	C_2H_2ClBr
C_i	only the identity operation (E) and a center of inversion (i)	$C_2H_2Cl_2Br$

High Symmetry Point Groups

High symmetry point groups include the T_d, O_h, I_h, $C_{\infty v}$, and $D_{\infty h}$ groups. The table below describes their characteristic symmetry operations. The full set of symmetry operations included in the point group is described in the corresponding character table.

Group	Description	Example
$C_{\infty v}$	linear molecule with an infinite number of rotation axes and vertical mirror planes (σ_v)	HBr
$D_{\infty h}$	linear molecule with an infinite number of rotation axes, vertical mirror planes (σ_v), perpendicular C_2 axes, a horizontal mirror plane (σ_h), and an inversion center (i)	CO_2
T_d	typically have tetrahedral geometry, with 4 C_4 axes, 3 C_2 axes, 3 S_4 axes, and 6 dihedral mirror planes (σ_d)	CH_4
O_h	typically have octahedral geometry, with 3 C_4 axes, 4 C_3 axes, and an inversion center (i) as characteristic symmetry operations	SF_6
I_h	typically have an icosahedral structure, with 6 C_5 axes as characteristic symmetry operations	$B_{12}H_{12}^{2-}$

See Also

Symmetry Gallery

5.3: Groups of Low and High Symmetry is shared under a not declared license and was authored, remixed, and/or curated by LibreTexts.

- **4.2.1: Groups of Low and High Symmetry** by Kathryn Haas has no license indicated.
- **1.2: Molecular Point Groups** by Wikipedia is licensed CC BY-SA 4.0. Original source: https://en.wikibooks.org/wiki/Advanced_Inorganic_Chemistry.

5.4: Other Groups

Click here to see a lecture on this topic.

D Groups

The D set of point groups is classified as D_{nh}, D_{nd}, or D_n, where n refers to the principal axis of rotation. Overall, the D groups are characterized by the presence of n C_2 axes perpendicular to the principal C_n axis. Further classification of a molecule in the D groups depends on the presence of horizontal or vertical/dihedral mirror planes.

Group	Description	Example
D_{nh}	n perpendicular C_2 axes, and a horizontal mirror plane (σ_h)	benzene, C_6H_6 is D_{6h}
D_{nd}	n perpendicular C_2 axes, and a vertical mirror plane (σ_v)	propadiene, C_3H_4 is D_{2d}
D_n	n perpendicular C_2 axes, no mirror planes	$[Co(en)_3]^{3+}$ is D_3

C Groups

The C set of point groups is classified as C_{nh}, C_{nv}, or C_n, where n refers to the principal axis of rotation. The C set of groups is characterized by the absence of n C_2 axes perpendicular to the principal C_n axis. Further classification of a molecule in the C groups depends on the presence of horizontal or vertical/dihedral mirror planes.

Group	Description	Example
C_{nh}	horizontal mirror plane (σ_h) perpendicular to the principal C_n axis	boric acid, H_3BO_3, is C_{3h}
C_{nv}	vertical mirror plane (σ_v) containing the principal C_n axis	ammonia, NH_3, is C_{3v}
C_n	no mirror planes	$P(C_6H_5)_3$ is C_3

S Groups

The S set of point groups is classified as S_{2n}, where n refers to the principal axis of rotation. The S set of groups is characterized by the absence of n C_2 axes perpendicular to the principal C_n axis, as well as the absence of horizontal and vertical/dihedral mirror planes. However, there is an improper rotation (or a rotation-reflection) axis collinear with the principal C_n axis.

Group	Description	Example
S_{2n}	improper rotation (or a rotation-reflection) axis collinear with the principal C_n axis	12-crown-4 is S_4

See Also

Symmetry Gallery

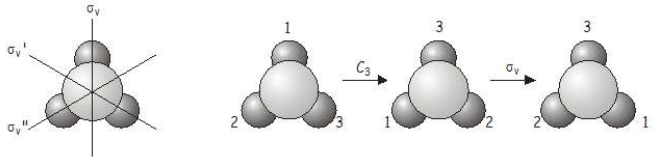
5.4: Other Groups is shared under a not declared license and was authored, remixed, and/or curated by LibreTexts.

- **4.2.2: Other Groups** by Kathryn Haas has no license indicated.
- **1.2: Molecular Point Groups** by Wikipedia is licensed CC BY-SA 4.0. Original source: https://en.wikibooks.org/wiki/Advanced_Inorganic_Chemistry.

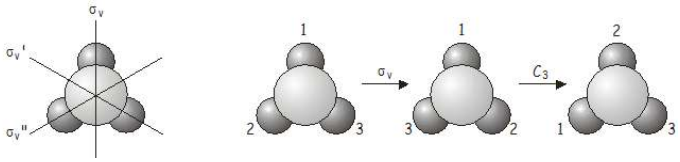
5.5: Properties and Representations of Groups

Group Multiplication

Now we will investigate what happens when we apply two symmetry operations in sequence. As an example, consider the NH_3 molecule, which belongs to the C_{3v} point group. Consider what happens if we apply a C_3rotation (120˚ counter-clockwise) followed by a σ_v reflection (reflection over the σ_v axis). We write this combined operation $\sigma_v C_3$ (when written, symmetry operations operate on the thing directly to their right, just as operators do in quantum mechanics – we therefore have to work backwards from right to left from the notation to get the correct order in which the operators are applied). As we shall soon see, the order in which the operations are applied is important.



The combined operation $\sigma_v C_3$ is equivalent to σ_v'' (note the double prime on σ_v''!), which is also a symmetry operation of the C_{3v} point group. Now let's see what happens if we apply the operators in the reverse order, i.e., $C_3\sigma_v$ is (σ_v followed by C_3).



Again, the combined operation $C_3\sigma_v$ is equivalent to another operation of the point group, this time σ_v' (note the single prime on σ_v'!).

There are two important points that are illustrated by this example:

1. The order in which two operations are applied is important. For two symmetry operations A and B, AB is not necessarily the same as BA, i.e. symmetry operations do not in general ***commute***. In some groups the symmetry elements do commute; such groups are said to be ***Abelian***.
2. If two operations from the same point group are applied in sequence, the result will be equivalent to another operation from the point group. Symmetry operations that are related to each other by other symmetry operations of the group are said to belong to the same ***class***. In NH_3, the three mirror planes σ_v, σ_v' and σ_v'' belong to the same class (related to each other through a C_3 rotation), as do the rotations C_3^+ and C_3^- (anticlockwise and clockwise rotations about the principal axis, related to each other by a vertical mirror plane).

Four Properties of Mathematical Groups

Now that we have explored some of the properties of symmetry operations and elements and their behavior within point groups, we are ready to introduce the formal mathematical definition of a group. The definitions below will be put into the context of *molecular* symmetry.

A mathematical group is defined as a set of elements (A_1, A_2, A_3...) together with a rule for forming combinations A_i,A_j... For our purposes, A_1, A_2, A_3, etc. are symmetry elements and A_i, A_j, etc. are symmetry operations described in a previous section. The elements of the group and the rule for combining them must satisfy the following four criteria.

1. The group must include the **identity** E, which commutes with other members of the group. In other terms, $EA_i = A_i$ for all the elements of the group. Application of the identity operation before or after another operation, A_i, results in the same outcome as A_i alone.
2. The elements must satisfy the group property that the combination of any pair of elements is also an element of the group. For example, in the C_{3v} point group, a C_3 rotation followed by a σ_v gives another operation that is already part of the group: a σ_v''.

3. Each symmetry operation A_i must have an inverse A_i^{-1} which is also an element of the group, such that

$$A_i A_i^{-1} = A_i^{-1} A_i = E$$

   The inverse g_i^{-1} effectively 'undoes' the effect of the symmetry operation g_i. For example, in the C_{3v} point group, the inverse of C_3^+ is C_3^-.
4. The rule of combination must be associative

$$(A_i A_j)(A_k) = A_i(A_j A_k)$$

   Or $A(BC) = (AB)C$. In other words, the order of operations should not matter.

Group theory is an important area in mathematics, and luckily for chemists the mathematicians have already done most of the work for us. Along with the formal definition of a group comes a comprehensive mathematical framework that allows us to carry out a rigorous treatment of symmetry in molecular systems and learn about its consequences.

Many problems involving operators or operations (such as those found in quantum mechanics or group theory) may be reformulated in terms of matrices. Any of you who have come across transformation matrices before will know that symmetry operations such as rotations and reflections may be represented by matrices. It turns out that the set of matrices representing the symmetry operations in a group obey all the conditions laid out above in the mathematical definition of a group, and using matrix representations of symmetry operations simplifies carrying out calculations in group theory. Before we learn how to use matrices in group theory, it will probably be helpful to review some basic definitions and properties of matrices.

*This page was adapted from here (click).

Contributors and Attributions

- Claire Vallance (University of Oxford)
- Curated or created by Kathryn Haas

5.5: Properties and Representations of Groups is shared under a not declared license and was authored, remixed, and/or curated by LibreTexts.

- **4.3: Properties and Representations of Groups** by Kathryn Haas is licensed CC BY-NC-SA 4.0.

5.6: Matrices

The symmetry of molecules is essential for understanding the structures and properties of organic and inorganic compounds. The properties of chemical compounds are often easily explained by consideration of symmetry. For example, the symmetry of a molecule determines whether the molecule has a permanent dipole moment or not. The theories that describe optical activity, infrared and ultraviolet spectroscopy, and crystal structure involve the application of symmetry considerations. Matrix algebra is the most important mathematical tool in the description of symmetry.

The properties of symmetry groups are organized in character tables (discussed later in this chapter). Character tables are constructed based on matrices. This page is a brief description of matrices and matrix multiplication.

What is a matrix?

An $m \times n$ matrix $\mathbf{A}$ is a rectangular array of numbers with m rows and n columns. The numbers m and n are the dimensions of $\mathbf{A}$. The numbers in the matrix are called its entries. The entry in row i and column j is called a_{ij}.

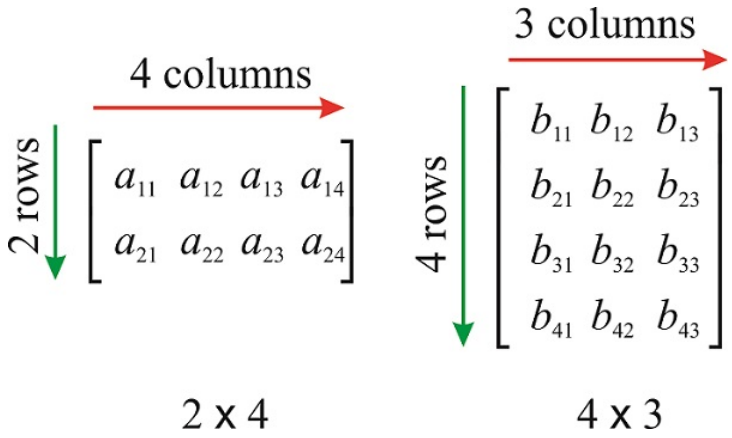


Figure **5.6.1**: Matrices of different dimensions

Some types of matrices have special names:

- A square matrix:

$$\begin{pmatrix} 3 & -2 & 4 \\ 5 & 3i & 3 \\ -i & 1/2 & 9 \end{pmatrix}$$

  with $m = n$
- A rectangular matrix:

$$\begin{pmatrix} 3 & -2 & 4 \\ 5 & 3i & 3 \end{pmatrix}$$

  with $m \neq n$
- A column vector:

$$\begin{pmatrix} 3 \\ 5 \\ -i \end{pmatrix}$$

  with $n = 1$
- A row vector:

$$\begin{pmatrix} 3 & -2 & 4 \end{pmatrix}$$

  with $m = 1$
- The identity matrix:

$$\begin{pmatrix} 1 & 0 & 0 \\ 0 & 1 & 0 \\ 0 & 0 & 1 \end{pmatrix}$$

with $a_{ij} = \delta_{i,j}$, where $\delta_{i,j}$ is a function defined as $\delta_{i,j} = 1$ if $i = j$ and $\delta_{i,j} = 0$ if $i \neq j$.

- A diagonal matrix:

$$\begin{pmatrix} a & 0 & 0 \\ 0 & b & 0 \\ 0 & 0 & c \end{pmatrix}$$

with $a_{ij} = c_i \delta_{i,j}$.

- An upper triangular matrix:

$$\begin{pmatrix} a & b & c \\ 0 & d & e \\ 0 & 0 & f \end{pmatrix}$$

All the entries below the main diagonal are zero.

- A lower triangular matrix:

$$\begin{pmatrix} a & 0 & 0 \\ b & c & 0 \\ d & e & f \end{pmatrix}$$

All the entries above the main diagonal are zero.

- A triangular matrix is one that is either lower triangular or upper triangular.

The Trace of a Matrix

The trace of an $n \times n$ square matrix $\mathbf{A}$ is the sum of the diagonal elements, and formally defined as $Tr(\mathbf{A}) = \sum_{i=1}^{n} a_{ii}$.

For example,

$$\mathbf{A} = \begin{pmatrix} 3 & -2 & 4 \\ 5 & 3i & 3 \\ -i & 1/2 & 9 \end{pmatrix} ; Tr(\mathbf{A}) = 12 + 3i$$

Singular and Nonsingular Matrices

A square matrix with nonzero determinant is called *nonsingular*. A matrix whose determinant is zero is called *singular*. (Note that you cannot calculate the determinant of a non-square matrix).

For a 2x2 matrix,

$$\mathbf{B} = \begin{pmatrix} a & b \\ c & d \end{pmatrix} ; det(\mathbf{B}) = ad - cb$$

For a 3x3 matrix,

$$\mathbf{C} = \begin{pmatrix} a & b & c \\ d & e & f \\ g & h & i \end{pmatrix}$$

$$det(\mathbf{C}) = a \begin{pmatrix} e & f \\ h & i \end{pmatrix} - b \begin{pmatrix} d & f \\ g & i \end{pmatrix} + c \begin{pmatrix} d & e \\ g & h \end{pmatrix}$$

$$det(\mathbf{C}) = aei - ahf - bdi + bgf + cdh - cge$$

The Matrix Transpose

The matrix transpose, most commonly written $\mathbf{A}^T$, is the matrix obtained by exchanging $\mathbf{A}$'s rows and columns. It is obtained by replacing all elements a_{ij} with a_{ji}. For example:

$$\mathbf{A} = \begin{pmatrix} 3 & -2 & 4 \\ 5 & 3i & 3 \end{pmatrix} \rightarrow \mathbf{A}^T = \begin{pmatrix} 3 & 5 \\ -2 & 3i \\ 4 & 3 \end{pmatrix}$$

Matrix Multiplication

To multiply two matrices, the number of vertical columns in the first matrix must be the same as the number of rows in the second matrix. If $\mathbf{A}$ has dimensions $m \times n$ and $\mathbf{B}$ has dimensions $n \times p$, then the product $\mathbf{AB}$ is defined, and has dimensions $m \times p$.

$$c_{ij} = \sum a_{ij} \times b_{ij}$$

The entry $a_{ij} \times b_{ij}$ is obtained by multiplying row i of $\mathbf{A}$ by column j of $\mathbf{B}$, which is done by multiplying corresponding entries together and then adding the results:

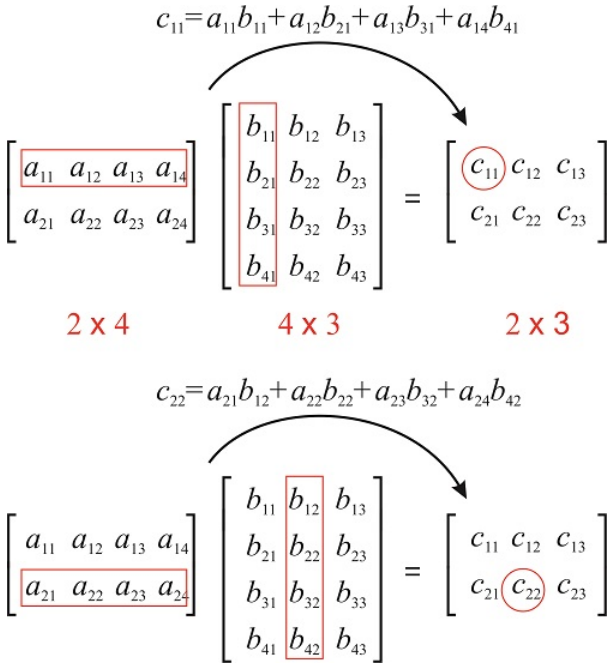


Figure 5.6.1: Matrix multiplication

Example 5.6.1

Calculate the product

$$\begin{pmatrix} 1 & -2 & 4 \\ 5 & 0 & 3 \\ 0 & 1/2 & 9 \end{pmatrix} \begin{pmatrix} 1 & 0 \\ 5 & 3 \\ -1 & 0 \end{pmatrix}$$

Solution

We need to multiply a 3×3 matrix by a 3×2 matrix, so we expect a 3×2 matrix as a result.

$$\begin{pmatrix} 1 & -2 & 4 \\ 5 & 0 & 3 \\ 0 & 1/2 & 9 \end{pmatrix} \begin{pmatrix} 1 & 0 \\ 5 & 3 \\ -1 & 0 \end{pmatrix} = \begin{pmatrix} a & b \\ c & d \\ e & f \end{pmatrix}$$

To calculate a, which is entry (1,1), we use row 1 of the matrix on the left and column 1 of the matrix on the right:

$$\begin{pmatrix} 1 & -2 & 4 \\ 5 & 0 & 3 \\ 0 & 1/2 & 9 \end{pmatrix} \begin{pmatrix} 1 & 0 \\ 5 & 3 \\ -1 & 0 \end{pmatrix} = \begin{pmatrix} a & b \\ c & d \\ e & f \end{pmatrix} \rightarrow a = 1 \times 1 + (-2) \times 5 + 4 \times (-1) = -13$$

To calculate b, which is entry (1,2), we use row 1 of the matrix on the left and column 2 of the matrix on the right:

$$\begin{pmatrix}1 & -2 & 4\\ 5 & 0 & 3\\ 0 & 1/2 & 9\end{pmatrix}\begin{pmatrix}1 & 0\\ 5 & 3\\ -1 & 0\end{pmatrix}=\begin{pmatrix}a & b\\ c & d\\ e & f\end{pmatrix}\rightarrow b=1\times 0+(-2)\times 3+4\times 0=-6$$

To calculate c, which is entry (2,1), we use row 2 of the matrix on the left and column 1 of the matrix on the right:

$$\begin{pmatrix}1 & -2 & 4\\ 5 & 0 & 3\\ 0 & 1/2 & 9\end{pmatrix}\begin{pmatrix}1 & 0\\ 5 & 3\\ -1 & 0\end{pmatrix}=\begin{pmatrix}a & b\\ c & d\\ e & f\end{pmatrix}\rightarrow c=5\times 1+0\times 5+3\times(-1)=2$$

To calculate d, which is entry (2,2), we use row 2 of the matrix on the left and column 2 of the matrix on the right:

$$\begin{pmatrix}1 & -2 & 4\\ 5 & 0 & 3\\ 0 & 1/2 & 9\end{pmatrix}\begin{pmatrix}1 & 0\\ 5 & 3\\ -1 & 0\end{pmatrix}=\begin{pmatrix}a & b\\ c & d\\ e & f\end{pmatrix}\rightarrow d=5\times 0+0\times 3+3\times 0=0$$

To calculate e, which is entry (3,1), we use row 3 of the matrix on the left and column 1 of the matrix on the right:

$$\begin{pmatrix}1 & -2 & 4\\ 5 & 0 & 3\\ 0 & 1/2 & 9\end{pmatrix}\begin{pmatrix}1 & 0\\ 5 & 3\\ -1 & 0\end{pmatrix}=\begin{pmatrix}a & b\\ c & d\\ e & f\end{pmatrix}\rightarrow e=0\times 1+1/2\times 5+9\times(-1)=-13/2$$

To calculate f, which is entry (3,2), we use row 3 of the matrix on the left and column 2 of the matrix on the right:

$$\begin{pmatrix}1 & -2 & 4\\ 5 & 0 & 3\\ 0 & 1/2 & 9\end{pmatrix}\begin{pmatrix}1 & 0\\ 5 & 3\\ -1 & 0\end{pmatrix}=\begin{pmatrix}a & b\\ c & d\\ e & f\end{pmatrix}\rightarrow f=0\times 0+1/2\times 3+9\times 0=3/2$$

The result is:

$$\begin{pmatrix}1 & -2 & 4\\ 5 & 0 & 3\\ 0 & 1/2 & 9\end{pmatrix}\begin{pmatrix}1 & 0\\ 5 & 3\\ -1 & 0\end{pmatrix}=\begin{pmatrix}-13 & -6\\ 2 & 0\\ -13/2 & 3/2\end{pmatrix}$$

Example 5.6.2

Calculate

$$\begin{pmatrix}1 & -2 & 4\\ 5 & 0 & 3\end{pmatrix}\begin{pmatrix}1\\ 5\\ -1\end{pmatrix}$$

Solution

We are asked to multiply a 2×3 matrix by a 3×1 matrix (a column vector). The result will be a 2×1 matrix (a vector).

$$\begin{pmatrix}1 & -2 & 4\\ 5 & 0 & 3\end{pmatrix}\begin{pmatrix}1\\ 5\\ -1\end{pmatrix}=\begin{pmatrix}a\\ b\end{pmatrix}$$

$$a=1\times 1+(-2)\times 5+4\times(-1)=-13$$

$$b=5\times 1+0\times 5+3\times(-1)=2$$

The solution is:

$$\begin{pmatrix}1 & -2 & 4\\ 5 & 0 & 3\end{pmatrix}\begin{pmatrix}1\\ 5\\ -1\end{pmatrix}=\begin{pmatrix}-13\\ 2\end{pmatrix}$$

Need help? The link below contains solved examples: Multiplying matrices of different shapes (three examples): http://tinyurl.com/kn8ysqq

External links:

- Multiplying matrices, example 1: http://patrickjmt.com/matrices-multiplying-a-matrix-by-another-matrix/
- Multiplying matrices, example 2: http://patrickjmt.com/multiplying-matrices-example-2/
- Multiplying matrices, example 3: http://patrickjmt.com/multiplying-matrices-example-3/

The Commutator

Matrix multiplication is not, in general, commutative. For example, we can perform

$$\begin{pmatrix} 1 & -2 & 4 \\ 5 & 0 & 3 \end{pmatrix} \begin{pmatrix} 1 \\ 5 \\ -1 \end{pmatrix} = \begin{pmatrix} -13 \\ 2 \end{pmatrix}$$

but cannot perform

$$\begin{pmatrix} 1 \\ 5 \\ -1 \end{pmatrix} \begin{pmatrix} 1 & -2 & 4 \\ 5 & 0 & 3 \end{pmatrix}$$

Even with square matrices, that can be multiplied both ways, multiplication is not commutative. In this case, it is useful to define the **commutator**, defined as:

$$[\mathbf{A}, \mathbf{B}] = \mathbf{AB} - \mathbf{BA}$$

Example 5.6.3

Given $\mathbf{A} = \begin{pmatrix} 3 & 1 \\ 2 & 0 \end{pmatrix}$ and $\mathbf{B} = \begin{pmatrix} 1 & 0 \\ -1 & 2 \end{pmatrix}$

Calculate the commutator $[\mathbf{A}, \mathbf{B}]$

Solution

$$[\mathbf{A}, \mathbf{B}] = \mathbf{AB} - \mathbf{BA}$$

$$\mathbf{AB} = \begin{pmatrix} 3 & 1 \\ 2 & 0 \end{pmatrix} \begin{pmatrix} 1 & 0 \\ -1 & 2 \end{pmatrix} = \begin{pmatrix} 3 \times 1 + 1 \times (-1) & 3 \times 0 + 1 \times 2 \\ 2 \times 1 + 0 \times (-1) & 2 \times 0 + 0 \times 2 \end{pmatrix} = \begin{pmatrix} 2 & 2 \\ 2 & 0 \end{pmatrix}$$

$$\mathbf{BA} = \begin{pmatrix} 1 & 0 \\ -1 & 2 \end{pmatrix} \begin{pmatrix} 3 & 1 \\ 2 & 0 \end{pmatrix} = \begin{pmatrix} 1 \times 3 + 0 \times 2 & 1 \times 1 + 0 \times 0 \\ -1 \times 3 + 2 \times 2 & -1 \times 1 + 2 \times 0 \end{pmatrix} = \begin{pmatrix} 3 & 1 \\ 1 & -1 \end{pmatrix}$$

$$[\mathbf{A}, \mathbf{B}] = \mathbf{AB} - \mathbf{BA} = \begin{pmatrix} 2 & 2 \\ 2 & 0 \end{pmatrix} - \begin{pmatrix} 3 & 1 \\ 1 & -1 \end{pmatrix} = \begin{pmatrix} -1 & 1 \\ 1 & 1 \end{pmatrix}$$

$$[\mathbf{A}, \mathbf{B}] = \begin{pmatrix} -1 & 1 \\ 1 & 1 \end{pmatrix}$$

Multiplication of a vector by a scalar

The multiplication of a vector $\vec{v}_1$ by a scalar n produces another vector of the same dimensions that lies in the same direction as $\vec{v}_1$;

$$n \begin{pmatrix} x \\ y \end{pmatrix} = \begin{pmatrix} nx \\ ny \end{pmatrix}$$

The scalar can stretch or compress the length of the vector, but cannot rotate it (figure [fig:vector_by_scalar]).

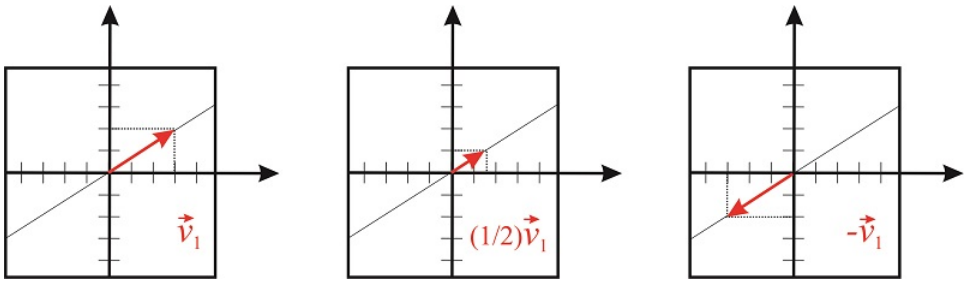


Figure **5.6.2**: Multiplication of a vector by a scalar

Multiplication of a square matrix by a vector

The multiplication of a vector $\vec{v_1}$ by a square matrix produces another vector of the same dimensions of $\vec{v_1}$. For example, we can multiply a 2×2 matrix and a 2-dimensional vector:

$$\begin{pmatrix} a & b \\ c & d \end{pmatrix} \begin{pmatrix} x \\ y \end{pmatrix} = \begin{pmatrix} ax + by \\ cx + dy \end{pmatrix}$$

For example, consider the matrix

$$\mathbf{A} = \begin{pmatrix} -2 & 0 \\ 0 & 1 \end{pmatrix}$$

The product

$$\begin{pmatrix} -2 & 0 \\ 0 & 1 \end{pmatrix} \begin{pmatrix} x \\ y \end{pmatrix}$$

is

$$\begin{pmatrix} -2x \\ y \end{pmatrix}$$

We see that 2×2 matrices act as operators that transform one 2-dimensional vector into another 2-dimensional vector. This particular matrix keeps the value of y constant and multiplies the value of x by -2 (Figure **5.6.3**).

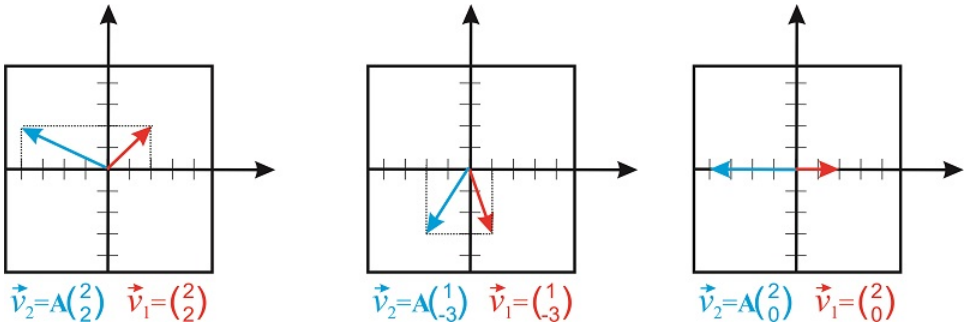


Figure **5.6.3**: Multiplication of a vector by a square matrix

Notice that matrices are useful ways of representing operators that change the orientation and size of a vector. An important class of operators that are of particular interest to chemists are the so-called symmetry operators.

Attribution

This page was adapted from Matrices (click here), contributed by Marcia Levitus, Associate Professor (Biodesign Institute) at Arizona State University.

Curated or created by Kathryn Haas

5.6: Matrices is shared under a not declared license and was authored, remixed, and/or curated by LibreTexts.

- **4.3.1: Matrices** by Kathryn Haas is licensed CC BY-NC-SA 4.0.

5.7: Representations of Point Groups

Symmetry Operations: Matrix Representations

A **symmetry operation**, such as a rotation around a symmetry axis or a reflection through a plane, is an operation that, when performed on an object, results in a new orientation of the object that is indistinguishable from the original. For example, if we rotate a square in the plane by $\pi/2$ or π, the new orientation of the square is superimposable on the original one (Figure 5.7.1).

If rotation by an angle θ of a molecule (or object) about some axis results in an orientation of the molecule (or object) that is superimposable on the original, the axis is called a rotation axis. The molecule (or object) is said to have an n-fold rotational axis, where n is $2\pi/\theta$. The axis is denoted as C_n. The square of Figure 5.7.1 has a C_4 axis perpendicular to the plane because a 90° rotation leaves the figure indistinguishable from the initial orientation. This axis is also a C_2 axis because a 180° degree rotation leaves the square indistinguishable from the original square. In addition, the figure has several other C_2 axis that lie on the same plane as the square:

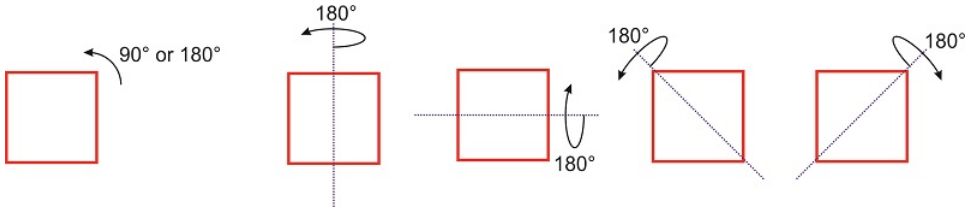


Figure 5.7.1: Symmetry operations performed on a square

A symmetry operation moves all the points of the object from one initial position to a final position, and that means that symmetry operators are 3×3 square matrices (or 2×2 in two dimensions). Each symmetry operation can be expressed as a **transformation matrix** where the vector (x', y', z') represents the new coordinates of the point (x, y, z) after the symmetry operation.

$$[\text{New Coordinates}(x', y', z')] = [\text{Transformation Matrix}] \times [\text{Old Coordinates}(x, y, z)]$$

We will use the example of water, which is in the C_{2v} point group, to illustrate how transformation matrices can be used to represent the symmetry of a group.

Figure 5.7.2 shows the three symmetry elements of the molecule of water (H_2O). This molecule has only one rotation axis, which is 2-fold, and therefore we call it a "C_2 axis." It also has two mirror planes, one that contains the two hydrogen atoms (σ_{yz}), and another one perpendicular to it (σ_{xz}). Both planes contain the C_2 axis.

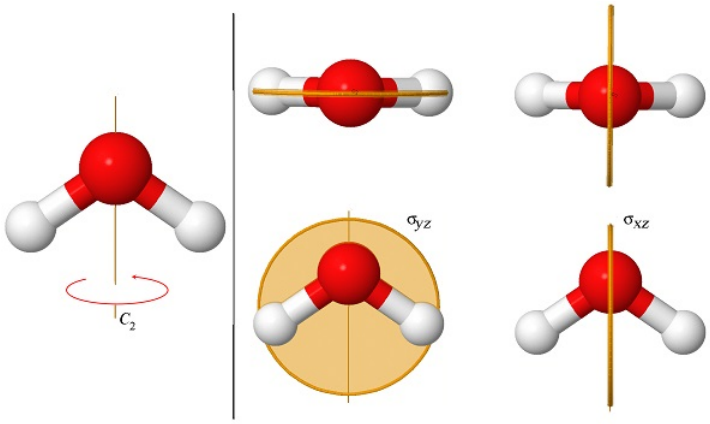


Figure 5.7.2: The symmetry elements of the molecule of water

Transformation Matrix of C_2 rotation

A 2-fold rotation around the z–axis changes the location of a point (x, y, z) to $(-x, -y, z)$ (see Figure 5.7.3). By convention, rotations are always taken in the counterclockwise direction.

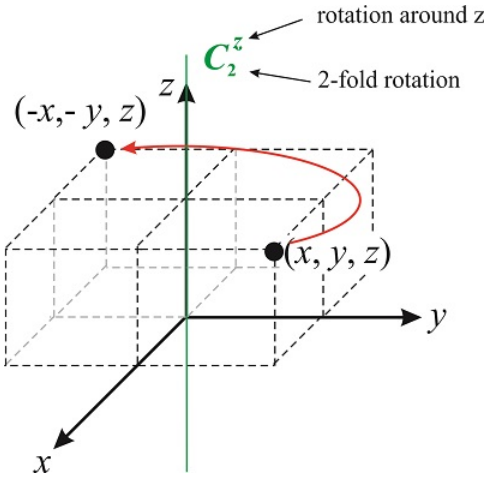


Figure 5.7.3: A 2-fold rotation around the z-axis

What is the matrix that represents the C_2 rotation? The matrix transforms the vector (x, y, z) into $(-x, -y, z)$, so

$$C_2(x, y, z) = (-x, -y, z)$$

$$\begin{pmatrix} a_{11} & a_{12} & a_{13} \\ a_{21} & a_{22} & a_{23} \\ a_{31} & a_{32} & a_{33} \end{pmatrix} \begin{pmatrix} x \\ y \\ z \end{pmatrix} = \begin{pmatrix} -x \\ -y \\ z \end{pmatrix}$$

We know the matrix is a 3×3 square matrix because it needs to multiply a 3-dimensional vector. In addition, we write the vector as a vertical column to satisfy the requirements of matrix multiplication.

$$\begin{pmatrix} a_{11} & a_{12} & a_{13} \\ a_{21} & a_{22} & a_{23} \\ a_{31} & a_{32} & a_{33} \end{pmatrix} \begin{pmatrix} x \\ y \\ z \end{pmatrix}$$

$$a_{11}x + a_{12}y + a_{13}z = -x$$

$$a_{21}x + a_{22}y + a_{23}z = -y$$

$$a_{31}x + a_{32}y + a_{33}z = z$$

and we conclude that $a_{11} = -1$, $a_{12} = a_{13} = 0$, $a_{22} = -1$, $a_{21} = a_{23} = 0$ and $a_{33} = 1$, $a_{31} = a_{32} = 0$. The transformation matrix of the C_2 operation of the C_{2v} point group is:

$$C_2 = \begin{pmatrix} -1 & 0 & 0 \\ 0 & -1 & 0 \\ 0 & 0 & 1 \end{pmatrix}$$

Transformation Matrix of σ_{xz} reflection

Rotations are not the only symmetry operations we can perform on a molecule. Figure 5.7.4 illustrates the reflection of a point through the xz plane. This operation transforms the vector (x, y, z) into the vector $(x, -y, z)$. Symmetry operators involving reflections through a plane are usually denoted with the letter σ, so the operator that reflects a point through the xz plane is $\hat{\sigma}_{xz}$:

$$\sigma_{xz}(x, y, z) = (x, -y, z)$$

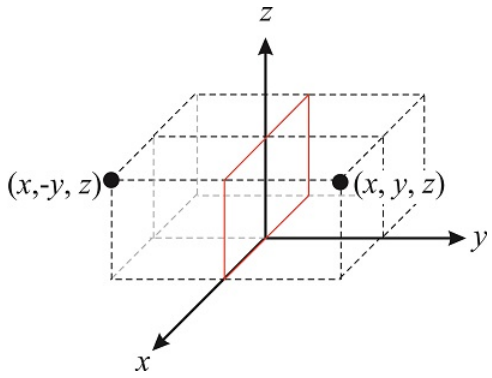


Figure 5.7.3: A reflection through the xz plane

Following the same logic we used for the rotation matrix, we can write the σ_{xz} transformation matrix as:

$$\sigma_{x,z} = \begin{pmatrix} 1 & 0 & 0 \\ 0 & -1 & 0 \\ 0 & 0 & 1 \end{pmatrix}$$

This is true because

$$\begin{pmatrix} 1 & 0 & 0 \\ 0 & -1 & 0 \\ 0 & 0 & 1 \end{pmatrix} \begin{pmatrix} x \\ y \\ z \end{pmatrix} = \begin{pmatrix} x \\ -y \\ z \end{pmatrix}$$

? Exercise 5.7.1

Find the transformation matrix of the identity (E) and the $\sigma_{y,z}$ operations under the C_{2v} point group.

Answer

The transformation matrix for E is $\begin{pmatrix} 1 & 0 & 0 \\ 0 & 1 & 0 \\ 0 & 0 & 1 \end{pmatrix}$.

The transformation matrix for $\sigma_{v(yz)''}$ is $\begin{pmatrix} -1 & 0 & 0 \\ 0 & 1 & 0 \\ 0 & 0 & 1 \end{pmatrix}$.

Characters

For a square matrix, the ***character*** is the trace of the matrix. For the C_2 operation, with the transformation matrix

$$\begin{pmatrix} -1 & 0 & 0 \\ 0 & -1 & 0 \\ 0 & 0 & 1 \end{pmatrix},$$

the trace is $(-1) + (-1) + 1 = -1$.

The set of characters for a point group is called a **reducible representation (Γ)**. The reducible representation for the C_{2v} point group is:

C_{2v}	E	C_2	σ_v	σ'_v
Γ	3	−1	1	1

? Exercise 5.7.1

Prove that the characters in the reducible representation for C_{2v} are correct:

C_{2v}	E	C_2	σ_v	σ'_v
Γ	3	−1	1	1

Answer

For the E operation, with the transformation matrix $\begin{pmatrix}1&0&0\\0&1&0\\0&0&1\end{pmatrix}$, the trace is $1+1+1=3$.

For the C_2^z operation, with the transformation matrix $\begin{pmatrix}-1&0&0\\0&-1&0\\0&0&1\end{pmatrix}$, the trace is $(-1)+(-1)+1=-1$.

For the $\sigma_{v(xz)'}$ operation, with the transformation matrix $\begin{pmatrix}1&0&0\\0&-1&0\\0&0&1\end{pmatrix}$, the trace is $1+(-1)+1=1$.

For the $\sigma_{v(yz)''}$ operation, with the transformation matrix $\begin{pmatrix}-1&0&0\\0&1&0\\0&0&1\end{pmatrix}$, the trace is $-1+1+1=1$.

This gives the reducible representation

C_{2v}	E	C_2	σ_v	σ_v'
Γ	3	−1	1	1

Reducible and Irreducible Representations

Let us now go back and look in more detail at the transformation matrices of the C_{2v} point group that we derived above. If we look at the matrices carefully we see that they all take the same block diagonal form (a square matrix is said to be **block diagonal** if all the elements are zero except for a set of submatrices lying along the diagonal).

$$E=\begin{pmatrix}[1]&0&0\\0&[1]&0\\0&0&[1]\end{pmatrix},\ C_2=\begin{pmatrix}[-1]&0&0\\0&[-1]&0\\0&0&[1]\end{pmatrix},$$
$$\sigma'_{v(xz)}=\begin{pmatrix}[1]&0&0\\0&[-1]&0\\0&0&[1]\end{pmatrix},\ \sigma_{v(yz)''}=\begin{pmatrix}[-1]&0&0\\0&[1]&0\\0&0&[1]\end{pmatrix}$$

All the non-zero elements become 1x1 matrices that each represent individual x, y, z coordinates. In other words, the element a_{11} represents x, a_{22} represents y, and a_{33} represents z. The matrix elements for x from each transformation matrix combine to form an irreducible representation of the C_{2v} point group. Likewise, the matrix elements for y combine to form a second irreducible representation, and the same is true for z elements. These irreducible representations are shown below:

C_{2v}	E	C_2	σ_v	σ_v'	Coordinate Used
	1	−1	1	−1	x
	1	−1	−1	1	y
	1	1	1	1	z
Γ	3	−1	1	1	

The irreducible representations add to form the reducible representation, Γ. This Γ, which is the set of 3x3 matrices, can be reduced to the set of 1x1 matrices of the irreducible representations. The irreducible representations cannot be reduced further, hence their name.

Sources & Attribution

- Parts of this page was adapted from Matrices (click here) (Symmetry Operators), contributed by Marcia Levitus, Associate Professor (Biodesign Institute) at Arizona State University.
- Parts of this page were adapted from Reductions of Representations, contributed by

  Claire Vallance (University of Oxford)
- Curated or created by Kathryn Haas

5.7: Representations of Point Groups is shared under a not declared license and was authored, remixed, and/or curated by LibreTexts.

- **4.3.2: Representations of Point Groups** by Kathryn Haas is licensed CC BY-NC-SA 4.0.

5.8: Character Tables

Introduction to Character Tables, using C_{2v} as example

A character table is the complete set of irreducible representations of a symmetry group. In the previous section, we derived three of the four irreducible representations for the C_{2v} point group. These three irreducible representations are labeled A_1, B_1, and B_2. The fourth irreducible representation, A_2, can be derived using the properties (or "rules") for irreducible representations listed below.

Properties of Characters of Irreducible Representations in Point Groups

1. There is always a totally symmetric representation in which all the characters are 1.
   e.g. In C_{2v}, A_1 is totally symmetric.
2. The order of the group (h) is the total number of symmetry operations in the group.
   e.g. In C_{2v}, $h = 4$
3. Similar operations are listed as classes (R) and appear as columns in the table.
   e.g. In C_{2v}, there are four classes of operations, E, C_2, $\sigma_{v(xz)}$, and $\sigma'_{v(yz)}$
4. The number of irreducible representations (rows) must equal the number of classes (columns). This results in all character tables being square.
   e.g. In C_{2v}, there are four classes and four irreducible representations.
5. The sum of squares of all characters under E is equal to the order of the group: $h = \sum [\chi_i]^2$
   e.g. In C_{2v}, $h = 1^2 + 1^2 + 1^2 + 1^2 = 4$
6. For any irreducible representation (i), the sum of squares of its characters multiplied by the number of operations in the class is the order of the group: $h = \sum [\chi_i(R)]^2$
   e.g. For A_2 in C_{2v}, $h = (1 \times 1)^2 + (1 \times 1)^2 + (-1 \times 1)^2 + (-1 \times 1)^2 = 4$
7. Irreducible representations are orthogonal. For any two representations (i and j): $\sum [\chi_i * (R) \chi_j(R)] = 0$
   e.g. For B_1 and B_2 of C_{2v}, $[1 \times 1] + [-1 \times -1] + [1 \times -1] + [-1 \times 1] = 0$

The complete character table for C_{2v} is given below.

C_{2v}	E	C_2	σ_v	σ'_v	$h = 4$	
A_1	1	1	1	1	z	x^2, y^2, z^2
A_2	1	1	−1	−1	R_z	xy
B_1	1	−1	1	−1	x, R_y	xz
B_2	1	−1	−1	1	y, R_x	yz

The various sections of the table are as follows:

i. The first element in the table gives the name of the point group, usually in Schoenflies (C_{2v}) notation.
ii. Along the first row are the symmetry operations of the group, E, C_2, σ_v and σ_v'', followed by the order of the group, h.
iii. In the first column are the irreducible representations of the group, represented by Mulliken Labels. In C_{2v} the irreducible representations are A_1, A_2, B_1 and B_2. The Mulliken labels indicate the symmetry of each representation (explained further below).
iv. The characters (χ) of the irreducible representations under each symmetry operation are given in the bulk of the table.
v. The final column(s) of the table lists a number of functions that transform as the various irreducible representations of the group. These are the Cartesian axes (x, y, z), the Cartesian products ($z^2, x^2 + y^2, xy, xz, yz$), and the rotations ($R_x, R_y, R_z$) (explained further below).

Another example: C_{3v}

Th C_{3v} point group has three classes of operations: E, C_3, and $\sigma_{v(xz)}$. The derivation of transformation matrices for E and $\sigma_{v(xz)}$ is similar to the case for C_{2v}. However, the C_{3v} operation does not give simple 1 or -1 characters. If we carry out a rotation about z by an angle θ, our x and y axes are transformed onto new axes x' and y'. The new axes can each be written as a linear combination of our original x and y axes. The derivation of the rotation matrices will not be covered in this text, but is described elsewhere:

$$x' = x\cos\theta + y\sin\theta$$
$$y' = -x\sin\theta + y\cos\theta$$

For a C_3 rotation counterclockwise through 120° (or $\frac{2\pi}{3}$):

$$x' = x\cos(2\pi/3) + y\sin(2\pi/3) = -\tfrac{1}{2}x - \tfrac{\sqrt{3}}{2}y$$
$$y' = -x\sin(2\pi/3) + y\cos(2\pi/3) = \tfrac{\sqrt{3}}{2}x - \tfrac{1}{2}y$$

The transformation matrices for symmetry operations of C_{3v} are as follows:

$$E = \begin{pmatrix} 1 & 0 & 0 \\ 0 & 1 & 0 \\ 0 & 0 & 1 \end{pmatrix} \quad C_3 = \begin{pmatrix} -\frac{1}{2} & -\frac{\sqrt{3}}{2} & 0 \\ \frac{\sqrt{3}}{2} & -\frac{1}{2} & 0 \\ 0 & 0 & 1 \end{pmatrix} \quad \sigma'_{v(xz)} = \begin{pmatrix} 1 & 0 & 0 \\ 0 & -1 & 0 \\ 0 & 0 & 1 \end{pmatrix}$$

The C_3 transformation matrix contains off-diagonal entries, and therefore it cannot be block diagonalized as 1x1 matrices. However, the first two lines can be diagonalized as a 2x2 and the last line as a 1x1 matrix (Figure 5.8.1):

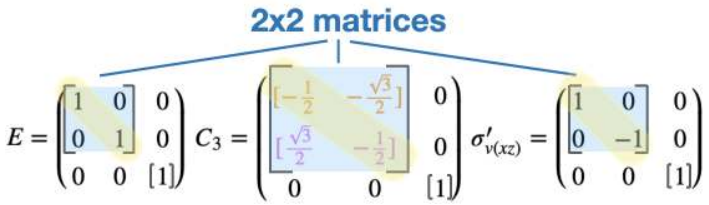


Figure 5.8.1: The C_3 transformation matrix contains off-diagonal entries, and therefore it cannot be block diagonalized as 1x1 matrices. However, the first two lines can be diagonalized as a 2x2 and the last line as a 1x1 matrix. (CC-BY-NC-SA; Kathryn Haas)

The character from a 2x2 matrix is the sum of the trace of that matrix. So, for the C_3 operation, the 2x2 matrix gives the character -1 (from $-\frac{1}{2} + -\frac{1}{2}$).

The character table for C_{3v} is shown below.

C_{3v}	E	$2C_3$	$3\sigma_v$	$h = 6$
A_1	1	1	1	$z, z^2, x^2 + y^2$
A_2	1	1	−1	R_z
E	2	−1	0	$(x, y), (xy, x^2 + y^2), (xz, yz), (R_x, R_y)$

Additional features of character tables

Additional Features of Character Tables

1. Symmetry operations of the same class are grouped into the same column (class) in the character table and not listed separately.
   e.g. In the C_{3v} point group, there are four operations: E, C_3, C_3^2, and σ_v. The C_3 and C_3^2 operations are listed together in the character table as $2C_3$.
2. IF there are multiple C_2 axes (in a D group), the C_2 axes that are perpendicular to the principle axis are labeled with primes (e.g. C_2' and C_2''); when there are multiple types of perpendicular C_2 axes, one prime (C_2') means that it passes through more atoms, while a double prime (C_2'') means it goes between atoms.
3. Mirror planes that are perpendicular to the principle axis are "horizontal" mirror planes and are designated with an h subscript (σ_h). Mirror planes that are in-plane with the principle axis are "vertical" mirror planes, σ_v. When there are two types of vertical mirror planes, those that run through more atoms are σ_v while those that run between atoms are "dihedral", σ_d.
4. Matching the symmetry operations listed in the character table to the symmetry operations of a molecule can confirm its point group.

5. Irreducible representations are each assigned a Mulliken label, listed in the left-hand column, that indicates the symmetry of that representation as follows:

Mulliken Labels	**meaning**
A	singly degenerate (1x1), symmetric to principle axis
B	singly degenerate (1x1), antisymmetric to principle axis
E	doubly degenerate (2x2)
T	triply degenerate (3x3)
Subscripts and superscripts	**meaning**
1	symmetric to $\sigma_v$or perpendicular to C_2
2	anti-symmetric to $\sigma_v$or perpendicular to C_2
g	symmetric to inversion center
u	anti-symmetric to inversion center
$'$	symmetric to σ_h
$''$	anti-symmetric to σ_h

6. The right-hand columns of the character table list a number of functions that transform as the various irreducible representations of the group. These are the Cartesian axes (x, y, z), the Cartesian products $(z^2, x^2 + y^2, xy, xz, yz)$, and the rotations (R_x, R_y, R_z). These expressions indicate the properties of orbitals within the symmetry group. The s-orbital, which is totally symmetric, corresponds to the irreducible representation that possesses symmetry of x^2, y^2 and z^2 combined. The p -orbitals each possess the symmetry of the corresponding axis (e.g. p_x corresponds to the x axis). Each of the d-orbitals possess the symmetry of the corresponding binary product (e.g. d_{xy} corresponds to the binary product, xy, in the character table).

The functions listed in the final column of the table are important in many chemical applications of group theory, particularly in spectroscopy. For example, by looking at the transformation properties of x, y and z (sometimes given in character tables as T_x, T_y, T_z) we can discover the symmetry of translations along the x, y, and z axes. Similarly, R_x, R_y and R_z represent rotations about the three Cartesian axes. The transformation properties of x, y, and z can be used to determine whether or not a molecule is IR-active or whether or not it can absorb a photon of x-, y-, or z-polarized light and undergo a spectroscopic transition. The Cartesian products play a similar role in determining selection rules for Raman transitions, which involve two photons.

A visual summary of the sections and their significance is given in Figure 5.8.2. Character tables for common point groups are given in the References section of LibreTexts Bookshelves.

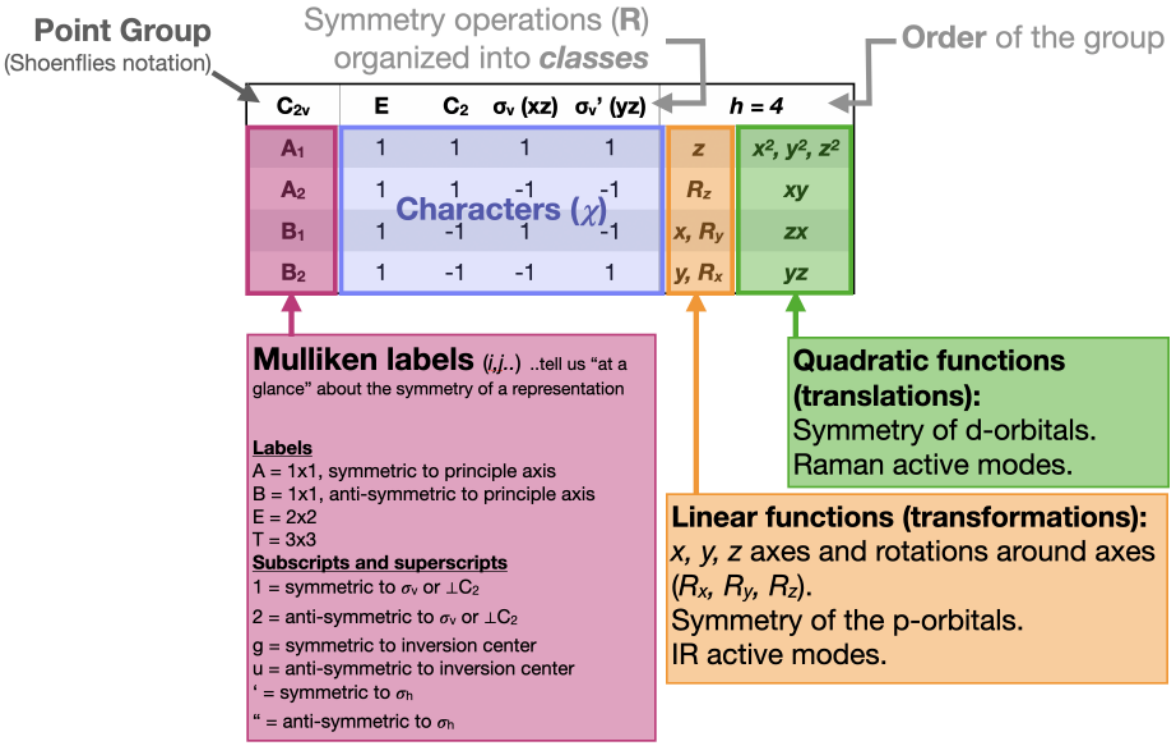


Figure 5.8.2: Visual summary of the sections of a character table and their meaning. (CC-BY-NC-SA; Kathryn Haas)

Contributors and Attributions

- Curated or created by Kathryn Haas
- Claire Vallance (University of Oxford)

  adapted from Character Tables (click here)

This page titled 5.8: Character Tables is shared under a not declared license and was authored, remixed, and/or curated by Kathryn Haas.

- **4.3.3: Character Tables** by Kathryn Haas is licensed CC BY-NC-SA 4.0.

SECTION OVERVIEW

5.9: Examples and Applications of Symmetry

The purpose of learning group theory is that molecular symmetry can be applied to understand the properties of molecules. This chapter introduces two applications of symmetry: chirality and molecular vibrations (in the context of analyzing IR and Raman spectra). An additional application of symmetry, to understand molecular bonding, deserves its own chapter and will be explored in Chapter 5.

5.9: Examples and Applications of Symmetry is shared under a not declared license and was authored, remixed, and/or curated by LibreTexts.

5.10: Chirality

Introduction

Around the year 1847, the French scientist Louis Pasteur provided an explanation for the optical activity of tartaric acid salts. When he carried out a particular reaction, Pasteur observed that two types of crystals precipitated. Patiently and carefully using tweezers, Pasteur was able to separate the two types of crystals. Pasteur noticed that the types rotated plane-polarized light by the same amount but in different directions. These two compounds are called enantiomers.

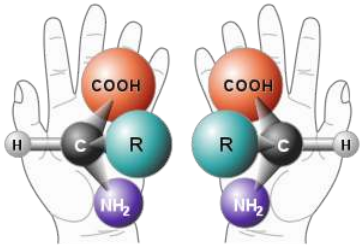


Figure 5.10.1: Two enantiomers of an amino acid (with side chain R).

What is chirality?

A molecule is **chiral** (or **dissymetric**) if it is non-superimposable on its mirror image. The two mirror images of a chiral molecule are called enantiomers. Enantiomers have the same physical properties (e.g., melting point, etc.). They differ in their ability to rotate plane polarized light and in their reactivity with other chiral molecules. Due to their ability to rotate plane polarized light, they are referred to as being *optically active*.

Using Symmetry to Determine Chirality

There are some general rules of thumb that help determine whether a molecule is chiral or achiral. The point group of the molecule, and the symmetry operations within that point group, can give clues as to whether the molecule is chiral.

Symmetry operations of chiral molecules

A chiral molecule cannot possess a plane of symmetry (σ), a center of inversion (i), or an improper rotation (S_n). Due to the fact that all groups that lack both σ and i also lack S_n, **a molecule that belongs to any group that lacks S_n is chiral**.

An example of an inorganic coordination complex is tris(ethylenediamine)cobalt(III) (Figure 5.10.1). Figure 5.10.1 shows the two enantiomers of tris(ethylenediamine)cobalt(III): the **Δ** and **Λ** isomers.

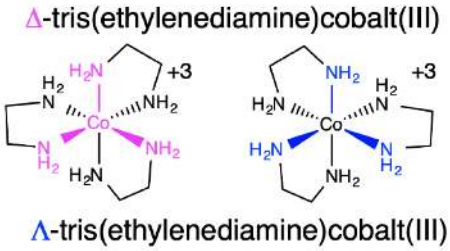


Figure 5.10.2: Two chiral enantiomers of tris(ethylenediamine)coalt(III).

You can visualize the **Λ** and **Δ** isomers by imagining that the ligands around the metal centers are blades of a fan. To push the air toward you, you would need to rotate the **Δ** isomer clockwise, and the **Λ** isomer counter-clockwise.

Exercise 5.10.1

Which point groups are possible for chiral molecules?

Answer

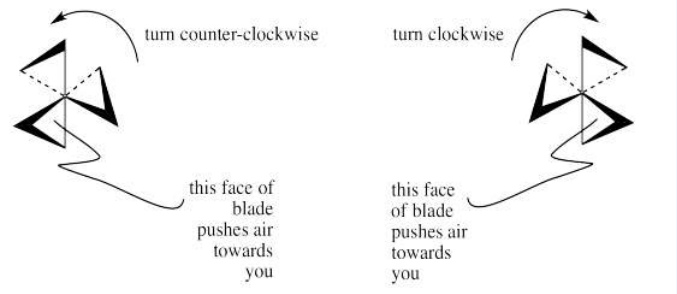


Figure **5.10.3**: Another way of thinking about the chirality of the two chiral enantiomers of tris(ethylenediamine)coalt(III) shown in Figure **5.10.2**. This figure was taken from Structure and Reactivity in Organic, Biological, and Inorganic Chemistry.

As a result of the previous discussion, there are a few classes of point groups that lack an improper axis. Those classes are C_1, C_n, and D_n.

5.10: Chirality is shared under a CC BY-NC 4.0 license and was authored, remixed, and/or curated by LibreTexts.

- **4.4.1: Chirality** by Kathryn Haas is licensed CC BY-NC 4.0.

5.11: Molecular Vibrations

Symmetry and group theory can be applied to understand molecular vibrations. This is particularly useful in the context of predicting the number of peaks expected in the infrared (IR) and Raman spectra of a given compound.

We will use water as a case study to illustrate how group theory is used to predict the number of peaks in IR and Raman spectra.

How many IR and Raman peaks would we expect for H_2O?

To answer this question with group theory, a pre-requisite is that you **assign the molecule's point group and assign an axis system** to the entire molecule. By convention, the z axis is collinear with the principle axis, the x axis is in-plane with the molecule or the most number of atoms. It is a good idea to stick with this convention (see Figure 5.11.1).

What is the point group for H_2O? (click to see answer)

H_2O has the following operations: E, C_2, σ_v, σ_v'. The point group is C_{2v}.

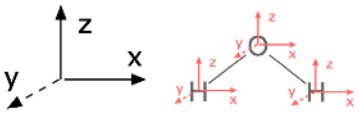


Figure 5.11.1: The first step to finding normal modes is to assign a consistent axis system to the entire molecule and to each atom. (CC-BY-SA; Kathryn Haas)

Now that we know the molecule's point group, we can use group theory to determine the symmetry of all motions in the molecule, or the symmetry of each of its degrees of freedom. Then we will subtract rotational and translational degrees of freedom to find the vibrational degrees of freedom. The number of degrees of freedom depends on the number of atoms (N) in a molecule. Each atom in the molecule can move in three dimensions (x, y, z), and so the number of degrees of freedom is three dimensions times N number of atoms, or $3N$. The total degrees of freedom include a number of vibrations, three translations (in x, y, and z), and either two or three rotations. Linear molecules have two rotational degrees of freedom, while non-linear molecules have three. The vibrational modes are represented by the following expressions:

$$\begin{aligned} \text{Linear Molecule Degrees of Freedom} &= 3N-5 \\ \text{Non-Linear Molecule Degrees of Freedom} &= 3N-6 \end{aligned}$$

Our goal is to find the symmetry of all degrees of freedom, and then determine which are vibrations that are IR- and Raman-active.

STEP 1: Find the reducible representation for all normal modes Γ_{modes}.

The first major step is to **find a reducible representation (Γ)** for the movement of all atoms in the molecule (including rotational, translational, and vibrational degrees of freedom). We'll refer to this as Γ_{modes}. To find normal modes using group theory, **assign an axis system** to each individual atom to represent the three dimensions in which each atom can move. Each axis on each atom should be consistent with the conventional axis system you previously assigned to the entire molecule (see Figure 5.11.1).

Γ_{modes} is the sum of the characters (trace) of the transformation matrix for the entire molecule (in the case of water, there are 9 degrees of freedom and this is now a 9x9 matrix). Let's walk through this step-by-step. The transformation matrix of E and C_2 are shown below:

$$E = \begin{pmatrix} 1 & 0 & 0 & 0 & 0 & 0 & 0 & 0 & 0 \\ 0 & 1 & 0 & 0 & 0 & 0 & 0 & 0 & 0 \\ 0 & 0 & 1 & 0 & 0 & 0 & 0 & 0 & 0 \\ 0 & 0 & 0 & 1 & 0 & 0 & 0 & 0 & 0 \\ 0 & 0 & 0 & 0 & 1 & 0 & 0 & 0 & 0 \\ 0 & 0 & 0 & 0 & 0 & 1 & 0 & 0 & 0 \\ 0 & 0 & 0 & 0 & 0 & 0 & 1 & 0 & 0 \\ 0 & 0 & 0 & 0 & 0 & 0 & 0 & 1 & 0 \\ 0 & 0 & 0 & 0 & 0 & 0 & 0 & 0 & 1 \end{pmatrix} \begin{pmatrix} x_{oxygen} \\ y_{oxygen} \\ z_{oxygen} \\ x_{hydrogen-a} \\ y_{hydrogen-a} \\ z_{hydrogen-a} \\ x_{hydrogen-b} \\ y_{hydrogen-b} \\ z_{hydrogen-b} \end{pmatrix} = \begin{pmatrix} x'_{oxygen} \\ y'_{oxygen} \\ z'_{oxygen} \\ x'_{hydrogen-a} \\ y'_{hydrogen-a} \\ z'_{hydrogen-a} \\ x'_{hydrogen-b} \\ y'_{hydrogen-b} \\ z'_{hydrogen-b} \end{pmatrix}, \chi = 9$$

$$C_2 = \begin{pmatrix} -1 & 0 & 0 & 0 & 0 & 0 & 0 & 0 & 0 \\ 0 & -1 & 0 & 0 & 0 & 0 & 0 & 0 & 0 \\ 0 & 0 & 1 & 0 & 0 & 0 & 0 & 0 & 0 \\ 0 & 0 & 0 & 0 & 0 & 0 & -1 & 0 & 0 \\ 0 & 0 & 0 & 0 & 0 & 0 & 0 & -1 & 0 \\ 0 & 0 & 0 & 0 & 0 & 0 & 0 & 0 & 1 \\ 0 & 0 & 0 & -1 & 0 & 0 & 0 & 0 & 0 \\ 0 & 0 & 0 & 0 & -1 & 0 & 0 & 0 & 0 \\ 0 & 0 & 0 & 0 & 0 & 1 & 0 & 0 & 0 \end{pmatrix} \begin{pmatrix} x_{oxygen} \\ y_{oxygen} \\ z_{oxygen} \\ x_{hydrogen-a} \\ y_{hydrogen-a} \\ z_{hydrogen-a} \\ x_{hydrogen-b} \\ y_{hydrogen-b} \\ z_{hydrogen-b} \end{pmatrix} = \begin{pmatrix} x'_{oxygen} \\ y'_{oxygen} \\ z'_{oxygen} \\ x'_{hydrogen-a} \\ y'_{hydrogen-a} \\ z'_{hydrogen-a} \\ x'_{hydrogen-b} \\ y'_{hydrogen-b} \\ z'_{hydrogen-b} \end{pmatrix}, \chi = 1$$

It is unnecessary to find the transformation matrix for each operation since it is only the TRACE that gives us the character, and any off-diagonal entries do not contribute to Γ_{modes}. The values that contribute to the trace can be found simply by performing each operation in the point group and assigning a value to each individual atom to represent how it is changed by that operation. If the atom moves away from itself, that atom gets a character of zero (this is because any non-zero characters of the transformation matrix are off of the diagonal). If the atom remains in place, each of its three dimensions is assigned a value of $\cos\theta$. For the example of H_2O under the C_{2v} point group, the axes that remain unchanged ($\theta = 0°$) are assigned a value of $\cos(0°) = 1$, while those that are moved into the negative of themselves (rotated or reflected to $\theta = 180°$) are assigned $\cos(180°) = -1$. The character for Γ is the sum of the values for each transformation.

Let's walk through the steps to assign characters of Γ_{modes} for H_2O to illustrate how this works:

For the operation E, performed on H_2O, all three atoms remain in place. The three axes x, y, z on each atom remain unchanged. Thus, each of the three axes on each of three atom (nine axes) is assigned the value $\cos(0°) = 1$, resulting in a sum of $\chi = 9$ for the Γ_{modes}.

For the operation C_2, the two hydrogen atoms are moved away from their original position, and so the hydrogens are assigned a value of zero. The oxygen remains in place; the z-axis on oxygen is unchanged ($\cos(0°) = 1$), while the x and y axes are inverted ($\cos(180°)$). The sum of these characters gives $\chi = -1$ in the Γ_{modes}.

Now you try! Find the characters of $\sigma_{v(xz)}$ and $\sigma_{v(yz)}$ under the C_{2v} point group. Compare what you find to the Γ_{modes} for all normal modes given below.

C_{2v}	E	C_2	σ_v	σ'_v
Γ_{modes}	9	−1	3	1

(5.11.1)

STEP 2: Break Γ_{modes} into its component irreducible representations.

Now that we've found the Γ_{modes} (5.11.1), we need to break it down into the individual irreducible representations ($i, j, k...$) for the point group. We can do this systematically using the following formula:

Misplaced '#'

In other words, the number of irreducible representations of type i is equal to the sum of the number of operations in the class × the character of the Γ_{modes} × the character of i, and that sum is divided by the order of the group (h).

Using equation ???, we find that for all normal modes of H_2O:

$$\Gamma_{modes} = 3A_1 + 1A_2 + 3B_1 + 2B_2 \tag{5.11.2}$$

.

Notice there are 9 irreducible representations in Equation 5.11.2. These irreducible representations represent the symmetries of all 9 motions of the molecule: vibrations, rotations, and translations.

? Exercise 5.11.1: Derive the irreducible representation in equation 5.11.2.

Derive the nine irreducible representations of Γ_{modes} for H_2O, expression 5.11.2.

Hint

To find the number of each kind of irreducible representation that combine to form the Γ_{modes}, we need the characters of Γ_{modes} that we found above (5.11.1), the C_{2v} character table (below), and equation ???.

C_{2v}	$1E$	$1C_2$	$1\sigma_v$	$1\sigma_v'$	$h=4$	
A_1	1	1	1	1	z	x^2, y^2, z^2
A_2	1	1	−1	−1	R_z	xy
B_1	1	−1	1	−1	x, R_y	xz
B_2	1	−1	−1	1	y, R_x	yz

In the C_{2v} point group, each class has only one operation, so the number of operations in each class (from equation ???) is 1 for each class. This has been explicitly added to the character table above for emphasis.

Answer

The number of $A_1 = \frac{1}{4}[(1\times 9\times 1) + (1\times(-1)\times 1) + (1\times 3\times 1) + (1\times 1\times 1)] = 3A_1$

The number of $A_2 = \frac{1}{4}[(1\times 9\times 1) + (1\times(-1)\times 1) + ((-1)\times 3\times 1) + ((-1)\times 1\times 1)] = 1A_2$

The number of $B_1 = \frac{1}{4}[(1\times 9\times 1) + ((-1)\times(-1)\times 1) + (1\times 3\times 1) + ((-1)\times 1\times 1)] = 3B_1$

The number of $B_2 = \frac{1}{4}[(1\times 9\times 1) + ((-1)\times(-1)\times 1) + ((-1)\times 3\times 1) + (1\times 1\times 1)] = 2B_2$

STEP 3: Subtract rotations and translations to find vibrational modes.

Because we are interested in molecular vibrations, we need to subtract the rotations and translations from the total degrees of freedom.

$$\text{Vibrations} = \Gamma_{modes} - \text{Rotations} - \text{Translations}$$

In the example of H_2O, the total degrees of freedom are given above in equation 5.11.2, and therefore the vibrational degrees of freedom can be found by:

$$H_2O \text{ vibrations} = (3A_1 + 1A_2 + 3B_1 + 2B_2) - \text{Rotations} - \text{Translations} \tag{5.11.3}$$

But which of the irreducible representations are ones that represent rotations and translations? The symmetry of rotational and translational degree modes can be found by inspecting the right-hand columns of any character table. Rotational modes correspond to irreducible representations that include R_x, R_y, and R_z in the table, while each of the three translational modes has the same symmetry as the x, y and z axes. For a non-linear molecule, subtract three rotational irreducible representations and three translational irreducible representations from the total Γ_{modes}.

In the specific case of water, we refer to the C_{2v} character table:

C_{2v}	E	C_2	σ_v	σ_v'	$h=4$	
A_1	1	1	1	1	z	x^2, y^2, z^2
A_2	1	1	−1	−1	R_z	xy
B_1	1	−1	1	−1	x, R_y	xz
B_2	1	−1	−1	1	y, R_x	yz

In C_{2v}, translations correspond to B_1, B_2, and A_1 (respectively for x, yz), and rotations correspond to B_2, B_1, and A_1 (respectively for R_x, R_y, R_z). Subtracting these six irreducible representations from Γ_{modes} will leave us with the irreducible representations for vibrations.

$$\begin{aligned} H_2O \text{ vibrations} &= \Gamma_{modes} - \text{Rotations} - \text{Translations} \\ &= (3A_1 + 1A_2 + 3B_1 + 2B_2) - (A_1 + B_1 + B_2) - (A_2 + B_1 + B_2) \\ &= 2A_1 + 1B_1 \end{aligned}$$

The three vibrational modes for H_2O are $2A_1 + 1B_1$. Note that we have the correct number of vibrational modes based on the expectation of $3N - 6$ vibrations for a non-linear molecule.

STEP 4: Determine which of the vibrational modes are IR-active and Raman-active.

The next step is to determine which of the vibrational modes is IR-active and Raman-active. To do this, we apply the IR and Raman Selection Rules below:

IR and Raman Selection Rules

Infrared selection rules:

If a vibration results in the change in the molecular dipole moment, it is IR-active. In the character table, we can recognize the vibrational modes that are IR-active by those with symmetry of the x, y, and z axes.

In C_{2v}, any vibrations with A_1, B_1 or B_2 symmetry would be IR-active.

Raman selection rules:

If a vibration results in a change in the molecular polarizability, it will be Raman-active. In the character table, we can recognize the vibrational modes that are Raman-active by those with symmetry of any of the binary products (xy, xz, yz, x^2, y^2, and z^2) or a linear combination of binary products (e.g. $x^2 - y^2$).

In C_{2v}, any vibrations with A_1, A_2, B_1 or B_2 symmetry would be Raman-active.

In our H_2O example, we found that of the three vibrational modes, two have A_1 and one has B_1 symmetry. Both A_1 and B_1 are IR-active, and both are also Raman-active. ***There are two possible IR peaks and three possible Raman peaks expected for water***.*

*It is important to note that this prediction tells only what is possible, but not what we might actually see in the IR and Raman spectra. For example, if the two IR peaks overlap, we might actually notice only one peak in the spectrum. Or, if one or more peaks is off-scale, we wouldn't see it in actual data. Group theory tells us what is *possible and allows us to make predictions or interpretations of spectra*.

Summary of Analysis for Water

Each molecular motion for water, or any molecule, can be assigned a symmetry under the molecule's point group. For water, we found that there are a total of 9 molecular motions; $3A_1 + A_2 + 3B_1 + 2B_2$. Six of these motions are not the translations and rotations. The remaining motions are vibrations; two with A_1 symmetry and one with B_1 symmetry.

We can tell what these vibrations would look like based on their symmetries. The two A_1 vibrations must be completely symmetric, while the B_1 vibration is antisymmetric with respect to the principal C_2 axis.

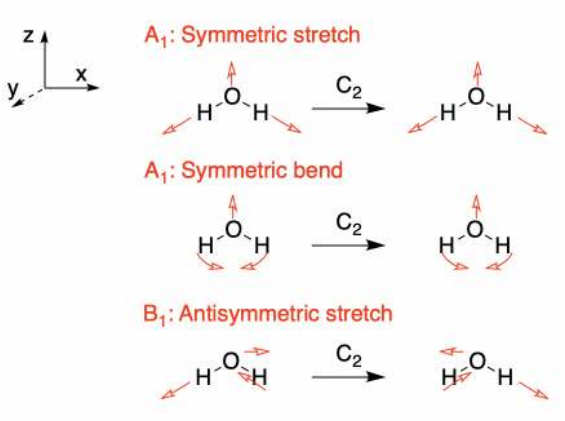


Figure 5.11.2: Illustration of the vibrational motions of water. The antisymmetric stretch has B_1 symmetry, while the symmetric stretch and symmetric bend both have A_1 symmetry. (Click here to see animation) (CC-BY-NC-SA; Kathryn Haas)

Table 5.11.1: Summary of the Symmetry of Molecular Motions for Water

All Motions (step 2 above)	Translations (x,y,z)	Rotations (R_x, R_y, R_z)	**Remaining Vibrations**	Description of Vibration
$3A_1$	$1A_1$		$2A_1$	One is a symmetric stretch. The other is a symmetric bend. Both are *IR-active* and *Raman-active*
A_2		$1A_2$		
$3B_1$	$1B_1$	$1B_1$	$1B_1$	Antisymmetric stretch that is *IR-active* and *Raman-active*.
$2B_2$	$1B_2$	$1B_2$		

? Exercise 5.11.2

Find the symmetries of all motions of the square planar complex, tetrachloroplatinate (II). Determine which are rotations, translations, and vibrations. Determine which vibrations are IR and Raman active.

Answer

The point group of $[PtCl_4]^{2-}$ is D_{4h} (refer to its character table). There are five atoms and 15 vectors (x, y, z for each atom × 5 atoms).

STEP 1: The first major step is to **find a reducible representation (Γ)** for the movement of all atoms in the molecule.

C_{2v}	E	$2C_4$	C_2	$2C_2'$	$2C_2''$	i	$2S_4$	σ_h	$2\sigma_v$	$2\sigma_d$
Γ_{modes}	15	1	−1	−3	−1	−3	−1	5	3	1

(5.11.4)

.

STEP 2: Break Γ_{modes} into its component irreducible representations.

Following the process described earlier, we come to $A_{1g} + A_{2g} + B_{1g} + B_{2g} + E_g + 2A_{2u} + B_{2u} + 3E_u$. This accounts for all modes of movement, including rotations and translations.

STEP 3: Subtract rotations and translations to find vibrational modes.

The translations are $A_{2u} + E_u$ and the rotations are $A_{2g} + E_g$.
The remaining normal modes are: $A_{1g} + B_{1g} + B_{2g} + A_{2u} + B_{2u} + 2E_u$

STEP 4: Determine which of the vibrational modes are IR-active and Raman-active:

$A_{2u} + E_u$ are IR-active. Since A_{2u} is singly degenerate and E_u is doubly degenerate, we expect three possible IR bands.
$A_{1g} + B_{1g} + B_{2g}$ are Raman-Active. Each of these is singly degenerate, so we expect three possible Raman bands.

Selected Vibrational Modes

The interpretation of CO stretching vibrations in an IR spectrum is particularly useful. Symmetry and group theory can be applied to predict the number of CO stretching bands that appear in a vibrational spectrum for a given metal coordination complex. A classic example of this application is in distinguishing isomers of metal-carbonyl complexes. For example, the *cis*- and *trans*-isomers of square planar metal dicarbonyl complexes ($ML_2(CO)_2$) have a different number of IR stretches that can be predicted and interpreted using symmetry and group theory. Another example is the case of *mer*- and *fac*- isomers of octahedral metal tricarbonyl complexes ($ML_3(CO)_3$). Structures of the two types of metal carbonyl configurations and their isomers are shown in Figure 5.11.1. The isomers in each case can be distinguished using vibrational spectroscopy.

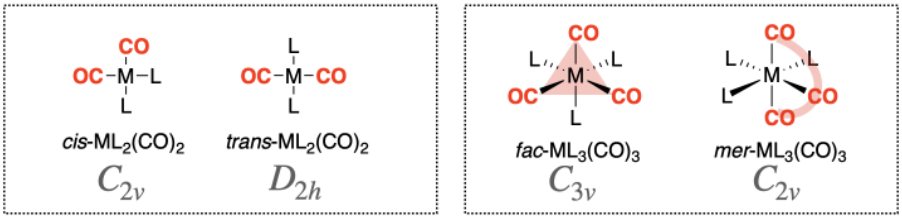


Figure 5.11.3: Cis- and *trans*- isomers of square planar metal dicarbonyl complexes ($ML_2(CO)_2$) are shown in the left box. *Mer*- and *fac*- isomers of octahedral metal tricarbonyl complexes ($ML_3(CO)_3$) are shown in the right box. The point group for each of the general structures is also shown. (CC-BY-NC-SA; Kathryn Haas)

EXAMPLE 1: Distinguishing *cis*- and *trans*- isomers of square planar metal dicarbonyl complexes

General structures of the *cis*- and *trans*- isomers of square planar metal dicarbonyl complexes ($ML_2(CO)_2$) are shown in the left box in Figure 5.11.1. We can use symmetry and group theory to predict how many carbonyl stretches we should expect for each isomer following the steps below.

Step 1: Assign the point group and Cartesian coordinates for each isomer.

The *cis*-isomer has C_{2v} symmetry and the *trans*-isomer has D_{2h} symmetry. We assign the Cartesian coordinates so that z is colinear with the principle axis in each case. For the D_2h isomer, there are several orientations of the z axis possible. The axes shown in Figure 5.11.2 will be used here.



Figure 5.11.4: Cis- and *trans*- isomers of square planar metal dicarbonyl complexes ($ML_2(CO)_2$) are shown and oriented with respect to the Cartesian coordinates shown at the left so that the highest-order rotation axis is colinear with z and the molecule is co-planar with the xz plane. The vector along each C—O bond is shown using a red arrow (→). These vectors represent the direction of C—O stretching motions. (CC-BY-NC-SA; Kathryn Haas)

Step 2: Produce a reducible representation (Γ) for CO stretches in each isomer

First, assign a vector along each C—O bond in the molecule to represent the direction of C—O stretching motions, as shown in Figure 5.11.2 (red arrows →). These vectors are used to produce a reducible representation (Γ) for the C—O stretching motions in each molecule. Using the symmetry operations under the appropriate character table, assign a value of 1 to each vector that remains in place during the operation, and a value of 0 if the vector moves out of place. There will be no occasion where a vector remains in place but is inverted, so a value of -1 will not occur.

cis- $ML_2(CO)_2$:

For *cis*- $ML_2(CO)_2$, the point group is C_{2v} and so we use the operations under the C_{2v} character table to create the Γ_{cis-CO}.

C_{2v}	E	C_2	$\sigma_v(xz)$	$\sigma_v'(yz)$
Γ_{cis-CO}	2	0	2	0

trans- $ML_2(CO)_2$:

For trans- $ML_2(CO)_2$, the point group is D_{2h} and so we use the operations under the D_{2h} character table to create the $\Gamma_{trans-CO}$.

D_{2h}	E	$C_2(z)$	$C_2(y)$	$C_2(x)$	i	$\sigma(xy)$	$\sigma(xz)$	$\sigma(yz)$
$\Gamma_{trans-CO}$	2	0	0	2	0	2	2	0

Step 3: Break each Γ into its component irreducible representations

Each Γ can be reduced using inspection or by the systematic method described previously.

In the case of the *cis*- $ML_2(CO)_2$, the CO stretching vibrations are represented by A_1 and B_1 irreducible representations:

C_{2v}	E	C_2	$\sigma_v(xz)$	$\sigma_v'(yz)$		
Γ_{cis-CO}	2	0	2	0		
A_1	1	1	1	1	z	x^2, y^2, z^2
B_1	1	−1	1	−1	x, R_y	xz

(5.11.5)

In the case of *trans*- $ML_2(CO)_2$, the CO stretching vibrations are represented by A_1 and B_{3u} irreducible representations:

D_{2h}	E	$C_2(z)$	$C_2(y)$	$C_2(x)$	i	$\sigma(xy)$	$\sigma(xz)$	$\sigma(yz)$	
$\Gamma_{trans-CO}$	2	0	0	2	0	2	2	0	
A_g	1	1	1	1	1	1	1	1	$x^2,\ y^2,\ z^2$
B_{3u}	1	−1	−1	1	−1	1	1	−1	x

These irreducible representations correspond to the symmetries of only the selected C—O vibrations. Since these motions are isolated to the C—O group, they do not include any rotations or translations of the entire molecule, and so we do not need to find and subtract rotationals or translations (unlike the previous cases where all motions were considered).

Step 4: Determine which vibrational modes are IR-active and/or Raman-active

Apply the infrared selection rules described previously to determine which of the CO vibrational motions are IR-active and Raman-active. The two isomers of $ML_2(CO)_2$ are described below.

In the case of the *cis*- $ML_2(CO)_2$, the CO stretching vibrations are represented by A_1 and B_1 irreducible representations. The characters of both representations and their functions are shown above, in 5.11.5 (and can be found in the C_{2v} character table). Under C_{2v}, both the A_1 and B_1 CO vibrational modes are IR-active and Raman-active. Therefore, two bands in the IR spectrum and two bands in the Raman spectrum are possible.

In the case of the trans- $ML_2(CO)_2$, the CO stretching vibrations are represented by A_g and B_{3u} irreducible representations. The characters of both representations and their functions are shown above, in 5.11.5 (and can be found in the D_{2h} character table). Under D_{2h}, the A_g vibrational mode is is Raman-active only, while the B_{3u} vibrational mode is IR-active only. Therefore, only one IR band and one Raman band are possible for this isomer.

Summary

It is possible to distinguish between the two isomers of square planar $ML_2(CO)_2$ using either IR or Raman vibrational spectroscopy. The *cis*- $ML_2(CO)_2$ can produce two CO stretches in an IR or Raman spectrum, while the *trans*- $ML_2(CO)_2$ isomer can produce only one band in either type of vibrational spectrum. If a sample of $ML_2(CO)_2$ produced two CO stretching bands, we could rule out the possibility of a pure sample of *trans*-$ML_2(CO)_2$.

Exercise 5.11.3

Repeat the steps outlined above to determine how many CO vibrations are possible for *mer*-$ML_3(CO)_3$ and *fac*-$ML_3(CO)_3$ isomers (see Figure **5.11.1**) in both IR and Raman spectra. Could either of these vibrational spectroscopies be used to distinguish the two isomers?

Answer

Step 1: Assign the point group and Cartesian coordinates for each isomer.
The *fac*-isomer is C_{3v}. The *mer*-isomer is C_{2v}.

Step 2: Produce a reducible representation for CO stretches in each isomer.

Step 3: Break each into its component irreducible representations.

Step 4: Determine which vibrational modes are IR-active and/or Raman-active.

***For fac*-$ML_3(CO)_3$**, the point group is C_{3v} and so we use the operations under the C_{3v} character table to create the Γ_{fac-CO}. Then break it into its irreducible representations and determine which are IR and Raman active:

C_{3v}	E	$2C_2$	$3\sigma_v$
Γ_{fac-CO}	3	0	1

This reduces to $A_1 + E$. Both of these are IR active, and since one is singly degenerate while the other is doubly degenerate, we expect three possible IR bands from this isomer. Both vibrational modes are also Raman active, and again we would expect three possible bands in the Raman spectrum.

For mer-$ML_3(CO)_3$, the point group is C_{2v} and so we use the operations under the C_{2v} character table to create the Γ_{mer-CO}. Then break it into its irreducible representations and determine which are IR and Raman active:

C_{2v}	E	C_2	$\sigma_v(xz)$	$\sigma'_v(yz)$
Γ_{mer-CO}	3	1	3	1

This reduces to $2A_1 + B_1$; both A_1 and B_1 are IR and Raman active. So this isomer would have three possible IR bands and three possible Raman Bands.

These two isomers have the same number of possible bands in both IR and Raman spectroscopy. It would not be straightforward to distinguish them from each other based on the number of possible bands in the vibrational spectrum.

This page titled 5.11: Molecular Vibrations is shared under a CC BY-NC 4.0 license and was authored, remixed, and/or curated by Kathryn Haas.

- **4.4.2: Molecular Vibrations** by Kathryn Haas is licensed CC BY-NC 4.0.

CHAPTER OVERVIEW

6: Molecular Orbitals

6.1: Formation of Molecular Orbitals from Atomic Orbitals
6.2: Molecular Orbitals from s Orbitals
6.3: Molecular Orbitals from p Orbitals
6.4: Molecular orbitals from d orbitals
6.5: Nonbonding Orbitals and Other Factors
6.6: Homonuclear Diatomic Molecules
6.7: Molecular Orbitals
6.8: Orbital Mixing
6.9: Diatomic Molecules of the First and Second Periods
6.10: Heteronuclear Diatomic Molecules
6.11: Orbital ionization energies
6.12: Polar bonds
6.13: Larger (Polyatomic) Molecules
6.14: Bifluoride anion
6.15: Carbon Dioxide
6.16: H_2O
6.17: NH_3
6.18: CO_2 (Revisted with Projection Operators)
6.19: BF_3
6.20: Ionic Compounds and Molecular Orbitals

6: Molecular Orbitals is shared under a not declared license and was authored, remixed, and/or curated by LibreTexts.

6.1: Formation of Molecular Orbitals from Atomic Orbitals

Molecular orbital theory extends from quantum theory and the atomic orbital wavefunctions (ψ) described by the Schrödinger equation. While the Schrödinger equation defines a Ψ for electrons in individual atoms, we can approximate the molecular wavefunction (what Ψ would look like if we combined the ψ of individual atoms). The addition or subtraction of wavefunctions is termed **linear combination of atomic orbitals** (LCAO). Molecular orbital theory is applied to LCAO to describe bonding.

The LCAO for the wavefunction of two atoms (ψ_a and ψ_b) is represented by the general expression below. The coefficients c_a and c_b quantify the contribution of each atomic ψ to the molecular Ψ.

$$\Psi = c_a\psi_a + c_b\psi_b$$

For two atomic ψs to form a bond, three conditions must be satisfied:

- First, the **distance between the atoms** must be small enough to provide good overlap. This is because the two orbitals must be able to overlap using regions of ψ^2 where the probability of finding electrons is significant. If atoms are not close enough, ψ_a and ψ_b cannot interact productively. At the same time, the atoms must be far enough apart that their nuclei do not repel each other.
- The **symmetry of the orbitals** must be compatible such that regions of ψ_a and ψ_b with the same sign constructively interfere more than regions with opposite sign destructively interfere. In other words, for a productive interaction, there must be a relatively high probability of finding an electron between the two nuclei, and this depends on the symmetry (and sign of the ψ) of the atomic orbitals.
- Third, the **energies of the atomic orbitals** must be similar. Orbitals with similar energy combine to make the most stable bonding molecular orbitals. Atomic orbitals with very different energies form less stable bonding interactions, and the larger the difference in the atomic orbitals, the weaker the bonding interaction will be.

Atomic orbitals combine to form molecular orbitals when these three conditions are met. The result is a set of bonding molecular orbitals that are lower in energy than the original atomic orbital energies.

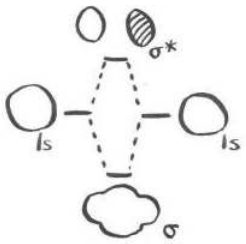
This page titled 6.1: Formation of Molecular Orbitals from Atomic Orbitals is shared under a CC BY-SA 4.0 license and was authored, remixed, and/or curated by Kathryn Haas.

- **5.1: Formation of Molecular Orbitals from Atomic Orbitals** by Kathryn Haas is licensed CC BY-SA 4.0.

6.2: Molecular Orbitals from s Orbitals

In the case of the hydrogen molecule, we took two atomic orbitals and combined them to form two molecular orbitals. These new molecular orbitals had different wavelengths than the two atomic orbitals: one had a longer wavelength and was a little lower in energy, while the other had a shorter wavelength and was a little higher in energy. If we take into account the energy of the two original atomic wavefunctions, and compare them to the total energy of the two new molecular wavefunctions, there is no change overall.

We started with two atomic orbitals, and by combining them we produced two molecular orbitals. Both of these ideas are useful in considering the formation of more complex molecules from individual atoms.

- - The average energy of the orbitals has remained almost constant.
  - Also, the number of wavefunctions has remained constant.
  - 

Of course, from the point of view of the two real electrons, some remarkable changes have occurred. Both of these electrons have adopted a longer wavelength and a lower energy and that has made all the difference. There is an occupied molecular orbital and an unoccupied molecular orbital; only the occupied orbital makes a real energetic contribution to the overall stability of the molecule. The unoccupied orbital is completely imaginary.

A bonding picture of He_2 would look exactly the same, because it would also involve the overlap of 1s electrons on one atom with 1s electrons on the other atom. There would be a different electronic energy, however. That difference would affect the prospects of helium-helium bond formation.

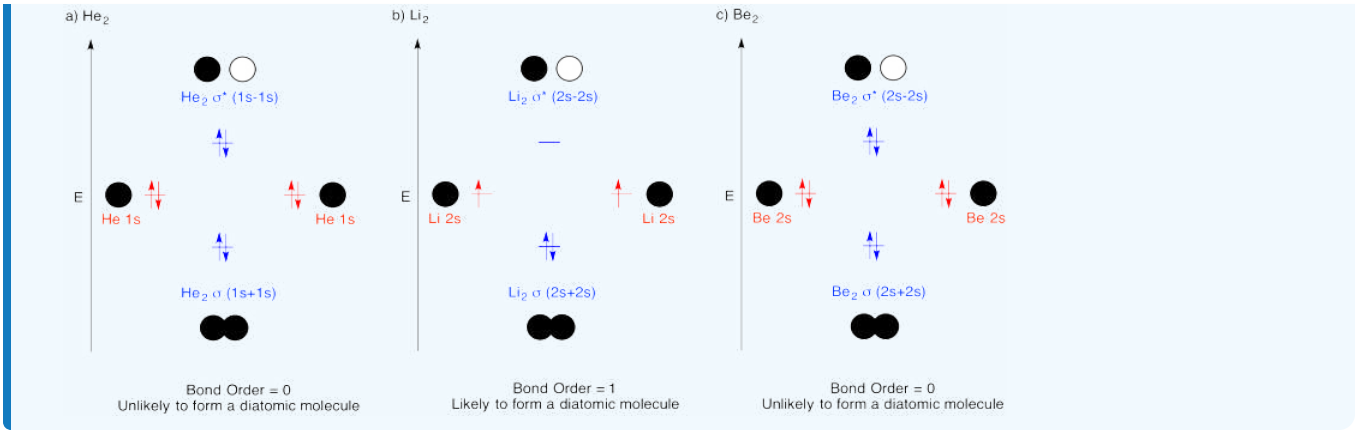
- The electrons have lower kinetic energy in the bond than they had before bonding.
- Electronic energy has decreased. A stable bond has formed.

? Exercise 6.2.1

Construct molecular orbital diagrams for the following diatomic species and discuss the likelihood of bond formation in each case.

a. He_2.
b. Li_2.
c. Be_2.

Answer



This page titled 6.2: Molecular Orbitals from s Orbitals is shared under a CC BY-SA 4.0 license and was authored, remixed, and/or curated by Chris Schaller & Kathryn Haas.

6.3: Molecular Orbitals from p Orbitals

Bonding with P-orbitals

Sigma bonding with p-orbitals

Other diatomic molecules in the upper right corner of the periodic table can be constructed in a similar way. Look at dinitrogen, N_2.

We can think about how dinitrogen would form if two nitrogen atoms were placed close enough together to share electrons. Nitrogen has more electrons than hydrogen, so this interaction is more complicated.

In our qualitative examination of bonding in main group diatomics, we will take the approach used in Lewis structures and just look at the valence electrons. A quantitative molecular orbital calculation with a computer would not take this shortcut, but would include all of the electrons in the atoms that are bonding together.

Nitrogen has five valence electrons, and these electrons are found in the 2s and 2p levels. There are three possible atomic orbitals in the 2p level where some of these electrons could be found: p_x, p_y and p_z. We need to look at the interaction between the s and p_x, p_y and p_z orbitals on one nitrogen atom with the s and p_x, p_y and p_z orbitals on the other nitrogen. That process could be extremely complicated, but:

- Orbital interactions are governed by symmetry.

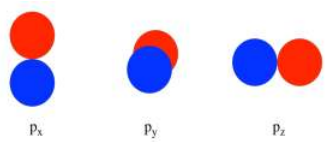
Orbitals interact most easily with other orbitals that have the same element of symmetry. For now, we can simplify and say that orbitals on one atom only interact with the same type of orbitals on the other atom.

- s orbitals interact with s orbitals. We can already see how that will work out in dinitrogen, because that is what happened in dihydrogen.
- p_x orbitals interact with p_x orbitals.
- p_y orbitals interact with p_y orbitals.
- p_z orbitals interact with p_z orbitals.

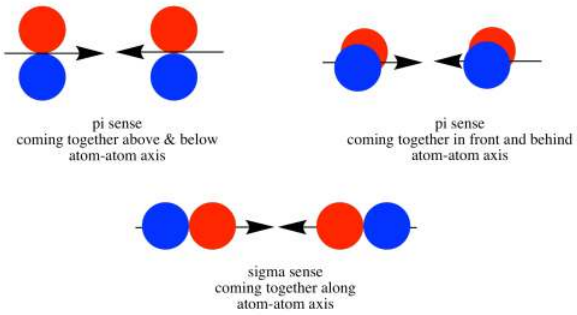
Another complication here is that the s and p orbitals do not start out at the same energy level. When the orbitals mix, one combination goes up in energy and one goes down. Does the s antibonding combination go higher in energy than the combinations from p orbitals? Do the p bonding combinations go lower in energy than the combinations from s orbitals? We will **simplify** and **assume** that the s and p levels remain completely separate from each other. This is not always true, but the situation varies depending on what atoms we are dealing with.

- The combination of one s orbital with another is just like in hydrogen. Two original orbitals will combine and rearrange to produce two new orbitals.
- There is a bonding combination in which the orbitals are in phase. The new orbital produced has a longer wavelength than the original orbital. It is lower in energy.
- There is an antibonding combination in which the orbitals are out of phase. The new orbital produced has a shorter wavelength than the original orbital. It is higher in energy.

In considering the interaction of two p orbitals, we have to keep in mind that p orbitals are directional. A p orbital lies along a particular axis: x, y or z. The three p orbitals on nitrogen are all mutually perpendicular (or orthogonal) to each other. That situation is in contrast to s orbitals, which are spherical and thus look the same from any direction.

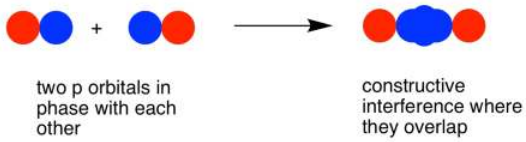


We first need to define one axis as lying along the N-N bond. It does not really matter which one. We arbitrarily say the N-N bond lies along the z axis. The p_z orbitals have a different spatial relationship to each other compared to the p_y and p_x. The p_z orbitals lie along the bond axis, whereas the p_y and p_x are orthogonal to it.

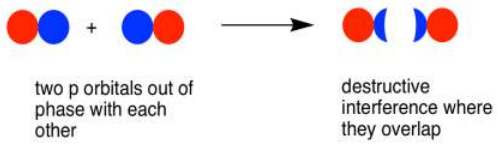


As the nitrogen atoms are brought together, one lobe on one p_z orbital overlaps strongly with one lobe on the other p_z orbital. The other lobes point away from each other and do not interact in any obvious way.

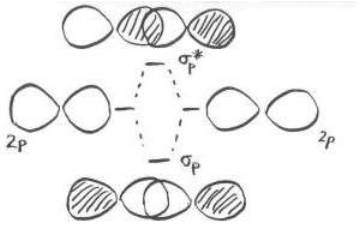
As with the s orbital, the p_z orbitals can be in-phase or out-of-phase. The in-phase combination results in constructive interference. (Here, "in-phase" means the lobes that overlap are in-phase; for that to happen the two p orbitals are actually completely out-of-phase with each other mathematically, so that one orbital is the mirror image of the other.) This combination is at a longer wavelength than the original orbital. It is a lower energy combination.



The out-of-phase combination (meaning in this case that the overlapping lobes are out-of-phase) results in destructive interference. This combination is at shorter wavelength than the original orbital. It is a higher energy combination.



As a result, we have two different combinations stemming from two different p orbitals coming together in two different ways. We get a low-energy, in-phase, bonding combination and a high-energy, out-of-phase, antibonding combination.

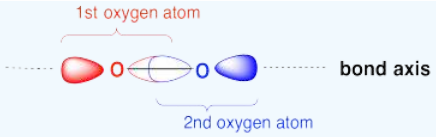


What about those other p orbitals, the ones that do not lie along the bond axis? We'll take a look at that problem on the next page.

? Exercise 6.3.2

Draw an MO cartoon of a sigma bonding orbital formed by the overlap of two p orbitals between two oxygen atoms. Label the positions of the oxygen nuclei with the symbol "O". Label the O-O bond axis.

Answer



Exercise 6.3.3

Chemical reactions can be described by MO diagrams too! Consider the following reaction in which a new sigma bond is formed.



Draw an MO diagram for the reaction above. In other words, start from the one frontier MO on each reactant to build the MO's of the new sigma bond in the product.

o Draw the orbital from the base (hydroxide) that is likely to donate its electrons.

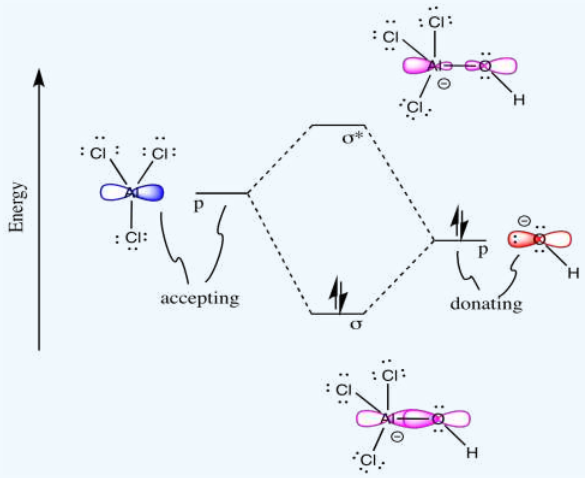
o Draw the orbital from the acid (aluminum chloride) that is likely to accept electrons.

o Complete the MO mixing diagram of these two orbitals:

- Label the electron donating orbital
- Label the electron accepting orbital
- Populate the MO mixing diagram with electrons

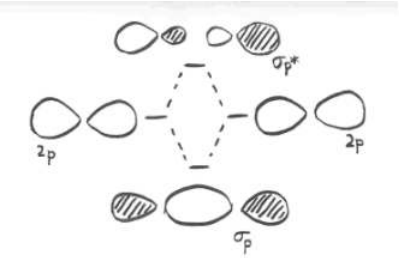
o Draw a cartoon showing each reactant and product MO that contributes to the bonding interaction.

Answer



Pi-bonding with p-orbitals

Earlier, we saw that p orbitals that lie along the same axis can interact to form bonds.



Parallel, but not collinear, p orbitals can also interact with each other. They would approach each other side by side, above and below the bond axis between the two atoms. They can be close enough to each other to overlap, although they do not overlap as strongly as orbitals lying along the bond axis. They can make an in-phase combination, as shown below.

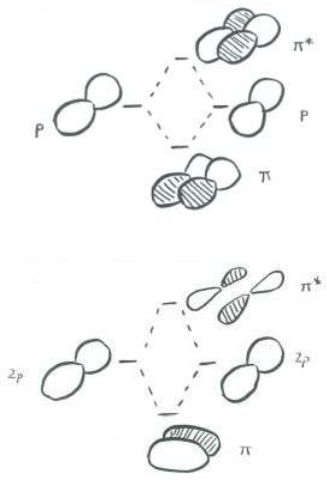


They could also make an out-of-phase combination, as shown below.



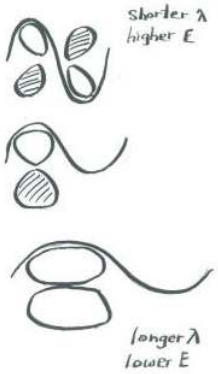
- parallel p orbitals can overlap to produce bonding and antibonding combinations.
- the resulting orbitals contain nodes along the bond axis.
- the electron density is found above and below the bond axis.
- this is called a p (pi) bond.

The illustration above is for one set of p orbitals that are orthogonal to the bond axis. The second picture shows the result of the constructive (or destructive) interference. A similar picture could be shown for the other set of p orbitals.

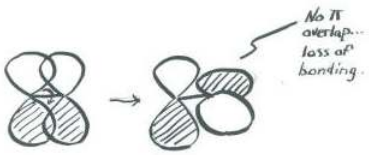


In a main group diatomic species like dinitrogen, one p orbital lying along the bond axis can engage in s bonding. The two p orbitals orthogonal to the bond axis can engage in p bonding. There will be both bonding and antibonding combinations.

Just as the sigma-bonding orbitals display progressively shorter wavelengths along the bonding axis as they go to higher energy, so do the pi bonding orbitals. In other words, there are more nodes in the higher-energy orbitals than in the lower-energy ones.



An important consequence of the spatial distribution or "shape" of a p orbital is that it is not symmetric with respect to the bond axis. An s orbital is not affected when the atom at one end of the bond is rotated with respect to the other. A p orbital is affected by such a rotation. If one atom turns with respect to the other, the p orbital would have to stretch to maintain the connection. The orbitals would not be able to overlap, so the connection between the atoms would be lost.



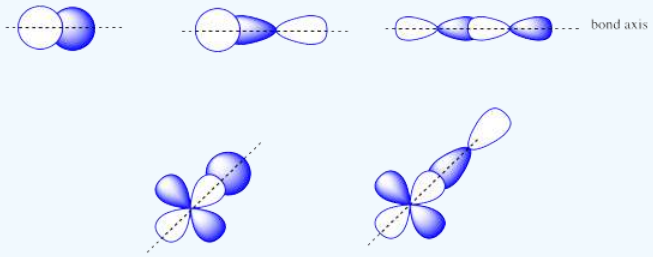
? Exercise 6.3.4

The combinations of _____ atomic orbitals leads to σ orbitals.

Draw pictures.

Answer

The combinations of ***s*** + ***s*** OR ***s*** + ***p*** OR ***p*** + ***p*** OR ***s*** + ***d*** OR ***p*** + ***d*** atomic orbitals can lead to σ orbitals.



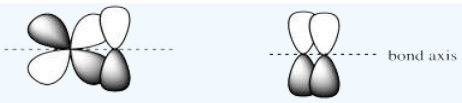
? Exercise 6.3.5

The combinations of _____ atomic orbitals leads to π orbitals.

Draw pictures.

Answer

The combinations of side by side p + p or p + d atomic orbitals leads to π orbitals.



Exercise 6.3.6

Which molecular orbital is typically the highest in energy?

a. p
b. σ
c. π*
d. π
e. σ*

Answer

e) σ*

Exercise 6.3.7

Why would a *core* 1s orbital not interact with a *valence* 2s orbital?

Hint: Why is a Li_2O bond stronger than a K_2O bond?

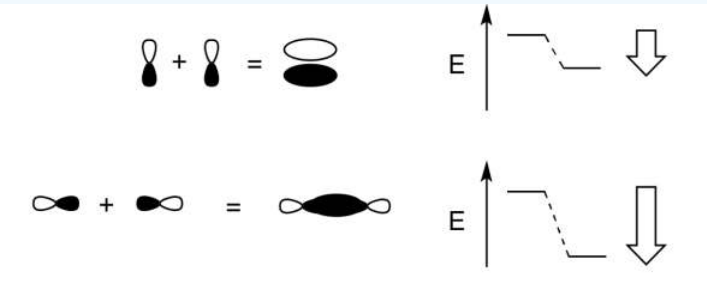
Answer

Li^+ and O^{2-} are more similar in size than K^+ and O^{2-}, so the bond between Li^+ and O^{2-} is stronger.

The energy difference between any core orbitals and valence orbitals is too large, so they cannot interact. In order for orbitals to interact, the orbitals need to have the same symmetry, be in the same plane, and be similar in energy.

Exercise 6.3.8

Add a few words to explain the ideas conveyed in these drawings.



Answer

When two parallel p orbitals combine out-of-phase, destructive interference occurs.

There is a node between the atoms.

The energy of the electrons increases.

When two parallel p orbitals combine in-phase, constructive interference occurs.

There is no node between the atoms; the electrons are found above and below the axis connecting the atoms.

The energy of the electrons decreases.

https://chem.libretexts.org/@go/page/403041

Attribution

Chris P Schaller, Ph.D., (College of Saint Benedict / Saint John's University)

Curated or created by Kathryn Haas

This page titled 6.3: Molecular Orbitals from p Orbitals is shared under a CC BY-SA 4.0 license and was authored, remixed, and/or curated by Chris Schaller.

- **5.1.2: Molecular Orbitals from p Orbitals** by Chris Schaller is licensed CC BY-NC 3.0.

6.4: Molecular orbitals from d orbitals

In transition metals and other heavier elements, the d orbitals may combine with other orbitals of compatible symmetry (and energy) to form molecular orbitals. Generally, there are three types of bonding and antibonding interactions that may occur with d orbitals: sigma (σ), pi (π), and delta (δ) bonds.

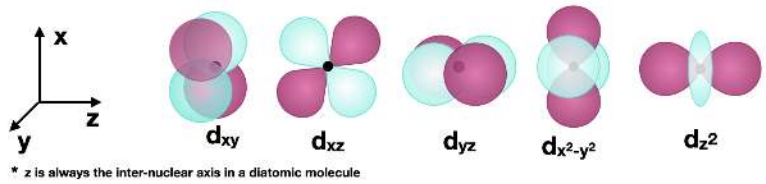


Figure 6.4.1: The five 3d orbitals are shown. The orientation of the axes is consistent and the z axis is horizontal for convenience in drawing bonding along the z axis (see examples below). (CC-BY-SA; Kathryn Haas)

Sigma (σ) bonding with d orbitals

σ bonds are symmetric with respect to the inter-nuclear axis (in a diatomic molecule, this is the z axis). An example of a σ bond formed by d orbitals is that of two d_{z^2} orbitals (see Figure 6.4.2). If a bonded atom is in a position other than on the z axis (in an octahedral geometry, for example), σ bonds can also form. For example, two $d_{x^2-y^2}$ orbitals on atoms bonded along the x or y axes could also form a σ bond.

d orbitals can also form σ bonds with other types of orbitals with the appropriate symmetry. Examples of orbitals with appropriate symmetry are the s orbital and certain p orbitals on another atom, as shown below in Figure 6.4.2.

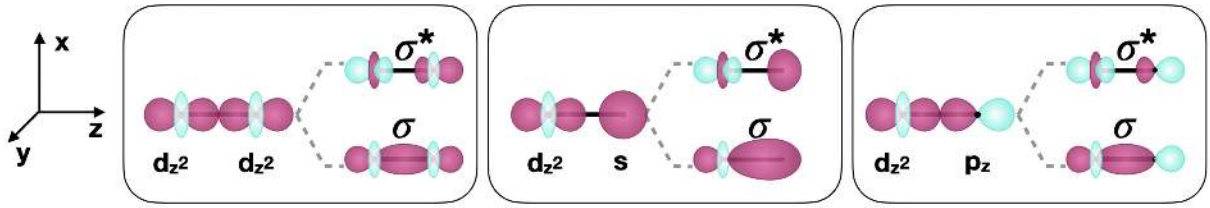


Figure 6.4.2: Selected examples of σ bonds involving d orbitals along the z internuclear axis (shown as a bold horizontal line) between two atoms. (CC-BY-SA; Kathryn Haas)

Pi (π) bonding with d orbitals

π bonds are those with one node that is in-plane with the internuclear axis. A π bond can form between two d orbitals or between d orbitals and other types of orbitals with comparable symmetry. An example of a π bond between two d orbitals is that formed by two d_{xz} orbitals along the z axis (shown in Figure 6.4.3). d orbitals can also form π bonds using p orbitals with compatible symmetry, as shown in Figure 6.4.3.

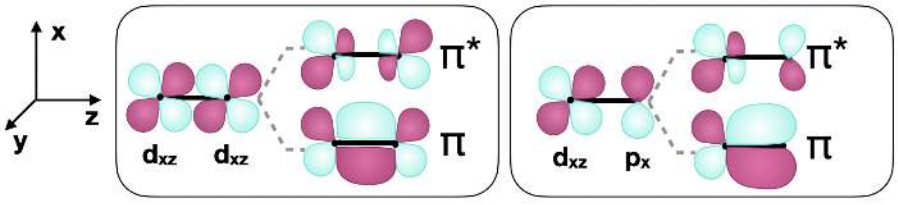


Figure 6.4.3: Selected examples of π bonds involving d orbitals along the z internuclear axis (shown as a bold horizontal line) between two atoms. (CC-BY-SA; Kathryn Haas)

Delta (δ) bonding with d orbitals

δ bonds are those with two nodes that are in-plane with the internuclear axis. δ bonds can form between two d orbitals with appropriate symmetry. For example, when two atoms bond along the z axis, the d_{xy} orbitals and the two $d_{x^2-y^2}$ orbitals can form δ bonds (Figure 6.4.4).

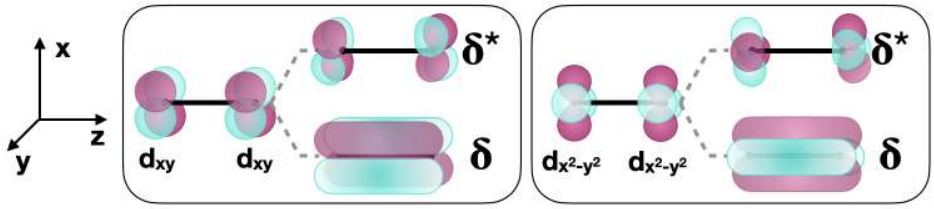


Figure **6.4.4**: Selected examples of δ bonds involving d orbitals along the z internuclear axis (shown in bold horizontal line) between two atoms. (CC-BY-SA; Kathryn Haas)

Incompatible orbitals

In the descriptions above, we focused on how bonds (and antibonds) can be formed with d orbitals. All bonding and non-bonding interactions require that orbitals have compatible symmetry to form productive interactions. It is worth mentioning that orbitals with symmetry that is incompatible with the d orbitals will not have bonding or antibonding interactions with d orbitals. The figure below shows several sets of orbitals that are incompatible for bonding.

Curated or created by Kathryn Haas

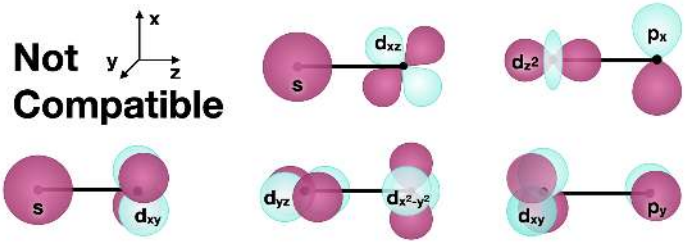


Figure **6.4.5**: Several incompatible pairs of orbitals. (CC-BY-SA; Kathryn Haas)

This page titled 6.4: Molecular orbitals from d orbitals is shared under a CC BY-SA 4.0 license and was authored, remixed, and/or curated by Kathryn Haas.

- **5.1.3: Molecular orbitals from d orbitals** by Kathryn Haas is licensed CC BY-SA 4.0.

6.5: Nonbonding Orbitals and Other Factors

The simplest case is when there is an even number of atomic orbitals that all combine to form strong bonding and antibonding orbitals. But what if there is an uneven number of atomic orbitals? Or what if there are some orbitals that don't meet the criteria for bonding? Or what if the bonding interactions are weak? In these cases, there will be molecular orbitals on the molecule that have non-bonding character.

It is important to note that the bonding, non-bonding, and antibonding nature of orbitals exist on a spectrum. Some bonding and anti-bonding orbitals may have some non-bonding character depending on where their energies lie with respect to the original atomic orbital energies. When molecular orbitals have energies similar to their original atomic orbitals, they will have some non-bonding character. The closer the energies of atomic and molecular orbitals, the more non-bonding the molecular orbitals.

Two major factors to consider

Uneven number of atomic orbitals: In the case that there is an uneven number of atomic orbitals with compatible symmetry, orbitals with non-bonding character will form. For example, in the case where three atomic orbitals combine, the most common result is formation of a low-energy bonding orbital, a high energy antibonding orbital, and a non-bonding orbital of intermediate energy (Figure 6.5.1).

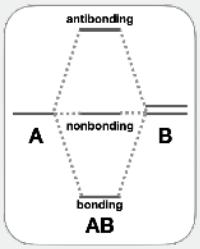


Figure 6.5.1. This figure illustrates the most common case for three atomic orbitals that combine to form three molecular orbitals; formation of one low-energy bonding, one high-energy antibonding, and one intermediate energy non-bonding molecular orbital. (CC-BY-NC-SA, Kathryn Haas)

Differences in energy: Combination of orbitals with different energies may lead to orbitals with non-bonding character. Atomic orbitals that have similar energies will have the strongest interactions, and result in bonding molecular orbitals with much lower energies than the component atomic orbitals. On the other hand, atomic orbitals with very unequal energies have a weaker interaction because the molecular orbitals are closer in energy to the atomic orbital energies, thus there is less energy benefit to putting electrons in the bonding molecular orbitals (Figure 6.5.2). When bonding or antibonding orbitals are close to the energies of the contributing atomic orbitals, those molecular orbitals may have some non-bonding character.

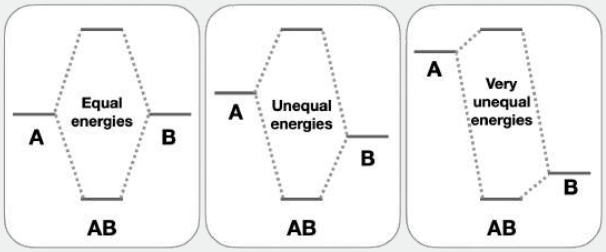


Figure 6.5.2. This figure illustrates how relative energies of atomic orbitals result in molecular orbitals that are more or less favorable. The greater the energy difference between atomic orbitals and the bonding molecular orbital, the more eneretically favorable it is for bonding to occur. (CC-BY-NC-SA, Kathryn Haas)

This page titled 6.5: Nonbonding Orbitals and Other Factors is shared under a CC BY-SA 4.0 license and was authored, remixed, and/or curated by Kathryn Haas.

- **5.1.4: Nonbonding Orbitals and Other Factors** by Kathryn Haas is licensed CC BY-SA 4.0.

SECTION OVERVIEW

6.6: Homonuclear Diatomic Molecules

In this section you will be introduced to the molecular orbital diagrams of several homonuclear diatomic molecules. Homonuclear diatomic molecules are molecules made of exactly two identical atoms, and they are relatively simple.

This page titled 6.6: Homonuclear Diatomic Molecules is shared under a CC BY-SA 4.0 license and was authored, remixed, and/or curated by Kathryn Haas.

6.7: Molecular Orbitals

There are several cases where our more elementary models of bonding (like Lewis Theory and Valence Bond Theory) fail to predict the actual molecular properties and reactivity. A classic example is the case of O_2 and its magnetic properties. At very cold temperatures, O_2 is attracted to a magnetic field, and thus it must be paramagnetic (unpaired electrons give rise to magnetism). Watch the video below!



The magnetic properties of O_2 are easily rationalized by its **molecular orbital diagram**. A molecular orbital diagram is a diagram that shows the relative energies and identities of each molecular orbital in a molecule. Figure 6.7.1 shows a simplified and generic molecular orbital diagram for a second-row homonuclear diatomic molecule. The diagram is simplified in that it assumes that interactions are limited to degenerate orbitals from two atoms (see next section).

There are some things you should note as you inspect Figure 6.7.1 (and keep these in mind as you draw your own diagrams!). First, notice that there are the **same number of molecular orbitals as there are atomic orbitals**. Second, notice that **each orbital in the diagram is rigorously labeled** using labels (σ and π) that include the subscripts u and g. These labels and subscripts indicate the symmetry of the orbitals. The σ symbol indicates that the orbital is symmetric with respect to the internuclear axis, while the π label indicates that there is one node along that axis. The g and u stand for *gerade* and *ungerade*, the German words for *even* and *uneven*, respectively. The subscript g is given to orbitals that are *even*, or *symmetric*, with respect to an inversion center. The subscript u is given to orbitals that are *uneven*, or *antisymetric*, with respect to an inversion center. The pictures of calculated molecular orbitals are shown in Figure 6.7.1 to illustrate the symmetry of each orbital.

Another important thing to notice is that the diagram in Figure 6.7.1 lacks electrons (because it is generic for any second-row diatomic molecule). If this were a *complete* molecular orbital diagram it would **include the electrons for each atom and for the molecule**. Electrons in molecular orbitals are filled in the same way an atomic orbital diagram would be filled, where electrons occupy lower energy orbitals before higher energy orbitals, and electrons occupy empty degenerate orbitals before pairing. A complete molecular orbital diagram would show whether the molecule is diamagnetic or paramagnetic. It can also be used to calculate the bond order of the molecule (the number of bonds between atoms) using the formula below:

$$\text{Bond order } = \frac{1}{2}\left[\left(\begin{array}{c}\text{number of electrons}\\ \text{in bonding orbitals}\end{array}\right) - \left(\begin{array}{c}\text{number of electrons}\\ \text{in antibonding orbitals}\end{array}\right)\right]$$

In general, non-valence (core) electrons can be ignored because they contribute nothing to the bond order. In fact, many molecular orbital diagrams will ignore the core orbitals, as they are insignificant for bonding interactions and reactivity.

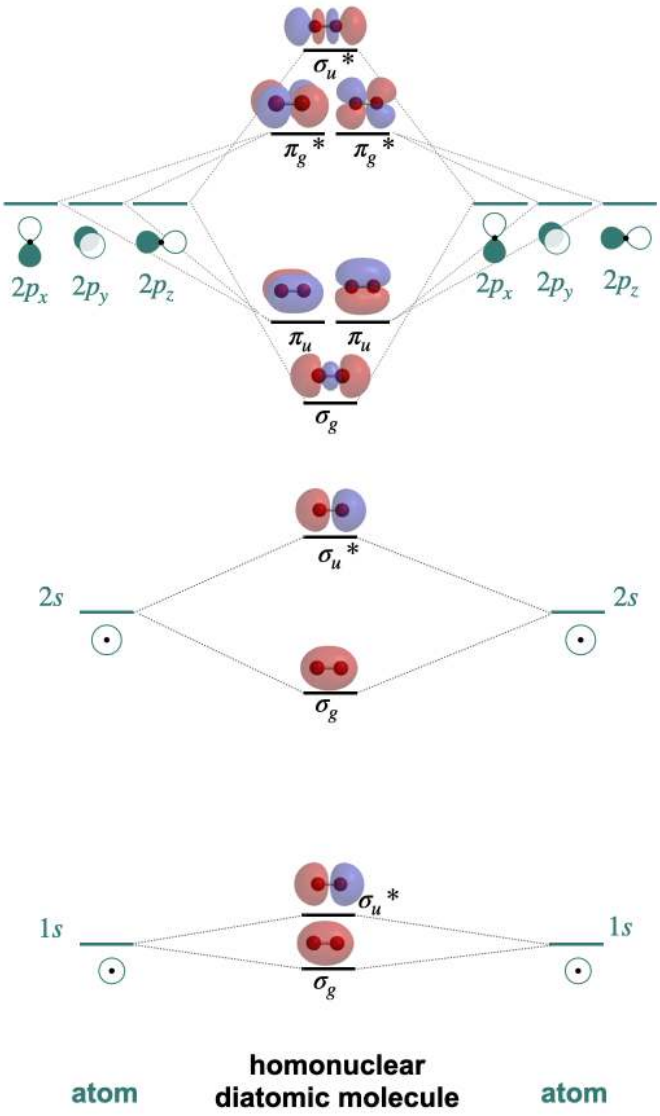


Figure **6.7.1**: A generic molecular orbital diagram for a homonuclear diatomic molecule of second-row elements assuming no orbital mixing (interactions are formed by orbitals of the same energy from each atom). (CC-BY-NC-SA, Kathryn Haas)

Now, to see how this molecular orbital diagram can explain the magnetic behaviour of O_2, complete the example below.

Example 6.7.1

Let's change Figure **6.7.1** to make it specific for O_2. Re-draw the MO diagram (no need to draw the shapes of orbitals). Fill in the correct number of electrons for each oxygen atom on either side of the diagram. Then, fill in the total molecular electrons in the center. Calculate the bond order and determine whether it is diamagnetic or paramagnetic.

Solution

The diagram in Figure **6.7.1** includes core orbitals (the 1s) and valence electrons (2s, 2p). Therefore, we will consider all the electrons in an oxygen atom and a dioxygen molecule. An oxygen atom has eight total electrons. So we fill eight electrons into the atomic orbitals for the oxygen atom on the right, and eight electrons into the atomic orbitals for oxygen on the left. The total number of electrons for the molecule is sixteen, so fill in 16 electrons into the molecular orbitals, being sure to apply Hund's rule and the Aufbau principle. The result is a diagram that looks like the one drawn below in Figure **6.7.2**.

The bond order is calculated using the molecular orbitals (we can ignore atomic orbitals). There are 10 electrons in binding orbitals and 6 electrons in antibonding orbitals). This gives a bond order of $\frac{1}{2}(10-6)=2$. This bond order is consistent with valence bond theory!

This diagram indicates that dioxygen is paramagnetic; it has two unpaired electrons in the π^* orbitals. This paramagnetic electron configuration explains why dioxygen is attacted to magnetic fields!

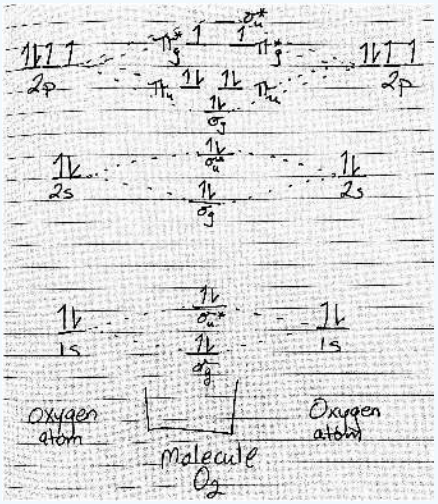


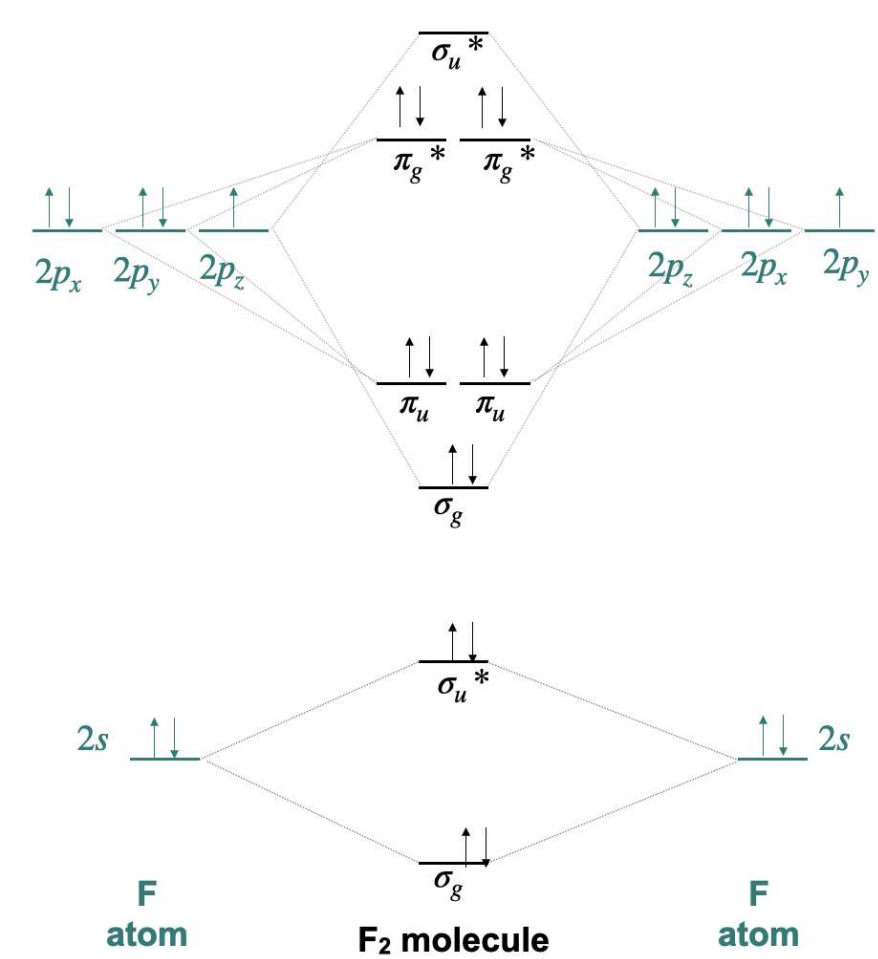
Figure 6.7.2: Hand-drawn molecular orbital diagram for dioxygen. (CC-BY-SA; Kathryn Haas)

? Exercise 6.7.1

Draw the molecular orbital diagram for $\mathbf{F_2}$; be sure to label your orbitals with the appropriate symmetry and count your orbitals to make sure that the total number of atomic orbitals and molecular orbitals is the same. As a shortcut, include only the valence orbitals and electrons. What is the bond order? Is the molecule diamagnetic or paramagnetic?

Answer

The valence orbitals on an F atom are 2s and 2p. And, there are seven valence electrons in F. This gives fourteen total valence electrons. The MO diagram of the valence molecular orbitals can be constructed by combining the valence 2s and valence 2p orbitals from each F atom. The bond order is 1 and the molecule is diamagnetic.



This page titled 6.7: Molecular Orbitals is shared under a CC BY-SA 4.0 license and was authored, remixed, and/or curated by Kathryn Haas.

- **5.2.1: Molecular Orbitals** by Kathryn Haas is licensed CC BY-SA 4.0.

6.8: Orbital Mixing

In the previous section, we introduced a simplified molecular orbital (MO) diagram, assuming that interactions were limited to degenerate orbitals of compatible symmetry. A version of that *simplified* diagram for second-row homonuclear diatomics is shown on the left side of Figure **6.8.1** (only valence orbitals shown).

In reality, orbitals of compatible symmetry can combine, or mix, even when they have different energies. When sets of orbitals mix, it has the effect of decreasing the energy of the lower-energy set and increasing the energy of the higher-energy set. There are two ways to explain mixing, described in the points below. The diagram on the right of side of Figure **6.8.1** shows how energy levels are affected by orbital mixing.

- **Starting from the simplified MO diagram and mixing molecular orbitals of like symmetry**: If we start with the "no mixing" simplified diagram shown on the left, we can pick out the orbitals with like symmetry and consider what will happen if these molecular orbitals mix. For example, starting from the MO diagram on the left side of Figure **6.8.1**, we see that there are two σ_g orbitals that have identical symmetry (hence they have identical symmetry labels). Upon mixing, the lower-energy $\sigma_g(2s)$ will decrease in energy while the higher-energy $\sigma_g(2p)$ will increase in energy. Likewise, there are two σ_u^* orbitals that will mix, decreasing the energy of $\sigma_u^*(2s)$ while increasing the energy of $\sigma_u^*(2p)$.
- **Starting from and mixing atomic orbitals of compatible symmetry**: Starting from the atomic orbitals, we can select the orbitals that have compatible symmetry to make productive interactions, and combine them as a set to make molecular orbitals. From the two sets of atomic orbitals on the right panel in Figure **6.8.1**, there are two sets of four orbitals with compatable symmetry; one is the set of two $2s$ and two $2p_z$ orbitals. These four orbitals can combine to form molecular orbitals with σ symmetry. They combine to form one lowest-energy bonding σ_g, a highest-energy σ_u^*, and two orbitals with intermediate energy (σ_g, and σ_u^*). This treatment can be expressed as the linear combination of four atomic orbitals:

  $$\Psi = c_1\psi(2s_a) \pm c_2\psi(2s_b) \pm c_3\psi(2p_a) \pm c_4\psi(2p_b)$$

  where the coefficients $c_1 = c_2$ and $c_3 = c_4$ for homonuclear diatomic molecules.

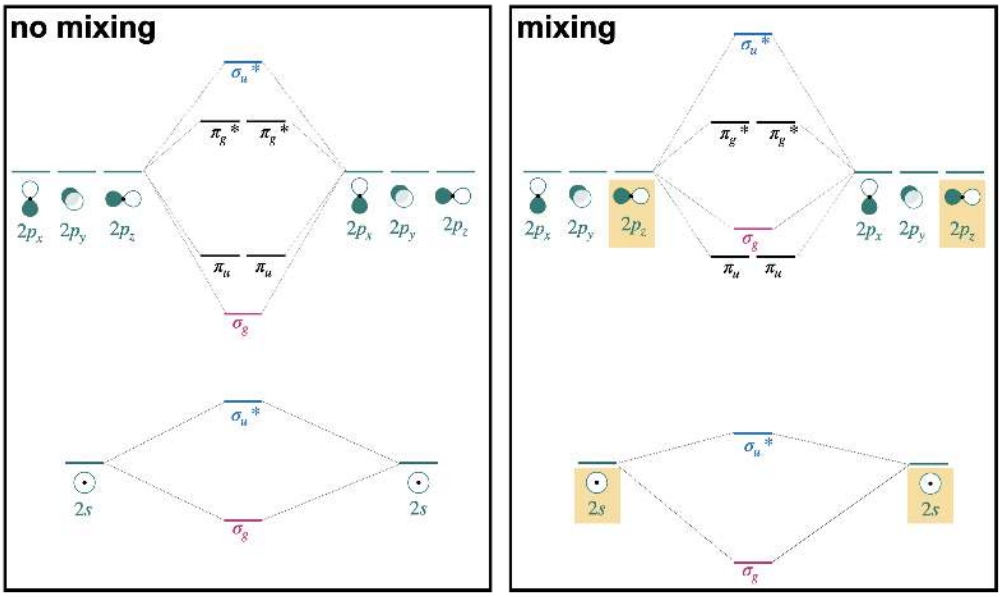


Figure **6.8.1**: Mixing of orbitals with like symmetry affects the energies of molecular orbitals. The simplified case where no mixing occurs is shown on the left. The effects of mixing are shown on the right. The σ_g orbitals of like symmetry are highlighted in fuschia and the σ_u^* orbitals of like symmetry are highlighted in blue. A group of atomic orbitals of similar symmetry are highlighted in yellow boxes; these atomic orbitals combine to give all σ molecular orbitals. (CC-BY-SA, Kathryn Haas)

In the case of homonuclear diatomic molecules of the second row, orbital mixing has important consequences for the energetic order of the $\sigma_g(2p)$ and $\pi_u(2p)$ orbitals. This will be discussed in the next section.

This page titled 6.8: Orbital Mixing is shared under a CC BY-SA 4.0 license and was authored, remixed, and/or curated by Kathryn Haas.

- **5.2.2: Orbital Mixing** by Kathryn Haas is licensed CC BY-SA 4.0.

https://chem.libretexts.org/@go/page/403046

6.9: Diatomic Molecules of the First and Second Periods

First Period Homonuclear Diatomic Molecules

In the first row of the periodic table, the valence atomic orbitals are $1s$. There are two possible homonuclear diatomic molecules of the first period:

Dihydrogen, H_2 [$\sigma_g^2(1s)$]: This is the simplest diatomic molecule. It has only two molecular orbitals (σ_g and σ_u^*), two electrons, a bond order of 1, and is diamagnetic. Its bond length is 74 pm. MO theory would lead us to expect bond order to decrease and bond length to increase if we either add or subtract one electron. The calculated bond length for the H_2^+ ion is approximately 105 pm.[1]

Dihelium, He_2 [$\sigma_g^2\sigma_u^{*2}(1s)$]: This molecule has a bond order of zero due to equal number of electrons in bonding and antibonding orbitals. Like other nobel gases, He exists in the atomic form and does not form bonds at ordinary temperatures and pressures.

Exercise 6.9.1

Draw the complete molecular orbital diagrams for H_2 and for He_2. Include sketches of the atomic and molecular orbitals.

Answer

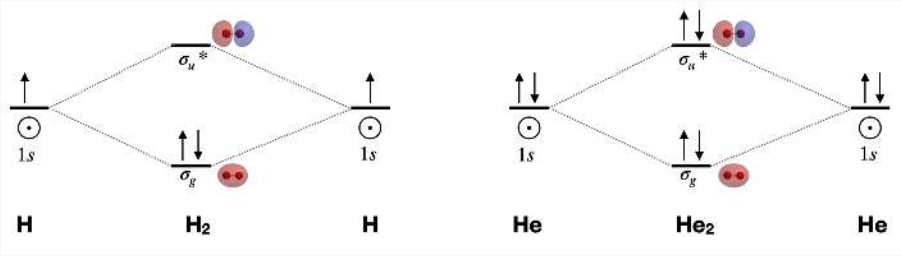


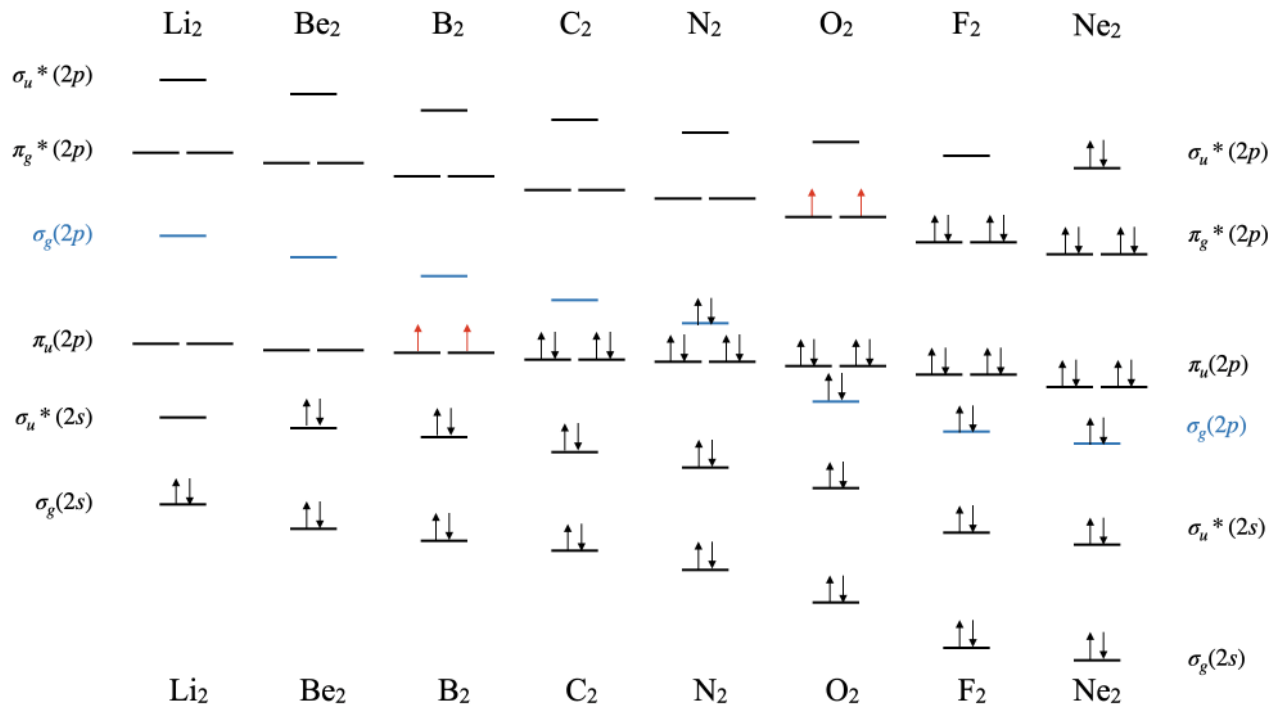
Figure for Exercise 6.9.1: Molecular orbital diagrams for dihydrogen and dihelium. Molecular orbital surfaces calculated using Spartan software. (CC-BY-NC-SA; Kathryn Haas)

A complete molecular orbital diagram includes all atomic orbitals and molecular orbitals, their symmetry labels, and electron filling.

Second Period Homonuclear Diatomic Molecules

The second period elements span from Li to Ne. The valence orbitals are 2s and 2p. In their molecular orbital diagrams, non-valence orbitals (1s in this case) are often disregarded in molecular orbital diagrams.

Orbital mixing has significant consequences for the magnetic and spectroscopic properties of second period homonuclear diatomic molecules because it affects the order of filling of the $\sigma_g(2p)$ and $\pi_u(2p)$ orbitals. Early in period 2 (up to and including nitrogen), the $\pi_u(2p)$ orbitals are lower in energy than the $\sigma_g(2p)$ (see Figure 6.9.1). However, later in period 2, the $\sigma_g(2p)$ orbitals are pulled to a lower energy. This lowering in energy of $\sigma_g(2p)$ is not unique; all of the σ orbitals in the molecule are pulled to lower energy due to the increasing positive charge of the nucleus. The π orbitals in the molecule are also affected, but to a much lesser extent than σ orbitals. The reason has to do with the high penetration of s atomic orbitals compared to p atomic orbitals (recall our previous discussion on penetration and shielding, and its effect on periodic trends). The σ molecular orbitals have more s character and thus their energy is more influenced by increasing nuclear charge. As nuclear charge increases, the energy of the $\sigma_g(2p)$ orbital is lowered significantly more than the energy of the $\pi_u(2p)$ orbitals (Figure 6.9.1).



	Li_2	Be_2	B_2	C_2	N_2	O_2	F_2	Ne_2
Unpaired e⁻	0	0	2	0	0	2	0	0
Bond Order	1	0	1	2	3	2	1	0
Experimental* Bond Length (pm)	267.3	246.0	159.0	124.3	109.8	120.8	141.2	310.0

*Experimental bond lengths from "List of Experimental Diatomic Bond Lengths", NIST, https://cccbdb.nist.gov/diatomicexpbondx.asp

Figure 6.9.1: Molecular orbital energy-level diagrams for the diatomic molecules of the period 2 elements. Unlike earlier diagrams, *only the valence molecular orbital energy levels for the* ***molecules*** *are shown here (atomic orbitals not shown for simplicity).* For Li_2 through N_2, the $\sigma_g(2p)$ orbital is higher in energy than the $\pi_u(2p)$ orbitals. In contrast, from O_2 onward, the $\sigma_g(2p)$ orbital is *lower* in energy than the $\pi_u(2p)$ orbitals because the nuclear charge increases across the row. The experimental bond lengths correlate with the calculated bond order. (CC-BY-NC-SA, Kathryn Haas)

Dilithium, Li_2 $[\sigma_g^2(2s)]$: This molecule has a bond order of one and is observed experimentally in the gas phase to have one Li-Li bond.

Diberylium, Be_2 $[\sigma_g^2\sigma_u^{*2}(2s)]$: This molecule has a bond order of zero due to the equal number of electrons in bonding and antibonding orbitals. Although Be_2 does not exist under ordinary conditions, it can be produced in a laboratory and its bond length measured (Figure 6.9.2). Although the bond is very weak, its bond length is surprisingly ordinary for a covalent bond of the second period elements.[2]

Diboron, B_2 $[\sigma_g^2\sigma_u^{*2}(2s)\pi_u^1\pi_u^1(2p)]$: The case of diboron is one that is much better described by molecular orbital theory than by Lewis structures or valence bond theory. This molecule has a bond order of one. The molecular orbital description of diboron also predicts, accurately, that diboron is paramagnetic. The paramagnetism is a consequence of orbital mixing, resulting in the σ_g orbital's being at a higher energy than the two degenerate π_u^* orbitals.

Dicarbon, C_2 $[\sigma_g^2\sigma_u^{*2}(2s)\pi_u^2\pi_u^2(2p)]$: This molecule has a bond order of two. Molecular orbital theory predicts two bonds with π symmetry, and no σ bonding. C_2 is rare in nature because its allotrope, diamond, is much more stable.

Dinitrogen, N_2 $[\sigma_g^2\sigma_u^{*2}(2s)\pi_u^2\pi_u^2\sigma_g^2(2p)]$: This molecule is predicted to have a triple bond. This prediction is consistent with its short bond length and bond dissociation energy. The energies of the $\sigma_g(2p)$ and $\pi_u(2p)$ orbitals are very close, and their relative energy levels have been a subject of some debate (see next section for discussion).

Dioxygen, O_2 $[\sigma_g^2\sigma_u^{*2}(2s)\sigma_g^2\pi_u^2\pi_u^2\pi_g^{*1}\pi_g^{*1}(2p)]$: This is another case where valence bond theory fails to predict actual properties. Molecular orbital theory correctly predicts that dioxygen is paramagnetic, with a bond order of two. Here, the molecular orbital diagram returns to its "normal" order of orbitals where orbital mixing could be somewhat ignored, and where $\sigma_g(2p)$ is lower in energy than $\pi_u(2p)$.

Difluorine, F_2 $[\sigma_g^2\sigma_u^{*2}(2s)\sigma_g^2\pi_u^2\pi_u^2\pi_g^{*2}\pi_g^{*2}(2p)]$: This molecule has a bond order of one and like oxygen, the $\sigma_g(2p)$ is lower in energy than $\pi_u(2p)$.

Dineon, Ne_2 $[\sigma_g^2\sigma_u^{*2}(2s)\sigma_g^2\pi_u^2\pi_u^2\pi_g^{*2}\pi_g^{*2}\sigma_u^{*2}(2p)]$: Like other noble gases, Ne exists in the atomic form and does not form bonds at ordinary temperatures and pressures. Like Be_2, Ne_2 is an unstable species that has been created in extreme laboratory conditions and its bond length has been measured (Figure **6.9.2**)

? Exercise 6.9.2

Draw the complete molecular orbital diagram for O_2. Show calculation of its bond order and tell whether it is diamagnetic or paramagnetic.

Answer

O_2 is paramagnetic with a bond order of 2. Its $\sigma_g(2p)$ molecular orbital is lower in energy that the set of $\pi_u(2p)$ orbitals.

$$\text{Bond order} = \frac{1}{2}\left[\left(\begin{array}{c}\textbf{8 electrons in}\\ \textbf{valence bonding orbitals}\end{array}\right) - \left(\begin{array}{c}\textbf{4 electrons in}\\ \textbf{valence antibonding orbitals}\end{array}\right)\right]$$

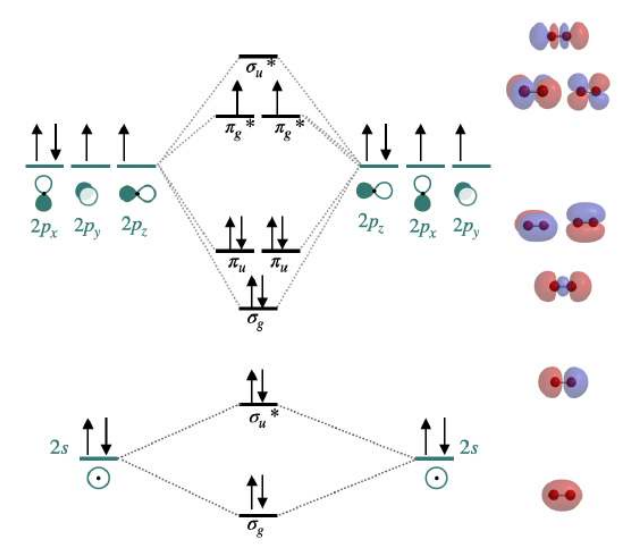


Figure for Exercise **6.9.2**. Molecular orbital diagram of O_2. (CC-BY-NC-SA, Kathryn Haas)

? Exercise 6.9.3: The Peroxide Ion

Use a qualitative molecular orbital energy-level diagram to predict the electron configuration, the bond order, and the number of unpaired electrons in the peroxide ion (O_2^{2-}).

Answer

This diagram looks similar to that of $\mathbf{O_2}$, except that there are two additional electrons.
$(\sigma_g(2s))^2\,(\sigma_u^*(2s))^2\,(\sigma_g(2p))^2\,(\pi_u(2p))^4\,(\pi_g(2p))^4$; bond order of 1; no unpaired electrons.

Bond Lengths in Homonuclear Diatomic Molecules

The trends in experimental bond lengths are predicted by molecular orbital theory, specifically by the calculated bond order. The values of bond order and experimental bond lengths for the second period diatomic molecules are given in Figure **6.9.1**, and shown

in graphical format on the plot in Figure **6.9.2**. From the plot, we can see that bond length correlates well with bond order, with a minimum bond length occurring where the bond order is greatest ($\mathbf{N_2}$). The shortest bond distance is at $\mathbf{N_2}$ due to its high bond order of 3. From $\mathbf{N_2}$ to $\mathbf{F_2}$ the bond distance increases despite the fact that atomic radius decreases.

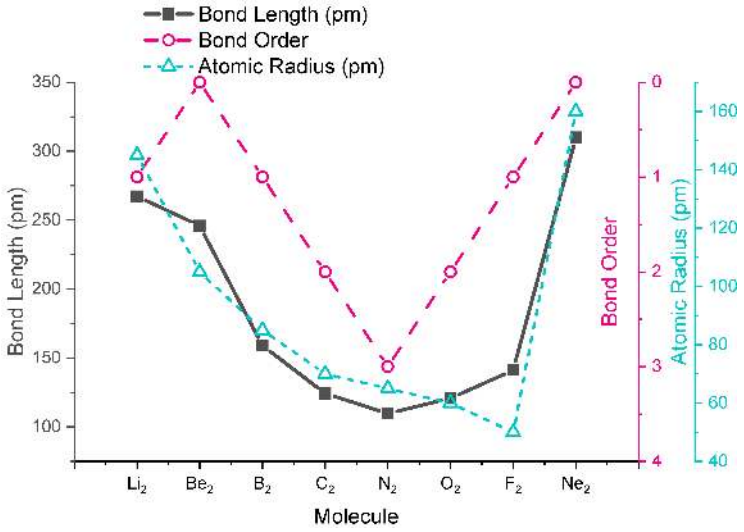


Figure **6.9.2**: Overlayed plots of bond length (black squares), bond order (pink circles), and atomic radius (teal triangles) versus atomic number for second period homonuclear diatomic molecules. (CC-BY-NC-SA; Kathryn Haas)

References

1. NIST, Calculated Geometries available for H_2^+ (Hydrogen cation) 2Σg+ D∞h, available at https://cccbdb.nist.gov/diatomicexpbondx.asp
2. Merritt, J. M.; Bondybey, V. E.; Heaven, M. C., Beryllium Dimer-Caught in the Act of Bonding. *Science* **2009,** *324* (5934), 1548-1551.

This page titled 6.9: Diatomic Molecules of the First and Second Periods is shared under a CC BY-SA 4.0 license and was authored, remixed, and/or curated by Kathryn Haas.

- **5.2.3: Diatomic Molecules of the First and Second Periods** by Kathryn Haas is licensed CC BY-SA 4.0.
- **5.P: Problems** is licensed CC BY-SA 4.0.

SECTION OVERVIEW

6.10: Heteronuclear Diatomic Molecules

Diatomic molecules with two non-identical atoms are called **heteronuclear** diatomic molecules. When atoms are not identical, the molecule forms by combining atomic orbitals of unequal energies. *The result is a polar bond in which atomic orbitals contribute unevenly to each molecular orbital*.

The application of molecular orbital theory to heteronuclear diatomic molecules is similar to the case of homonuclear diatomics, except that the atomic orbitals from each atom have different energies and contribute unequally to molecular orbitals. Recall that atomic orbitals must have compatible symmetry and similar energy to combine into molecular orbitals. In the case where atomic orbitals of like symmetry have different energies, they combine less favorably than orbitals that are closer to one another in energy. As a general rule, orbitals that have energy differences of greater than 10-14 eV do not combine favorably. In the molecular orbital diagram, the closer a molecular orbital is to an atomic orbital, the more that atomic orbital contributes to the molecular orbital. This last point is helpful for back-of-the napkin estimations of what the molecular orbitals "look" like.

In this section, you should learn how to generate molecular orbital diagrams of heteronuclear diatomic molecules. To approach such a problem, we must start with a knowledge of the relative energies of electrons in different atomic orbitals. In other words, we need knowledge of the orbital potential energies (or orbital ionization energies).

Sources:

- Gray, Harry. *Electrons and Chemical Bonding*, Benjamin, 1964.
- Miessler, Gary L, and Donald A. Tarr. *Inorganic Chemistry*. Upper Saddle River, N.J: Pearson Education, 2014. Print.

This page titled 6.10: Heteronuclear Diatomic Molecules is shared under a CC BY-SA 4.0 license and was authored, remixed, and/or curated by Kathryn Haas.

6.11: Orbital ionization energies

To generate molecular orbital diagrams of heteronuclear diatomic molecules, we must start with a knowledge of the relative energies of electrons in different atomic orbitals. In other words, we need knowledge of the orbital potential energies (or orbital ionization energies).

Orbital Ionization Energies

There are two approaches you can use to "know" or estimate the atomic orbital energy levels.

1. Use a table of atomic orbital ionization energies, like those found in Table **6.11.1**.
2. When you do not have access to a table of values like the one below, use periodic trends in electronegativity and/or ionization energies as your guide to approximate relative values for different atoms.

Table **6.11.1**: These are one-electron ionization energies of the valence orbitals calculated by average energies of both the ground-state and ionized-state configurations. (From Harry Gray, "Electrons and Chemical Bonding," Benjamin, 1964, Appendix) Values are expressed in eV.

Atom	1*s*	2*s*	2*p*	3*s*	3*p*	4*s*	4*p*	*Atom*	3*d*	4*s*	4*p*
H	−13.64							*Sc*	−4.71	−5.70	−3.22
He	−24.55							*Ti*	−5.58	−6.08	−3.35
Li		−5.46						*V*	−6.32	−6.32	−3.47
Be		−9.30						*Cr*	−7.19	−6.57	−3.47
B		−14.01	−8.31					*Mn*	−7.93	−6.82	−3.60
C		−19.47	−10.66					*Fe*	−8.68	−7.07	−3.72
N		−25.54	−13.14					*Ni*	−10.04	−7.56	−3.84
O		−32.36	−15.87					*Cu*	−10.66	−7.69	−3.97
F		−46.37	−18.72								
Ne		−48.48	−21.57								
Na				−5.21							
Mg				−7.69							
Al				−11.28	−5.95						
Si				−15.00	−7.81						
P				−18.72	−10.17						
S				−20.71	−11.65						
Cl				−25.29	−13.76						
Ar				−29.26	−15.87						
K						−4.34					
Ca						−6.08					
Zn						−9.42					
Ga						−12.65	−5.95				
Ge						−15.62	−7.56				
As						−17.61	−9.05				
Se						−20.83	−10.79				
Br						−24.05	−12.52				
Kr						−27.52	−14.26				

This page titled 6.11: Orbital ionization energies is shared under a CC BY-SA license and was authored, remixed, and/or curated by Kathryn Haas.

- **5.3: Heteronuclear Diatomic Molecules** by Kathryn Haas is licensed CC BY-SA 4.0.

6.12: Polar bonds

Molecular orbital diagrams for heteronuclear diatomic molecules

The molecular orbital diagram of a heteronuclear diatomic molecule is approached in a way similar to that of a homonuclear diatomic molecule. The orbital diagrams may also look similar. A major difference is that the more electronegative atom will have orbitals at a lower energy level. Two examples of heteronuclear diatomic molecules will be explored below as illustrative examples.

Carbon monoxide MO diagram

Carbon monoxide is an example of a heteronuclear diatomic molecule where both atoms are second-row elements. The valence molecular orbitals in both atoms are the $2s$ and $2p$ orbitals. The molecular orbital diagram for carbon monoxide (Figure **6.12.1**) is constructed in a way similar to how you would construct dicarbon or dioxygen, except that the oxygen orbitals have a lower potential energy than analogous carbon orbitals. The labeling of molecular orbitals in this diagram follows a convention by which orbitals are given serial labels according to type of orbital (σ, π, etc.). The lowest energy orbitals of any type are assigned a value of 1 and higher energy orbitals of the same type are assigned by increasing intervals (..2, 3, 4...). The orbital labeling system described previously is inappropriate for heteronuclear diatomic molecules that cannot be assigned g and u subscripts.

A consequence of unequal atomic orbital energy levels is that orbital mixing is significant. Notice the order of the molecular orbitals labeled 1π and 3σ in Figure **6.12.1**. This is a similar order of π and σ orbitals to the one we saw in the case of the σ_g and π_u orbitals of N_2 and lighter diatomics of the second period. Because the oxygen $2p_z$ orbital is close in energy to both the carbon $2p_z$ and carbon $2s$, these three orbitals will have significant interaction (mixing). The result is an increase in the energy of the 3σ orbital and a decrease in energy of the $2\sigma^*$ orbital, resulting in the diagram shown in Figure **6.12.1**.

In the case of carbon monoxide (Figure **6.12.1**), atomic orbitals contribute unequally to each molecular orbital. For example, because the $2s$ orbital of oxygen is very close in energy to the 2σ moelcular orbital, it contributes to that molecular orbital more than the $2s$ orbital from carbon. Notice the shape of this 2σ orbital and how it is unevenly distributed over the two atoms; it is more heavily distributed on the oxygen because it is most like the oxygen $2s$. This is in line with the assumption that electron density is distributed more on oxygen because it is more electronegative than carbon. Likewise, the 1π orbitals are unevenly distributed, with more distribution close to the oxygen.

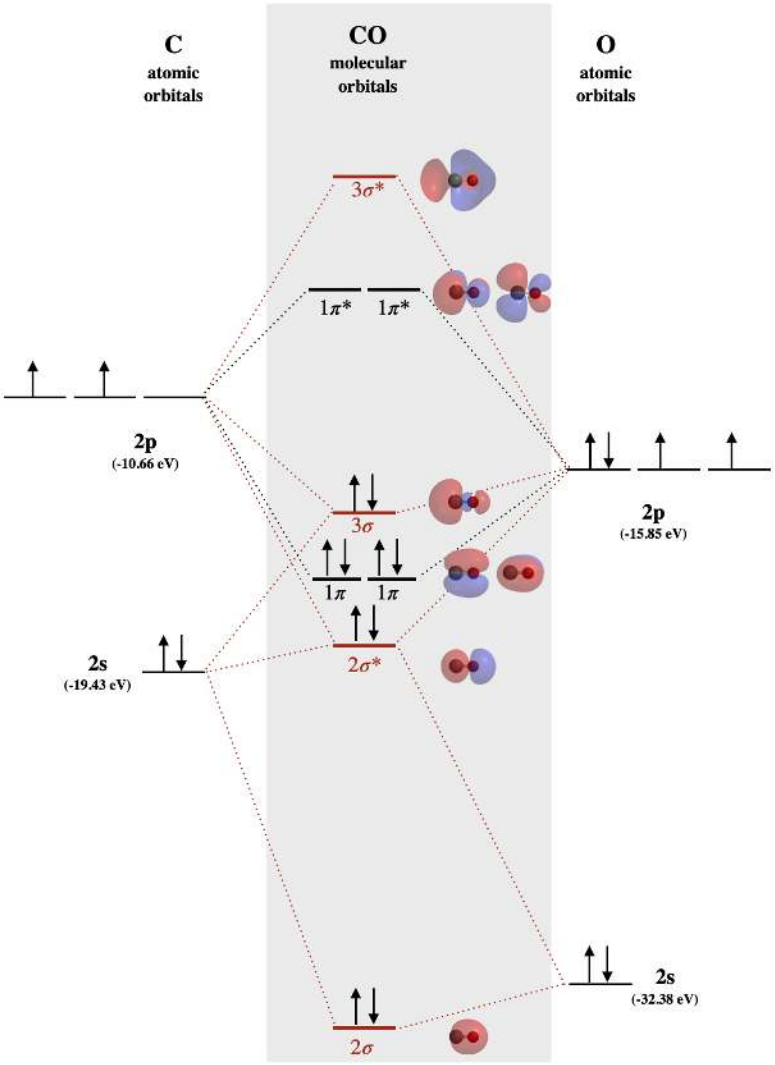
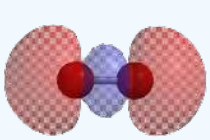


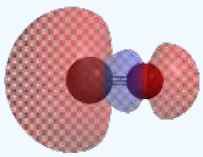
Figure 6.12.1: Molecular orbital diagram of carbon monoxide. The labeling of molecular orbitals in this diagram follows a convention by which orbitals are given serial names according to the type of orbital (σ, π, etc.). The lowest energy orbitals of any type are assigned a value of 1 and higher energy orbitals of the same type are assigned by increasing intervals (..2, 3, 4...). The orbital labeling system described previously is inappropriate for heteronuclear diatomic molecules that cannot be assigned g and u subscripts. Molecular orbital surfaces were calculated using Spartan software. (Kathryn Haas, CC-BY-NC-SA)

? Exercise 6.12.1

Examine the shape of the 3σ orbital of carbon monoxide in Figure 6.12.1. Describe what ways this shape is different from the shape of the σ_g orbitals from second period homonuclear diatomic molecules (see Fig. 5.2.1.1). Rationalize these differences. Both orbitals are re-created below for convenience.



σ_g of homonuclear diatomic



3σ of CO

Answer

https://chem.libretexts.org/@go/page/403050

The 3σ orbital is like the σ_g in that it has three lobes and two nodes distributed along the internuclear bond. They are different in their distribution. The two external lobes of σ_g are evenly distributed because they are an equal combination of two p_z orbitals (one from each atom). The 3σ orbital is more heavily distributed toward the carbon atom, the less electronegative atom, than toward the oxygen. The unequal distribution of 3σ is apparent in the unequal sizes of its exterior lobes and the uneven shape of the interior lobe. The heavier distribution within the exterior lobe on carbon is caused by the mixing of the carbon $2s$ orbital with carbon and oxygen $2p_z$ orbitals. The uneven shape of the interior lobe, where it leans toward oxygen, is best explained by the fact that the 3σ orbital is closer in energy to the oxygen $2p_z$ than the carbon $2p_z$.

Hydrogen fluoride MO diagram

Hydrogen fluoride is an example of a heteronuclear diatomic molecule in which the two atoms are from different periods. In this case, the valence orbital of H is $1s$ while those of F are $2s$ and $2p$. The molecular orbital diagram for HF is shown in Figure 6.12.2.

Three of these orbitals have compatible symmetry for mixing; these are the hydrogen $1s$, fluorine $2s$, and fluorine $2p$. However, the extent to which they will interact depends on their relative energies. Fluorine is more electronegative than H, and the fluorine atom has a higher first ionization energy than does hydrogen. From these trends, we can expect that the fluorine valence orbitals are lower in energy than that of hydrogen. From Table 5.3.1, we find that the 1s orbital of H (-13.6 eV) is higher in energy than both fluorine orbitals (-18.7 and -40.2 eV, respectively for $2p$ and $2s$). The energies of hydrogen $1s$ and fluorine $2p$ are a good match for combination; however, the fluorine $2s$ orbital is much too different to create a productive interaction. Therefore, we expect that the fluorine $2s$ will create a non-bonding molecular orbital, while the $1s$ and $2p_z$ orbitals combine to make σ bonding and σ^* antibonding molecular orbitals. The remaining $2p_x$ and $2p_y$ orbitals do not have compatible symmetry for bonding with hydrogen, and they will form non-bonding π molecular orbitals. The non-bonding orbitals will have similar energy and character as their component atomic orbitals.

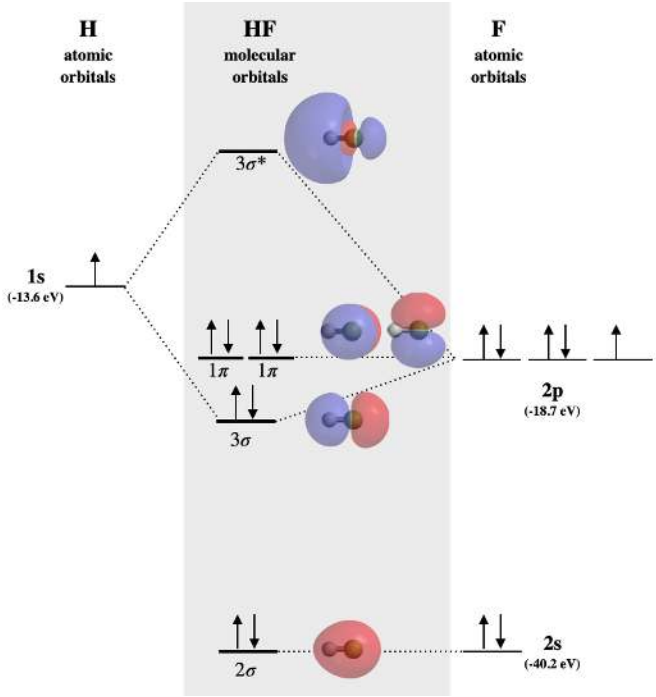


Figure 6.12.2: Molecular Orbital diagram of hydrogen fluoride. Molecular orbitals calculated using Spartan software. (Kathryn Haas, CC-BY-NC-SA)

Chemical reactions take place at the HOMO and LUMO orbitals

Knowledge of molecular orbital diagrams, and the shapes of molecular orbitals, can be used to accurately explain and predict chemical reactivity. Chemical reactions take place using the highest occupied molecular orbitals (HOMO) of a nucleophile or Lewis base, and the lowest unoccupied molecular orbital (LUMO) of an electrophile or Lewis acid.

> *Lewis bases react using electrons in the HOMO, while Lewis acids react using the empty LUMO.*

Example: Reactivity of CO with metal ions

CO is an excellent ligand for many metal ions. In fact, the strong affinity between CO and the heme iron (Fe) ions in hemoglobin can explain the mechanism of carbon monoxide poisoning. When CO binds in place of O_2 to hemoglobin, that hemoglobin can no longer carry O_2 to tissue cells. CO binding to hemoglobin is strong and practically irreversible. When CO binds to metal ions, it does so through the carbon atom. This is contrary to expectations based on the Lewis structure and the known bond polarity, where electron density is polarized toward oxygen. The distribution of the electron density of the HOMO of CO can explain this observation!

? Exercise 6.12.2

Refer to the MO diagram for CO. Identify the HOMO and explain why CO bonds to metal ions through the carbon atom rather than through the oxygen atom.

Answer

In the interaction between CO and a metal ion, CO would act as a Lewis base; thus it will react using electrons in its HOMO. The MO diagram for CO is shown in Figure 6.12.1: the HOMO is the 3σ orbital (also discussed in ? Exercise 6.12.1). The electron density of that MO is centered around the carbon atom, thus the carbon atom will be a better Lewis base than the O atom.

This page titled 6.12: Polar bonds is shared under a CC BY-SA 4.0 license and was authored, remixed, and/or curated by Kathryn Haas.

- **5.3.2: Polar bonds** by Kathryn Haas is licensed CC BY-SA 4.0.

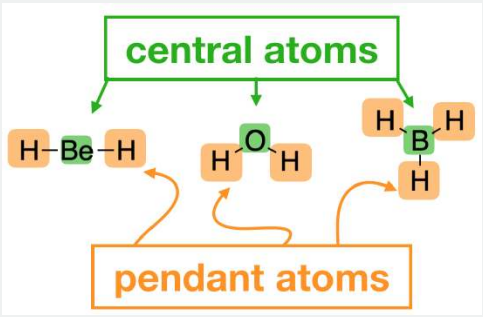
SECTION OVERVIEW

6.13: Larger (Polyatomic) Molecules

We can extend the method we used for diatomic molecules to draw the molecular orbitals of more complicated, polyatomic molecules (molecules with more than two atoms). To combine several different atoms in a molecular orbital diagram, we will group orbitals from different atoms into sets that match the symmetry of a central atom. These **group orbitals** are also referred to as **symmetry adapted linear combinations (SALCs)**. We'll use a stepwise approach to do this as summarized below.

Symmetry adapted linear combinations (SALCs)

We need SALCs (aka group orbitals) to draw molecular orbital (MO) diagrams of *polyatomic* molecules. SALCs are groups of orbitals on **pendant atoms**. These groups of orbitals much match the symmetry of valence orbitals on the **central atom** in order to create a productive interaction. When we combine SALCs with the atomic orbitals on the central atom, we can generate an MO diagram that gives us information about the molecule's bonding and electronic states.



Below is a set of steps you can follow to find SALCs and draw an MO Diagram. Each step will be illustrated in detail through the examples in the subsections that follow this page.

1. Find the **point group** of the molecule and assign Cartesian coordinates so that z is the principal axis.
   Sometimes we can simplify things by looking only at the point group of the relevant orbitals. Only simplify when instructed to do so.*
2. Identify and count the pendant atoms' valence orbitals.
   Is there more than 1 type for each atom (ex. just s, or s and p?) We expect 1 SALC for each ligand orbital.
3. Generate a **reducible representation (Γ)** for the group of pendant atom orbitals using the appropriate character table.
   You have to do this for each set of orbital types. If you only have s orbitals for each ligand, you only need to generate 1 reducible representation. If you have p orbitals, you would generate additional Γ*'s for p_x, p_y, and p_z.*
4. Break the Γ into its component **irreducible representations** from the character table. Note the symmetry of each irreducible representation, its associated orbitals, and their degeneracy.
5. If you are asked to sketch the shapes of SALCs, determine what they "look like" using one of the following strategies.
   (a) Shortcut: if the reducible representations are listed with s, p, or d orbitals in the character table, just draw them (… and skip steps b-c)
   (b) Systematic (Projection Operator) method: Draw an expanded character table and draw your molecule with each ligand identified by letters or numbers (*a,b,c...* or *i,j,k...* or *1,2,3...*) Determine where each pendant atom/orbital ends up under each of the operations of your expanded table. Project the values for each irreducible representation onto the chart you created and then add up the values. Positive and negative values are opposite signed orbitals.
6. Draw the MO diagram by combining SALCs with AO's of like symmetry. When drawing SALC energy levels, remember that the more nodal planes in your SALC orbital drawing, the higher the energy for that SALC orbital.

** When we are focused on orbitals, as in the case for finding group orbitals and drawing molecular orbital diagrams, the symmetry of the orbitals is what we are interested in. In the case of high-symmetry point groups, like $D_{\infty h}$ and $C_{\infty v}$, even though the molecule may have a C_∞ axis, the orbitals do not necessarily retain this symmetry element. For example, the p_x orbital would not have a C_∞ axis, but rather a C_2 axis. It is sufficient and useful to substitute D_{2h} for $D_{\infty h}$ and C_{2v} for $C_{\infty v}$ to simplify the problem.*

6.13: Larger (Polyatomic) Molecules is shared under a CC BY-SA 4.0 license and was authored, remixed, and/or curated by LibreTexts.

https://chem.libretexts.org/@go/page/403052

6.14: Bifluoride anion

Finding SALCs and drawing the MO diagram for [F-H-F]$^-$

The linear anion [F-H-F]$^-$ is a good place to start as an example to illustrate the process of generating pendant atom SALCs and then constructing a molecular orbital diagram for a polyatomic molecule. We will proceed using the steps outlined on the previous page for generating SALCs and a molecular orbital diagram.

Step 1. Find the point group of the molecule and assign Cartesian coordinates so that z is the principal axis.

We begin by assigning the appropriate point group for this molecule: $D_{\infty h}$ (Figure 6.14.1). As mentioned in the previous page, it is useful to substitute D_{2h} for $D_{\infty h}$ when generating SALCs and molecular orbital diagrams. The z axis is assigned to be colinear with the principal axis, and in this case is the same as the C_∞ axis (Figure 6.14.1).

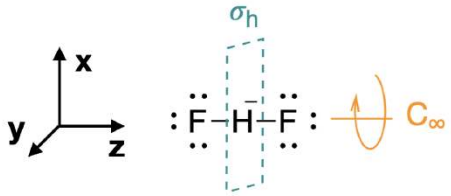


Figure 6.14.1: The [FHF]$^-$ anion belongs to the $D_{\infty h}$ point group. (CC-BY-NC-SA; Kathryn Haas)

Step 2. Identify and count the pendant atoms' valence orbitals.

The next step is to identify the valence orbitals on the pendant F atoms that will form SALCs. In most cases, you should consider all of the valence orbitals. In this case, each of the fluorine atoms has four valence orbitals ($2s$, $2p_x$, $2p_y$, and $2p_z$). From these eight fluorine valence orbitals, we should expect eight group orbitals (SALCs).

3. - 5. Generate SALCS (shortcut)

To draw these SALCs for this molecule is rather simple, and we don't need to follow all the steps of finding the Γ's and reducing them. Rather, you can proceed as if you are creating bonding and antibonding molecular orbitals between the two F atoms, except that the F orbitals are separated by the H atom. Approximate sketches of the eight SALCs from F valence orbitals are shown in Figure 6.14.2.

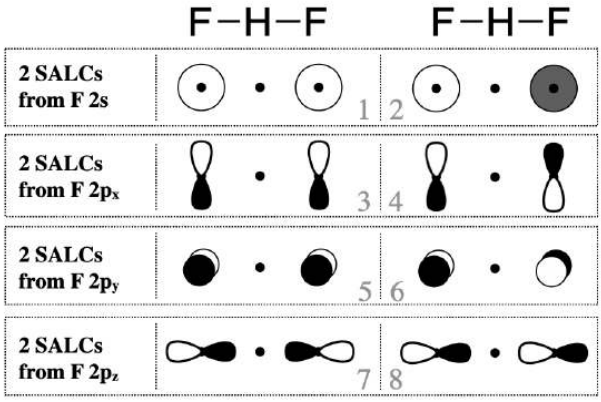


Figure 6.14.2: Eight SALCs from the valence orbitals of two fluorine atoms. (CC-BY-NC-SA; Kathryn Haas)

6. Draw the MO diagram by combining SALCs with AO's of like symmetry.

SALCs can productively interact with the central atom only when symmetry is compatible. Just some of the groups of orbitals in Figure 6.14.2 possess appropriate symmetry to combine with the hydrogen atom valence orbital (the H $1s$). In this simple case, you can decide whether orbitals have compatible symmetry by visually inspecting the shapes of the group orbitals. The F $2p_y$ and $2p_x$ orbitals do not have appropriate symmetry to bond to the H $1s$ orbital because the nodes of these orbitals run through the center of the H $1s$ orbital, thus we can eliminate all SALCs composed from F $2p_x$ and $2p_y$ (*these are SALCs numbered 3-6 in Figure* 6.14.2). On the other hand, the F $2s$ and $2p_z$ orbitals individually do have appropriate shape and direction in space for productive interaction

with an H $1s$ orbital. However only SALCs where the *entire group* has appropriate symmetry will combine with H $1s$ to produce bonding or antibonding molecular orbitals. Only the SALCs labeled with numbers 1 and 7 can combine with an s orbital in the center of the group. The ways in which these SALCs are able to combine with H $1s$ are illustrated in Figure **6.14.3**.

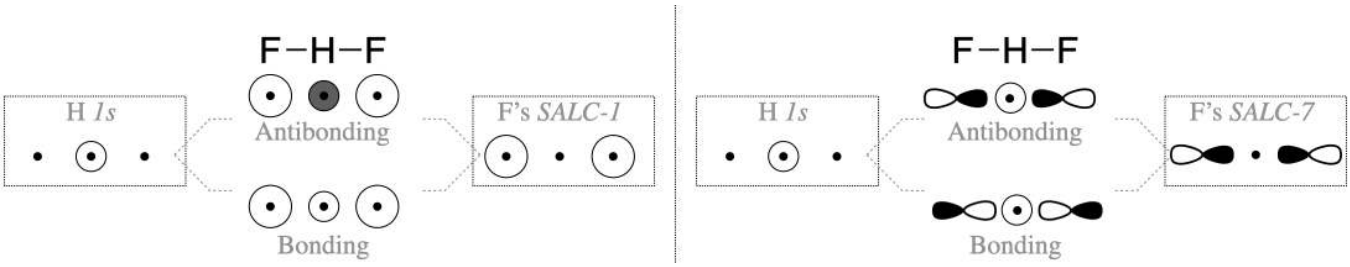
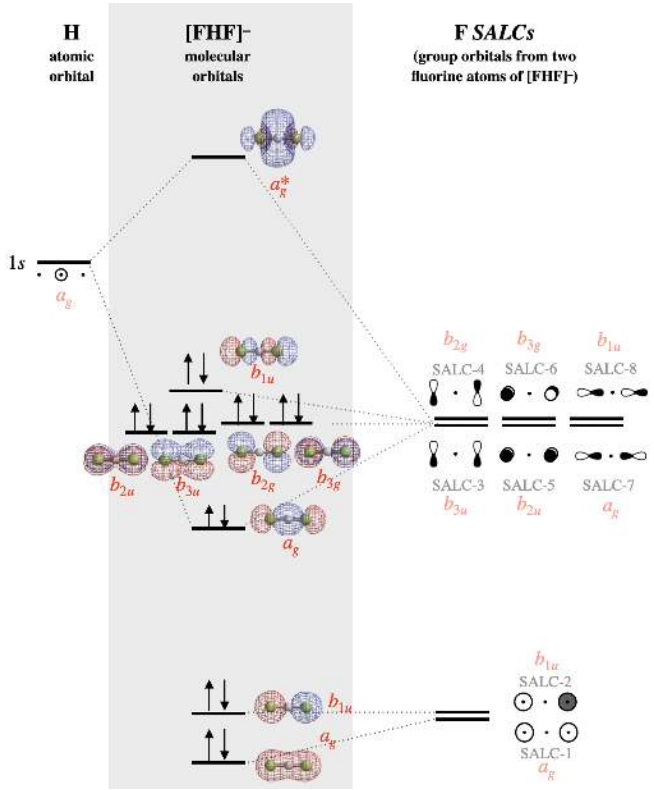


Figure **6.14.3**: Combinations of a central H $1s$ orbital with the group orbitals, SALC-1 and SALC-7 from Figure **6.14.2**, to create bonding and antibonding interactions. (CC-BY-NC-SA; Kathryn Haas)

Before we assume that both SALC-1 and SALC-7 will combine with the H $1s$ orbital, we must consider the energies of all atomic orbitals. The F $2p_z$ orbital has a potential energy of -18.7 eV (see Table 5.3.1). This is a good match for the H $1s$ orbital (-13.6 eV). However, the F $2s$ orbital has a much lower energy of -46.37 eV and would have weak interaction with the H $1s$.

The molecular orbital diagram for $[F\text{-}H\text{-}F]^-$ is shown in Figure **6.14.4**. Notice that all atomic orbitals, group orbitals (SALCs), and molecular orbitals in Figure **6.14.4** are assigned a symmetry label that corresponds to each element's symmetry under the D_{2h} point group. The molecular orbital labels correspond to **lower-case Mulliken Labels** of individual reducible representations from the D_{2h} character table. Upper-case symbols are used to indicate symmetry and irreducible representations, while lower-case symbols are used to indicate the identity of an orbital with that symmetry. The labeling methods described for simple diatomic linear molecules (σ, π) are not sufficient to indicate the more complex symmetries of the molecular orbitals in polyatomic molecules. The use of lower-case Mulliken symbols is the most rigorous way to label the orbitals. Refer to your instructor for how you should label orbitals for any graded work.

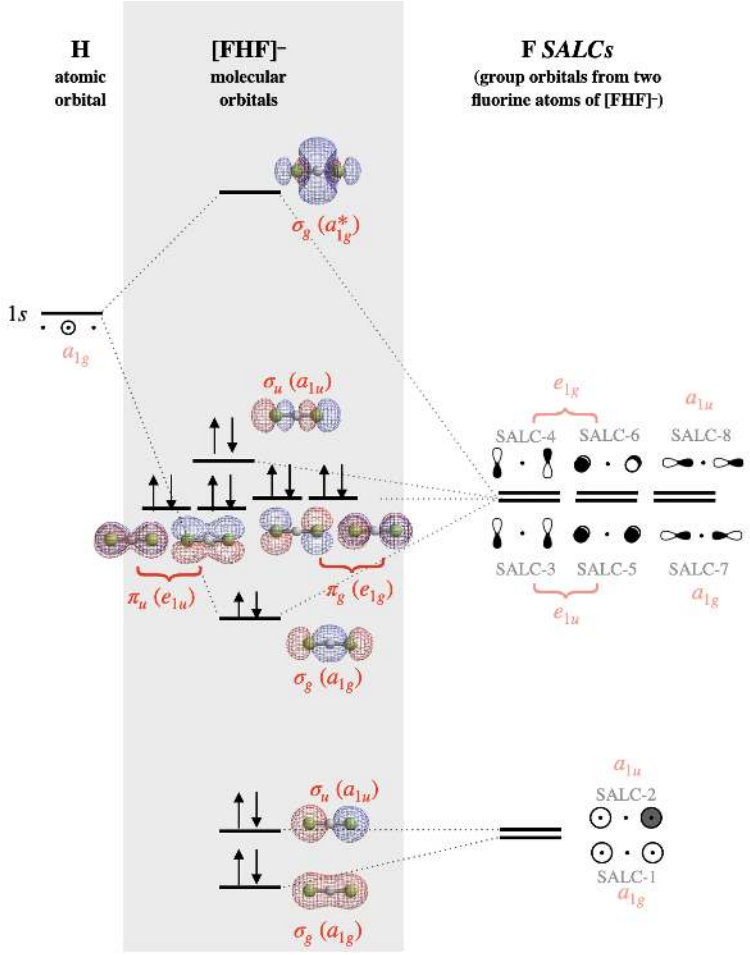


https://chem.libretexts.org/@go/page/403053

Figure **6.14.4**:The molecular orbital diagram for [F-H-F]⁻. The molecular orbital surfaces and relative energy levels were calculated using Spartan software. SALCs are labeled according to numbers assigned in Figure **6.14.2**. The symmetry of each SALC and orbital under the D_{2h} **point group** is shown in red font. (CC-BY-NC-SA; Kathryn Haas)

Click here for a version of Figure 6.14.4 using $D_{\infty h}$ labeling:

For high-symmetry groups, a shortcut is to use a lower-symmetry group that maintains the critical symmetry elements. In the case of the $D_{\infty h}$ point group, it is often sufficient to use the approximation of the D_{2h} point group and character table. This is the same MO diagram as shown above, but using the symmetry labels appropriate for the D_{2h} approximation.



Alternate Figure **6.14.4**: The molecular orbital diagram for [F-H-F]⁻. The molecular orbital surfaces and relative energy levels were calculated using Spartan software. SALCs are labeled according to numbers assigned in Figure **6.14.2**. The symmetry of each SALC and orbital under the D_{2h} **point group** is shown in red font. (CC-BY-NC-SA; Kathryn Haas)

Constructing the MO diagram

After identifying the atomic orbitals and constructing SALCs, place the atomic orbitals of H on one side of the diagram and all SALCs from F on the other side. Molecular orbitals are in the center.

The lowest-energy fluorine SALCs will be those composed of the lowest-energy atomic orbitals of fluorine; these would be SALC-1 (a_{1g}) and SALC-2 (a_{1u}) that are constructed from fluorine s atomic orbitals. Of these two orbitals, the one with zero nodes would be slightly lower in energy than the one with one node. When these two orbitals form molecular orbitals, the completely symmetric SALC-1 will be mostly non-bonding with slight bonding character from minor combination with the hydrogen $1s$ orbital. SALC-2, however is symmetrically incompatible with hydrogen $1s$ and will be a truly non-bonding orbital distributed over both F atoms.

The six SALCs constructed of fluorine p orbitals will have higher energy since the fluorine p atomic orbitals are higher in energy than the s orbitals (SALC-3 through SALC-8). Again, we expect SALCs with more nodes (SALC-4, -6, -8) to have slightly higher

energy than those with fewer nodes (SALC-3, -5, -7). SALC-7 will form a bonding and antibonding interaction with the hydrogen **1*s*** orbital. All other SALCS are truly non-bonding, but are non-degenerate non-bonding orbitals.

In bifluoride, there is an important distinction between the Lewis structure and molecular orbital description of lone pairs. In Lewis theory, the lone pairs are localized to individual fluorine atoms, while in the molecular orbital description each lone pair is distributed over both fluorine atoms at once (see surface depiction of each molecular orbital in Figure **6.14.4**).

6.14: Bifluoride anion is shared under a CC BY-SA 4.0 license and was authored, remixed, and/or curated by LibreTexts.

- **5.4.1: Bifluoride anion** is licensed CC BY-SA 4.0.

6.15: Carbon Dioxide

Construct SALCs and the molecular orbital diagram for CO_2

Carbon dioxide is another linear molecule. This example is slightly more complex than the previous example of the bifluoride anion. While bifluoride had only one valence orbital to consider in its central H atom (the $1s$ orbital), carbon dioxide has a larger central atom, and thus more valence orbitals that will interact with SALCs.

Preliminary Steps

Step 1. Find the point group of the molecule and assign Cartesian coordinates so that z is the principal axis.

The CO_2 molecule is linear and its point group is $D_{\infty h}$. The z axis is collinear with the C_∞ axis. We will use the D_{2h} point group as a substitute since the orbital symmetries are retained in the D_{2h} point group.

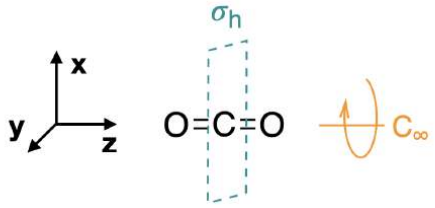


Figure 6.15.1: CO_2 belongs to the $D_{\infty h}$ point group. (CC_BY-NC-SA; Kathryn Haas)

Step 2. Identify and count the pendant atoms' valence orbitals.

Each of the two pendant oxygen atoms has four valence orbitals; $2s$, $2p_x$, $2p_y$, and $2p_z$. Thus, we can expect a total of eight SALCs.

Generate SALCs

The SALCs for CO_2 are identical in shape and symmetry to those described in the previous example for the bifluoride anion. But instead of cutting to the shortcut, we will systematically derive the SALCs here to demonstrate the process.

Step 3. Generate the Γ's

Use the D_{2h} character table to generate four reducible representations ($\Gamma's$); one for each of the four types of pendant atom orbitals (s, p_x, p_y, p_z). For each s orbital, assign a value of 1 if it remains in place during the operation or zero if it moves out of its original place. For each p orbital, assign 1 if there is no change, -1 if it remains in place but is inverted, and 0 if it moves out of its original position. The four Γ's are given below:

D_{2h}	E	$C_2(z)$	$C_2(y)$	$C_2(x)$	i	$\sigma(xy)$	$\sigma(xz)$	$\sigma(yz)$
Γ_{2s}	2	2	0	0	0	0	2	2
Γ_{2p_x}	2	−2	0	0	0	0	2	−2
Γ_{2p_y}	2	−2	0	0	0	0	−2	2
Γ_{2p_z}	2	2	0	0	0	0	2	2

Step 4. Break Γ's into irreducible representations for individual SALCs

Reduce each Γ into its component irreducible representations. There are two strategies that can be used to do this. The quick and easy way is to do it "by inspection", but this only works well for simple cases. The other is by using the systematic approach for breaking a Γ into reducible representations described previously in section 4.4.2 using the following formula:

$$\text{number of } i = \frac{1}{h}\sum(\text{number of operations in class}) \times (\chi_\Gamma) \times (\chi_i) \tag{6.15.1}$$

In other words, the number of irreducible representations of type i is equal to the sum of the number of operations in the class × the character of the Γ_{modes} × the character of i, and that sum is divided by the order of the group (h).

Using either approach results in the following eight irreducible representations ($2A_g + 2B_{1u} + B_{2g} + B_{3u} + B_{3g} + B_{2u}$):

$\mathbf{D_{2h}}$	E	$C_2(z)$	$C_2(y)$	$C_2(x)$	i	$\sigma(xy)$	$\sigma(xz)$	$\sigma(yz)$	
$\mathbf{\Gamma_{2s} = A_g + B_{1u}}$	$\mathbf{\Gamma_{2s}}$	**2**	**2**	**0**	**0**	**0**	**0**	**2**	**2**
	A_g	1	1	1	1	1	1	1	1
	B_{1u}	1	1	−1	−1	−1	−1	1	1
$\mathbf{\Gamma_{2p_x} = B_{2g} + B_{3u}}$	$\mathbf{\Gamma_{2p_x}}$	**2**	**−2**	**0**	**0**	**0**	**0**	**2**	**−2**
	B_{2g}	1	−1	1	−1	1	−1	1	−1
	B_{3u}	1	−1	−1	1	−1	1	1	−1
$\mathbf{\Gamma_{2p_y} = B_{3g} + B_{2u}}$	$\mathbf{\Gamma_{2p_y}}$	**2**	**−2**	**0**	**0**	**0**	**0**	**−2**	**2**
	B_{3g}	1	−1	−1	1	1	−1	−1	1
	B_{2u}	1	−1	1	−1	−1	1	−1	1
$\mathbf{\Gamma_{2p_z} = A_g + B_{1u}}$	$\mathbf{\Gamma_{2p_z}}$	**2**	**2**	**0**	**0**	**0**	**0**	**2**	**2**
	A_g	1	1	1	1	1	1	1	1
	B_{1u}	1	1	−1	−1	−1	−1	1	1

Step 5. Sketch the SALCs

From the systematic process above, you have found the symmetries (the irreducible representations) of all eight SALCs under the D_{2h} point group. To sketch the SALC that corresponds to each irreducible representation, again we use the D_{2h} character table, and specifically the functions listed on the right side columns of the table.

Two A_g SALCs (one from s and one from p_z): The A_g SALCs are each singly degenerate and symmetric with respect to both the principal axis (z) and the inversion center (i) (based on its Mulliken Label). We can look at the functions in the D_{2h} character table that correspond to A_g and see that it is completely symmetric under the group (because the combination of x^2, y^2, z^2 shows that it is totally symmetric). This would be the same symmetry as an s orbital on the central atom. From this information, we know that these SALCs must have symmetry compatible with an s orbital on the central atom, and we can draw the two A_g SALCs shown in Figure 6.15.2.

Two B_{1u} SALCs (one from s and one from p_z): The Mulliken Label tells us that the B_{1u} SALCs are each antisymmetric with respect to both the principal axis and the inversion center. The function, z, appearing with B_{1u} in the character table tells us that these SALCs have the same symmetry as the z axis, or a p_z orbital on the central atom. From this information, we know that these two SALCs should be compatible with a p_z orbital on the central atom, and we can draw the two B_{1u} SALCs shown in Figure 6.15.2.

All other SALCs shown below are derived using a strategy similar to the one in the two cases described above.

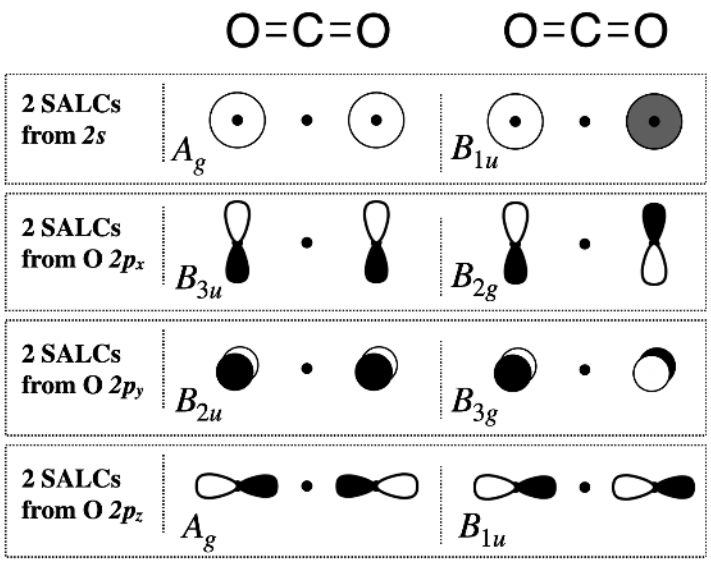


Figure 6.15.2: SALCs from the valence orbitals of oxygen atoms in CO_2. (CC-BY-NC-SA; Kathryn Haas)

Draw the MO diagram for CO_2

Step 6. Combine SALCs with AO's of like symmetry.

First we identify the valence orbitals on carbon: there are four including $2s$, $2p_x$, $2p_y$, and $2p_z$. Now we identify the symmetry of each using the D_{2h} character table. The symmetry of a central s orbital corresponds to the combination of functions x^2, y^2, and z^2 in the character table; this is A_g. The p_z orbital corresponds to the symmetry of the linear function z in the character table; this is B_{1u}. And so on... The symmetries of the C valence orbitals are listed below.

$$2s = A_g$$
$$2p_x = B_{3u}$$
$$2p_y = B_{2u}$$
$$2p_z = B_{1u}$$

Now that we have identified the symmetries of the eight oxygen SALCs and the four valence orbitals on carbon, we know which atomic orbitals and SALCs may combine based on compatible symmetries. We also need to know the relative orbital energy levels so that we can predict the relative strength of orbital interactions. The orbital ionization energies are listed in Section 5.3.

With knowledge of both orbital symmetries and energies, we can construct the molecular orbital diagram. The carbon atom goes on one side of the diagram while the oxygen SALCs are drawn on the opposite side. Molecular orbitals are drawn in the center column of the diagram:

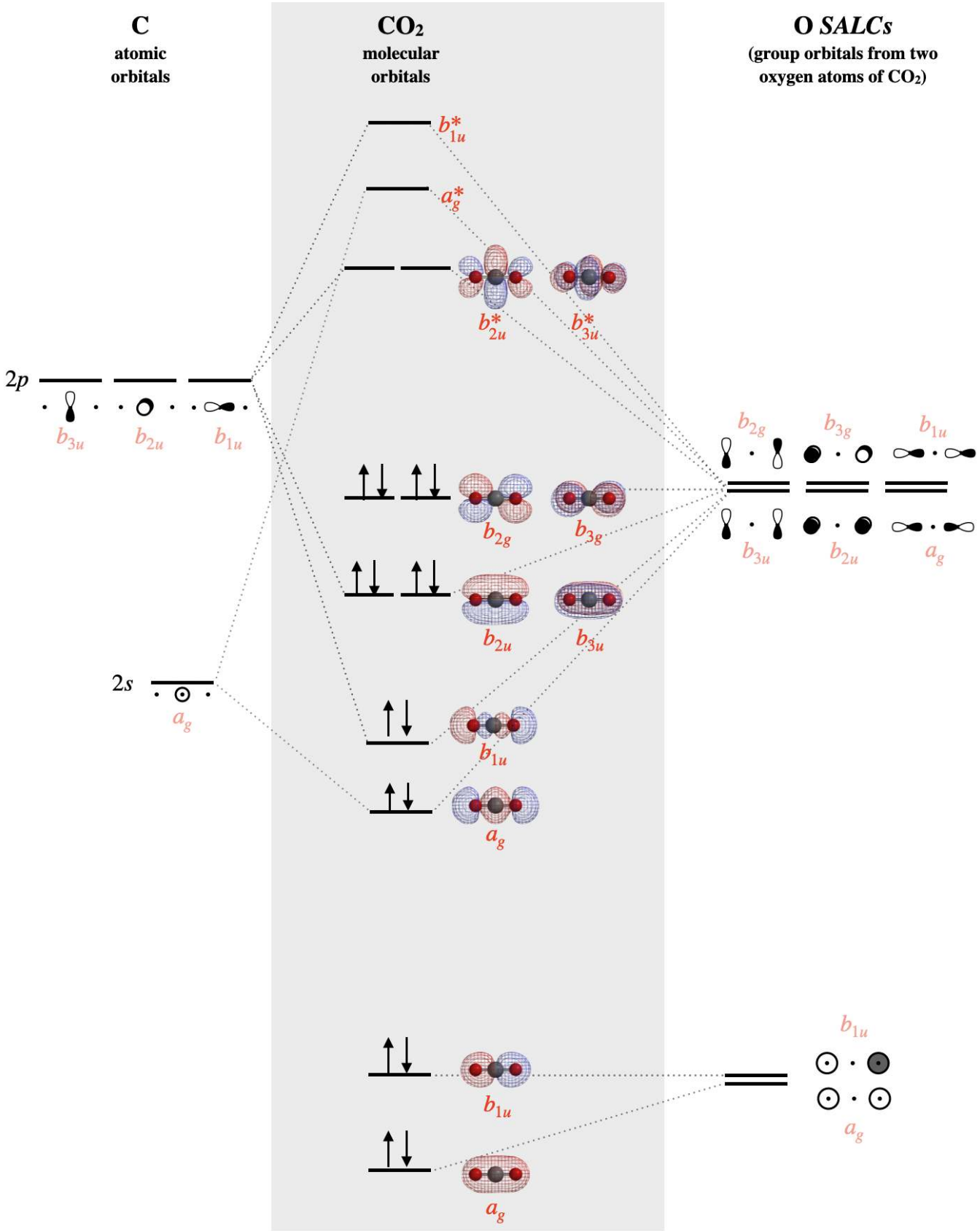


Figure 6.15.3: Molecular orbital diagram for carbon dioxide. (CC-BY-NC-SA; Kathryn Haas)

The SALCs on the right side of the diagram above are constructed from groups of either the $2s$ atomic orbitals of oxygen, or the $2p$ atomic orbitals of oxygen. Each SALC will combine with the atomic orbitals of carbon that have compatible symmetry; but the strength of the interaction depends on their relative energies. The individual valence atomic orbitals of oxygen have energies of $-32.36eV$ ($2s$) and $-15.87eV$ ($2p$), while the valence orbitals of carbon have energies of $-19.47eV$ ($2s$) and $-10.66eV$ ($2p$). The $2s$ orbitals of the oxygen are far lower in energy ($-32.36eV$) than all other valence orbitals, and so we should expect that molecular orbitals that are constructed from these oxygen $2s$ will be mostly non-bonding. These mostly non-bonding orbitals are the a_{1g} and b_{1g} orbitals shown at the bottom of Figure $6.15.3$. The a_g orbital is lower in energy than the b_{1u} due to slight mixing with other orbitals of a_g symmetry.

The bonding orbitals of CO_2 include two $sigma$ molecular orbitals of a_g and b_{1u} symmetry and two π molecular orbitals of b_{2u} and b_{3u} symmetry. Each of these bonding molecular orbitals possesses a higher-energy antibonding partner. The b_{2g} and b_{3g} SALCs that are formed from oxygen $2p_x$ and $2p_y$ orbitals have no compatible match with carbon valence orbitals; thus they form two b_{2g} and b_{3g} molecular orbitals, which are truly non-bonding and mostly oxygen in character. Still, notice that each orbital is spread across both oxygen atoms at once, and again we see that each non-bonding electron pair in the HOMO is very different in molecular orbital theory compared to Lewis theory. Each non-bonding pair is distributed over both oxygen atoms at once in molecular orbital theory, while in Lewis theory each lone pair is isolated to one atom or to localized bonds attached to that atom.

This page titled 6.15: Carbon Dioxide is shared under a CC BY-SA 4.0 license and was authored, remixed, and/or curated by Kathryn Haas.

- **5.4.2: Carbon Dioxide** by Kathryn Haas is licensed CC BY-SA 4.0.

6.16: H_2O

Construct SALCs and the molecular orbital diagram for H_2O.

This is the first example so far that is not a linear molecule. Water is a bent molecule, and so it is important to remember that interactions of pendant ligands are dependent on their positions in space. You should consider the positions of the three atoms in water to be essentially fixed in relation to each other. The process for constructing the molecular orbital diagram *for a non-linear molecule*, like water, is similar to the process for linear molecules. We will walk through the steps below to construct the molecular orbital diagram of water.

Preliminary Steps

Step 1. Find the point group of the molecule and assign Cartesian coordinates so that z is the principal axis.

The H_2O molecule is bent and its point group is C_{2v}. The z axis is collinear with the principal axis, the C_2 axis. There is no need to simplify this problem, as we had done for previous examples. The C_{2v} point group is simple enough.

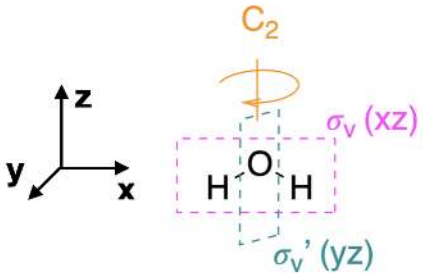


Figure **6.16.1**: The water molecular is in the C_{2v} point group. (CC-BY-NC-SA; Kathryn Haas)

Step 2. Identify and count the pendant atoms' valence orbitals.

Each of the two pendant hydrogen atoms has one valence orbital, the $1s$. Thus, we can expect a total of two SALCs from these two atoms.

Generate SALCs

The SALCs for H_2O are quite simple, yet we will systematically derive the SALCs here to demonstrate the process.

Step 3. Generate the Γ's

Use the C_{2v} character table to generate one reducible representation (Γ); in this case we need only one Γ because there is only one type of valence orbital (the $1s$). For each s orbital, assign a value of 1 if it remains in place during the operation or zero if it moves out of its original place. The Γ is given below:

C_{2v}	E	C_2	$\sigma_v(xz)$	$\sigma_v'(yz)$
Γ_{1s}	2	0	2	0

Step 4. Break Γ's into irreducible representations for individual SALCs

Reduce each Γ into its component irreducible representations. Using either of the processes described previously, we find that the Γ reduces to the two irreducible representations A_1 and B_1 under the C_{2v} point group.

C_{2v}	E	C_2	$\sigma_v(xz)$	$\sigma_v'(yz)$
Γ_{1s}	**2**	**0**	**2**	**0**
A_1	1	1	1	1
B_1	1	−1	1	−1

Step 5. Sketch the SALCs

From the systematic process above, you have found the symmetries (the irreducible representations) of both SALCs under the C_{2v} point group. To sketch the SALC that corresponds to each irreducible representation, again we use the C_{2v} character table, and

specifically the functions listed on the right side columns of the table.

One A_1 SALC: The A_1 SALC is singly degenerate and symmetric with respect to both the principle axis (z) and the inversion center (i) (based on its Mulliken Label). We can look at the functions in the C_{2v} character table that correspond to A_1 and see that it is completely symmetric under the group (because the combination of x^2, y^2, z^2 shows that it is totally symmetric). This would be the same symmetry as an s orbital on the central oxygen atom. From this information, we know that this SALC must have symmetry compatible with an s orbital on the central atom. We can also see from the character table that the z axis, and thus a p_z orbital on oxygen, also possesses A_1 symmetry. This tells us that in addition to being compatible with the oxygen s orbital, it should also be compatible with the oxygen p_z orbital. From this information we can draw the A_1 SALC shown in Figure **6.16.2**. *If it is not obvious how the A_1 sketch in Fig.* **6.16.2** *is compatible with the s and p_z orbitals of oxygen, inspect the drawings corresponding to molecular orbitals $2a_1$ and $3a_1$ in Fig.* **6.16.3**.

One B_1 SALC: The Mulliken Label tells us that the B_1 SALC is singly degenerate and antisymmetric with respect to both the principal axis and the inversion center. The function, x, appearing with B_1 in the character table tells us that this SALC has the same symmetry as the x axis, or a p_x orbital on the central oxygen atom. From this information, we know that this SALC should be compatible with a p_x orbital on the central atom, and we can draw the B_1 SALCs shown in Figure **6.16.2**. *If it is not obvious how the B_1 sketch in Fig.* **6.16.2** *is compatible with the p_x orbital of oxygen, inspect the drawing corresponding to molecular orbital $1b_1$ in Fig.* **6.16.3**.

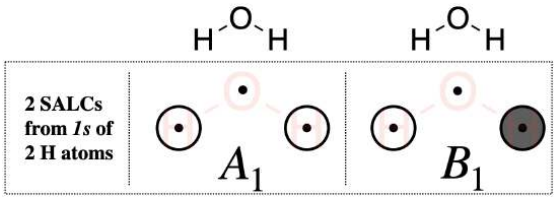


Figure **6.16.2**: Sketch of the A_1 and B_1 hydrogen SALCs of water. (CC-BY-NC-SA; Kathryn Haas)

Not convinced about the sketches of these SALCs? You can convince yourself by putting them to the test. Try the exercise below.

? Exercise 6.16.1

Perform all operations of the C_{2v} point group on the two sketches of H SALCs shown in Figure **6.16.2**, and convince yourself that each sketch does possess the A_1 and B_1 symmetries assigned to them, respectively, under the C_{2v} point group.

Answer

Add texts here. Do not delete this text first.

Draw the MO diagram for H_2O

Step 6. Combine SALCs with AO's of like symmetry.

First we must identify the valence orbitals on the central oxygen: there are four including $2s$, $2p_x$, $2p_y$, and $2p_z$. Now we identify the symmetry of each using the C_{2v} character table. The symmetry of a central $2s$ orbital corresponds to the combination of functions x^2, y^2, and z^2 in the character table; this is A_1. The p_z orbital also corresponds to A_1. And so on... The symmetries of oxygen valence orbitals are listed below.

$$2s = A_1$$
$$2p_x = B_1$$
$$2p_y = B_2$$
$$2p_z = A_1$$

Now that we have identified the symmetries of the two hydrogen SALCs and the four valence orbitals on oxygen, we know which atomic orbitals and SALCs may combine based on compatible symmetries. We also need to know the relative orbital energy levels so that we can predict the relative strength of orbital interactions. The orbital ionization energies are listed in Section 5.3.1.

With knowledge of both orbital symmetries and energies, we can construct the molecular orbital diagram. The valence orbitals of oxygen go on one side of the diagram while the hydrogen group orbitals are drawn on the opposite side. Molecular orbitals are

drawn in the center column of the diagram, as shown in Figure **6.16.3**:

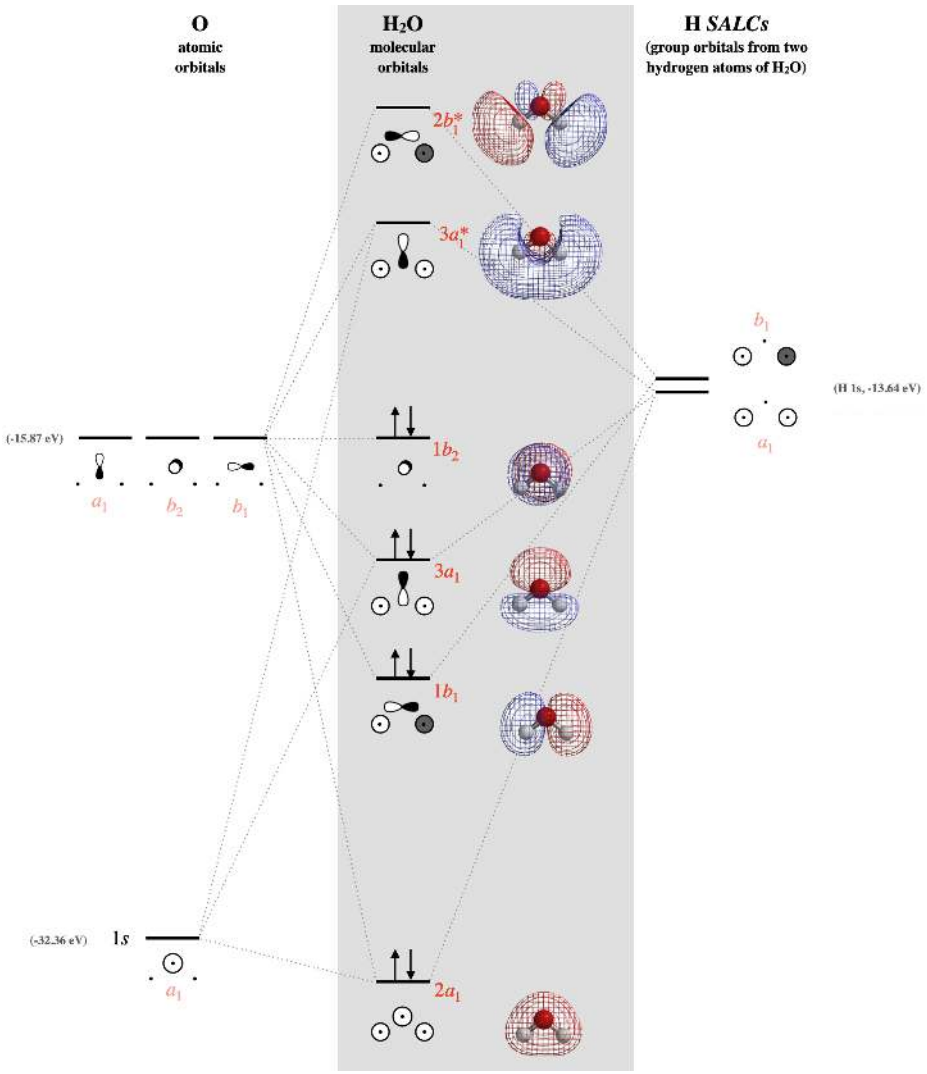


Figure **6.16.3**: The molecular orbital diagram of water. Molecular orbital surfaces calculated using Spartan software. The surface of the $3a_1^*$ orbital has been trimmed. (CC-BY-NC-SA; Kathryn Haas)

Example 6.16.1

In the previous examples shown for the molecular orbital diagrams of the bifluoride anion and carbon dioxide, we discussed differences in the understanding of those molecules from molecular orbital theory compared to Lewis structures. Water contains two lone pairs in its Lewis structure. Compare the predictions about water's lone pairs of electrons and its reactivity based on (1) the combination of elementary models (Lewis, Valence Bond, and Hybridized Orbital theories) and (2) Molecular Orbital theory. Specifically address and explain how the elementary models differ from molecular orbital theory in the following respects:

a. Where are the lone pairs in water?
b. Are the two lone pairs equivalent or are they different?
c. Where are sites on the molecule that will undergo reaction with electrophiles and nucleophiles?

Solution

1) Elementary models: The Lewis structure predicts that two lone pairs are (a) localized on the oxygen atom of water and that (b) both lone pairs are equivalent. The Lewis structure, combined with Valence Bond Theory, would predict that lone pairs occupy two equivalent hybridized sp^3 atomic orbitals on oxygen. (c) Lewis theory would predict that the oxygen lone pairs are

nucleophiles; thus an electrophile would react with the oxygen atom lone pairs. The polarized O-H bond leaves the H atoms as the most electrophilic locations on the water molecule; thus nucleophiles would react at the H atoms of water.

2) Molecular orbital theory: The molecular orbitals predict that (a) the two lone pairs of water are not equivalent, and that (b) each is distributed over the entire molecule. One lone pair is in the truly non-bonding $1b_2$ orbital (Figure **6.16.3**), which is also the HOMO. There is not another truly non-bonding orbital in the molecule, but the lowest-energy $2a_1$ orbital could be considered mostly non-bonding due to the large energy difference between it and other valence orbitals. (c) Although the $2a_1$ orbital can be considered mostly non-bonding, we cannot expect the electrons in $2a_1$ to react readily, as they are in the lowest-energy molecular orbital. Molecular orbital theory predicts that reactions occur at the HOMO and LUMO orbitals. The HOMO reacts with electrophiles, and in this case, the HOMO is distributed over the top and bottom faces of the molecule, and is centered on the oxygen atom. The LUMO would react with nucleophiles. The LUMO is the orbital labeled $3a_1^*$ in Figure **6.16.3**, and has a major lobe that is distributed more heavily over the H atoms, and from this we should predict H atoms to be the preferred site of reaction for nucleophiles.

Expressing molecular orbitals in terms of Ψ

The general expression for a molecular orbital, or the linear combination of atomic orbitals (LCAO), was given previously as $\Psi = c_a\psi_a + c_b\psi_b$. In this expression, the wavefunction of two atoms (ψ_a and ψ_b) is combined to form the wavefunction of the molecular orbital. The coefficients c_a and c_b quantify the contribution of each atomic ψ to the molecular Ψ.

$$\Psi = c_a\psi_a + c_b\psi_b$$

In the case of polyatomic orbitals, each LCAO is constructed of atomic orbitals from a central atom and group orbitals (SALCs) from the pendent atoms. In the case of water, the expression above could be modified to give the expression below.

$$\Psi = c_{oxygen}\,(\psi_{oxygen}) + c_{SALCs}\,(N(\psi_{H_a} \pm \psi_{H_b}))$$

N represents the normalizing requirement that was mentioned previously in reference to the requirements for electron wavefunctions and probability functions. The normalizing requirement simply stated is the requirement that the probability of finding the electron in any orbital, including group orbitals, is 1. In general, the value of N for a group orbital is...

$$N = \frac{1}{\sum c_i^2}$$

...where c_i is the coefficient of each unique atomic orbital that contributes to the group. For the hydrogen SALCs of water, there are two atomic orbitals that contribute to equally to each SALC, and so the coefficient on each of the two orbitals is 1. This gives $N = \left(\frac{1}{\sqrt{1^2+1^2}}\right) = \frac{1}{\sqrt{2}}$ for the H SALCs of water.

There are only two hydrogen SALCs: the one in which the hydrogen wavefunctions are added ($N(\psi_{H_a} + \psi_{H_b})$) has A_1 symmetry, and the one in which the hydrogen wavefunctions are subtracted ($N(\psi_{H_a} - \psi_{H_b})$) has B_1 symmetry.

The molecular orbitals from Figure **6.16.3** are expressed below in terms of their LCAO of individual wavefunctions. Yet, note that these expressions are simplifications that ignore orbital mixing. For example, as expressed below, they ignore contributions of oxygen $2s$ to the higher energy moelcular orbitals with A_1 symmetry (the $3a_1$ and $3a_1^*$ in Figure **6.16.3**).

MO		*OxygenAO*		*HydrogenSALC*	*Description*
Ψ_{2a_1}	=	$c_{(ox1)}\psi_{(2s)}$	+	$c_{(hy1)}[N(\psi_{H_a} + \psi_{H_b})]$	$c_{(hy1)}$ is positive; bonding, slightly nonbonding
Ψ_{1b_1}	=	$c_{(ox2)}\psi_{(2p_x)}$	+	$c_{(hy2)}[N(\psi_{H_a} - \psi_{H_b})]$	$c_{(hy2)}$ is positive; bonding
Ψ_{3a_1}	=	$c_{(ox3)}\psi_{(2p_z)}$	+	$c_{(hy3)}[N(\psi_{H_a} + \psi_{H_b})]$	$c_{(hy3)}$ is positive; bonding
Ψ_{1b_2}	=	$\psi_{(2p_y)}$			nonbonding
$\Psi^*_{3a_1}$	=	$c_{(ox4)}\psi_{(2p_z)}$	+	$c_{(hy4)}[N(\psi_{H_a} + \psi_{H_b})]$	$c_{(hy4)}$ is negative; antibonding
$\Psi^*_{1b_1}$	=	$c_{(ox5)}\psi_{(2p_x)}$	+	$c_{(hy5)}[N(\psi_{H_a} - \psi_{H_b})]$	$c_{(hy5)}$ is negative; antibonding

6.16: H_2O is shared under a CC BY-SA 4.0 license and was authored, remixed, and/or curated by LibreTexts.

- **5.4.3: H_2O** is licensed CC BY-SA 4.0.

6.17: NH_3

Construct SALCs and the molecular orbital diagram for NH_3

This is the first example so far that has more than two pendant atoms and the first example in which the molecule has atoms that lie in three dimensions (i.e., it is not flat). Ammonia is a trigonal pyramidal molecule, with three pendant hydrogen atoms. The three-dimensional shape and the odd number of pendant atoms makes this example more complicated than the previous cases of water, carbon dioxide, and bifluoride. In this case, sketching the shapes (step 5) of pendant atom SALCs is less straightforward; rather, an alternative method, the **projection operator method**, is preferred for generating pictorial representations of the SALCs.

As in previous examples, it is important to remember that interactions of pendant ligands are dependent on their positions in three-dimensional space. You should consider the positions of the four atoms in ammonia to be essentially fixed in relation to each other. We will walk through the steps used to construct the molecular orbital diagram of ammonia. The first few steps are the same as you've seen before:

Step 1. Find the point group of the molecule and assign Cartesian coordinates so that z is the principal axis.

The NH_3 molecule is trigonal pyramidal and its point group is C_{3v}. The z axis is collinear with the principal axis, the C_3 axis.

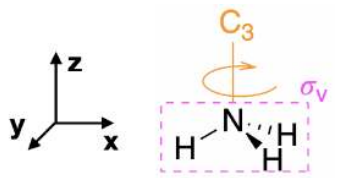


Figure **6.17.1**: The ammonia molecule is in the C_{3v} point group. (CC-BY-NC-SA; Kathryn Haas)

Step 2. Identify and count the pendant atoms' valence orbitals.

Each of the three pendant hydrogen atoms has one valence orbital; the $1s$. Thus, we can expect a total of three SALCs from these three atoms.

Step 3. Generate the Γ's

Use the C_{3v} character table to generate one reducible representation (Γ); in this case we need only one Γ because there is only one type of valence orbital (the $1s$). For each s orbital, assign a value of 1 if it remains in place during the operation or zero if it moves out of its original place. The Γ is given below:

C_{3v}	E	$2C_3$	$3\sigma_v$
Γ_{1s}	3	0	1

Step 4. Break Γ's into irreducible representations for individual SALCs

Reduce each Γ into its component irreducible representations. Using either of the processes described previously, we find that the Γ reduces to the two irreducible representations A_1 and E under the C_{3v} point group.

C_{3v}	E	$2C_3$	$3\sigma_v$
Γ_{1s}	3	0	2
A_1	1	1	1
E	2	−1	0

Notice that we only found TWO irreducible representations. But, in fact we have THREE different SALCs. The E irreducible representation is doubly degenerate, which in this context means that it corresponds to two degenerate SALCs. Thus, we have already found the symmetries of the three SALCs for ammonia: Two of the SALCs are degenerate with E symmetry under the C_{3v} point group, while the third SALC has A_1 symmetry.

Step 5. Sketch the SALCs using the PROJECTION OPERATOR METHOD

From the first four steps (described above), you have found the symmetries (the irreducible representations) of all three SALCs under the C_{3v} point group. To sketch the SALC that corresponds to each irreducible representation, again we use the C_{3v} character

table. But now we will introduce the **projection operator method** to derive the surface representation of each SALC.

Step 5.1: Label the pendent atoms

In the projection operator method, first **label each of the pendant atoms so that we can distinguish identical atoms from one another**; for example, identify the three hydrogen atoms on ammonia as H_a, H_b, and H_c (Figure 6.17.2).

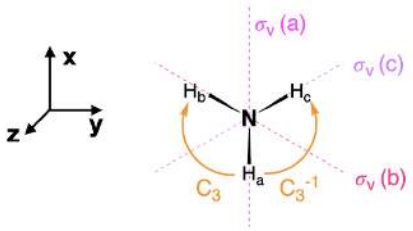


Figure 6.17.2: The three H's in NH_3 are chemically identical, but we can distinguish them using labels for the purpose of applying the projection operator method. In this figure, we have placed the z axis along the principal C_3 axis and placed the x axis colinear with one H. Each of the three H atoms has been labeled as H_a, H_b, or H_c. The σ_v that is coplanar with each H is labeled similarly (a, b, c) to keep account of each individual plane of symmetry. (CC-BY-NC-SA; Kathryn Haas)

Step 5.2: Create an expanded character table with one pendant atom's projected position after each operation

We will **perform each operation of the C_{3v} point group on this labeled molecule** and follow where one of the atoms is projected after the operation is complete. We will arbitrarily choose H_a. For example, upon performing the identity operation, E, the H_a atom is projected onto itself. On the other hand, H_a is projected onto H_b upon a clockwise C_3 rotation (as drawn in Figure 6.17.2). We take into account the result of each operation using an expanded character table (refer to the table below, 6.17.1). In the expanded character table, each operation within each class is written separately (i.e., $2C_3$ is accounted for separately as C_3 and C_3^{-1}).

Table 6.17.1: The expanded character table, and the projection of H_a by each operation is shown below.

$\mathbf{C_{3v}}$	E	C_3	C_3^{-1}	$\sigma_v(a)$	$\sigma_v(b)$	$\sigma_v(c)$
Projection of $\mathbf{H_a}$	H_a	H_b	H_c	H_a	H_c	H_b

(6.17.1)

Step 5.3: Find the contribution of each pendant atom to each SALC

Next, **create a linear combination of the projections for each of the SALCs** (the irreducible representations found in step 4). For each of the irreducible representations, multiply the projection by the respective character of the operation.

$$\text{Contribution of each atom to the SALC } = \sum(\text{Projection of } H_a \times \chi)$$

The linear combination for all irreducible representations of C_3v is shown below.

Table 6.17.2: The symmetry adapted linear combination (SALC) for each irreducible representation of C_3v is shown.

$\mathbf{C_{3v}}$	E	C_3	C_3^{-1}	$\sigma_v(a)$	$\sigma_v(b)$	$\sigma_v(c)$	Linear Combination
Projection of $\mathbf{H_a}$	$\mathbf{H_a}$	$\mathbf{H_b}$	$\mathbf{H_c}$	$\mathbf{H_a}$	$\mathbf{H_c}$	$\mathbf{H_b}$	
A_1	1	1	1	1	1	1	$= \mathbf{2H_a + 2H_b + 2H_c}$
A_2	1	1	1	−1	−1	−1	$= 0$
E	2	−1	−1	0	0	0	$= \mathbf{2H_a - H_b - H_c}$

(6.17.2)

Notice that there are only two irreducible representations that produce SALCs, and these are the same that were found in Step 4, above. This illustrates the fact that only the irreducible representations found through the reduction of the Γ will produce SALCs. We can ignore any irreducible representations that were not found in Step 4. Or, you can check your work in Step 4 by applying the projection operator to any irreducible representations not found in Step 4, and finding that they produce a sum of zero.

Step 5.4: Sketch the SALCs

The meaning of the linear combinations found in Table 6.17.2 is as follows:

- **Sketch the SALC with A_1 symmetry:** The linear combination $2H_a + 2H_b + 2H_c$ indicates all contributions to this SALC are of the same sign (of the wavefunction). Qualitatively, this means there is no node in this SALC. We can take this SALC almost literally to assume that all three H 1s wavefunctions contribute equally to the SALC. We can also use the fact that the A_1 representation possesses the full symmetry of the C_3v point group, is compatible with an s orbital on N, and thus is a totally symmetric SALC.

  Quantitatively, we can apply the normalizing factor, N, for this SALC. The linear combination for the A_1 SALC in Table 6.17.2 shows us that the coefficient for each orbital is 1. Thus, the normalizing factor for the A_1 SALC is $N = \left(\frac{1}{\sqrt{1^2+1^2+1^2}}\right) = \frac{1}{\sqrt{3}}$. This tells us that H_a, H_b, and H_c each contribute $\frac{1}{\sqrt{3}}$ to the normalized A_1 group orbital:

  $$A_1 \text{ group orbital } = \frac{1}{\sqrt{3}}\left[\psi_{H_a} + \psi_{H_b} + \psi_{H_c}\right]$$

  This is shown visually in Figure **6.17.3**.
- **Sketch two SALCs with E symmetry:** The linear combination $2H_a - H_b - H_c$ indicates that there are contributions with both positive and negative sign to the wavefunction for each of the E group orbitals. Qualitatively, this tells us that there is a node within each of these two SALCs, and that the total contribution of the positive portion of the wavefunction is equal to the contribution of the negative portion.
  - **Finding the first E SALC:**
    For one of the SALCs, we can take the linear combination from Table 6.17.2 almost literally: The contribution from H_a is equal and opposite to the sum of the contributions from $H_b + H_c$. This would result in a SALC as shown in Figure **6.17.3** (E, left), that would have symmetry of the x axis and that would be compatible with the p_x orbital on N. The node exists in the yz plane and there is an equal contribution of positive and negative parts of the total wavefunction.

    We can also apply the normalizing factor, N, to find this SALC. The linear combination for the E SALC in Table 6.17.2 shows us that the coefficients for orbital contributions are 2, -1, and -1. Thus, the normalizing factor for the first E SALC is $N = \left(\frac{1}{\sqrt{2^2+(-1)^2+(-1)^2}}\right) = \frac{1}{\sqrt{6}}$. This normalized E group orbital is:

    $$\text{First } E \text{ group orbital } = \frac{1}{\sqrt{6}}\left[2\psi_{H_a} - \psi_{H_b} - \psi_{H_c}\right]$$

    This is shown visually in Figure **6.17.3** (E, left).
  - **Finding the second E SALC:**
    The second SALC is less obvious at first glance. We must use clues from the character table to help us determine what it should "look like". Since the E representation transforms as the group, (x, y), we know that one of the SALCs will have the symmetry of the x axis and p_x orbital on the central nitrogen atom, while the other should possess the symmetry of the y axis and be compatible with the p_y orbital on nitrogen. This alone could lead you to the sketch of the second SALC with E symmetry shown in Figure **6.17.3** (E, right). This second E SALC must have a node in the xz plane, and because H_a lies in this node, H_a cannot contribute to this group orbital. Retaining the fact that the positive and negative contributions of the linear combination must be equal, we can arrive at a SALC that has equal but opposite contributions of H_b and H_c, and no contribution by H_c (Figure **6.17.3**, right).

    We can also apply the normalizing factor, N, to find this SALC. But we must apply the fact that H_a cannot contribute to the SALC with "y" symmetry. We remove the contribution of H_a, leaving us with coefficients of 0 for H_a and 1 for H_b and H_c. Thus, the normalizing factor for the second E SALC is $N = \left(\frac{1}{\sqrt{0^2+1^2+1^2}}\right) = \frac{1}{\sqrt{2}}$. To this, we must add positive and negative coefficients so that the entire wavefunction of this SALC is normalized. The result for this normalized E group orbital is:

    $$\text{Second } E \text{ group orbital } = \frac{1}{\sqrt{2}}\left[\psi_{H_b} - \psi_{H_c}\right]$$

    This is shown visually in Figure **6.17.3**.

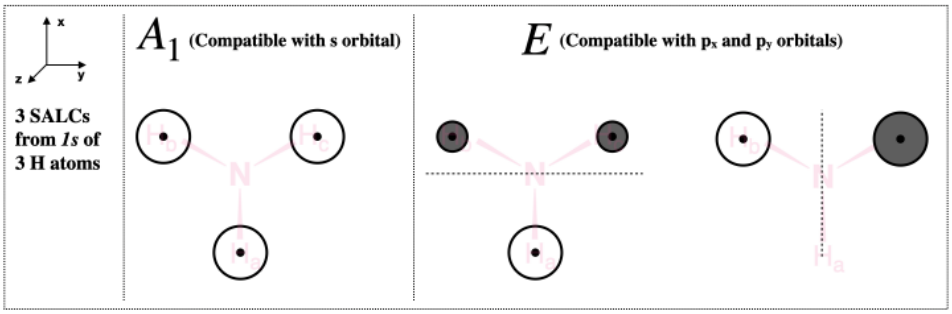


Figure **6.17.3**: Sketches of H SALCs of ammonia from the perspective of the C_3 axiz (z axis). The A_1 SALC is shown at the left, while two degenerate SALCs with E symmetry are shown on the right. Nodes for E group orbitals are shown as dashed lines. (CC-BY-NC-SA; Kathryn Haas)

Step 6. Combine SALCs with AO's of like symmetry to draw the MO diagram for NH_3

First we must identify the valence orbitals on the central nitrogen: there are four including $2s$, $2p_x$, $2p_y$, and $2p_z$. Now we identify the symmetry of each using the C_{3v} character table. The symmetry of a central $2s$ orbital corresponds to the combination of functions x^2, y^2, and z^2 in the character table; this is A_1. The p_z orbital also corresponds to A_1. And so on... The symmetries of nitrogen valence orbitals are listed below.

$$2s = A_1$$
$$(2p_x,\ 2p_y) = E$$
$$2p_z = A_1$$

The next step is to get a sense of the relative energies of valence atomic orbitals for nitrogen and hydrogen, and then construct the molecular orbital diagram. The nitrogen $2s$ orbital is about 12 eV lower in energy than a H $1s$. This difference is an acceptable energy-match for the H orbitals to interact, but would not usually result in a strong interaction. On the other hand, the nitrogen 2p orbitals have an energy very close to the hydrogen 1s, different by only 0.5 eV. Knowledge of the relative energies of the atomic orbitals tells us that, when constructing a diagram, we can place the H SALCs at an energy similar to that of the N $2p$ orbitals, while the N $2s$ is much lower (Figure **6.17.4**).

The $2s$ and $2p_z$ orbitals have A_1 symmetry and can combine with the A_1 SALC. These orbitals will give three molecular orbitals. The $2s$ orbital will not have strong interactions with the other orbitals of A_1 symmetry due to the large energy difference. The $2p_z$ orbital will not have good overlap with the wavefunctions for the three hydrogen orbitals due to their positions in space: The $2p_z$ orbital has half of its angular distribution pointed away from the hydrogen orbitals, and half pointed toward the center of a triangle formed by the three hydrogen atoms. The nitrogen $2s$ and $2p_z$ will combine with the hydrogen SALC of A_1 symmetry to give three molecular orbitals; one low-energy bonding orbital, one mid-energy non-bonding orbital, and one high-energy antibonding orbital. The mid-level non-bonding a_1 molecular orbital is close in energy to, and resembles, the nitrogen $2p_z$ orbital. The lowest energy a_1 molecular orbital will be lower in energy, but be similar to the nitrogen $2s$.

The remaining two $2p$ orbitals are degenerate and possess E symmetry under the C_{3v} point group. Although these orbitals are a good energy match, again, their orientation and positions in space do not allow for good orbital overlap, and their bonding and antibonding interactions are relatively weak compared to what we might otherwise expect from such a good energy match. The e atomic orbitals of nitrogen will combine with the e SALCs to give a set of two degenerate bonding molecular orbitals and a set of two degenerate antibonding orbitals (four total molecular orbitals of e symmetry). The MO diagram for NH_3 is shown in Figure **6.17.4**, with calculated electron density surfaces of each MO shown.

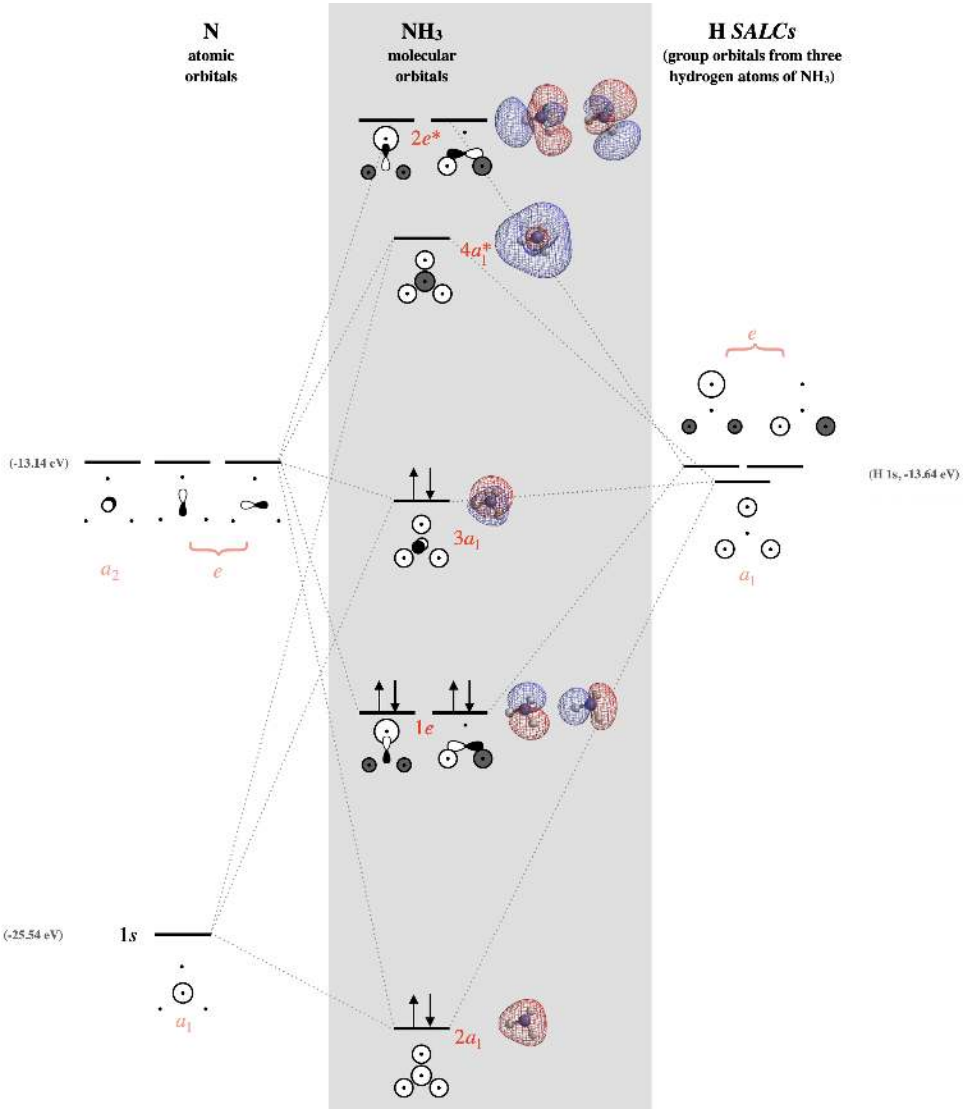


Figure **6.17.4**: The molecular orbital diagram of ammonia. Molecular orbitals surfaces calculated using Spartan software. (CC-BY-NC-SA; Kathryn Haas)

6.17: NH3 is shared under a CC BY-SA 4.0 license and was authored, remixed, and/or curated by LibreTexts.

- **5.4.4: NH3** by Kathryn Haas is licensed CC BY-SA 4.0.

6.18: CO_2 (Revisted with Projection Operators)

The process for finding SALCs and constructing the molecular orbital diagram for carbon dioxide was described in a previous section (Section 5.4.2). However, we also just presented an alternative strategy, the projection operator method, to finding the shapes of SALCs in Section 5.4.4. Let's revisit carbon dioxide and demonstrate how you can use the projection operator method to find SALCs for carbon dioxide.

Just as before, we can simplify the problem by approximating the $D_{\infty h}$point group using D_{2h}. The first four steps for constructing the MO diagram would be the same as described in Section 5.4.2. and we will pick up from that point (with Step 5) to find what the SALCs look like using the projection operator method.

The projection operator method applied to CO_2

Step 5.1: Label the pendent atoms.

We can label the pendant atoms as O_a and O_b, as in Figure 6.18.1.

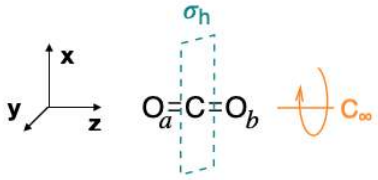


Figure 6.18.1: The structure of carbon dioxide with pendant oxygen atoms distinguished with labels a and b. Note that we will approximate the C_∞ axis as a C_2 axis to simplify the process of finding the SALCs. (CC-BY-SA; Kathryn Haas)

Step 5.2: Create an expanded character table with one pendant atom's projected position for each operation

The D_{2h} character table needs no expansion because each operation is in its own class. We will arbitrarily choose to determine the new position of O_a after each operation.

D_{2h}	E	$C_2(z)$	$C_2(y)$	$C_2(x)$	i	$\sigma(xy)$	$\sigma(xz)$	$\sigma(yz)$
Projection of O_a	O_a	O_a	O_b	O_b	O_b	O_b	O_a	O_a

Step 5.3: Find the contribution of each pendant atom to each SALC

Create a linear combination of the projections for each or the SALCs. The irreducible representations were found in step 4 in Section 5.4.2. Eight irreducible representations were found to be: $2A_g + 2B_{1u} + B_{2g} + B_{3u} + B_{3g} + B_{2u}$. For each of the irreducible representations, multiply the projection by the respective character of the operation.

$$\text{Contribution of each atom to the SALC } = \sum(\text{Projection of } H_a \times \chi)$$

The linear combination for all irreducible representations of D_{2h} are shown below.

Table 6.18.1: The symmetry adapted linear combination (SALC) for each irreducible representations of C_3v are shown.

D_{2h}	E	$C_2(z)$	$C_2(y)$	$C_2(x)$	i	$\sigma(xy)$	$\sigma(xz)$	$\sigma(yz)$	Linear Combination
Projection of O_a	O_a	O_a	O_b	O_b	O_b	O_b	O_a	O_a	
A_g	1	1	1	1	1	1	1	1	$= 4O_a + 4O_b$
B_{1u}	1	1	−1	−1	−1	−1	1	1	$= 4O_a - 4O_b$
B_{2g}	1	−1	1	−1	1	−1	1	−1	$= 0$
B_{3u}	1	−1	−1	1	−1	1	1	−1	$= 0$
B_{3g}	1	−1	−1	1	1	−1	−1	1	$= 0$
B_{2u}	1	−1	1	−1	−1	1	−1	1	$= 0$

(6.18.1)

Notice that there are only two irreducible representations that produce SALCs, the A_g and the B_{1u}. Since we found two of each ($2A_g + 2B_{1u}$) when we found the irreducible representations, we know that there will be two SALCs of A_g symmetry and two of B_{1u}

symmetry; that is four total SALCs from the pendant oxygens. This is the same as what we found in Section 5.4.2 using a different method.

Step 5.4: Sketch the SALCs

The SALCs with A_g symmetry: Quantitatively, we can apply the normalizing factor, N, for these SALCs. Each atom contributes equally to the SALCs, thus the normalizing factor for the A_g SALC is $N = \left(\frac{1}{\sqrt{1^2+1^2}}\right) = \frac{1}{\sqrt{2}}$. This tells us that each oxygen contributes $\frac{1}{\sqrt{2}}$ to each of the normalized A_g group orbitals:

$$A_g \text{ group orbital } = \frac{1}{\sqrt{2}}\left[\psi_{O_a} + \psi_{O_b}\right]$$

The linear combination $4O_a + 4O_b$ indicates that wavefunctions from each oxygen atom contribute equally to each of the two SALCs, with the same sign of the wavefunction for each. Because we know that A_g is totally symmetric (all 1's in the characters), we can assume that the SALC's will look like a symmetric arrangement of oxygen orbitals. But which orbitals contribute? We could peek at the character table to get a hint. But we'll treat this problem systematically.

The SALCs with B_{1u} symmetry: The linear combination $4O_a - 4O_b$ indicates that each oxygen atom contributes equally, but that they have opposite wavefunctions. Application of the normalizing factor would give us:

$$B_{1u} \text{ group orbital } = \frac{1}{\sqrt{2}}\left[\psi_{O_a} + \psi_{O_b}\right]$$

But how do we know what the SALCs look like? Again, the character table can give us some hints, but we'll use a systematic process, below.

What do the SALCs look like? One way to systematically derive the SALC shapes is to perform the projection (Step 5.3) on specific groups of orbitals on the oxygen atom. For example, if we replicate Table 6.18.1 using just the group of oxygen 2s orbitals and the A_g and B_{1u} representations, we get the following:

D_{2h}	E	$C_2(z)$	$C_2(y)$	$C_2(x)$	i	$\sigma(xy)$	$\sigma(xz)$	$\sigma(yz)$	Linear Combination
Projection of 2s orbital of O_a	$O1s_a$	$O1s_a$	$O1s_b$	$O1s_b$	$O1s_b$	$O1s_b$	$O1s_a$	$O1s_a$	
A_g	1	1	1	1	1	1	1	1	$= 4O1s_a + 4O1s_b$
B_{1u}	1	1	−1	−1	−1	−1	1	1	$= 4O1s_a - 4O1s_b$

(6.18.2)

This tells us that one of the A_g SALCs looks like two oxygen 1s orbitals with equal signs and contributions. It also tells us that one of the B_{1u} SALCs looks like two s orbitals with opposite signs and equal magnitudes. These two SALCs are shown in Figure 6.18.2.

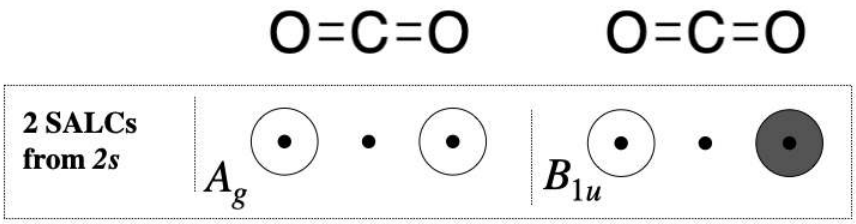


Figure 6.18.2: SALCs derived from two oxygen $2s$ orbitals from carbon dioxide. Compare to Section 5.4.2. (CC-BY-SA; Kathryn Haas)

If we do the same for the $2p_z$ orbitals, we need to pay attention to the orientation of the p orbital lobes. If the orbital is moved into the opposite orientation, it would get a negative sign in the projection (see below).

$\mathbf{D_{2h}}$	E	C_2 (z)	C_2 (y)	C_2 (x)	i	$\sigma(x$ $y)$	$\sigma(x$ $z)$	$\sigma(yz)$	Linear Combination
Projection of 2px orbital of O_a	$+O2$ pz_a	$+O2$ pz_a	$-O2$ pz_b	$+O2$ pz_b	$-O2$ pz_b	$-O2$ pz_b	$+O2$ pz_a	$+O2$ pz_a	
A_g	1	1	1	1	1	1	1	1	$= 4O2pz_a$ $- 4O2pz_b$
B_{1u}	1	1	−1	−1	−1	−1	1	1	$= 4O2pz_a$ $+ 4O2pz_b$

(6.18.3)

This tells us that one of the A_g SALCs is derived from two $2p_z$ orbitals of opposite sign but equal magnitude. In other words, the two p orbitals are pointing in opposite directions, but the lobes that are facing one another are of the same sign (see Figure **6.18.3**, left). This also tells us that one of the B_{1u} orbitals is derived from two p_z orbitals of equal magnitude and equal sign (pointing in the same directions, with lobes facing one another of opposite sign!) (see Figure **6.18.3**, right).

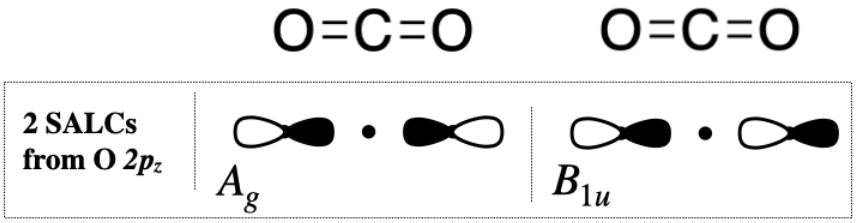


Figure **6.18.3**: SALCs derived from two oxygen $2p_z$ orbitals from carbon dioxide. Compare to Section 5.4.2. (CC-BY-SA; Kathryn Haas)

Now we have reached the same SALCs that we found previously in Section 5.4.2, but by an alternate method.

6.18: CO_2 (Revisted with Projection Operators) is shared under a CC BY-SA 4.0 license and was authored, remixed, and/or curated by LibreTexts.

- **5.4.4: NH_3** by Kathryn Haas is licensed CC BY-SA 4.0.

6.19: BF_3

The case of boron trifluoride (BF_3) is an example of a molecule with one more layer of complexity than the other examples we have seen in previous sections in this chapter. (BF_3) is more complex than previous examples because it is the first case in which there are multiple types of valence orbitals on the pendant atoms. (BF_3) possesses s and p orbitals on *both* the central atom and all of the pendant atoms. We can follow the same steps that we have previously to derive other molecular orbital diagrams; however, there is one important difference: we will treat each type of pendant orbital as an individual set of SALCs.

Step 1. Find the point group of the molecule and assign Cartesian coordinates so that z is the principal axis.

The BH_3 molecule is trigonal planar, and its point group is D_{3h}. The z axis is colinear with the principle axis, the C_3 axis.

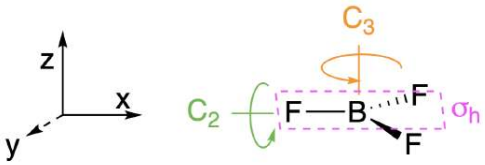


Figure **6.19.1**: The molecule is in the D_{3h} point group. (CC-BY-NC-SA; Kathryn Haas)

Step 2. Identify and count the pendant atoms' valence orbitals.

Each of the three pendant fluorine atoms has four valence orbitals: one $2s$ and three $2p$ orbitals. Thus, we can expect a total of twelve SALCs from the three atoms. However, we will treat each type of orbital from the F atoms as its own set; each will have its own set of coordinates, with the y axis along the M-L bond. Thus we expect the following:

- One set of $2s$ SALCs: there is one 2s orbital on each of three atoms. This set will have three SALCs.
- One set of $2p_x$ SALCs: there is one $2p_x$ orbital on each of three atoms. Each of these individual orbitals is perpendicular to the M-L bond and coplanar with the molecule. This set will have three SALCs.
- One set of $2p_y$ SALCs: there is one $2p_y$ orbital on each of three atoms. Each of these individual orbitals is colinear with the M-L bond. This set will have three SALCs.
- One set of $2p_z$ SALCs: there is one $2p_z$ orbital on each of three atoms. Each of these individual orbitals is perpendicular to the M-L bond and parallel with the principal axis of the molecule. This set will have three SALCs.

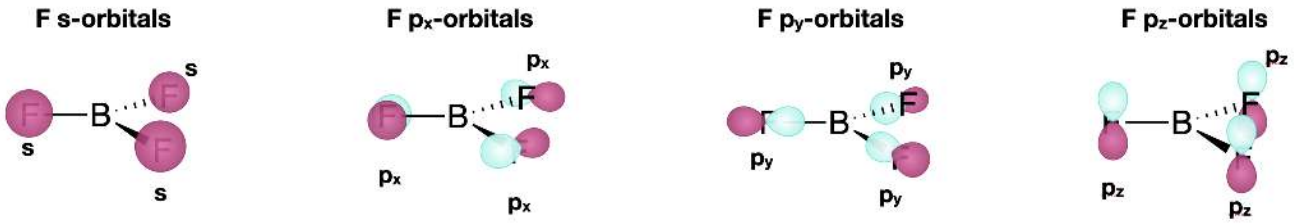


Figure **6.19.2**: Individual sets of pendant fluorine atomic orbitals will create separate sets of SALCs. (CC-BY-SA; Kathryn Haas)

Step 3. Generate the Γ's for each set of SALCs

Use the D_{3h} character table to generate one reducible representation (Γ) for each of the four sets of pendant atomic orbitals shown in Figure **6.19.2**; in this case we need four Γ because there are four types of valence orbital (the s, p_x, p_y, p_z).

- For the set of s orbitals: perform the operation for each class in the character table. Each s orbital is assigned a value depending on whether it moves or not: assign a value of 1 if it remains in place during the operation, or 0 (zero) if it moves out of its original place.
- for each set of p orbitals: Now there are phases (signs of the wavefunction), so a negative value is possible. Assign a value of 1 to each p orbital if it remains in place and in phase during the operation; assign a -1 if the atom's position remains, while the phase of the orbital is inverted (the positive lobe moves to the position of the negative lobe and vice versa); assign a 0 if it moves out of its original position.

The Γ for each type is given below:

$\mathbf{D_{3h}}$	E	$2C_3$	$3C_2$	σ_h	$2S_3$	$3\sigma_v$
$\mathbf{\Gamma_{2s}}$	3	0	1	3	0	1
$\mathbf{\Gamma_{2p_x}}$	3	0	−1	3	0	−1
$\mathbf{\Gamma_{2p_y}}$	3	0	1	3	0	1
$\mathbf{\Gamma_{2p_z}}$	3	0	−1	−3	0	1

Step 4. Break Γ's into irreducible representations for individual SALCs

Reduce each $\mathbf{\Gamma}$ into its component irreducible representations. Using either of the processes described previously, we find that each of the $\mathbf{\Gamma}$ reduces to two irreducible representations under the $\boldsymbol{D_{3h}}$ point group; in each case one is singly degenerate ($\boldsymbol{A}$) and the other doubly degenerate ($\boldsymbol{E}$). This equates to three SALCs for each $\mathbf{\Gamma}$ (orbital type) and a total of twelve SALCs. This should give us confidence! We were in fact expecting 12 SALCs because we found that there were twelve pendant atomic orbitals to start with.

D_{3h}	E	$2C_3$	$3C_2$	σ_h	$2S_3$	$3\sigma_v$
$\mathbf{\Gamma_{2s}}$	**3**	**0**	**1**	**3**	**0**	**1**
A_1'	1	1	1	1	1	1
E'	2	−1	0	2	−1	0

D_{3h}	E	$2C_3$	$3C_2$	σ_h	$2S_3$	$3\sigma_v$
$\mathbf{\Gamma_{2p_x}}$	**3**	**0**	**−1**	**3**	**0**	**−1**
A_2'	1	1	−1	1	1	−1
E'	2	−1	0	2	−1	0

D_{3h}	E	$2C_3$	$3C_2$	σ_h	$2S_3$	$3\sigma_v$
$\mathbf{\Gamma_{2p_y}}$	**3**	**0**	**1**	**3**	**0**	**1**
A_1'	1	1	1	1	1	1
E'	2	−1	0	2	−1	0

D_{3h}	E	$2C_3$	$3C_2$	σ_h	$2S_3$	$3\sigma_v$
$\mathbf{\Gamma_{2p_z}}$	**3**	**0**	**−1**	**−3**	**0**	**1**
A_2''	1	1	−1	−1	−1	1
E''	2	−1	0	−2	1	0

Step 5: Sketch the SALCs

We'll skip this step for now to make this problem simpler.

Step 6: Draw the MO diagram by combining SALCs with AO's of like symmetry.

We now know the symmetries of different pendant orbital SALCs - and it is helpful if we also know their relative energies, and the energies of the valence orbitals on the central boron atom. We can make predictions based on periodic trends, or we can use a table of ionization energies as a guide. The symmetries of the boron $\boldsymbol{2s}$ and $\boldsymbol{2p}$ orbitals can be found from the $\boldsymbol{D_{3h}}$ character table.

6.19: BF_3 is shared under a CC BY-SA 4.0 license and was authored, remixed, and/or curated by LibreTexts.

- **5.4.4: NH_3** by Kathryn Haas is licensed CC BY-SA 4.0.

6.20: Ionic Compounds and Molecular Orbitals

Ionic interactions lie at one extreme on a spectrum of bonding. On the opposite end of the spectrum are the non-polar covalent bonds (e.g., homonuclear diatomics). In these molecules, molecular orbitals are formed by equal-energy atomic orbitals, resulting in electron density evenly distributed over the molecule. In the middle of the spectrum are the cases of polar covalent bonds (e.g., heteronuclear diatomics), in which atomic orbitals of unequal energies contribute unequally to molecular orbitals, resulting in uneven distribution of electron density across the molecule. In the case of polar bonds, the electron density is shifted toward the more electronegative atom since that atom contributes more to the lowest energy bonding molecular orbitals. Molecular orbital diagrams can be drawn for ionic compounds as if they are extremely polar bonds in which electrons are not only shifted toward, but are transferred completely to the more electronegative atom.

Example: NaCl

In **NaCl**, the sodium **3*s*** orbital (-5.2 eV) is significantly higher in energy than the chlorine valence orbitals. The chlorine **3*s*** and **3p_z** orbitals have compatible symmetry, yet only the **3p_z** orbital (-13.8 eV) is close enough in energy to interact with the Na **3*s***; still, the energy difference is large enough to make bonding weak. The Na **3*s*** orbital combines with Cl **3p_z** to form the molecular orbitals labeled **4σ** and **4σ*** in Figure **6.20.1**. The **4σ** orbital is weakly bonding, but is very close in energy to the Cl **3p_z** orbital, and is mostly Cl-like in character. Notice that all **σ** orbitals look very much like either **s** or **p** orbitals centered on the **Cl** atom, while the **4σ*** orbital is centered almost entirely on Na. The lack of molecular orbitals that are distributed over both atoms at once is consistent with a lack of significant covalent bond character in **NaCl**. The bonding here is characterized by transfer of one electron from **Na** to **Cl** and is almost entirely electrostatic. Bonding that is mostly electrostatic in character is non-directional, unlike true covalent bonding.

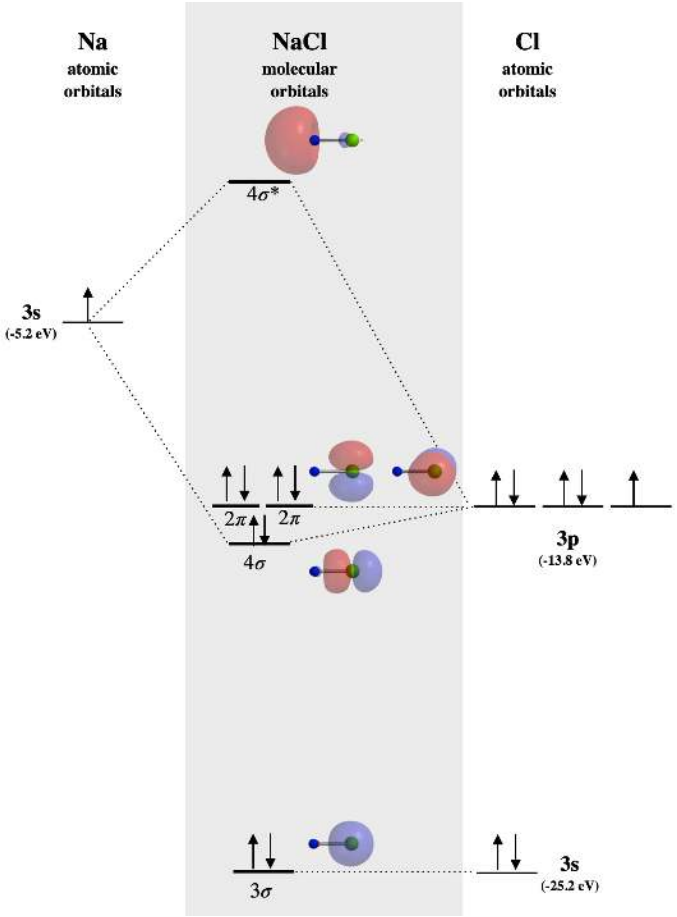


Figure **6.20.1**: The molecular orbital diagram for sodium chloride. Molecular orbital surfaces calculated using Spartan software indicate almost no covalent nature of bonding. (CC-BY-NC-SA, Kathryn Haas)

Exercise 6.20.1

Draw the molecular orbital diagram for **LiF**. Make sure to label all molecular orbitals appropriately, and specify whether they are mostly bonding, non-bonding, or antibonding. Identify the HOMO and LUMO. Sketch the approximate shapes of all orbitals.

Answer

We expect **LiF** to be an ionic compound because the energy difference in valence orbitals is at least 10-14 eV. (See Table 5.3.1) There are a variety of ways used to label molecular orbitals. In the figure below, we are using the convention of labeling each type of orbital with numbers starting from the lowest-energy orbitals. The 1σ orbital would be mostly F $1s$ in character and is not shown. The 2σ orbital is mostly non-bonding in nature, although it has a very small contribution from $2s$ of Li due to compatible symmetry. The 3σ orbital is slightly bonding but it is mostly F$2p$ in character. The two 1π orbitals are completely non-bonding. The $3\sigma^*$ orbital is antibonding.

- HOMO is 1π
- LUMO is $3\sigma^*$

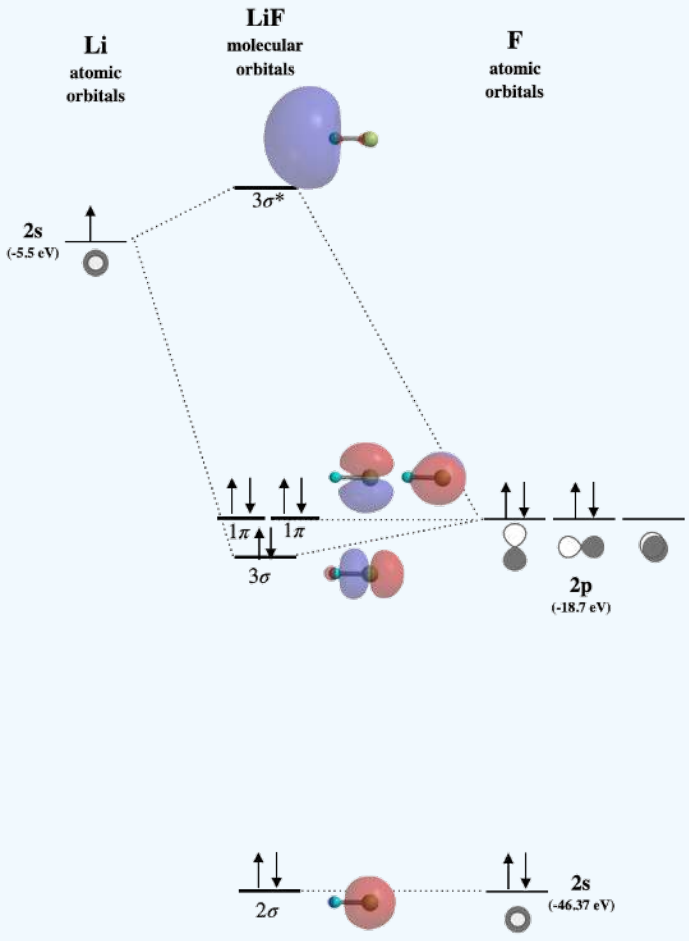


Figure for Exercise 6.20.1: Molecular orbital diagram for the ionic compund, LiF. (CC-BY-NC-SA, Kathryn Haas)

This page titled 6.20: Ionic Compounds and Molecular Orbitals is shared under a CC BY-SA 4.0 license and was authored, remixed, and/or curated by Kathryn Haas.

- **5.3.3: Ionic Compounds and Molecular Orbitals** by Kathryn Haas is licensed CC BY-SA 4.0.

CHAPTER OVERVIEW

7: Acid-Base and Donor-Acceptor Chemistry

7.1: Lewis Concept and Frontier Orbitals

7.2: The frontier orbital approach considers Lewis acid base reactions in terms of the donation of electrons from the base's highest occupied orbital into the acid's lowest unoccupied orbital.

7.3: All other things being equal electron withdrawing groups tend to make Lewis acids stronger and bases weaker while electron donating groups tend to make Lewis bases stronger and acids weaker

7.4: The electronic spectra of charge transfer complexes illustrate the impact of frontier orbital interactions on the electronic structure of Lewis-Acid base adducts

7.5: Hard and Soft Acids and Bases

7.6: Quantitative Measures of Hardness, Softness, and Acid-Base Interactions from a Hard Soft Acid-Base Principle perspective involve orbital energies and or apportioning acid-base bonding in terms of electrostatic and covalent factors

7.7: Hard-Hard and Soft-Soft preferences may be explained and quantified in terms of electrostatic and covalent and electronic stabilization on the stability of Lewis acid-base adducts

---

7: Acid-Base and Donor-Acceptor Chemistry is shared under a not declared license and was authored, remixed, and/or curated by LibreTexts.

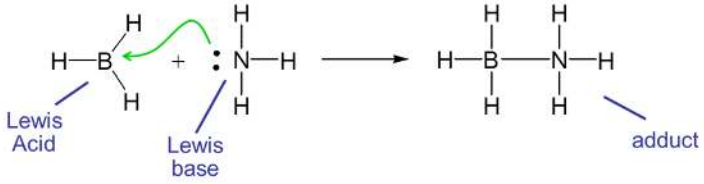
7.1: Lewis Concept and Frontier Orbitals

The Lewis acid-base concept generalizes the Brønsted and solvent system acid base concepts by describing acid-base reactions in terms of the donation and acceptance of an electron pair.

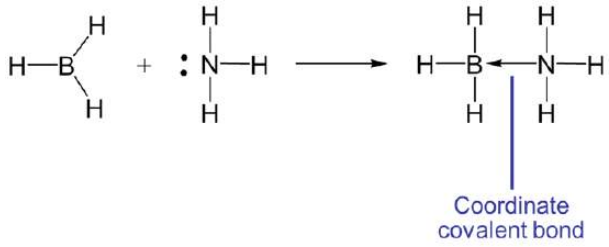
Under the Lewis definition

- **Lewis acids** are electron pair acceptors
- **Lewis bases** are electron pair donors

and in Lewis acid-base reactions, a Lewis base donates an electron pair to the Lewis acid, which accepts it. The reaction between borane, BH_3, and NH_3 is the classic example:

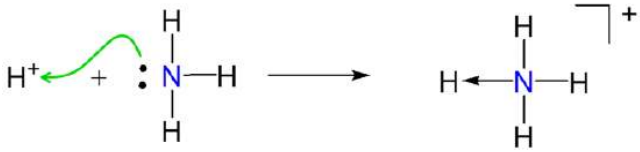


In this case the Lewis acid-base reaction results in the formation of a bond between BH_3, and NH_3. When the acid and base combine to form a larger unit, that unit is said to be an adduct, and the resulting bond is said to be a coordinate covalent or dative bond. Such coordinate covalent bonds are often represented by an arrow that indicates the direction of electron donation from the base to the acid. For instance, the reaction between BH_3 and NH_3 could also have been written as

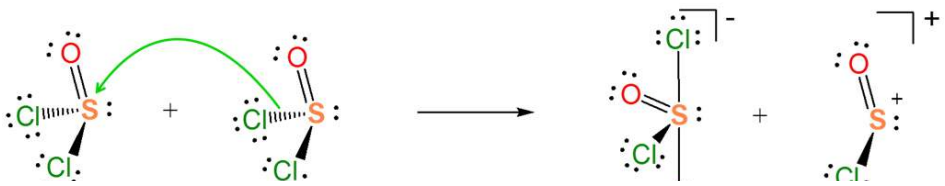


The arrow notation for the coordinate covalent bond is really just a convenient formalism - a bookkeeping tool to help keep track of where the electrons came from and where they might return if the reverse reaction occurs. In actuality a coordinate covalent bond is just an ordinary covalent bond like any other.

For example, in Brønsted acid-base reactions, the hydrogen ion is an acid because it accepts an electron pair from the Brønsted base. Consequently, under the Lewis acid-base concept, Brønsted acid-base reactions involve the formation of an adduct between H^+ and a base.



The Lewis acid-base concept nicely explains ionization reactions involving nonaqueous solvents. For instance, the autoionization of $SOCl_2$ is an acid-base reaction between two $SOCl_2$ molecules.



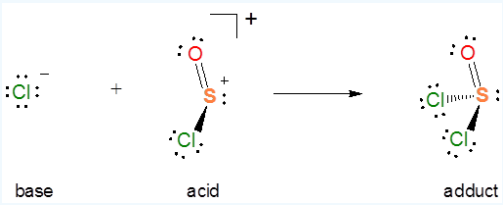


Example 7.1.1

Explain how the autoionization of $SOCl_2$ is a Lewis acid-base displacement reaction.

Solution

In the autoionization of $SOCl_2$ the pair of electrons donated comes from the S-Cl bond, and the S-Cl bond is broken to give a lone pair bearing a Cl^- base and an $SOCl^+$ Lewis acid fragment. If you are having trouble seeing how this works, it can be instructive to consider the reverse of this process. It is a Lewis acid-base reaction to give a Lewis acid-base adduct:

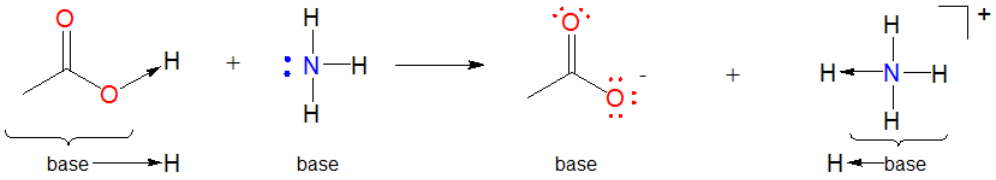


From the autoionization reaction it is also apparent that $SOCl_2$ itself acts as a Lewis acid towards the liberated Cl^-. So the autoionization reaction involves a transfer of the Cl^- base between the two Lewis acids - a Lewis acid-base displacement reaction.



It can be helpful to keep several distinctions in mind when using the Lewis acid-base concept to describe chemical reactions.

1. Many Lewis-Acid base reactions are displacement reactions. This is because the hydrogen ion is usually bound to something at the start of the reaction. In such cases the Lewis acid H^+ unit is transferred from one Lewis base to another :



Such acid-base reactions are sometimes called displacement reactions since the base group in the initial Lewis acid-base complex is displaced by the incoming Lewis base to generate another complex.

2. Substances are sometimes considered amphoteric because they exhibit Lewis acidity and basicity at different types of atomic centers. The classic example is aluminum hydroxide, $Al(OH)_3$. In water $Al(OH)_3$ can act as a Lewis acid towards OH^- ion. The reaction occurs by formation of an adduct at $Al(OH)_3$'s Al^{3+} center:

$$Al(OH)_3 + OH^- \rightarrow Al(OH)_4^-$$

Notice that in addition to acting as a Lewis acid, in this reaction $Al(OH)_3$

- does not act as a Brønsted acid or base since no H^+ ion transfer occurs
- but does act as an Arrhenius acid since OH^- ion is consumed from solution, decreasing $[OH^-]$ and increasing $[H^+]$

In water $Al(OH)_3$ also acts as a Lewis base towards H^+ through the lone pairs on its hydroxide ligands.

$$Al(OH)_3 + 3H^+ + 3H_2O \rightarrow Al(H_2O)_6^{3+}$$

Notice that in addition to acting as a Lewis base, in this reaction $Al(OH)_3$ also acts as a

- Brønsted base, since a H^+ ion is transferred onto the OH^- ligand
- Arrhenius base, since H^+ ion is consumed from solution, decreasing $[H^+]$
- Lewis acid at its Al^{3+} center, since Al-O metal-ligand bonds are formed

Substances that rapidly undergo Lewis acid-base reactions are called nucleophiles and electrophiles.

Two factors govern the course of chemical reactions - thermodynamics and kinetics. Thermodyamics determines what possible fates of the reaction can take place while kinetics determines which among those possible fates will take place quickly under a particular set of reaction conditions. Because of this, it can be helpful to distinguish Lewis acids and bases that tend to undergo reaction quickly with one another from those which do so more slowly. For this reason, synthetic chemists use the terms electrophile and nucleophile to refer to Lewis acids and bases that react quickly:

- electrophile - Lewis acids that rapidly react with a given Lewis base or class of Lewis bases are said to be good electrophiles
- nucleophile - Lewis bases that rapidly react with a given Lewis acid or class of Lewis acids are said to be good nucleophiles

The electrophile-nucleophile concept is sometimes referred to as the Ingold-Robinson acid-base concept after two organic chemists who did much to illustrate the utility of thinking about Lewis acid-base reactions in kinetic terms.

Several distinctions that should be kept in mind when using the electrophile-nucleophile/Ingold-Robinson concept to think about chemical reactivity:

1. Whether a given Lewis acid or base is able to react rapidly depends on the reaction conditions and the substrate (substance it is reacting with). This means that in principle, the terms nucleophile and electrophile should not be used without appropriately qualifying what the substances act as a nucleophile or electrophile towards and under what conditions. Unfortunately this is rarely done. In such cases, the conditions and substrate must be inferred from the context. For instance, when you learned that the chloride ion is a good nucleophile when studying organic chemistry, what was meant is that chloride is a good nucleophile towards electrophilic carbon atoms in organic molecules.

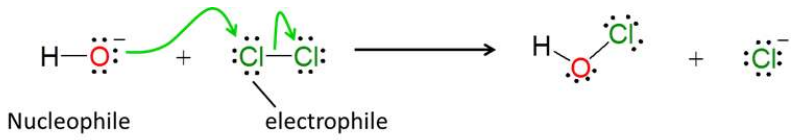
2. Acid and base strength and electrophilicity-nucleophilicity are not exactly the same thing. In many contexts where Lewis acids and bases are classified as electrophilic and nucleophilic substances, it is common to also refer to substances as being good acids or bases on the basis of their Brønsted acidity and basicity. In these contexts, the terms acid and base typically refer to the thermodynamic propensity of a substance to give and accept hydrogen ions while the terms nucleophile and electrophile refer to a substance's kinetic propensity to react with carbon-based Lewis acids and bases, respectively.

A substance may be both a good nucleophile and a strong Brønsted base. For instance, alkyllithium carbanion reagents and alkali metal hydrides are strong bases and good nucleophiles towards electrophilic carbon atoms in organic solvents at moderate temperatures. However, this is not always the case. Under such conditions iodide ion, I^-, is a good nucleophile towards electrophilic carbon atoms but is a poor Brønsted base (it is the conjugate of the strong acid HI). In fact, for the halide ions the order of Brønsted basicity is the opposite of the order of nucleophilicity towards electrophilic carbon:

stronger Brønsted base: F^-, Cl^-, Br^-, I^-: weaker Brønsted base

better nucleophlie: I^-, Br^-, Cl^-, F^-: poorer nucleophile

3. Although the nucleophile-electrophile concept is most often used to describe organic reactions, it is also useful for describing inorganic reactions as well. For instance, the formation of hypochlorite ion in chlorine water possibly involves nucleophilic attack of hydroxide on an electrophilic chlorine atom in an S_N2 type process:



The Usanovich Acid-base Concept

The Usanovich Acid-base concept encompasses a wider range of reactions than the Lewis acid-base concept but is perhaps too general to serve as a convenient framework for understanding reaction chemistry. The Usanovich acid-base concept was developed by the Russian chemist Mikhail Usanovich and extends the Lewis acid-base concept's definition of acids and bases as electron pair donors and acceptors even further. Within the Usanovich definition:

- Acids are anything that accepts electrons, increases cation concentrations, decreases anion concentrations, or reacts with bases
- Bases are anything that donates electrons, increases anion concentrations, decreases cation concentrations, or reacts with acids

These definitions essentially expand the Lewis definition by removing the requirement that the electrons donated or accepted be a pair and practically mean that Usanovich acid-base reactions include Lewis acid-base reactions plus oxidation-reduction reactions. In other words:

- Usanovich acids are Lewis acids plus oxidants
- Usanovich bases are Lewis bases plus reductants

Under this definition BF_3, Fe^{3+}, and $[Fe(CN)_6]^{3-}$ all act as acids, and : NH_3, CN^-, and Zn are all bases:

$$\underset{acid}{BF_3} + \underset{base}{NH_3} \rightarrow F_3B-NH_3$$

$$\underset{acid}{Fe^{3+}} + 6\underset{base}{CN:^-} \rightarrow [Fe(CN)_6]^{3-}$$

$$2\underset{acid}{[Fe(CN)_6]^{3-}} + \underset{base}{Zn} \rightarrow 2[Fe(CN)_6]^{3-} + Zn^{2+}$$

However, notice that while it is easy to think about how any acids might interchangeably react with a given base (and vice versa), under the other acid-base concepts chemists have found it more difficult to think about reactions between oxidants/reductants and Lewis acids and bases. For example, it is difficult to think about how a reaction between BF_3 and Zn metal might occur. Would two Zn donate a pair of electrons to the BF_3? For this reason, most chemists find it more convenient to think about Lewis acid-base and redox reactions under separate categories rather than unite them under the Usanovich definition.

$$2\underset{oxidant}{[Fe(CN)_6]^{3-}} + \underset{reductant}{Zn} \rightarrow 2[Fe(CN)_6]^{3-} + Zn^{2+}$$

Again, it can be helpful to remember Huheey's dictum that deciding between acid-base concepts is not a matter of which concept is the most correct but rather of which is more convenient for a given application.

7.1: Lewis Concept and Frontier Orbitals is shared under a CC BY-NC 4.0 license and was authored, remixed, and/or curated by Stephen M. Contakes.

- **6.4: Lewis Concept and Frontier Orbitals** by Stephen M. Contakes is licensed CC BY 4.0.

7.2: The frontier orbital approach considers Lewis acid base reactions in terms of the donation of electrons from the base's highest occupied orbital into the acid's lowest unoccupied orbital.

Another way the Lewis-Acid base concept is widely employed for understanding chemical reactivity is through the frontier orbital approach to chemical reactions. The frontier orbital concept conceptualizes chemical bonding and reactivity in terms of the interactions between frontier orbitals on the chemical species undergoing an interaction (*e.g.* molecules, atoms, ions, or groups as they interact to form a bond or undergo a reaction). Frontier orbitals are those at the frontier between occupied and unoccupied. They are often taken to be the highest energy occupied and lowest energy unoccupied molecular orbitals, called the HOMO and LUMO levels. However, it can sometimes be more convenient to think about them as atomic orbitals or Valence Bond approach-derived orbitals. When developing rough qualitative frontier orbital descriptions of the orbital interactions involved in a given system, the choice of what types of orbitals to use is often a matter of what is the most informative and convenient.

In particular, the frontier orbital concept envisions a Lewis acid-base interaction as involving an interaction between some of the frontier orbitals of the Lewis acid and base, specifically the donation of electrons from the base's HOMO level into the acid's LUMO level. For example, in the frontier orbital approach, adduct formation between $\boldsymbol{NH_3}$ and $\boldsymbol{BH_3}$ involves the donation of electrons from ammonia's a_1 HOMO into BH_3's a_2'' LUMO level.

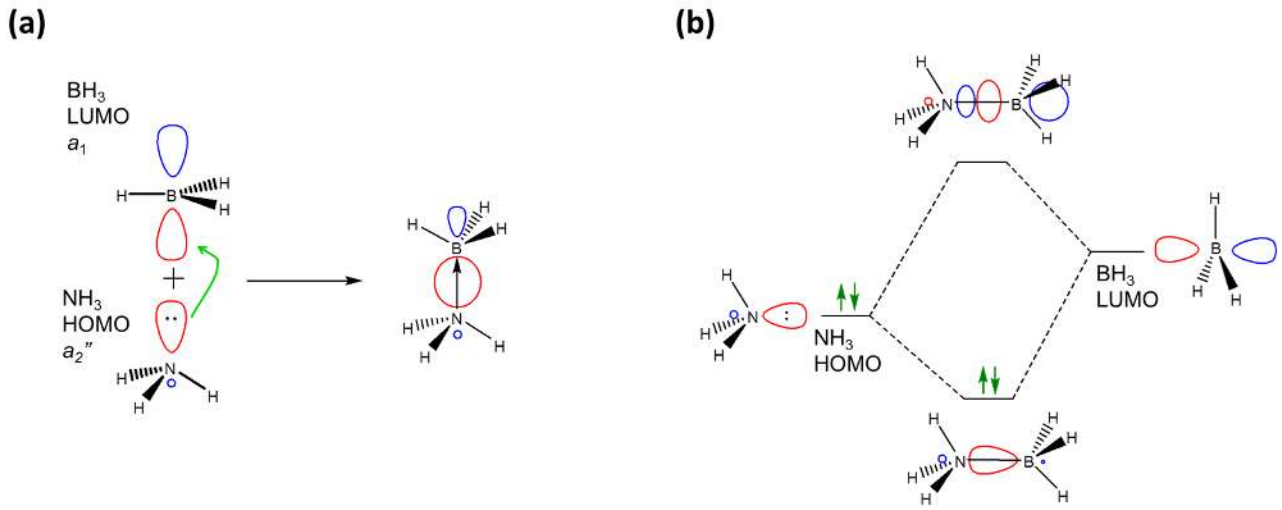


Figure **7.2.1**. Frontier orbital picture of adduct formation between ammonia and borane. (a) As $\boldsymbol{NH_3}$ and $\boldsymbol{BH_3}$ approach one another, interaction between the $\boldsymbol{NH_3}$ HOMO and $\boldsymbol{BH_3}$ LUMO gives a bonding MO. (b) Partial molecular orbital diagram for $\boldsymbol{NH_3 \rightarrow BH_3}$ showing the stabilization of the base ($\boldsymbol{NH_3}$) lone pair in a sigma bonding MO upon adduct formation.

As expected when two orbitals of the appropriate symmetry combine, the result of the interaction is the formation of a lower energy bonding orbital between the acid and base (Figure **7.2.1**). Since it is occupied by an electron, the net result of the interaction is the lowering of the base's lone pair energy as it interacts with the Lewis acid. In this case the interaction just follows the general pattern for Lewis-Acid base adduct formation, which is:

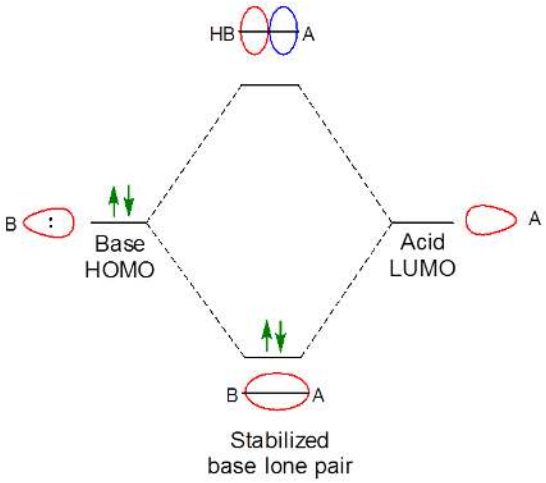
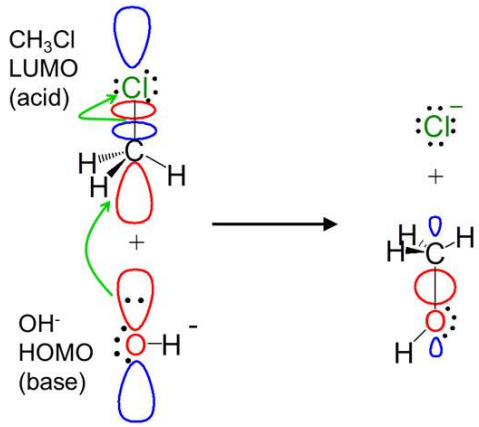


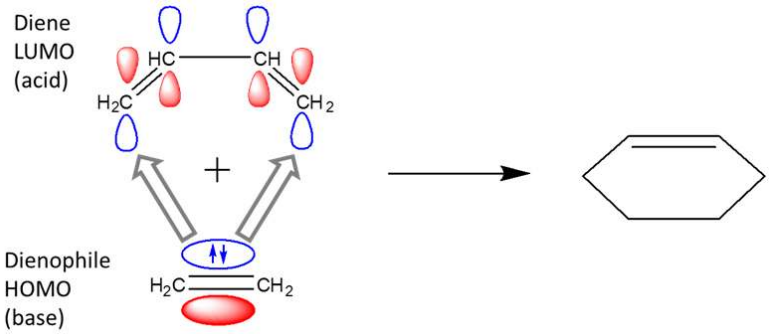
Figure **7.2.2**. Generalized frontier orbital picture for adduct formation between a Lewis base (B) and a Lewis acid (A) involving stabilization of the lone pair of the base HOMO by formation of a bonding orbital with the acid LUMO. The relative energies of the acid LUMO and base HOMO affect the character of the bonding and antibonding MOs but are otherwise unimportant in determining the general features of the interaction. In some cases the base HOMO is higher in energy; in others the acid LUMO is higher in energy; in still others they are equal in energy. In any case the net result is the stabilization of the base lone pair.

The frontier orbital concept illuminates the orbital interactions involved in reactions. For instance, from a frontier orbital perspective the alkyl halide substitution reaction between hydroxide and CH_3Cl via the S_N2 mechanism involves a Lewis acid-base interaction:

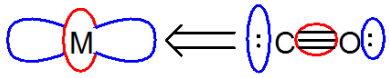


Notice how the frontier orbital approach even explains the displacement of the chloride leaving group. The donation of electrons from the hydroxide HOMO populates the antibonding CH_3Cl LUMO, breaking the C-Cl bond.

With the frontier orbital approach, it becomes apparent that pericyclic reactions are Lewis acid-base reactions. For example, in the Diels-Alder reaction, the dienophile acts as a Lewis base and the diene as a Lewis acid.



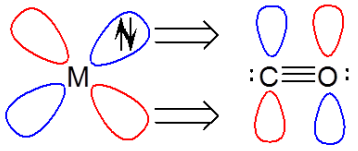
The orbital interactions involved in a given reaction can include both reactants acting as both an acid and base. In these cases the HOMO of each reactant interacts with the LUMO of the other. A good example of this involves **Π**-type interactions between a metal ion with occupied *d* orbitals and a pi-acceptor ligand. The ligand acts as a base and the metal as an acid to give a M-CO single bond:



Metal LUMO (d_{z^2}) acts as an acid

Carbon monoxide HOMO acts as a base

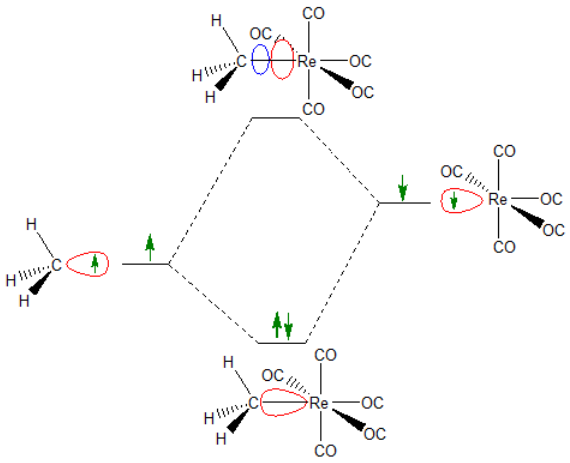
However, the metal can also act as a base towards the ligand LUMO (π^*) orbitals.



Metal HOMO (d_{xz}, d_{xz}) acts as a base

Carbon monoxide LUMO (π^*) acts as an acid

The frontier orbital concept can also be used to describe interactions between one or more singly occupied frontier orbitals. In fact, when approximate molecular orbital diagrams are being constructed, it can often be helpful to focus on one or two particularly instructive interactions. In these cases, it is sometimes convenient to think about a chemical bond as involving the formation of bonding and antibonding interactions between singly occupied frontier orbitals on different molecular fragments. For instance, when thinking about the chemistry of $CH_3Re(CO)_5$ it can sometimes be helpful to think about the C-Re bond as arising from the interaction between a singly-occupied sp^3 type orbital on a CH_3 group and a singly occupied d^2sp^3 orbital on the Re.



In introducing singly occupied orbitals, the frontier orbital concept formally handles interactions that the Lewis acid-base concept does not, since Lewis acid-base behavior is formally confined to the acceptance and donation of electron *pairs*.

7.2: The frontier orbital approach considers Lewis acid base reactions in terms of the donation of electrons from the base's highest occupied orbital into the acid's lowest unoccupied orbital. is shared under a not declared license and was authored, remixed, and/or curated by Stephen M. Contakes.

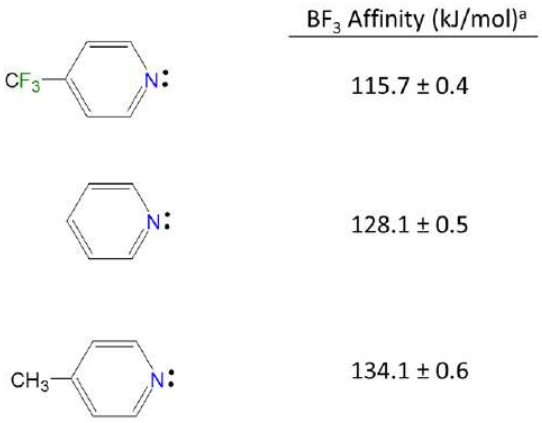
- **6.4.1: The frontier orbital approach considers Lewis acid-base reactions in terms of the donation of electrons from the base's highest occupied orbital into the acid's lowest unoccupied orbital.** by Stephen M. Contakes is licensed CC BY 4.0.

7.3: All other things being equal electron withdrawing groups tend to make Lewis acids stronger and bases weaker while electron donating groups tend to make Lewis bases stronger and acids weaker

The electrons donated from a Lewis base to a Lewis acid in a Lewis acid-base reaction are donated and accepted at particular atomic centers. For instance, the formation of an adduct between ammonia and BF_3 involves the donation of the lone pair on the ammonia nitrogen atom to the Lewis acid site on BF_3.



Because Lewis acid-base reactions involve electron donation and acceptance at particular sites, substituent groups which alter the electron density at a site through inductively donating or withdrawing electron density will affect the Lewis acid-base properties of that site. For instance, the BF_3 affinities of 4-substituted pyridines increase slightly as the substituent on the aromatic ring is changed from electron donating Me to electron withdrawing CF_3.



a) Data from Laurence, C.; Gal, J.-F. o., *Lewis basicity and Affinity Scales: Data and Measurement. John Wiley: Chichester, West Sussex, U.K., 2010; pp. 91-101.*

Substituent inductive effects are much as one might predict. Since Lewis bases donate electron pairs and Lewis acids accept them:

- electron withdrawing substituents tend to decrease the Lewis basicity of basic sites while electron donating substituents increase site Lewis basicity by making them more electron rich.
- electron withdrawing substituents increase the Lewis acidity of acidic sites by making those sites more electron deficient while electron donating substituents tend to decrease Lewis acidity by making sites less electron deficient.

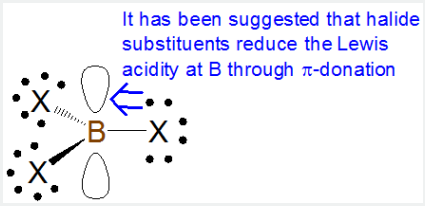
Nevertheless it can be difficult to predict substituent-based trends in Lewis acidity and basicity by inductive effects alone. This is because inductive effects are modest and often exists in competition with other substituent effects, such as

- Steric effects, discussed in section 6.4.7
- Hardness effects, discussed in section 6.6
- π-donation and acceptance effects, which can increase or decrease electron density at a given site as well as create an energy barrier for any structural distortions that might occur upon adduct formation.

Avoid misconceptions about the impact of π donation and acceptance on Lewis acid-base affinity

As with σ-based induction effects, π-donation tends to increase Lewis basicity and decrease Lewis acidity while π-withdrawal tends to decrease Lewis basicity and increase Lewis acidity. However, care needs to be taken in assessing the effect of π-

donation effects on Lewis acidity and basicity. For example, some textbooks claim that the Lewis acidity of boron trihalides is dominated by the reduction of boron acidity through π-donation from the halide substituents:

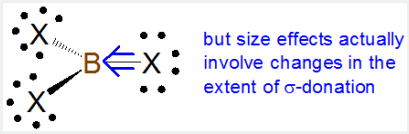


According to this explanation, the extent of this π-donation decreases down the halogen group as the boron-halogen bond distance decreases. This is consistent with the observed trend in Lewis acidity of the boron trihalides towards most bases, which runs counter to that suggested by inductive effects alone:

$$BI_3 > BBr_3 > BCl_3 >> BF_3$$

However, computational work suggests that this explanation is incorrect, since

- atomic size effects are important mainly for substituents in which the connected atom is in row 3+ or higher;
- atomic size effects mainly involve changes in the extent of σ-overlap. In other words, the larger halogens are less able to reduce the electron deficiency at the boron center through σ interactions while π-interactions play little or no role.



References:

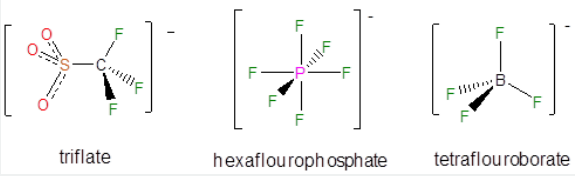
1. Plumley, J. A.; Evanseck, J. D., Periodic Trends and Index of Boron Lewis Acidity. *The Journal of Physical Chemistry A* 2009, 113 (20), 5985-5992.

2. Jupp, A. R.; Johnstone, T. C.; Stephan, D. W., Improving the Global Electrophilicity Index (GEI) as a Measure of Lewis Acidity. *Inorganic Chemistry* 2018, 57 (23), 14764-14771.

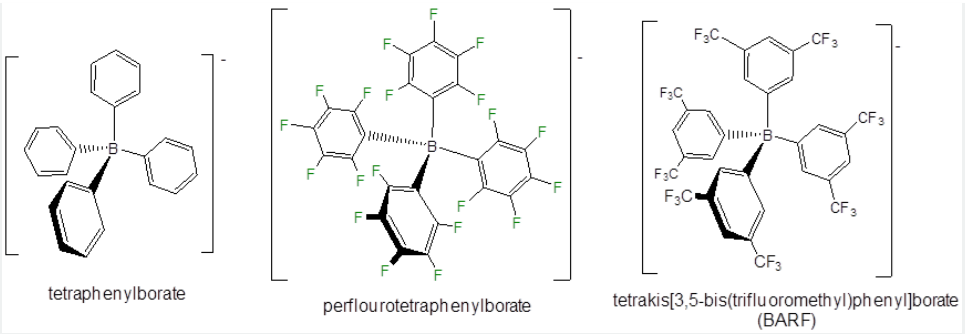
The conjugate bases of many Brønsted superacids have electron-withdrawing substituents that make them such poor Lewis bases that they are useful as noncoordinating anions.

The nonreactivity of Brønsted superacids' conjugate bases towards hydrogen ions is often mirrored in nonreactivity towards other Lewis Acids/electrophiles, most notably metals. This makes these substances useful as inert or noncoordinating ions, although since all are reactive towards suitably electrophilic centers, they are perhaps better understood as weakly coordinating.

A number of noncoordinating anions are commonly used in synthetic and other applications. The conjugate base of perchloric acid, perchlorate, was a common noncoordinating inert anion in classical coordination chemistry and continues to be used widely in electrochemistry. In contrast, the conjugate bases of triflic acid, hexafluoroboric acid, and tetrafluoroboric acid are now more commonly used as counterions for isolating reactive cations.



Even less reactive noncoordination anions include derivatives of tetraphenylborate, particularly those with electron withdrawing substituents.



Other classes of noncoordinating ions include fluoroantimonate clusters, derivatives of the carborane anion ($CB_{11}H_{11}^-$), and fluorinated aluminum tetraalkoxides.

References

Engesser, T. A.; Lichtenthaler, M. R.; Schleep, M.; Krossing, I., Reactive p-block cations stabilized by weakly coordinating anions. *Chemical Society reviews* **2016**, *45 (4)*, 789-899.

7.3: All other things being equal electron withdrawing groups tend to make Lewis acids stronger and bases weaker while electron donating groups tend to make Lewis bases stronger and acids weaker is shared under a not declared license and was authored, remixed, and/or curated by Stephen M. Contakes.

- **6.4.2: All other things being equal, electron withdrawing groups tend to make Lewis acids stronger and bases weaker while electron donating groups tend to make Lewis bases stronger and acids weaker** by Stephen M. Contakes is licensed CC BY 4.0.

7.4: The electronic spectra of charge transfer complexes illustrate the impact of frontier orbital interactions on the electronic structure of Lewis-Acid base adducts

When a Lewis acid-base adduct is formed, electron density and negative charge are transferred from the Lewis base to the acid.

The formation of a Lewis-acid base complex involves the transfer of electron density from the base to the acid.

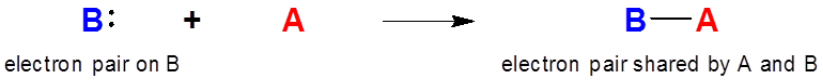


Figure 6.4.2.**7.4.1**.

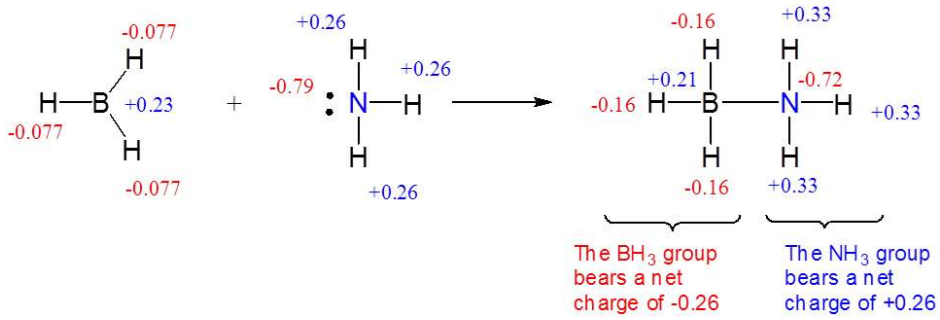


Figure 6.4.2.**7.4.1**. Calculated change in atomic charge distribution upon formation of an adduct between BH_3 and NH_3 in the gas phase. All partial charges were calculated for geometry-optimized molecules at the 6-31G** level.

Weakly bound Lewis acid-base adducts in which charge is incompletely transferred are called charge transfer complexes.

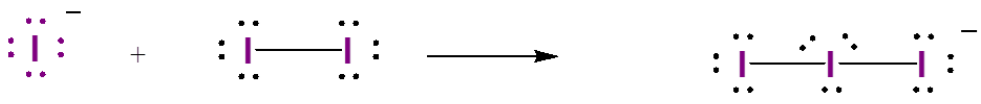
In many weakly bound Lewis acid-base complexes, the transfer of electron density and, consequently, charge from the base group to the acid group is only partial:

$$A + B \rightleftharpoons A^{\delta-}B^{\delta+}$$

Such Lewis acid-base adducts are commonly called **charge transfer complexes (CT complexes)** or **donor-acceptor complexes (DA complexes)**. In these

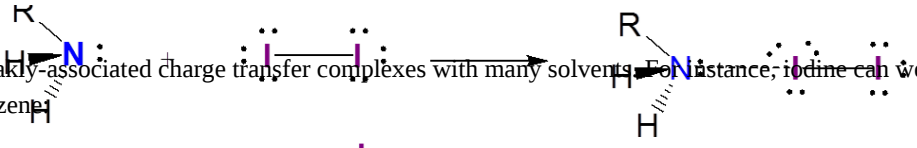
- the base is called the **donor (D)** since it is a net donor of electrons and, consequently, their negative charge
- the acid is called the **acceptor (A)** since it is a net acceptor of electrons and, consequently, their negative charge

A particularly well-known class of charge transfer complexes is the iodine charge transfer complexes. In iodine charge transfer complexes the I_2 acts as a Lewis acid. This is possible since iodine is a Row 3+ element and so is capable of forming hypervalent complexes on reaction with a Lewis base. For example, I_2 reacts with I^- to give the triiodide ion.

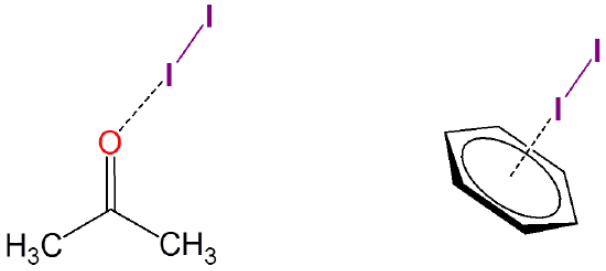


Triiodide is well-known from introductory chemistry from the bright blue color that appears when the triiodide complexes with starch to give the dark blue starch-iodide complex.

In contrast to the stable triiodide anion, iodine charge transfer complexes are only weakly associated. Complexes between iodine and amines are a well known example:

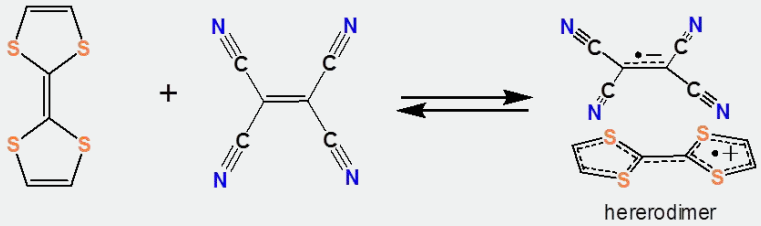


Iodine also forms weakly-associated charge transfer complexes with many solvents. For instance, iodine can weakly associate with both acetone and benzene:

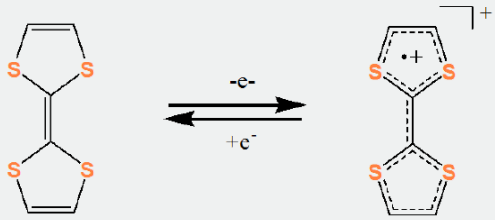


Organic Charge Transfer Complexes

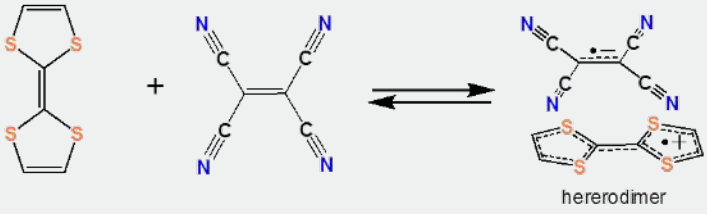
It is worth noting in passing that several organic charge transfer complex systems have been developed in which organic electron donors and acceptors weakly associate with each other. These are of considerable interest for use in molecular electronics applications, and as a result, a large variety of organic electron donors and acceptors have been developed. An example of an organic electron acceptor is tetracyanoethylene (TCNE):



and an example of an organic electron acceptor is tetrathiofulvalene (TTF).



Together they form a charge transfer complex:



Similar organic charge transfer systems have been investigated for use in organic photovoltaic cells. There is considerable interest in developing such organic photovoltaic devices owing to the ease with which organic materials may be fabricated from organic solutions and suspensions.

Charge transfer complexes exhibit charge transfer transitions in which absorption triggers the transfer of an electron from the donor to the acceptor.

When iodine is dissolved in solutions of donor solvents, the striking purple color of molecular iodine is replaced by a yellow-brown color. This is because charge transfer complexes like those formed by I_2 can absorb light in ways that neither the donor nor the

acceptor can on their own. Specifically, charge transfer complexes exhibit **charge transfer bands (CT bands)** in their absorption spectra. In the charge transfer transition the initial partial transfer of charge from the donor Lewis base to the acceptor Lewis acid in the charge transfer complex is pushed further by photoexcitation.

$$D^{\delta+} - A^{\delta-} \xrightarrow{h\nu_{CT}} D^{+} - A^{-}$$

The nature of these charge transfer transitions is seen from the orbital description of binding for iodine charge transfer complexes. When a donor-I_2 complex forms, the formation of donor-I_2 bonding and antibonding orbitals results in a shift in the $I2\sigma \rightarrow \sigma*$ transition to higher energy, as a new charge transfer band is formed, associated with the excitation of an electron from the largely amine-centered amine-I_2 σ orbital to the largely I_2-centered amine-I_2 $\sigma*$ orbital.

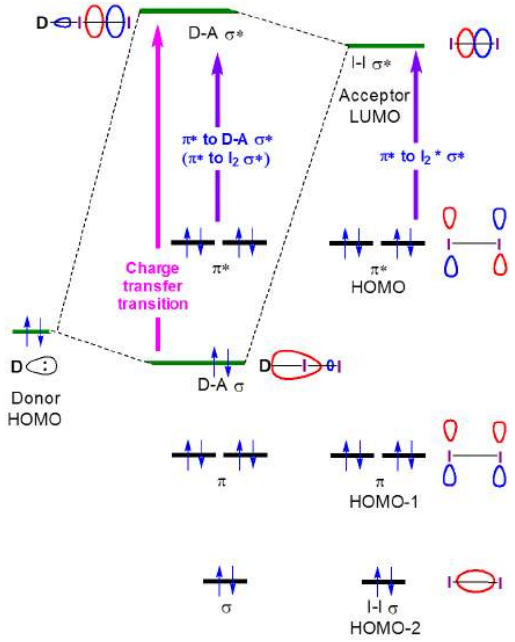


Figure 6.4.2.**7.4.2**. Frontier orbital interactions that give rise to changes in the absorption spectra of iodine when it forms a charge transfer complex with a Lewis base donor.

Solutions of I_2 as mixtures with Lewis bases such as amines and in donor solvents clearly have charge transfer bands in their absorption spectra. Several such spectra are given in Figure 6.4.2.3.

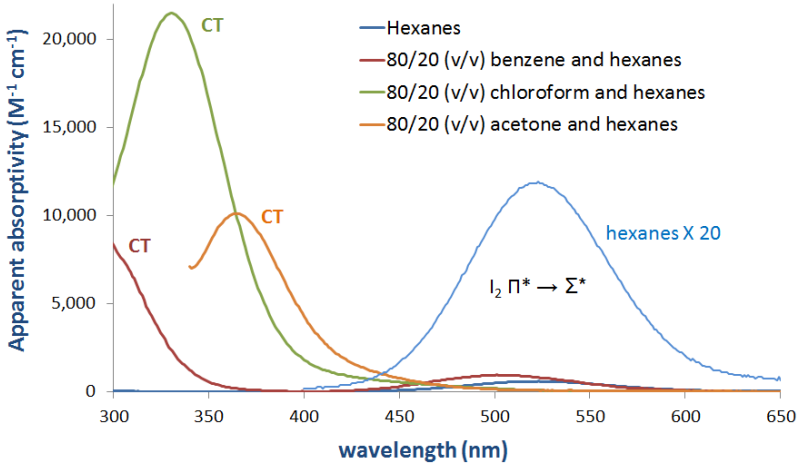


Figure **7.4.3**. Absorption spectrum of molecular iodine (I_2) in various solvents showing the appearance of a CT band in donor solvents.*

In principle, the energies of both the charge transfer and $I_2\ \pi* \rightarrow D-A\ \sigma*$ transitions both increase with donor strength, as shown in Figure 6.4.2.4.

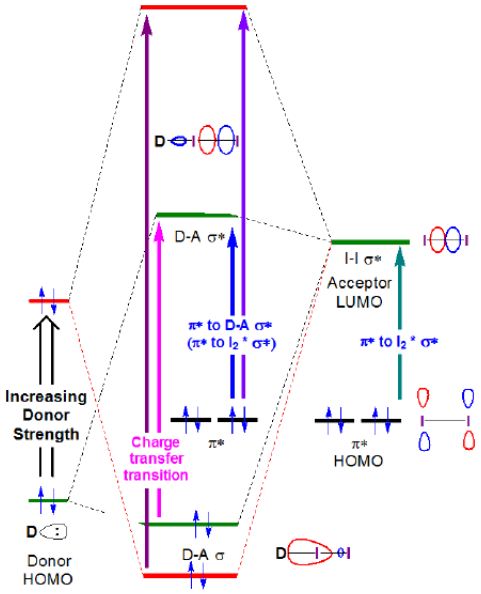


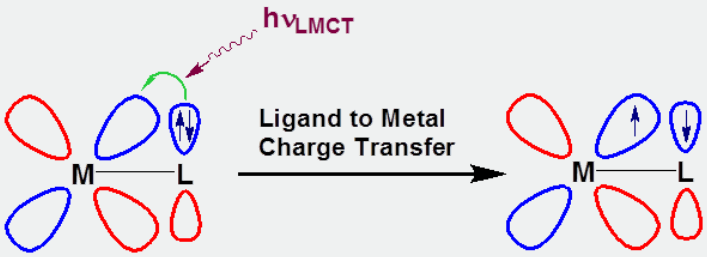
Figure **7.4.4**. Expected change in the frontier orbital energies associated with I_2 donor acceptor complex formation when the HOMO energy of the donor is increased.

As can be seen in Figure 6.4.2, the charge transfer band energy might be expected to increase as the donor HOMO increases in energy to become closer in energy to the acceptor LUMO. Although care should be taken when interpreting the solution phase spectra of I_2, this expectation is borne out by a cursory and qualitative analysis of the spectra in Figure 6.4.2.3. The CT transition energy shifts towards lower wavelengths (and thus higher energy) as the highest occupied atomic orbital energy for the donor atom increases on going from acetone (oxygen, -15.85 eV) to chloroform (chlorine, -13.67eV) and finally benzene (carbon, -10.66 eV).**

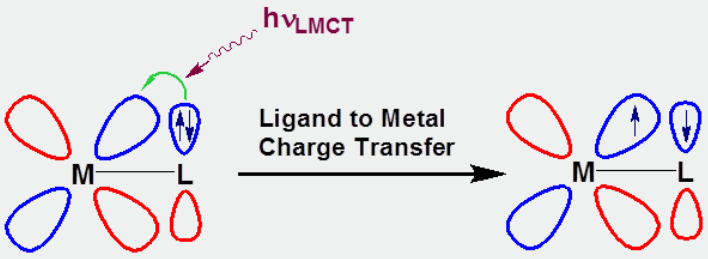
Charge Transfer Bands in Transition Metal Chemistry

Charge transfer transitions are responsible for the intense color of many transition metal complexes. In these cases, however, the weak Lewis acid-base interaction involves incomplete electron donation and acceptance in a $p\pi - d\pi$ (or $p\pi - d\pi*$)-bond between a metal and ligand. The charge transfer bands in the absorption spectra of these complexes involve the transfer of electrons between the metal and ligand. In particular,

- Metal to ligand charge transfer (MLCT or CTTL) bands involve the transfer of an electron from a filled or partly filled metal *d* orbital to a ligand $\pi*$-type orbital.



- Ligand to metal charge transfer (LMCT or CTTM) bands involve the transfer of an electron from a filled or partly filled ligand orbital to a metal *d*-orbital.



- Metal to metal charge transfer bands can be observed in some bimetallic complexes. However, these are usually thought of only as an electron transfer rather than as a shift in the status of a Lewis acid-base interaction.

Because metal-ligand charge transfer bands involve intermolecular electron transfer between the metal and ligand to generate a high energy redox state, the CT excited state is both a better oxidant and reductant than the ground state. Consequently there has been intense research into the development of metal complexes whose charge transfer excited states are powerful oxidants and reductants in the expectation that they will be able to drive the photocatalytic oxidation and reduction of substrates.

* The apparent absorptivity of I_2 in hexanes was calculated from the absorption spectrum of 215 μM I_2 in hexanes. All other apparent absorptivities were calculated from absorption spectra of solutions that were 44 μM in I_2.

** The band positions are not the CT band energies, and the HOMO energies given are atomic energy levels and do not necessarily correspond to the HOMO of the donor in solution. Because of this and other simplifications this analysis is not intended to replace a rigorous computational analysis of the factors that give rise to CT band positions.

References

1. Meyerstein, D.; Treinin, A., Charge-transfer complexes of iodine and inorganic anions in solution. Transactions of the Faraday Society 1963, 59 (0), 1114-1120.
2. Baskar, A. J. A.; Rajpurohit, A. S.; Panneerselvam, M.; Jaccobb, M.; RoopSingh, D.; Kannappan, V., Experimental and theoretical analysis of substituent effect on charge transfer complexes of iodine and some alkylbenzenes in n-hexane solution at 303K. Chemical Data Collections 2017, 7-8, 80-92.

7.4: The electronic spectra of charge transfer complexes illustrate the impact of frontier orbital interactions on the electronic structure of Lewis-Acid base adducts is shared under a CC BY-NC 4.0 license and was authored, remixed, and/or curated by Stephen M. Contakes.

- **6.4.3: The electronic spectra of charge transfer complexes illustrate the impact of frontier orbital interactions on the electronic structure of Lewis acid-base adducts** by Stephen M. Contakes is licensed CC BY 4.0.

7.5: Hard and Soft Acids and Bases

Origin of the Hard-Soft Acid-Base Principle

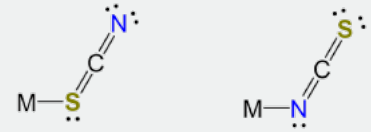
One of the strengths of the Lewis acid-base concept is the readiness with which it illuminates the role that covalent and electrostatic interactions in acid base behavior, specifically through its ability to explain chemical interactions in terms of frontier orbitals and the interactions between charged groups as electrons are donated from a base to an acid. However, simply acknowledging the presence of such interactions does little to illuminate the degree to which each mode of explanation best explains the bonding in a given system? To what extent is a given adduct better described as held together by covalent bonds as opposed to ionic ones - *e.g.* better described as a molecule rather than an ion pair? Moreover, does it even matter, given that the orbitals of quantum mechanics result from the combination of electrons' wavelike behavior with their electrostatic attraction to nuclei in either case?[1] These questions and more are addressed by one of the most important conceptual tools in contemporary inorganic chemistry, the Hard-Soft acid-base principle.

The **Hard-Soft acid-base principle (HSAB principle)** stems from the recognition that some Lewis acids and bases seem to have a natural affinity for one another.* Consider the following:

- Some metals are commonly found in nature as salts of chloride or as oxide ores while others are found in combination with sulfur. Geochemists even use the Goldschmidtt classification scheme to classify the halide and oxide formers as lithophiles and the sulfide formers as chalcophiles.
- In living systems small highly charged metals ions like Fe^{3+} are usually found bound to N and O atoms while larger metals with lower charges such as Zn^{2+} are often found attached to at least one S atom. Similarly, metals prefer to bind to one coordination site over the other when forming complexes with ambidentate ligands. The most well-known instances involve complexes of cyanate and thiocyanate, which can coordinate metals through either the N or chalcogen atom. For instance, Cu^{2+} and Zn^{2+} form *N*-thiocyanato complexes in species like $[Cu(NCS)_2(py)_2]$ and $[Zn(NCS)_4]^{2-}$ while their larger cogeners Au^{3+} and Hg^{2+} preferentially forms *S*-thiocyanato complexes, giving species like $[Hg(SCN)_4]^{2-}$.

Ambidentate ligands

Ambidentate ligands possess multiple coordination sites through which a metal may bind. For instance, thiocyanate may coordinate metals (M) at either the S or N to give *S*-thiocyanato or *N*-thiocyanato complexes.



S-thiocyanato *N*-thiocyanato

- The solubility trends for the alklai metal halides and silver halides are opposite, even though both involve salts of formula M^+X^- (salts can be thought of as involving Lewis acid-base adduct formation between the anions and cations). Specifically, although the silver halides are all relatively insoluble in water, the very modest solubility they possess follows the order:

$$X = F >> Cl > Br > I \text{ (for the solubility of AgX)}$$

In contrast, the much more ample solubility of the alkali metal halides** follows the opposite order. For example, the order for the lithium halides is

$$X = F << Cl < Br << I \text{ (for the solubility of LiX)}$$

Notes

1. Albeit suitably fudged through such niceties as the Aufbau principle and other approximations.

* Despite the fruitfulness of this observation, in general it is important to reduce the potential for observer bias by checking observations like these against compounds reported in the chemical literature and databases like the Inorganic Crystal Structure and Cambridge Crystallographic Databases.

** These are very soluble in water, to the point where some solutions are perhaps better described as solutions of water in the halide.

† This can be predicted based on the relative hardness of BF_3, BR_3, and BH_3 in the list of hard and soft acids. However, for those of you who may be confused as to why H is considered a better electron donor for the purposes of softening a Lewis acid center while alkyl groups are better electron donors for the purposes of stabilizing carbocations in organic chemistry, the dominant effect is the lower electronegativity of H relative to carbon (in CH_3). The effect of electron donation due to hyperconjugation isn't as great for thermodynamically stable bases like BX_3/BR_3.

7.5: Hard and Soft Acids and Bases is shared under a not declared license and was authored, remixed, and/or curated by Stephen M. Contakes.

- **6.6: Hard and Soft Acids and Bases** by Stephen M. Contakes is licensed CC BY 4.0.

7.6: Quantitative Measures of Hardness, Softness, and Acid-Base Interactions from a Hard Soft Acid-Base Principle perspective involve orbital energies and or apportioning acid-base bonding in terms of electrostatic and covalent factors

Pearson Absolute Hardness is a useful metric of hardness based on orbital energies

The recognition that hard acids and bases possess a large HOMO-LUMO gap suggests that the gap size itself might serve as a useful index of hardness. The basis for this idea may be found by considering Pearson's definition of absolute hardness, η.[1] **Pearson's absolute hardness, η**, is half the second derivative of a species' energy with respect to changes in total number of electrons, N_{e^-}.

$$\text{Pearson's absolute hardness} = \eta = \frac{1}{2}\frac{d^2E}{dN_{e^-}^2}$$

$$(in \;\; eV)$$

and, since acids' and bases' hardness and softness are inversely related, Pearson's absolute softness, σ, is just the inverse of hardness.

$$\text{Pearson's softness} = \frac{1}{\eta}$$

Of these, Pearson's absolute hardness is related to the **Mulliken definition of electronegativity** as the first derivative of a species' energy with respect to changes in total number of electrons.

$$\text{Mulliken electronegativity} = \chi = \frac{dE}{dN_{e^-}}$$

$$(in \;\; eV)$$

Operationally, both the Pearson hardness and Mulliken electronegativity are approximated in terms of the energies associated with unit changes in the number of electrons – *i.e.*, in terms of ionization energies and electronegativities. Specifically,

$$\text{Pearson's absolute hardness} = \eta \approx \frac{IE - EA}{2}$$

$$\text{Mulliken electronegativity} = \chi \approx \frac{IE + EA}{2}$$

where IE and EA are in eV.

The connection between Pearson's absolute hardness/softness and the HOMO-LUMO gap then follows from Koopman's theorem, in which the ionization energy (IE) is just the opposite of the HOMO energy.

$$IE = -E_{HOMO}$$

Similarly, the electron affinity (EA), defined as the opposite of the energy released on absorption of an electron, may be taken as an approximation of the LUMO energy.

$$E_{LUMO} \approx -EA$$

So Pearson's absolute hardness is just half the HOMO-LUMO gap (band gap) size in electron volts:

$$\text{Pearson's absolute hardness} = \eta \approx \frac{E_{LUMO} - E_{HOMO}}{2}$$

where all values are given in eV,

and the Mulliken electronegativity is just the average of the HOMO and LUMO energies (~Fermi energy):

$$Mulliken\ electronegativity, \chi \approx -\frac{E_{LUMO} + E_{HOMO}}{2}$$

$$where\ all\ values\ are\ given\ in\ eV$$

The relationships between the Pearson absolute hardness, Mulliken electronegativity, and HOMO and LUMO energies are depicted schematically for the group 1A monocations in Figure **7.6.1**.

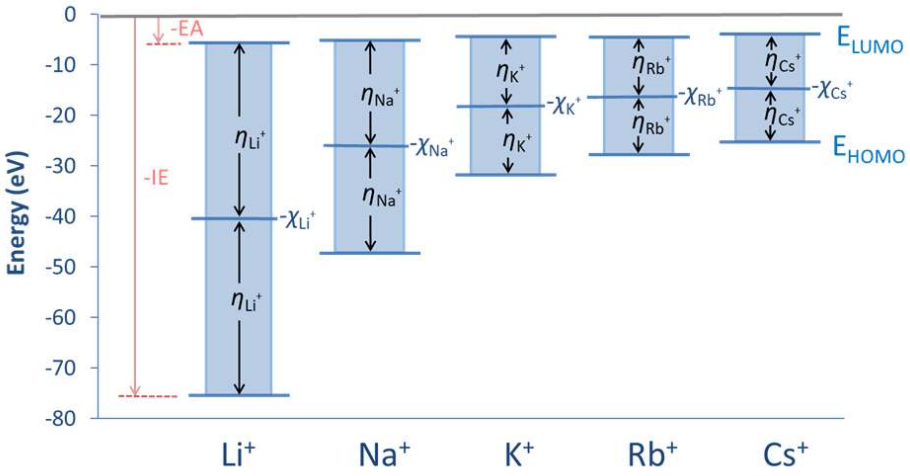


Figure **7.6.1**. Relationships between Pearson absolute hardness, Mulliken electronegativity, and HOMO and LUMO energies for the group 1A monocations.

Values of the Pearson hardness and Mulliken electronegativity for several acids and bases are given in Table **7.6.1**. The values in the table confirm the expected trends, showing an increase in hardness with size (down a group), with increasing charge, and as substituent electronegativity increases for a series of isolobal ions.

Table **7.6.1**: Pearson Absolute Hardness and Related Parameters for Selected Acids and Bases.[2] Taken from Pearson, R. G., Absolute electronegativity and hardness: application to inorganic chemistry. Inorganic Chemistry 1988, 27 (4), 734-740.

Species	Ionization Energy, IE or I (eV)	Electron Affinity, EA or A (eV)	Mulliken Electronegativity, χ (eV)	Pearson Absolute Hardness, η (eV)
Selected Acids				
Group 1A monocations				
Li^+	75.64	5.39	40.52	35.12
Na^+	47.29	5.14	26.21	21.08
K^+	31.63	4.34	17.99	13.64
Rb^+	27.28	4.18	15.77	11.55
Cs^+	25.1	3.89	14.5	10.6
Group 11 monocations				
Cu^+	20.29	7.73	14.01	6.28
Ag^+	21.49	7.58	14.53	6.96
Au^+	20.5	9.23	14.9	5.6
Isoelectronic Row 3 Metal Cations				
Na^+	47.29	5.14	26.21	21.08
Mg^{2+}	80.14	15.04	47.59	32.55
Al^{3+}	119.99	28.45	74.22	45.77
Changes with Transition Metal Ion Charge				
Fe^{2+}	30.65	16.18	23.42	7.24
Fe^{3+}	54.8	30.65	42.73	12.08
Co^{2+}	33.50	17.06	25.28	8.22
Co^{3+}	51.3	22.5	42.4	8.9
Boron trihalides				
BF_3	15.81	-3.5	6.2	9.7
BCl_3	11.60	0.33	5.97	5.64
BBr_3	10.51	0.82	5.67	4.85
CO_2	13.8	-3.8	5.0	8.8
CS_2	10.08	0.62	5.35	5.56
Selected Bases				
Group 17 monoanions (taken to be identical to the free atom values; for arguments as to why this is reasonable see Pearson, R. G., Inorg. Chem. 1988, 27 (4), 734-740.)				
F^-	17.42	3.40	10.41	7.01
Cl^-	13.01	3.62	8.31	4.70
Br^-	11.84	3.36	7.60	4.24
I^-	10.45	3.06	6.76	3.70

Species	Ionization Energy, IE or I (eV)	Electron Affinity, EA or A (eV)	Mulliken Electronegativity, χ (eV)	Pearson Absolute Hardness, η (eV)
Group 15 hydrides				
NH_3	10.7	-5.6	2.6	8.2
PH_3	10.0	-1.9	4.1	6.0
Trimethylpnictides				
NMe_3	7.8	-4.8	1.5	6.3
PMe_3	8.6	-3.1	2.8	5.9
$AsMe_3$	8.7	-2.7	3.0	5.7
Group 16 hydrides				
H_2O	12.6	-6.4	3.1	9.5
H_2S	10.5	-2.1	4.2	6.2
Phosphorous trihalides				
PF_3	12.3	-1.0	5.7	6.7
$PC1_3$	10.2	0.8	5.5	4.7
PBr_3	9.9	1.6	5.6	4.2

Drago-Wayland Acid-Base Parameters allow for estimation of the electrostatic and covalent contributions to the enthalpy of formation of a Lewis acid-base adduct.

Although Pearson hardness values are a useful metric of acids' and bases' hardness, they cannot easily be used to estimate the Lewis acid-base interaction energy. This is not the case for the EC model developed by Drago and Wayland.[3] In the **Drago and Wayland's EC Model,** the enthalpy of formation of an acid-base adduct, AB,

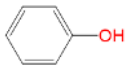
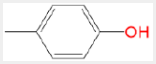
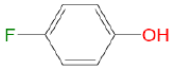
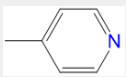
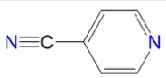
$$A + B \rightleftharpoons AB \qquad \Delta H_{AB\ adduct}$$

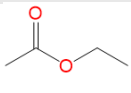
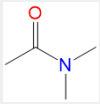
from the acid (A) and base (B) can be calculated as the sum of products of electrostatic (E) and covalent (C) factors that reflect the propensity of the acid and base to engage in strong electrostatic and covalent interactions with one another:

$$-\Delta H_{AB\ adduct} = E_A E_B + C_A C_B$$

where E_A and C_A are the electrostatic and covalent parameters for the acid and E_B and C_B the electrostatic and covalent parameters for the base given in units of $kcal^{½}\ mol^{-½}$. E and C parameters for selected acids and bases are given in Table **7.6.2** .

Table **7.6.2**: E and C Parameters for selected Lewis acids and bases according to the ECW model.[4,5] Taken from Vogel, G. C.; Drago, R. S., The ECW Model. *Journal of Chemical Education* 1996, 73 (8), 701 and Drago, R. S. A modern approach to acid-base chemistry. *Journal of Chemical Education* 1974, 51 (5), 300 (for BF_3).

Species	E (kcal^{½} mol$^{-½}$)	C (kcal^{½} mol$^{-½}$)	W (kcal mol^{-1})	C/E
Acids				
I_2	0.5†	2†	0	4
ICl	2.92	1.66	0	0.57
H_2O	1.31	0.78	0	0.59
SO_2	0.51	1.56	0	3.1
$HCCl_3$ (chloroform)	1.56	0.44	0	0.28
$(CH_3)_3COH$	1.07	0.69	0	0.65
$(CF_3)_3COH$	3.06	1.88	-0.87	0.61
	2.27	1.07	0	0.47
	2.23	1.03	0	0.46
	2.30	1.11	0	0.48
	1.38	0.68	0	0.49
BF_3	1.62	9.88		6.10
$B(CH_3)_3$	2.90	3.60	0	1.2
$Al(CH_3)_3$	8.66	3.68	0	0.43
$Ga(C_2H_5)_3$	6.95	1.48	0	0.21
$In(CH_3)_3$	6.60	2.15	0	0.33
$Zn[N(Si(CH_3)_3)]_2$	2.75	2.32	0	0.84
$Cd[N(Si(CH_3)_3)]_2$	2.50	1.83	0	0.73
Bases				
NH_3	2.31	2.04		0.88
CH_3NH_2	2.16	3.13		1.4
$(CH_3)_2NH$	1.80	4.21		2.3
$(CH_3)_3N$	1.21	5.61		4.6
	1.78	3.54		2.0
	1.81	3.73		2.0
	1.53	2.94		1.9

Species	E ($kcal^{½}$ $mol^{-½}$)	C ($kcal^{½}$ $mol^{-½}$)	W ($kcal$ mol^{-1})	C/E
CH_3CN	1.64	0.71		0.43
$ClCH_2CN$	1.67	0.33		0.20
$CH_3C(O)CH_3$	1.74	1.26		0.72
$(C_2H_5)_2O$	1.80	1.63		0.91
	1.64	2.18		1.3
 (EtOAc)	1.63	0.95		0.58
	2.35†	1.31		0.56
$(CH_3)_2S$	0.25	3.75		15
$(CH_3CH_2)_2S$	0.24	3.92†		15
	0.26	4.07		16
$(CH_3)_2Se$	0.05	4.24		83
$(CH_3)_2SO$	2.4	1.47		0.61
$(CH_3)_3P$	0.25	5.81		24
$(CH_3O)_3P$	0.13	4.83		37
$(C_6H_5)_3PO$	2.59	1.67		0.64
$(C_6H_5)_3PS$	0.35	3.65		10
C_6H_6	0.70	0.45		0.64

† These values were fixed to parameterize the rest of the E and C parameters.

Trends in the relative values of C and E for the acids and bases in Table **7.6.2** are very roughly consistent with the trends in hardness and softness outlined earlier. However, the parameters suggest that some trends in hardness reflect changes in species' ability to engage in ionic interactions while others reflect changes in species' ability to engage in strong covalent interactions. For example, C_B for the dimethylchalcogenides increases steadily from 1.5 to 4.25 $kcal^{½}$ $mol^{-½}$ on going from Me_2O to Me_2Se while E_B decreases from 1.68 to 0.05 $kcal^{½}$ $mol^{-½}$, suggesting that electrostatic and covalent factors are both involved in a decrease in base hardness down group 16. However, in the case of phosphines and amines it appears that electrostatic factors are primarily responsible for the decrease in hardness down group 15. On going from Me_3N to Me_3P, C_B only increases slightly from 5.61 to 5.81 $kcal^{½}$ $mol^{-½}$ while E_B decreases from 1.21 to 0.25 $kcal^{½}$ $mol^{-½}$ - *i.e.*, to 20% of the Me_3N value.

However, some species tend to have very high values for both E and C, reflecting their ability to engage in strong electrostatic and covalent interactions, while others have small values for both, reflecting their relative stability as free species in solution.

As can be seen by comparing the acids and bases listed in the absolute hardness table (Table **7.6.1**) and the EC parameters table (Table **7.6.2**). The EC model has primarily been applied to organic and main group organometallic acids and bases. However, a variety of extensions have been proposed that enable its wider applicability.

The simple EC model only includes electrostatic and covalent considerations and thus ignores steric, lattice energy, and other contributions to the interaction energy. Thus it is only useful for analyzing the interaction energies of sterically unhindered adducts in which solvation energy and other contributions to the overall interaction energy are insignificant. However, additional refinements of the model attempt to extend its usefulness by accomodating various factors, such as

- *Steric strain.* Specifically, Hancock and Martell[6] introduced a D parameter to account for any additional steric strain introduced upon adduct formation,* giving

$$-\Delta H_{AB\ adduct} = E_A E_B + C_A C_B - D_A D_B$$

- *Charge transfer upon adduct formation.* As discussed in section 6.4.2, the formation of a Lewis acid-base complex results in a net transfer of electron density from the electron donor (base) to the acceptor (acid). Drago and Wong[7] extended the EC model to include that charge transfer by adding what they called receptance factors that account for the acid's ability to receive electron density (R_A) and transference factors that account for the base's ability to donate electron density (T_B), giving

$$-\Delta H_{AB\ adduct} = E_A E_B + C_A C_B + R_A T_B$$

  This extension of the EC model is called the **electrostatic-covalent-transfer or ECT model**. Notably, it has been applied successfully to adducts involving ions, for which the $R_A T_B$ term can account for as much as 31% of the interaction energy.

- *Any constant energy term, such as the energy needed to cleave a dimer in order to make the Lewis acid (e.g., $Al_2Cl_6 \rightarrow 2AlCl_3$).* Drago and Vogel[4] extended the EC model to accommodate these constant energy terms, which they designated W. The resulting model is called the **ECW model,** for which

$$-\Delta H_{AB\ adduct} = E_A E_B + C_A C_B + W$$

where

$$W = W_A + W_B$$

A simple application of EC and extended EC models is that they allow the enthalpy of adduct formation to be calculated. These enthalpy calculations based on the EC model are consistent with the superior interaction energy of hard-hard and soft-soft interactions compared to hard-soft ones. Consider, for example, the transfer of I_2 between BF_3 and $InMe_3$, H_3N-BF_3, and H_3N-$InMe_3$.

$$H_3N - BF_3 + InMe_3 \rightleftharpoons BF_3 + H_3N - InMe_3$$

Since H_3N is a hard base and BF_3 and $InMe_3$ are harder and softer acids, respectively, the equilibrium is expected to favor the reactant, H_3N-BF_3. Assuming the equilbrium is enthalpically driven, this qualitative analysis is consistent with the expected endothermic enthalpy of the reaction, as may be seen from the calculated enthalpies of adduct formation for both H_3N-BF_3 and H_3N-$InMe_3$.

For H_3N-BF_3:

$$-\Delta H_{H_3N-BF_3} = E_{BF_3} E_{NH_3} + C_{BF_3} C_{NH_3}$$

$$-\Delta H_{H_3N-BF_3} = (1.62)(2.31) + (9.88)(2.04)$$

$$-\Delta H_{H_3N-BF_3} = 3.74\ kcal/mol + 20.1\ kcal/mol = 23.8\ kcal/mol$$

$$\Delta H_{H_3N-BF_3} = -23.8\ kcal/mol$$

For H_3N-$InMe_3$:

$$-\Delta H_{H_3N-InMe_3} = E_{InMe_3} E_{NH_3} + C_{InMe_3} C_{NH_3}$$

$$-\Delta H_{H_3N-InMe_3} = (6.6)(2.31) + (2.15)(2.04)$$

$$-\Delta H_{H_3N-InMe_3} = 15.25\ kcal/mol + 4.39\ kcal/mol = 19.63\ kcal/mol$$

$$\Delta H_{H_3N-InMe_3} = -19.63\ kcal/mol$$

So H_3N-BF_3 is enthalpically favored by -4.2 kcal/mol [=-23.8 kcal/mol - (-19.63 kcal/mol) according to Hess' Law].

In addition to their utility for estimating enthalpies of Lewis acid-base complex formation, EC and related models serve as a useful tool for estimating the relative importance of ionic, covalent, and steric factors in complex formation. Specifically,

- The relative contributions of ionic and covalent factors can be calculated directly, as from the E and C terms. This can provide insight into why some complexes are more stable than others. Such calculations reveal that the hard-hard adduct H_3N-BF_3 is favored over the hard-soft adduct H_3N-$InMe_3$ because of the strong covalent interaction holding together H_3N-BF_3. The covalent term accounts for 84% of the energy of the H_3N-BF_3 interaction and is largely lost upon formation of H_3N-$InMe_3$, for which it contributes only 22% of the interaction energy. When the electrostatic term is accounted for, it can be seen that the formation of H_3N-$InMe_3$ from H_3N-BF_3 is disfavored, since it would result in a loss of 15.7 kcal/mol of covalent stabilization that would be incompletely compensated for by a gain of 11.5 kcal/mol of electrostatic stabilization.
- The role of other contributions to the bonding in a Lewis acid-base complex may be estimated from the discrepancy between the experimental and EC model calculated stabilization energies. This is because the EC parameters assume sigma bonding and so any deviation between the calculated and experimental enthalpies of complex formation can be attributed to non-sigma contributions.
    - This is done explicitly in extensions of the EC model. For instance, in the case of the Hancock and Martell, ECT, and ECW extensions of the EC model, the contributions of the steric, charge transfer, and constant energy factors (like dimer dissociation) are directly computed in the model.
    - Comparisons of the difference between the energies calculated using ordinary EC parameters and the observed enthalpies has also been used as an estimate of the
        - steric strain energy in strained adducts, which exhibit a less exothermic heat of adduct formation than expected
        - π-backbonding energy in adducts which are capable of such interactions and exhibit a more exothermic heat of formation than expected.[8-10]
    - For examples see (a) Drago, R. S., The interpretation of reactivity in chemical and biological systems with the E and C model. Coordination Chemistry Reviews 1980, 33 (3), 251-277; (b) Drago, R. S.; Bilgrien, C. J., Inductive transfer and coordination of ligands in metal—metal bonded systems. Polyhedron 1988, 7 (16), 1453-1468; (c) Drago, R. S., The question of a synergistic metal-metal interaction leading to .pi.-back-bond stabilization in dirhodium tetrabutyrate adducts. Inorganic Chemistry 1982, 21 (4), 1697-1698.
- The role of electrostatic, covalent, and other contributions to the spectroscopic behavior of Lewis acid-base complexes can be assessed similarly using specialized versions of the ECW or ECT model that allow for calculation of changes in spectroscopic parameters upon adduct formation - *e.g.*, OH stretching frequencies. Details are beyond the scope of this text but may be found in the original literature,[11] for example, Drago, R. S.; Vogel, G. C. *JACS* 1992, 114 (24), 9527-9532; Vogel, G. C.; Drago, R. S., *J. Chem. Educ.* 1996, 73 (8), 701; Drago, R. S.; Wong, N. M., *J. Chem. Educ.* 1996, 73 (2), 123.).

Pearson Softness Parameters have been proposed as a means of calculating the equilibrium constant for formation of a Lewis acid-base adduct, although they are more commonly used to estimate metal toxicity

Pearson also proposed a softness parameter that can be used to estimate the thermodynamics of Lewis acid-base complex formation, this time in the form of the equilibrium constant for

$$A + B \overset{K}{\rightleftharpoons} AB$$

for which Pearson proposed

$$logK = S_A S_B + \sigma_A \sigma_B$$

where S_A and S_B are acid and base parameters related to the strength of the acid-base interaction and σ_A and σ_B are acid and base parameters related to softness. This approach hasn't found as wide an acceptance in studies of chemical reactivity as the Drago-Wayland and absolute hardness parameters. However, because the toxicity of metal ions sometimes depends on their propensity to bind soft Lewis bases in living systems, the softness parameters which Pearson and Mawby subsequently proposed based on the relative energies of metal fluorine and metal iodine bonds[12] have been widely used as a tool for predicting metal ion toxicity.[13]

References

1. Pearson, R. G., Absolute electronegativity and absolute hardness of Lewis acids and bases. *Journal of the American Chemical Society* 1985, 107 (24), 6801-6806.

2. Pearson, R. G., Absolute electronegativity and hardness: application to inorganic chemistry. *Inorganic Chemistry* 1988, 27 (4), 734-740.

3. Drago, R. S.; Wayland, B. B., A Double-Scale Equation for Correlating Enthalpies of Lewis Acid-Base Interactions. *Journal of the American Chemical Society* 1965, 87 (16), 3571-3577.

4. Vogel, G. C.; Drago, R. S., The ECW Model. *Journal of Chemical Education* 1996, 73 (8), 701.

5. Drago, R. S. A modern approach to acid-base chemistry. *Journal of Chemical Education* 1974, 51 (5), 300

6. Hancock, R. D.; Martell, A. E., Hard and Soft Acid-Base Behavior in Aqueous Solution: Steric Effects Make Some Metal Ions Hard: A Quantitative Scale of Hardness-Softness for Acids and Bases. *Journal of Chemical Education* 1996, 73 (7), 654.

7. Drago, R. S.; Wong, N. M., The Role of Electron-Density Transfer and Electronegativity in Understanding Chemical Reactivity and Bonding. *Journal of Chemical Education* 1996, 73 (2), 123.

8. Drago, R. S., The interpretation of reactivity in chemical and biological systems with the E and C model. Coordination Chemistry Reviews 1980, 33 (3), 251-277.

9. Drago, R. S.; Bilgrien, C. J., Inductive transfer and coordination of ligands in metal—metal bonded systems. Polyhedron 1988, 7 (16), 1453-1468.

10. Drago, R. S., The question of a synergistic metal-metal interaction leading to .pi.-back-bond stabilization in dirhodium tetrabutyrate adducts. Inorganic Chemistry 1982, 21 (4), 1697-1698.

11. Drago, R. S.; Vogel, G. C., Interpretation of spectroscopic changes upon adduct formation and their use to determine electrostatic and covalent (E and C) parameters. *Journal of the American Chemical Society* 1992, 114 (24), 9527-9532.

12. Pearson, R. G.; Mawby, R. J. The Nature of Metal-Halogen Bonds in Gutmann, V. *Halogen Chemistry, vol. 3.* Academic Press: London, 1967, pp. 55-84.

13. Kinraide, T. B. Improved Scales for Metal Ion Softness and Toxicity *Environmental Toxicology and Chemistry* 2009, 28 (3), 525-533.

Notes

* More precisely, the D parameters account for the difference in steric strain in the adduct relative to a water adduct of the Lewis acid.

7.6: Quantitative Measures of Hardness, Softness, and Acid-Base Interactions from a Hard Soft Acid-Base Principle perspective involve orbital energies and or apportioning acid-base bonding in terms of electrostatic and covalent factors is shared under a CC BY-NC 4.0 license and was authored, remixed, and/or curated by Stephen M. Contakes.

- **6.6.1: Quantitative Measures of Hardness, Softness, and Acid-Base Interactions from a Hard Soft Acid-Base Principle Perspective Involve Orbital Energies and/or Apportioning Acid-Base Bonding in Terms of Electrostatic and Covalent Factors** by Stephen M. Contakes is licensed CC BY 4.0.

7.7: Hard-Hard and Soft-Soft preferences may be explained and quantified in terms of electrostatic and covalent and electronic stabilization on the stability of Lewis acid-base adducts

The Hard Soft Acid Base Principle is a Conceptual Tool for Thinking About Patterns of Lewis Acid-Base Reactivity

The explanation of the trends in metal distribution, halide salt solubility, and preferred metal coordination patterns is rooted in Arland, Chatt, and Davies' observation that *Lewis acids and bases could be classified into two groups based on their propensity to form stable compounds with one another* (*e.g.* acids in a class tend to form more stable adducts with bases in the same class than they did with bases in the other).[1] Arland, Chatt, and Davies somewhat boringly termed these groups class a and class b but today they are known by Ralph Pearson's name for them. Pearson called the class a acids and bases hard and class b acids and bases soft. These terms reflect how "soft" these substance's electron clouds are towards distortion or, in other words, their polarizability (Figure **7.7.1**). Pearson terms acids and bases which are relatively polarizable **soft** and those which are difficult to polarize **hard.**

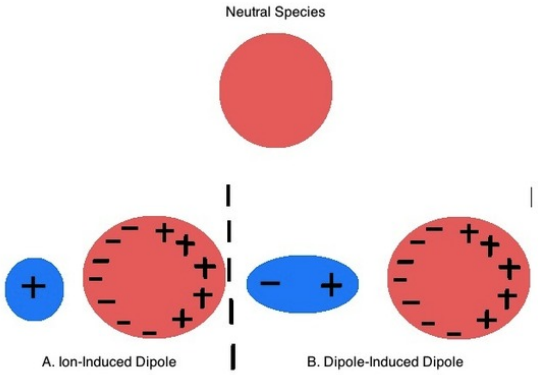


Figure **7.7.1**: Polarizability refers to the ease with which a substance's electron cloud may be distorted under the action of an electric field. A fragment's polarizability determines the degree to which its electron cloud is distorted by A.) an Ion and B.) a polar molecule to induce a dipole moment. The figure is taken from (and the caption expanded from) Cox, Kelly and Dana Reusser "Polarizability"

Recognizing Hard and Soft Acids and Bases

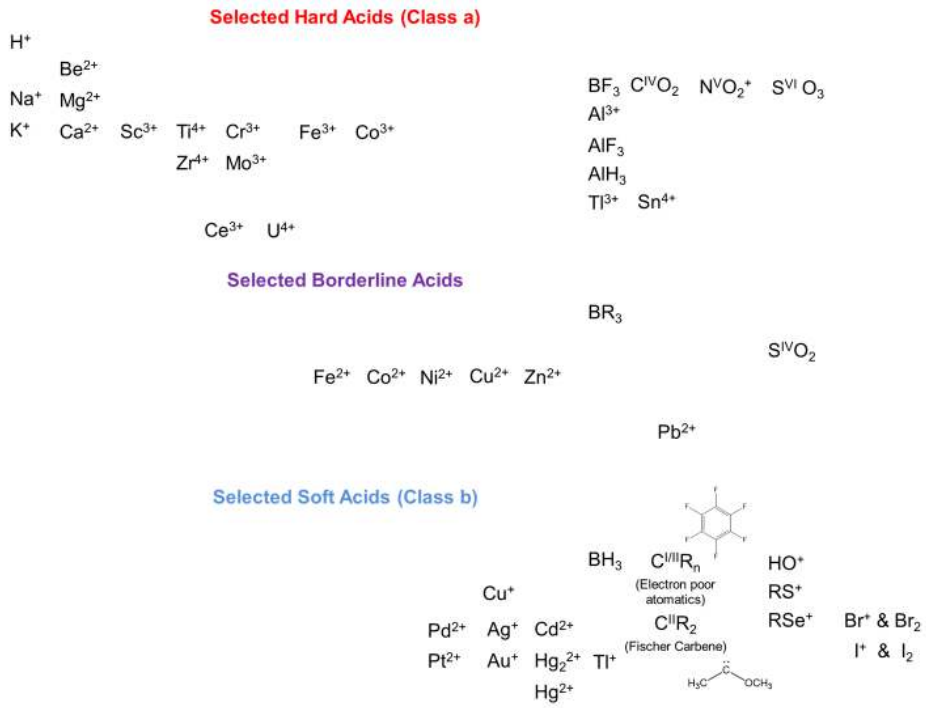
Hard acids and bases come in two varieties:

1. hard acid and base sites that possess few valence electrons and for which polarization therefore involves distorting core electrons, which are difficult to distort because they are close to the nucleus and experience a high nuclear charge. The most common examples of such substances are Lewis acid hard acids towards the left of the periodic table.
2. hard acid and base sites with a high charge density (highly charged relative to size) and/or which are electron deficient. In these cases polarization involves distorting electrons that already experience strong unshielded electrostatic interactions.

Soft acids and bases also come in two varieties

1. soft acids and bases which posses many valence electrons and so are more readily polarized. In consequence, all other things being equal, soft acids and bases are more likely to be found towards the middle or right of the periodic table.
2. soft acids and bases with little charge density and/or which are relatively electron rich.

Note that the hard-soft classification should not be thought of as if all hard acids and bases are equally hard and all soft acids and bases equally soft. There is a graduation in hardness and softness and a number of intermediate acids and bases which do not fit neatly in either category. With this caveat in mind, representative **hard, soft, and borderline acids** are given below. Notice how they illustrate the trends just outlined.



As expected, hard acids tend to be found towards the left side of the periodic table and involve higher oxidation states and/or electron donating substituents while soft acids are more common to the right of the periodic table and involve lower oxidation states and/or electron donating substituents.

Illustrative hard, soft, and borderline bases are given below. Again, notice how these substances illustrate the general trends.

Selected Hard Bases (Class a)

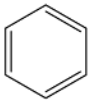
Nitrogen bases	Oxygen bases		small halides
NH_2^-	OH^-	CO_3^{2-}	F^-
NH_3	H_2O	RCO_2^-	Cl^-
RNH_2	ROH	NO_3^-	
NH_2NH_2	ROR	PO_4^{3-}	
		SO_4^{2-}	

Selected Borderline Bases

electron-poor Nitrogen bases		low oxidation state element oxyanions	intermediate halides
N_3^-		NO_2^-	
NO_2^-			Br^-
SCN^-		SO_3^{2-}	
N_2			

Selected Soft Bases (Class b)

Carbon bases	P and As bases	Sulfur bases	large halides & pseudohalides
R^-	PR_3	RS^-	H^-
CO	$P(OR)_3$	RSH	I^-
CN^-	AsR_3	RSR	
RNC		SCN^-	
$R_2C{=}CR_2$ (alkenes)			



(electron-rich aromatics)

Qualitative Estimation of the Relative Hardness and Softness of Lewis Acids and Bases

As can be seen from the examples above, **hard acids are relatively electron-poor and hard bases electron-rich** since they have comparatively

- small frontier orbitals, reflective of their relatively small atom/ion/fragment sizes
- high (for acids) or low (for bases) oxidation states on the base atom, reflected in a large positive formal charge (for acids) or negative formal charge (for bases)
- low polarizability, due to loss or gain of substantial numbers of electrons, or the localization of
  - positive charge on an electropositive element or an atom bearing electron-withdrawing substituents
  - negative charge on an electronegative element or an atom bearing electron-donating substituents

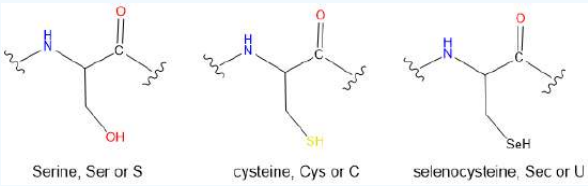
In contrast to hard acids and bases, **soft acids are relatively electron-rich and soft bases larger and more electron poor** since they have comparatively

- large frontier orbitals, reflective of their relatively large atom/ion/fragment sizes
- low oxidation states, often resulting in small or nonexistent atomic charges
- high polarizability, as might be expected of species in which electron-electron repulsions are lower and electrons are spread over a large volume. Sometimes this is indicated by
  - positive charge on an electronegative element or an atom bearing electron-donating substituents
  - negative charge on an electropositive element or an atom bearing electron-withdrawing substituents

Exercise 7.7.1

Rank the acids or bases in each set in increasing order of expected hardness.

a. Cr^{2+} and Cr^{3+}
b. H^+, Cs^+, and Tl^+
c. SCN^- (acting as a base at N) and SCN^- (acting as a base at S)
d. AlF_3, AlH_3, $AlMe_3$
e. The side chains of the following proteinogenic amino acids

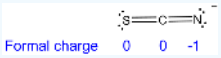


Answer

(a) $Cr^{2+} < Cr^{3+}$ All other things being equal, hardness increases with oxidation state.

(b) $Tl^+ < Cs^+ < H^+$ The order reflects Cs^+ and Tl^+'s larger size relative to H^+ (which doesn't possess any electrons that can be polarized anyway) and that Tl^+ still possesses two valence electrons while Cs^+ possesses none.

(c) SCN^- (acting as a base at S) < SCN^- (acting as a base at N). The order reflects the greater electronegativity of N than S and N's possession of a more negative formal charge of -1.



(d) $AlH_3 < AlMe_3 < AlF_3$. The hardness increases as the substituents on the Lewis acid Al center become less electron donating and more electron withdrawing (and, incidentally, harder bases) as their electronegativity increases in the order $H^- < CH_3^- < F^-$. Note that the order of electron donating ability for H^- and CH_3^- is the opposite observed for carbocations, for which hyperconjugation plays a larger role.

(e) Sec < Cys < Ser. The hardness increases as the electronegativity of the Lewis base chalcogen increases on going from a selenol to a thiol to an alcohol.

The Hard-Soft Acid-Base Principle (HSAB Principle)

The **Hard-Soft acid-base principle (HSAB Principle) explains patterns in Lewis acid-base reactivity in terms of a *like reacts with like preference***. Both thermodynamically and kinetically, hard acids prefer hard bases and soft acids soft bases. Specifically,

- Thermodynamically, hard acids form stronger acid-base complexes with hard bases while soft acids form stronger complexes with soft bases.
- Kinetically, hard acids/electrophiles react more quickly with hard bases/nucleophiles while soft acids/electrophiles react more quickly with soft bases/neucleophiles.

Applications of the HSAB principle include

1. Predicting the equilibrium or speed of *Lewis acid-base metathesis and displacement reactions.* In a Lewis acid-base **metathesis reaction** the acids and bases swap partners

$$\mathbf{A_1 : B_1 + A_2 : B_2 \overset{k_1,\, K_{eq_1}}{\rightleftharpoons} A_1 : B_2 + A_2 : B_1}$$

For example, the equilibrium position of the metathesis reaction between $\mathbf{TlF}$ and $\mathbf{K_2S}$ favors the products:

$$\mathbf{2\,TlF + H_2S \rightleftharpoons Tl_2S + 2\,KF}$$

consistent with the HSAB's hard-hard and soft-soft preference.



The HSAB principle also allows for prediction of the position of displacement reactions, in which a Lewis acid or base forms an adduct using a base or acid from an existing Lewis acid-base complex. In these reactions, the displacement of acid or base from the reactant complex may be thought of as a sort of metathesis reaction, one in which in the unbound acid or base switches places with one in the complex. For example, the reaction between **HI** and methylmercury cation

$$\mathbf{HI + HgSCH_3^+ \rightleftharpoons CH_3SHgI + H^+}$$

involves displacement of an iodide from **HI** to give $\mathbf{CH_3HgI}$. The position of the equilibrium favors $\mathbf{CH_3HgI}$ since both $\mathbf{CH_3Hg^+}$ and $\mathbf{I^-}$ are soft, while $\mathbf{H^+}$ is a hard acid.



Exercise 7.7.2

Predict the position of equilibrium for the following reaction.

$$\mathbf{Fe_2O_3 + 3\,Ag_2S \rightleftharpoons Fe_2S_3 + 3\,Ag_2O}$$

Answer

The equilibrium will favor the reactants (K<1) since the hard-hard and soft-soft interactions in the reactants are more stable than the hard-soft interactions in the products.



Exercise 7.7.3

Predict whether K for the following equilibria will be <<1, ~1, or >>1.

a. $\mathbf{2\,HF + (CH_3Hg)_2S \rightleftharpoons 2\,CH_3HgF + H_2S}$
b. $\mathbf{Ag(NH_3)_2^+ + 2\,PH_3 \rightleftharpoons Ag(PH_3)_2^+ + 2\,NH_3}$
c. $\mathbf{Ag(PH_3)_2^+ + 2\,H_3B{-}SH_2 \rightleftharpoons 2\,H_3B{-}PH_3 + Ag(SH_2)_2^+}$
d. $\mathbf{H_3B{-}NH_3 + F_3B{-}SH_2 \rightleftharpoons H_3B{-}SH_2 + F_3B{-}NH_3}$

Answer

a. K< < 1 since the reactant adducts are hard-hard and soft-soft while the products involve hard-soft interactions.

b. K>>1 since the reactant complex, diamine silver(I), is a complex of a hard base, NH_3, with the soft acid, Ag^+, while the product is a complex of the same soft acid with the soft base phosphine.

c. K~1 since all the adducts amongst the reactants and products involve soft acids and bases.

d. K>>1 since BH_3 is a softer acid than BF_3, so it will form a stronger complex with the softer base H_2S while the harder BF_3 forms a stronger complex with the harder base NH_3.

2. Predicting the relative strengths of a given set of *Lewis acids or bases towards a particular substrate*. Consider, for example, the relative strengths of a BH_3, BMe_3, and BF_3 towards group 15 hydrides like NH_3, PH_3, and AsH_3. Of the

boranes listed, the hardest acid BF_3 is the strongest acid towards the hard base NH_3 while BH_3 is the strongest towards AsH_3.[†]

? Exercise 7.7.4

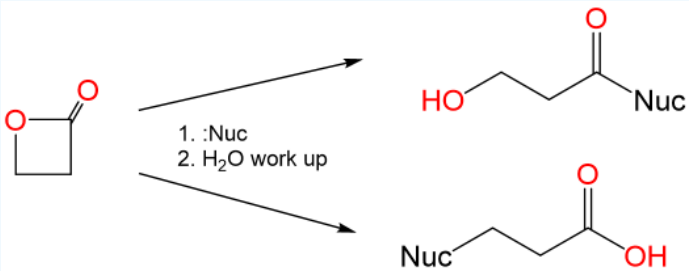
Which acid will form the most stable complex with **CO**: $\mathbf{BH_3}$, $\mathbf{BF_3}$, or $\mathbf{BMe_3}$?

Answer

$\mathbf{BH_3}$. Since **CO** forms complexes primarily through its carbon lone pair, it is a soft base and so will form the strongest complex with the softest Lewis acid.

? Exercise 7.7.5

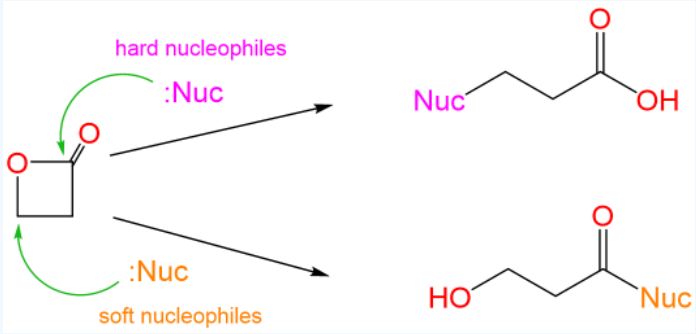
When lactones react with nucleophiles, they can undergo ring opening reactions to give either an alcohol or a carboxylic acid, as shown for propiolactone below:



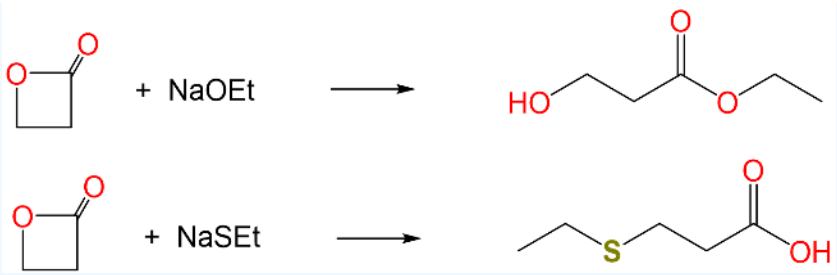
In the reaction above, sterically unhindered alkoxides give one product and sterically unhindered thioalkoxides the other. Explain why this is the case and predict the products of the reaction between propiolactone and the sodium salts of ethoxide and thioethoxide.

Answer

The two reaction products correspond to nucleophilic attack at the lactones' two electrophilic carbon centers. Specifically, the acid is produced by attack at the softer C^{I} center of the CH_2 directly attached to the ester oxygen and the alcohol by nucleophilic attack at the harder C^{III} center of the ester carbonyl.



Consequently, it is reasonable to expect that the harder base ethoxide will nucleophilically attack the harder carbonyl carbon while the softer thioethoxide will attack the softer methylene carbon.



The theoretical interpretation of the hard-soft acid-base principle is that hard-hard preferences reflect superior electrostatic stabilization while soft-soft preferences reflect superior covalent stabilization.

The hard-hard and soft-soft preferences in Lewis acid-base interactions reflect that

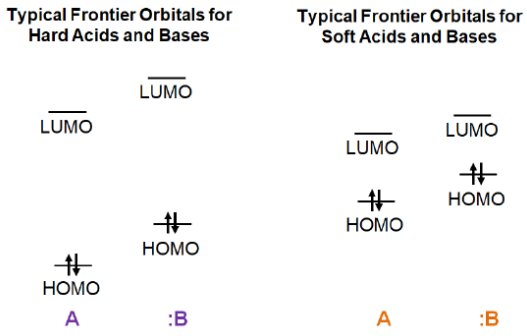
- The lone pair of a hard base is strongly stabilized electrostatically by a hard acid.
- The lone pair of a soft base is strongly stabilized by forming a covalent bond with a soft acid.
- The lone pair of a hard or soft base is comparatively weakly stabilized by an acid opposite to it in hardness or softness since the overall electrostatic and covalent stabilization of the adduct is comparatively weak.

To see why this is the case it is helpful to divide the contributions to the interaction energy between an acid and a base as follows:

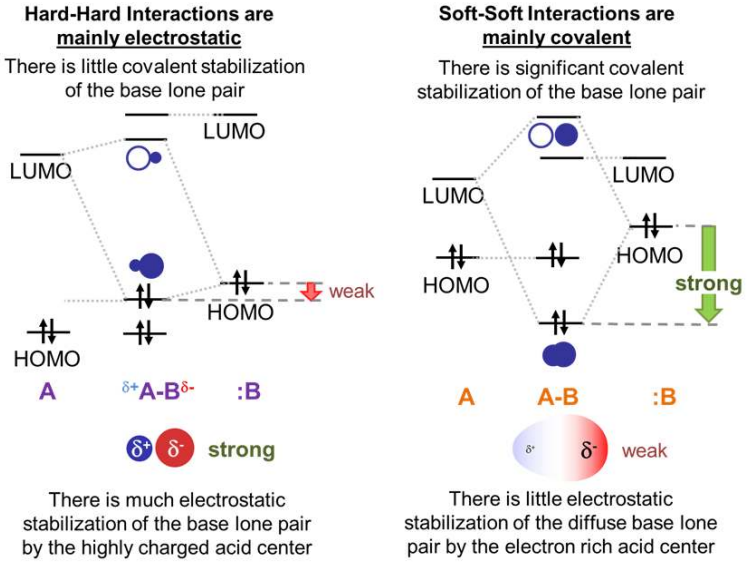
$$\text{Interaction Energy} = \underbrace{\text{Electrostatic attractions and repulsions of partial atomic charges}}_{\text{Ionic term}} + \underbrace{\text{Interactions between filled orbitals on one fragment and unfilled orbitals on the other}}_{\text{Covalent term}} + \underbrace{\text{Electrostatic repulsions between filled orbitals on the two fragments}}_{\text{Steric term}}$$

Of the three contributions to the interaction energy, only the ionic and covalent terms directly relate to the hardness of the interacting acid and base. One approach to thinking about how hardness influences the ionic and covalent contributions is to consider the frontier orbitals involved in the acid-base interaction. This is sometimes done through the use of the Salem-Klopman equation,[1,*] although in the treatment which follows a more qualitative approach will be employed.

Both hard acids and bases will have comparatively low energy HOMO levels and high energy LUMO levels, with a correspondingly high HOMO-LUMO gap. In contrast, soft acids and bases will have comparatively high-energy HOMO levels and low-energy LUMO levels, giving a comparatively smaller HOMO-LUMO gap.



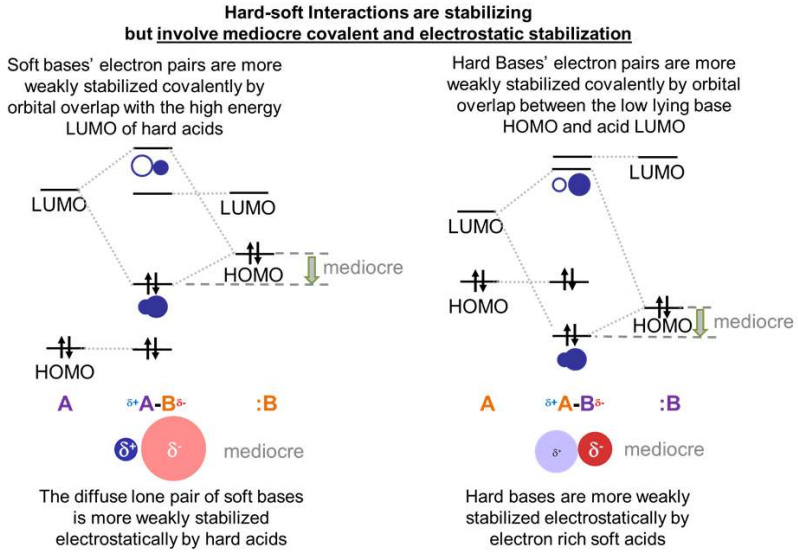
Given this, consider the frontier orbital interactions involved in the formation of an acid-base complex for the possible cases, as illustrated schematically below.



The large gap in energy between hard bases' highly stabilized HOMO lone pairs and the high energy LUMO of hard acids ensures that in **hard acid-hard base adducts the dominant stabilizing interaction will involve electrostatic attraction between the base lone pair and the electropositive Lewis acid center**. Fortunately, since the electron clouds in hard bases are relatively dense and electron rich while hard Lewis acids are highly charged and small, these electrostatic interactions are strong.

In contrast, in **soft acid-soft base adducts, the dominant stabilizing interaction will be covalent.** This is because the small gap in energy between a soft base HOMO and soft acid LUMO enables the formation of a well-stabilized bonding orbital with significant electron density between the acid and base.

The orbitals' interactions between hard acids and soft bases and soft acids and hard bases are intermediate between the hard acid-hard base and soft acid-soft base cases.



This means that the adducts are stable relative to free acid and base – just not as well stabilized as in the hard acid and hard base case. In the case of hard acids and soft bases the hard acids are less able to stabilize the soft bases' relatively diffuse electron pair electrostatically and there isn't as much covalent stabilization as in adducts of soft acids and bases due to the hard acid's high energy.

References

1. Ahrland, S.; Chatt, J.; Davies, N. R., The relative affinities of ligand atoms for acceptor molecules and ions. Quarterly Reviews, Chemical Society 1958, 12 (3), 265-276.

2. Pearson, R. G., Hard and Soft Acids and Bases. Journal of the American Chemical Society 1963, 85 (22), 3533-3539.

3. Fleming, I., Molecular orbitals and organic chemical reactions. Reference ed.; Wiley: Hoboken, N.J., 2010.

Notes

* Despite the fruitfulness of this observation, in general it is important to reduce the potential for observer bias by checking observations like these against compounds reported in the chemical literature and databases like the Inorganic Crystal Structure and Cambridge Crystallographic Databases.

** These are very soluble in water, to the point where some solutions are perhaps better described as solutions of water in the halide.

† This can be predicted based on the relative hardness of BF_3, BR_3, and BH_3 in the list of hard and soft acids. However, for those of you who may be confused as to why H is considered a better electron donor for the purposes of softening a Lewis acid center while alkyl groups are better electron donors for the purposes of stabilizing carbocations in organic chemistry, the dominant effect is the lower electronegativity of H relative to carbon (in CH_3). The effect of electron donation due to hyperconjugation isn't as great for thermodynamically stable bases like BX_3/BR_3.

†† For more on the Salem-Klopman equation see Fleming, I., Molecular orbitals and organic chemical reactions. Reference ed.; Wiley: Hoboken, N.J., 2010; pp. 138-143.

7.7: Hard-Hard and Soft-Soft preferences may be explained and quantified in terms of electrostatic and covalent and electronic stabilization on the stability of Lewis acid-base adducts is shared under a CC BY-NC 4.0 license and was authored, remixed, and/or curated by Stephen M. Contakes.

- **6.6.2: Hard-Hard and Soft-Soft preferences may be explained and quantified in terms of electrostatic and covalent and electronic stabilization on the stability of Lewis acid-base adducts** by Stephen M. Contakes is licensed CC BY 4.0.

CHAPTER OVERVIEW

8: The Crystalline Solid State

8.1: Molecular Orbitals and Band Structure

8.2: Prelude to Electronic Properties of Materials - Superconductors and Semiconductors

8.3: Metal-Insulator Transitions

8.4: Periodic Trends- Metals, Semiconductors, and Insulators

8.5: Semiconductors- Band Gaps, Colors, Conductivity and Doping

8.6: Semiconductor p-n Junctions

8.7: Diodes, LEDs and Solar Cells

8.8: Lattice Structures in Crystalline Solids

8.9: Superconductors

8: The Crystalline Solid State is shared under a not declared license and was authored, remixed, and/or curated by LibreTexts.

SECTION OVERVIEW

8.1: Molecular Orbitals and Band Structure

Learning Objectives

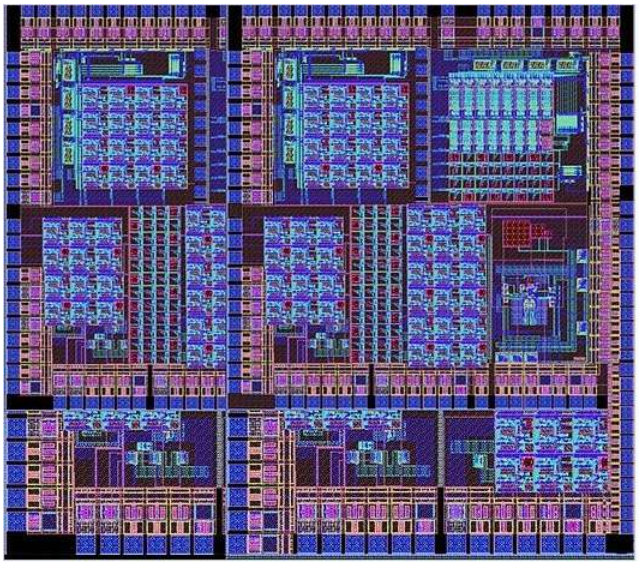
- Explain the physical basis of the Hubbard and Mott models of metal-insulator transitions.
- Understand why good superconductors derive from bad metals.
- Know the structures and the periodic trends in band gaps and colors of semiconductors.
- Obtain the band gap of an intrinsic semiconductor from the temperature dependence of the conductivity.
- Predict the doping type when impurities or defects are introduced into a semiconductor.
- Correlate the band picture and Fermi level with n- or p-type doping.
- Understand the physical principles of operation of diodes, LEDs, solar cells, and FETs.
- Explain the differences in structures and electronic properties of crystalline and amorphous semiconductors.

The band model (like MO theory) is based on a *one-electron* model. This was an approximation we made at the very beginning of our discussion of MO theory: we used hydrogen-like (one-electron) solutions to the Schrödinger equation to give us the shapes of s, p, d, and f atomic orbitals. In a one-electron atom, these orbitals are degenerate within a given shell, and the energy differences between, e.g., 2s and 2p orbitals arise only when we consider the energy of an electron in the field of other electrons in the atom. Moving from atoms to molecules, we made linear combinations to generate one-electron molecular orbitals (and, in solids, one-electron energy bands). But as in multi-electron atoms, life is not so simple for real molecules and solids that contain many electrons. Electrons repel each other, and so their movement in molecules and in solids is ***correlated***.

8.1: Molecular Orbitals and Band Structure is shared under a CC BY-SA 4.0 license and was authored, remixed, and/or curated by LibreTexts.

8.2: Prelude to Electronic Properties of Materials - Superconductors and Semiconductors

In Chapter 6 we developed an energy band picture for metals, starting from atomic orbitals and building up the molecular orbitals of the solid metallic crystal. This treatment gave us a useful picture of how electrons behave in metals, moving at very fast speed between scattering events, and migrating in an electric field at a slow drift velocity. It also taught us that a metal is something with a partially filled band, meaning that the Fermi level cuts through one of its bands of orbitals. An insulator or a semiconductor has a similar band picture, except that the bands are either completely full or completely empty. In this case the Fermi level lies in the gap between fully occupied and unoccupied bands. We will see in this chapter that the properties of semiconductors (along with their useful electronic applications) depend on the addition of small amounts of impurities ("dopants") that change the position of the Fermi level, resulting in conduction by electrons or "holes."



Modern integrated circuits contain billions of nanoscale transistors and diodes that are essential for logic and memory functions. Both kinds of devices rely on junctions between crystalline silicon regions that contain a few parts per million of boron or phosphorus impurities.

While the band picture works well for most crystalline materials, it does not tell us the whole story of conduction in solids. That is because the band model (like MO theory) is based on a *one-electron* model. This was an approximation we made at the very beginning of our discussion of MO theory: we used hydrogen-like (one-electron) solutions to the Schrödinger equation to give us the shapes of s, p, d, and f atomic orbitals. In a one-electron atom, these orbitals are degenerate within a given shell, and the energy differences between, e.g., 2s and 2p orbitals arise only when we consider the energy of an electron in the field of other electrons in the atom. Moving from atoms to molecules, we made linear combinations to generate one-electron molecular orbitals (and, in solids, one-electron energy bands). But as in multi-electron atoms, life is not so simple for real molecules and solids that contain many electrons. Electrons repel each other and so their movement in molecules and in solids is ***correlated***. While this effect is weak in a "good" metal such as sodium - where the wavefunctions are highly delocalized - it can be quite important in other materials such as transition metal oxides. Correlated electron effects give rise to **metal-insulator transitions** that are driven by small changes in temperature, pressure, or composition, as well as to **superconductivity** - the passage of current with zero resistance at low temperatures. In this chapter we will develop some simple models to understand these interesting and important electronic properties of solids.

8.2: Prelude to Electronic Properties of Materials - Superconductors and Semiconductors is shared under a CC BY-SA 4.0 license and was authored, remixed, and/or curated by LibreTexts.

- **10.1: Prelude to Electronic Properties of Materials - Superconductors and Semiconductors** by Chemistry 310 is licensed CC BY-SA 4.0. Original source: https://en.wikibooks.org/wiki/Introduction_to_Inorganic_Chemistry.

8.3: Metal-Insulator Transitions

In Chapter 6 we learned that metals and insulators not only have different electrical properties but also have very different crystal structures. Metals tend to have high coordination numbers (typically 8 or 12) whereas insulators have low coordination numbers that can be rationalized as "octet" bonding arrangements. For example, in crystalline Si or Ge (diamond structure), each atom has four nearest neighbors. There are two electrons per bond, and thus each atom has eight electrons in its valence shell. Sn, the element below Ge, exists in two different forms, one (gray tin) with the diamond structure that is a brittle narrow-gap semiconductor, and the other (white tin) with a body-centered tetragonal structure that is a malleable metal. These two forms are very close in energy, and in fact metallic white tin transforms to the brittle semiconducting gray form at low temperature. Extremely cold weather in 18th century Europe caused many tin organ pipes to break and eventually turn to dust. This transformation has been called tin blight, tin disease, tin pest or tin leprosy. The dust is actually grey tin, which lacks the malleability of its metallic cousin white tin.

Under experimentally accessible temperatures and pressures, Si and Ge are always semiconducting (i.e., insulating), and Pb is always metallic. Why is Sn different? The reason has to do with orbital overlap. Theory tells us in fact that any (and all) insulators should become metallic at high enough pressure, or more to the point, at high enough density. For most insulators, however, the pressures required are far beyond those that we can achieve in the laboratory.



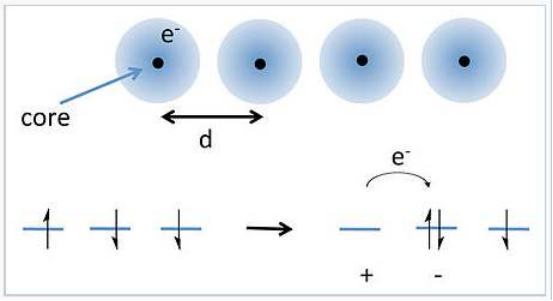
Figure **8.3.1**: Organ pipes destroyed by "tin blight"

How can we rationalize the transition of insulators to the metallic state? Indeed, how can we understand the existence of insulators at all?

The Hubbard Model

Let's consider a chain of a large number (N) of atoms as we did in Chapter 6. For convenience, we can say that these are atoms such as H, Na, or Cs that have one valence electron. The simple band model we developed earlier suggests that the chain should be metallic, because N atoms combine to make N orbitals, and the N valence electrons only fill the band of orbitals halfway. But this

conclusion doesn't depend on the density, which creates a paradox. If atoms in the chain are very far apart, we suspect that the electrons should localize on the atoms.

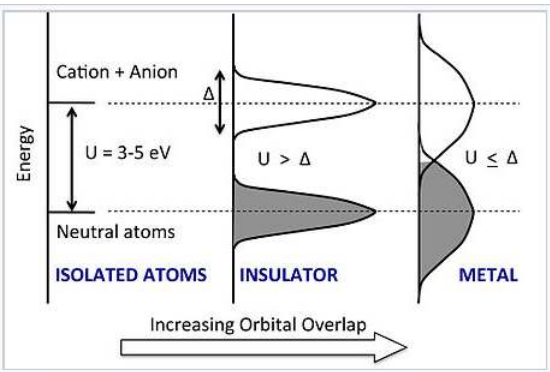


Electron hopping in a 1-D chain of atoms.

A solution to this problem was proposed by J. Hubbard in 1963.[1] Hubbard considered the energy required to transfer an electron from an atom to its nearest neighbor, as shown in the picture at the right. Because each atom already has one electron (with random spin), moving an electron over by one atom requires overcoming the energy of electron-electron repulsion to make a cation-anion pair. For well-separated atoms this energy (U) is given by:

$$U = IP - Ea - \frac{e^2}{4\pi\varepsilon_0 d} \tag{8.3.1}$$

where IP and EA are the ionization energy and electron affinity, ε_0 is the permittivity of free space, and the last term in the equation represents the coulombic attraction between the cation and the anion. For atoms such as alkali metals, U is on the order of 3–5 eV, which is much larger than the thermal energy kT. Thus we expect there to be very few anion-cation pairs at room temperature, and the chain of atoms should be insulating.

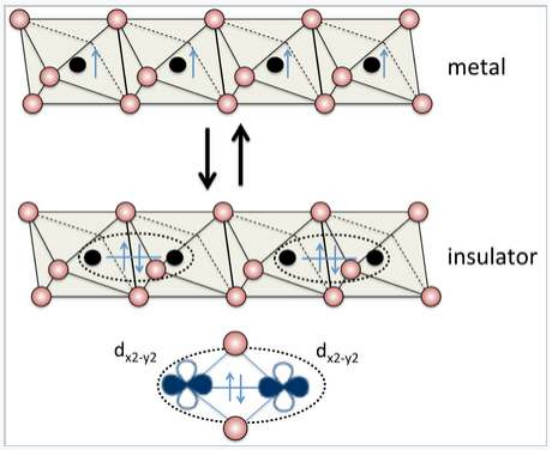


Energy vs. DOS for the chain of atoms as the density and degree of orbital overlap between atoms increases. Increasing overlap broadens the neutral atom and anion-cation states into bands, each of which has a bandwidth Δ. A transition to the metallic state occurs abruptly when Δ exceeds the Hubbard gap U.

What happens when we squeeze the atoms together? In the Hubbard model, as the distance between atoms decreases, the energies of both the neutral atom states and the anion-cation states broaden into bands, each of which has a band width Δ. The lower band can accommodate exactly *N* electrons (not *2N* as in the MO picture we developed earlier) because each orbital can only take one electron without spin-pairing. Thus for small Δ the lower band is full and the upper band is empty. However, as we continue to compress the chain, the orbital overlap becomes so strong that Δ ≈ U. At this point, the bands overlap and some of the electrons fill the anion-cation states. The chain then becomes conducting and the material is metallic.

Some materials, such as Sn and VO_2, happen to have just the right degree of orbital overlap to make the Hubbard transition occur by changing the temperature or pressure. Such materials can be very useful for electrical switching, as illustrated at the right for rutile structure VO_2. Most materials are far away from the transition, either on the metallic or insulating side. An interesting periodic trend that illustrates this concept can be seen among the transition metal monoxides, MO (M = Ti, V, Cr, Mn, Fe, Co, Ni),

all of which have the NaCl structure. TiO and VO are metallic, because the 3d orbitals have significant overlap in the structure. However, CrO, MnO, FeO, CoO, and NiO are all insulators, because the 3d orbitals contract (and therefore $\Delta < U$) going across the transition metal series. In contrast, the analogous sulfides (TiS, VS,....NiS) are all metallic. The sulfides have the NiAs structure, in which all the metal atoms are eclipsed along the stacking axis (the hexagonal c-axis). The short metal-metal distances along that axis result in strong orbital overlap, making $\Delta > U$.



Vanadium dioxide has the rutile structure, and in its undistorted form it is metallic, with one valence electron per V atom. Distortion of the lattice makes pairs of V atoms, resulting in an electronically insulating state. The metal-insulator transition can be driven reversibly by changing the temperature, pressure, or orbital occupancy. Electrical switching of this transition in VO_2 is being studied for applications in high performance thin film transistors[2]

The Mott Model

A simpler, less atomistic model of the metal-insulator transition was formulated by Neville Mott.[3] The Mott model considers the behavior of an electron in a material as a function of the density of all the other valence electrons. We know for a one-electron hydrogen-like atom (H, Na, Cs, etc.) the Schrödinger equation contains a potential energy term:

$$V(r) = -(\frac{e^2}{4\pi\varepsilon_0 r}) \tag{8.3.2}$$

This potential energy function gives rise to familiar ladder of allowed energy levels in the hydrogen atom. However, in a metal, this Coulomb potential must be modified to include the screening of nuclear charge by the other electrons in the solid. In this case there is a **screened Coulomb potential**:

$$V(r) = -(\frac{e^2}{4\pi\varepsilon_0 r})exp(-qr) \tag{8.3.3}$$

where q, which is the inverse of the **screening length**, is given by:

$$q^2 = 4m_e^2(\frac{3n}{\pi})^{\frac{1}{3}}(\frac{2\pi}{h}) \tag{8.3.4}$$

Here n is the density of atoms (or valence electrons), m_e is the electron mass, and h is Planck's constant. At distances much larger than the screening length q^{-1}, the electron no longer "feels" the charge on the nucleus. Mott showed that there is a critical density of electrons n_c above which the valence electrons are no longer bound by individual nuclei and are free to roam the crystal. This critical density marks the transition to the metallic state, and is given by the Mott criterion:

$$\mathbf{n_c^{\frac{1}{3}} a_H \approx 0.26} \tag{8.3.5}$$

In this equation, a_H is an effective Bohr radius for the valence electrons in the low-density limit, e.g. the average orbital radius of electrons in the 6s shell of a Cs atom when computing the value for Cs metal.



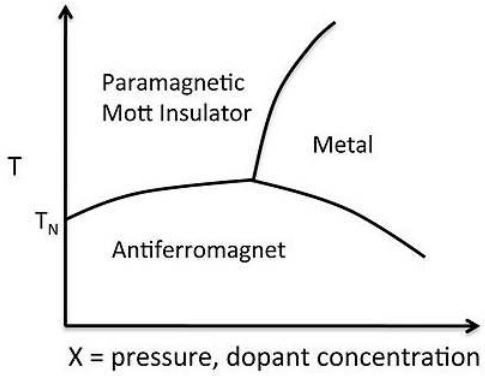
Solutions of lithium metal in liquid ammonia at low (top, ionic conductor) and higher (bottom, metal) Li concentration. From a video by Joshua Judkins

The important concept from the Mott model is that the metal-insulator transition depends very strongly on the **density of valence electrons.** This is consistent with the orbital overlap model of Hubbard, but also more general in the sense that it does not depend on a periodic structure of atoms. The Mott model is thus applicable to such diverse systems as metal atoms dissolved in liquid ammonia, metal atoms trapped in frozen gas matrices, and dopants in semiconductors.[4] In some systems, it is possible to continuously tune the density of valence electrons with rather striking results. For example, dissolving alkali metal (Li, Na, ...) in liquid ammonia (bp -33 ^oC) produces a blue liquid. The solvated alkali cations and negatively charged electrons impart ionic conductivity (as in a salt solution) but not electronic conductivity to the blue liquid ammonia solution. But as the concentration of electrons increases, a reflective, bronze-colored liquid phase forms that floats over the blue phase. This bronze phase is metallic and highly conducting. Eventually, with enough alkali metal added, the entire liquid is converted to the electronically conducting bronze phase.

The electrical switching of VO_2 between insulating and metallic phases (see above) can also be rationalized in terms of the Mott transition. Adding more electron density (by chemical or electric field doping) increases the concentration of valence electrons, driving the phase transition to the metallic state.

Thermodynamics and phase transitions

Thermodynamically, the metal-insulator transition is a **first-order phase transition**. In such a transition, the structure and properties change abruptly (think of the breakfast-to-lunch transition at McDonalds - there is just no way to get pancakes after, or hamburgers before 10:30 AM![5]). Thus in the case of Sn metal, the changes in structure (from four- to eight-coordination) and in electronic conductivity (insulator to metal) occur simultaneously. As in other first order phase transitions such as ice to water to steam, there is a latent heat associated with the transition and a discontinuity in derivative properties such as the heat capacity.



A typical phase diagram for a metal-insulator transition is shown at the right for V_2O_3. The octahedrally coordinated V^{3+} ion has a d^2 electron count, so there are two unpaired spins per atom, and at low temperature the spins in the lattice order antiferromagnetically. As we learned in Chapter 8, above the Néel temperature an antiferromagnet becomes a paramagnet, which is also a Mott insulator. Increasing the pressure, or doping with electrons (e.g., by substituting some d^3 Cr^{3+} for V^{3+}) pushes the electron density over the Mott transition, the spins pair, and the solid becomes metallic.

This page titled 8.3: Metal-Insulator Transitions is shared under a CC BY-SA 4.0 license and was authored, remixed, and/or curated by Chemistry 310 (Wikibook) via source content that was edited to the style and standards of the LibreTexts platform.

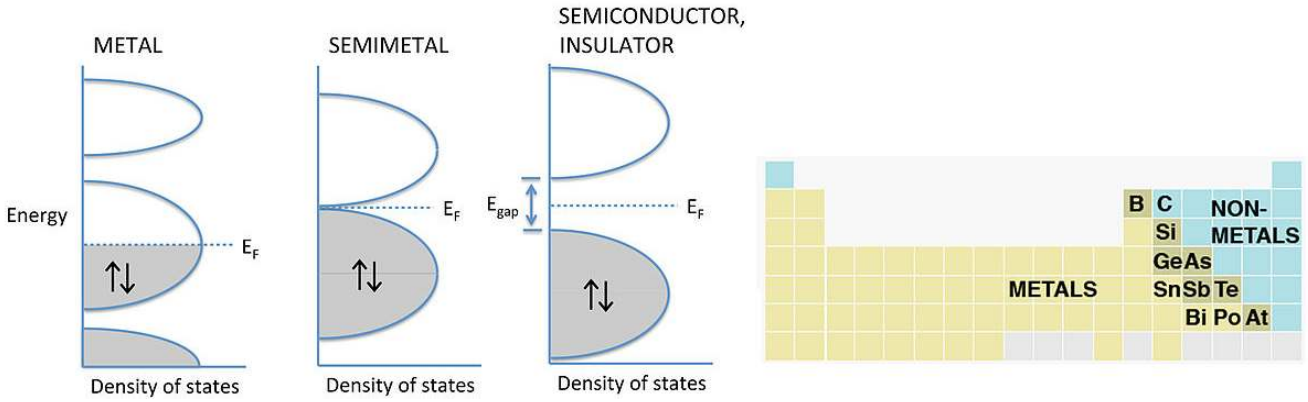
- **10.2: Metal-Insulator Transitions** by Chemistry 310 is licensed CC BY-SA 4.0. Original source: https://en.wikibooks.org/wiki/Introduction_to_Inorganic_Chemistry.

8.4: Periodic Trends- Metals, Semiconductors, and Insulators

As we consider periodic trends in the electronic properties of materials, it is important to review some of the key bonding trends we have learned in earlier chapters:

- Going down the periodic table, atoms in solids tend to adopt structures with higher coordination numbers.
- The second row of the periodic table is special, with strong s-p hybridization and π-bonding between atoms.
- Electrons in higher quantum shells are less strongly bound, so the energy difference between bonding and antibonding orbitals becomes smaller for heavier atoms.

We also know that most of the elements in the periodic table are metals, but the elements in the top right corner are insulating under ordinary conditions (1 atm. pressure) and tend to obey the octet rule in their compounds.



At the transition between metals and non-metals in the periodic table we encounter a crossover in electronic properties, as well as in other properties such as the acidity of the oxides (see Ch. 3). The group of elements at the border is loosely referred to as the metalloids. Several of these elements (such as C, Sn, and As) can exist as different allotropes that can be metals, insulators, or something in between.

A more rigorous delineation of the electronic properties of these elements (and of many compounds) can be made by considering their band structures and the **temperature dependence of the electronic conductivity**. As we have previously discussed, metals have partially filled energy bands, meaning that the Fermi level intersects a partially filled band. With increasing temperature, metals become poorer conductors because lattice vibrations (which are called phonons in the physics literature) scatter the mobile valence electrons. In contrast, semiconductors and insulators, which have filled and empty bands, become better conductors at higher temperature, since some electrons are thermally excited to the lowest empty band. The distinction between insulators and semiconductors is arbitrary, and from the point of view of metal-insulator transitions, all semiconductors are insulators. We typically call an insulator a semiconductor if its band gap (E_{gap}) is less than about 3 eV. A semimetal is a material that has a band gap near zero, examples being single sheets of sp^2-bonded carbon (graphene) and elemental Bi. Like a narrow gap semiconductor, a semimetal has higher conductivity at higher temperature.

8.4: Periodic Trends- Metals, Semiconductors, and Insulators is shared under a CC BY-SA 4.0 license and was authored, remixed, and/or curated by LibreTexts.

- **10.4: Periodic Trends- Metals, Semiconductors, and Insulators** by Chemistry 310 is licensed CC BY-SA 4.0. Original source: https://en.wikibooks.org/wiki/Introduction_to_Inorganic_Chemistry.

8.5: Semiconductors- Band Gaps, Colors, Conductivity and Doping

Semiconductors, as we noted above, are somewhat arbitrarily defined as insulators with **band gap energy ≤ 3.0 eV** (~290 kJ/mol). This cutoff is chosen because, as we will see, the conductivity of undoped semiconductors drops off exponentially with the band gap energy and at 3.0 eV it is very low. Also, materials with wider band gaps (e.g. $SrTiO_3$, E_{gap} = 3.2 eV) do not absorb light in the visible part of the spectrum

There are a number of places where we find semiconductors in the periodic table:

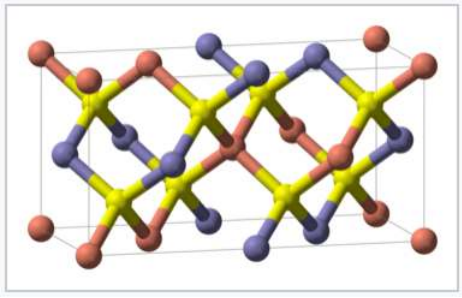
- Early transition metal oxides and nitrides, especially those with d^0 electron counts such as TiO_2, TaON, and WO_3
- Oxides of later 3d elements such as Fe_2O_3, NiO, and Cu_2O
- Layered transition metal chalcogenides with d^0, d^2 and d^6 electron counts including TiS_2, ZrS_2, MoS_2, WSe_2, and PtS_2
- d^{10} copper and sliver halides, e.g., CuI, AgBr, and AgI
- Zincblende- and wurtzite-structure compounds of the p-block elements, especially those that are isoelectronic with Si or Ge, such as GaAs and CdTe. While these are most common, there are other p-block semiconductors that are not isoelectronic and have different structures, including GaS, PbS, and Se.



A 2" wafer cut from a GaAs single crystal. GaAs, like many p-block semiconductors, has the zincblende structure.

The **p-block octet semiconductors** are by far the most studied and important for technological applications, and are the ones that we will discuss in detail.

Zincblende- and wurtzite-structure semiconductors have 8 valence electrons per 2 atoms. These combinations include 4-4 (Si, Ge, SiC,…), 3-5 (GaAs, AlSb, InP,…), 2-6 (CdSe, HgTe, ZnO,…), and 1-7 (AgCl, CuBr,…) semiconductors. Other variations that add up to an octet configuration are also possible, such as $Cu^{I}In^{III}Se_2$, which has the **chalcopyrite** structure, shown at the right.



The **chalcopyrite structure** is adopted by ABX_2 octet semiconductors such as $Cu^{I}In^{III}Se_2$ and $Cd^{II}Sn^{IV}P_2$. The unit cell is doubled relative to the parent **zincblende structure** because of the ordered arrangement of cations. Each anion (yellow) is coordinated by two cations of each type (blue and red).

How does the **band gap energy** vary with **composition**? There are two important trends

(1) Going **down a group** in the periodic table, the gap **decreases**:

C (diamond) > Si > Ge > α-Sn

E_{gap} (eV): 5.4 1.1 0.7 0.0

This trend can be understood by recalling that E_{gap} is related to the **energy splitting between bonding and antibonding orbitals**. This difference decreases (and bonds become weaker) as the principal quantum number increases.

(2) For isoelectronic compounds, **increasing ionicity** results in a **larger band gap**.

Ge < GaAs < ZnSe

0.7 1.4 2.8 eV

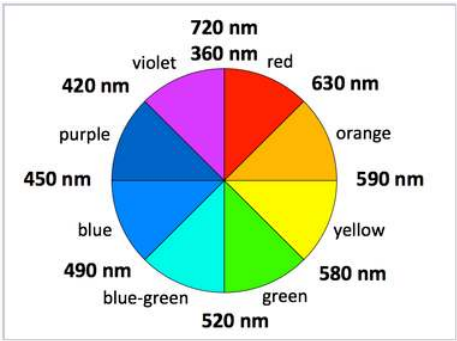
Sn < InSb < CdTe < AgI

0.0 0.2 1.6 2.8 eV

This trend can also be understood from a simple MO picture, as we discussed in Ch. 2. As the electronegativity difference Δχ increases, so does the energy difference between bonding and antibonding orbitals.

The band gap is a very important property of a semiconductor because it determines its color and conductivity. Many of the applications of semiconductors are related to band gaps:

- Narrow gap materials ($Hg_xCd_{1-x}Te$, VO_2, InSb, Bi_2Te_3) are used as infrared photodetectors and thermoelectrics (which convert heat to electricity).
- Wider gap materials (Si, GaAs, GaP, GaN, CdTe, $CuIn_xGa_{1-x}Se_2$) are used in electronics, light-emitting diodes, and solar cells.



Color wheel showing the colors and wavelengths of emitted light.

Semiconductor solid solutions such as $GaAs_{1-x}P_x$ have band gaps that are intermediate between the end member compounds, in this case GaAs and GaP (both zincblende structure). Often, there is a linear relation between composition and band gap, which is referred to as **Vegard's Law**. This "law" is often violated in real materials, but nevertheless offers useful guidance for designing materials with specific band gaps. For example, red and orange light-emitting diodes (LED's) are made from solid solutions with compositions of $GaP_{0.40}As_{0.60}$ and $GaP_{0.65}As_{0.35}$, respectively. Increasing the mole fraction of the lighter element (P) results in a larger band gap, and thus a higher energy of emitted photons.

Colors of semiconductors

The color of absorbed and emitted light both depend on the band gap of the semiconductor. Visible light covers the range of approximately 390-700 nm, or 1.8-3.1 eV. The **color of emitted light** from an LED or semiconductor laser corresponds to the band gap energy and can be read off the color wheel shown at the right.



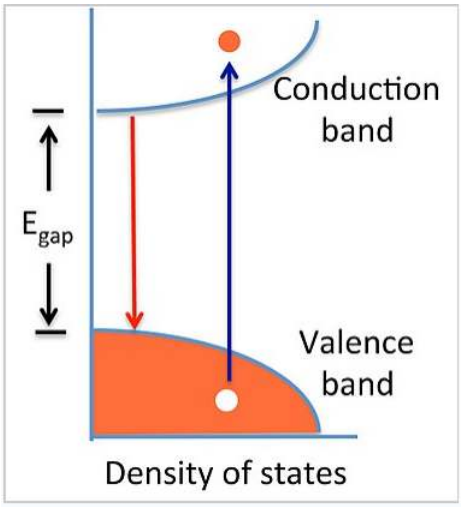
Fe_2O_3 powder is reddish orange because of its 2.2 eV band gap

The color of **absorbed light** includes the band gap energy, but also all colors of higher energy (shorter wavelength), because electrons can be excited from the valence band to a range of energies in the conduction band. Thus semiconductors with band gaps in the infrared (e.g., Si, 1.1 eV and GaAs, 1.4 eV) appear black because they absorb all colors of visible light. Wide band gap semiconductors such as TiO_2 (3.0 eV) are white because they absorb only in the UV. Fe_2O_3 has a band gap of 2.2 eV and thus absorbs light with $\lambda < 560$ nm. It thus appears reddish-orange (the colors of light reflected from Fe_2O_3) because it absorbs green, blue, and violet light. Similarly, CdS (E_{gap} = 2.6 eV) is yellow because it absorbs blue and violet light.

Electrons and holes in semiconductors

Pure (undoped) semiconductors can conduct electricity when electrons are promoted, either by heat or light, from the valence band to the conduction band. The promotion of an **electron** (e^-) leaves behind a **hole** (h^+) in the valence band. The hole, which is the absence of an electron in a bonding orbital, is also a mobile charge carrier, but with a positive charge. The motion of holes in the lattice can be pictured as analogous to the movement of an empty seat in a crowded theater. An empty seat in the middle of a row can move to the end of the row (to accommodate a person arriving late to the movie) if everyone moves over by one seat. Because the movement of the hole is in the opposite direction of electron movement, it acts as a positive charge carrier in an electric field.

The opposite process of excitation, which creates an electron-hole pair, is their recombination. When a conduction band electron drops down to recombine with a valence band hole, both are annihilated and energy is released. This release of energy is responsible for the emission of light in LEDs.



An electron-hole pair is created by adding heat or light energy E ≥ E_{gap} to a semiconductor (blue arrow). The electron-hole pair recombines to release energy equal to E_{gap} (red arrow).

At equilibrium, the creation and annihilation of electron-hole pairs proceed at equal rates. This dynamic equilibrium is analogous to the dissociation-association equilibrium of H^+ and OH^- ions in water. We can write a mass action expression:

$$n \times p = K_{eq} = n_i^2$$

where n and p represent the number density of electrons and holes, respectively, in units of cm^{-3}. The intrinsic carrier concentration, n_i, is equal to the number density of electrons or holes in an undoped semiconductor, where $n = p = n_i$.

Note the similarity to the equation for water autodissociation:

$$[H^+][OH^-] = K_w$$

By analogy, we will see that when we increase n (e.g., by doping), p will decrease, and vice-versa, but their product will remain constant at a given temperature.

Temperature dependence of the carrier concentration. Using the equations $K_{eq} = e^{(\frac{-\Delta G^o}{RT})}$ and $\Delta G^o = \Delta H^o - T\Delta S^o$, we can write:

$$n \times p = n_i^2 = e^{(\frac{\Delta S^o}{R})} e^{(\frac{-\Delta H^o}{RT})} \tag{8.5.1}$$

The entropy change for creating electron hole pairs is given by:

$$\Delta S^o = Rln(N_V) + Rln(N_V) = Rln(N_C N_V) \tag{8.5.2}$$

where N_V and N_C are the effective density of states in the valence and conduction bands, respectively.

and thus we obtain

$$n_i^2 = N_C N_V e^{(-\Delta H^o RT)} \tag{8.5.3}$$

Since the volume change is negligible, $\Delta H^o \approx \Delta E^o$, and therefore $\frac{\Delta H^o}{R} \approx \frac{E_{gap}}{k}$, from which we obtain

$$n_i^2 = N_C N_V e^{(\frac{-E_{gap}}{kT})} \tag{8.5.4}$$

and finally

$$\mathbf{n = p = n_i = (N_C N_V)^{\frac{1}{2}} e^{(\frac{-E_{gap}}{2kT})}} \tag{8.5.5}$$

For pure Si (E_{gap} = 1.1 eV) with N ≈ 10^{22}/cm^3, we can calculate from this equation a carrier density n_i of approximately 10^{10}/cm^3 at 300 K. This is about 12 orders of magnitude lower than the valence electron density of Al, the element just to the left of Si in the periodic table. Thus we expect the conductivity of pure semiconductors to be many orders of magnitude lower than those of metals.

Conductivity of intrinsic semiconductors

The conductivity (σ) is the product of the number density of carriers (n or p), their charge (e), and their mobility (μ). Recall from Chapter 6 that μ is the ratio of the carrier drift velocity to the electric field and has units of cm^2/Volt-second. Typically electrons and holes have somewhat different mobilities (μ_e and μ_h, respectively) so the conductivity is given by:

$$\sigma = ne\mu_e + pe\mu_h \tag{8.5.6}$$

For either type of charge carrier, we recall from Ch. 6 that the mobility μ is given by:

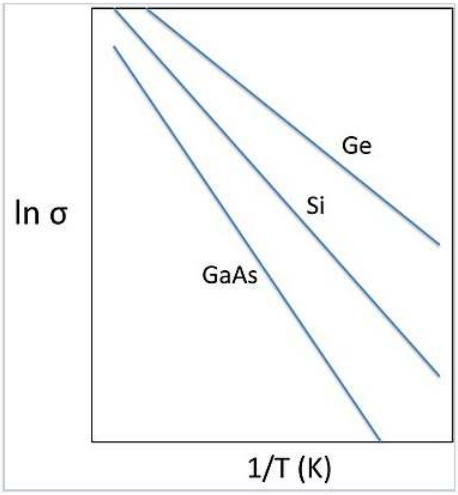
$$\mu = \frac{v_{drift}}{E} = \frac{e\tau}{m} \tag{8.5.7}$$

where e is the fundamental unit of charge, τ is the scattering time, and m is the effective mass of the charge carrier.

Taking an average of the electron and hole mobilities, and using n = p, we obtain

$$\sigma = \sigma_o e^{\left(\frac{-E_{gap}}{2kT}\right)},\ where\ \sigma_o = 2(N_C N_V)^{\frac{1}{2}} e\mu \tag{8.5.8}$$

By measuring the conductivity as a function of temperature, it is possible to obtain the activation energy for conduction, which is $E_{gap}/2$. This kind of plot, which resembles an Arrhenius plot, is shown at the right for three different undoped semiconductors. The slope of the line in each case is $-E_{gap}/2k$.



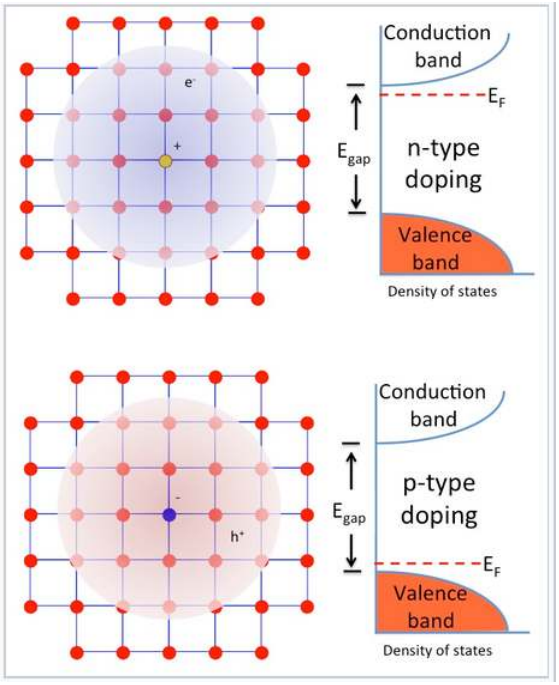
Plots of ln(σ) vs. inverse temperature for intrinsic semiconductors Ge (E_{gap} = 0.7 eV), Si (1.1 eV) and GaAs (1.4 eV). The slope of the line is $-E_{gap}/2k$.

Doping of semiconductors. Almost all applications of semiconductors involve controlled **doping**, which is the substitution of impurity atoms, into the lattice. Very small amounts of dopants (in the parts-per-million range) dramatically affect the conductivity of semiconductors. For this reason, very pure semiconductor materials that are carefully doped - both in terms of the concentration and spatial distribution of impurity atoms - are needed.

n- and p-type doping. In crystalline Si, each atom has four valence electrons and makes four bonds to its neighbors. This is exactly the right number of electrons to completely fill the valence band of the semiconductor. Introducing a phosphorus atom into the lattice (the positively charged atom in the figure at the right) adds an extra electron, because P has five valence electrons and only needs four to make bonds to its neighbors. The extra electron, at low temperature, is bound to the phosphorus atom in a hydrogen-like molecular orbital that is much larger than the 3s orbital of an isolated P atom because of the high dielectric constant of the semiconductor. In silicon, this "expanded" Bohr radius is about 42 Å, i.e., 80 times larger than in the hydrogen atom. The energy needed to ionize this electron – to allow it to move freely in the lattice - is only about 40–50 meV, which is not much larger

the thermal energy (26 meV) at room temperature. Therefore the Fermi level lies just below the conduction band edge, and a large fraction of these extra electrons are promoted to the conduction band at room temperature, leaving behind fixed positive charges on the P atom sites. The crystal is **n-doped**, meaning that the majority carrier (electron) is negatively charged.

Alternatively, boron can be substituted for silicon in the lattice, resulting in **p-type** doping, in which the majority carrier (hole) is positively charged. Boron has only three valence electrons, and "borrows" one from the Si lattice, creating a positively charged hole that exists in a large hydrogen-like orbital around the B atom. This hole can become delocalized by promoting an electron from the valence band to fill the localized hole state. Again, this process requires only 40–50 meV, and so at room temperature a large fraction of the holes introduced by boron doping exist in delocalized valence band states. The Fermi level (the electron energy level that has a 50% probability of occupancy at zero temperature) lies just above the valence band edge in a p-type semiconductor.



n- and p-type doping of semiconductors involves substitution of electron donor atoms (light orange) or acceptor atoms (blue) into the lattice. These substitutions introduce extra electrons or holes, respectively, which are easily ionized by thermal energy to become free carriers. The Fermi level of a doped semiconductor is a few tens of mV below the conduction band (n-type) or above the valence band (p-type).

As noted above, the doping of semiconductors dramatically changes their conductivity. For example, the intrinsic carrier concentration in Si at 300 K is about 10^{10} cm^{-3}. The mass action equilibrium for electrons and holes also applies to doped semiconductors, so we can write:

$$n \times p = n_i^2 = 10^{20} cm^{-6} \; at \; 300K \tag{8.5.9}$$

If we substitute P for Si at the level of one part-per-million, the concentration of electrons is about 10^{16} cm^{-3}, since there are approximately 10^{22} Si atoms/cm^3 in the crystal. According to the mass action equation, if n = 10^{16}, then p = 10^4 cm^{-3}. There are three consequences of this calculation:

- The density of carriers in the doped semiconductor (10^{16} cm^{-3}) is much higher than in the undoped material (~10^{10} cm^{-3}), so the conductivity is also many orders of magnitude higher.
- The activation energy for conduction is only 40–50 meV, so the conductivity does not change much with temperature (unlike in the intrinsic semiconductor)
- The minority carriers (in this case holes) do not contribute to the conductivity, because their concentration is so much lower than that of the majority carrier (electrons).

Similarly, for p-type materials, the conductivity is dominated by holes, and is also much higher than that of the intrinsic semiconductor.

Chemistry of semiconductor doping. Sometimes it is not immediately obvious what kind of doping (n- or p-type) is induced by "messing up" a semiconductor crystal lattice. In addition to substitution of impurity atoms on normal lattice sites (the examples given above for Si), it is also possible to dope with vacancies - missing atoms - and with interstitials - extra atoms on sites that are not ordinarily occupied. Some simple rules are as follows:

- For substitutions, adding an **atom to the right** in the periodic table results in **n-type** doping, and an atom to the **left** in **p-type** doping.

  For example, when TiO_2 is doped with Nb on some of the Ti sites, or with F on O sites, the result is n-type doping. In both cases, the impurity atom has one more valence electron than the atom for which it was substituted. Similarly, substituting a small amount of Zn for Ga in GaAs, or a small amount of Li for Ni in NiO, results in p-type doping.

- **Anion vacancies** result in **n-type** doping, and **cation vacancies** in **p-type** doping.

  Examples are anion vacancies in CdS_{1-x} and WO_{3-x}, both of which give n-type semiconductors, and copper vacancies in $Cu_{1-x}O$, which gives a p-type semiconductor.

- **Interstitial cations** (e.g. Li) donate electrons to the lattice resulting in **n-type** doping. Interstitial anions are rather rare but would result in p-type doping.

Sometimes, there can be both p- and n-type dopants in the same crystal, for example B and P impurities in a Si lattice, or cation and anion vacancies in a metal oxide lattice. In this case, the two kinds of doping **compensate** each other, and the doping type is determined by the one that is in higher concentration. A dopant can also be present on more than one site. For example, Si can occupy both the Ga and As sites in GaAs, and the two substitutions compensate each other. Si has a slight preference for the Ga site, however, resulting in n-type doping.

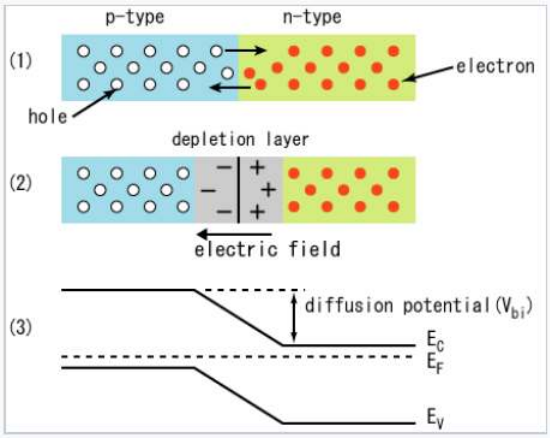
8.5: Semiconductors- Band Gaps, Colors, Conductivity and Doping is shared under a CC BY-SA 4.0 license and was authored, remixed, and/or curated by LibreTexts.

- **10.5: Semiconductors- Band Gaps, Colors, Conductivity and Doping** by Chemistry 310 is licensed CC BY-SA 4.0. Original source: https://en.wikibooks.org/wiki/Introduction_to_Inorganic_Chemistry.

8.6: Semiconductor p-n Junctions

Semiconductor p-n junctions are important in many kinds of electronic devices, including diodes, transistors, light-emitting diodes, and photovoltaic cells. To understand the operation of these devices, we first need to look at what happens to electrons and holes when we bring p-type and n-type semiconductors together. At the junction between the two materials, mobile electrons and holes annihilate each other, leaving behind the fixed + and - charges of the electron donor and electron acceptor dopants, respectively. For example, on the n-side of a silicon p-n junction, the positively charged dopants are P^+ ions and on the p-side the negatively charged dopants are B^-. The presence of these uncompensated electrical charges creates an electric field, the **built-in field** of the p-n junction. The region that contains these charges (and a very low density of mobile electrons or holes) is called the **depletion region**.

The electric field, which is created in the depletion region by electron-hole recombination, repels both the electrons (on the n-side) and holes (on the p-side) away from the junction. The concentration gradient of electrons and holes, however, tends to move them in the opposite direction by diffusion. At equilibrium, the flux of mobile carriers is zero because the field-driven migration flux is equal and opposite to the concentration-driven diffusion flux.



When p-type and n-type semiconductors are joined, electrons and holes are annihilated at the interface, leaving a depletion region that contains positively and negatively charged donor and acceptor atoms, respectively. At equilibrium, the Fermi level (E_F) is uniform throughout the junction. E_F lies just above the valence band on the p-type side of the junction and just below the conduction band on the n-type side.

The width of the depletion layer depends on the screening length in the semiconductor, which in turn depends on the dopant density. At high doping levels, the depletion layer is narrow (tens of nanometers across), whereas at low doping density it can be as thick as 1 μm. The depletion region is the only place where the electric field is nonzero, and the only place where the bands bend. Elsewhere in the semiconductor the field is zero and the bands are flat.

In the middle of p-n junction, the Fermi level energy, E_F, is halfway between the valence band, VB, and the conduction band, CB, and the semiconductor is intrinsic ($n = p = n_i$)

8.6: Semiconductor p-n Junctions is shared under a CC BY-SA 4.0 license and was authored, remixed, and/or curated by LibreTexts.

- **10.6: Semiconductor p-n Junctions** by Chemistry 310 is licensed CC BY-SA 4.0. Original source: https://en.wikibooks.org/wiki/Introduction_to_Inorganic_Chemistry.

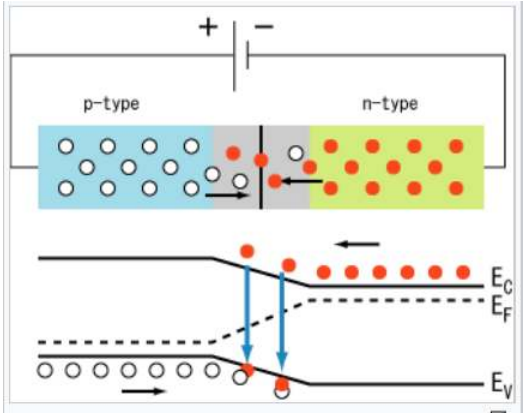
8.7: Diodes, LEDs and Solar Cells

Diodes are semiconductor devices that allow current to flow in only one direction. Diodes act as rectifiers in electronic circuits, and also as efficient light emitters (in LEDs) and solar cells (in photovoltaics). The basic structure of a diode is a junction between a p-type and an n-type semiconductor, called a p-n junction. Typically, diodes are made from a single semiconductor crystal into which p- and n- dopants are introduced.



Closeup of a diode, showing the square-shaped semiconductor crystal *(black object on left)* (John Maushammer, Wikipedia, CC-BY-SA)

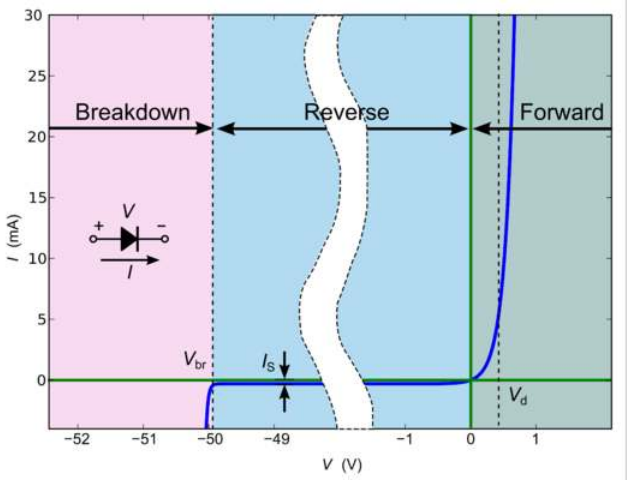
If the n-side of a diode is biased at positive potential and the p-side is biased negative, electrons are drawn to the n-side and holes to the p-side. This reinforces the built in potential of the p-n junction, the width of the depletion layer increases, and very little current flows. This polarization direction is referred to as "back bias." If the diode is biased the other way, carriers are driven into the junction where they recombine. The electric field is diminished, the bands are flattened, and current flows easily since the applied bias lowers the built-in potential. This is called "forward bias."



Electrons (red) and holes (white) in a forward-biased diode. (S-kei. Wikipedia, CC-BY-SA)

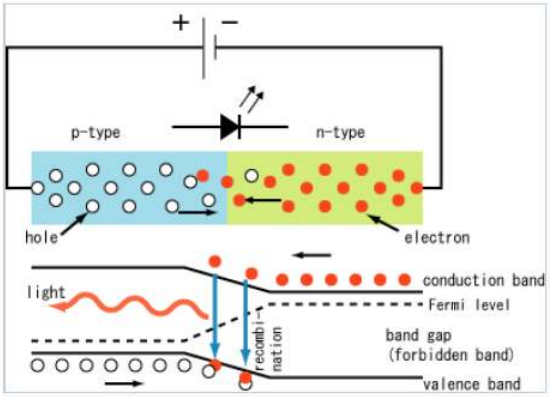
The figure on the left illustrates a forward-biased diode, through which current flows easily. As electrons and holes are driven into the junction (black arrows in lower left figure), they recombine (downward blue arrows), producing light and/or heat. The Fermi level in the diode is indicated as the dotted line. There is a drop in the Fermi level (equal to the applied bias) across the depletion layer. The corresponding diode i-V curve is shown on the right. The current rises exponentially with applied voltage in the forward

bias direction, and there is very little leakage current under reverse bias. At very high reverse bias (typically tens of volts) diodes undergo avalanche breakdown and a large reverse current flows.



Diode i-V curve

A **light-emitting diode** or **LED** is a kind of diode that converts some of the energy of electron-hole recombination into light. This radiative recombination process always occurs in competition with non-radiative recombination, in which the energy is simply converted to heat. When light is emitted from an LED, the photon energy is equal to the bandgap energy. Because of this, LED lights have pure colors and narrow emission spectra relative to other light sources, such as incandescent and fluorescent lights. LED lights are energy-efficient and thus are typically cool to the touch.



Light-emitting diode (LED). (S-kei. Wikipedia, CC-BY-SA)

Direct-gap semiconductors such as GaAs and GaP have efficient luminescence and are also good light absorbers. In direct gap semiconductors, there is no momentum change involved in electron-hole creation or recombination. That is, the electrons and holes originate at the same value of the momentum wavevector **k**, which we encountered in Ch. 6. **k** is related to the momentum (also a vector quantity) by **p** = h**k**/2π. In a direct-gap semiconductor, the top of the valence band and the bottom of the conduction band most typically both occur at **k** = 0. Since the momentum of the photon is close to zero, photon absorption and emission are strongly allowed (and thus kinetically fast). Polar semiconductors such as GaAs, GaN, and CdSe are typically direct-gap materials. **Indirect-gap** semiconductors such as Si and Ge absorb and emit light very weakly because the valence band maximum and conduction band minimum do not occur at the same point in k-space. This means that a lattice vibration (a phonon) must also be created or annihilated in order to conserve momentum. Since this "three body" (electron, hole, phonon) process has low probability, the radiative recombination of electrons and holes is slow relative to non-radiative decay - the thermalization of electron-hole

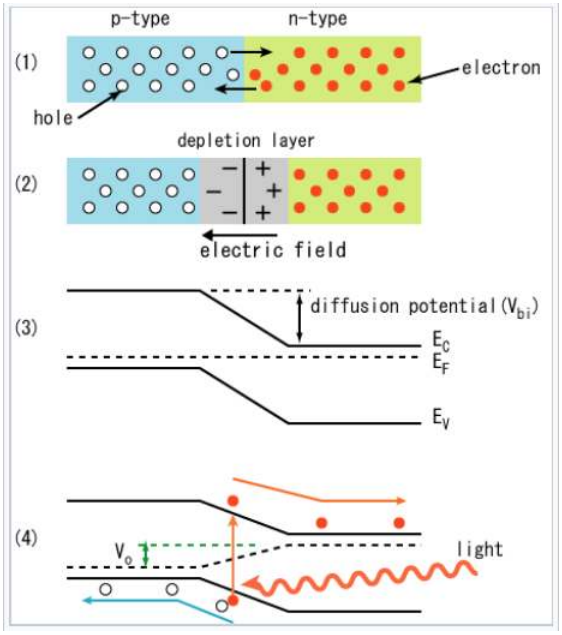
energy as lattice vibrations - in indirect-gap semiconductors. The momentum selection rule thus prevents light absorption/emission and there are no pure Si LEDs or Si-based lasers.



Prof. Shuji Nakamura holding a blue LED.

While red, orange, yellow, and green LEDs can be fabricated relatively easily from AlP-GaAs solid solutions, it was initially very difficult to fabricate blue LEDs because the best direct gap semiconductor with a bandgap in the right energy range is a nitride, GaN, which is difficult to make and to dope p-type. Working at Nichia Corporation in Japan, Shuji Nakamura succeeded in developing a manufacturable process for p-GaN, which is the basis of the blue LED. Because of the importance of this work in the development of information storage (Blu-Ray technology) and full-spectrum, energy-efficient LED lighting, Nakamura shared the 2014 Nobel Prize in Physics with Isamu Asaki and Hiroshi Amano, both of whom had made earlier contributions to the development of GaN diodes.

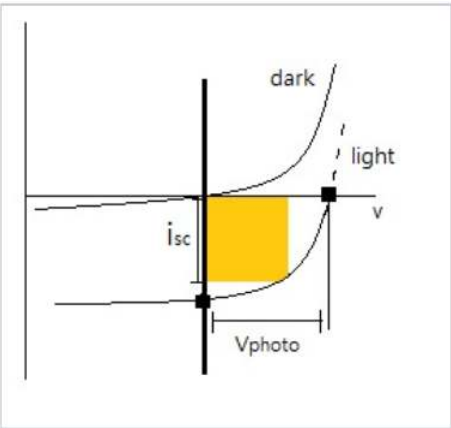
A **Solar cell**, or photovoltaic cell, converts light absorbed in a p-n junction directly to electricity by the photovoltaic effect. Photovoltaics is the field of technology and research related to the development of solar cells for conversion of solar energy to electricity. Sometimes the term solar cell is reserved for devices intended specifically to capture energy from sunlight, whereas the term photovoltaic cell is used when the light source is unspecified.



Photovoltaic effect in a semiconductor p-n junction. (S-kei. Wikipedia, CC-BY-SA)

Photocurrent in p-n junction solar cells flows in the diode reverse bias direction. In the dark, the solar cell simply acts as a diode. In the light, the photocurrent can be thought of as a constant current source, which is added to the i-V characteristic of the diode. The

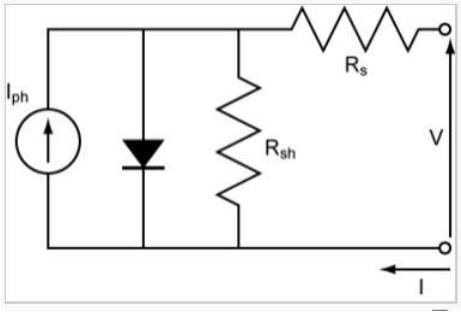
relationship between the dark and light current in a photovoltaic cell is shown in the diagram at the left.



Current-voltage characteristic of a solar cell in the dark and under illumination with band gap light. The short-circuit photocurrent is indicated as i_{sc}, and the open-circuit photovoltage is V_{photo}. The maximum power generated by the solar cell is determined by the area of the orange box.

The built-in electric field of the p-n junction separates e^- h^+ pairs that are formed by absorption of bandgap light in the depletion region. The electrons flow downhill, towards the n-type side of the junction, the holes flow uphill towards the p-side. If $h\nu \geq E_{gap}$, light can be absorbed by promoting an electron from the valence band to the conduction band. Any excess energy is rapidly thermalized. Light with $h\nu > E_g$ thus can store only E_g worth of energy in an e^- h^+ pair. If light is absorbed outside of depletion region, i.e., on the n- or p-side of the junction where there is no electric field, minority carriers must diffuse into the junction in order to be collected. This process occurs in competition with electron-hole recombination. Because impurity atoms and lattice defects make efficient recombination centers, semiconductors used in solar cells (especially indirect-gap materials such as Si, which must be relatively thick in order to absorb most of the solar spectrum) must be very pure. Most of the cost of silicon solar cells is associated with the process of purifying elemental silicon and growing large single crystals from the melt.

In the photodiode i-V curve above, V_{photo} is typically only about 70% of the bandgap energy E_{gap}. The photocurrent is limited by the photon flux, the recombination rate, and the re-emission of absorbed light.[6] The area of the orange rectangle indicates the power generated by the solar cell, which can be calculated as P = i x V. In good single crystal or polycrystalline solar cells made of Si, GaAs, CdTe, $CuIn_xGa_{1-x}Se_2$, or $(CH_3NH_3)PbI_3$ the quantum yield (the ratio of short circuit photocurrent to photon flux) is close to unity.

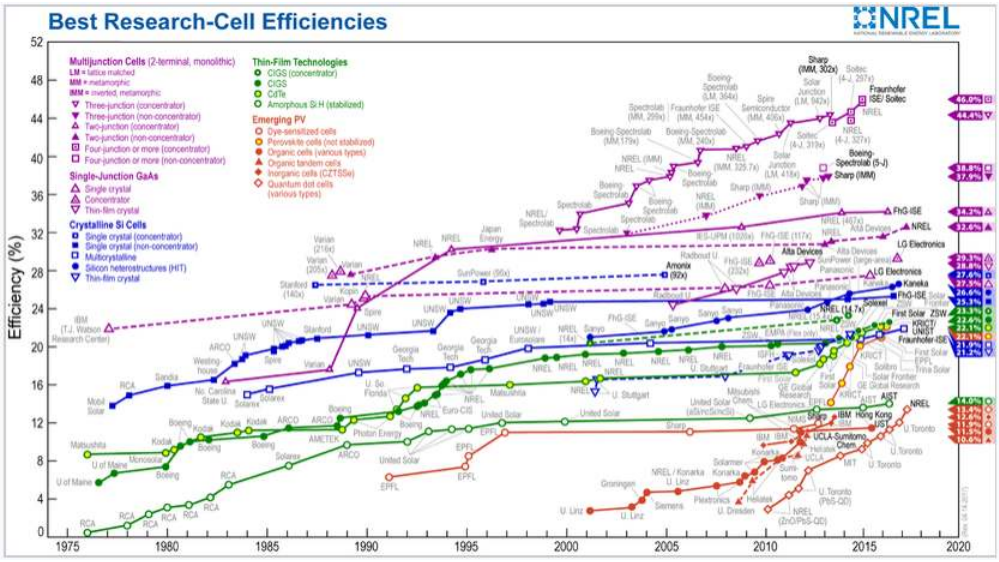


The equivalent circuit of a p-n junction solar cell, which results in the "light" i-V curve shown in the figure above. The solar cell is effectively a diode with a reverse-bias current source provided by light-generated electrons and holes. The shunt resistance (R_{sh}) in the equivalent circuit represents parasitic electron-hole recombination. A high shunt resistance (low recombination rate) and low series resistance (R_s) are needed for high solar cell efficiency.

Solar cells have many current applications. Individual cells are used for powering small devices such as electronic calculators. Photovoltaic arrays generate a form of renewable electricity, particularly useful in situations where electrical power from the grid is

unavailable such as in remote area power systems, Earth-orbiting satellites and space probes, remote radio-telephones and water pumping applications. Photovoltaic electricity is also increasingly deployed in grid-tied electrical systems.

The cost of installed photovoltaics (calculated on a per-watt basis) has dropped over the past decade at a rate of about 13% per year, and has already reached grid parity in Germany and a number of other countries.[7] Photovoltaic grid parity is anticipated in U.S. power markets in the 2020 timeframe.[8] A major driver in the progressively lower cost of photovoltaic power is the steadily increasing efficiency of solar cells, which is shown in the graphic at the right. Higher efficiency solar cells require less area to deliver the same amount of power, and this lowers the "balance of system" costs such as wiring, roof mounting, etc., which scale as the area of the solar panels. Progress towards higher efficiency reflects improved processes for making photovoltaic materials such as silicon and gallium arsenide, as well as the discovery of new materials. Silicon solar cells are a mature technology, so they are now in the flat part of the learning curve and are approaching their maximum theoretical efficiencies. Newer technologies such as organic photovoltaics, quantum dot solar cells, and lead halide perovskite cells are still in the rising part of the learning curve.

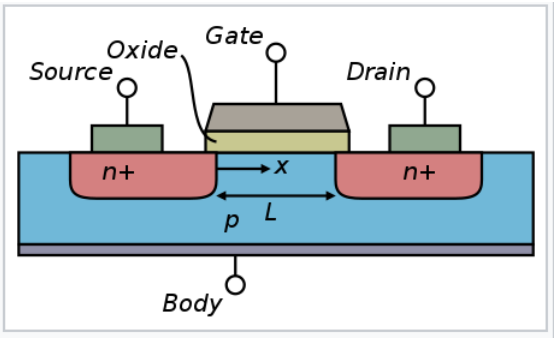


Reported timeline of solar cell energy conversion efficiencies since 1976 (National Renewable Energy Laboratory)

A **field effect transistor (FET)** is a transistor that uses an electric field to control the width of a conducting channel and thus the current in a semiconductor material. It is classified as unipolar transistor, in contrast to bipolar transistors.

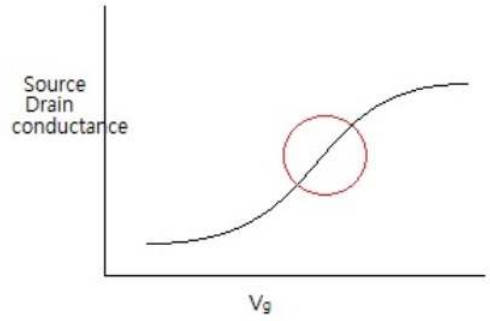
Field effect transistors function as current amplifiers. The typical structure of Si-based FETs is one in which two n-type regions (the source and the drain) are separated by a p-type region. An oxide insulator over the p-type region separates a metal gate lead from the semiconductor. This structure is called a metal-oxide-semiconductor FET (or MOSFET). When voltage is applied between source and drain, current cannot flow because either the n-p or the p-n junction is back-biased. When a positive potential is applied to the gate, however, electrons are driven towards the gate, and locally the semiconductor is "inverted" to n-type. Then the current flows easily between the n-type source and drain through the n-channel. The current flow between the source and drain is many

times larger than the current through the gate, and thus the FET can act as an amplifier. Current flow can also represent a logical "1," so FETs are also used in digital logic.



Cross section of an n-type MOSFET

In electronic devices such as microprocessors, field-effect transistors are kept in the off-state most of the time in order to minimize background current and power consumption. The FET shown above, which has n-type source and drain regions, is called an NMOS transistor. In a PMOS transistor, the source and drain regions are p-type and the gate is n-type. In **CMOS** (complementary metal-oxide semiconductor) integrated circuits, both NMOS and PMOS transistors are used. CMOS circuits are constructed in such a way that all PMOS transistors must have either an input from the voltage source or from another PMOS transistor. Similarly, all NMOS transistors must have either an input from ground or from another NMOS transistor. This arrangement results in low static power consumption.



Transistors are most useful in the range of gate voltage (indicated by the red circle in the figure at the left) where the source-drain current changes rapidly. In this region it is possible to effect a large change in current between source and drain when a small signal is applied to the gate. An important figure of merit for FETs is the **subthreshold slope**, which is the slope a plot of log(current) vs. V_{gate}. An ideal subthreshold slope is one decade of current per 60 mV of gate bias. Typically, a decade change in source-drain current can be achieved with a change in gate voltage of ~70 mV. The performance of FETs as switches and amplifiers is limited by the subthreshold slope, which in turn is limited by the capacitance of the gate. It is desirable to have a very high gate capacitance, which requires a thin insulating oxide, but also to have a small leakage current, which requires a thick oxide. A current challenge in the semiconductor industry is to continue to scale FETs to even smaller nanoscale dimensions while maintaining acceptable values of these parameters. This is being done by developing new gate insulator materials that have higher dielectric constants than silicon oxide and do not undergo redox reactions with silicon or with metal gate leads. Only a few known materials (such as hafnium oxynitride and hafnium silicates) currently meet these stringent requirements.

8.7: Diodes, LEDs and Solar Cells is shared under a CC BY-SA 4.0 license and was authored, remixed, and/or curated by LibreTexts.

- **10.7: Diodes, LEDs and Solar Cells** by Chemistry 310 is licensed CC BY-SA 4.0. Original source: https://en.wikibooks.org/wiki/Introduction_to_Inorganic_Chemistry.

8.8: Lattice Structures in Crystalline Solids

Learning Objectives

- Describe the arrangement of atoms and ions in crystalline structures
- Compute ionic radii using unit cell dimensions
- Explain the use of X-ray diffraction measurements in determining crystalline structures

Over 90% of naturally occurring and man-made solids are crystalline. Most solids form with a regular arrangement of their particles because the overall attractive interactions between particles are maximized, and the total intermolecular energy is minimized, when the particles pack in the most efficient manner. The regular arrangement at an atomic level is often reflected at a macroscopic level. In this module, we will explore some of the details about the structures of metallic and ionic crystalline solids, and learn how these structures are determined experimentally.

The Structures of Metals

We will begin our discussion of crystalline solids by considering elemental metals, which are relatively simple because each contains only one type of atom. A pure metal is a crystalline solid with metal atoms packed closely together in a repeating pattern. Some of the properties of metals in general, such as their malleability and ductility, are largely due to having identical atoms arranged in a regular pattern. The different properties of one metal compared to another partially depend on the sizes of their atoms and the specifics of their spatial arrangements. We will explore the similarities and differences of four of the most common metal crystal geometries in the sections that follow.

Unit Cells of Metals

The structure of a crystalline solid, whether a metal or not, is best described by considering its simplest repeating unit, which is referred to as its unit cell. The unit cell consists of lattice points that represent the locations of atoms or ions. The entire structure then consists of this unit cell repeating in three dimensions, as illustrated in Figure 8.8.1.

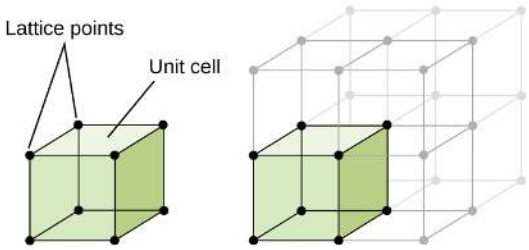


Figure 8.8.1: A unit cell shows the locations of lattice points repeating in all directions.

A diagram of two images is shown. In the first image, a cube with a sphere at each corner is shown. The cube is labeled “Unit cell” and the spheres at the corners are labeled “Lattice points.” The second image shows the same cube, but this time it is one cube amongst eight that make up a larger cube. The original cube is shaded a color while the other cubes are not.

Let us begin our investigation of crystal lattice structure and unit cells with the most straightforward structure and the most basic unit cell. To visualize this, imagine taking a large number of identical spheres, such as tennis balls, and arranging them uniformly in a container. The simplest way to do this would be to make layers in which the spheres in one layer are directly above those in the layer below, as illustrated in Figure 8.8.2. This arrangement is called simple cubic structure, and the unit cell is called the simple cubic unit cell or primitive cubic unit cell.

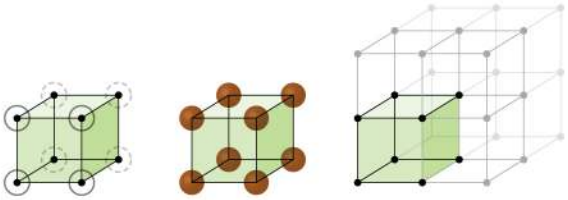


Figure 8.8.2: .When metal atoms are arranged with spheres in one layer directly above or below spheres in another layer, the lattice structure is called simple cubic. Note that the spheres are in contact.

A diagram of three images is shown. In the first image, a cube with a sphere at each corner is shown. The spheres at the corners are circled. The second image shows the same cube, but this time the spheres at the corners are larger and shaded in. In the third image, the cube is one cube amongst eight that make up a larger cube. The original cube is shaded a color while the other cubes are not.

In a simple cubic structure, the spheres are not packed as closely as they could be, and they only "fill" about 52% of the volume of the container. This is a relatively inefficient arrangement, and only one metal (polonium, Po) crystallizes in a simple cubic structure. As shown in Figure 8.8.3, a solid with this type of arrangement consists of planes (or layers) in which each atom contacts only the four nearest neighbors in its layer; one atom directly above it in the layer above; and one atom directly below it in the layer below. The number of other particles that each particle in a crystalline solid contacts is known as its coordination number. For a polonium atom in a simple cubic array, the coordination number is, therefore, six.

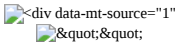


Figure 8.8.3: An atom in a simple cubic lattice structure contacts six other atoms, so it has a coordination number of six.

In a simple cubic lattice, the unit cell that repeats in all directions is a cube defined by the centers of eight atoms, as shown in Figure 8.8.4. Atoms at adjacent corners of this unit cell contact each other, so the edge length of this cell is equal to two atomic radii, or one atomic diameter. A cubic unit cell contains only the parts of these atoms that are within it. Since an atom at a corner of a simple cubic unit cell is contained by a total of eight unit cells, only one-eighth of that atom is within a specific unit cell. And since each simple cubic unit cell has one atom at each of its eight "corners," there is $8 \times \frac{1}{8} = 1$ atom within one simple cubic unit cell.

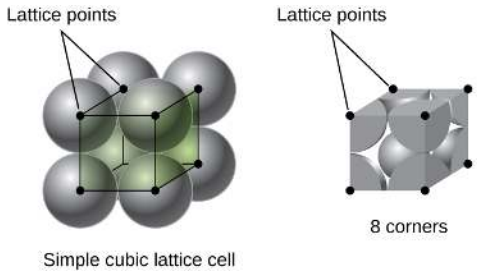


Figure 8.8.4: A simple cubic lattice unit cell contains one-eighth of an atom at each of its eight corners, so it contains one atom total.

A diagram of two images is shown. In the first image, eight spheres are stacked together to form a cube and dots at the center of each sphere are connected to form a cube shape. The dots are labeled "Lattice points" while a label under the image reads "Simple cubic lattice cell." The second image shows the portion of each sphere that lie inside the cube. The corners of the cube are shown with small circles labeled "Lattice points" and the phrase "8 corners" is written below the image.

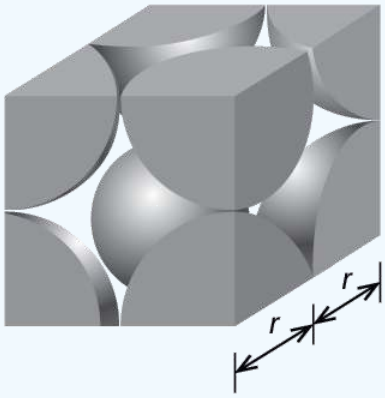
✔ Example 8.8.1: Calculating Atomic Radius and Density for Metals (Part 1)

The edge length of the unit cell of alpha polonium is 336 pm.

a. Determine the radius of a polonium atom.
b. Determine the density of alpha polonium.

Solution

Alpha polonium crystallizes in a simple cubic unit cell:



(a) Two adjacent Po atoms contact each other, so the edge length of this cell is equal to two Po atomic radii: $l = 2r$. Therefore, the radius of Po is

$$r = \frac{l}{2} = \frac{336\ \text{pm}}{2} = 168\ \text{pm}$$

(b) Density is given by

$$\text{density} = \frac{\text{mass}}{\text{volume}}.$$

The density of polonium can be found by determining the density of its unit cell (the mass contained within a unit cell divided by the volume of the unit cell). Since a Po unit cell contains one-eighth of a Po atom at each of its eight corners, a unit cell contains one Po atom.

The mass of a Po unit cell can be found by:

$$1\ \text{Po unit cell} \times \frac{1\ \text{Po atom}}{1\ \text{Po unit cell}} \times \frac{1\ \text{mol Po}}{6.022 \times 10^{23}\ \text{Po atoms}} \times \frac{208.998\ \text{g}}{1\ \text{mol Po}} = 3.47 \times 10^{-22}\ \text{g}$$

The volume of a Po unit cell can be found by:

$$V = l^3 = (336 \times 10^{-10}\ \text{cm})^3 = 3.79 \times 10^{-23}\ \text{cm}^3$$

(Note that the edge length was converted from pm to cm to get the usual volume units for density.)

Therefore, the density of

$$\text{Po} = \frac{3.471 \times 10^{-22}\ \text{g}}{3.79 \times 10^{-23}\ \text{cm}^3} = 9.16\ \text{g/cm}^3$$

? Exercise 8.8.1

The edge length of the unit cell for nickel is 0.3524 nm. The density of Ni is 8.90 g/cm^3. Does nickel crystallize in a simple cubic structure? Explain.

Answer

No. If Ni were simple cubic, its density would be given by:

$$1\ \text{Ni atom} \times \frac{1\ \text{mol Ni}}{6.022 \times 10^{23}\ \text{Ni atoms}} \times \frac{58.693\ \text{g}}{1\ \text{mol Ni}} = 9.746 \times 10^{-23}\ \text{g}$$

$$V = l^3 = (3.524 \times 10^{-8}\ \text{cm})^3 = 4.376 \times 10^{-23}\ \text{cm}^3$$

Then the density of Ni would be

$$(= \frac{9.746 \times 10^{-23}\ \text{g}}{4.376 \times 10^{-23}\ \text{cm}^3} = 2.23\ \text{g/cm}^3$$

Since the actual density of Ni is not close to this, Ni does not form a simple cubic structure.

Most metal crystals are one of the four major types of unit cells. For now, we will focus on the three cubic unit cells: simple cubic (which we have already seen), body-centered cubic unit cell, and face-centered cubic unit cell—all of which are illustrated in Figure 8.8.5. (Note that there are actually seven different lattice systems, some of which have more than one type of lattice, for a total of 14 different types of unit cells. We leave the more complicated geometries for later in this module.)

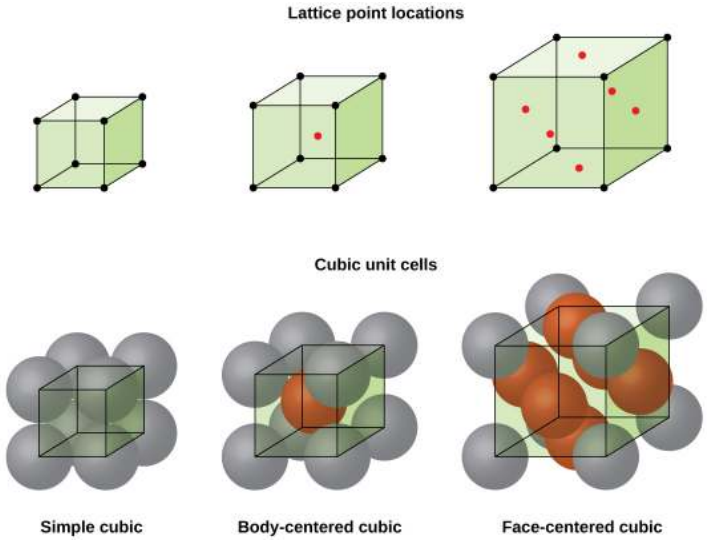


Figure 8.8.5: Cubic unit cells of metals show (in the upper figures) the locations of lattice points and (in the lower figures) metal atoms located in the unit cell.

Three pairs of images are shown. The first three images are in a row and are labeled “Lattice point locations” while the second three images are in a row labeled “Cubic unit cells.” The first image in the top row shows a cube with black dots at each corner while the first image in the second row is composed of eight spheres that are stacked together to form a cube and dots at the center of each sphere are connected to form a cube shape. The name under this image reads “Simple cubic.” The second image in the top row shows a cube with black dots at each corner and a red dot in the center while the second image in the second row is composed of eight spheres that are stacked together to form a cube with one sphere in the center of the cube and dots at the center of each corner sphere connected to form a cube shape. The name under this image reads “Body-centered cubic.” The third image in the top row shows a cube with black dots at each corner and red dots in the center of each face while the third image in the second row is composed of eight spheres that are stacked together to form a cube with six more spheres located in the center of each face of the cube. Dots at the center of each corner sphere are connected to form a cube shape. The name under this image reads “Face-centered cubic.”

Some metals crystallize in an arrangement that has a cubic unit cell with atoms at all of the corners and an atom in the center, as shown in Figure 8.8.6. This is called a body-centered cubic (BCC) solid. Atoms in the corners of a BCC unit cell do not contact each other but contact the atom in the center. A BCC unit cell contains two atoms: one-eighth of an atom at each of the eight corners ($8 \times \frac{1}{8} = 1$ atom from the corners) plus one atom from the center. Any atom in this structure touches four atoms in the layer above it and four atoms in the layer below it. Thus, an atom in a BCC structure has a coordination number of eight.

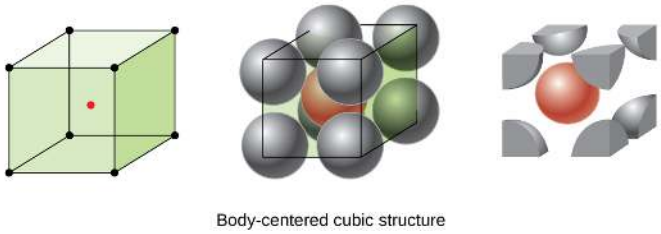


Figure 8.8.6: In a body-centered cubic structure, atoms in a specific layer do not touch each other. Each atom touches four atoms in the layer above it and four atoms in the layer below it.

Three images are shown. The first image shows a cube with black dots at each corner and a red dot in the center while the second image is composed of eight spheres that are stacked together to form a cube with one sphere in the center of the cube and dots at the center of each corner sphere connected to form a cube shape. The name under this image reads “Body-centered cubic structure.” The third image is the same as the second, but only shows the portions of the spheres that lie inside the cube shape.

Atoms in BCC arrangements are much more efficiently packed than in a simple cubic structure, occupying about 68% of the total volume. Isomorphous metals with a BCC structure include K, Ba, Cr, Mo, W, and Fe at room temperature. (Elements or compounds that crystallize with the same structure are said to be isomorphous.)

Many other metals, such as aluminum, copper, and lead, crystallize in an arrangement that has a cubic unit cell with atoms at all of the corners and at the centers of each face, as illustrated in Figure 8.8.7. This arrangement is called a face-centered cubic (FCC) solid. A FCC unit cell contains four atoms: one-eighth of an atom at each of the eight corners ($8 \times \frac{1}{8} = 1$ atom from the corners) and one-half of an atom on each of the six faces ($6 \times \frac{1}{2} = 3$ atoms from the faces). The atoms at the corners touch the atoms in the centers of the adjacent faces along the face diagonals of the cube. Because the atoms are on identical lattice points, they have identical environments.

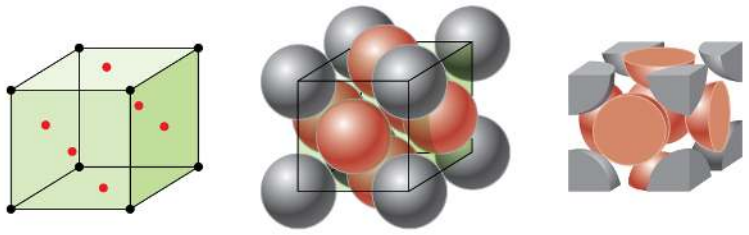


Figure 8.8.7:A face-centered cubic solid has atoms at the corners and, as the name implies, at the centers of the faces of its unit cells.

Three images are shown. The first image shows a cube with black dots at each corner and red dots in the center of each face of the cube while the second image is composed of eight spheres that are stacked together to form a cube with six more spheres, one located on each face of the structure. Dots at the center of each corner sphere are connected to form a cube shape. The name under this image reads “Face-centered cubic structure.” The third image is the same as the second, but only shows the portions of the spheres that lie inside the cube shape.

Atoms in an FCC arrangement are packed as closely together as possible, with atoms occupying 74% of the volume. This structure is also called cubic closest packing (CCP). In CCP, there are three repeating layers of hexagonally arranged atoms. Each atom contacts six atoms in its own layer, three in the layer above, and three in the layer below. In this arrangement, each atom touches 12 near neighbors, and therefore has a coordination number of 12. The fact that FCC and CCP arrangements are equivalent may not be immediately obvious, but why they are actually the same structure is illustrated in Figure 8.8.8.

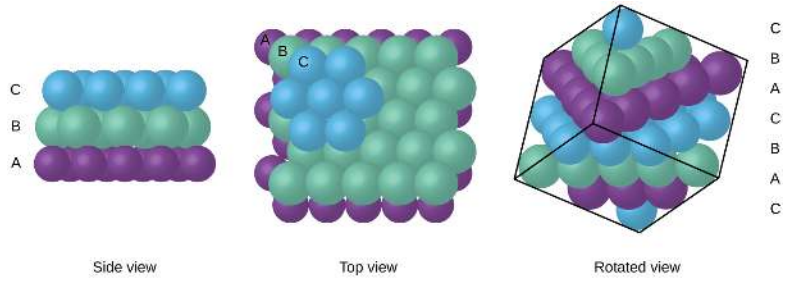


Figure 8.8.8: A CCP arrangement consists of three repeating layers (ABCABC…) of hexagonally arranged atoms. Atoms in a CCP structure have a coordination number of 12 because they contact six atoms in their layer, plus three atoms in the layer above and three atoms in the layer below. By rotating our perspective, we can see that a CCP structure has a unit cell with a face containing an atom from layer A at one corner, atoms from layer B across a diagonal (at two corners and in the middle of the face), and an atom from layer C at the remaining corner. This is the same as a face-centered cubic arrangement.

Three images are shown. In the first image, a side view shows a layer of blue spheres, labeled “C” stacked on top of, and sitting in between the gaps in a second layer that is composed of green spheres, labeled “B,” which are sitting atop a purple layer of spheres labeled “A.” A label below this image reads “Side view.” The second image shows a top view of the same layers of spheres, where the top layer is “C,” the second layer is “B” and the lowest layer is “C.” This image is labeled “Top view” and written under this is the phrase “Cubic closest packed structure.” The third image shows an upper view of the side of a cube composed of two sets of the repeating layers shown in the other images. The layers are arranged “C, B, A, C, B, A, C” and the phrase written under this image reads “Rotated view.”

Because closer packing maximizes the overall attractions between atoms and minimizes the total intermolecular energy, the atoms in most metals pack in this manner. We find two types of closest packing in simple metallic crystalline structures: CCP, which we have already encountered, and hexagonal closest packing (HCP) shown in Figure **8.8.9**. Both consist of repeating layers of hexagonally arranged atoms. In both types, a second layer (B) is placed on the first layer (A) so that each atom in the second layer is in contact with three atoms in the first layer. The third layer is positioned in one of two ways. In HCP, atoms in the third layer are directly above atoms in the first layer (i.e., the third layer is also type A), and the stacking consists of alternating type A and type B close-packed layers (i.e., ABABAB⋯). In CCP, atoms in the third layer are not above atoms in either of the first two layers (i.e., the third layer is type C), and the stacking consists of alternating type A, type B, and type C close-packed layers (i.e., ABCABCABC⋯). About two–thirds of all metals crystallize in closest-packed arrays with coordination numbers of 12. Metals that crystallize in an HCP structure include Cd, Co, Li, Mg, Na, and Zn, and metals that crystallize in a CCP structure include Ag, Al, Ca, Cu, Ni, Pb, and Pt.

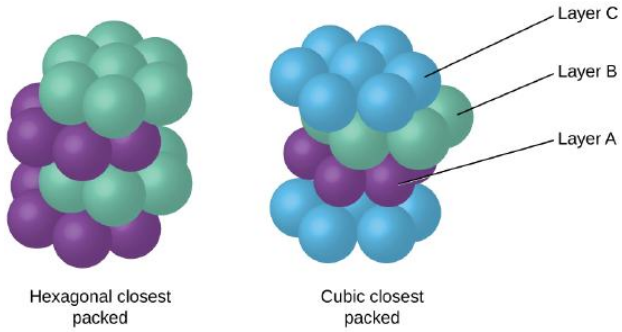


Figure **8.8.9**: In both types of closest packing, atoms are packed as compactly as possible. Hexagonal closest packing consists of two alternating layers (ABABAB…). Cubic closest packing consists of three alternating layers (ABCABCABC…).

Two images are shown. The first image, labeled “Hexagonal closest packed,” shows seven green spheres arranged in a circular sheet lying atop another sheet that is the same except the spheres are purple. The second sheet is offset just a bit so that the spheres of the top sheet lie in the grooves of the second sheet. Two more alternating green and purple layers of spheres lie below the first pair. The second image shows seven blue spheres, labeled “Layer C,” arranged in a circular sheet laying atop another sheet, labeled “Layer B” that is the same except the spheres are green. The second sheet is offset just a bit so that the spheres of the top sheet lie in the grooves of the second sheet. Two more alternating purple and then blue layers of spheres lie below the first pair. The purple layer is labeled “Layer A” and the phrase written below this image reads “Cubic closest packed.”

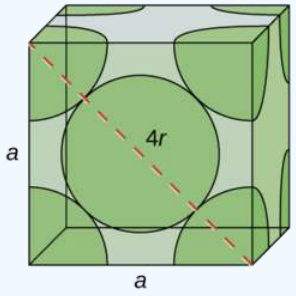
✔ Example 8.8.2: Calculating Atomic Radius and Density for Metals (Part 2)

Calcium crystallizes in a face-centered cubic structure. The edge length of its unit cell is 558.8 pm.

a. What is the atomic radius of Ca in this structure?
b. Calculate the density of Ca.

Solution

(a) In an FCC structure, Ca atoms contact each other across the diagonal of the face, so the length of the diagonal is equal to four Ca atomic radii (d = 4*r*).



Two adjacent edges and the diagonal of the face form a right triangle, with the length of each side equal to 558.8 pm and the length of the hypotenuse equal to four Ca atomic radii:

$$a^2 + a^2 = d^2$$

$$(558.8\ \text{pm})^2 + (558.5\ \text{pm})^2 = (4r)^2$$

Solving this gives

$$r = \sqrt{\frac{(558.8\ \text{pm})^2 + (558.5\ \text{pm})^2}{16}} = 197.6\ \text{pmg for a Ca radius.}$$

(b) Density is given by $\textbf{density} = \frac{\textbf{mass}}{\textbf{volume}}$. The density of calcium can be found by determining the density of its unit cell: for example, the mass contained within a unit cell divided by the volume of the unit cell. A face-centered Ca unit cell has one-eighth of an atom at each of the eight corners ($8 \times \frac{1}{8} = 1$atom) and one-half of an atom on each of the six faces $6 \times \frac{1}{2} = 3$ atoms), for a total of four atoms in the unit cell.

The mass of the unit cell can be found by:

$$1\ \text{Ca unit cell} \times \frac{4\ \text{Ca atoms}}{1\ \text{Ca unit cell}} \times \frac{1\ \text{mol Ca}}{6.022 \times 10^{23}\ \text{Ca atoms}} \times \frac{40.078\ \text{g}}{1\ \text{mol Ca}} = 2.662 \times 10^{-22}\ \text{g}$$

The volume of a Ca unit cell can be found by:

$$V = a^3 = (558.8 \times 10^{-10}\ \text{cm})^3 = 1.745 \times 10^{-22}\ \text{cm}^3$$

(Note that the edge length was converted from pm to cm to get the usual volume units for density.)

Then, the density of polonium:

$$\text{Po} = \frac{2.662 \times 10^{-22}\ \text{g}}{1.745 \times 10^{-22}\ \text{cm}^3} = 1.53\ \text{g/cm}^3$$

? Exercise 8.8.2

Silver crystallizes in an FCC structure. The edge length of its unit cell is 409 pm.

a. What is the atomic radius of Ag in this structure?
b. Calculate the density of Ag.

Answer a

144 pm

Answer b

10.5 g/cm^3

In general, a unit cell is defined by the lengths of three axes (*a*, *b*, and *c*) and the angles (*α*, *β*, and *γ*) between them, as illustrated in Figure 8.8.10. The axes are defined as being the lengths between points in the space lattice. Consequently, unit cell axes join points with identical environments.

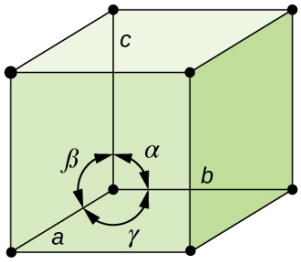


Figure 8.8.10: A unit cell is defined by the lengths of its three axes (a, b, and c) and the angles (α, β, and γ) between the axes.

A cube is shown where each corner has a black dot drawn on it. A circle in the bottom of the cube is composed of three double-ended arrows. The left top of this circle is labeled “alpha,” the top right is labeled “beta” and the bottom is labeled “gamma.” The bottom left corner of the cube is labeled “a” while the bottom of the back face is labeled “b” and the top, back, left corner is labeled “c.”

There are seven different lattice systems, some of which have more than one type of lattice, for a total of fourteen different unit cells, which have the shapes shown in Figure 8.8.11.

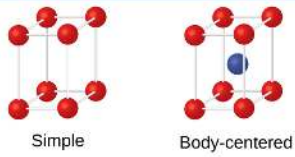
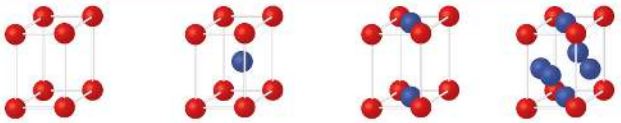
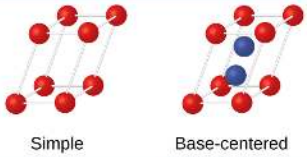
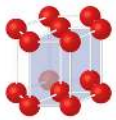
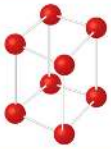
System/Axes/Angles	Unit Cells
Cubic $a = b = c$ $\alpha = \beta = \gamma = 90^\circ$	
Tetragonal $a = b \neq c$ $\alpha = \beta = \gamma = 90^\circ$	
Orthorhombic $a \neq b \neq c$ $\alpha = \beta = \gamma = 90^\circ$	
Monoclinic $a \neq b \neq c$ $\alpha = \gamma = 90^\circ; \beta \neq 90^\circ$	
Triclinic $a \neq b \neq c$ $\alpha \neq \beta \neq \gamma \neq 90^\circ$	
Hexagonal $a = b \neq c$ $\alpha = \beta = 90^\circ; \gamma = 120^\circ$	
Rhombohedral $a = b = c$ $\alpha = \beta = \gamma \neq 90^\circ$	

Figure **8.8.11**:There are seven different lattice systems and 14 different unit cells.

A table is composed of two columns and eight rows. The header row reads “System / Axes / Angles” and “Unit Cells .” The first column reads “Cubic, a equals b equals c, alpha equals beta equals gamma equals 90 degrees,” “Tetragonal, a equals b does not equal c, alpha equals beta equals gamma equals 90 degrees,” “Orthorhombic, a does not equal b does not equal c, alpha equals beta equals gamma equals 90 degrees,” “Monoclinic, a does not equal b does not equal c, alpha equals gamma equals 90 degrees, beta does not equal 90 degrees,” “Triclinic, a does not equal b does not equal c, alpha does not equal beta does not equal gamma does not equal 90 degrees,” “Hexagonal, a equals b does not equal c, alpha equals beta equals 90 degrees, gamma equals 120 degrees,” “Rhombohedral, a equals b equals c, alpha equals beta equals gamma does not equal 90 degrees.” The second column is composed of diagrams. The first set of diagrams in the first cell show a cube with spheres at each corner labeled “Simple,” a cube with spheres in each corner and on each face labeled “Face-centered” and a cube with spheres in each corner and one in the center labeled “Body-centered.” The second set of diagrams in the second cell show a vertical rectangle with spheres at each corner labeled “Simple” and a vertical rectangle with spheres in each corner and one in the center labeled “Body-centered.” The third set of diagrams in the third cell show a vertical rectangle with spheres at each corner labeled “Simple,” a vertical rectangle with spheres in each corner and one in the center labeled “Body-centered,” a vertical rectangle with spheres in each corner and one on the top and bottom faces labeled “Base-centered,” and a vertical rectangle with spheres in each corner and one on each face labeled “Face-centered.” The fourth set of diagrams in the fourth cell show a vertical rectangle with spheres at each corner that is slanted to one side labeled “Simple” and a vertical rectangle with spheres in each corner that is slanted to one side and has two spheres in the center is labeled “Body-centered.” The fifth diagrams in the fifth cell show a cube that is slanted with spheres at each corner while the sixth diagram in the sixth cell shows a pair of hexagonal rings that are connected together to form a six-sided shape with spheres at each corner. The seventh diagram in the seventh cell shows a rectangle that is slanted with spheres at each corner.

The Structures of Ionic Crystals

Ionic crystals consist of two or more different kinds of ions that usually have different sizes. The packing of these ions into a crystal structure is more complex than the packing of metal atoms that are the same size. Most monatomic ions behave as charged spheres, and their attraction for ions of opposite charge is the same in every direction. Consequently, stable structures for ionic compounds result (1) when ions of one charge are surrounded by as many ions as possible of the opposite charge and (2) when the cations and anions are in contact with each other. Structures are determined by two principal factors: the relative sizes of the ions and the ratio of the numbers of positive and negative ions in the compound.

In simple ionic structures, we usually find the anions, which are normally larger than the cations, arranged in a closest-packed array. (As seen previously, additional electrons attracted to the same nucleus make anions larger and fewer electrons attracted to the same nucleus make cations smaller when compared to the atoms from which they are formed.) The smaller cations commonly occupy one of two types of holes (or interstices) remaining between the anions. The smaller of the holes is found between three anions in one plane and one anion in an adjacent plane. The four anions surrounding this hole are arranged at the corners of a tetrahedron, so the hole is called a tetrahedral hole. The larger type of hole is found at the center of six anions (three in one layer and three in an adjacent layer) located at the corners of an octahedron; this is called an octahedral hole. Figure **8.8.12** illustrates both of these types of holes.

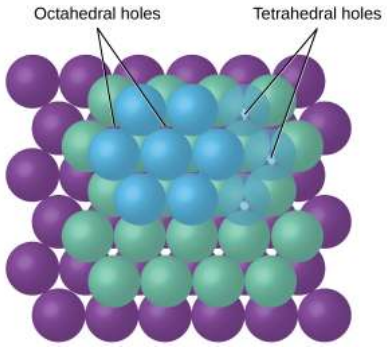


Figure **8.8.12**: Cations may occupy two types of holes between anions: octahedral holes or tetrahedral holes.

An image shows a top-view of a layer of blue spheres arranged in a sheet lying atop another sheet that is the same except the spheres are green. The second sheet is offset just a bit so that the spheres of the top sheet lie in the grooves of the second sheet. A third sheet composed of purple spheres lies at the bottom. The spaces created between the spheres in each layer are labeled “Octahedral holes” and “Tetrahedral holes.”

Depending on the relative sizes of the cations and anions, the cations of an ionic compound may occupy tetrahedral or octahedral holes, as illustrated in Figure **8.8.13**. Relatively small cations occupy tetrahedral holes, and larger cations occupy octahedral holes. If the cations are too large to fit into the octahedral holes, the anions may adopt a more open structure, such as a simple cubic array. The larger cations can then occupy the larger cubic holes made possible by the more open spacing.

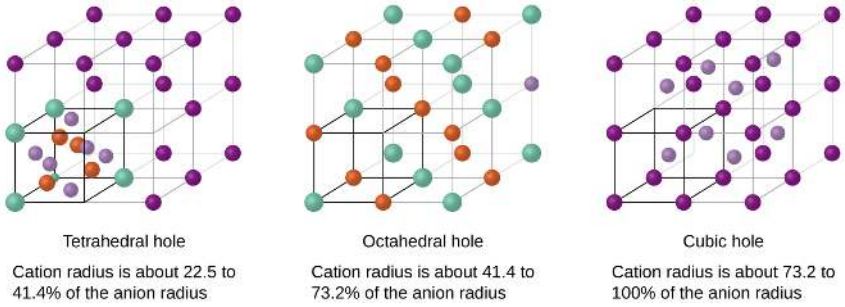


Figure **8.8.13**:A cation's size and the shape of the hole occupied by the compound are directly related.

A diagram of three images is shown. In the first image, eight stacked cubes, with purple spheres at each corner, that make up one large cube are shown. The bottom left cube is different. It has green spheres at each corner and has four orange and six light purple spheres located on the faces of the cube. Labels below this structure read "Tetrahedral hole" and "Cation radius is about 22.5 to 41.4 percent of the anion radius. In the second image, eight stacked cubes, with alternating orange and green spheres at each corner, make up one large cube that is shown. The bottom left cube has darker lines that connect the spheres together. Labels below this structure read "Octahedral hole" and "Cation radius is about 41.4 to 73.2 percent of the anion radius. In the third image, eight stacked cubes, with purple spheres at each corner and light purple spheres on their interior faces, make up one large cube that is shown. Labels below this structure read "Cubic hole" and "Cation radius is about 73.2 to 100 percent of the anion radius."

There are two tetrahedral holes for each anion in either an HCP or CCP array of anions. A compound that crystallizes in a closest-packed array of anions with cations in the tetrahedral holes can have a maximum cation:anion ratio of 2:1; all of the tetrahedral holes are filled at this ratio. Examples include Li_2O, Na_2O, Li_2S, and Na_2S. Compounds with a ratio of less than 2:1 may also crystallize in a closest-packed array of anions with cations in the tetrahedral holes, if the ionic sizes fit. In these compounds, however, some of the tetrahedral holes remain vacant.

✔ Example 8.8.3: Occupancy of Tetrahedral Holes

Zinc sulfide is an important industrial source of zinc and is also used as a white pigment in paint. Zinc sulfide crystallizes with zinc ions occupying one-half of the tetrahedral holes in a closest-packed array of sulfide ions. What is the formula of zinc sulfide?

Solution

Because there are two tetrahedral holes per anion (sulfide ion) and one-half of these holes are occupied by zinc ions, there must be $\frac{1}{2} \times 2$, or 1, zinc ion per sulfide ion. Thus, the formula is ZnS.

? Exercise 8.8.3: Lithium selenide

Lithium selenide can be described as a closest-packed array of selenide ions with lithium ions in all of the tetrahedral holes. What it the formula of lithium selenide?

Answer

Li_2Se

The ratio of octahedral holes to anions in either an HCP or CCP structure is 1:1. Thus, compounds with cations in octahedral holes in a closest-packed array of anions can have a maximum cation:anion ratio of 1:1. In NiO, MnS, NaCl, and KH, for example, all of the octahedral holes are filled. Ratios of less than 1:1 are observed when some of the octahedral holes remain empty.

✔ Example 8.8.4: Stoichiometry of Ionic Compounds Sapphire

Aluminum oxide crystallizes with aluminum ions in two-thirds of the octahedral holes in a closest-packed array of oxide ions. What is the formula of aluminum oxide?

Solution

Because there is one octahedral hole per anion (oxide ion) and only two-thirds of these holes are occupied, the ratio of aluminum to oxygen must be $\frac{2}{3}$:1, which would give $\mathbf{Al_{2/3}O}$. The simplest whole number ratio is 2:3, so the formula is Al_2O_3.

? Exercise 8.8.4

The white pigment titanium oxide crystallizes with titanium ions in one-half of the octahedral holes in a closest-packed array of oxide ions. What is the formula of titanium oxide?

Answer

$\mathbf{TiO_2}$

In a simple cubic array of anions, there is one cubic hole that can be occupied by a cation for each anion in the array. In CsCl, and in other compounds with the same structure, all of the cubic holes are occupied. Half of the cubic holes are occupied in SrH_2, UO_2, $SrCl_2$, and CaF_2.

Different types of ionic compounds often crystallize in the same structure when the relative sizes of their ions and their stoichiometries (the two principal features that determine structure) are similar.

Unit Cells of Ionic Compounds

Many ionic compounds crystallize with cubic unit cells, and we will use these compounds to describe the general features of ionic structures. When an ionic compound is composed of cations and anions of similar size in a 1:1 ratio, it typically forms a simple cubic structure. Cesium chloride, CsCl, (Figure **8.8.14**) is an example of this, with Cs^+ and Cl^- having radii of 174 pm and 181 pm, respectively. We can think of this as chloride ions forming a simple cubic unit cell, with a cesium ion in the center; or as cesium ions forming a unit cell with a chloride ion in the center; or as simple cubic unit cells formed by Cs^+ ions overlapping unit cells formed by Cl^- ions. Cesium ions and chloride ions touch along the body diagonals of the unit cells. One cesium ion and one chloride ion are present per unit cell, giving the l:l stoichiometry required by the formula for cesium chloride. Note that there is no lattice point in the center of the cell, and CsCl is not a BCC structure because a cesium ion is not identical to a chloride ion.



Figure **8.8.14**: Ionic compounds with similar-sized cations and anions, such as CsCl, usually form a simple cubic structure. They can be described by unit cells with either cations at the corners or anions at the corners.

Three images are shown. The first image shows a cube with black dots at each corner and a red dot in the center. This cube is stacked with seven others that are not colored to form a larger cube. The second image is composed of eight spheres that are grouped together to form a cube with one smaller sphere in the center. The name under this image reads “Body-centered simple cubic structure.” The third image shows five horizontal layers of purple spheres with layers of smaller green spheres in between.

We have said that the location of lattice points is arbitrary. This is illustrated by an alternate description of the CsCl structure in which the lattice points are located in the centers of the cesium ions. In this description, the cesium ions are located on the lattice points at the corners of the cell, and the chloride ion is located at the center of the cell. The two unit cells are different, but they describe identical structures.

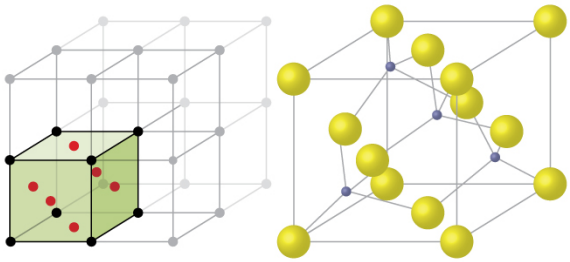
When an ionic compound is composed of a 1:1 ratio of cations and anions that differ significantly in size, it typically crystallizes with an FCC unit cell, like that shown in Figure **8.8.15**. Sodium chloride, NaCl, is an example of this, with Na^+ and Cl^- having radii of 102 pm and 181 pm, respectively. We can think of this as chloride ions forming an FCC cell, with sodium ions located in the octahedral holes in the middle of the cell edges and in the center of the cell. The sodium and chloride ions touch each other along the cell edges. The unit cell contains four sodium ions and four chloride ions, giving the 1:1 stoichiometry required by the formula, NaCl.



Figure 8.8.15: Ionic compounds with anions that are much larger than cations, such as NaCl, usually form an FCC structure. They can be described by FCC unit cells with cations in the octahedral holes.

Three images are shown. The first image shows a cube with black dots at each corner and a red dot in the center. This cube is stacked with seven others that are not colored to form a larger cube. The second image is composed of eight spheres that are grouped together to form a cube with one much larger sphere in the center. The name under this image reads “Body-centered simple cubic structure.” The third image shows seven horizontal layers of alternating purple and green spheres that are slightly offset with one another and form a large cube.

The cubic form of zinc sulfide, zinc blende, also crystallizes in an FCC unit cell, as illustrated in Figure 8.8.16. This structure contains sulfide ions on the lattice points of an FCC lattice. (The arrangement of sulfide ions is identical to the arrangement of chloride ions in sodium chloride.) The radius of a zinc ion is only about 40% of the radius of a sulfide ion, so these small Zn^{2+} ions are located in alternating tetrahedral holes, that is, in one half of the tetrahedral holes. There are four zinc ions and four sulfide ions in the unit cell, giving the empirical formula ZnS.

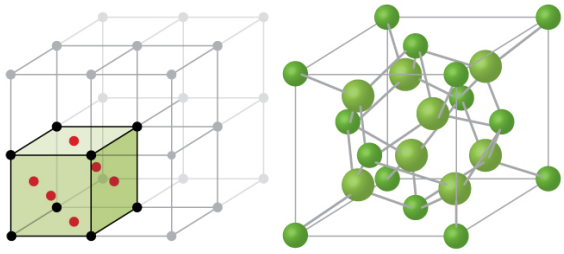


ZnS face-centered unit cell

Figure 8.8.16: ZnS, zinc sulfide (or zinc blende) forms an FCC unit cell with sulfide ions at the lattice points and much smaller zinc ions occupying half of the tetrahedral holes in the structure.

Two images are shown. The first image shows a cube with black dots at each corner and a red dot in the center of each face of the cube. This cube is stacked with seven others that are not colored to form a larger cube. The second image is composed of eight spheres that form the corners of a cube with six other spheres located in the face of the cube. The spheres are connected to one another by lines. The name under this image reads “Z n S, face-centered unit cell.”

A calcium fluoride unit cell, like that shown in Figure 8.8.17, is also an FCC unit cell, but in this case, the cations are located on the lattice points; equivalent calcium ions are located on the lattice points of an FCC lattice. All of the tetrahedral sites in the FCC array of calcium ions are occupied by fluoride ions. There are four calcium ions and eight fluoride ions in a unit cell, giving a calcium:fluorine ratio of 1:2, as required by the chemical formula, CaF_2. Close examination of Figure 8.8.17 will reveal a simple cubic array of fluoride ions with calcium ions in one half of the cubic holes. The structure cannot be described in terms of a space lattice of points on the fluoride ions because the fluoride ions do not all have identical environments. The orientation of the four calcium ions about the fluoride ions differs.



CaF_2 face-centered unit cell

Figure 8.8.17: Calcium fluoride, CaF_2, forms an FCC unit cell with calcium ions (green) at the lattice points and fluoride ions (red) occupying all of the tetrahedral sites between them.

Two images are shown. The first image shows a cube with black dots at each corner and a red dot in the center of each face of the cube. This cube is stacked with seven others that are not colored to form a larger cube. The second image is composed of eight small green spheres that form the corners of a cube with six other small green spheres located in the faces of the cube. Eight larger green spheres are spaced inside the cube and all of the spheres are connect to one another by lines. The name under this image reads “C a F, subscript 2, face-centered unit cell.”

Calculation of Ionic Radii

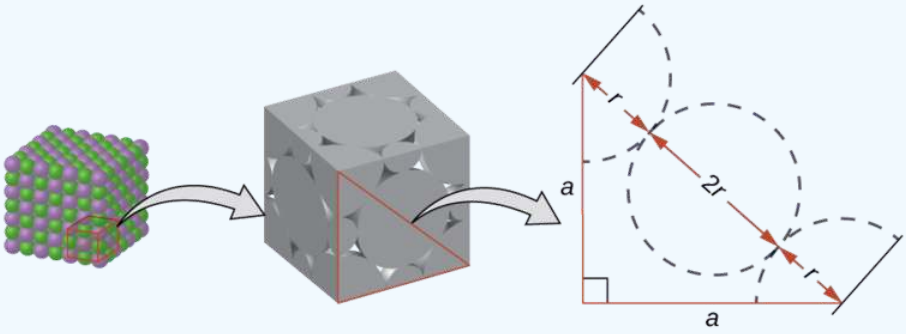
If we know the edge length of a unit cell of an ionic compound and the position of the ions in the cell, we can calculate ionic radii for the ions in the compound if we make assumptions about individual ionic shapes and contacts.

Example 8.8.5: Calculation of Ionic Radii

The edge length of the unit cell of LiCl (NaCl-like structure, FCC) is 0.514 nm or 5.14 Å. Assuming that the lithium ion is small enough so that the chloride ions are in contact, calculate the ionic radius for the chloride ion. Note: The length unit angstrom, Å, is often used to represent atomic-scale dimensions and is equivalent to 10^{-10} m.

Solution

On the face of a LiCl unit cell, chloride ions contact each other across the diagonal of the face:



Drawing a right triangle on the face of the unit cell, we see that the length of the diagonal is equal to four chloride radii (one radius from each corner chloride and one diameter—which equals two radii—from the chloride ion in the center of the face), so $d = 4r$. From the Pythagorean theorem, we have:

$$a^2 + a^2 = d^2$$

which yields:

$$(0.514\ \text{nm})^2 + (0.514\ \text{nm})^2 = (4r)^2 = 16r^2$$

Solving this gives:

$$r = \sqrt{\frac{(0.514\ \text{nm})^2 + (0.514\ \text{nm})^2}{16}} = 0.182\ \text{nm}\ (1.82\ \text{Å})\ \text{for a}\ Cl^-\ \text{radius.}$$

Exercise 8.8.6

The edge length of the unit cell of KCl (NaCl-like structure, FCC) is 6.28 Å. Assuming anion-cation contact along the cell edge, calculate the radius of the potassium ion. The radius of the chloride ion is 1.82 Å.

Answer

The radius of the potassium ion is 1.33 Å.

It is important to realize that values for ionic radii calculated from the edge lengths of unit cells depend on numerous assumptions, such as a perfect spherical shape for ions, which are approximations at best. Hence, such calculated values are themselves approximate and comparisons cannot be pushed too far. Nevertheless, this method has proved useful for calculating ionic radii from experimental measurements such as X-ray crystallographic determinations.

X-Ray Crystallography

The size of the unit cell and the arrangement of atoms in a crystal may be determined from measurements of the *diffraction* of X-rays by the crystal, termed X-ray crystallography. Diffraction is the change in the direction of travel experienced by an electromagnetic wave when it encounters a physical barrier whose dimensions are comparable to those of the wavelength of the light. X-rays are electromagnetic radiation with wavelengths about as long as the distance between neighboring atoms in crystals (on the order of a few Å).

When a beam of monochromatic X-rays strikes a crystal, its rays are scattered in all directions by the atoms within the crystal. When scattered waves traveling in the same direction encounter one another, they undergo *interference*, a process by which the waves combine to yield either an increase or a decrease in amplitude (intensity) depending upon the extent to which the combining waves' maxima are separated (Figure 8.8.18).

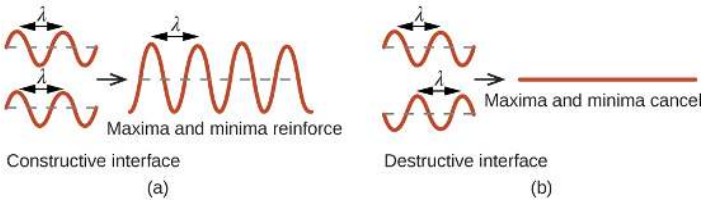


Figure 8.8.18: Light waves occupying the same space experience interference, combining to yield waves of greater (a) or lesser (b) intensity, depending upon the separation of their maxima and minima.

A pair of images is shown that has four sections. In the first section, two sinusoidal waves are shown, one drawn above the other, and a section from the top of one curve to the top of the next curve is labeled "lambda." The curves align with one another. The phrase below this reads "Constructive interference." A right facing arrow leads from the first section to the second, which shows one larger sinusoidal curve that has higher and lower peaks and troughs. A section from the top of one curve to the top of the next curve is labeled "lambda" and the phrase below this reads "Maxima and minima reinforce." In the second section, two sinusoidal waves are shown, one drawn above the other, and a section from the top of one curve to the top of the next curve is labeled "lambda." The curves do not align with one another. The phrase below this reads "Destructive interference." A right facing arrow leads from the first section to the second, which shows one flat line. The phrase below this reads "Maxima and minima cancel."

When X-rays of a certain wavelength, λ, are scattered by atoms in adjacent crystal planes separated by a distance, d, they may undergo constructive interference when the difference between the distances traveled by the two waves prior to their combination is an integer factor, n, of the wavelength. This condition is satisfied when the angle of the diffracted beam, θ, is related to the wavelength and interatomic distance by the equation:

$$n\lambda = 2d\sin\theta \tag{8.8.1}$$

This relation is known as the Bragg equation in honor of W. H. Bragg, the English physicist who first explained this phenomenon. Figure 8.8.18 illustrates two examples of diffracted waves from the same two crystal planes. The figure on the left depicts waves diffracted at the Bragg angle, resulting in constructive interference, while that on the right shows diffraction and a different angle that does not satisfy the Bragg condition, resulting in destructive interference.

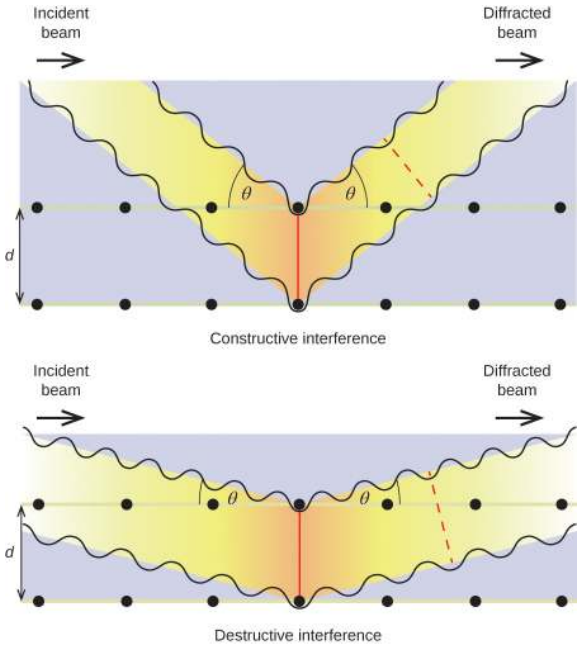


Figure 8.8.19: The diffraction of X-rays scattered by the atoms within a crystal permits the determination of the distance between the atoms. The top image depicts constructive interference between two scattered waves and a resultant diffracted wave of high intensity. The bottom image depicts destructive interference and a low intensity diffracted wave.

Two similar figures are shown. The first figure, labeled “Constructive Interference,” shows two horizontal rows of seven black dots with a line passing through them. The fourth dots of each row have a vertical line connecting them. The distance between these rows is labeled “d.” A beam labeled “Incident beam” descends at an angle labeled “theta” until it hits the line connecting the fourth dots, after which a diffracted beam ascends at the same angle “theta.” A dotted line is drawn across the diffracted beam. The second figure, labeled “Destructive interference,” is very similar, except that the angles “theta” are far more acute, making the slopes of the beams more shallow.

An X-ray diffractometer, such as the one illustrated in Figure 8.8.20, may be used to measure the angles at which X-rays are diffracted when interacting with a crystal as described earlier. From such measurements, the Bragg equation may be used to compute distances between atoms as demonstrated in the following example exercise.

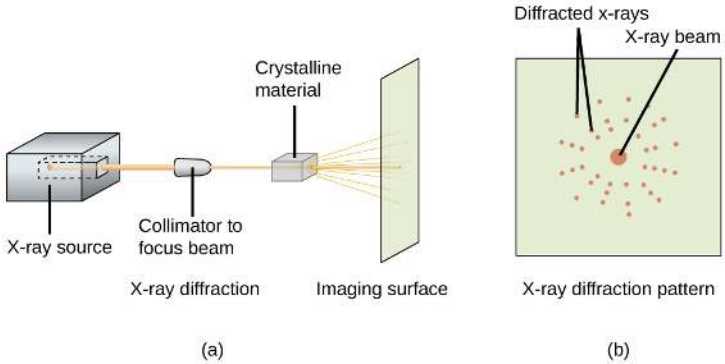


Figure 8.8.20: (a) In a diffractometer, a beam of X-rays strikes a crystalline material, producing (b) an X-ray diffraction pattern that can be analyzed to determine the crystal structure.

A diagram, labeled “a” shows a cube on the left with a channel bored into its right side labeled “X dash ray source.” A beam is leaving from this channel and traveling in a horizontal line toward an oval-shaped, short tube, labeled “Collimator to focus beam” and “X dash ray diffraction,” where it passes through a cube labeled “Crystalline material” and scatters onto a vertical sheet labeled “Imaging surface.” A second diagram, labeled “b,” shows a square sheet with a large dot in the center labeled “X dash ray beam,” that is surrounded by smaller dots arranged in rings and labeled “Diffracted X dash rays.”

Example 8.8.6: Using the Bragg Equation

In a diffractometer, X-rays with a wavelength of 0.1315 nm were used to produce a diffraction pattern for copper. The first order diffraction (n = 1) occurred at an angle θ = 25.25°. Determine the spacing between the diffracting planes in copper.

https://chem.libretexts.org/@go/page/403075

Solution

The distance between the planes is found by solving the Bragg equation (Equation 8.8.1) for d.

This gives

$$d = \frac{n\lambda}{2\sin\theta} = \frac{1(0.1315\ \text{nm})}{2\sin(25.25°)} = 0.154\ \text{nm}$$

Exercise 8.8.6

A crystal with spacing between planes equal to 0.394 nm diffracts X-rays with a wavelength of 0.147 nm. What is the angle for the first order diffraction?

Answer

21.9°

X-ray Crystallographer Rosalind Franklin

The discovery of the structure of DNA in 1953 by Francis Crick and James Watson is one of the great achievements in the history of science. They were awarded the 1962 Nobel Prize in Physiology or Medicine, along with Maurice Wilkins, who provided experimental proof of DNA's structure. British chemist Rosalind Franklin made invaluable contributions to this monumental achievement through her work in measuring X-ray diffraction images of DNA. Early in her career, Franklin's research on the structure of coals proved helpful to the British war effort. After shifting her focus to biological systems in the early 1950s, Franklin and doctoral student Raymond Gosling discovered that DNA consists of two forms: a long, thin fiber formed when wet (type "B") and a short, wide fiber formed when dried (type "A"). Her X-ray diffraction images of DNA provided the crucial information that allowed Watson and Crick to confirm that DNA forms a double helix, and to determine details of its size and structure. Franklin also conducted pioneering research on viruses and the RNA that contains their genetic information, uncovering new information that radically changed the body of knowledge in the field. After developing ovarian cancer, Franklin continued to work until her death in 1958 at age 37. Among many posthumous recognitions of her work, the Chicago Medical School of Finch University of Health Sciences changed its name to the Rosalind Franklin University of Medicine and Science in 2004, and adopted an image of her famous X-ray diffraction image of DNA as its official university logo.

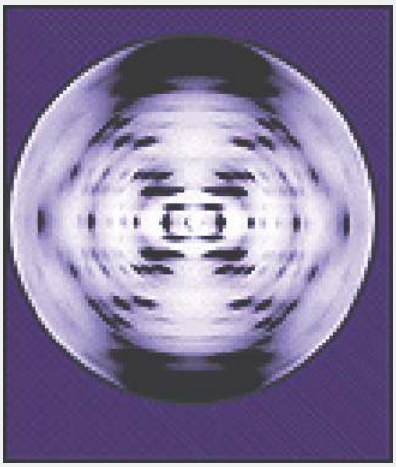


Figure 8.8.7.This illustration shows an X-ray diffraction image similar to the one Franklin found in her research. (credit: National Institutes of Health)

Key Concepts and Summary

The structures of crystalline metals and simple ionic compounds can be described in terms of packing of spheres. Metal atoms can pack in hexagonal closest-packed structures, cubic closest-packed structures, body-centered structures, and simple cubic structures.

The anions in simple ionic structures commonly adopt one of these structures, and the cations occupy the spaces remaining between the anions. Small cations usually occupy tetrahedral holes in a closest-packed array of anions. Larger cations usually occupy octahedral holes. Still larger cations can occupy cubic holes in a simple cubic array of anions. The structure of a solid can be described by indicating the size and shape of a unit cell and the contents of the cell. The type of structure and dimensions of the unit cell can be determined by X-ray diffraction measurements.

Glossary

body-centered cubic (BCC) solid
crystalline structure that has a cubic unit cell with lattice points at the corners and in the center of the cell

body-centered cubic unit cell
simplest repeating unit of a body-centered cubic crystal; it is a cube containing lattice points at each corner and in the center of the cube

Bragg equation
equation that relates the angles at which X-rays are diffracted by the atoms within a crystal

coordination number
number of atoms closest to any given atom in a crystal or to the central metal atom in a complex

cubic closest packing (CCP)
crystalline structure in which planes of closely packed atoms or ions are stacked as a series of three alternating layers of different relative orientations (ABC)

diffraction
redirection of electromagnetic radiation that occurs when it encounters a physical barrier of appropriate dimensions

face-centered cubic (FCC) solid
crystalline structure consisting of a cubic unit cell with lattice points on the corners and in the center of each face

face-centered cubic unit cell
simplest repeating unit of a face-centered cubic crystal; it is a cube containing lattice points at each corner and in the center of each face

hexagonal closest packing (HCP)
crystalline structure in which close packed layers of atoms or ions are stacked as a series of two alternating layers of different relative orientations (AB)

hole
(also, interstice) space between atoms within a crystal

isomorphous
possessing the same crystalline structure

octahedral hole
open space in a crystal at the center of six particles located at the corners of an octahedron

simple cubic unit cell
(also, primitive cubic unit cell) unit cell in the simple cubic structure

simple cubic structure
crystalline structure with a cubic unit cell with lattice points only at the corners

space lattice

all points within a crystal that have identical environments

tetrahedral hole

tetrahedral space formed by four atoms or ions in a crystal

unit cell

smallest portion of a space lattice that is repeated in three dimensions to form the entire lattice

X-ray crystallography

experimental technique for determining distances between atoms in a crystal by measuring the angles at which X-rays are diffracted when passing through the crystal

Paul Flowers (University of North Carolina - Pembroke), Klaus Theopold (University of Delaware) and Richard Langley (Stephen F. Austin State University) with contributing authors. Textbook content produced by OpenStax College is licensed under a Creative Commons Attribution License 4.0 license. Download for free at http://cnx.org/contents/85abf193-2bd...a7ac8df6@9.110).

This page titled 8.8: Lattice Structures in Crystalline Solids is shared under a CC BY 4.0 license and was authored, remixed, and/or curated by OpenStax.

- **10.7: Lattice Structures in Crystalline Solids** by OpenStax is licensed CC BY 4.0. Original source: https://openstax.org/details/books/chemistry-2e.

8.9: Superconductors

Superconductivity refers to the flow of electrical current in a material with zero resistance. Such materials are very important for use in electromagnets, e.g., in magnetic resonance imaging (MRI) and nuclear magnetic resonance (NMR) machines, because once the current starts flowing in the coils of these magnets it doesn't stop. Magnetic levitation using superconductors - which, below a critical field strength, are perfect diamagnets that are not penetrated by magnetic flux lines - is also potentially relevant to future technologies such as magnetically levitated trains.

The phenomenon of superconductivity, first discovered in Hg metal in 1911 by Onnes, continues to be only partially understood. It is of great interest to physicists as a macroscopic quantum phenomenon, and to chemists and materials scientists who try to make better superconductors (especially those that superconduct at higher temperatures) and devices derived from them, such as superconducting quantum interference devices (SQUIDs), which are extremely sensitive magnetometers.

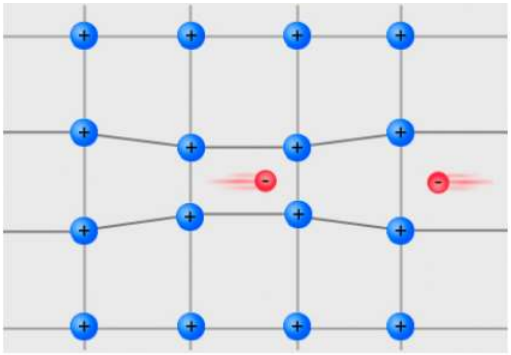


A magnet levitating above a high-temperature superconductor, cooled with liquid nitrogen. Persistent electric current flows on the surface of the superconductor, excluding the magnetic field of the magnet. This current effectively forms an electromagnet that repels the magnet.

Spin pairing and zero resistance

The transition from the metallic to the superconducting state is related to the quantum phenomena of Bose-Einstein condensation and superfluidity. Individual electrons have spin = 1/2, and as such are fermions (particles with half-integer spin). Because of the Pauli exclusion principle, no more than two fermions can occupy the same quantum state (such as an orbital in a molecule or a solid). The familiar consequence of this rule is the aufbau filling of orbitals with spin-paired electrons in each energy level. In contrast, particles with integer spins - which are called bosons - do not have this restriction, and any number of bosons can occupy the same quantized energy level.

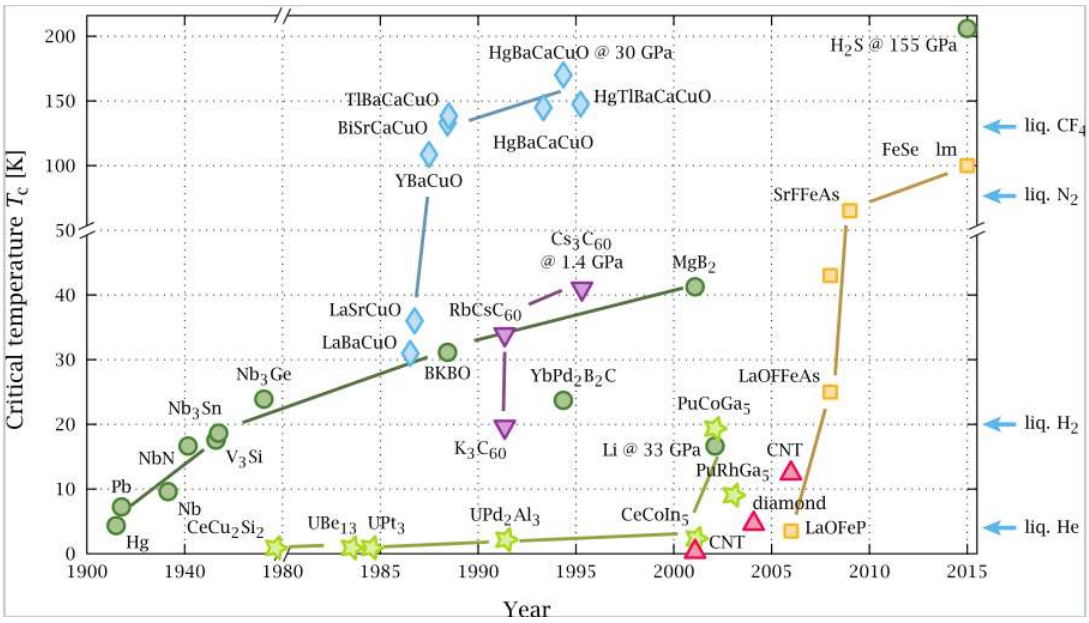
Superconductivity occurs when electrons spin pair into so-called Cooper pairs, which can travel through the lattice together. The electrons in a Cooper pair, although spin-paired, have a long-distance relationship: the spatial extent of a Cooper pair is a few nanometers in cuprate superconductors, and up to one micron in low T_c superconductors such as aluminum. Because its overall spin angular momentum is zero, a Cooper pair is a boson. When the temperature is low enough, the Cooper pairs "condense" into the lowest energy level. The second lowest energy level - which is typically a few meV above the ground state - is not accessible to them as long as the energy gap is larger than the thermal energy, kT. The scattering of electrons by the lattice then becomes forbidden by energy conservation because scattering dissipates energy, and the Cooper pairs cannot change their energy state. Thus the resistance (which arises from scattering, as we learned in Ch. 6) drops abruptly to zero below T_c. However, the Cooper pairs can be broken apart when they move fast, and thus superconductors turn back into normal metals (even below T_c) above some critical current density j_c. This phenomenon is also related to the critical magnetic field, H_c, that quenches superconductivity.



A trampoline for electrons

What causes electrons, which repel each other because of their negative charge, to pair up and travel together in superconductors? The mechanism - which must involve some kind of attractive interaction between electrons - is well understood for "conventional" superconductors which have relatively low transition temperatures, but is not yet known with certainty for high temperature oxide superconductors. In conventional, or BCS superconductors, the spin pairing is mediated by the lattice as shown in the figure at the left. A strong electron-lattice interaction causes a distortion in the lattice as an electron moves through. This elastic deformation is felt as an attractive force by a second electron moving in the opposite direction. This can be thought of as analogous to the interaction of two people jumping on a trampoline. The weight of the first person on the trampoline creates a "well" that attracts the second one, and they tend to move together (even if they don't like each other). Strange as this interaction seems, it is supported experimentally by isotope effects on T_c and by quantitative predictions of T_c values in conventional superconductors.

Bad metals make good superconductors. All superconductors are "normal" metals - with finite electrical resistance - above their critical transition temperature, T_c. If you ask where in the periodic table one might look for superconductors, the answer is surprising. The most conductive metals (Ag, Au, Cu, Cs, etc.) make the worst superconductors, i.e., they have the lowest superconducting transition temperatures, in many cases below 0.01 K. Conversely "bad" metals, such as niobium alloys, certain copper oxides, $K_xBa_{1-x}BiO_3$, MgB_2, FeSe, and alkali salts of C_{60}^{n-} anions, can have relatively high transition temperatures.

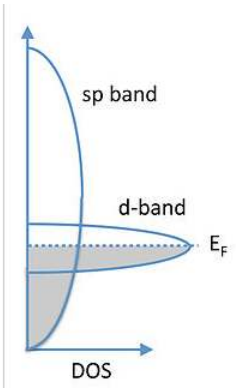


Timeline of superconducting materials, showing T_c vs. year of discovery.

We observe that most good superconductors appear in composition space very **near a metal-insulator transition**. In terms of our microscopic picture, orbital overlap in superconductors is poor, just barely enough to make them act as metals ($\Delta \approx U$) above T_c. In the normal state, superconductors with high T_c - which can be as high as 150 K - are typically "bad" metals. An important

characteristic of such metals is that the **mean free path** of electrons (in the normal state, above T_c) is on the order of the lattice spacing, i.e., **only a few Å**. In contrast, we learned in Ch. 6 that good metals such as Au, Ag, and Cu have electron mean free paths that are two orders of magnitude longer (ca. 40 nm). In a bad metal, the electron "feels" the lattice rather strongly, whereas in a good metal, the electrons are insensitive to small changes in the distance between metals atoms.

What does the band picture look like for a bad metal? The key point is that because orbital overlap is poor, the metal has a **high density of states** at the Fermi level. This is a universal property of high temperature superconductors and provides a clue of where to look for new and improved superconducting materials. Recall that transition elements in the middle of the 3d series (Cr, Fe, Co, Ni) were magnetic because of poor orbital overlap and weak d-d bonding. The elements below these - especially Nb, Ta, and W - have just barely enough d-d orbital overlap to be on the metallic side of the metal-insulator transition and to be "bad" metals. Carbides and nitrides of these elements are typically superconducting, with the carbon and nitrogen atoms serving to adjust the valence electron density, as illustrated in the table below.



Generic E vs. DOS for a bad metal.

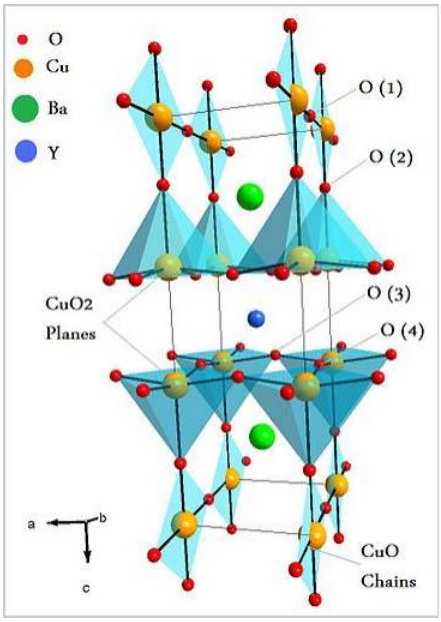
Compound	NbC	Mo_2N	TaC	VN	NbN	TaN	Nb_3Ge
T_c (K)	11.1	5.0	9.7	7.5	15.2	17.8	22.3

High T_c superconductors

In addition to having weak orbital overlap in the metallic state - which results in a high DOS at E_F - high temperature superconductors also typically contain elements in mixed oxidation states (for example, $Cu^{2+/3+}$ or $Bi^{3+/5+}$) that are close in energy to the O^{2-}/O^- couple in the lattice. At ambient pressure, cuprate superconductors have the highest known T_c values, ranging between about 35 and 150 K. The crystal structures of these materials are almost all variants of the perovskite lattice, as shown at the right for the 1-2-3 superconductor $YBa_2Cu_3O_{7-\delta}$. An ideal perovskite lattice would have formula $ABO_3 = A_3B_3O_9$. In $YBa_2Cu_3O_{7-\delta}$, Y and Ba occupy the A cation sites, Cu occupies the B sites, and two of the nine O atoms are missing.

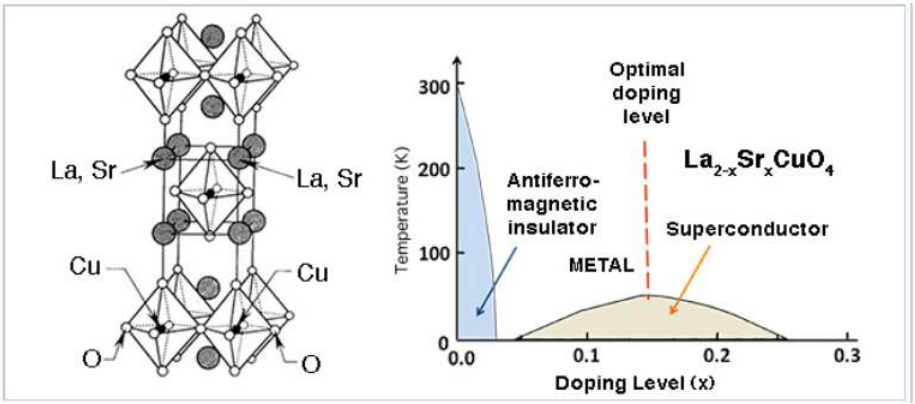
The $YBa_2Cu_3O_{7-\delta}$ lattice consists of mixed-valent copper(II/III) oxide sheets capped by oxygen atoms to form CuO_5 square pyramids. These sheets encapsulate the Y^{3+} cations. Copper(II) oxide ribbons that share the apical oxygen atoms of the square pyramids run in one direction through the structure. In $YBa_2Cu_3O_{7-\delta}$ and related materials, one component of the structure (here the Cu-O ribbons) acts as a **charge reservoir** to control the doping of the planar CuO_2 sheets, which are the elements of the structure

that carry the supercurrent. Cuprate superconductors with Bi, Tl, or Hg-containing charge reservoir layers and multiple, eclipsed CuO_2 sheets in the unit cell tend to have the highest T_c values.



Crystal structure of $YBa_2Cu_3O_{7-\delta}$ (YBCO), the first superconductor with T_c above the boiling point of liquid nitrogen.

The connection between the metal-insulator transtion and superconductivity is nicely illustrated in the phase diagram of $La_{2-x}Sr_xCuO_4$, the first cuprate superconductor, which was discovered in 1986 by Georg Bednorz and K. Alex Müller. This compound has a rather simple structure in which rocksalt La(Sr)O layers are intergrown with perovskite La(Sr)CuO_3 layers. Undoped La_2CuO_4 contains only Cu^{2+} ions and is an antiferromagnetic insulator. As a small amount of Sr^{2+} is substituted for La^{3+}, some of the Cu^{2+} is oxidized to Cu^{3+}, and the lattice is doped with holes. As the doping level increases, the antiferromagnetic phase undergoes a first-order phase transition to a "bad" metal, and at slightly higher doping density the superconducting phase appears. The proximity of the superconducting phase to the metal-insulator transition is a hallmark of cuprate superconductors. A maximum T_c of 35K is observed at x = 0.15. Doping at higher levels moves the Fermi level beyond the point of highest DOS in the d-band of Cu and the superconducting phase then gradually disappears. It is interesting to compare this phase diagram with that of V_2O_3 (above), which also undergoes an antiferromagnetic insulator to "bad" metal transition as it is doped.



Crystal structure and phase diagram of the cuprate superconductor $La_{2-x}Sr_xCuO_4$. (LSCO)

8.9: Superconductors is shared under a CC BY-SA 4.0 license and was authored, remixed, and/or curated by LibreTexts.

- **10.3: Superconductors** by Chemistry 310 is licensed CC BY-SA 4.0. Original source: https://en.wikibooks.org/wiki/Introduction_to_Inorganic_Chemistry.

CHAPTER OVERVIEW

9: Coordination Chemistry II- Bonding

9.1: Evidence for Electronic Structures
9.2: Thermodynamic Data
9.3: Magnetic Susceptibility
9.4: Crystal Field Theory
9.5: Ligand Field Theory
9.6: Ligand Field Theory - Molecular Orbitals for an Octahedral Complex
9.7: Orbital Splitting and Electron Spin
9.8: Ligand Field Stabilization Energy
9.9: Tetrahedral Complexes
9.10: Ligand Field Theory New Page
9.11: Angular Overlap
9.12: Sigma Bonding in the Angular Overlap Model
9.13: Pi Acceptors in the Angular Overlap Model
9.14: Pi Donors in the Angular Overlap Model
9.15: The Spectrochemical Series
9.16: The Magnitude of Parameters $e\sigma$, $e\pi$ and Δ
9.17: The Jahn-Teller Effect

9: Coordination Chemistry II- Bonding is shared under a not declared license and was authored, remixed, and/or curated by LibreTexts.

SECTION OVERVIEW

9.1: Evidence for Electronic Structures

This section describes the types of experimental data that give us hints about the electronic structure of coordination complexes (ie the molecular orbitals, their energy levels, and electron configurations). The types of experimental observations discussed here have been used to generate the theories of bonding that are described later in this chapter.

Introduction

The frontier (valence) electrons and orbitals define the chemical and physical properties of any compound. In the transition metals and their coordination compounds, the ***d*** orbitals and ***d*** electrons are the ones of interest. Thus, the ***d*** orbitals and electrons will be the focus of this chapter.

One of the first things you might notice about valence ***d*** orbitals is the order of orbital energy levels of atoms and ions in the transition metals. For example, in the first row of transition metals, the 4s orbital fills before the **3*d*** *in the atoms*. This indicates that **4*s*** is lower in energy than **3*d*** *in these atoms*. However, *in the ions* of the same elements, the **3*d*** orbital is occupied while the **4*s*** orbital is empty. This indicates the opposite, that the **3*d*** orbital is lower in energy than **4*s*** *in these ions*. The change in the relative energy levels of the **3*d*** and **4*s*** orbitals in atoms compared to ions is a result of the combined effects of shielding and penetration, as discussed in a previous chapter. The result is that the 3d and 4s orbital energy levels are close enough in energy that subtle changes in the environment can reverse the order.

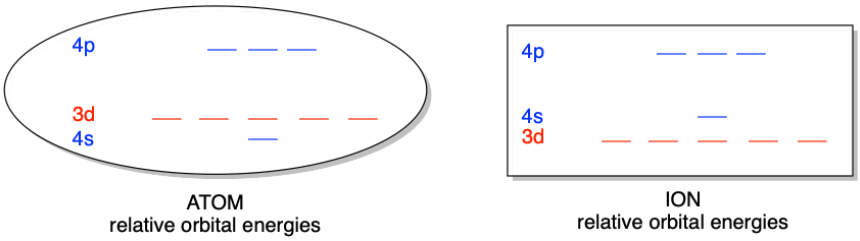


Figure **9.1.1**: In early period 4 of the periodic table, the **4*s*** orbital energy level is lower than **3*d*** for atoms. However, in the ions of the same elements, the **3*d*** is lower in energy than **4*s***. (CC-BY-NC; Chris Schaller)

Furthermore, you are going to see that once the atom is surrounded by ligands, the five ***d*** orbitals are no longer degenerate. In a coordination compound, with ligands bound in a specific geometry, the ***d*** orbitals become split into slightly different energy levels. The splitting pattern depends on where the ligands are in space; in other words it depends on the coordination geometry. The patterns of splitting for tetrahedral and octahedral geometries are shown below. Notice that the splitting is reversed between metals in a tetrahedral coordination environment compared to an octahedral environment.

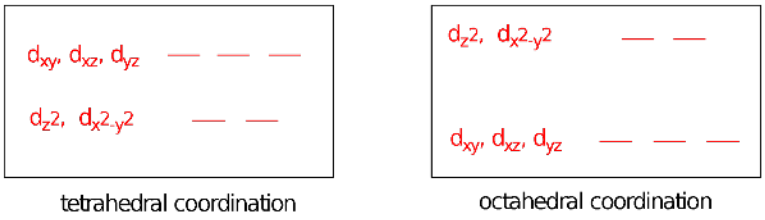


Figure **9.1.2**: Splitting of d orbitals for (left) tetrahedral and (right) octahedral ligand geometries. (CC-BY-NC; Chris Schaller)

When the orbitals of a coordination compound are filled with electrons, the electron configuration depends on the energy difference between the lower and higher energy levels. For example, given five ***d*** electrons in an octahedral environment, there are two possible electron configurations. All five electrons may occupy the lower level of ***d*** orbitals (Fig. **9.1.3**, left), so that some electrons are paired. Another possibility is that all the electrons will be unpaired if they populate both levels of the d orbitals (Fig. **9.1.3**, right).

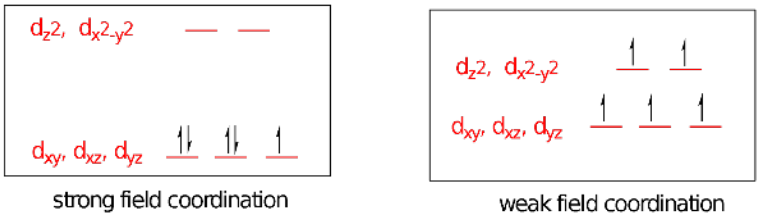


Figure **9.1.3**: Two possible electron configurations for five electrons in an octahedral ligand field. (CC-BY-NC; Chris Schaller)

A number of factors determine which case results, including the identity of the metal ion and the nature of the ligands involved. These different filling orders have consequences, too. The magnetic properties of the complex, its propensity to undergo reactions, and its optical properties all depend on the configuration of these frontier electrons.

This chapter is an exploration of the nature of the metal-ligand bond and how both geometry and the mode of bonding influence the properties of coordination complexes.

This page titled 9.1: Evidence for Electronic Structures is shared under a CC BY-NC 4.0 license and was authored, remixed, and/or curated by Chris Schaller.

9.2: Thermodynamic Data

We can get some insight into the stability of coordination complexes by looking at their formation constants. The formation constant is the equilibrium constant for the reaction leading to the formation of a coordination complex. The greater the formation constant, the more thermodynamically stable the product complex compared to the reactant complex.

Many complexation reactions take place in aqueous solution by dissolving a metal ion in water to produce the "aqueous metal ion". An aqueous metal ion is one that is coordinated by a number of water molecules, and since it is charged, there must be counter ions to balance that charge. When an aqueous metal ion reacts to form a new complex, its formation constant indicates the stability of the product compared to the aqueous complex. Depending on the number of ligands that are replaced in the product compared to the reactant, the formation complex is defined as either a **stepwise formation constant** (K) or an **overall formation constant** (β).

For example, the formation of $[Cu(NH_3)(OH_2)_5]^{2+}$ complex ion from $Cu^{2+}_{(aq)}$ can be represented by the following *stepwise* reaction:[1]

$$[Cu(OH_2)_6]^{2+} + NH_3 \rightleftharpoons [Cu(NH_3)(OH_2)_5]^{2+} + H_2O \qquad K_1 = 1.9 \times 10^4$$

The formation constant, K_1, is a stepwise formation constant because it represents the substitution of a single aquo ligand (a coordinated water) by an ammine ligand. Another example is the reaction below that represents the substitution of four aquo ligands for four ammine ligands. The *overall* formation of the $[Cu(NH_3)_4(OH_2)_2]^{2+}$ complex ion from $Cu^{2+}_{(aq)}$ would be represented by this equation:

$$[Cu(OH_2)_6]^{2+} + 4\,NH_3 \rightleftharpoons [Cu(NH_3)_4(OH_2)_2]^{2+} + 4\,H_2O \qquad \beta_4 = 1.1 \times 10^{13}$$

This time, the formation constant represents the substitution of four ammine ligands for four aquo ligands. This transformation does not happen in one step, so the formation constant, β_4 is a composite of the equilibrium constants for four individual steps:

$$[Cu(OH_2)_6]^{2+} + NH_3 \rightleftharpoons [Cu(NH_3)(OH_2)_5]^{2+} + H_2O \qquad K_1 = \frac{[Cu(NH_3)(OH_2)_5{}^{2+}]}{[Cu(OH_2)_6{}^{2+}][NH_3]} = 1.9 \times 10^4$$

$$[Cu(NH_3)(OH_2)_5]^{2+} + NH_3 \rightleftharpoons [Cu(NH_3)_2(OH_2)_4]^{2+} + H_2O \qquad K_2 = \frac{[Cu(NH_3)_2(OH_2)_4{}^{2+}]}{[Cu(NH_3)(OH_2)_5{}^{2+}][NH_3]} = 3.9 \times 10^3$$

$$[Cu(NH_3)_2(OH_2)_4]^{2+} + NH_3 \rightleftharpoons [Cu(NH_3)_3(OH_2)_3]^{2+} + H_2O \qquad K_3 = \frac{[Cu(NH_3)_3(OH_2)_3{}^{2+}]}{[Cu(NH_3)_2(OH_2)_4{}^{2+}][NH_3]} = 1.0 \times 10^3$$

$$[Cu(NH_3)_3(OH_2)_3]^{2+} + NH_3 \rightleftharpoons [Cu(NH_3)_4(OH_2)_2]^{2+} + H_2O \qquad K_4 = \frac{[Cu(NH_3)_4(OH_2)_2{}^{2+}]}{[Cu(NH_3)_3(OH_2)_3{}^{2+}][NH_3]} = 1.5 \times 10^2$$

$$\beta_4 = K_1 \times K_2 \times K_3 \times K_4 = (1.9 \times 10^4)(3.9 \times 10^3)(1.0 \times 10^3)(1.5 \times 10^2) = 1.1 \times 10^{13}$$

(\beta\) notation

The β notation is used to distinguish an overall formation constant from a stepwise formation constant. However, sometimes alternative notation will be used. You may see other texts, the literature, or your instructor using alternative ways to distinguish an overall formation constant like β_4 from the stepwise formation constant, like K_4. The important thing is to understand the conventions used for whatever source you are reading.

In both the examples above, the equilibrium lies to the right (in other words, the formation constant is >> 1). Another way to interpret this is that Cu(II) has a higher affinity for ammonia than for water, and thus the ammine complex is more stable than the aqueous metal ion. In the case of the copper tetraammine complex, replacement of each individual water by ammonia is favorable, so the aggregate formation constant β_4 becomes very large. The preference of Cu(II) for ammonia can be explained by the increased basicity of ammonia compared to water.

Formation constants can provide valuable insight into factors that contribute to the stability of coordination complexes, but we may need a more extensive set of data to build a more complete picture. If we look at formation constants in a series of complexes that have something in common, we may get an idea about additional factors that play a role in complex stability. Take a look at these examples:[2]

$$\mathrm{Cu^+(aq) + 2\,Cl^- \rightleftharpoons [CuCl_2]^-} \quad K = 3.0 \times 10^5$$
$$\mathrm{Cu^+(aq) + 2\,Br^- \xrightleftharpoons{CuBr_2} -} \quad K = 8.0 \times 10^5$$
$$\mathrm{Cu^+(aq) + 2\,I^- \xrightleftharpoons{CuI_2} -} \quad K = 8.0 \times 10^8$$

The reactions above are simplified by abbreviating the aqueous metal ion, $\mathrm{[Cu(OH_2)n]^+}$ as $\mathrm{Cu^+(aq)}$. This time, we are dealing with Cu(I) rather than Cu(II). Note that basicity does not seem to play a role in this series. The pK_a's of the conjugate acids HCl, HBr, and HI are -6.7, -8.7, and -9.3, respectively. If basicity were important, chloride should bind most tightly, followed by bromide, and then iodide; that trend is reversed here. Instead, this case can be explained by an application of Pearson's hard-soft acid-base theory (HSAB). HSAB theory predicts that small, charge-dense bases will bind more tightly with small, charge-dense acids. Archetypically, hard bases have N, O, or F donor atoms. Conversely, larger, more polarizable bases bind more tightly with larger, more polarizable acids. Soft bases archetypically have P or S donor atoms. In this series of copper complexes, the iodide is the softest, most polarizable of the three halide ions shown, whereas the chloride is the hardest (although not as hard as fluoride). Cu(I) has a relatively low charge density, so it can be considered a soft acid. Soft acids and soft bases form strong bonds because of the pronounced covalency between the donor and acceptor. Of the three halides, iodide is the most capable of providing that soft-soft interaction with the Cu(I) ion.

Let's look at another major contributor to complex stability. In this case, aqueous nickel ion reacts with ammonia to produce the hexaammine complex, $\mathrm{[Ni(NH_3)_6]^{2+}}$. That's similar to the reaction of aqueous copper ion with ammonia; ammonia is a better donor in this case than water. However, ammine is easily displaced by ethylenediamine ($\mathrm{H_2NCH_2CH_2NH_2}$, abbreviated en) to provide an ethylenediamine complex, $\mathrm{[Ni(en)_3]_2^+}$.[2,3]

$$\mathrm{[Ni(OH_2)_6]^{2+} + 6\,NH_3 \xrightleftharpoons{Ni(NH_3)_6} {}^{2}+} \quad K = 2.0 \times 10^8$$
$$\mathrm{[Ni(NH_3)_6]^{2+} + 3\,en \xrightleftharpoons{Ni(en)_3} {}^{2} + + 6\,NH_3} \quad K = 4.7 \times 10^9$$

Once again, we see that an ammine ligand is a much more effective donor than an aquo ligand. The ethylenediamine ligand, however, binds exceptionally tightly, and can even displace ammine ligands. To gain insight into why a metal ion would have higher affinity toward $\mathrm{H_2NCH_2CH_2NH_2}$ (en) than $\mathrm{NH_3}$, despite the fact that the two ligands have similar donor atoms, we can look at the thermodynamic parameters (the entropy and enthalpy) of the reaction for the formation of $\mathrm{[Ni(en)_3]^{2+}}$ from $\mathrm{[Ni(NH_3)_6]^{2+}}$:

$$\begin{aligned} \Delta H^\circ &= -12.1\ \mathrm{kJ\ mol^{-1}} \\ \Delta S^\circ &= 184.9\ \mathrm{J\ mol^{-1} K^{-1}} \\ \text{and at 298 K}, -T\Delta S^\circ &= -55.1\ \mathrm{kJ\ mol^{-1}} \end{aligned}$$

That last term, $-T\Delta S^\circ$, is included for easier comparison to the enthalpy contribution, since these two factors are evaluated via the Gibbs free energy equation, $\Delta G = \Delta H - T\Delta S$. We see that the formation of $\mathrm{[Ni(en)_3]^{2+}}$ from $\mathrm{[Ni(NH_3)_6]^{2+}}$ is slightly favored enthalpically (by $\Delta H^\circ = -12.1\mathrm{kJ\ mol^{-1}}$), even though there are nitrogen atom donor ligands in both reactant and product complexes. However, this small preference is not likely the most important driving force for the large formation constant. The entropy factor is much larger in comparison ($T\Delta S^\circ = -55.1\ \mathrm{kJ\ mol^{-1}}$), indicating entropy is driving the huge formation constant for the ethylenediamine complex.

How do we interpret that large $T\Delta S^\circ$? The simplest approach to interpreting a change in entropy of a reaction is to evaluate the number of molecules in the reactants compared to the products. If there is an increase in the number of molecules, there is an increase in disorder (entropy).

In the replacement of aquo ligands with ammine ligands, there are seven species on either side of the equation:

$$\begin{array}{ccc} \mathrm{[Ni(OH_2)_6]^{2+} + 6\,NH_3} & \rightleftharpoons & \mathrm{[Ni(NH_3)_6]^{2+}} \\ \text{7 molecules} & & \text{7 molecules} \end{array}$$

We might not expect this reaction to have a large entropic driving force because the number of molecules is the same in the reactants and products.

On the other hand, in the replacement of ammine ligands with ethylenediamine ligands, there are four molecules on the reactant side, and seven on the products side.

$$\underset{\text{4 molecules}}{[Ni(NH_3)_6]^{2+} + 3\,en} \rightleftharpoons \underset{\text{7 molecules}}{[Ni(en)_3]^{2+} + 6\,NH_3}$$

That means there is a net increase in the number of molecules in solution when the ethylenediamine replaces the ammines. An increase in the number of molecules represents an increase in the partitioning of energy, which is entropically favorable. The underlying reason for this difference is that each ethylenediamine ligand has two nitrogen donors, allowing one ethylenediamine to replace two ammines. The high formation constant for ligands that contain multiple donor atoms is called the **chelate effect**, from the Greek word for "crab" (which has two claws with which it can grab things). We call donors capable of binding through multiple atoms “polydentate” ligands (for “many-toothed”, indicating they can bite more strongly into the metal and hold on).

Formation constants of coordination complexes affect important processes ranging from industrial catalysis to biology. For example, most people are aware of carbon monoxide poisoning. Carbon monoxide leads to suffocation by displacing molecular oxygen from hemoglobin (Hb), the oxygen-carrying protein in blood cells. Hemoglobin has an Fe(II) ion bound in its active site which in turn coordinates molecular oxygen, increasing the oxygen-carrying capacity of a blood cell. The two relevant equilibria are:[4]

$$Hb + O_2 \rightleftharpoons HbO_2 \quad K = 3.2\ \mu M^{-1}$$
$$Hb + CO \rightleftharpoons HbCO \quad K = 750\ \mu M^{-1}$$

Here, Hb is just a shorthand for hemoglobin. The formation constants shown above indicate that carbon monoxide binds to hemoglobin hundreds of times more tightly than does oxygen. This difference can’t be caused by a chelate effect; both **CO** and O_2 are monodentate donors in this case. The origin for this difference comes from more subtle differences in metal-ligand binding that we will develop later in this chapter.

Problems

Exercise 9.2.1

Show how we can combine the formation constants given above for $[Ni(NH_3)_6]^{2+}$ and $[Ni(en)_3]^{2+}$ from $[Ni(HO_2)_6]^{2+}$ to determine the formation constant for the ethylenediamine complex from aqueous nickel ion.

$$[Ni(OH_2)_6]^{2+} + 3\,en \rightleftarrows [Ni(en)_3]^{2+} + 6\,H_2O \qquad K = ?$$

Answer

We know the formation constants of $[Ni(NH_3)_6]^{2+}$ and $[Ni(en)_3]^{2+}$. Let's call them "reactions i and j":

$$\text{Reaction } i: \quad [Ni(OH_2)_6]^{2+} + 6\,NH_3 \overset{Ni(NH_3)_6}{\rightleftharpoons} {}^{2+} \qquad K_i = \frac{[Ni(NH_3)_6]}{[Ni(OH_2)_6][NH_3]} = 2.0 \times 10^8$$

$$\text{Reaction } j: \quad [Ni(NH_3)_6]^{2+} + 3\,en \overset{Ni(en)_3}{\rightleftharpoons} {}^{2+} + 6\,NH_3 \qquad K_j = \frac{[Ni(en)_3][NH_3]^6}{[Ni(NH_3)_6][en]^3} = 4.7 \times 10^9$$

and we want to find the equilibrium constant for the formation of $[Ni(en)_3]^{2+}$ from $[Ni(HO_2)_6]^{2+}$. We'll call this "reaction k".

$$\text{Reaction } k: \quad [Ni(OH_2)_6]^{2+} + 3\,en \rightleftarrows [Ni(en)_3]^{2+} + 6\,H_2O \qquad K_k = ?$$

Reaction "k" is the sum of reaction "i" followed by reaction "j".

$$\begin{aligned} K_k &= K_i \times K_j \\ &= \frac{[Ni(NH_3)_6]}{[Ni(OH_2)_6][NH_3]} \times \frac{[Ni(en)_3][NH_3]^6}{[Ni(NH_3)_6][en]^3} = \frac{[Ni(en)_3]}{[Ni(OH_2)_6][en]^3} \\ &= (2.0 \times 10^8)(4.7 \times 10^9) = 9.4 \times 10^{17} \end{aligned}$$

Exercise 9.2.2

The formation constants shown below correspond to the substitution of one ligand on aqueous Cu(II) ion.[5] Propose a trend that explains the different stabilities of the complexes.

$$\begin{array}{ll} NH_3 & K = 2.0 \times 10^3 \\ F^- & K = 8.0 \\ Cl^- & K = 1.2 \\ Br^- & K = 0.9 \end{array}$$

Answer

This trend could be explained by basicity, since ammonium ion is a weak base and the acidity of the hydrogen halides increase in the order HF < HCl < HBr. The ammine ligand is a better donor than any of the halides to the nickel ion, but fluoride is better than chloride and chloride is better than bromide. The reason for the acidity trend varies in the midst of this series. Among the halides, fluoride is the best donor because it is the least polarizable and least stable ion. However, in the second row of the periodic table, the nitrogen in ammonia is a better donor than fluoride because nitrogen is less electronegative than fluorine. This difference is enough to compensate for the fact that ammine is a neutral ligand, presumably with less Coulombic attraction to the copper ion than fluoride.

Note that this trend is very different for Cu(II) than for a similar series of ligands with Cu(I). Cu(II), with greater charge density, is harder in character than Cu(I). Thus, it doesn't necessarily bind more tightly to softer donors the way Cu(I) does.

? Exercise 9.2.3

Ethylenediamine can be displaced from nickel by tren, (NH2CH2CH2)3N, another polydentate ligand.[3]

$$[Ni(en)_2(OH_2)_2]^{2+} + \text{tren} \rightleftarrows [Ni(\text{tren})(H_2O)_2]^{2+} + 2\,\text{en} \qquad K = 76$$

a. What is the denticity of tren?
b. It is reported that $\Delta H° = +13.0$ kJ mol^{-1} and $\Delta S° = 79.5$ J mol^{-1} K^{-1}. Propose a reason for the moderately large formation constant.

Answer

a) Tren has a denticity of 4; it is sometimes described as a tetradentate ligand.

b) The enthalpy of reaction $\Delta H° = +13.0$ kJ mol-1 and at 298 K, $-T\Delta S° = -23.7$ kJ mol-1. That means there are no arguments based on the donor-acceptor strength, such as HSAB or basicity, because the enthalpy of reaction is positive. The tightness of binding must result from the positive entropy, which comes from the net increase in the number of molecules as the reaction proceeds (the chelate effect).

The moderately positive enthalpy change is probably related to ring strain in the multidentate complex.

References

1. Complex-Ion Equilibria https://chem.libretexts.org/@go/page/516 (accessed Jun 25, 2021).
2. Complex Ion Formation Constants https://chem.libretexts.org/@go/page/6648 (accessed Jun 25, 2021).
3. Cotton, F.A.; Wilkinson, G. *Advanced Inorganic Chemistry*, 4th Ed. John Wiley & Sons: New York, 1980, pp 71-73.
4. Wilbur S, Williams M, Williams R, et al. Toxicological Profile for Carbon Monoxide. Atlanta (GA): Agency for Toxic Substances and Disease Registry (US); 2012 Jun. Table 3-12, Hemoglobin and Myoglobin Binding Kinetics and Equilibrium Constants for Oxygen and Carbon Monoxide. Available from: https://www.ncbi.nlm.nih.gov/books/NBK153687/table/T22/ (accessed Jun 26, 2021).
5. Miessler, G. L.; Fischer, P. J.; Tarr, D. A. *Inorganic Chemistry*, 5th Ed. Pearson: Upper Saddle River, NJ, p. 358.

This page titled 9.2: Thermodynamic Data is shared under a CC BY-NC 4.0 license and was authored, remixed, and/or curated by Chris Schaller.

- **10.1.1: Thermodynamic Data** by Chris Schaller is licensed CC BY-NC 4.0.

9.3: Magnetic Susceptibility

Electronic Structure

The electronic structure of coordination complexes can lead to several different properties that involve different responses to magnetic fields. These properties can vary between related compounds because of differences in electron counts, geometry, or donor strength. As a result, magnetic measurement of these materials can be used as a tool to provide insight into the structure of a coordination complex.

Diamagnetic and paramagnetic compounds are two common categories defined by interaction with a magnetic field. Diamagnetic compounds display a very slight repulsion from magnetic fields. The interaction is quite subtle and requires the proper instrumentation if it is to be observed; it's not something you would normally notice by waving a magnet in front of a vial of coordination complex. In contrast, paramagnetic compounds display a very slight attraction to magnetic fields. In terms of electronic structure, diamagnetic compounds have all of their electrons in pairs whereas paramagnetic compounds have one or more unpaired electrons. These definitions are not limited to coordination complexes. Atmospheric oxygen, O_2, is a common example of a paramagnetic compound. Atmospheric nitrogen, N_2, is a common example of a diamagnetic compound.

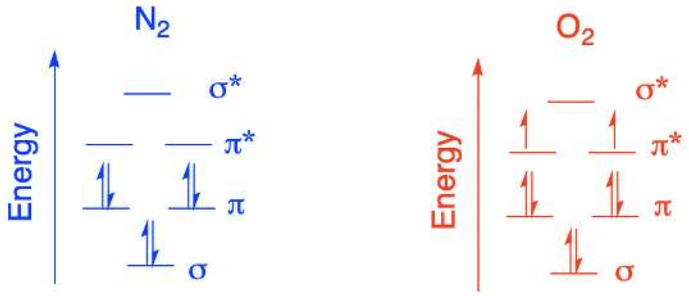


Figure **9.3.1**: Valence molecular orbital diagrams of N_2 and O_2 show that N_2 is diamagnetic while O_2 is paramagnetic. (CC-BY-NC; Chris Schaller)

These differences arise because of a quantum mechanical property of electrons and other subatomic particles: spin. Spin does not have a direct macroscopic analogy; physical chemists often urge caution about equating it to a phenomenon on the level at which we observe the universe. However, we do know that spin is related to magnetic phenomena. We can think of an electron as having a magnetic moment. There are two allowed values of this magnetic moment ($+\frac{1}{2}$ and $-\frac{1}{2}$) that differ in orientation; spin is a vector quantity. Normally, there is no preference for one orientation over the other. If a coordination complex has one unpaired electron, and we have a million of those coordination complexes in a very tiny sample, about 500,000 of the unpaired electrons would have spin = $+\frac{1}{2}$ and about 500,000 of them would have spin = $-\frac{1}{2}$. The spin of each electron is randomly oriented. As a result, the material would have no net magnetic moment. In the presence of a magnetic field, however, there is a small energy difference between those two spin states. As a result, a majority of the spins adopt the energetically more favorable orientation. Although the material by itself has no net magnetic field, one has temporarily been induced by the influence of an external magnetic field. This is what we mean by magnetic susceptibility.

Measuring Magnetic Susceptibility

All diamagnetic compounds have a roughly similar response to a magnetic field; either their electrons are all paired or they are not. Paramagnetic compounds, however, can respond quite differently to a magnetic field, depending on the number of unpaired electrons. The more unpaired electrons there are, the stronger the magnetic susceptibility will be, and so the stronger the attraction between the compound and the magnetic field. For this reason, measuring the strength of attraction of a compound for a magnetic field can reveal the number of unpaired electrons in the compound. This relationship is most straightforward for complexes of first row transition metals (**3*d*** metals), becoming a little more complicated for the **4*d*** and **5*d*** series.

A Guoy balance is probably the simplest example of a method for determining the presence of unpaired electrons in a coordination complex.[1] It uses a balance, a sample holder and a magnet. Essentially, the magnet is weighed in the presence and absence of the sample. The discrepancy between the two measurements arises because of the interaction of the sample with the magnetic field. Any diamagnetic sample causes slight downward repulsion, registering as a heavier weight. A paramagnetic sample suspended

between the poles of the magnet causes a slight upward pull on the magnet, which registers as a lighter weight. The more unpaired electrons there are, the greater the induced magnetic moment, and so the lighter the weight becomes.

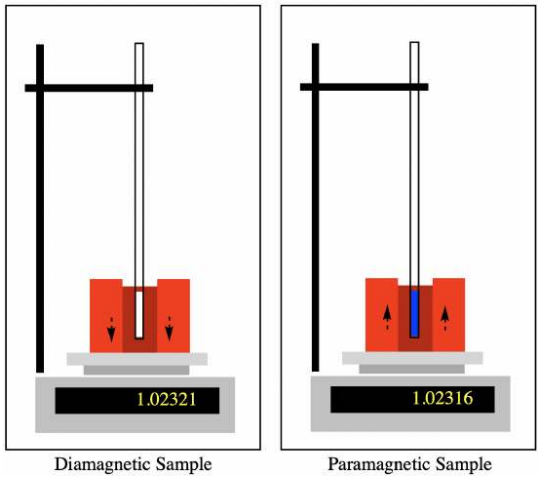


Figure **9.3.2**: Diagram of a Guoy balance. A magnet (red) sits on a balance and a sample tube is placed in the center cavity of the magnet. (CC-BY-NC; Chris Schaller)

From that measurement, we can extract a parameter that we normally refer to as the effective magnetic moment of the material, μ_{eff}. The magnetic moment is expressed in units called Bohr magnetons. A Bohr magneton (BM or μ_B) is defined as:

$$1\text{BM} = \frac{eh}{4\pi mc}$$

in which e is the charge on an electron; h is Planck's constant; m is the mass of the electron; c is the speed of light.

This experimental quantity is fitted to a simple relationship that depends on the number of unpaired electrons. This mathematical model gives a prediction of the "spin-only" magnetic moment. If the magnetic moment arises purely from the number of unpaired electrons without additional complicating factors, the fit to the experimental data is pretty good.

$$\mu_{eff} \approx \mu_{so} = g\sqrt{S(S+1)}$$

Here, g is the gyromagnetic ratio, which is a proportionality constant between the angular momentum of the electron and the magnetic moment. It has a value of 2.00023, or approximately 2.0. The term $\sqrt{S(S+1)}$ is the value of the angular momentum, which depends on the number of unpaired electrons; S is the absolute value of the sum of the individual spins of the valence electrons. Of course, the spins would cancel out in electrons that were paired, because one would have $m_s = \frac{1}{2}$ and the other would have $m_s = -\frac{1}{2}$. For unpaired electrons, Hund's rule states that they would have parallel spins; for example, two unpaired electrons gives $S = 1$.

Number of unpaired electrons, n	Maximum total spin, S	Spin-only magnetic moment, $\mu_{so}(BM)$
1	$\frac{1}{2}$	1.73
2	1	2.83
3	$\frac{3}{2}$	3.87
4	2	4.90
5	$\frac{5}{2}$	5.92

The table above shows how the magnetic moment changes with the number of unpaired electrons. The maximum number of unpaired electrons given is five, because for a transition metal a sixth electron would have to pair up in a previously occupied orbital. In f-block elements, there could be seven unpaired electrons before pairing occurs because there are seven f orbitals rather than just five d orbitals.

Note that the expression for spin-only magnetic moment is sometimes written in an alternative way, based directly on the number of unpaired electrons, n, rather than S.

$$\mu_{eff} \approx \mu_{so} = \sqrt{n(n+2)}$$

There is an additional approximation in these cases, based on how the values of the spin-only magnetic moment correlate with the number of unpaired electrons. If we always round the value of μ_{so}, then it is one greater than the number of unpaired electrons. Thus, $\mu_{so} \approx n+1$, provided of course that there are any unpaired electrons at all; the relationship doesn't hold if n = 0 because then $\mu_{so} = 0$, not 1.

In reality, observed magnetic moments are slightly different than spin-only magnetic moments. In some cases, the observed magnetic moment is smaller than expected, but those cases are more complicated and we won't consider them here. Very often, the observed magnetic moments are larger than predicted because orbital angular momentum also plays a role in determining the magnitude of the overall magnetic moment. We may use a modified expression that takes this part into account.

$$\mu_{eff} \approx \mu_{s+L} = g\sqrt{S(S+1) + \frac{1}{4}L(L+1)}$$

Just as *S* is the absolute value of the sum of the spin quantum numbers in the ion, m_s, *L* is the absolute value of the sum of the orbital quantum numbers, m_l. There are five d orbitals, with $m_l = 2, 1, 0, -1, -2$, and the value of *L* has to be maximized according to Hund's rule. That means the value of *L* can be 3, 2, or 0.

As an example, suppose we have a Co^{2+} ion. Co^{2+} ion has a d^7 configuration. It has five d orbitals, so four of these electrons are paired, leaving only three unpaired electrons with parallel spins, so $S = 3/2$. In order to maximize the orbital quantum number, L, two electrons will be in an orbital with $m_l = 2$, two electrons will be in an orbital with $m_l = 1$, and one electron will be in each orbital with m_l = 0, -1, and -2. When we take the sum, we find $L = 2+2+1+1+0-1-2 = 3$. That gives us:

$$\mu_{s+L} = g\sqrt{3/2(3/2+1) + \frac{1}{4}3(3+1)} = 5.20$$

In comparison, $m_{so} = 3.87$ in this case. Observed values of μ_{eff} vary between different Co^{2+} complexes but are generally in the range 4.1 – 5.2 BM.[2] The orbital contribution is often smaller than expected, so magnetic susceptibilities frequently fall somewhere between μ_{so} and μ_{S+L}.

The use of a simple Guoy balance is an historically important method of determining magnetic susceptibility, and it is sometimes used in undergraduate laboratory experiments. Other methods are frequently used to measure magnetic susceptibility in the research laboratory. A magnetic susceptibility balance operates on a similar principle to the one behind the Guoy balance. A sample is placed within the poles of an electromagnet, causing the electromagnet to move very slightly. The current in the electromagnet is adjusted, changing its magnetic field, until the magnet comes back to its initial position. The magnitude of the current adjustment is proportional to the magnetic susceptibility of the sample.

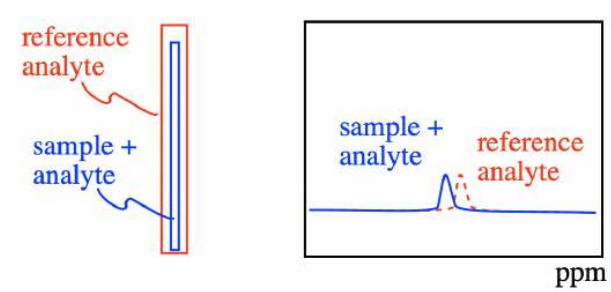


Figure **9.3.3**: The Evans Method uses chemical shifts (from NMR) to measure magnetic susceptibility. Left: A capillary tube containing sample and a reference analyte is bathed in a larger tube containing reference analyte solution. Right: The NMR signal of a reference analyte (red) is shifted when that analyte is mixed with a paramagnetic sample (blue). (CC-BY-NC; Chris Schaller)

A superconducting quantum interference device (SQUID) uses a superconducting loop in an external magnetic field to measure magnetic susceptibility of a sample.[3] The sample is mechanically moved though the superconducting loop, inducing a change in current and magnetic field that are proportional to the magnetic susceptibility of the sample. Commercially produced SQUID magnetometers often have variable temperature controls, allowing magnetic susceptibility to be measured across a range of temperatures.

The Evans NMR method is quite common because of the widespread availability of high-field NMR spectrometers in research labs. A capillary containing the paramagnetic sample and a reference analyte is placed in an NMR tube containing the same reference analyte but without the paramagnetic sample. The analyte in the presence of the paramagnetic material will experience a local, induced magnetic field owing to the effect of the superconducting magnet of the NMR instrument on the paramagnetic sample. Its NMR signals will shift as a result. The NMR signal of the analyte outside the capillary will undergo no such shift, and the difference in the two signals is an indicator of the magnetic susceptibility of the sample.

There are other types of magnetic behavior in addition to diamagnetism and paramagnetism. Ferromagnetic materials have long-range order with spins oriented parallel to each other, even in the absence of an external magnetic field. Common, permanent magnets are made from ferromagnetic materials. Antiferromagnetic materials also have long-range order, but the magnetic moments are arranged in opposing pairs. These three different magnetic behaviors are diagnosed by the temperature dependence of the magnetic susceptibility. Paramagnetic materials display magnetic susceptibility (χ_M, related to μ_{eff}) that increases with the inverse of temperature. Ferromagnetic materials have a critical temperature below which magnetic susceptibility rapidly rises. Antiferromagnetic materials have a critical temperature below which magnetic susceptibility rapidly falls. However, these behaviors are largely beyond the scope of the current discussion.

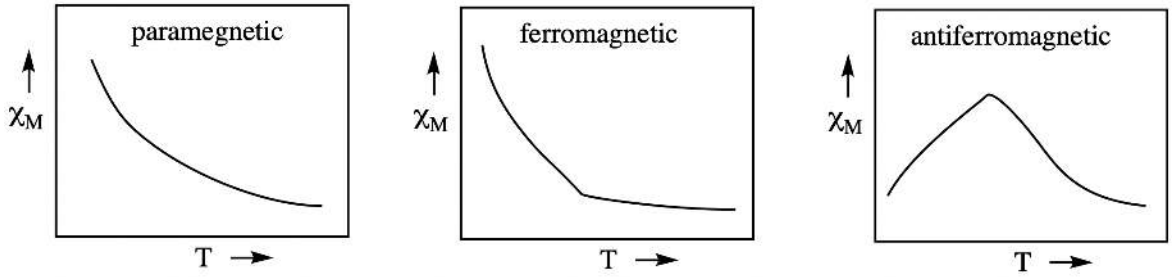


Figure **9.3.4**: Magnetic behavior depends on temperature. Shown are plots of magnetic behaviour in terms of magnetic susceptibility χ_M versus temperature (T). (CC-BY-NC; Chris Schaller)

Problems

? Exercise 9.3.1

Show that, given g = 2.0, then $g\sqrt{S(S+1)} = \sqrt{n(n+2)}$.

Answer

$$\begin{aligned}\mu_{so} &= g\sqrt{S(S+1)} \\ &= 2\sqrt{S(S+1)} \\ &= \sqrt{4S(S+1)} \\ &= \sqrt{2S(2S+2)}\end{aligned}$$

but $S = n(1/2)$ or $n = 2S$ then

$$\mu_{so} = \sqrt{n(n+2)}$$

? Exercise 9.3.2

Calculate the value of μ_{so} in the following cases:

a) V^{4+} b) Cr^{2+} c) Ni^{2+} d) Co^{3+} e) Mn^{2+} f) Fe^{2+}

Answer

a) V^{4+} is $d^1; n = 1; \sqrt{n(n+2)} = 1.73$
b) Cr^{2+} is $d^4; n = 4; \sqrt{n(n+2)} = 4.90$

c) Ni^{2+} is $d^8; n = 2; \sqrt{n(n+2)} = 2.83$
d) Co^{3+} is $d^6; n = 0; \sqrt{n(n+2)} = 0$
e) Mn^{2+} is $d^5; n = 5; \sqrt{n(n+2)} = 5.92$
f) Fe^{2+} is $d^6; n = 4; \sqrt{n(n+2)} = 4.90$
g) Cr^{3+} is $d^3; n = 3; \sqrt{n(n+2)} = 3.87$
h) V^{3+} is $d^2; n = 2; \sqrt{n(n+2)} = 2.83$

Exercise 9.3.3

Calculate the value of μ_{eff} in the following cases:

a) V^{4+} b) Cr^{2+} c) Ni^{2+} d) Co^{3+} e) Mn^{2+} f) Fe^{2+}

g) Cr^{3+} h) V^{3+}

Answer

a) V^{4+} is $d^1; S = 1/2; L = 2; \mu_{s+L} = g\sqrt{1/2(1/2+1) + \frac{1}{4}2(2+1)} = 3.00$
b) Cr^{2+} is $d^4; S = 2; L = 2+1+0-1 = 2; \mu_{s+L} = g\sqrt{2(2+1) + \frac{1}{4}2(2+1)} = 5.48$
c) Ni^{2+} is $d^8; S = 1; L = 2+2+1+1+0+0-1-2 = 3; \mu_{s+L} = g\sqrt{1(1+1) + \frac{1}{4}3(3+1)} = 2.24$
d) Co^{3+} is $d^6; S = 2; L = 2+2+1+0-1-2 = 2; \mu_{s+L} = g\sqrt{(2+1) + \frac{1}{4}2(2+1)} = 5.48$
e) Mn^{2+} is $d^5; S = 5/2; L = 2+1+0-1-2 = 0; \mu_{s+L} = g\sqrt{5/2(5/2+1) + \frac{1}{4}0(0+1)} = 5.92$
f) Fe^{2+} is $d^6; S = 2; L = 2+2+1+0-1-2 = 2; \mu_{s+L} = g\sqrt{2(2+1) + \frac{1}{4}2(2+1)} = 5.48$
g) Cr^{3+} is $d^3; S = 3/2; L = 2+1+0 = 3; \mu_{s+L} = g\sqrt{3/2(3/2+1) + \frac{1}{4}3(3+1)} = 5.20$
h) V^{3+} is $d^2; S = 1; L = 2+1 = 3; \mu_{s+L} = g\sqrt{1(1+1) + \frac{1}{4}3(3+1)} = 2.24$

References

1. Lancashire, R. J. Magnetic Susceptibility https://chem.libretexts.org/Bookshelves/Inorganic_Chemistry/Map%3A_Inorganic_Chemistry_(Housecroft)/04%3A_Experimental_techniques/4.14%3A_Magnetism/Magnetic_Susceptibility_Measurements (accessed Jun 27, 2021).
2. Cotton, F.A.; Wilkinson, G. *Advanced Inorganic Chemistry*, 4th Ed. John Wiley & Sons: New York, 1980, p 628.
3. Raja, P. M. V.; Barron, A. R. Magnetism https://chem.libretexts.org/@go/page/55872 (accessed Jun 27, 2021).

This page titled 9.3: Magnetic Susceptibility is shared under a CC BY-NC 4.0 license and was authored, remixed, and/or curated by Chris Schaller.

- **10.1.2: Magnetic Susceptibility** by Chris Schaller is licensed CC BY-NC 4.0.

9.4: Crystal Field Theory

As the name implies, crystal field theory was developed as a way of explaining phenomena in ionic crystalline solids. Bethe and van Vleck wished to provide a rationale for the magnetic properties of these materials, as well as their colors. The latter resulted from the wavelength of light absorbed, revealing something about differences in electronic energy levels in the ions of the crystalline solid. The magnetic properties also depended on electronic energy levels, because magnetism depended upon whether electrons were paired, and whether or not electrons are paired depends on the presence or absence of orbitals at the same energy level.

They first considered a transition metal ion in an octahedral hole formed between layers of counterions packed in a crystalline lattice. The metal ion would have six near neighbors: three above and three below. Of course, the ions would be held together by electrostatics: the negative charges on the counterions would be attracted to the positive charge on the metal ion.

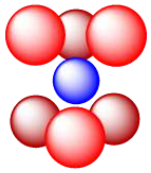


Figure **9.4.1**: Illustration of a positively charged metal ion (blue) surrounded by six near neighbors with negative charges (red). (CC-BY-NC; Chris Schaller)

But in addition to that positive charge, the metal ion also has electrons of its own. How did the electrons of those neighboring counterions affect the energy of those metal electrons? "...If we're going to work this out carefully, we need to consider three different situations", thought the physicists. "We need to start by considering the energy of the metal valence orbitals in the absence of counterions. Since these are transition metal ions, we will pay close attention to the five d orbitals. What happens when those d orbitals are placed in a field of surrounding electrons, if the field is evenly distributed around them? In other words, what happens to them in a spherical field of negative charge? And then, what happens if those electrons are not evenly distributed? What happens if the surrounding electrons approach only along the Cartesian axes?"

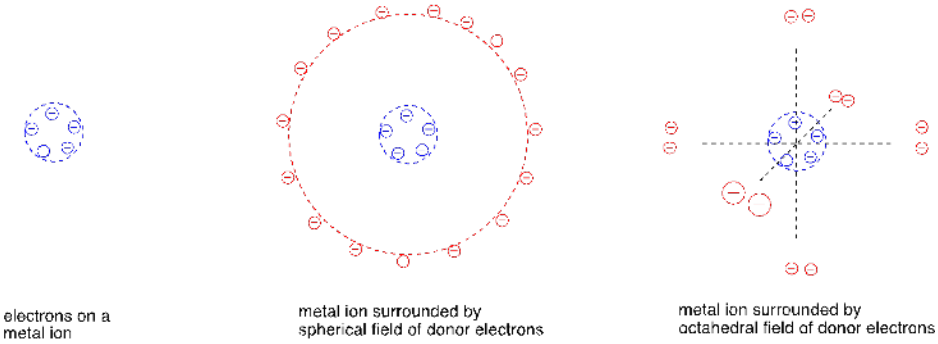


Figure **9.4.2**: Illustration of the electrostatic charges to consider in idealized situations. (Left) imaginary situation of a "lone" metal ion with five d electrons in its valence shell. (Middle) Imaginary situation where a d^5 metal ion is surrounded by a spherical distribution of donor (Lewis base) electrons from a set of ligands. (Right) Imaginary situation where a d^5 metal ion is surrounded by a set of ligand donor electrons that are located along Cartesian coordinates (in an octahedral geometry). (CC-BY-NC; Chris Schaller)

The Cartesian axes are important here because, in an octahedron, the six ligands are ninety degrees (**90°**) apart from each other in space. We can think of two of those ligand electrons as lying in either direction from the metal ion along the z axis; two of them along the x axis; and the last two along the y axis.

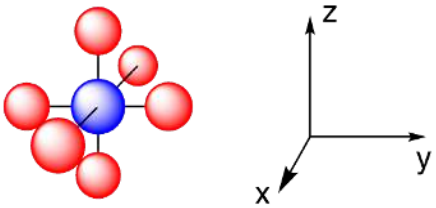


Figure 9.4.3: Illustration of a positively charged metal ion (blue) surrounded by six ligands (red) in an octahedral geometry where each ligand lies along the Cartesian axes. (CC-BY-NC; Chris Schaller)

Of course, when these metal electrons are placed in a field of negative charge, repulsion results, and the electrons on the metal go up in energy. They all increase in energy by the same amount.

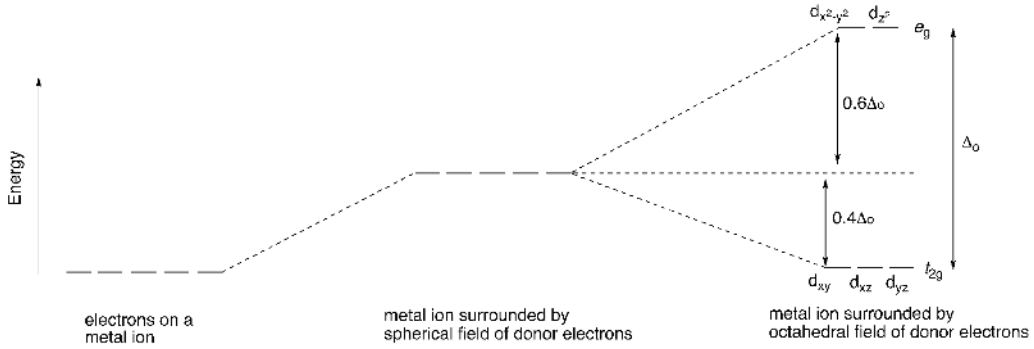


Figure 9.4.4: The relative energy levels of the valence d orbitals corresponding to the imaginary situations pictured in Figure 9.4.2 above. (Left) The five valence d orbitals of a "lone" metal ion are degenerate. (Middle) The electrons in the five valence d orbitals of a metal ion would be uniformly repelled by a spherical distribution of negative charge, and thus would be higher in energy than a "lone" metal ion. (Right) The electrons in each of the five valence d orbitals of a metal ion would interact to different extents with ligands located along each of the Cartesian coordinates, and thus their energies would be raised or lowered compared to the situation where charge was distributed in a uniform sphere. (CC-BY-NC; Chris Schaller)

The octahedral field is a different question, however, because the five d orbitals have different spatial distributions. Two of them (the d_{z^2} and $d_{x^2-y^2}$) lie along the axes. These orbitals are referred to as having e_g symmetry. The other three (the d_{xy}, d_{xz}, and d_{yz}) lie in between the axes. These three are referred to as having t_{2g} symmetry.

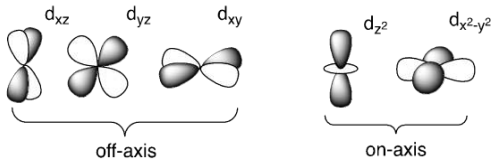


Figure 9.4.5: Illustration of the boundary surfaces of the five d orbitals. (CC-BY-NC; Chris Schaller)

Those two orbitals along the axes experience repulsion from the neighboring anions. Because all of the negative charge is focused in six positions rather than being uniformly distributed, the repulsion experienced by these orbitals is greater than it would be in a spherical field. On the other hand, the three orbitals between the axes experience very little repulsion; their energy is actually much lower than it would be in a spherical field of negative charge.

These two sets of orbitals are therefore found at two different energy levels. The energy difference between them is called the octahedral field splitting, Δ_o. Because the total amount of repulsion is the same in the octahedral field and the spherical field – it is just distributed differently – the average energy level of the orbitals should be the same in the two fields. This average energy of the orbitals is called the **barycenter**, a term borrowed from astronomy. Because two of the orbitals are raised above the barycenter in the octahedral field and three are lowered below the barycenter, then the e_g set must be $\frac{3}{5}\Delta_o$ $(= 0.6\Delta_o)$ above the barycenter and the t_{2g} set must be $\frac{2}{5}\Delta_o$ $(= 0.4\Delta_o)$ below the barycenter. That means the average energy lies at the barycenter.

A parameter called the crystal field stabilization energy (CFSE) was developed to assess the energy difference between the metal ion in an octahedral coordination geometry and a spherical field. To determine CFSE, we simply add up the energy of all the electrons relative to the energy level of electrons in the spherical field, in units of Δ_o. For an octahedral case:

Misplaced '#'

Problems

Exercise 9.4.1

Determine the crystal field stabilization energy (CFSE) in the following octahedral ions:

a) V^{3+} b) Ni^{2+} c) Cr^{3+} d) Zn^{2+}

Answer a

V^{3+} is d^2, with two electrons in the t_{2g} and zero electrons in e_g.

CFSE = $[2(-0.4) + 0(0.6)] \times \Delta_o = -0.8\Delta_o$

Answer b

Ni^{2+} is d^8, with six electrons in t_{2g} and two electrons in e_g.

CFSE = $[6(-0.4) + 2(0.6)] \times \Delta_o = -1.2\Delta_o$

Answer c

Cr^{3+} is d^3, with three electrons in t_{2g} and zero electrons in e_g.

CFSE = $[3(-0.4) + 0(0.6)] \times \Delta_o = -1.2\Delta_o$

Answer d

Zn^{2+} is d^{10}, with six electrons in t_{2g} and four electrons in e_g.

CFSE = $[6(-0.4) + 4(0.6)] \times \Delta_o = 0\Delta_o$.

This page titled 9.4: Crystal Field Theory is shared under a CC BY-NC 4.0 license and was authored, remixed, and/or curated by Chris Schaller.

- **10.2.1: Crystal Field Theory** by Chris Schaller is licensed CC BY-NC 4.0.

SECTION OVERVIEW

9.5: Ligand Field Theory

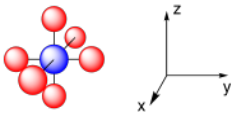
This page titled 9.5: Ligand Field Theory is shared under a CC BY-NC 4.0 license and was authored, remixed, and/or curated by Chris Schaller.

9.6: Ligand Field Theory - Molecular Orbitals for an Octahedral Complex

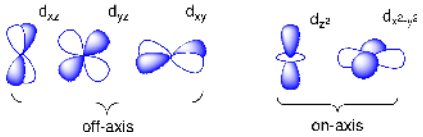
Crystal field theory is successful at providing some general insights into the differing energy levels of d orbitals in coordination complexes. That knowledge can help us to understand some of the magnetic properties of these compounds, which are determined by the number of unpaired electrons. It can also help us to understand some of the absorbed wavelengths of light in the UV-visible spectrum, which in some cases depends on the energy difference between different sets of d orbitals.

Ligand field theory picks up where crystal field theory left off by taking into consideration the importance of orbital overlap for covalent bonding. That factor adds another level of detail to our model of metal complex behavior, and it provides additional nuance to our understanding of why two related complexes may have very different properties.

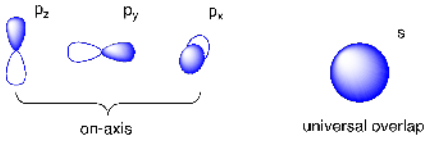
We can start by taking another look at octahedral coordination geometry. That's probably the most common coordination geometry. It's also the one we looked at when we considered crystal field theory. In this geometry, all six ligands are located along the x, y, or z axes.



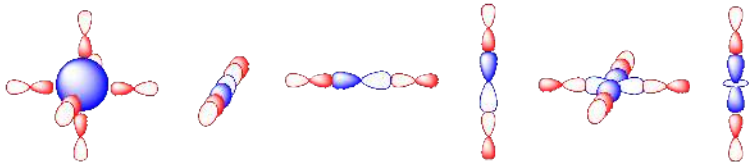
Once again, only two of the valence d orbitals are located along those axes. In crystal field theory, we considered that orientation as an opportunity for electron-electron repulsion between ligand lone pairs (or charges on neighboring anions) and the d electrons. This time, we'll think about the opportunity for covalent bonding that exists between ligand orbitals and the d orbitals along these axes.



In addition to the d orbitals, we should also think about the potential for bonding with the metal's valence s and p orbitals. All three p orbitals are located along the axes where we find the ligands. They are ideally located for bonding with ligand orbitals along those axes. The s orbital is different: it is non-directional. No matter where a ligand is located, if it has sigma bonding, it will have the same overlap with that spherical s orbital. That means the s orbital is a good candidate for forming a covalent sigma bond with any ligand, no matter what the geometry.

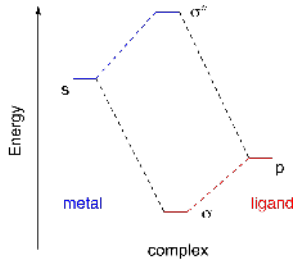


That leaves us with six possible metal orbitals that could potentially overlap with the six ligands. Each metal orbital could potentially interact with any one of a number of these ligands. In the illustration below, we've made the assumption that the ligand orbitals are p orbitals. That's not a bad bet given that we are generally considering p-block elements as donor atoms in most ligands. The s orbital could presumably interact with up to six ligands. The metal p orbitals could interact with ligand orbitals in either direction along the axis. By inspection, it appears that the d orbitals could interact with two or four orbitals.



That ratio of six ligand orbitals to six ligand orbitals is coincidental. A one-to-one correspondence between metal orbitals and ligand orbitals isn't strictly required, but it's easier to think about that way. Let's begin by assuming that the s orbital interacts with just one donor orbital. Just like in MO construction for main group diatomics, if we start with two atomic orbitals and combine

them, we get two molecular orbitals. One of them is the in-phase combination and the other one is the out-of-phase combination. The number of molecular orbitals we obtain is the same as the number of atomic orbitals we start with.



We can think of these two combinations as the addition of two orbitals together, with a positive coefficient if they are in phase and a negative coefficient if they are out of phase.

$$\psi M\text{-}L = a\psi M(s) + b\psi L(p)$$

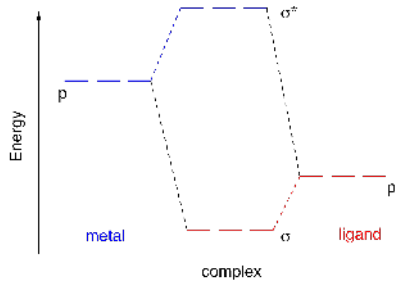
$$\psi^* M\text{-}L = c\psi M(s) - d\psi L(p)$$

Notice that the molecular orbital interaction diagram is asymmetric. The ligand orbital is at lower energy than the metal orbital. The donor atom is a p block element; it's to the right of the transition metals in the periodic table. The donor atom is more electronegative than the transition metal, so its electrons are at lower energy. In a case like that, the coefficients in the orbital combination follow a pattern. In the in-phase combination, the more electronegative element gets a larger coefficient than the less electronegative element ($b > a$). The opposite is true in the out-of-phase combination ($c > d$).

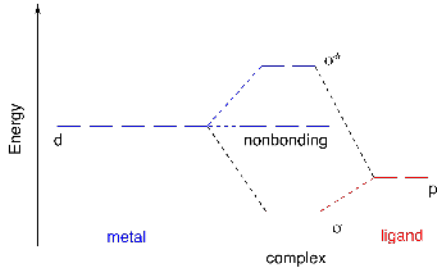


The molecular orbital more closely resembles the atomic orbital to which it is closest in energy, both spatially and energetically. Consequently, we often talk about the bonding orbital, σ, as though it is still a ligand p orbital, and the antibonding orbital, σ, as though it is still a metal s orbital. The bonding orbital is ligand-centered and the antibonding orbital is metal-centered.

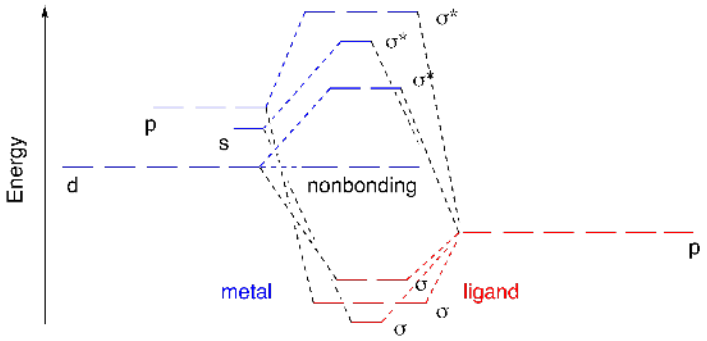
If we consider the three metal p orbitals and their overlap with three of the ligand donor orbitals, we find a very similar outcome. The three σ* orbitals are metal-centered, whereas the three σ orbitals are ligand-centered.



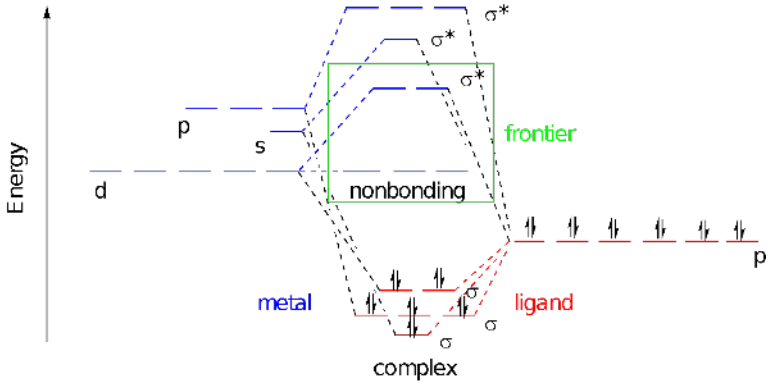
The d orbitals, on the other hand, present a significant variation. Only two of them appear to be capable of overlap with ligand p orbitals. If we pair those two d orbitals off with the remaining two ligand donor orbitals, we have three leftover metal d orbitals. Those three metal orbitals do not overlap with the ligand and so they are non-bonding.



We can superimpose those three pictures to get a look at the full molecular orbital interaction diagram. It is still somewhat simplified. We are ignoring any core orbitals on the metal and we are also ignoring any ligand orbitals that aren't involved in sigma bonding to the metal. Maybe we have ammine ligands but we are ignoring all of those N-H bonds and focusing solely on the M-N bonds.

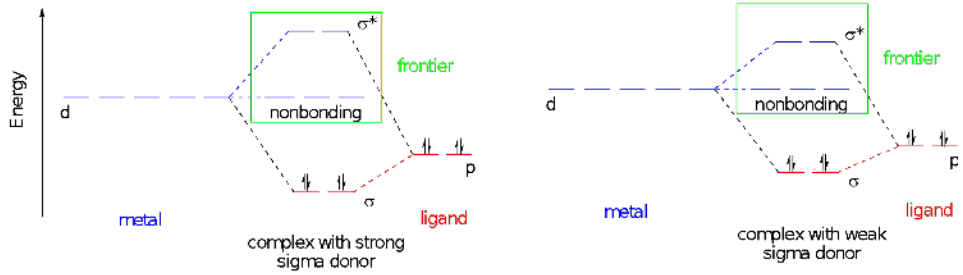


The six donor atoms are each donating a pair of electrons to the metal. Upon covalent bond formation, each of those lone pairs slides down into an energy well; they are stabilized by formation of the metal-ligand bond.

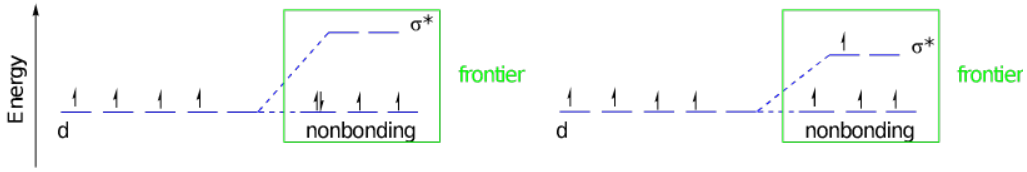


So far, we have ignored the electrons on the metal because we are looking at a general case. There could be anywhere from zero to ten electrons in the atomic d orbitals, depending on the metal and its oxidation state. These electrons will be crucial to many aspects of the behavior of the complex because they are found at the frontier. Frontier orbitals are often the key to understanding reactivity as well as physical properties such as magnetism and interaction with light.

We often consider only these frontier orbitals when we consider the properties of transition metal complexes. We ignore what seems like the most important part of the picture: the bonding orbitals. We do that because those bonding orbitals are not frontier orbitals. Furthermore, the stability of those bonding orbitals is reflected in the antibonding level. The lower the bonding electrons sink, the higher the antibonding levels rise. One immediate consequence of that connection is that the bond strength may control the gap between nonbonding and antibonding d orbitals. Strong sigma donors provide a large d-d gap, whereas weak sigma donors give a smaller d-d gap. Understanding donor strength can be a difficult task, but remember for example that more basic ligands are often stronger donors.



If we think about a specific case of metal ion, we can add some d electrons to the picture. Suppose we have a d^4 metal ion. Maybe it's a Cr^{2+} ion. This ion can take on two different electron configurations in an octahedral environment. With stronger donors, the d-d gap is potentially too large to promote a fourth electron into the next energy level, so the complex is left with two unpaired electrons. With weaker donors, the relatively small d-d gap may be smaller than the energy it takes to put two electrons into the same orbital, so there are four unpaired electrons. We'll return to the consequences of these situations on an upcoming page.



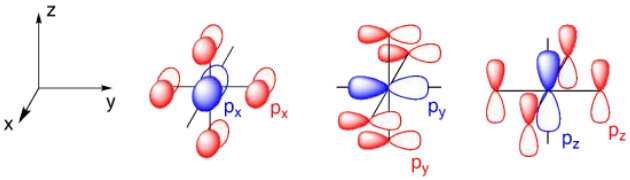
Pi Donor Ligands

The sigma donor strength of the ligand can have an appreciable effect on the d orbital splitting in the complex, and that might influence the properties of the complex. That's not something that we considered in crystal field theory, but thinking about bonding interactions has provided another layer of information. What other variations in ligand donation might play a role in the d orbital splitting?

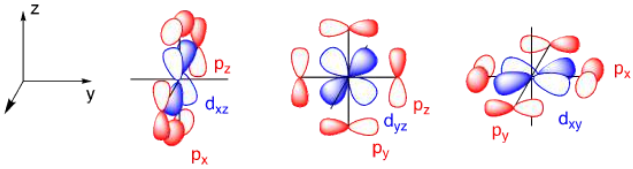
Suppose a donor atom had more than one lone pair. Could it donate a second? On paper, that makes another bond between the ligand and the metal. Bond formation is energy-releasing and stabilizing, although sometimes we get in trouble when we draw too many bonds, because we've run out of orbitals to interact with each other.



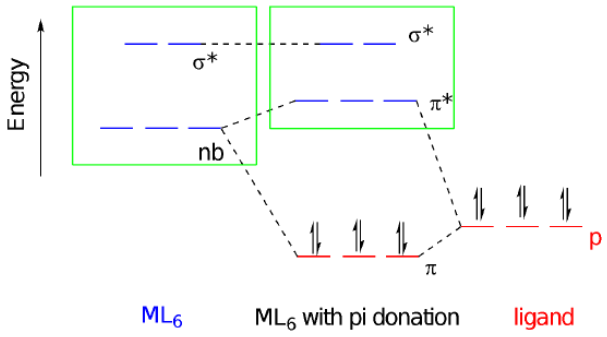
When we draw a pair of bonds between two atoms, we usually think of the first bond as a sigma bond and the second one as a pi bond. The question here is, can bromine form a pi bond with a transition metal? When we learn about pi bonds, we start by looking at two nitrogen atoms or two carbon atoms using parallel p orbitals to bond with each other. The resulting pi bond avoids the sigma bond because it is above and below the bond axis. We have already established that the metal can use its p orbitals for bonding. On paper, a metal p orbital in an octahedral complex could pi bond with four different ligands.



The trouble with that scheme is that we are already using these metal p orbitals for sigma bonding. We have other metal orbitals that could overlap with these ligand p orbitals, however, and we aren't using them for sigma bonding. These are the d_{xy}, d_{xz}, and d_{yz} orbitals. This set looks even more promising for pi bonding; the d orbitals reach out towards the ligand p orbitals, maximizing overlap. Once again, each d orbital could potentially form pi bonds with up to four ligands.



Let's consider the consequences of pi bond formation using the molecular orbital interaction diagram. This time we're just considering lone pairs on three ligands that could donate to the three different d orbitals of appropriate symmetry: the d_{xy}, d_{yz}, and d_{xz}. We get a bonding and an antibonding combination, but the three ligand pairs all go down in energy. As long as there are fewer than six d orbitals there is a net decrease in energy. Just like before, when these orbitals combine, the bonding combination has more ligand character whereas the antibonding combination has more metal character. The key change in terms of the frontier orbitals is that the d orbital splitting becomes smaller than in the case of the simple sigma bond donor.

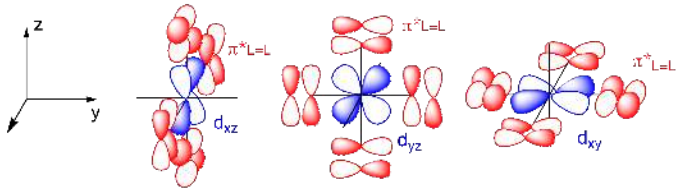


Ligand-to-metal donation is just one way to make a metal-ligand double bond. In those cases in which the metal has d electrons, the double bond could also be formed by donation from the metal to the ligand. The d electrons are most likely to occupy the d_{xy}, d_{xz}, and d_{yz}, as those orbitals are the lowest available ones. Those are the same orbitals that were involved in π bonding in ligand-to-metal donation. In addition to d electrons, there must also be an acceptor orbital on the ligand. That is to say, there must be an empty orbital on the ligand with π symmetry. Instead of a lone pair, this acceptor takes the form of a π* orbital on the ligand. That means there has to be a π bond between the donor atom and a second atom within the ligand. Carbon monoxide is the classic example of such a ligand.

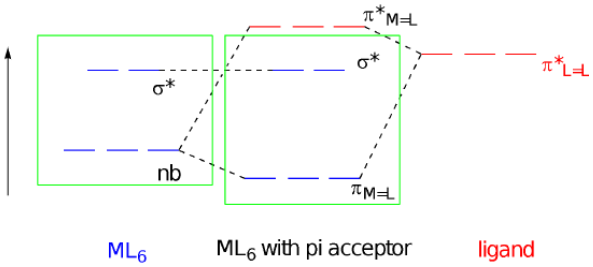


Metal-to-ligand π donation has the effect of breaking a π bond in the ligand because of the fact that electrons are donated into a ligand π* orbital. In terms of Lewis structures, this looks like an interaction that would strengthen the metal-ligand bond but weaken bonds within the ligand itself. When a metal π donates into a carbon monoxide, populating the CO π* orbital, the CO bond gets weaker.

Because we are still looking at π bond formation, the orbital pictures look somewhat similar to the ones for ligand-to-metal π donation, but with π* molecular orbitals instead of p atomic orbitals.



This time, the relevant ligand orbitals are higher in energy than the metal orbitals because they are antibonding. Antibonding orbitals are typically higher in energy than atomic orbitals. That means that when we construct orbital combinations from these pairs, the metal-ligand pi bonding orbital has more metal character. Conversely, the metal-ligand pi antibonding orbital has more ligand character. If there are any d electrons, they will drop into a lower energy well through formation of the pi bond. The ligand π* molecular orbitals are raised in energy, but that change has no energetic consequences since there aren't any electrons there.



In contrast to ligand-to-metal pi bond donation, metal-to-ligand pi bond formation has the effect of increasing the d orbital splitting. That gives us three different magnitudes of d orbital splitting for three different categories of ligand. The splitting follows the order

pi donors < sigma donors < pi acceptors, at least as a rough trend; individual ligands may deviate from this trend for other reasons, such as the strength of sigma donation.

Group Theory as a Tool in Ligand Field Theory

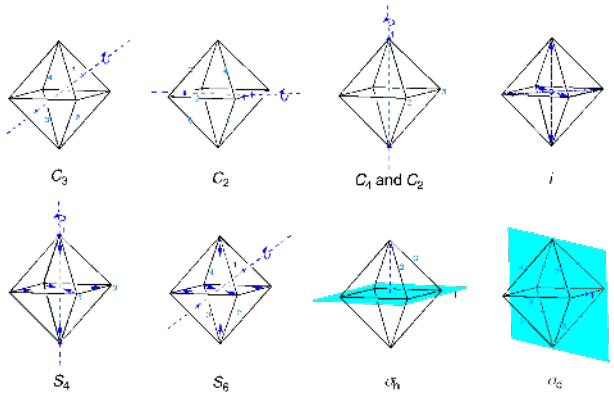
What if the orbital combinations are not obvious? What if you can't decide by inspection which ligand orbital would overlap with which metal orbital? There is a more general method of evaluating these things using group theory. We should use that approach for the octahedral geometry, because we already have a concrete example of what that should look like. We can use our knowledge of that outcome to build confidence in our results from group theory. Group theory may be a newer approach to us, and so it will be helpful to validate the results.

To get started, we are going to need a character table for an octahedral geometry, and we will need to consider how the bonding orbitals behave under the symmetry operations of this group. You can brush up on point groups and symmetry here.1

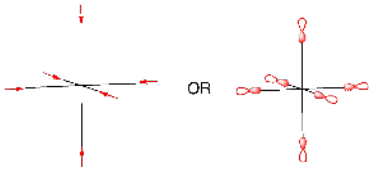
The top row of the character table for the octahedral point group organizes the symmetry operations and tells us how many of each operation we can find.

O_h	E	$8C_3$	$6C_2$	$6C_4$	$3C_2\ (=C_4^2)$	i	$6S_4$	$8S_6$	$3\sigma_h$	$3\sigma_d$

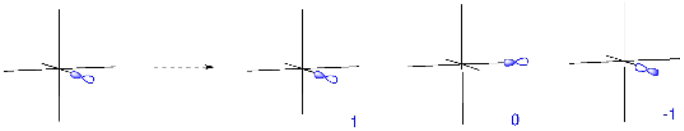
Apart from the identity element, there are ten additional symmetry elements in this point group. The C_3 axis passes through the four pairs of opposite faces of the octahedron. We can rotate by either 120 degrees or 240 degrees, making a total of eight operations. Six different C_2 axes pass through opposite edges of the octahedron. Additional C_2 axes are coincident with the C_4 axis passing through opposite corners of the octahedron (because $C_2 = C_4^2$, but not C_4^1 or C_4^3). There is an inversion center at the position of the metal ion. That inversion element makes possible an S_4 axis coincident with the C_4 axis and an S_6 axis coincident with the C_3 axis. Finally, there are two sets of mirror planes, one set in the equatorial planes and one set bisecting the faces of the octahedron.



We can use the character table to determine appropriate orbitals for bonding with the ligands. A set of vectors is often used for this purpose but p orbitals can be used just as well. We consider how each of the p orbitals will change under a particular symmetry element.



Has a p orbital remained in place, unchanged? That counts as 1. Has it moved into an entirely different position? That counts as 0. Has it remained in place, but with the opposite orientation? That counts as -1.



Looking at each of the symmetry elements gives us a reducible representation.

O_h	E	$8C_3$	$6C_2$	$6C_4$	$3C_2 (= C_4^2)$	i	$6S_4$	$8S_6$	$3\sigma_h$	$3\sigma_d$
Γ	6	0	0	2	2	0	0	0	4	2

If we look at the complete character table, we can find the irreducible representations that this reducible representation is composed of.

O_h	E	$8C_3$	$6C_2$	$6C_4$	$3C_2 (= C_4^2)$	i	$6S_4$	$8S_6$	$3\sigma_h$	$3\sigma_d$		
A_{1g}	1	1	1	1	1	1	1	1	1	1		$x^2 + y^2 + z^2$
A_{2g}	1	1	-1	-1	1	1	-1	1	1	-1		
E_g	2	-1	0	0	2	2	0	-1	2	0		$(2z^2 - x^2 - y^2, x^2 - y^2)$
T_{1g}	3	0	-1	1	-1	3	1	0	-1	-1	(R_x, R_y, R_z)	
T_{2g}	3	0	1	-1	-1	3	-1	0	-1	1		(xz, yz, xy)
A_{1u}	1	1	1	1	1	-1	-1	-1	-1	-1		
A_{2u}	1	1	-1	-1	1	-1	1	-1	-1	1		
E_u	2	-1	0	0	2	-1	0	1	-2	0		
T_{1u}	3	0	-1	1	-1	-3	-1	0	1	1	(x, y, z)	
T_{2u}	3	0	1	-1	-1	-3	1	0	1	-1		

We find that $\Gamma = A_{1g} + T_{1u} + E_g$. If we add together the characters for each of the symmetry elements in those three representations, we get the characters in our reducible representation for the ligand p orbitals.

The A_{1g} representation corresponds to the metal s orbital. The T_{1u} representation corresponds to the three metal p orbitals. The E_g representation corresponds to two of the d orbitals: $2z^2 - x^2 - y^2$ (usually abbreviated as z^2) and $x^2 - y^2$. The other three d orbitals (d_{xy}, d_{xz}, and d_{yz}) have T_{1u} symmetry and are not a match for the set of ligand orbitals that we examined. This is exactly the outcome that we established by looking at metal orbitals and ligand orbitals and deciding which ones would overlap. The match between the two approaches should provide some confidence about the use of character tables to make decisions about symmetry-appropriate bonding.

References

(1) Point Groups https://chem.libretexts.org/@go/page/269925 (accessed Jul 2, 2021).

Example 9.6.1

The formula for decomposing a reducible representation is based on taking the dot product and normalizing:

$$ai = 1hQN \bullet \chi(R) \bullet \chi(R)Q$$

in which ai is the number of times the irreducible representation appears in the reducible representation; h is the order of the point group (the total number of symmetry operations); N is the number of operations for a given symmetry element, Q; $\chi(R)$is the character of the reducible representation and $\chi(R)$is the character of the irreducible representation.

Use the formula to confirm the finding that, for sigma bonding in an octahedral geometry:

$$\Gamma = A_{1g} + T_{1u} + E_g.$$

Solution

ai = 1h QN· χ(R)·χ(R)Q

A_{1g}: ai = 148 [1·6·1+8·0·1+6·0·1+6·2·1+3·2·1+ 1·0·1+6·0·1 + 8·0·1+3·4·1+6·2·1] = 148 (6+12+ 6+12+12)= 148·48=1

A_{2g}: ai = 148 [1·6·1+8·0·1+6·0·(-1)+6·2·(-1)+3·2·1+ 1·0·1+6·0·(-1) + 8·0·1+3·4·1+6·2·(-1)] = 148 (6-12+ 6+12-12)= 148·0=0

E_g: ai = 148 [1·6·2+8·0·(-1)+6·0·0+6·2·0+3·2·2+ 1·0·2+6·0·0 + 8·0·(-1)+3·4·2+6·2·0] = 148 (12+12+ 24)= 148·48=1

T_{1g}: ai = 148 [1·6·3+8·0·0+6·0·(-1)+6·2·1+3·2·(-1)+ 1·0·3+6·0·1 + 8·0·0+3·4·(-1)+6·2·(-1)] = 148 (18+12- 6-12-12)= 148·0=0

T_{2g}: ai = 148 [1·6·3+8·0·0+6·0·1+6·2·(-1)+3·2·(-1)+ 1·0·3+6·0·(-1) + 8·0·0+3·4·(-1)+6·2·1] = 148 (18-12- 6-12+12)= 148·0=0

A_{1u}: ai = 148 [1·6·1+8·0·1+6·0·1+6·2·1+3·2·1+ 1·0·(-1)+6·0·(-1) + 8·0·(-1)+3·4·(-1)+6·2·(-1)] = 148 (6+12+ 6-12-12)= 148·0=0

A_{2u}: ai = 148 [1·6·1+8·0·1+6·0·(-1)+6·2·(-1)+3·2·1+ 1·0·(-1)+6·0·1 + 8·0·(-1)+3·4·(-1)+6·2·1] = 148 (6-12+ 6-12+12)= 148·0=0

E_u: ai = 148 [1·6·2+8·0·(-1)+6·0·0+6·2·0+3·2·2+ 1·0·(-2)+6·0·0 + 8·0·1+3·4·(-2)+6·2·0] = 148 (12+12- 24)= 148·0=0

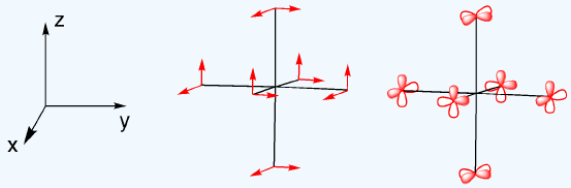
T_{1u}: ai = 148 [1·6·3+8·0·0+6·0·(-1)+6·2·1+3·2·(-1)+ 1·0·(-3)+6·0·(-1) + 8·0·0+3·4·1+6·2·1] = 148 (18+12- 6+12+12)= 148·48=1

T_{2u}: ai = 148 [1·6·3+8·0·0+6·0·1+6·2·(-1)+3·2·(-1)+ 1·0·(-3)+6·0·1 + 8·0·0+3·4·1+6·2·(-1)] = 148 (18-12- 6+12-12)= 148·0=0

$$\Gamma = A_{1g} + T_{1u} + E_g.$$

Example 9.6.1

Determine the reducible representation for the symmetry of the pi-bonding orbitals in an octahedral geometry. You can use simple vectors to represent the bias of the p orbitals.



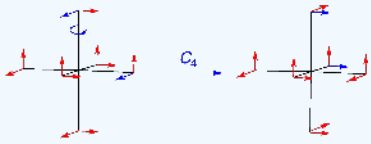
Solution

E: All 12 vectors remain in same place in same orientation. The character is 12.

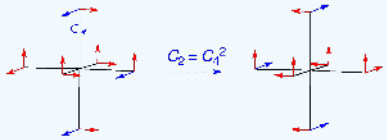
C_3: An off-axis rotation, so all vectors have moved. The character is 0.

C_2: An off-axis rotation, so all vectors have moved. The character is 0.

C_4: An on-axis rotation, but the vectors are off-axis. Note how the labeled vectors make the movement out of position clear. The character is 0.

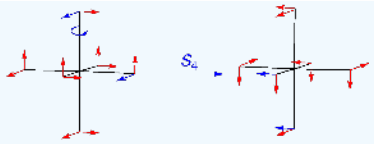


C_2 (= C_4^2): An on-axis rotation, but this time the four vectors located along the rotational axis just switch bias. The others move out of position. The character is -4.



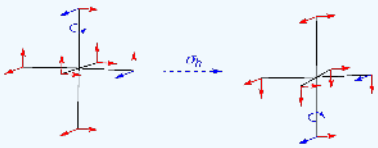
i: All 12 vectors move to the opposite side of the structure. The character is 0.

S_4: An on-axis rotation, followed by inversion. Note how the labeled vectors make the movement out of position clear. The character is 0.



S_6: An off-axis rotation, so all vectors have moved. The character is 0.

σ_h: Four vectors change position (character is 0); four vectors remain in position and keep original bias (character is 4); four vectors remain in position and switch bias (character is -4); net character is 0.



σ_d: An off-axis reflection, so all vectors have moved. The character is 0.

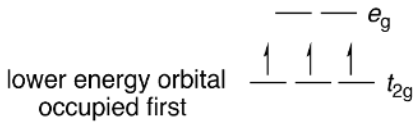
O_h	E	$8C_3$	$6C_2$	$6C_4$	$3C_2$ (= C_4^2)	i	$6S_4$	$8S_6$	$3\sigma_h$	$3\sigma_d$
Γ	12	0	0	0	-4	0	0	0	0	0

This page titled 9.6: Ligand Field Theory - Molecular Orbitals for an Octahedral Complex is shared under a CC BY-NC 4.0 license and was authored, remixed, and/or curated by Chris Schaller.

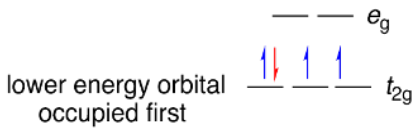
- **10.3.1: Ligand Field Theory - Molecular Orbitals for an Octahedral Complex** by Chris Schaller is licensed CC BY-NC 4.0.

9.7: Orbital Splitting and Electron Spin

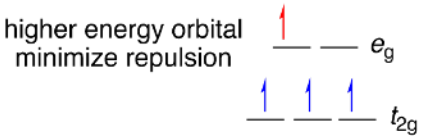
Once we have a d orbital splitting diagram for a particular geometry of a complex, we can populate the diagram with the known number of d electrons for a specific metal ion. If the complex is octahedral and the metal ion has 1, 2, or 3 d electrons, then the electrons will simply go in the lower level, the t_{2g} orbitals. For the d^3 case, one electron will occupy each orbital, with parallel spins.



What about a fourth electron? If the metal ion has a d^4 configuration, we could imagine two situations. The electron may also occupy one of the t_{2g} orbitals, which lie at lower energy. To do so, the fourth electron must be spin-paired with the other occupant of that orbital.



That's the low-spin configuration. The fourth electron has gone into the lower possible orbital rather than the higher possible one. Alternatively, the fourth electron could occupy one of the e_g orbitals. It would be at a higher energy level, but it would avoid that repulsive interaction with the other electron in the t_{2g} orbital. That would be the high-spin case. The fourth electron has gone into the higher possible orbital rather than the lower one.



The terms "high-spin" and "low-spin" really refer to the net spin of the atom. Each electron has a spin of a certain magnitude, but spin is a vector quantity. If two spins are pointing in the same direction, they add together, so the overall spin of the atom increases. If two spins are pointing in opposite directions, they cancel out, so the overall spin of the atom decreases. Having electrons paired in the same orbital leads to a lower spin for the atom.

The electron configuration of a d^4 metal ion in an octahedral complex depends broadly on two factors: the difference in energy between the t_{2g} and e_g levels (the octahedral field splitting, Δ_o) and the energy associated with pairing two electrons in the same orbital. We have already looked at some of the factors that influence the field splitting, so let's start by looking at that factor.

It is useful to be aware of some general trends in Δ_o. First, comparison between Δ_o measured for +3 cations and for +2 cations of the first-row transition metals manganese, iron, and cobalt shows that charge exerts a significant influence. The higher the charge on an ion, the larger Δ_o becomes. These examples are illustrated in Table 1.

Table 1. Comparison of Octahedral Field Splitting Between M(II) and M(III) Ions[1]

Complex	Δ_o (cm^{-1})	Complex	Δ_o (cm^{-1})
$Cr(OH_2)_6^{2+}$	14,000	$Cr(OH_2)_6^{3+}$	17,600
$Mn(OH_2)_6^{2+}$	7,500	$Mn(OH_2)_6^{3+}$	21,000
$Fe(OH_2)_6^{2+}$	10,000	$Fe(OH_2)_6^{3+}$	14,000

In each case, the M(III) ion has an octahedral field splitting that is significantly larger than the corresponding value in the M(II) case. However, comparisons of the field splitting between metals in different columns is complicated, with no simple trend.

Second, Δ_o is much larger for second-row than for first-row metals of the same group, as shown in Table 2. The value of Δ_o is even larger for third-row transition metals than second-row transition metals. As a result, transition metal ions from the second and third rows are usually low-spin. First-row transition metal ions, with their smaller Δ_o values, are often high spin, but they can also be low spin, and charge is an important factor in determining which case will occur.

Table 2. Comparison of Octahedral Field Splitting Between Ions from Different Periods of the Periodic Table[2]

Complex	Δ_o (cm^{-1})	Complex	Δ_o (cm^{-1})
$CoCl_6^{3-}$	Not available	$Co(NH_3)_6^{3+}$	23,000
$RhCl_6^{3-}$	20,300	$Rh(NH_3)_6^{3+}$	33,900
$IrCl_6^{3-}$	24,900	$Ir(NH_3)_6^{3+}$	Not available

Although the available data is limited here, second-row rhodium has a larger octahedral field splitting than first-row cobalt, and third-row iridium displays a larger field splitting than second-row rhodium. Note that these examples are compared using complexes with identical ligands.

The configuration of first-row transition metals is also strongly influenced by the ligands in the complex, indicated in Table 3. For a given ion, we would expect π-acceptors to give relatively large values of Δ_o, whereas σ-donors would give a smaller Δ_o and π-donors would give a smaller value still. There may be some overlap between these groups, because there are stronger and weaker π-acceptors, for example, or stronger and weaker σ-donors, but that is the general trend that we would expect.

Table 3. Comparison of Octahedral Field Splitting Between Ions from Different Periods of the Periodic Table[2]

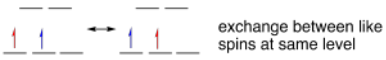
Complex	Δ_o (cm^{-1})	Complex	Δ_o (cm^{-1})
$CrBr_6^{3-}$	Not available	$NiBr_6^{2-}$	7,000
$CrCl_6^{3-}$	13,600	$NiCl_6^{2-}$	7,300
$Cr(OH_2)_6^{3+}$	17,400	$Ni(OH_2)_6^{2+}$	8,500
$Cr(NH_3)_6^{3+}$	21,600	$Ni(NH_3)_6^{2+}$	10,800
$Cr(CN)_6^{3-}$	26,300	$Ni(CN)_6^{2-}$	Not available

Among the chromium complexes, the π-accepting cyanide gives a much larger value of Δ_o than the π-donating chloride, as expected from molecular orbital considerations. In both the chromium and nickel cases, the ammine ligand, a simple σ-donor, provides a larger splitting that the aquo ligand, which is a π-donor. We may not be able to make predictions about electron configuration based solely on the type of ligand, but generally we would expect that a complex with π-accepting ligandswould be more likely to be low-spin than a complex with π-donating ligands.

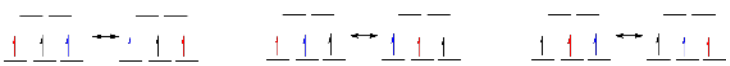
In addition to comparing ligands of different classes, we may also want to look at differences between ligands of the same class. Frequently, among σ-donors and π-donors, basicity of the ligand plays a valuable predictive role. For example, when coordinated to Ni(II), chloride results in a larger field splitting than bromide. Chloride is more basic than bromide, as shown by the pKa of the conjugate acids (pK_a = -6 for HCl vs. -9 for HBr), leading to stronger coordination in the case of chloride; that means a lower energy for the donor electrons but a higher energy for the σ* orbital compared to bromide coordination.

Let's take a look at the other factor that plays a role in determining the electron configuration: the pairing energy. We refer generally to the pairing energy as Π, but it actually has two components. Π_c is the coulombic portion of this energy. It arises from repulsion between two electrons that occupy the same region of space (the same orbital). Repulsion between the electrons causes energy to increase, so Π_c is a positive unit of energy.

The second component involves quantum mechanical exchange between like spins: Π_e is a stabilizing factor. When two electrons of like spin can exchange with each other, energy decreases: Π_e is a negative unit of energy. For example, in a d^2 octahedral metal, the two electrons are both at the t_{2g} level and have the same spin; that situation allows them to freely exchange with each other, which results in a decrease in energy.



In a d^3 system, the addition of just one more electron leads to a significant lowering of energy because the amount of exchange triples. Now, the electron in the first orbital can exchange with either the electron in the second or the third orbital. The electrons in the second and third orbitals can also exchange with each other. That makes a total of three possible exchanges.



These two factors, repulsion and exchange, contribute to an overall or total pairing energy. Some values of total pairing energy are shown in Table 4.

Table 4. Comparison of Total Pairing Energies Between M(II) and M(III) Ions[3]

Complex	Π (cm^{-1})	Complex	Π (cm^{-1})
$Mn(OH_2)_6^{2+}$	25,500	$Mn(OH_2)_6^{3+}$	28,000
$Fe(OH_2)_6^{2+}$	17,600	$Fe(OH_2)_6^{3+}$	30,000
$Co(OH_2)_6^{2+}$	22,500	$Co(OH_2)_6^{3+}$	21,000

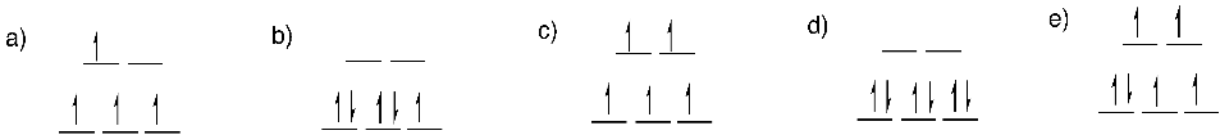
Like the field splitting, pairing energy is somewhat complex and is governed by more than one factor. However, it is worth pointing out that pairing energy is frequently (but not always) larger for more highly charged ions. For example, the pairing energy for both Mn(III) and Fe(III) are greater than the respective values for Mn(II) and Fe(II). That fact reflects the contraction of the more highly-charged ions. Confined to a smaller volume, repulsion between the electrons becomes greater.

In general, notice that the magnitudes of these pairing energies are pretty large compared to many of the octahedral field splitting values in the previous tables. In particular, they are larger than most of the values of Δ_o for first-row transition metals. That's why many first-row ions are high spin: the energy required to pair electrons in a low-spin configuration is often greater than the energy required to place an electron in the e_g level. The pairing energies are not that large compared to Δ_o for second- and third-row transition metals, so ions of those metals are more likely to be low spin.

So, if we are comparing the energy difference between two configurations, we need to take into account both the energy difference between the two orbital energy levels and the energy difference resulting from spin pairing. That could include both differences in electron-electron repulsion and differences in energy because of exchange.

Problems

1. Demonstrate the exchanges possible in the following configurations.



2. Determine the difference in Π_c between the high spin and low spin configuration in each of the following cases:

a) d^4 b) d^5 c) d^6

3. Determine the difference in Π_e between the high spin and low spin configuration in each of the following cases:

a) d^5 b) d^6 c) d^7

4. Given the value of Δ_o and Π in each case, predict whether the complex will be high spin or low spin.

a) $[Mn(OH_2)_6]^{2+}$

b) $[Mn(OH_2)_6]^{3+}$

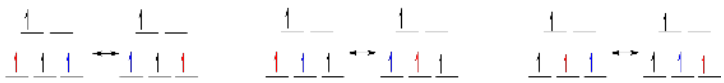
c) $[Co(OH_2)_6]^{2+}$ (Δ_o = 14,000 cm^{-1})4

d) $[Co(OH_2)_6]^{3+}$ (Δ_o = 19,000 cm^{-1})4

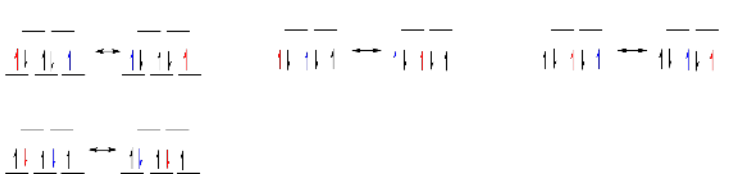
Solutions

1.

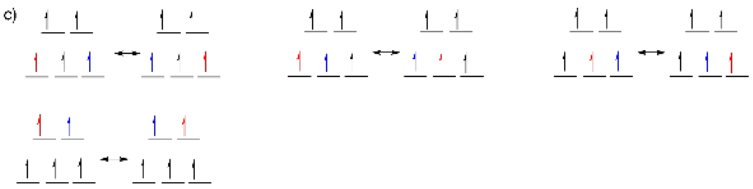
a)



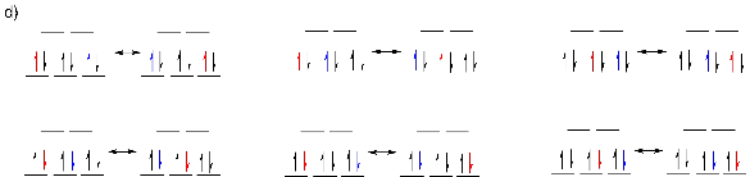
b)



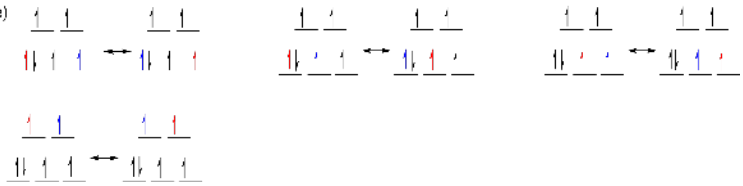
c)



d)



e)



2. Determine the difference in Π_c between the high spin and low spin configuration in each of the following cases:

a) d^4



The difference is: ΔE = ls – hs = Π_c – 0 = Π_c.

b) d^5



The difference is: ΔE = ls – hs = $2\Pi_c$ – 0 = $2\Pi_c$.

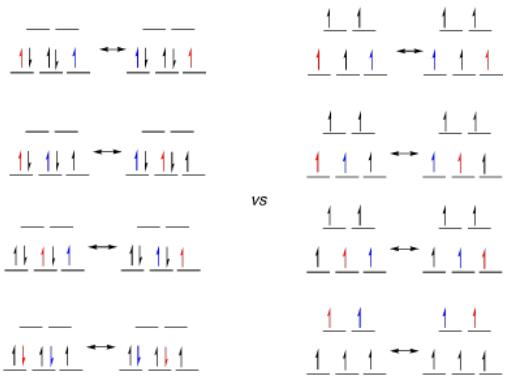
c) d^6



The difference is: ΔE = ls – hs = $2\Pi_c$ – 0 = $2\Pi_c$.

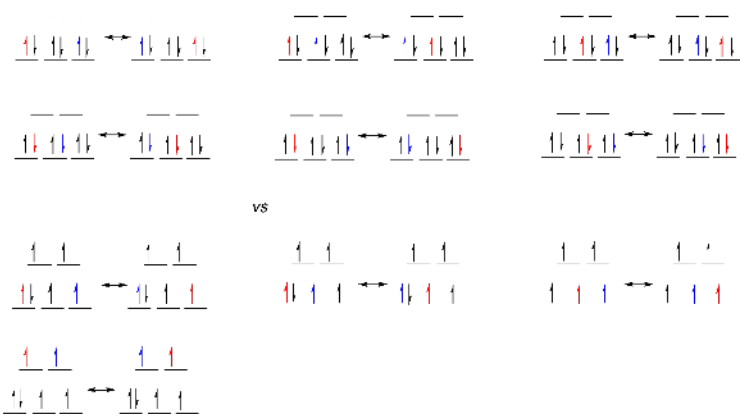
3. Determine the difference in Π_e between the high spin and low spin configuration in each of the following cases:

a) d^5



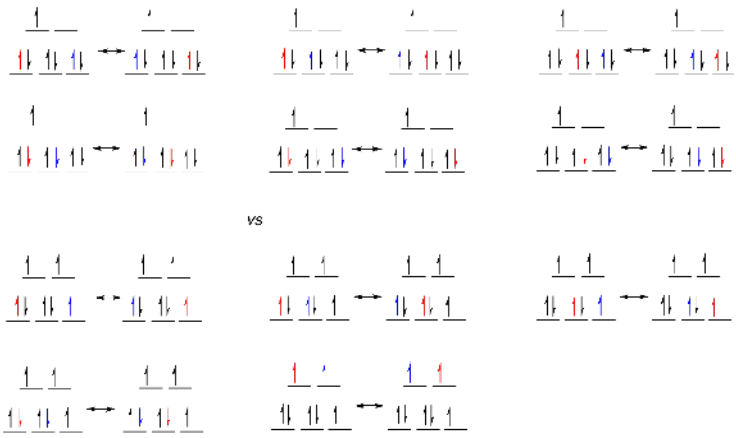
The difference is: ΔE = ls – hs = $4\Pi_e - 4\Pi_e = 0$

b) d_6



The difference is: ΔE = ls – hs = $6\Pi_e - 4\Pi_e = 2\Pi_e$

c) d^7



The difference is: ΔE = ls – hs = $6\Pi_e - 5\Pi_e = \Pi_e$

4. Given the value of Δ_o and Π in each case, predict whether the complex will be high spin or low spin.

a) $[Mn(OH_2)_6]^{2+}$

Δ_o = 7,500 cm^{-1} and Π = 25,500 cm^{-1}; because it costs more to pair electrons than to promote one, this complex will be high spin.

b) $[Mn(OH_2)_6]^{3+}$

Δ_o = 21,000 cm^{-1} and Π = 28,000 cm^{-1}; because it costs more to pair electrons than to promote one, this complex will be high spin.

c) $[Co(OH_2)_6]^{2+}$ (Δ_o = 10,000 cm^{-1})4

Δ_o = 10,000 cm^{-1} and Π = 22,500 cm^{-1}; because it costs more to pair electrons than to promote one, this complex will be high spin.

d) $[Co(OH_2)_6]^{3+}$ (Δ_o = 19,000 cm^{-1})4

Δ_o = 19,000 cm^{-1} and Π = 21,000 cm^{-1}; because it costs more to pair electrons than to promote one, this complex will be high spin, but note how similar the values are. Many Co(III) complexes are low spin.

References.

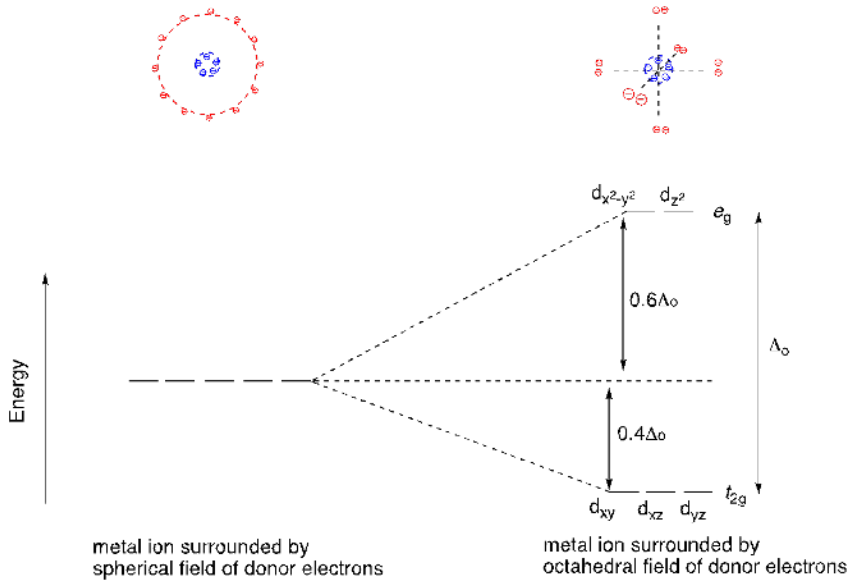
1. Dunn, T. M.; McClure, D. S.; Pearson, R. G. *Some Aspects of Crystal Field Theory*. Harper & Row: New York, 1965, p.82.
2. Sienko, M. A.; Plane, R. A. *Physical Inorganic Chemistry*. W. A. Benjamin: New York, 1963, p. 56.
3. Miessler, G. L.; Fischer, P. J.; Tarr, D. A. *Inorganic Chemistry, 5th Ed*. Pearson: Boston, 2014, p. 374.
4. Figgis, B. N.; Hitchman, M. A, *Ligand Field Theory and Its Applications*. Wiley-VCH: Brisbane, 2000, p. 215

This page titled 9.7: Orbital Splitting and Electron Spin is shared under a CC BY-NC 4.0 license and was authored, remixed, and/or curated by Chris Schaller.

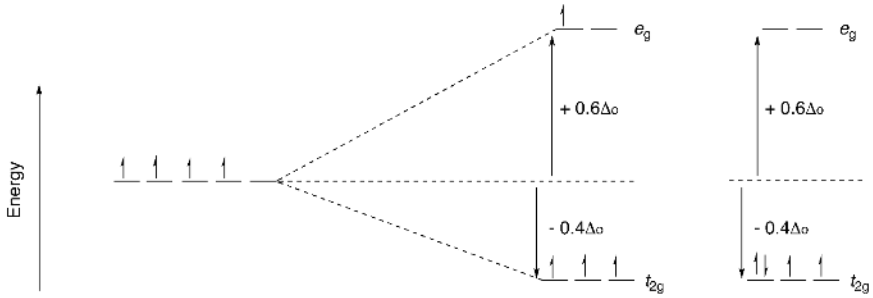
- **10.3.2: Orbital Splitting and Electron Spin** by Chris Schaller is licensed CC BY-NC 4.0.

9.8: Ligand Field Stabilization Energy

If we want to compare the stability of a particular electron configuration compared to the imaginary d electron configuration in a spherical electric field, we can calculate the ligand field stabilization energy. Remember, in crystal field theory, we compared the d electrons in a spherical field to the situation in which ligands approached in an octahedral geometry. The e_g level is destabilized by $0.6\Delta_o$ compared to undifferentiated d orbitals in a spherical field, whereas the t_{2g} level is $0.4\Delta_o$ lower in energy than the d orbitals in a spherical field.



Let's look at the case of a d^4 complex. That's an interesting case, because as we fill in the d electrons one by one, it is the first example in which there is the possibility of either a high spin or a low spin configuration. If we first consider the high-spin case, then we see that three of the electrons drop into the t_{2g} level and the last one goes into the e_g level.



The ligand field stabilization energy is the difference between energy in a spherical field and in an octahedral field. In the high spin d^4 case, that means three electrons are lower in energy and one is higher in an octahedral environment.

- High spin d^4:

$$\begin{aligned} \textbf{LFSE} &= [0.6(1)–0.4(3)]\Delta_o \\ &= [0.6–1.2]\Delta_o \\ &= -0.6\Delta_o \end{aligned}$$

For comparison, in the low spin case, all four of the electrons are lower in energy in the presence of the octahedral field.

- Low spin d^4:

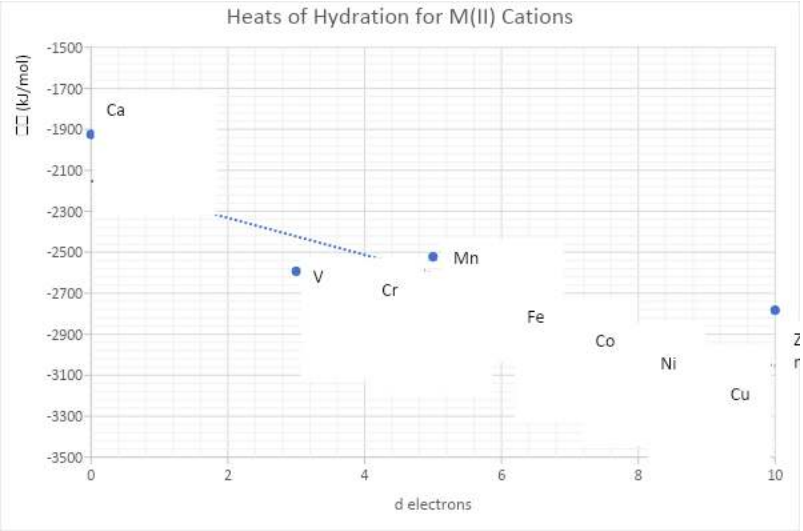
$$\begin{aligned} \textbf{LFSE} &= [0.6(0)–0.4(4)]\Delta_o \\ &= -1.6\Delta_o \end{aligned}$$

Of course, the ligand field stabilization energy isn't the only contributor to energetic differences between possible electron configurations. Pairing energy will also play a role, including Coulombic or repulsive terms as well as exchange terms. The total energy difference between a high spin and low spin configuration will compare those energies as well. For the d^4 case:

$$\Delta E(\text{low spin} - \text{high spin}) = (-1.6\Delta_o + \Pi_c + 3\Pi_e) - (-0.6\Delta_o + 3\Pi_e)$$
$$= -\Delta_o + \Pi_c$$

One application of ligand field stabilization energy is found in the hydration energies of metal ions. As a first approximation, we might expect that the energy released when a bond is formed between a ligand and a metal ion would be related to Coulomb's Law. If we look at values for the hydration of gas-phase ions, we expect the energies of reaction to become more negative as we move across the transition metals from left to right. That increase in magnitude of the exothermicity of hydration reflects the periodic trend in sizes of the ions. Ions of the same charge get smaller as we go to the right because of the increasing number of protons in the nucleus. As the radius of the atom decreases, the energy released upon binding a ligand increases.

The following graph illustrates this general phenomenon for a series of M^{2+} ions. There are gaps in the graph where data was unavailable. Some of the early transition metals are rarely observed as divalent ions.

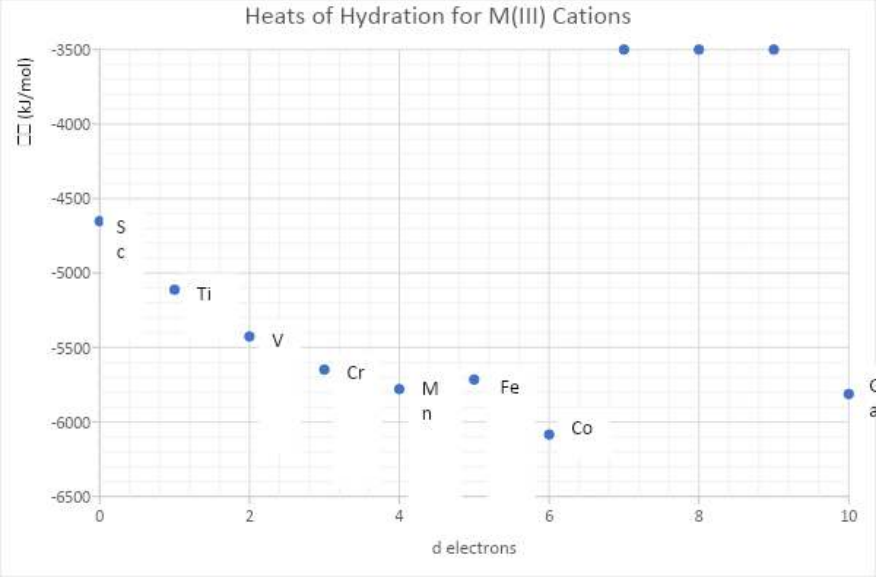


Overall, we can see a general progression towards more negative heats of hydration as we move across the series. That observation is consistent with Coulomb's Law. However, if we look carefully, we can see that some of the data points are a little higher compared to the rest (or a little lower, depending on your perspective). The higher data points occur at d^0, d^5 and d^{10} (Ca^{2+}, Mn^{2+} and Zn^{2+}). Assuming we are dealing with high spin configurations, which is often the case for the first row of transition metals, then these are exactly the cases in which we expect ligand field stabilization energy to be absent. The table below illustrates that point.

Table 3.3.1. Ligand Field Stabilization Energy for High Spin Configuration

Electron count (dn)	LFSE (Δo)
0	0
1	-0.2
2	-0.4
3	-0.6
4	-0.3
5	0
6	-0.2
7	-0.4
8	-0.6
9	-0.3
10	0

We can confirm that what we are seeing is related to the d electron count, rather than some intrinsic property of individual metals, by looking at a similar series of M^{3+} ions. Once again, we observe the overall agreement with Coulomb's Law, and we see that the d^0 cases display a lower heat of hydration than the others because of a lack of ligand field stabilization energy.



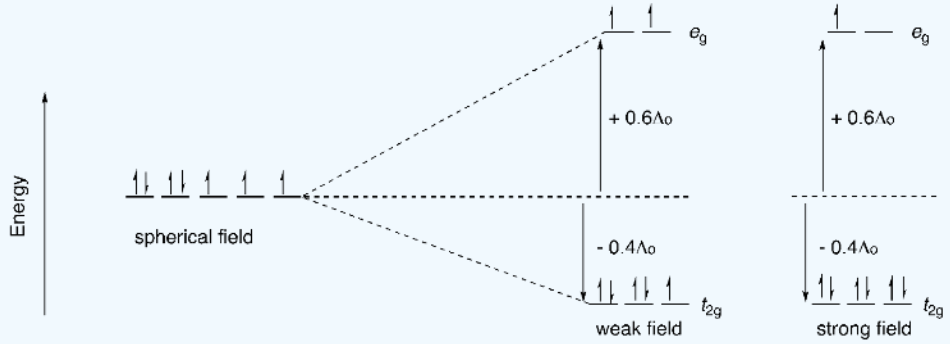
This time, Fe^{3+} is an outlier because it is d^5, rather than the d^4 Mn^{3+}. Again, some of the data is missing here because some of the later transition metals are rarely found as trivalent ions. Conversely, the ions that exhibit ligand field stabilization energies are depressed from the overall trend, displaying additional stabilization in an octahedral coordination environment.

Neither the hydration energies for the M^{2+} ions nor the hydration energies for the M^{3+} ions track perfectly with ligand field stabilization energies. There are a number of other factors that also impact these observed hydration energies, but they are beyond the scope of the current discussion. These factors include the nephelauxetic ("cloud-expanding") effect, in which interelectron repulsion in complexes can be lower than in free ions based on the degree of covalency in the complex.

Example 9.8.1

Draw a diagram showing the energetic differences between d^7 metal ions in a spherical field, a weak field octahedral environment, and a strong field octahedral environment.

Solution



Example 9.8.2

Show how you would calculate the ligand field stabilization energy in the following cases:

a. Low-spin d^5
b. High-spin d^5
c. Low-spin d^7
d. High-spin d^7

Solution

a. Low-spin d^5: LFSE = $[0.6\ (0) – 0.4\ (5)]\Delta_o = -2.0\Delta_o$
b. High-spin d^5: LFSE = $[0.6\ (2) – 0.4\ (3)]\Delta_o = [1.2 - 1.2]\Delta_o = 0\Delta_o$
c. Low-spin d^7: LFSE = $[0.6\ (1) – 0.4\ (6)]\Delta_o = [0.6 - 2.4]\Delta_o = -1.8\Delta_o$
d. High-spin d^7: LFSE = $[0.6\ (2) – 0.4\ (5)]\Delta_o = [1.2 - 2.0]\Delta_o = -0.8\Delta_o$

Example 9.8.3

Calculate the difference between low spin and high spin electronic configurations in the following cases:

a. d^5
b. d^7

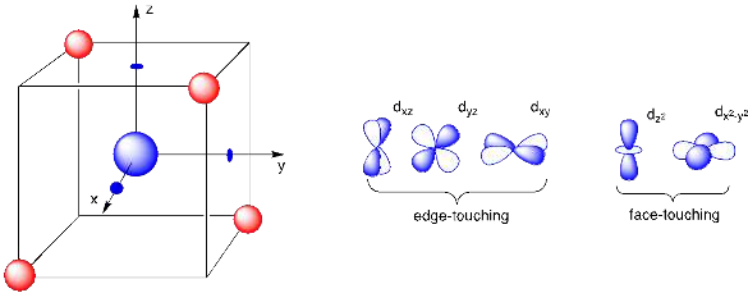
Solution

1. d^5: ΔE low spin – high spin = $(-2.0\Delta_o + 2\Pi_c + 4\Pi_e) - (0\Delta_o + 4\Pi_e) = -2\Delta_o$
2. d^7: ΔE low spin – high spin = $(-1.8\Delta_o + 3\Pi_c + 6\Pi_e) - (-0.8\Delta_o + 2\Pi_c + 5\Pi_e) = -\Delta_o + \Pi_c + \Pi_e$

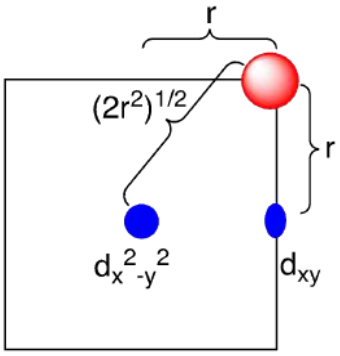
This page titled 9.8: Ligand Field Stabilization Energy is shared under a CC BY-NC 4.0 license and was authored, remixed, and/or curated by Chris Schaller.

9.9: Tetrahedral Complexes

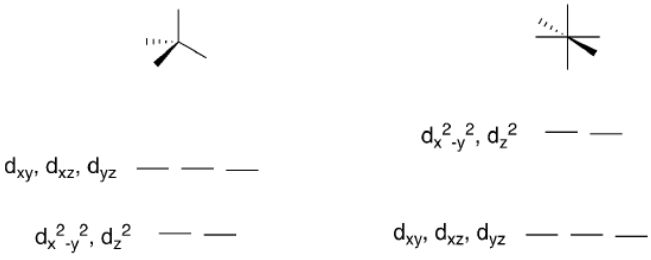
Tetrahedral geometry is even more common in chemistry than square planar geometry. Assessing the orbital interactions in tetrahedral geometry is somewhat more complicated, however, and it is common to proceed directly to a group theory approach. Nevertheless, let's take a look at this geometry and see what we can determine through simple observation before we see the results from a more rigorous approach. To begin, it helps to know that a tetrahedral geometry is defined as having four atoms arranged at alternating corners of a cube around a central atom.



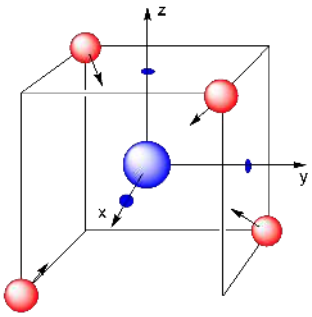
If we consider the orientation of the d orbitals, we find that they fall into two different groups. Although all five orbitals lie off-axis with respect to the ligands, some of them are pointed directly at the edges of the cube (d_{xy}, d_{xz}, d_{yz}) whereas the others point at the faces of the cube ($d_{x^2-y^2}$, d_{z^2}). The edge-touching orbitals lie a little closer to the ligands; we'll define this distance as *r*, which in this case is half the edge length of the cube. The face-touching orbitals are slightly farther away: based on the Pythagorean theorem, they are $r^2 + r^2 = 2\,r^2 = r^2$ away from the ligands.



Based on that simple observation, we might start to think about the dxy, dxz and dyz group as forming the antibonding orbitals upon interaction with the ligands. The dz2 and dx2-y2 would be left as non-bonding orbitals. This result would be exactly the opposite of the octahedral case. We would therefore expect an orbital splitting diagram that is exactly the inverse of the octahedral one. Maybe the splitting between orbital levels would be a little smaller, though, because of the lack of direct overlap between the ligands and the metal orbitals. After all, even the closest set of metal orbitals don't point directly at the ligands like in the octahedral case.

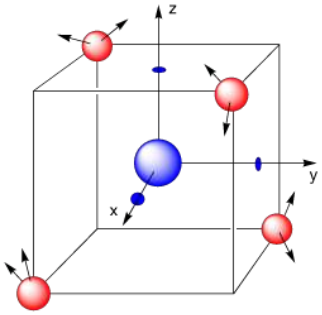


This supposition is confirmed through a group theory approach. We can use vectors pointing along the ligand-metal axes to examine sigma bonding, as shown below. We would subject these vectors to the symmetry transformations in the tetrahedral space group, T_d, shown in the table.



T_d	E	$8C_3$	$6C_2$	$6S_4$	$6\sigma_d$		
A_1	1	1	1	1	1		$x^2 + y^2 + z^2$
A_2	1	1	1	-1	-1		
E	2	-1	2	0	0		$(2z^2 - x^2 - y^2, x^2 - y^2)$
T_1	3	0	-1	1	-1	(R_x, R_y, R_z)	
T_2	3	0	-1	-1	1	(x, y, z)	(xy, xz, yz)
Γ_σ	4	1	0	0	2		$A_1 + T_2$
Γ_π	8	-1	0	0	0		$E + T_1 + T_2$

That analysis leads to the reducible representation for sigma bonding, Γ_σ , shown in the table. This representation reduces to the irreducible representations, $A_1 + T_2$. The d orbitals represented here, the T_2 set, are indeed the d_{xy}, d_{xz} and d_{yz}. The non-bonding d orbitals are the E group, corresponding to d_{z^2} and $d_{x^2-y^2}$.



We can go further with the group theory approach and to determine the reducible representation for pi bonding, Γ_π , also shown in the table. Pi bonding is otherwise even more difficult to assess via simple inspection than was sigma bonding. The resulting representation reduces to $E + T_1 + T_2$. The d orbitals represented here include the expected d_{z^2} and $d_{x^2-y^2}$. Note, however, that they also include the d_{xy}, d_{xz}, and d_{yz} orbitals. That means that in the presence of a pi-donor ligand, the latter set are antibonding with respect to both sigma and pi bonding.

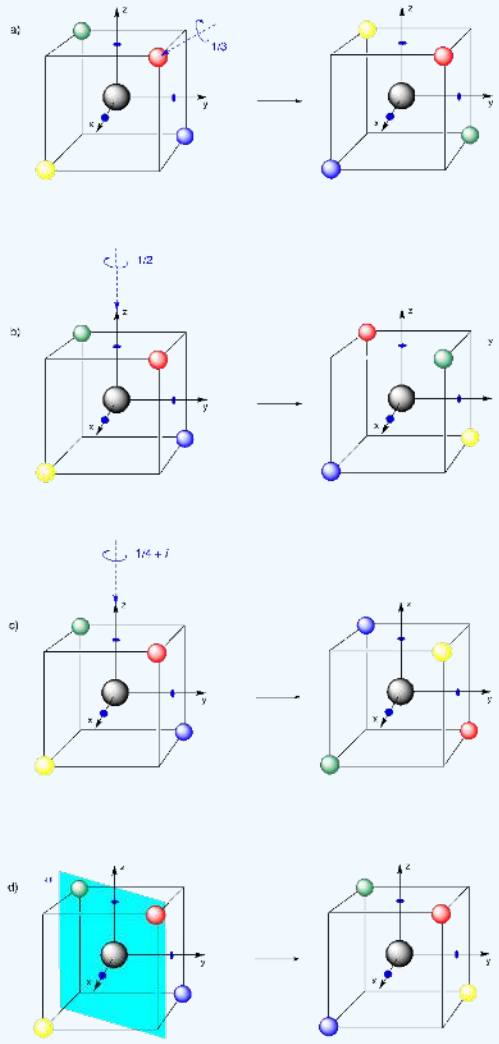
Example 9.9.1

Demonstrate these symmetry operations on the drawing of the tetrahedron within a cube shown above.

a. C_3
b. C_2
c. S_4
d. σ_d

https://chem.libretexts.org/@go/page/403086

Solution



This page titled 9.9: Tetrahedral Complexes is shared under a CC BY-NC 4.0 license and was authored, remixed, and/or curated by Chris Schaller.

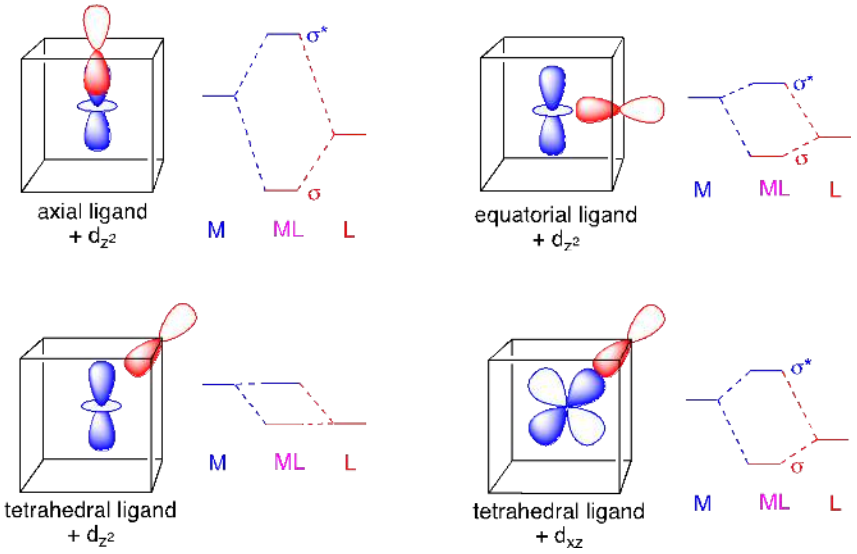
9.10: Ligand Field Theory New Page

9.10: Ligand Field Theory New Page is shared under a not declared license and was authored, remixed, and/or curated by LibreTexts.

9.11: Angular Overlap

The angular overlap model is an approach to quantifying the interaction between metal and ligand orbitals in different geometries, with a focus on the metal d orbitals. Although developed in the 1970's, this approach is still used as a starting point for theoretical calculations using advanced computational chemistry methods available today.1

The core concept of the angular overlap model is that different ligand orbitals will overlap with metal d orbitals to different extents because of the variety of angles at which these orbitals would approach each other. Stronger overlap leads to greater interaction. That means both greater stabilization of the ligand-centered bonding orbital and greater destabilization of the metal-centered antibonding orbital.



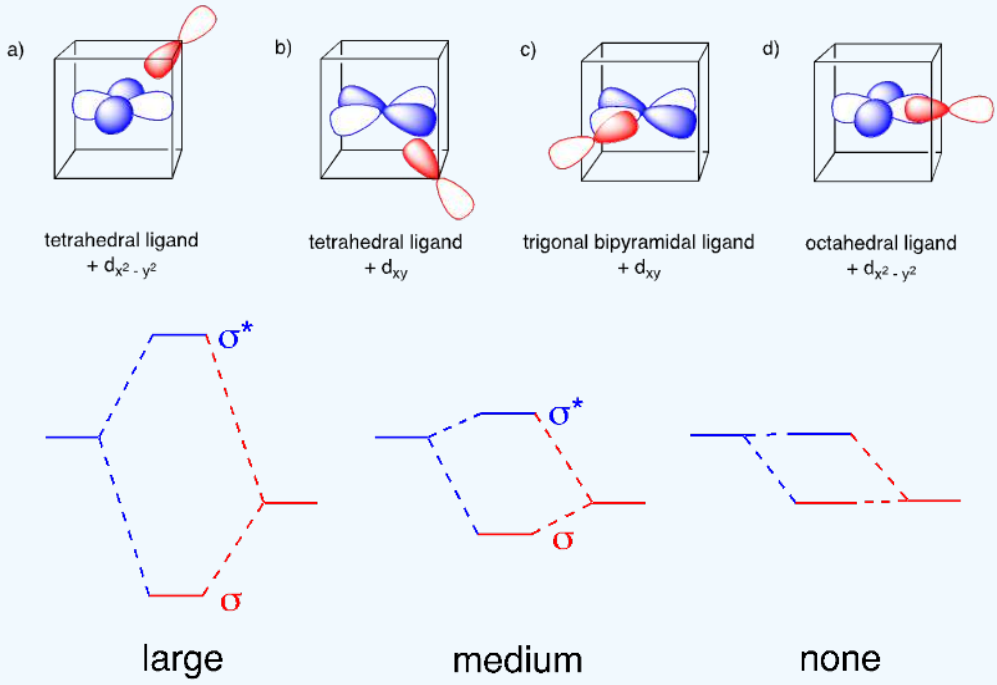
Let's look at some examples. Consider the overlap of the d_{z^2} orbital with an axial ligand in octahedral geometry, with the assumption that the d_{z^2} orbital lies in the axial direction. There should be considerable overlap between the metal and ligand orbitals, leading to both significant stabilization of the ligand donor electrons and similar destabilization of an electrons in the metal d_{z^2} orbital. By comparison, an equatorial ligand would have significantly less overlap with the d_{z^2} orbital. Instead of overlapping with the substantial lobe along the z axis, the ligand would be interacting with the minimal d_{z^2} toroid in the xy plane. The bonding orbital would be stabilized to a significantly lesser extent compared to the axial ligand. The antibonding orbital would be destabilized by a correspondingly smaller amount.

In the case of a tetrahedral ligand, there is essentially no overlap with the d_{z^2} orbital because its on-axis lobe is too far away from the cubic corner positions occupied by ligands in a tetrahedral array. There is really no bonding or antibonding in this case. On the other hand, the dxz orbital reaches a little closer to that corner position, allowing for some overlap with the ligand orbital. Consequently, there is some stabilization of the bonding electrons and destabilization of the antibonding d orbital. At first glance, the amount of overlap in this case, and the amount of stabilization or destabilization, appears much more similar to the case of the equatorial ligand with the d_{z^2} orbital than the axial ligand with the d_{z^2} orbital.

We will not go into the mathematics that explore the exact extent of overlap expected in each case. Instead, we will go straight to a summary of the results in the next section.

? Exercise 9.11.1

Estimate the degree of interaction between the ligand and metal orbital: large, medium, or none.



Answer

a) none b) medium c) medium (although it may appear greater than in (b), and it is) d) large

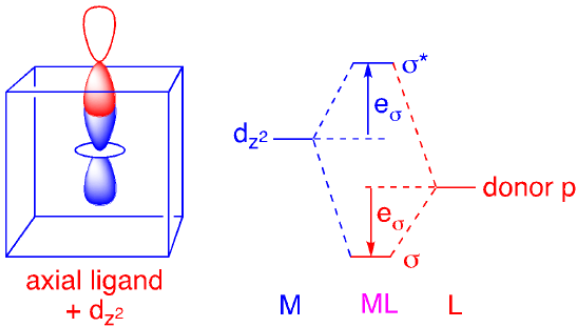
References

1. For example: Chilkuri, V. G.; DeBeer, S.; Neese, F. Ligand Field Theory and Angular Overlap Model Based Analysis of the Electronic Structure of Homovalent Iron–Sulfur Dimers. *Inorg. Chem.* **2020**, *59*(2), 984-995.

This page titled 9.11: Angular Overlap is shared under a CC BY-NC 4.0 license and was authored, remixed, and/or curated by Chris Schaller.

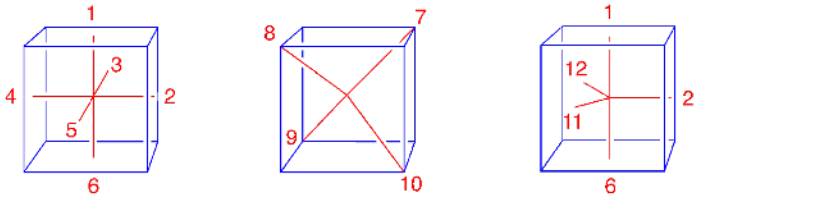
9.12: Sigma Bonding in the Angular Overlap Model

The pictures we considered previously explicitly addressed sigma overlap between the ligand donor orbital and the metal d acceptor orbital. The donor electrons drop in energy into the new sigma bonding combination and any electrons in the d orbital are raised into the new sigma antibonding combination. For example, when an axial ligand interacts with a metal dz2 orbital, the in-phase, bonding combination drops in energy by a quantity that we will call eσ. At the same time, the out-of-phase, antibonding combination is raised in energy by the same quantity, eσ. A real computational treatment would reveal that this is not exactly true; the amount of energy by which the bonding orbital is stabilized is slightly different from the amount by which the antibonding orbital is destabilized. However, the distinction is pretty minor for our purposes.



From the interactions we have already looked at, we know that this specific interaction is a strong one. Other metal-ligand interactions may involve less overlap than this one and will lead to smaller changes in energy. For this reason, other metal-ligand interactions are expressed as fractions of the quantity, eσ, found in the case of the dz2 orbital interacting with an axial ligand.

Our first task is to label the positions that will be occupied by ligands in a number of different geometries. To avoid a cluttered diagram of these positions, we can use three separate illustrations to illustrate the ligand positions in some common geometries. The first drawing below includes all the geometries in which ligands are found along Cartesian coordinates. The second drawing describes tetrahedral geometry, whereas the third one describes trigonal structures.



Given those ligand positions, we can assess the interactions that would occur if ligands were purely sigma donors. For reference, the dz2 orbital is assumed to lie along the axis between positions 1 and 6 and the magnitudes of the interactions are all scaled relative to the interaction of a ligand at position 1 or 6 with the dz2 orbital. We will not address the approach that was taken to arrive at these relative numbers; we will simply use the results tabulated here.

Sigma Interactions of Ligands with Metal d Orbitals (units of eσ)

Ligand Positions	dz2	dx2-y2	dxy	dxz	dyz
1	1	0	0	0	0
2	1/4	3/4	0	0	0
3	1/4	3/4	0	0	0
4	1/4	3/4	0	0	0
5	1/4	3/4	0	0	0
6	1	0	0	0	0
7	0	0	1/3	1/3	1/3
8	0	0	1/3	1/3	1/3
9	0	0	1/3	1/3	1/3
10	0	0	1/3	1/3	1/3
11	1/4	3/16	9/16	0	0
12	1/4	3/16	9/16	0	0

In order to quantify the interactions between ligands and metal orbitals, we simply tally up the interactions for each orbital. For example, consider a complex like hexaamminecobalt(III) chloride, [Co(NH3)6]Cl3. It has six sigma donor ligands, forming an octahedral structure. The total interactions with each orbital in this geometry would be calculated by totaling the interactions at all the ligand positions for each orbital.

Looking under the dz2 column and totaling only the values for positions 1 through 6, we find:

dz2: (1 + 1/4 + 1/4 + 1/4 + 1/4 + 1) eσ = 3eσ

A similar approach using the dx2-y2 column leads to:

dx2-y2: (0 + 3/4 + 3/4 + 3/4 + 3/4 + 0) eσ = 3eσ

However, the remaining three d orbitals have no interactions with the ligands in these six positions:

dxy: 0; dxz: 0; dyz: 0

So, we find that the dz2 and dx2-y2 orbitals are both raised in energy by 3eσ. At the same time, we know that the ligand donor orbitals are stabilized by their interaction with the metal orbitals. To see how much, we can tally up the interaction for each ligand at its position. That is, for the ligand in position 1, we would add in its interaction with each of the five d orbitals to determine the amount by which it is stabilized by bonding. We simply add up the values across that row.

Ligand in position 1: - (1 + 0 + 0 + 0 + 0) eσ = - eσ

Ligand in position 2: - (1/4 + 3/4 + 0 + 0 + 0) eσ = - eσ

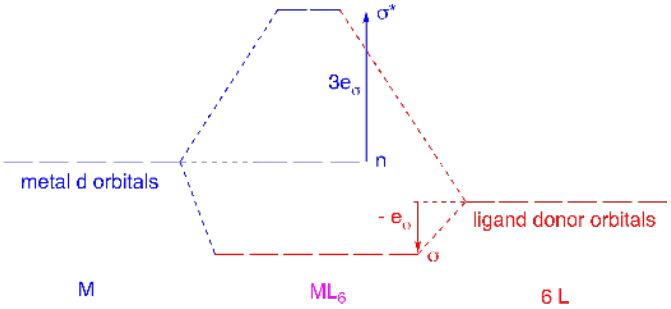
Ligand in position 3: - (1/4 + 3/4 + 0 + 0 + 0) eσ = - eσ

Ligand in position 4: - (1/4 + 3/4 + 0 + 0 + 0) eσ = - eσ

Ligand in position 5: - (1/4 + 3/4 + 0 + 0 + 0) eσ = - eσ

Ligand in position 6: - (1 + 0 + 0 + 0 + 0) eσ = - eσ

We have now generated a diagram that looks very much like what we saw from ligand field theory. We see the familiar d orbital splitting diagram for octahedral geometry as well as stabilization of the ligand donor orbitals in sigma bonds.



The results from the angular overlap model are somewhat simplified compared to the results from ligand field theory. For example, they completely neglect any interaction between ligand orbitals and metal s or p orbitals. However, this model allows a very straightforward calculation of the relative d orbital energy levels.

Problems

1. Use the results of the calculation for the octahedral geometry to calculate the net stabilization due to bonding (in units of eσ) for the following complexes.

a) [Co(NH3)6]Cl3 (assume low spin) b) [Fe(NH3)6](NO3)3 (assume high spin)

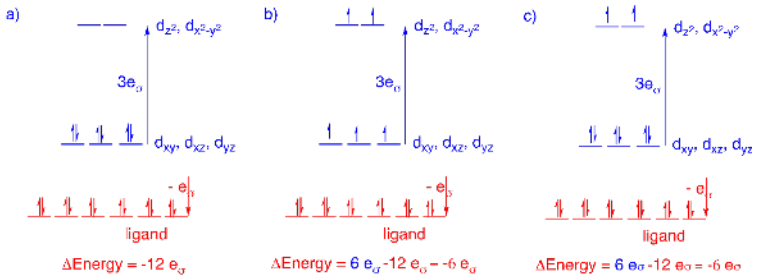
c) [Ni(NH3)6]Cl2

2. Use the table of sigma interactions to calculate orbital energy stabilization or destabilization for the following geometries.

a) trigonal planar ML3 b) square planar ML4 c) trigonal bipyramidal ML5

Solutions

1.



2. a) Positions 2, 11, 12.

dz2: (1/4 + 1/4 + 1/4) eσ = 3/4 eσ

dx2-y2: (3/4 + 3/16 + 3/16) eσ = 18/16 = 9/8 eσ

dxy: (0 + 9/16 + 9/16) eσ = 18/16 = 9/8 eσ

dxz: 0

dyz: 0

Ligand in position 2: - (1/4 + 3/4 + 0 + 0 + 0) eσ = - eσ

Ligand in position 11: - (1/4 + 3/16 + 9/16 + 0 + 0) eσ = - eσ

Ligand in position 12: - (1/4 + 3/4 + 9/16 + 0 + 0) eσ = - eσ

b) Positions 2, 3, 4, 5.

dz2: (1/4 + 1/4 + 1/4 + 1/4) eσ = eσ

dx2-y2: (3/4 + 3/4 + 3/4 + 3/4) eσ = 3 eσ

dxy: 0

dxz: 0

dyz: 0

Ligand in position 2: - (1/4 + 3/4 + 0 + 0 + 0) eσ = - eσ

Ligand in position 3: - (1/4 + 3/4 + 0 + 0 + 0) eσ = - eσ

Ligand in position 4: - (1/4 + 3/4 + 0 + 0 + 0) eσ = - eσ

Ligand in position 5: - (1/4 + 3/4 + 0 + 0 + 0) eσ = - eσ

c) Positions 1, 2, 6, 11, 12.

dz2: (1 + 1/4 + 1+ 1/4 + 1/4) eσ = 11/4 eσ

dx2-y2: (0 + 3/4 + 0 + 3/16 + 3/16) eσ = 18/16 = 9/8 eσ

dxy: (0 + 0 + 0 + 9/16 + 9/16) eσ = 18/16 = 9/8 eσ

dxz: 0

dyz: 0

Ligand in position 1: - (1 + 0 + 0 + 0 + 0) eσ = - eσ

Ligand in position 2: - (1/4 + 3/4 + 0 + 0 + 0) eσ = - eσ

Ligand in position 6: - (1 + 0 + 0 + 0 + 0) eσ = - eσ

Ligand in position 11: - (1/4 + 3/16 + 9/16 + 0 + 0) eσ = - eσ

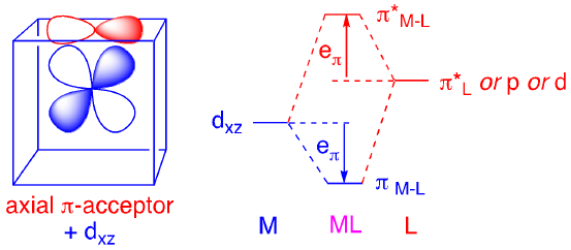
Ligand in position 12: - (1/4 + 3/4 + 9/16 + 0 + 0) eσ = - eσ

This page titled 9.12: Sigma Bonding in the Angular Overlap Model is shared under a CC BY-NC 4.0 license and was authored, remixed, and/or curated by Chris Schaller.

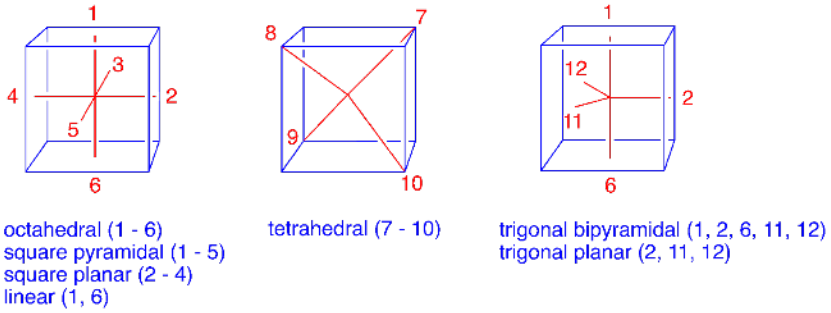
9.13: Pi Acceptors in the Angular Overlap Model

So far, we have considered only the effects of sigma donation on the d orbital splitting diagram using the angular overlap model. When we looked at ligand field theory, we saw that pi-donor and pi-acceptor effects produced significant changes in these diagrams. We generally see these effects in any ligands that have orbitals that can accept electron density from the metal (back-bonding). The paradigm of a pi acceptor is carbon monoxide, of course. Similar effects can be found in related ligands in which the donor atoms participate in pi bonding with another atom in the ligand, thus making a pi* orbital available for back-bonding. In addition, back-bonding is a feature of phosphine ligands and some N-heterocyclic carbenes.

We usually think about this interaction as illustrated below. The empty ligand orbital approaches so that it is perpendicular to the bond axis, allowing overlap with the filled metal d orbital. The interaction lowers the energy of the d electrons, which become bonding in nature, and raises the energy of the empty ligand orbital.



We can use the same ligand positions for pi acceptors that we already used for sigma donors. The orbitals will be oriented differently than the sigma donor orbitals but they will approach from the same directions..

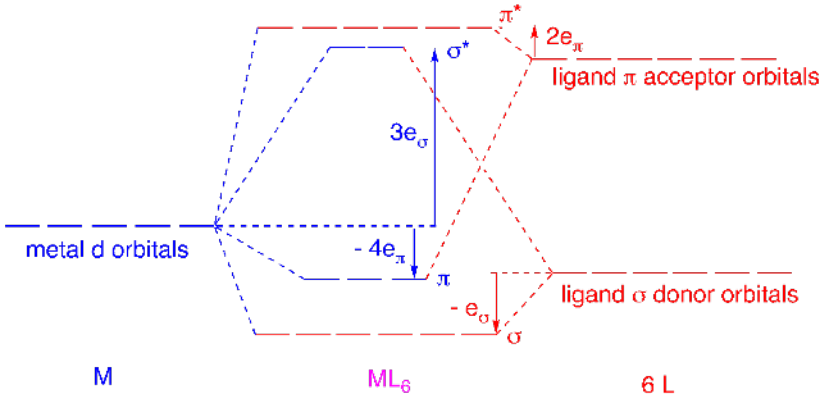


As before, we can use the results of calculations of the strengths of these interactions based on the amount of overlap; we don't need to know exactly how the numbers in the table below came about. This time, the maximum overlap occurs between a dxz orbital and a p orbital approaching in position 1, perpendicular to the bond axis. Several other combinations will be equally strong. This time, the stabilization is expressed in terms of eπ rather that eσ. The amount of energy in this case is somewhat smaller than in sigma donation because of a lesser degree of metal-ligand orbital overlap.

Sigma Interactions of Ligands with Metal d Orbitals (units of eπ)

Ligand Positions	dz2	dx2-y2	dxy	dxz	dyz
1	0	0	0	1	1
2	0	0	1	1	0
3	0	0	1	0	1
4	0	0	1	1	0
5	0	0	1	0	1
6	0	0	0	1	1
7	2/3	2/3	2/9	2/9	2/9
8	2/3	2/3	2/9	2/9	2/9
9	2/3	2/3	2/9	2/9	2/9
10	2/3	2/3	2/9	2/9	2/9
11	0	3/4	1/4	1/4	3/4
12	0	3/4	1/4	1/4	3/4

These interactions modify the picture we built previously for simple sigma donors. In the new interaction diagram, a second set of ligand p orbitals is destabilized by the pi interaction. At the same time, some of the d orbitals are stabilized by the additional interaction. This modification is illustrated below for octahedral geometry.



Problems

1. Use the table of pi interactions to calculate orbital energy stabilization or destabilization for the following geometries.

a) trigonal planar ML3 b) square planar ML4 c) trigonal bipyramidal ML5

Solutions

1. a) Positions 2, 11, 12.

dz2: 0

dx2-y2: - (0 + 3/4 + 3/4) eπ = 6/4 = - 3/2 eπ

dxy: - (1 + 1/4 + 1/4) eσ = 6/4 = - 3/2 eπ

dxz: - (1 + 1/4 + 1/4) eσ = 6/4 = - 3/2 eπ

dyz: - (0 + 3/4 + 3/4) eσ = 6/4 = - 3/2 eπ

Ligand in position 2: (0 + 0 + 0 + 1 + 1) eπ = 2eπ

Ligand in position 11: (0 + 3/4 + 1/4 + 1/4 + 3/4) eπ = 2eπ

Ligand in position 12: (0 + 3/4 + 1/4 + 1/4 + 3/4) eπ = 2eπ

b) Positions 2, 3, 4, 5.

dz2: 0

dx2-y2: 0

dxy: - (1 + 1 + 1 + 1) = -4 eπ

dxz: - (1 + 0 + 1 + 0) = -2 eπ

dyz: - (0 + 1 + 0 + 1) = -2 eπ

Ligand in position 2: (0 + 0 + 1 + 1 + 0) eπ = 2 eπ

Ligand in position 3: (0 + 0 + 1 + 0 + 1) eπ = 2 eπ

Ligand in position 4: (0 + 0 + 1 + 1 + 0) eπ = 2 eπ

Ligand in position 5: (0 + 0 + 1 + 0 + 1) eπ = 2 eπ

c) Positions 1, 2, 6, 11, 12.

dz2: 0

dx2-y2: - (0 + 0 + 0 + 3/4 + 3/4) eπ = -3/2 eπ

dxy: - (0 + 1 + 0 + 1/4 + 1/4) eπ = -3/2 eπ

dxz: - (1 + 1 + 1 + 1/4 + 1/4) eπ = -7/2 eπ

dyz: - (1 + 0 + 1 + 3/4 + 4/4) eπ = -7/2 eπ

Ligand in position 1: (0 + 0 + 0 + 1 + 1) eπ = 2 eπ

Ligand in position 2: (0 + 0 + 1 + 1 + 0) eπ = 2 eπ

Ligand in position 6: (0 + 0 + 0 + 1 + 1) eπ = 2 eπ

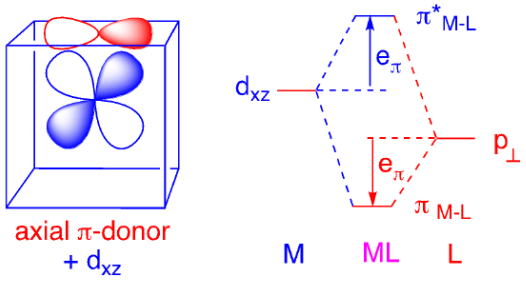
Ligand in position 11: (0 + 3/4 + 1/4 + 1/4 + 3/4) eπ = 2 eπ

Ligand in position 12: (0 + 3/4 + 1/4 + 1/4 + 3/4) eπ = 2 eπ

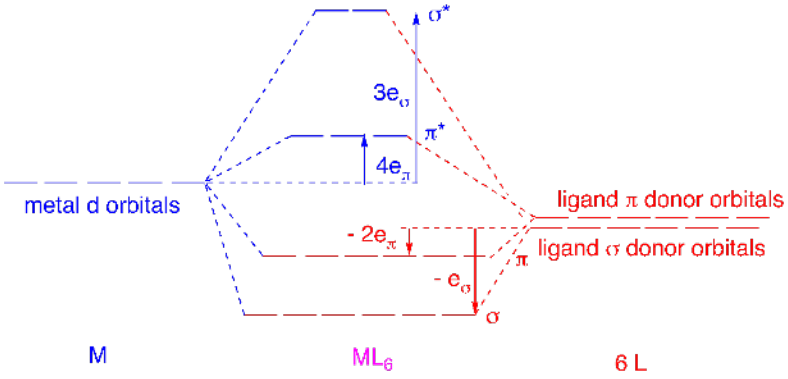
This page titled 9.13: Pi Acceptors in the Angular Overlap Model is shared under a CC BY-NC 4.0 license and was authored, remixed, and/or curated by Chris Schaller.

9.14: Pi Donors in the Angular Overlap Model

Ligands in which the donor atom has more than one lone pair are capable of pi donation to the metal. Common examples include halide and alkoxide ligands. The overlap question in this case is exactly the same as in the case of pi acceptors; the same table of interactions applies here. However, since the ligand electrons are forming the pi bond in this case, the ligand electrons are stabilized and the d orbitals with which they overlap are destabilized.



In octahedral geometry, for example, we see the off-axis d orbitals raised modestly in energy in the presence of pi donor ligands. The angular overlap model allows us to quantify the relative changes in energy because of these ligand interactions.



Example 9.14.1

Confirm the stabilization and destabilization of orbitals due to pi donation in the octahedral interaction diagram shown above.

Solution

Positions 1, 2, 3, 4, 5, 6.

- dz2: 0
- dx2-y2: 0
- dxy: (0 + 1 + 1 + 1 + 1 + 0) = 4 eπ
- dxz: (1 + 1 + 0 + 1 + 0 + 1) = 4 eπ
- dyz: (1 + 0 + 1 + 0 + 1 + 1) = 4 eπ

- Ligand in position 1: (0 + 0 + 0 + 1 + 1) eπ = 2 eπ
- Ligand in position 2: (0 + 0 + 1 + 1 + 0) eπ = 2 eπ
- Ligand in position 3: (0 + 0 + 1 + 0 + 1) eπ = 2 eπ
- Ligand in position 4: (0 + 0 + 1 + 1 + 0) eπ = 2 eπ
- Ligand in position 5: (0 + 0 + 1 + 0 + 1) eπ = 2 eπ
- Ligand in position 6: (0 + 0 + 0 + 1 + 1) eπ = 2 eπ

This page titled 9.14: Pi Donors in the Angular Overlap Model is shared under a CC BY-NC 4.0 license and was authored, remixed, and/or curated by Chris Schaller.

9.15: The Spectrochemical Series

The spectrochemical series was determined through an examination of the absorption spectra of a series of octahedral $Co(III)$ complexes by Tsuchida in the 1930's. The position of the d-d absorption band is influenced by the field strength of the ligand, which leads to greater or lesser values of Δ_o. That interaction depends on both the relative energies of the metal and ligand orbitals and the degree of overlap between these orbitals. The closer in energy the two orbitals are to each other, the greater the interaction. Also, the greater the overlap between the two orbitals, the greater the interaction.

Recall that sigma donors simply donate a lone pair to the metal but do not have additional metal-ligand interactions. The classic example is ammonia. The nitrogen in ammonia has only one lone pair to donate and is a simple sigma donor. Ethylenediamine, $NH_2CH_2CH_2NH_2$ (en), is also a sigma donor because it has a single lone pair on each nitrogen atom. The en ligand is a slightly stronger sigma donor than ammonia. The difference is explained by the slightly stronger basicity of en compared to ammonia; the nitrogen lone pairs in en are better donors to both protons and metal ions.

en > NH3 (basicity)

The common pi donors include the halides and some oxygen donors. In these cases, the donor atom has an additional lone pair (or more) which may engage in formation of a pi bond by donation to a metal d orbital. Among the halides, fluoride produces the largest field splitting and iodide the smallest. This trend is also explained in terms of the relative basicity of these halides; fluoride is more basic than bromide. In addition, there is also understood to be better overlap between fluorine's p orbital and the d acceptor of a positively charged metal ion, compared to larger halides such as iodine.

F- > Cl- > Br- > I- (basicity)

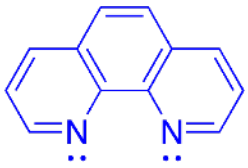
Oxygen donors do not follow this basicity trend. Hydroxide is thought to act as a better pi donor than water, partly because of its negative charge. A carboxylate ligand is not quite as strong a pi donor as hydroxide, probably because its lone pair is delocalized into the carbonyl group.

H20 > RCO2- > HO- (pi donation anion vs neutral)

The pi acceptors include familiar examples such as carbon monoxide (carbonyl ligand) as well as the aromatic phenanthroline.

CO > -CN > phenanthroline > NO2- > SCN-

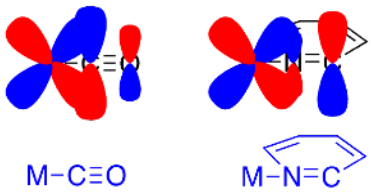
The phenanthroline may be an unfamiliar ligand. It is an aromatic amine, like pyridine. Other aromatic ligands, if they donate through a lone pair such as a phenyl, $C_6H_5^-$, can also be considered pi acceptors. These compounds feature a pi bond that includes the donor atom, so there is a pi* orbital at that position capable of undergoing back-donation from the metal.



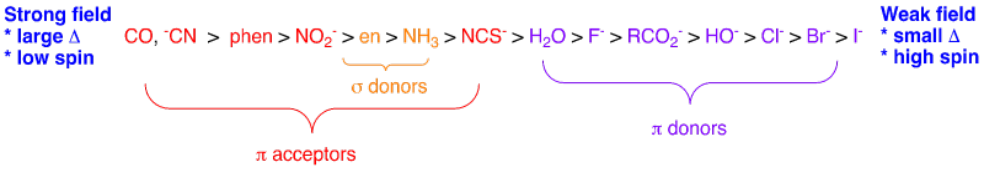
phenanthroline (phen)

Again, there are subtle variations among the field strengths exhibited by these pi acceptors, and there may be several factors contributing to those differences. For example, the cyanide is only slightly weaker field than the isoelectronic carbon monoxide. That small difference may be due to the negative charge on the cyanide rendering it a weaker electron acceptor. On the other hand, phenanthroline is neutral, but it is still a weaker donor than carbon monoxide. That weaker field may be due to the smaller lobe on the nitrogen atom in the pi* orbital in phenanthroline. Because nitrogen is more electronegative than carbon, it makes a greater contribution to the C=N pi bonding orbital than carbon; the opposite is true in the antibonding orbital. Carbon monoxide, in contrast, features a larger lobe on carbon in its pi* orbital. The result is better metal-ligand pi overlap with carbon monoxide than with phenanthroline.

Phosphines are also commonly considered to be pi acceptors, for subtle reasons that have been subject to some debate.1

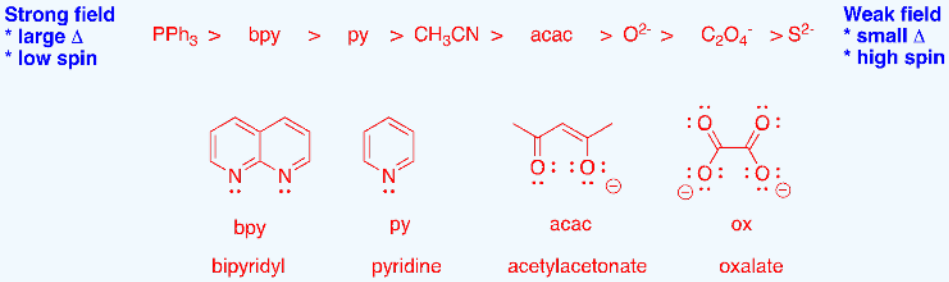


All three of these series can be collated to arrive at a combined list, which is a more complete spectrochemical series. Note that there may be some overlap between the different types of donors. Nevertheless, the overall trend holds: pi acceptors lead to the greatest field splitting on average, whereas di donors lead to the smallest.



Example 9.15.1

Some additional common ligands are displayed according to field strength, below. Classify these ligands as pi donors, sigma donors, or pi acceptors.



Solution

Ph3, based on its structure, appears to be a sigma donor only because it has just one lone pair on the donor atom. However, phosphines tend to behave as pi acceptors; that is, they appear to withdraw some electron density from the metal as indicated by the response of reporter ligands such as CO.

Bpy, py and CH3CN (acetonitrile) all appear to be pi acceptors. Like phen, they behave as weak pi acceptors.

Acac, oxide, oxalate and sulfide are all pi donors. The donor atom in each case has a lone pair in addition to the sigma donor pair.

References

1. Wolczanski, P. T. "Flipping the Oxidation State Formalism: Charge Distribution in Organometallic Complexes as Reported by Carbon Monoxide". *Organometallics* **2017**, *36*, 622-631.

This page titled 9.15: The Spectrochemical Series is shared under a CC BY-NC 4.0 license and was authored, remixed, and/or curated by Chris Schaller.

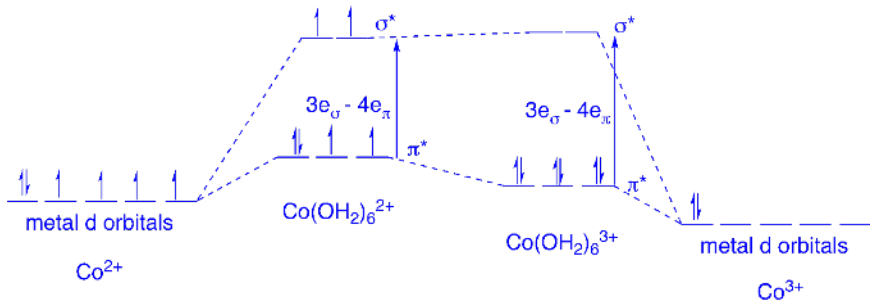
9.16: The Magnitude of Parameters eσ, eπ and Δ

In the angular overlap model (AOM), the field splitting, Δ, can be shown to result from a combination of the interaction parameters eσ and eπ. For example, in octahedral geometry,

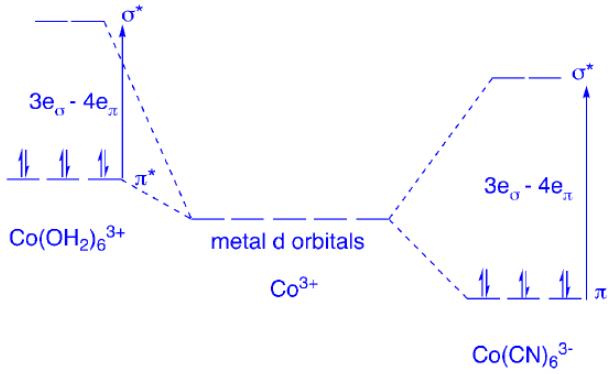
$$\Delta = 3e\sigma - 4e\pi \tag{9.16.1}$$

in which the value of eπ is positive for a pi donor but negative for a pi acceptor.

The magnitude of these parameters varies from one complex to another. As we have seen previously in examination of ligand field theory, both the metal ion and the identity of the ligand play a role in determining the magnitude of the field splitting. As outlined in the previous section on ligand field theory, the identity of the metal influences the d orbital splitting. Even for the same element, an increase in charge translates into a significant increase in the splitting parameter. For this reason, aqueous $\mathrm{Co(II)}$ ion is high spin, whereas the aqueous $\mathrm{Co(III)}$ ion is low spin.



The spectrochemical series tells us that the ligands also play a major role in determining the magnitude of the field splitting, with pi donors producing a smaller splitting than pi acceptors. The splitting produced by an aquo ligand is much smaller than the produced by a cyano ligand, for example.



Spectroscopic data can be used to determine the parameters eσ and eπ. A series of examples for different ligands coordinated to the $\mathrm{Cr^{3+}}$ ion are outlines in Table 9.16.1.

Table 9.16.1: Angular Overlap Parameters in Octahedral Cr(III) Complexes[1]

Ligand	eσ	eπ	Δ (cm-1)
		π acceptors	
-CN	7,530	-930	26,310
pyridine	6,150	-330	19,770
		σ donors	
en	7,260	assumed 0	21,780
NH3	7,180	assumed 0	21,540
		π donors	
HO-	8,600	2,150	17,200
H2O	7,550	1,850	15,250
F-	8,200	2,000	16,600
Cl-	5,700	980	13,180
Br-	5,380	950	12,430
I-	4,100	670	9,620

It is worth noting that the parameters observed for Cr(III), although mostly consistent with the spectrochemical series, are not identical to those seen in Co(III). In particular, the places of water and hydroxide are switched in the series. Once again, the identity of the metal plays a role in the strength of interaction with the ligand, and certain ligands may be observed to interact more strongly with some metals than with others.

Example 9.16.1

Calculate Δ for tetrahedral $\mathbf{Ni^{2+}}$ when coordinated with the following ligands, given the parameters eσ and eπ.[1]

a. $\mathbf{PPh_3}$ with $e\sigma = 5,000\ \mathbf{cm^{-1}}$ and $e\pi = -1,750\ \mathbf{cm^{-1}}$
b. $\mathbf{Cl^-}$ with $e\sigma = 3,900\ \mathbf{cm^{-1}}$ and $e\pi = 1,500\ \mathbf{cm^{-1}}$
c. $\mathbf{Br^-}$ with $e\sigma = 3,600\ \mathbf{cm^{-1}}$ and $e\pi = -1,000\ \mathbf{cm^{-1}}$

Solution

This question is a direct application of Equation 9.16.1:

a. $\mathbf{PPh_3}$:

$$\begin{aligned}\Delta &= 3e\sigma - 4e\pi \\ &= 3(5,000) - 4(-1,750)cm^{-1} \\ &= 22,000\ \mathbf{cm^{-1}}.\end{aligned}$$

b. $\mathbf{Cl^-}$:

$$\begin{aligned}\Delta &= 3(3,900) - 4(1,500) \\ &= 5,700\ \mathbf{cm^{-1}}.\end{aligned}$$

c. $\mathbf{Br^-}$:

$$\begin{aligned}\Delta &= 3(3,600) - 4(1,000) \\ &= 6,800\ \mathbf{cm^{-1}}.\end{aligned}$$

Example 9.16.2

AOM parameters eσ were calculated from spectroscopic data for a series of bidentate nickel complexes with octahedral geometry, $Ni(en')_2(NCS)_2$.[2]

- en' = $H_2NCH_2CH_2NH_2$ with eσ = 4,010 cm-1
- en' = $(CH_3)_2NCH_2CH_2N(CH_3)_2$ with eσ = 3,165 cm-1
- en' = $(CH_3CH_2)_2NCH_2CH_2NH_2$ with eσ = 2,485 cm-1 ($-NEt_2$); eσ = 4,650 cm-1 ($-NH_2$)

Explain the reasons for the differences in the eσ values.

Solution

Greater steric hindrance appears to decrease the interaction between the sigma donor and the metal. Thus, the magnitude of eσ decreases from the least hindered $-NH_2$ group to the most hindered NEt_2 group.

References

1. Figgis, B. N.; Hitchman, M. A. *Ligand Field Theory and Its Applications*. Wiley-VCH: New York, 2000, p. 71.
2. Lever, A. B. P.; Walker, I. M.; McCarthy, P. J.; Mertes, K. B.; Jircitano, A.; Sheldon, R. "Crystallographic and Spectroscopic Studies of Low-Symmetry Nickel(II) Complexes Possessing Ling Nickel-Nitrogen Bonds", *Inorg. Chem.* **1983**, *22*, 2252-8.

This page titled 9.16: The Magnitude of Parameters eσ, eπ and Δ is shared under a CC BY-NC 4.0 license and was authored, remixed, and/or curated by Chris Schaller.

9.17: The Jahn-Teller Effect

Certain metal ions frequently display distortions from ideal geometry, such that the symmetry of the compound is lowered. In tetragonal distortions of octahedral complexes, for example, the metal-ligand bond distances of two axial ligands may be significantly longer than the distances of the equatorial ligands. Alternatively, two of the metal-ligand distances may be compressed compared to others.

Sometimes, these distortions can be experimentally observed. For example, EXAFS (X-ray absorption fine structure) data for [Cu(OH2)6](BrO3)2, an octahedral complex in which all six Cu-O bonds ought to be the same length, show two different Cu-O distances of 1.96(1) and 2.32(2) Å (the digit in parentheses is used to convey the degree of uncertainty in X-ray measurements).1 That's an approximately 20% difference between the same kind of metal-ligand bond distances within the same complex.

These distortions, often called **Jahn-Teller distortions**, are observed in complexes of transition metals with specific electron configurations: high spin d4, low spin d7, and d9 (for which there is neither a low nor high spin case). These configurations give rise to unequally occupied degenerate orbitals. Degenerate orbitals are multiple orbitals at the same energy. The three p orbitals in an atomic shell are degenerate, for example. In contrast, non-degenerate orbitals occur at different energy levels. These two cases are illustrated below with the simplest conceivable case, a pair of orbitals.

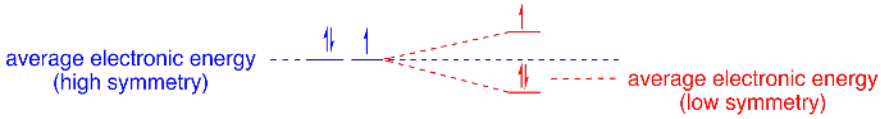


A set of degenerate orbitals might be equally or unequally occupied depending on the number of available electrons. For example, in the simple case of two degenerate orbitals, equal occupancy would occur if there were two electrons or four electrons because those even numbers of electrons could be divided evenly between the two orbitals. Either one or three electrons would lead to unequally occupied orbitals; there is no way to put the same number of electrons in each orbital in this case.

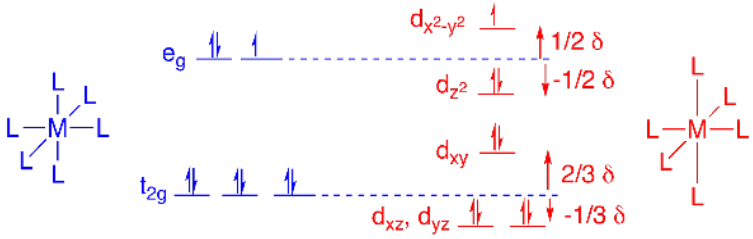




These cases of unequally occupied degenerate orbitals can lead to opportunities for distortion. When the symmetry of a complex drops, two otherwise degenerate orbitals might no longer exist at the same energy as each other. That means, for example, that instead of having three electrons at the same energy, we would have two electrons at lower energy and one at higher. There would be a net decrease in energy in the non-symmetric, distorted case.

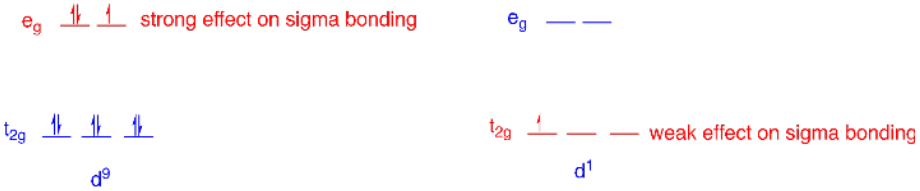


In the context of an octahedral d9 complex, elongation of the bonds to the axial ligands leads to a very slight lowering of the d orbitals that interact with ligands along the z axis: the dz2 and the dxz and dyz. The other orbitals are shown increasing slightly according to the principle that the average energy of the orbitals is preserved at the orbital barycenter (as opposed to the energy of the electrons, which decreases in this case).



Not all cases of unequally occupied degenerate orbitals produce measurable Jahn Teller distortions. In octahedral geometry, examples of strong Jahn Teller effects are seen when the unequally occupied orbitals are in the eg set rather than the t2g set. The eg

set is the one that is linked to sigma bonding, after all, so the orbitals in that level are strongly influenced by the strength of that sigma bonding interaction, and hence the bond length.



Changes in bond length are not the only observable result of the Jahn Teller effect. The absorption spectra of some octahedral complexes show two distinct d-d bands rather than the one band absorbed for pure octahedral symmetry. This observation is a consequence of having additional orbital levels giving rise to distinct electronic transitions. This phenomenon is also seen if the excited state, rather than the ground state, experiences Jahn Teller distortion.

The Jahn Teller effect also plays a role in reactivity. For example, it is thought to promote the lability of octahedral Cu(II) complexes by weakening the bonds to axial ligands via the tetragonal distortion.

References

1. Persson, I.; Persson, P.; Sandstrom, M.; Ullström, A.-S. "Structure of Jahn–Teller distorted solvated copper(ii) ions in solution, and in solids with apparently regular octahedral coordination geometry." *J. Chem. Soc. Dalton* **2002**, 1256-1265.

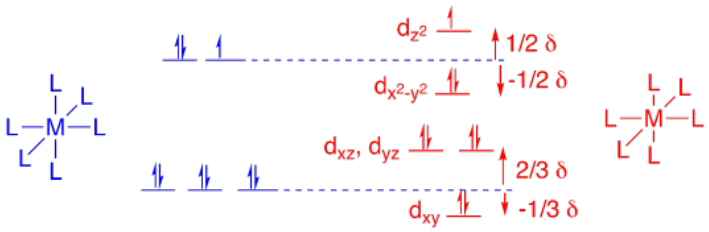
Problems

1. Given the effect of axial bond elongation on the d orbital energy levels in an octahedral complex, show the corresponding effects that would result from shortening of the axial metal ligand bonds.

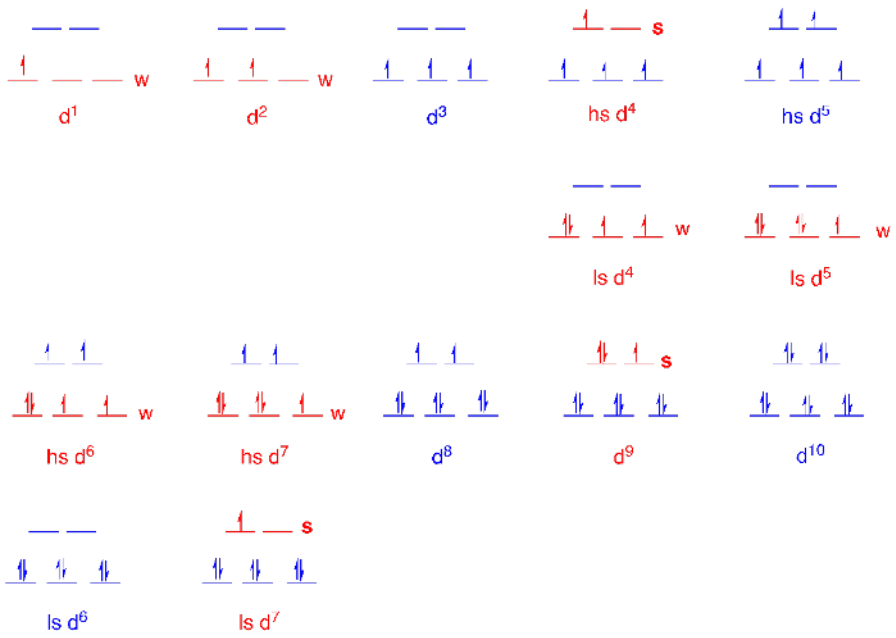
2. Fill in octahedral d orbital splitting diagrams for d1 to d10 configurations to show why only high spin d4, low spin d7 and d9 configurations exhibit strong Jahn Teller distortions.

Solutions

1. This time, dz2 is elevated, along with the dxz and dyx.



2. The w indicates a weak Jahn Teller effect. The s indicates a strong Jahn Teller effect.



This page titled 9.17: The Jahn-Teller Effect is shared under a CC BY-NC 4.0 license and was authored, remixed, and/or curated by Chris Schaller.

Index

A

atomic radius
- 2.11: Lanthanide Contraction

Aufbau principle
- 2.6: Aufbau Principle

B

barycenter
- 9.4: Crystal Field Theory

bent
- 3.6: Valence Shell Electron-Pair Repulsion

beryllium
- 3.5: Lewis Fails to Predict Unusual Cases - Boron and Beryllium

block diagonal
- 5.7: Representations of Point Groups

bond angle
- 3.6: Valence Shell Electron-Pair Repulsion

Bragg equation
- 8.8: Lattice Structures in Crystalline Solids

bridging ligands
- 4.6: Coordination Frameworks

C

character (matrix)
- 5.7: Representations of Point Groups

character table
- 5.8: Character Tables

charge transfer band
- 7.4: The electronic spectra of charge transfer complexes illustrate the impact of frontier orbital interactions on the electronic structure of Lewis-Acid base adducts

chelate ring
- 4.4: Isomerism

chirality
- 5.10: Chirality

coordinate covalent bond
- 4.1: Prelude to Coordination Chemistry I - Structure and Isomers

coordination compounds
- 4.1: Prelude to Coordination Chemistry I - Structure and Isomers

coordination number
- 8.8: Lattice Structures in Crystalline Solids

crystal field stabilization energy
- 9.4: Crystal Field Theory

crystal field theory
- 9.4: Crystal Field Theory

cubic closest packing
- 8.8: Lattice Structures in Crystalline Solids

D

D Block Contraction
- 2.11: Lanthanide Contraction

diffraction
- 8.8: Lattice Structures in Crystalline Solids

Diode
- 8.7: Diodes, LEDs and Solar Cells

dipole moment
- 3.6: Valence Shell Electron-Pair Repulsion
- 3.11: Molecular Polarity

Drago and Wayland's EC Model
- 7.6: Quantitative Measures of Hardness, Softness, and Acid-Base Interactions from a Hard Soft Acid-Base Principle perspective involve orbital energies and or apportioning acid-base bonding in terms of electrostatic and covalent factors

E

ECW model
- 7.6: Quantitative Measures of Hardness, Softness, and Acid-Base Interactions from a Hard Soft Acid-Base Principle perspective involve orbital energies and or apportioning acid-base bonding in terms of electrostatic and covalent factors

effective nuclear charge
- 2.7: Shielding

electron affinity
- 2.10: Electron Affinity

electronegativity (Mulliken)
- 7.6: Quantitative Measures of Hardness, Softness, and Acid-Base Interactions from a Hard Soft Acid-Base Principle perspective involve orbital energies and or apportioning acid-base bonding in terms of electrostatic and covalent factors

electronegativity
- 3.9: Electronegativity and Atomic Size Effects

electrophile
- 7.1: Lewis Concept and Frontier Orbitals

enantiomers
- 5.10: Chirality

F

formal charge
- 3.4: Formal Charge

frontier orbitals
- 7.2: The frontier orbital approach considers Lewis acid base reactions in terms of the donation of electrons from the base's highest occupied orbital into the acid's lowest unoccupied orbital.

H

hexagonal closest packing
- 8.8: Lattice Structures in Crystalline Solids

hole
- 8.8: Lattice Structures in Crystalline Solids

hydrogen bonding
- 3.12: Hydrogen Bonding

hypervalency
- 3.1: Lewis Electron-Dot Diagrams

hypervalent molecule
- 3.3: Breaking the octet rule with higher electron counts (hypervalent atoms)

hypovalency
- 3.1: Lewis Electron-Dot Diagrams

I

ionization energy
- 2.11: Lanthanide Contraction

isomerism
- 4.4: Isomerism

isomorphous
- 8.8: Lattice Structures in Crystalline Solids

K

Kepert Model
- 4.5: Coordination Numbers and Structures

L

Lanthanide Contraction
- 2.11: Lanthanide Contraction

Ligand Close Packing (LCP)
- 3.10: Ligand Close Packing

Ligand Field Stabilization Energy
- 9.8: Ligand Field Stabilization Energy

linear
- 3.6: Valence Shell Electron-Pair Repulsion

Linear Combination of Atomic Orbitals (LCAO)
- 6.1: Formation of Molecular Orbitals from Atomic Orbitals

M

Magnetic Susceptibility
- 9.3: Magnetic Susceptibility

N

nucleophile
- 7.1: Lewis Concept and Frontier Orbitals

O

octahedral
- 3.6: Valence Shell Electron-Pair Repulsion

octahedral hole
- 8.8: Lattice Structures in Crystalline Solids

orbital mixing
- 6.8: Orbital Mixing

P

particle in a box
- 2.4.1: Particle in a Box

Pearson's absolute hardness
- 7.6: Quantitative Measures of Hardness, Softness, and Acid-Base Interactions from a Hard Soft Acid-Base Principle perspective involve orbital energies and or apportioning acid-base bonding in terms of electrostatic and covalent factors

penetration
- 2.7: Shielding

philosopher's stone
- 1.2: History of Inorganic Chemistry

point groups
- 5.2: Point Groups

R

resonance
- 3.2: Resonance

resonance structures
- 3.2: Resonance

rotation axis
- 5.7: Representations of Point Groups

S

SALC
- 6.15: Carbon Dioxide

Scandide Contraction
2.11: Lanthanide Contraction
seesaw
3.6: Valence Shell Electron-Pair Repulsion
shielding
2.7: Shielding
shielding effect
2.11: Lanthanide Contraction
simple cubic structure
8.8: Lattice Structures in Crystalline Solids
simple cubic unit cell
8.8: Lattice Structures in Crystalline Solids
space lattice
8.8: Lattice Structures in Crystalline Solids
spectrochemical series
9.15: The Spectrochemical Series
square pyramidal
3.6: Valence Shell Electron-Pair Repulsion
superconductor
8.9: Superconductors
Symmetry Adapted Linear Combinations
6.13: Larger (Polyatomic) Molecules
symmetry elements
5.1: Symmetry Elements and Operations
symmetry operation
5.7: Representations of Point Groups
symmetry operations
5.1: Symmetry Elements and Operations

T

tetrahedral
3.6: Valence Shell Electron-Pair Repulsion
tetrahedral hole
8.8: Lattice Structures in Crystalline Solids
trigonal bipyramidal
3.6: Valence Shell Electron-Pair Repulsion
trigonal planar
3.6: Valence Shell Electron-Pair Repulsion
trigonal prismatic coordination
4.5: Coordination Numbers and Structures
trigonal pyramidal
3.6: Valence Shell Electron-Pair Repulsion

U

unit cell
8.8: Lattice Structures in Crystalline Solids
Usanovich acids
7.1: Lewis Concept and Frontier Orbitals
Usanovich bases
7.1: Lewis Concept and Frontier Orbitals

V

valence shell electron pair repulsion theory
3.6: Valence Shell Electron-Pair Repulsion
VSEPR
3.6: Valence Shell Electron-Pair Repulsion

Z

zeroth ionization energy
2.10: Electron Affinity

Glossary

Sample Word 1 | Sample Definition 1

Detailed Licensing

Overview

Title: CHE360: Inorganic Chemistry

Webpages: 116

Applicable Restrictions: Noncommercial

All licenses found:

- Undeclared: 38.8% (45 pages)
- CC BY-NC 4.0: 24.1% (28 pages)
- CC BY-SA 4.0: 24.1% (28 pages)
- CC BY-NC-SA 4.0: 6.9% (8 pages)
- CC BY 4.0: 4.3% (5 pages)
- CC BY-NC-SA 3.0: 0.9% (1 page)
- CC BY-NC 3.0: 0.9% (1 page)

By Page

- CHE360: Inorganic Chemistry - *Undeclared*
  - Front Matter - *Undeclared*
    - TitlePage - *Undeclared*
    - InfoPage - *Undeclared*
    - Table of Contents - *Undeclared*
    - Licensing - *Undeclared*
  - 1: Introduction to Inorganic Chemistry - *Undeclared*
    - 1.1: What is Inorganic Chemistry? - *Undeclared*
    - 1.2: History of Inorganic Chemistry - *CC BY-NC-SA 4.0*
  - 2: Atomic Structure - *Undeclared*
    - 2.1: Historical Development of Atomic Theory - *Undeclared*
    - 2.2: The Periodic Table - *Undeclared*
    - 2.3: Discovery of Subatomic Particles and the Bohr Atom - *CC BY-NC-SA 3.0*
    - 2.4: The Schrödinger equation, particle in a box, and atomic wavefunctions - *CC BY-NC-SA 4.0*
      - 2.4.1: Particle in a Box - *CC BY-NC-SA 4.0*
    - 2.5: Quantum Numbers and Atomic Wave Functions - *CC BY-NC-SA 4.0*
    - 2.6: Aufbau Principle - *CC BY-NC-SA 4.0*
    - 2.7: Shielding - *CC BY-NC-SA 4.0*
    - 2.8: Periodic Properties of Atoms - *Undeclared*
      - 2.8.1: Covalent and Ionic Radii - *CC BY-NC 4.0*
    - 2.9: Ionization energy - *Undeclared*
    - 2.10: Electron Affinity - *CC BY-NC 4.0*
    - 2.11: Lanthanide Contraction - *Undeclared*
  - 3: Simple Bonding Theory - *Undeclared*
    - 3.1: Lewis Electron-Dot Diagrams - *CC BY-NC 4.0*
    - 3.2: Resonance - *CC BY-NC 3.0*
    - 3.3: Breaking the octet rule with higher electron counts (hypervalent atoms) - *CC BY-NC 4.0*
    - 3.4: Formal Charge - *CC BY-NC 4.0*
    - 3.5: Lewis Fails to Predict Unusual Cases - Boron and Beryllium - *CC BY-NC 4.0*
    - 3.6: Valence Shell Electron-Pair Repulsion - *CC BY-NC-SA 4.0*
    - 3.7: Lone Pair Repulsion - *Undeclared*
    - 3.8: Multiple Bonds - *Undeclared*
    - 3.9: Electronegativity and Atomic Size Effects - *Undeclared*
    - 3.10: Ligand Close Packing - *Undeclared*
    - 3.11: Molecular Polarity - *Undeclared*
    - 3.12: Hydrogen Bonding - *Undeclared*
  - 4: Coordination Chemistry I- Structures and Isomers - *Undeclared*
    - 4.1: Prelude to Coordination Chemistry I - Structure and Isomers - *CC BY 4.0*
    - 4.2: History - *CC BY-NC-SA 4.0*
    - 4.3: Nomenclature and Ligands - *Undeclared*
    - 4.4: Isomerism - *CC BY 4.0*
    - 4.5: Coordination Numbers and Structures - *CC BY 4.0*
    - 4.6: Coordination Frameworks - *CC BY 4.0*
  - 5: Symmetry and Group Theory - *Undeclared*
    - 5.1: Symmetry Elements and Operations - *Undeclared*
    - 5.2: Point Groups - *Undeclared*

- 5.3: Groups of Low and High Symmetry - *Undeclared*
- 5.4: Other Groups - *Undeclared*
- 5.5: Properties and Representations of Groups - *Undeclared*
- 5.6: Matrices - *Undeclared*
- 5.7: Representations of Point Groups - *Undeclared*
- 5.8: Character Tables - *Undeclared*
- 5.9: Examples and Applications of Symmetry - *Undeclared*
- 5.10: Chirality - *CC BY-NC 4.0*
- 5.11: Molecular Vibrations - *CC BY-NC 4.0*

6: Molecular Orbitals - *Undeclared*

- 6.1: Formation of Molecular Orbitals from Atomic Orbitals - *CC BY-SA 4.0*
- 6.2: Molecular Orbitals from s Orbitals - *CC BY-SA 4.0*
- 6.3: Molecular Orbitals from p Orbitals - *CC BY-SA 4.0*
- 6.4: Molecular orbitals from d orbitals - *CC BY-SA 4.0*
- 6.5: Nonbonding Orbitals and Other Factors - *CC BY-SA 4.0*
- 6.6: Homonuclear Diatomic Molecules - *CC BY-SA 4.0*
- 6.7: Molecular Orbitals - *CC BY-SA 4.0*
- 6.8: Orbital Mixing - *CC BY-SA 4.0*
- 6.9: Diatomic Molecules of the First and Second Periods - *CC BY-SA 4.0*
- 6.10: Heteronuclear Diatomic Molecules - *CC BY-SA 4.0*
- 6.11: Orbital ionization energies - *CC BY-SA 4.0*
- 6.12: Polar bonds - *CC BY-SA 4.0*
- 6.13: Larger (Polyatomic) Molecules - *CC BY-SA 4.0*
- 6.14: Bifluoride anion - *CC BY-SA 4.0*
- 6.15: Carbon Dioxide - *CC BY-SA 4.0*
- 6.16: H_2O - *CC BY-SA 4.0*
- 6.17: NH_3 - *CC BY-SA 4.0*
- 6.18: CO_2 (Revisted with Projection Operators) - *CC BY-SA 4.0*
- 6.19: BF_3 - *CC BY-SA 4.0*
- 6.20: Ionic Compounds and Molecular Orbitals - *CC BY-SA 4.0*

7: Acid-Base and Donor-Acceptor Chemistry - *Undeclared*

- 7.1: Lewis Concept and Frontier Orbitals - *CC BY-NC 4.0*
- 7.2: The frontier orbital approach considers Lewis acid base reactions in terms of the donation of electrons from the base's highest occupied orbital into the acid's lowest unoccupied orbital. - *Undeclared*
- 7.3: All other things being equal electron withdrawing groups tend to make Lewis acids stronger and bases weaker while electron donating groups tend to make Lewis bases stronger and acids weaker - *Undeclared*
- 7.4: The electronic spectra of charge transfer complexes illustrate the impact of frontier orbital interactions on the electronic structure of Lewis-Acid base adducts - *CC BY-NC 4.0*
- 7.5: Hard and Soft Acids and Bases - *Undeclared*
- 7.6: Quantitative Measures of Hardness, Softness, and Acid-Base Interactions from a Hard Soft Acid-Base Principle perspective involve orbital energies and or apportioning acid-base bonding in terms of electrostatic and covalent factors - *CC BY-NC 4.0*
- 7.7: Hard-Hard and Soft-Soft preferences may be explained and quantified in terms of electrostatic and covalent and electronic stabilization on the stability of Lewis acid-base adducts - *CC BY-NC 4.0*

8: The Crystalline Solid State - *Undeclared*

- 8.1: Molecular Orbitals and Band Structure - *CC BY-SA 4.0*
- 8.2: Prelude to Electronic Properties of Materials - Superconductors and Semiconductors - *CC BY-SA 4.0*
- 8.3: Metal-Insulator Transitions - *CC BY-SA 4.0*
- 8.4: Periodic Trends- Metals, Semiconductors, and Insulators - *CC BY-SA 4.0*
- 8.5: Semiconductors- Band Gaps, Colors, Conductivity and Doping - *CC BY-SA 4.0*
- 8.6: Semiconductor p-n Junctions - *CC BY-SA 4.0*
- 8.7: Diodes, LEDs and Solar Cells - *CC BY-SA 4.0*
- 8.8: Lattice Structures in Crystalline Solids - *CC BY 4.0*
- 8.9: Superconductors - *CC BY-SA 4.0*

9: Coordination Chemistry II- Bonding - *Undeclared*

- 9.1: Evidence for Electronic Structures - *CC BY-NC 4.0*
- 9.2: Thermodynamic Data - *CC BY-NC 4.0*
- 9.3: Magnetic Susceptibility - *CC BY-NC 4.0*
- 9.4: Crystal Field Theory - *CC BY-NC 4.0*
- 9.5: Ligand Field Theory - *CC BY-NC 4.0*
- 9.6: Ligand Field Theory - Molecular Orbitals for an Octahedral Complex - *CC BY-NC 4.0*
- 9.7: Orbital Splitting and Electron Spin - *CC BY-NC 4.0*
- 9.8: Ligand Field Stabilization Energy - *CC BY-NC 4.0*
- 9.9: Tetrahedral Complexes - *CC BY-NC 4.0*

- 9.10: Ligand Field Theory New Page - *Undeclared*
- 9.11: Angular Overlap - *CC BY-NC 4.0*
- 9.12: Sigma Bonding in the Angular Overlap Model - *CC BY-NC 4.0*
- 9.13: Pi Acceptors in the Angular Overlap Model - *CC BY-NC 4.0*
- 9.14: Pi Donors in the Angular Overlap Model - *CC BY-NC 4.0*
- 9.15: The Spectrochemical Series - *CC BY-NC 4.0*
- 9.16: The Magnitude of Parameters eσ, eπ and Δ - *CC BY-NC 4.0*
- 9.17: The Jahn-Teller Effect - *CC BY-NC 4.0*

Back Matter - *Undeclared*

- Index - *Undeclared*
- Glossary - *Undeclared*
- Detailed Licensing - *Undeclared*